

Copyright is owned by the Author of the thesis. Permission is given for a copy to be downloaded by an individual for the purpose of research and private study only. The thesis may not be reproduced elsewhere without the permission of the Author.

**INSTITUTE OF FOOD, NUTRITION AND HUMAN HEALTH  
MASSEY UNIVERISTY  
PALMERSTON NORTH  
NEW ZEALAND**

**RHEOLOGICAL  
CHARACTERISATION OF AGE  
THICKENING IN MILK  
CONCENTRATES**

**A THESIS PRESENTED IN PARTIAL FULFILMENT OF THE  
REQUIREMENTS FOR THE DEGREE OF DOCTOR OF  
PHILOSOPHY IN FOOD ENGINEERING AT MASSEY  
UNIVERSITY**

**BINH TRINH  
2006**

## SUMMARY

This project investigates the time-dependent rheological behaviour of fresh and reconstituted milk concentrates.

New experimental protocols, including sampling and measurement techniques, as well as equipment calibration and data analysis procedures were developed for both the industrial surveys and controlled rheology experiments.

The controlled rheology experiments were mainly carried out on reconstituted milk concentrates to minimise the variation in composition of fresh milk. A new recombination rig was built which could minimise the age thickening process by mixing at 35°C and recirculating at 40,000 s<sup>-1</sup> to break down the structure completely. This is the essence of this project, where age thickening is studied from a starting point of a fully broken down structure in contrast to past research. Using this method, the replicate milk concentrate samples had reproducible rheological behaviour, with a maximum reproducible error of 10%.

Age thickening involves two stages, a slow initial increase in apparent viscosity with storage time, followed by a sudden sharp rise which marks the onset of gelation.

The age thickening behaviour of milk concentrates is dependent on the processing variables prior to rheological measurement. These include solids content, shear rate and temperature during recombination, shear rate and residence time in the plate heat exchanger, and most importantly the raw material. The viscosity at the gelling point is an important characteristic of the age thickening process, and seems to depend mainly on the powder used, rather than the process treatments applied.

Industrial surveys exhibited similar trends, even under varying conditions that could not be completely controlled.

It is proposed that two types of age thickening phenomena can be distinguished: type I occurs below the temperature at minimum viscosity (65°C in this case), where weak

interactions take place between the casein micelles; type II occurs above the temperature at minimum viscosity, where additional stronger covalent bonds are formed, primarily due to the denaturation of whey proteins.

No mathematical model for the time-dependent rheology was developed. However, some important issues that must be taken into account during modelling were discussed.

The results showed that the age thickening process is more complex than had previously been envisaged. The knowledge of the interactions between the operating conditions, rheology of fresh concentrates and powder properties should be invaluable in the improvement of plant efficiency and quality control.

## ACKNOWLEDGEMENTS

I would like to dedicate this PhD to my loving father, I will forever be in his debt for his love, kindness, perseverance, and faith in me, and to my caring mother for always supporting me throughout my life.

I wish to express my deepest appreciation and gratitude to my supervisor, Dr Derek Haisman for his supervision, guidance and patience during the course of this project. I would also wish to extend my appreciation to my co-supervisors, Dr Mike Weeks, and Mr Brent Prankerd for their support and invaluable help, particularly during the plant visits.

I would like to thank Mr Byron McKillop for his valuable assistance, particularly during the design and commission work on the recombination rig, Mr. Steve Glassgow, Mr. Garry Radford, Mr. Aaron Hicks for their technical assistance during the experimental work at Massey University, Mr. Darren Johnson and Mr. Carrigan Trower for making the industrial surveys trouble free and enjoyable.

I wish to extend my gratitude to the Foundation for Research, Science and Technology, New Zealand and Fonterra Co-operative Ltd for their generous financial support without which this project would not have been possible.

I sincerely thank the staff of the Institute of Food, Nutrition and Human Health for their assistance. I would also like to mention the enjoyable company and memorable moments provided by my fellow post-graduate students during the course of this project.

Finally, I would like to express my special thanks to my sincere friend, Laura Clouston, for her love, encouragement, patience and invaluable help.

## TABLE OF CONTENTS

<b>ABSTRACT</b>	ii
<b>ACKNOWLEDGEMENTS</b>	iv
<b>TABLE OF CONTENTS</b>	v
<b>LIST OF FIGURES</b>	xv
<b>LIST OF TABLES</b>	xxxv
<b>LIST OF SYMBOLS</b>	xxxix
<b>NOMENCLATURE</b>	xli
<b>LIST OF PUBLICATIONS</b>	xlii
<b>1 INTRODUCTION</b>	1
<b>2 LITERATURE REVIEW</b>	5
2.1 Milk concentrate rheology	6
2.1.1 Milk composition	10
2.1.1.1 Total solids content	10
2.1.1.2 Protein	14
2.1.1.3 Fat	19
2.1.1.4 Salts and minerals	21
2.1.1.5 Urea	22
2.1.1.6 Seasonal variation and stage of lactation	23
2.1.2 pH	26
2.1.3 Temperature during processing	29
2.1.4 Preheat treatment	34
2.1.5 Reconstituted versus fresh milk	36
2.1.6 Effect of rheological behaviour of concentrate	36

	systems on processing conditions and milk powder properties	
2.1.7	Rheological modelling	37
2.1.8	Postulated mechanism of age thickening	40
2.1.9	Summary	42
2.2	Recombination	44
2.2.1	Raw ingredients	45
2.2.2	Recombining technology	45
2.2.3	Equipment	46
2.3	Conclusion of literature review	46
<b>3</b>	<b>MATERIALS AND METHODS</b>	<b>49</b>
3.1	Introduction	50
3.2	Recombination rig	53
3.2.1	Principle of design	53
3.2.2	Commissioning experiments	57
3.2.2.1	Viscosity data during recombination	57
3.2.2.2	Viscosity data during storage at 65°C	60
3.2.2.3	Effect of bacteria	62
3.2.2.4	Replicate error	67
3.2.3	Recombination protocol	67
3.3	Performance characterisation of the Paar Physica MC1	68
3.3.1	Minimum reliable spindle speed	73
3.3.1.1	Cause of scattering error	80
3.3.1.2	Effect of measurement time on the performance of the MC1	84

3.3.2	Minimum reliable torque	86
3.3.2.1	Accuracy and stress correction protocol	89
3.3.3	Rheological measurement protocol for the Paar Physica MC1	93
3.4	Industrial surveys	94
3.4.1	Sampling method	97
3.4.2	Rheological measurement protocol for Brookfield viscometer	99
3.4.3	Brookfield versus Paar Physica MC1	100
3.4.3.1	Comparison of Brookfield and Paar Physica MC1 measurements	101
3.4.3.2	Time-dependent analysis	104
3.5	Controlled rheology experimental protocols	108
3.5.1	Materials	109
3.5.2	Generalised experimental procedures for reconstituted samples	110
3.5.3	TEM protocol	111
3.5.4	Particle size distribution (PSD) analysis	112
3.5.5	Total solids content measurement	112
3.6	Data analysis	113
3.6.1	Brookfield LVTD data	113
3.6.1.1	Shear stress and shear rate calculations	113
3.6.2	Paar Physica MC1 data	115
3.6.2.1	Shear stress and shear rate calculations	115
3.6.2.2	Non-Newtonian corrections	118
3.6.2.3	Model fitting and data analysis	122

<b>4</b>	<b>INDUSTRIAL SURVEYS</b>	124
4.1	Effect of plant operation on the rheology of fresh milk concentrate systems	125
4.2	Effect of plant design on the rheology of fresh milk concentrate systems	134
4.3	Effect of solids content on the rheology of fresh milk concentrate systems	145
4.4	Effect of preheat treatment on the rheology of fresh milk concentrate systems	147
4.5	Effect of protein content on the rheology of fresh milk concentrate systems	152
4.6	Effect of shear rate during sampling on the rheology of fresh milk concentrate systems	155
<b>5</b>	<b>CONTROLLED RHEOLOGY EXPERIMENTS</b>	162
5.1	Rheological characterisation of whole milk concentrate systems	165
5.1.1	Materials and methods	166
5.1.2	Results	166
5.1.2.1	Basic flow curve	166
5.1.2.2	Rheological descriptors of time-dependent fluids	167
5.1.2.2.1	Apparent viscosity	167
5.1.2.2.2	Extrapolated viscosity at infinite shear rate	170
5.1.2.2.3	Hysteresis loop area	173
5.1.2.2.4	Rheological modelling	178
5.1.2.3	Limitations	180
5.2	Comparative rheology of fresh and reconstituted whole milk concentrates	183

5.2.1	Materials and methods	185
5.2.1.1	Fresh versus reconstituted milk with different shear history using the Brookfield LVTD and the Paar Physica MCI	185
5.2.1.2	Fresh versus reconstituted milk with different shear history using the Paar Physica MCI	186
5.2.1.3	Fresh versus reconstituted milk with the same shear history using the Paar Physica MCI	186
5.2.2	Results	188
5.2.2.1	Fresh versus reconstituted milk with different shear history using the Brookfield LVTD and the Paar Physica MCI	188
5.2.2.2	Fresh versus reconstituted milk with different shear history using the Paar Physica MCI	190
5.2.2.3	Fresh versus reconstituted milk with the same shear history using the Paar Physica MCI	192
5.3	Effect of solids content on the rheology, pH and PSD of the reconstituted whole milk concentrates	196
5.3.1	Materials and methods	196
5.3.2	Results	197
5.4	Effect of solids content and temperature on the rheology of reconstituted whole milk concentrates	202
5.4.1	Materials and methods	202
5.4.2	Powder A results	204
5.4.2.1	Effect of solids content and temperature on the initial viscosity	204
5.4.2.2	Effect of solids content and temperature on age thickening	209
5.4.2.3	Rheological modelling	219
5.4.3	Powder B results	225

5.4.3.1	Effect of solids content and temperature on age thickening	225
5.4.3.2	Rheological modelling	228
5.4.3.3	Changes in PSD of powder A reconstituted concentrates during age thickening	230
5.4.4	Data summary	233
5.5	Effect of shear rate during recirculation on the rheological behaviour of reconstituted whole milk concentrates during reconstitution and subsequent heating and storage	234
5.5.1	Materials and methods	234
5.5.2	Results	236
5.5.2.1	Effect of recirculation shear rate on the inline rheological behaviour	236
5.5.2.2	Effect of recirculation shear rate on the rheological behaviour of heated reconstituted milk concentrates during storage at 65°C for powder A concentrates and 75°C for powder B concentrates	242
5.5.2.3	Effect of recirculation time and shear rate on the rheology of heated reconstituted milk concentrates made from powder A during storage at 65°C	248
5.5.2.4	Changes in PSD of powder A reconstituted concentrates during recirculation and storage	250
5.5.3	Data summary	254
5.6	Effect of temperature during recirculation on the rheological behaviour of reconstituted whole milk concentrates during reconstitution and subsequent heating and storage	255
5.6.1	Materials and methods	255
5.6.2	Powder A results	257

5.6.2.1	Effect of recirculation temperature on the inline rheological behaviour	257
5.6.2.2	Effect of recirculation temperature on the rheological behaviour of stored samples at 65°C	258
5.6.3	Powder B results	259
5.6.3.1	Effect of recirculation temperature on the inline rheological behaviour	259
5.6.3.2	Effect of recirculation temperature on the rheological behaviour of stored samples at 75°C	260
5.6.4	Data summary	261
5.7	Effect of shear and residence time during heating on the rheology of reconstituted whole milk concentrates	262
5.7.1	Materials and methods	262
5.7.2	Results	263
5.7.2.1	Age thickening during storage	263
5.7.2.2	Rheological modelling	267
5.7.2.3	Changes in PSD during age thickening	268
5.7.3	Data summary	270
5.8	Age thickening of skim and whole milk concentrates- TEM, rheology, PSD	271
5.8.1	Materials and methods	271
5.8.2	Results	272
5.8.2.1	Age thickening in reconstituted whole milk concentrates	272
5.8.2.1.1	Rheological measurement	272
5.8.2.1.2	PSD	275

5.8.2.1.3	TEM	276
5.8.2.2	Age thickening in reconstituted skim milk concentrates	280
5.8.3	Data summar	283
5.9	Direct experimental proof of irreversible changes during age thickening	284
5.9.1	Materials and methods	285
5.9.2	Results	286
5.9.2.1	Irreversibility at 35°C	286
5.9.2.2	Irreversibility at 75°C	293
5.9.3	Data summary	299
<b>6</b>	<b>DISCUSSION</b>	<b>300</b>
6.1	Data analysis	301
6.1.1	Data collection and measurement procedures	301
6.1.1.1	Oscillatory versus flow curve tests	301
6.1.1.2	Structure breakdown and build up	302
6.1.2	Measurement with the Brookfield LVDT viscometer and the Paar Physica MCI rheometer	303
6.1.3	Techniques for rheology characterisation of time dependent milk concentrates	304
6.1.4	Bias and short comings of the modelling technique	306
6.2	Methods of recombination	309
6.3	Controlled rheology experiments	312
6.3.1	Use of reconstituted powder solutions versus fresh milk concentrates	312
6.3.2	Effects of solids content and temperature on the transition of rheological behaviour in reconstituted	312

whole milk concentrates	
6.3.3 Behaviour of milk concentrates observed during age thickening	314
6.3.4 Effect of solids content and temperature on the rheology of reconstituted milk concentrates	316
6.3.4.1 Solids Content	316
6.3.4.2 Temperature	317
6.3.5 Effect of sample preparation techniques on the rheology of reconstituted milk concentrates	319
6.3.5.1 Effect of recombination shear rate	319
6.3.5.2 Effect of recombination temperature	322
6.3.6 Effect of powder origin	322
6.4 Industrial surveys	324
6.5 Mechanism for age thickening	325
6.5.1 Physical changes during concentration and heating	326
6.5.1.1 Volume fraction	327
6.5.1.2 PSD	327
6.5.2 Reversible and irreversible changes during age thickening	329
6.5.2.1 Changes not reversed by dilution	329
6.5.2.2 Changes not reversed by shearing	329
6.5.3 Milk components and chemical changes involved in the age thickening process	331
6.5.4 Types of age thickening	333
6.5.5 Proposed mechanisms of age thickening	335
6.5.5.1 Physical interactions in type I mechanism	335
6.5.5.2 Aggregation in type II mechanism	337

6.5.5.3	Particle interactions	338
6.5.6	Modelling of the age thickening process	342
<b>7</b>	<b>CONCLUSIONS AND RECOMMENDATIONS</b>	<b>346</b>
7.1	Calibration of the Paar Physica MC1	347
7.2	Controlled rheology experiments	347
7.2.1	Rheology of milk concentrates	347
7.2.1.1	Effect of solids content and temperature on the viscosity of reconstituted milk concentrates	348
7.2.2	Age thickening behaviour	348
7.2.2.1	Processing conditions affecting the age thickening behaviour	349
7.2.2.2	Effect of powder origin	349
7.3	Industrial surveys	349
7.4	Mechanisms of age thickening	350
7.5	Recommendations for future studies	350
7.5.1	Improvements to the recombination rig	350
7.5.2	Industrial surveys	351
7.5.3	Factors affecting the age thickening behaviour of reconstituted milk concentrates	351
7.6	Concluding remarks	351
<b>8</b>	<b>REFERENCES</b>	<b>353</b>
	<b>APPENDICES</b>	<b>A1</b>
A.1.	Milk system literature review	A2
A.2.	Time-dependent rheology: Thixotropy review	A16

A.3.	Ratios of change in the Herschel-Bulkley parameters during age thickening	A82
A.4.	Comparison of consistency coefficient versus apparent viscosity	A84

## LIST OF FIGURES

- Figure 2.1: Relative change in viscosity of whey protein free milk with various concentrations of  $\beta$ -lactoglobulin ( $\beta$ -lg) as a function of the holding time at 90°C: o,  $\beta$ -lg = 0.2g/L; •,  $\beta$ -lg = 3.3g/L;  $\Delta$ ,  $\beta$ -lg = 6.6g/L. (Jeurnink & Dekruif, 1993)..... 15
- Figure 2.2: Schematic representation of the casein/whey protein acid gels. (A) casein/native whey protein heated to 20°C, (B) casein/native whey protein heated to 80°C, (C) casein/pre-denatured whey protein, which has been heated to 80°C, heated to 20°C, (D) casein-pre-denatured whey protein, which has been heated to 80°C, heated to 80°C. (Schorsch et al. 2001) ..... 17
- Figure 2.4: Schematic representation of the thickening of non-homogenised concentrate (A) and of homogenized concentrate (B). (Snoeren et al., 1984) ..... 22
- Figure 2.5: pH-HCT profile of a Type A milk. (McCrae, 1999)..... 28
- Figure 2.6: pH-HCT profile of a Type B milk. (McCrae, 1999)..... 29
- Figure 2.7: A schematic representation of the interactions between casein micelles and whey proteins occurring in milk during heat treatment for 10 minutes at 80°C at pH values ranging from 6.35 to 6.9. The small circles represent denatured whey proteins, the large circles the casein micelles. The whey proteins are either present in aggregates or covalently associated with the casein micelle. Native whey proteins are not included in the figure. (Vasbinder & de Kruif, 2003)..... 32
- Figure 2.8: Variation of apparent viscosity with temperature and storage time. (Trinh and Shrakeenrad, 2002) ..... 34
- Figure 3.1: Schematic layout of the recombination rig..... 54
- Figure 3.2: Accurate Dry Material Feeder. .... 55

Figure 3.3:	Mixing tank equipped with four baffles and a central baffle disc. ....	55
Figure 3.4:	Powder mixing system .....	56
Figure 3.5:	Capillary tubes system.....	57
Figure 3.6:	Shear sweep curve for a 47%TS reconstituted sample of medium heat whole powder just after complete mixing. Experiment A1, Paar Physica MC1, Z2.1, CSS, 35°C.....	58
Figure 3.7:	Viscosity at 105.3 Pa against recirculation time for reconstituted samples of medium whole milk powder at 47.1 %TS (A1) and 45.8 %TS (A2). Paar Physica MC1, Z2.1, CSS, 35 °C. ....	59
Figure 3.8:	Effect of recirculation time at 35°C on the viscosity during storage for a heated reconstituted whole milk concentrate solution. Experiment A3, Paar Physica MC1, Z2.1, CSS, 48%TS, 65°C.....	61
Figure 3.9:	Change in in-line viscosity with recirculation time at 35°C for three reconstituted solutions at three concentrations, 45.1%TS (A6), 46.5%TS (A7), 47%TS (A8). Paar Physica MC1, Z2.1, CSS, 35°C. ....	65
Figure 3.10:	Effect of recirculation time at 35°C on the viscosity during storage for heated reconstituted whole milk concentrates. Experiment A9, Paar Physica MC1, Z2.1, CSS, 48%TS, 65°C. ....	66
Figure 3.11:	Paar Physica MC1 and Julabo water bath .....	70
Figure 3.12:	Paar Physica MC1 spindles Z2,1 (left bob and cup) and Z3 (right bob and cup).....	71
Figure 3.13:	Flow curve of a S60 oil at 20°C using a Z2.1 spindle in CSS mode. Experiment A32. ....	72

Figure 3.14: Viscosity against shear rate for a S60 oil at 20°C using a Z2.1 spindle in CSS mode. Experiment A32. ....	73
Figure 3.15: Shear sweep curves for S200 oil at several temperatures. (a) viscosity versus spindle speed, (b) viscosity versus torque. Experiment A33-A36, Paar Physica MC1, Z1, CSR. ....	75
Figure 3.16: Comparison between shear sweep and shear step tests for S200 oil using the Z1 spindle at 40°C in CSR mode. Experiment A37-A40, Paar Physica MC1, Z1, CSR. Solid line represents the data from a single shear sweep test. The data points represent the data from three replicate shear step tests. ....	76
Figure 3.17: Coefficient of variation (COV) against spindle speed at different temperatures for S200 oil. Experiments A41-A44, Paar Physica MC1, Z1, CSR.....	78
Figure 3.18: Coefficient of variation (COV) against spindle speed at different temperatures for S2000 oil. Experiments A45-A49, Paar Physica MC1, Z3, CSR....	79
Figure 3.19: Variation in viscosity over 5 minutes of constant shear of 4rpm and 90 rpm for an S200 oil at 40°C. Experiment A74, Paar Physica MC1, Z1, CSR.....	81
Figure 3.20: Viscosity and relative position versus spindle speed for an S200 oil at 40°C. Experiment A74, Paar Physica MC1, Z1, CSR. ....	82
Figure 3.21: Viscosity versus rotational position at 4rpm and 90 rpm, for an S200 oil at 40°C. Experiment A74, Paar Physica MC1, Z1, CSR.....	83
Figure 3.22: Effect of measurement time on the COV versus spindle speed plot of a S60 oil at 20°C. Experiments A73-A77, Paar Physica MC1, Z2.1, CSR. ....	85
Figure 3.23: Effect of measurement time on the COV versus torque plot of a S60 oil at 20°C. Experiments A81-A85, Paar Physica MC1, Z2.1, CSR. ....	85

Figure 3.24: Normalised viscosity for S2000 oil at different temperatures. (a) normalised viscosity versus spindle speed (b) normalised viscosity versus torque. Experiments A102-A106, Paar Physica MC1, Z3, CSR. ....	88
Figure 3.25: Viscosity against shear stress for the S60 oil at different temperatures without stress correction. Experiments A107-A118, Paar Physica MC1, Z2.1, CSS. ....	90
Figure 3.26: Stress correction coefficient versus spindle speed for S60 oil at different temperatures. Experiments A107-A118, Paar Physica MC1, Z2.1, CSS.....	91
Figure 3.27: Corrected viscosity against shear stress for the S60 oil at different temperatures with stress correction. Experiments A107-A118, Paar Physica MC1, Z2.1, CSS.....	92
Figure 3.28: General process flow chart during skim milk powder processing.....	95
Figure 3.29: Brookfield LVTD viscometer and LV1 spindle .....	98
Figure 3.30: Change in viscosity with shearing time for fresh infant milk concentrate samples taken after the evaporator (47.4%TS, 52°C) at the Waitoa milk powder plant with the Brookfield LVTD viscometer. Experiment A119. ....	102
Figure 3.31: Change in viscosity with shearing time for fresh infant milk concentrate samples taken after the concentrate heater (47.12%TS, 72°C) at the Waitoa milk powder plant with the Brookfield LVTD viscometer. Experiment A119.....	102
Figure 3.32: Change in viscosity at 105.3 Pa with storage time for fresh infant milk concentrate samples taken after the evaporator (47.4 %TS, 52°C) and concentrate heater (47.4%TS, 74°C) at the Waitoa milk powder plant. Experiment A119, Paar Physica MC1.....	103

Figure 3.33: Change in  $\tau_y$  with storage time for fresh infant milk concentrate samples collected after the concentrate heater data at the Waitoa milk powder plant. Experiment A119, Paar Physica MC1, 47.5%TS, 75°C.....107

Figure 3.34: Change in  $K$  with storage time for fresh infant milk concentrate samples collected after the concentrate heater data at the Waitoa milk powder plant. Experiment A119, Paar Physica MC1, 47.5%TS, 75°C.....107

Figure 3.35: Change in  $n$  with storage time for fresh infant milk concentrate samples collected after the concentrate heater data at the Waitoa milk powder plant. Experiment A119, Paar Physica MC1, 47.5%TS, 75°C.....108

Figure 3.36: Effect of non-Newtonian correction on the rheological data measured in fresh milk concentrates collected after the concentrate heater (47.6%TS, 75°C) at the Waitoa milk powder plant with the Paar Physica MC1 rheometer. Experiment A119.....120

Figure 3.37: Effect of non-Newtonian correction on rheological data measured in a reconstituted whole milk concentrate sample (48%TS, 75°C) with the Paar Physica MC1 rheometer.....121

Figure 4.1: Change in viscosity with shearing time for fresh skim milk concentrate samples (46.5%TS) taken after the evaporator #4 (64°C) and concentrate heater (65°C) at the Te Awamutu skim milk powder plant. Experiment B1, Brookfield LVTD.....126

Figure 4.2: Comparison of replicate values in the age thickening profiles after the evaporator at 30 rpm and the concentrate heater at 6 rpm for experiments B1 and B2 at the Te Awamutu skim milk plant. ....127

Figure 4.3: Variation in total solids content of milk concentrate samples after the evaporator for experiments B1 and B2 at the Te Awamutu skim milk powder plant.....129

Figure 4.4: Variation in milk concentrates temperature after the evaporator for experiments B1 and B2 at the Te Awamutu skim milk powder plant. ....	130
Figure 4.5: Change in viscosity with shearing time for fresh skim milk concentrate samples taken after the evaporator #1 at the Te Awamutu skim milk powder plant. Experiment B3, Brookfield LVTD, 50%TS, 48°C. ....	131
Figure 4.6: Change in viscosity with shearing time for fresh skim milk concentrate samples taken after the concentrate heater at the Te Awamutu skim milk powder plant. Experiment B3, Brookfield LVTD, 50%TS, 62°C. ....	131
Figure 4.7: Change in viscosity with shearing time for fresh skim milk concentrate samples taken after the evaporator #1 at the Te Awamutu skim milk powder plant. Experiment B6, Brookfield LVTD, 50%TS, 47.5°C. ....	135
Figure 4.8: Change in viscosity with shearing time for fresh skim milk concentrate samples taken after the evaporator #4 at the Te Awamutu skim milk powder plant. Experiment B5, Brookfield LVTD, 50%TS, 55.5°C. ....	136
Figure 4.9: Change in viscosity with shearing time for fresh skim milk concentrate samples taken after the density meter #1 at the Waitoa milk powder plant. Experiment B7, Brookfield LVTD, 48%TS, 54°C. ....	139
Figure 4.10: Change in viscosity with shearing time for fresh skim milk concentrate samples taken after the density meter #3 at the Waitoa milk powder plant. Experiment B7, Brookfield LVTD, 48%TS, 54°C. ....	139
Figure 4.11: Change in viscosity with shearing time for fresh skim milk concentrate samples taken after the filter #1 at the Waitoa milk powder plant. Experiment B7, Brookfield LVTD, 48%TS, 54°C. ....	140

Figure 4.12: Change in viscosity with shearing time for fresh skim milk concentrate samples taken after the filter #3 at the Waitoa milk powder plant. Experiment B7, Brookfield LVTD, 48%TS, 54°C.....140

Figure 4.13: Change in viscosity with shearing time for fresh skim milk concentrate samples taken after the evaporator #2 at the Te Awamutu skim milk powder plant. Experiment B8, Brookfield LVTD, 46.2%TS, 47.5°C. ....143

Figure 4.14: Change in viscosity with shearing time for fresh skim milk concentrate samples taken after the evaporator #4 at the Te Awamutu skim milk powder plant. Experiment B8, Brookfield LVTD, 46.4%TS, 60°C. ....143

Figure 4.15: Change in viscosity with shearing time for fresh skim milk concentrate samples taken after the concentrate heater #2 at the Te Awamutu skim milk powder plant. Experiment B8, Brookfield LVTD, 46%TS, 66°C.....144

Figure 4.16: Change in viscosity with shearing time for fresh skim milk concentrate samples taken after the concentrate heater #3 at the Te Awamutu skim milk powder plant. Experiment B8, Brookfield LVTD, 46%TS, 66°C.....144

Figure 4.17: Change in viscosity with shearing time for fresh skim milk concentrate samples (50%TS, 66°C) taken after the concentrate heater at the Te Awamutu skim milk powder plant. Experiment B5, Brookfield LVTD,. ....146

Figure 4.18: Change in viscosity with shearing time for fresh skim milk concentrate samples taken (52%TS, 66°C) after the concentrate heater at the Te Awamutu skim milk powder plant. Experiment B6, Brookfield LVTD, .....146

Figure 4.19: Change in viscosity with shearing time for fresh infant milk concentrate samples taken after the concentrate heater at the Waitoa milk powder plant. Experiment B11, Brookfield LVTD, 48%TS, 72°C.....151

Figure 4.20: Change in viscosity with shearing time for fresh infant milk concentrate samples taken after the concentrate heater at the Waitoa milk powder plant. Experiment B12, Brookfield LVTD, 48%TS, 78°C.....	151
Figure 4.21: Change in viscosity with shearing time for fresh skim milk concentrate samples taken after the concentrate heater at the Te Awamutu whole milk powder plant. Experiment B9, Brookfield LVTD, 47.5%TS, 55°C.....	154
Figure 4.22: Change in viscosity with shearing time for fresh skim milk concentrate samples taken after the concentrate heater at the Te Awamutu whole milk powder plant. Experiment B13, Brookfield LVTD, 46%TS, 55°C.....	154
Figure 4.23: Schematic diagram of the low shear sampler at the Waitoa milk powder plant.....	156
Figure 4.24: Effect of shear level during sampling on the rate of age thickening of fresh infant milk concentrate samples taken after the concentrate heater at the Waitoa milk powder plant. Experiment B14, Paar Physica MC1, 47.2%TS, 72°C.....	158
Figure 4.25: Changes in the Herschel Bulkley model parameters for 47.5%TS with storage time at 75°C. (a) yield stress $\tau_y$ ; (b) consistency coefficient K; (c) behaviour index $n$ .....	160
Figure 5.1: Shear sweep curves for 48%TS heated reconstituted whole milk concentrates after 150 minutes of storage at 65°C. Run C1.....	169
Figure 5.2: Apparent viscosity of 48%TS reconstituted whole milk concentrate sample during storage at 65°C at three different shear stress values. Calculated from the shear-up legs.....	171
Figure 5.3: Apparent viscosities calculated for shear up and shear down legs of the flow curves at the reference shear stress of 105.3 Pa. Run C1.....	171

Figure 5.4: Changes in apparent viscosity with (a) shear rate and (b)  $\frac{1}{\text{Shear Rate}}$  for a 48%TS reconstituted whole milk concentrate sample during 148 minutes of storage at 65°C. Run C1... .....172

Figure 5.5: Comparison between the extrapolated apparent viscosity at infinite shear and apparent viscosity at 105.3 Pa of a 48%TS reconstituted whole milk concentrate sample during 148 minutes of storage at 65°C. Run C1.....173

Figure 5.6: Flow curve of the reconstituted milk concentrate sample after 90 minutes of storage. C1, powder A, 48%TS, 65°C. ....174

Figure 5.7: Changes in thixotropy hysteresis area and apparent viscosity of the 48%TS reconstituted whole milk concentrate sample during storage at 65°C. Run C1.....175

Figure 5.8: Changes in the maximum shear rate of the shear up curve and the HLA with storage time in the reconstituted milk concentrate sample after 90 minutes of storage. Run C1, powder A, 48%TS, 65°C. ....176

Figure 5.9: Changes in the flow curves of the shear up and down tests of the reconstituted milk concentrate samples after 90 and 120 minutes of storage. Run C1, powder A, 48%TS, 65°C. ....176

Figure 5.10: Changes in the standardised and intrinsic HLA with storage time. Run C1, powder A, 48%TS, 65°C.....177

Figure 5.11: Changes in the Herschel Bulkley model parameters for 48%TS with storage time at 65°C. (a) yield stress  $\tau_y$ ; (b) consistency coefficient K; (c) behaviour index  $n$  Run C1. ....179

Figure 5.12: The effect of the number of data points on the apparent viscosity when conducting a shear sweep test on yoghurt samples at 10°C in CSS mode using the Paar Physica MC1. Runs C2-C12. ....181

Figure 5.13: Apparent viscosity against storage time for the reconstituted concentrates with the Paar Physica MC1 and measurement time for the fresh concentrates with the Brookfield LVTD. 47.5%TS and 75°C. C22..... 189

Figure 5.14: Apparent viscosity against storage time for fresh (B14) and reconstituted (C26) concentrates using the Paar Physica MC1. 47.5%TS and 75°C.....190

Figure 5.15: Changes in the Herschel-Bulkley model parameters with storage time for fresh (B14) and reconstituted concentrates (C26) using the Paar Physica MC1. 47.5%TS and 75°C. (a)  $\tau_y$ ; (b)  $K$ ; (c)  $n$ .....191

Figure 5.16: Apparent viscosity against storage time for fresh (C28) and reconstituted (C29) concentrates using the Paar Physica MC1. 47.5%TS and 75°C. Paar Physica MC1.....194

Figure 5.17: Changes in the Herschel Bulkley model parameters with storage time for fresh (C28) and reconstituted milk concentrates (C29) with storage time. 47.5%TS and 75°C. Paar Physica MC1. (a) yield stress  $\tau_y$ ; (b) consistency coefficient  $K$ ; (c) behaviour index  $n$ .....195

Figure 5.18: Effect of solids content on the apparent viscosity at 105.3 Pa of the reconstituted whole milk solutions. 35°C.....197

Figure 5.19: Effect of solids content on the Herschel-Bulkley model parameters of the reconstituted whole milk solutions. (a)  $\tau_y$ ; (b)  $K$ ; (c)  $n$  .....199

Figure 5.20: Effect of solids content on the pH of the reconstituted whole milk solutions at 35°C.....	200
Figure 5.21: Effect of solids content on the particle size distribution of the reconstituted whole milk solutions at 35°C.....	201
Figure 5.22: Effect of solids content on the volume percentage of particles > 2µm at 35°C.....	201
Figure 5.23: Effect of solids content on the initial (0 hr) viscosity of reconstituted whole milk concentrates at 45°C (runs C31, C33, C35, C37, C45, C50). ....	205
Figure 5.24: Effect of concentration and storage time on the viscosity of reconstituted whole milk concentrates during storage at 45°C. Runs C31 (10%TS), C33 (20%TS), C35 (30%TS), C37 (35%TS), powder A, 45°C.....	206
Figure 5.25: Effect of concentration and storage time on the viscosity of reconstituted whole milk concentrates during storage at 85°C. Runs C31 (10%TS), C33 (20%TS), C35 (30%TS), C37 (35%TS), powder A, 85°C.....	207
Figure 5.26: Initial apparent viscosity values of various reconstituted whole milk concentrates as a function of temperature. Powder A. ....	208
Figure 5.27: Apparent viscosities of various reconstituted whole milk concentrates as a function of temperature after 60 minutes of storage. Powder A. ....	209
Figure 5.28: Changes in the apparent viscosity with shear rate at different storage times. Run C52, powder A, 48%TS, 65°C. ....	210
Figure 5.29: Effect of heating and storage temperature on the changes in apparent viscosity with storage time in 44%TS reconstituted milk concentrates. Powder A...	211

Figure 5.30: Effect of heating and storage temperature on the changes in apparent viscosity with storage time in 46%TS reconstituted milk concentrates. Powder A...211

Figure 5.31: Effect of heating and storage temperature on the changes in apparent viscosity with storage time in 48%TS reconstituted milk concentrates. Powder A...212

Figure 5.32: Changes in the apparent viscosity with storage time up to the gelling point at two heating and storage temperatures. Runs C46 (55°C) and C47 (65°C), powder A, 46%TS.....214

Figure 5.33: Effect of solids content on the changes in apparent viscosity with storage time in reconstituted milk concentrate solutions that were heated and stored at 65°C. Powder A.....215

Figure 5.34: Effect of solids content on the changes in apparent viscosity with storage time in reconstituted milk concentrate solutions that were heated and stored at 75°C. Powder A.....216

Figure 5.35: Effect of solids content on the changes in apparent viscosity with storage time in reconstituted milk concentrate solutions that were heated and stored at 85°C. Powder A.....216

Figure 5.36: Effects of solids content and temperature on the gelling time of the reconstituted concentrates made from powder A. (a) gelling time versus heating and storage temperature at different solids contents, (b) gelling time versus solids content at different heating and storage temperatures. ....218

Figure 5.37: Variation of consistency coefficient  $K$  with time-temperature for 48%TS reconstituted whole milk concentrates. Powder A.....221

Figure 5.38: Variation of yield stress  $\tau_y$  with time-temperature for 48%TS reconstituted whole milk concentrates. Powder A.....221

Figure 5.39: Variation of behaviour index  $n$  with time-temperature for 48%TS reconstituted whole milk concentrates. Powder A.....222

Figure 5.40: Variation of consistency coefficient  $K$  with time-concentration at 75 °C for powder A reconstituted whole milk concentrates .....222

Figure 5.41: Variation of yield stress  $\tau_y$  with time-concentration at 75 °C for powder A reconstituted whole milk concentrates.....223

Figure 5.42: Variation of behaviour index with time-concentration at 75 °C for powder A reconstituted whole milk concentrates.....223

Figure 5.43: Effect of heating and storage temperature on the changes in apparent viscosity with storage time in 50%TS reconstituted milk concentrate solutions. Runs C55-C58, powder B.....226

Figure 5.44: Effects of solids content and temperature on the gelling time of the reconstituted concentrates made from powders A and B. ....227

Figure 5.45: The effect of powder type on the rate of age thickening (RAT) up to the gelling point of reconstituted concentrate samples made from powders A and B.....228

Figure 5.46: Effect of heating and storage temperature on the changes in the Herschel-Bulkley model parameters with storage time in reconstituted whole milk concentrates made from powder B. (a)  $\tau_y$ ; (b)  $K$ ; (c)  $n$ . Runs C55-C58, powder B, 50%TS.....229

Figure 5.47: Changes in particle size distribution with storage time. Run C55, powder B, 50%TS, 35°C.....231

Figure 5.48: Changes in particle size distribution with storage time. Run C58, powder B, 50%TS, 75°C.....232

Figure 5.49: Comparison of the change in apparent viscosity and aggregation profile with storage time. Run C55, powder B, 50%TS, 35°C.....	233
Figure 5.50: Comparison of the change in apparent viscosity and aggregation profile with storage time. Run C58, powder B, 50%TS, 75°C.....	233
Figure 5.51: Effect of recirculation shear rate on the inline apparent viscosity with recirculation time of the reconstituted milk concentrates. C59-C62, powder B, 50%TS, 35°C. ....	237
Figure 5.52: Changes in the in-line Herschel-Bulkley model parameters during recirculation at different shear rate for reconstituted whole milk concentrates. (a) $\tau_y$ ; (b) $K$ ; (c) $n$ . C59-C62, powder B, 48%TS, 35°C. ....	239
Figure 5.53: Effect of recirculation shear rate on the inline apparent viscosity during recirculation at 35°C. C63-C67, powder A, 48%TS, 35°C.....	240
Figure 5.54: Changes in rates of age thickening with nominal shear rates during recirculation in reconstituted milk concentrates made from powders A and B.....	241
Figure 5.55: Effect of shear rate during recirculation at 35°C on the rheology of heated reconstituted whole milk concentrates during storage at 75°C. C78-C79, powder B, 50%TS, 75°C.....	243
Figure 5.56: Effect of recirculation shear rate on the hysteresis loop area of the reconstituted whole milk concentrates during storage at 75°C. C78-C79, powder B, 50%TS, 75°C.....	243
Figure 5.57: Effect of recirculation shear rate on the Herschel-Bulkley model parameters during storage at 75°C. (a) $\tau_y$ ; (b) $K$ ; (c) $n$ . C78-C79, powder B, 50%TS, 75°C. ....	245

Figure 5.58: Effect of shear rate during recirculation on the rheology of heated reconstituted whole milk concentrates during storage at 65°C. C73-C77, powder A, 48%TS, 65°C.....	247
Figure 5.59: Effect of recirculating shear rate on the gelling time of heated reconstituted whole milk concentrates during storage at 65°C. C73-C77, powder A, 48%TS, 65°C.....	247
Figure 5.60: Effects of recirculation time on the apparent viscosity with storage time at 65°C for 47%TS reconstituted milk concentrates that had been sheared at 40,000s <sup>-1</sup> during recirculation at 35°C. C80, powder A, 47%TS.....	248
Figure 5.61: Effects of recirculation time on the apparent viscosity with storage time at 65°C of 47%TS reconstituted milk concentrates that had been sheared at 600s <sup>-1</sup> during recirculation at 35°C. C81, powder A, 47%TS. ....	249
Figure 5.62: Changes in particle size distribution with recirculation time during recirculation at 600s <sup>-1</sup> at 35°C. Run C67, powder A, 48%TS, 35°C. ....	250
Figure 5.63: Changes in particle size distribution with storage time at 65°C when the milk concentrates were sheared at 40,000s <sup>-1</sup> at 35°C. Run C80, powder A, 47%TS, 65°C.....	251
Figure 5.64: Changes in particle size distribution with storage time at 65°C when the milk concentrates were sheared at 600s <sup>-1</sup> at 35°C. Run C81, powder A, 47%TS, 65°C.....	251
Figure 5.65: Comparison of the changes in apparent viscosity with the aggregation profile during recirculation at 600 s <sup>-1</sup> at 35°C. Run C67, powder A, 48%TS, 35°C.....	253

Figure 5.66: Comparison changes in apparent viscosity with the aggregation profile during storage at 65°C. Recirculation was carried out at 600s <sup>-1</sup> for 60 minutes. C80, powder A, 47%TS, 65°C.....	253
Figure 5.67: Comparison of changes in apparent viscosity with the aggregation profile during storage at 65°C. Recirculation was carried out at 40,000s <sup>-1</sup> for 60 minutes. C81, powder A, 47%TS, 65°C.....	254
Figure 5.68: Effect of recirculation temperature on the inline apparent viscosity with recirculation time at shear level of 40,000s <sup>-1</sup> . C82-C83, powder A, 48%TS.....	258
Figure 5.69: Effect of recirculation temperature on the apparent viscosity during storage at 65°C. C87-C90, powder A, 48%TS. ....	259
Figure 5.70: Effect of recirculation temperature on the inline apparent viscosity with recirculation time at shear level of 40,000s <sup>-1</sup> . C84-C86, powder B, 50%TS.....	260
Figure 5.71: Effect of recirculation temperature on the apparent viscosity during storage at 75°C. C91-C92, powder B, 50%TS.....	261
Figure 5.72: Effect of flow rate during heating on the rheology of reconstituted milk concentrates during storage at 75°C. C96-97, powder B, 50%TS, 6 plates. ....	264
Figure 5.73: Effect of flow rate during heating on the rheology of reconstituted milk concentrates during storage at 75°C. C98-99, powder B, 50%TS, 10 plates. ....	264
Figure 5.74: Effect of flow rate during heating on the rheology of reconstituted milk concentrates during storage at 75°C. C100-101, powder B, 50%TS, 20 plates. ....	265
Figure 5.75: Effect of shear rate and number of plates during heating on the gelling time of heated products during storage. ....	266

Figure 5.76: Effect of flow rate during heating on the Herschel-Bulkley model parameters during storage at 75°C in a hot water bath. (a) $\tau_y$ ; (b) $K$ ; (c) $n$ . C90-C91, powder B, 50%TS, 20 plates. ....	267
Figure 5.77: Change in particle size distribution during storage of heated reconstituted whole milk concentrates. C97, powder B, 50%TS, 75°C, 6 plates, 40 L/hour.....	269
Figure 5.78: Comparison of the changes in the apparent viscosity and the aggregation profile with storage time during age thickening at 75°C. C97, powder B, 50%TS, 75°C, 6 plates, 40 L/hour. ....	270
Figure 5.79: Changes in the apparent viscosity at 105.3 Pa with storage time during age thickening at 75°C. Run C103, whole milk powder B, 50%TS. ....	272
Figure 5.80: Changes in the behaviour index, $n$ , of the Herschel-Bulkley model with time for a 50%TS reconstituted whole milk concentrate during storage at 75°C. Run C103, whole milk powder B, 50%TS.....	274
Figure 5.81: Change in particle size distribution of the 50%TS reconstituted whole milk concentrates during storage at 75°C. Run C103, whole milk powder B.....	275
Figure 5.82: Comparison of the changes in the aggregation profile and apparent viscosity with storage time at 75°C during age thickening for the 50%TS reconstituted whole milk concentrates. Run C103, whole milk powder B.....	276
Figure 5.83: Age thickening in reconstituted whole milk concentrates during storage at 75°C. Magnification 3200x. Storage time: (a) 0 min, (b) 150 min, (c) 270 min, (d) 340 min. Run C103, whole milk powder B, 50%TS.....	277
Figure 5.84: Age thickening in reconstituted whole milk concentrates during storage at 75°C. Magnification 9100x. Storage time: (a) 0 min, (b) 150 min, (c) 270 min, (d) 340 min. Run C103, whole milk powder B, 50%TS.....	278

Figure 5.85: Age thickening in reconstituted whole milk concentrates during storage at 75°C. Magnification 20600x. Storage time: (a) 0 min, (b) 150 min, (c) 270 min, (d) 340 min. Run C103, whole milk powder B, 50%TS. ....	280
Figure 5.86: Age thickening in reconstituted skim milk concentrates during storage at 65°C. Magnification 3200x. Storage time: (a) 1 hour, (b) 2 hours, (c) 4 hours. Run C104, skim milk powder C, 50%TS.....	281
Figure 5.87: Age thickening in reconstituted skim milk concentrates during storage at 65°C. Magnification 20600x. Storage time: (a) 1 hour, (b) 2 hours, (c) 4 hours. Run C104, skim milk powder C, 50%TS. ....	283
Figure 5.88: Change in apparent viscosity with storage time during age thickening at 35°C. Run C105, powder B, 49.4%TS, 35°C. ....	287
Figure 5.89: Change in pH with storage time during age thickening at 35°C. Run C105, powder B, 49.4%TS, 35°C. ....	288
Figure 5.90: Change in standardised HLA with storage time during age thickening at 35°C. Run C105, powder B, 49.4%TS, 35°C. ....	289
Figure 5.91: Effect of heating and storage temperature on the Herschel-Bulkley model parameters with storage time in concentrates made from powder B. (a) $\tau_y$ ; (b) $K$ ; (c) $n$ . Run C105, powder B, 49.4%TS, 35°C. ....	290
Figure 5.92: Changes in PSD with storage time after the first recirculation step. Run C105, powder B, 49.4%TS, 35°C.....	291
Figure 5.93: Changes in PSD with storage time after the second recirculation step. Run C105, powder B, 49.4%TS, 35°C.....	291

Figure 5.94: Changes in volume percentage of particles >2 $\mu$ m with storage time. Run C105, powder B, 49.4%TS, 35 $^{\circ}$ C.....	292
Figure 5.95: Change in apparent viscosity with storage time during age thickening at 35 $^{\circ}$ C. Run C106, powder B, 47.5%TS, 75 $^{\circ}$ C. ....	294
Figure 5.96: Change in standardised HLA with storage time during age thickening at 35 $^{\circ}$ C. Run C106, powder B, 47.5%TS, 75 $^{\circ}$ C. ....	295
Figure 5.97: Comparison of standardised HLA between runs C105 at 35 $^{\circ}$ C and C106 at 75 $^{\circ}$ C.....	295
Figure 5.98: Effect of heating and storage temperature on the Herschel-Bulkley model parameters with storage time in reconstituted milk concentrates made from powder B. (a) $\tau_y$ ; (b) $K$ ; (c) $n$ . Run C106, powder B, 47.5%TS, 75 $^{\circ}$ C. ....	297
Figure 5.99: Changes in PSD with storage time after the first recirculation step. Run C106, powder B, 47.5%TS, 75 $^{\circ}$ C.....	298
Figure 5.100: Changes in PSD with storage time after the second recirculation step. Run C106, powder B, 47.5%TS, 75 $^{\circ}$ C.....	298
Figure 5.101: Changes in volume percentage of particles >2 $\mu$ m with storage time. Run C106, powder B, 47.5%TS, 75 $^{\circ}$ C.....	299
Figure 6.1: Typical flow curves drawn as torque versus spindle speed for two typical Newtonian solutions.....	305
Figure 6.2: Changes in the flow curve during age thickening in run C100. Powder B, 50%TS, 75 $^{\circ}$ C.....	308
Figure 6.3: The changes in apparent viscosity with shear rate after different duration of recirculation. Runs C63-C67, powder A, 48%TS, 35 $^{\circ}$ C.....	310

Figure 6.4: Effect of shear rate on the ratio of increase in the extrapolated apparent viscosity at infinite shear rate during recirculation. ....321

Figure 6.5: Proposed types of age-thickening .....335

Figure 6.6: Proposed mechanisms of age thickening.....340

## LIST OF TABLES

Table 2.1: Methods for eliminating the minimum from the HCT-pH profiles of Type A milks (Singh, 2004).....	29
Table 3.1: Mesophilic bacteria count during a recombination experiment A4...	63
Table 3.2: Effect of cleaning and addition of sodium azide on bacterial count during a recombination experiment A5.....	64
Table 3.3: Background data on the Paar Physica MC1 (quoted by Physica Messtechnik GmbH, 1993).....	69
Table 3.4: Dimensions for several spindle geometries for the Paar Physica MC1 (Physica Messtechnik GmbH, 1993).....	70
Table 3.5: Viscosity-temperature data for three Cannon Instrument Company's Newtonian standard oils.....	74
Table 3.6: Spindle speeds and measured torques at critical COV of 0.001 for Z3 spindle with S2000 oil at various temperatures. Experiments A45-A49.....	86
Table 3.7: Viscosity values for the S60 Newtonian oil (lot 03201) (Cannon Instrument Company, USA), manufactured in 24 February 2003, expires on 08 February 2005.....	90
Table 3.8: Measuring protocol for shear sweep test using the Paar Physica MC1.....	93
Table 3.9: Technical data for several Brookfield spindles (Brookfield Engineering Labs).....	99
Table 3.10: General composition of the infant milk concentrates in experiment A 119 at the Waitoa milk powder plant.....	100

Table 3.11: Plant operating conditions in experiment A119 at the Waitoa milk powder plant.....	101
Table 3.12: General compositional specifications for several tested powder used in the controlled rheology experiments.....	109
Table 3.13: Effects of data corrections and truncation during rheological modeling.....	120
Table 4.1: General composition of the skim milk concentrates in experiment B1 at the Te Awamutu skim milk powder plant.....	126
Table 4.2: Solids contents and temperatures of milk concentrate samples from the Te Awamutu skim milk powder plant for experiments B1 and B1.....	128
Table 4.3: Variation in temperature and total solid content for experiments B3 and B4 at the Te Awamutu skim milk powder plant.....	133
Table 4.4: Plant processing conditions in experiment B5 at the Te Awamutu skim milk powder plant.....	135
Table 4.5: General composition of the skim milk concentrates in experiment B7 at the Waitoa milk powder plant.....	138
Table 4.6: Plant processing conditions in experiment B7 at the Waitoa milk powder plant.....	138
Table 4.7: Plant processing conditions in experiment B8 at the Te Awamutu skim milk powder plant.....	142
Table 4.8: General composition of skim milk concentrates in experiments B9, B1, B8 and B10 at the Te Awamutu skim milk and whole milk powder plants.....	148

Table 4.9: Plant processing conditions in experiments B9, B1, B8 and B10 at the Te Awamutu skim and whole milk powder plants.....	148
Table 4.10: General composition of the infant milk concentrates in experiments B11 and B12 at the Waitoa milk powder plant.....	149
Table 4.11: Plant processing conditions in experiments B11 and B12 at the Waitoa powder plant.....	149
Table 4.12: General composition of the skim milk concentrates in experiments B9 and B13 at the Te Awamutu whole milk powder plant.....	152
Table 4.13: Plant operating conditions in experiments B9 and B13 at the Te Awamutu whole milk powder plant.....	153
Table 4.14: General composition of the infant milk concentrates in experiment B14 at the Waitoa milk powder plant.....	157
Table 4.15: Plant operating conditions in experiment B14 at the Waitoa milk powder plant.....	157
Table 5.1: The effect of the number of data points on the Herschel-Bulkley model parameters when conducting a shear sweep test on yoghurt samples at 10°C in CSS mode using the Paar Physica MC1. Runs C2-C12.....	181
Table 5.2: The effect of the minimum shear stress on the Herschel-Bulkley model parameters when conducting a shear sweep test on yoghurt samples at 10°C in CSS mode using the Paar Physica MC1. Runs C13-C21.....	182
Table 5.3: General composition of the infant milk concentrates in experiments C28 & C29 at the Pahiatua milk powder plant.....	187
Table 5.4: Plant operating conditions in experiments C28 & C29 at the Pahiatua milk powder plant.....	188

Table 5.5: Experimental conditions to study the effect of solids content and temperature on the rheology of reconstituted whole milk concentrates made from powder A.....	203
Table 5.6: Experimental run conditions to study the effect of solids content and temperature on the rheology of reconstituted whole milk concentrates made from powder B.....	204
Table 5.7: Typical values for the Herschel-Bulkley parameters at the gelling points in reconstituted concentrates made from powder A.....	224
Table 5.8: Changes in the apparent viscosity and the Herschel-Bulkley parameters at the gelling points in reconstituted concentrates made from powder B at different heating temperatures.....	230
Table 5.9: Experimental conditions to study the effect of shear rate on the rheology of reconstituted whole milk concentrates during recirculation at 35°C.....	235
Table 5.10: Reconstitution conditions for experiments C82-C92.....	257
Table 5.11: Operating parameters during heating experiments.....	263
Table 5.12: Changes in solids content after recirculation.....	286
Table 6.1: Changes in the HLA and the Herschel-Bulkley parameters with shear rate range in three concentrate samples. Run C100, powder B, 50%TS, 75°C.....	307
Table 6.2: General composition of the two whole milk powders used in the controlled rheology experiments.....	323

## LIST OF SYMBOLS

<b>Roman letters</b>		<b>Unit</b>
<b>A</b>	Empirical constant A in the Weltman model	Dimensionless
<b>B</b>	Empirical constant B in the Weltman model	Dimensionless
$f_{ss}$	Shear stress conversion factor	Dimensionless
$f_{sr}$	Shear rate conversion factor	Dimensionless
<b>K</b>	Consistency coefficient	$\text{Pa}\cdot\text{s}^n$
<b>L</b>	Length of bob	m
<b>m</b>	slope of the logarithmic plot of $\ln N$ versus $\ln \tau_b$	$\text{rpm}\cdot\text{Pa}^{-1}$
<b>M</b>	Torque	Nm
<b>n</b>	Behaviour index	Dimensionless
<b>n"</b>	Slope of a logarithmic plot of torque versus rotational speed	$\text{Nm}\cdot\text{rpm}^{-1}$
<b>N</b>	Spindle speed	rpm
$R_b$	Radius of bob	m
$R_c$	Radius of cup	m
<b>t</b>	Time	s or min or hour

<b>Greek Symbol</b>		<b>Unit</b>
$\varepsilon$	Ratio of $Rb/R_c$	Dimensionless
$\phi$	Volume fraction	Dimensionless
$\phi_{\max}$	Maximum volume fraction of the dispersed phase	Dimensionless
$\tau$	Shear stress	Pa
$\tau_B$	Baxter interaction parameter	Pa
$\tau_b$	Shear stress at the surface of the spindle	Pa
$\tau_y$	Yield stress	Pa
$\tau_e$	Elastic stress	Pa
$\tau_t$	Total stress	Pa
$\tau_v$	Viscous stress	Pa
$\mu$	Viscosity	Pa.s
$\mu_{app}$	Apparent viscosity	Pa.s
$\mu_s$	Viscosity of the solvent	Pa.s
$[\mu]$	Intrinsic viscosity	Pa.s
$\mu_{normalised}$	Normalised viscosity	Dimensionless
$\mu_{high\ shear}$	Steady viscosity attained at high shear rates	Pa.s
$\mu_{\infty}$	Viscosity at infinite shear rate	Pa.s
$\mu_{\infty ad}$	Adjusted extrapolated viscosity at infinite shear rate	Pa.s
$\gamma_e$	Elastic strain associated with the flow structure	Dimensionless
$\dot{\gamma}$	Shear rate	$s^{-1}$
$\dot{\gamma}_b$	Shear rate at the surface of the spindle	$s^{-1}$
COV	Coefficient of variation	Dimensionless

## LIST OF ABBREVIATIONS

$\beta$ -lg	$\beta$ -lactoglobulin
CCP	Colloidal calcium phosphate
CIP	Cleaning-in-place
COV	Coefficient of variation
DFGM	Damaged fat globule membrane
HCT	Heat coagulation time
HLA	Hysteresis loop area
NEM	N-ethylmaleimide
NFGM	Native fat globule membrane
PHE	Plate heat exchanger
PSD	Particle size distribution
RAT	Rate of age thickening
RSCM	Recombined sweetened condensed milk
SCM	Sweetened condensed milk
SDS-PAGE	Sodium dodecyl sulphate polyacrylamide gel electrophoresis
SNF	Solids non-fat
TASMP	Te Awamutu skim milk powder
TAWMP	Te Awamutu whole milk powder
TEM	Transmission electron microscopy

## LIST OF PUBLICATIONS

Trinh, B., Haisman, D., Trinh, K. T., Croy, R. J., Hemar, Y., Weeks, M., Chen, H., (2002) Effect of total solids content and temperature on the rheology profile of reconstituted milk concentrates. 9th APCCChE Congress and Chemeca, Christchurch, New Zealand.

Trinh, B., Haisman, D., Trinh, K. T., Weeks, M., (2002) Design of a recombination system for time-dependent food systems. 9th APCCChE Congress and Chemeca, Christchurch, New Zealand.

Trinh, B., Haisman, D., Trinh, K. T., Prankerd, B., (2004) Effect of heater design and operation during heating on the rheology of whole milk concentrate. . 9<sup>th</sup> World Congress of Engineering and Food , Montpellier, France.

Trinh, B., Haisman, D., Trinh, K. T., Prankerd, B., (2004) Effect of shear during recombination of time-dependent food products. 9<sup>th</sup> World Congress of Engineering and Food , Montpellier, France.

Trinh, B., Haisman, D., Trinh, K. T., Prankerd, B., (2004) Effect of temperature during recombination of time-dependent food products. 9<sup>th</sup> World Congress of Engineering and Food , Montpellier, France.

Trinh, B., Haisman, D., Trinh, K. T., (2005) Characterisation of a commercial controlled shear stress rheometer. 7th World Congress of Chemical Engineering, Glasgow, Scotland.

Trinh, B., Haisman, D., Trinh, K. T., (2005) A new technique for the rheological study of time-dependent colloidal systems. 7th World Congress of Chemical Engineering, Glasgow, Scotland.

Trinh, B., Haisman, D., Trinh, K. T., (2005) Structural behaviour in heated milk concentrate. 7th World Congress of Chemical Engineering, Glasgow, Scotland.

---

# **CHAPTER 1**

# **INTRODUCTION**

---

# CHAPTER 1: INTRODUCTION

Annual global cow milk production in 2004 was estimated to be 490 billion litres. Major producers include the European Union (EU) (125.5 billion), India (91.3 billion), USA (77.5 billion) and Russia (32 billion) ([www.fao.org](http://www.fao.org)).

The EU is the world's major dairy exporter accounting for 36 per cent of all export sales on a milk equivalent basis. Although accounting for only 3 per cent of world milk output (15 billion litres), New Zealand is the second largest supplier of manufactured milk products to the world market with a 31 per cent share. This contributes to over NZ\$7 billion worth of exports, earning approximately 25% of the New Zealand total exports value. The Fonterra Co-operative Group is the biggest dairy company in New Zealand, controlling 95% of milk supply. Milk powder is the biggest export product with \$3 billion dollars worth of sales from 700 million kilograms of products, contributing to nearly 25% of the total revenue.

Milk is a complex colloidal dispersion containing fat globules, casein micelles and whey proteins in an aqueous solution of lactose, minerals and other minor compounds. Its physical, chemical and functional properties are dependent on a combination of composition and processing factors.

During the production of milk powder, raw milk with solids content of 10-12%TS is concentrated to 45-50%TS by evaporation, before being transported to the spray drier. Milk concentrates display time-dependent rheological behaviour where the viscosity is dependent on the applied shear rate, temperature and time. In other words, previous processing treatments affect the current rheological behaviour of the milk concentrate system, which has a significant effect on both the plant operating efficiency and the quality of the resultant powder product (Vilder et al., 1979; Bloore & Boag, 1981; Snoeren et al., 1982).

There are numerous reports on the rheology of milk based products, including raw milk and acidified products such as yoghurt and cheese. However, there have been

few studies on concentrated systems. In the case of milk concentrates, the published results have been conflicting, leaving more questions than answers.

There is a real need to develop a better understanding of the rheological behaviour of milk concentrates, as well as other time-dependent fluid systems. The aim of this project was to develop new tools and methods for studying time-dependent rheology of milk concentrates. The specific objectives were

1. To develop a method for recombination of dairy products with reproducible rheological profiles
2. To master, and if necessary develop new rheometry techniques applicable to the study of milk concentrates
3. To develop a new methodology for analysing the rheology of time-dependent systems
4. To conduct a survey of milk concentrate rheological behaviour in industrial plants
5. To compare the rheological behaviour of fresh and reconstituted milk concentrates
6. To study the effects of shear and temperature history on the rheological behaviour of reconstituted milk concentrates
7. To give an overall description of the combined effect of concentration, time and temperature on concentrate rheology in samples with a known shear history
8. To obtain structural measurements of milk concentrates during age-thickening
9. To provide a better understanding of the age-thickening process

This thesis begins with a comprehensive literature review that focuses primarily on the rheology of milk concentrate systems. The review discusses the effect of product variables (e.g. solids content, protein level) and processing variables (e.g. temperature, pH) on the rheology of milk concentrates. A short review of recombination follows, which looks at the available recombination techniques that are being used in the dairy industry.

Materials and methods are documented in Chapter 3. New experimental techniques were developed to cope with the complexity of the exercise. The techniques

developed include sample preparation, measurement techniques, recombination equipment design and protocols, and data analysis. The experimental runs in this chapter are labelled as “A” series followed by the run number, e.g. A1-A100.

The experimental results are divided into two separate sections, those data obtained from the industrial surveys (Chapter 4) and those collected in the laboratory under controlled conditions (Chapter 5). The experimental runs in these two chapters are labelled as “B” and “C” series respectively, followed by the run number.

The industrial survey provided an insight into the change in rheological behaviour of the fresh milk concentrate system during processing. The survey investigated the effect of several processing variables, such as solids content and temperature, on the viscosity and rate of age thickening in fresh milk concentrates.

The work carried out in the laboratory focused on the effect of recombination processing parameters on the rheology of reconstituted milk concentrates. Chapter 5 begins with a discussion on new methods of analysing the rheological behaviour of time-dependent systems. The next section in chapter 5 compares the rheology of fresh and reconstituted milk concentrate systems in order to validate the use of powder and reconstituted milk concentrates as a substitute for fresh milk systems. The remaining sections of chapter 5 investigate the effect of processing variables on the rheology of reconstituted milk concentrates. These include solids content, storage temperature, shear level and temperature during recirculation. The results illustrate the importance of preparation techniques and their impact on the rheology of the final reconstituted milk concentrates.

Chapter 6 provides a summary of the findings and discusses their significance. The implications of the results from a fundamental research perspective and industrial applications are reviewed. Special attention is given to any information that can shed light on the age thickening phenomenon in an attempt to answer two important questions. “What causes age thickening?” and “What happens to the structure of milk systems during age thickening?”

---

# **CHAPTER 2**

# **LITERATURE REVIEW**

---

## CHAPTER 2: LITERATURE REVIEW

This literature review focuses mainly on the rheological behaviour of milk concentrates. However, background knowledge of the milk system and time-dependent rheology are also essential. Extensive reviews on these two topics have been carried out. However, due to the university size constraint on the thesis, these two reviews are not included in this section, and have been attached as appendices A1 and A2. The reader may wish to browse these two documents before proceeding further into this review.

### 2.1 Milk Concentrate Rheology

In the production of milk powders, the viscosity of the milk concentrate has a significant influence on the plant and its performance (Vilder & Moermans, 1983). The interaction between processing conditions and rheological behaviour also controls the quality and shelf life of the end powder products. The understanding of these interactions provides an invaluable quality control tool that can be applied during processing to make products with desirable and consistent properties, as well as giving rise to the potential for new products with different textural and functional properties.

The term viscosity is commonly used in the literature to refer either to the apparent viscosity of the milk during transportation in the pipeline, or to the initial measurement obtained after sampling.

Under appropriate conditions, such as a high temperature and high total solids content, milk concentrates are widely known to exhibit time-dependent behaviour. In these systems, the change in viscosity is dependent on both shear and time. If during storage at rest, the viscosity increases with time, this time-dependent phenomenon, when associated with dairy products, is more commonly known as age thickening (Upadhyay, 1998).

Snoeren et al. (1982a, 1984) described age thickening by providing two viscosity definitions for milk concentrate systems:

- Basic viscosity,  $\mu_{\infty}$ , is the viscosity at infinite shear at zero time
- Structural viscosity, is the contribution to the increase in concentrate viscosity during storage.

At any given time, the apparent viscosity consists of the basic viscosity and the structural viscosity. Similar definitions were given by Samel & Muers (1962) who believed that the observed viscosity of sweetened condensed milk is the sum of an “initial” viscosity (determined by the dispersion of casein, whey proteins, and fat in the continuous phase) and an aggregation-network viscosity. The change in structural viscosity (terminology of Snoeren et al. (1982a) or the aggregation viscosity (Samel & Muers, 1962) with time defines the rate of age thickening.

The initial viscosity and the time-dependent behaviour constitute the rheological characteristics of milk concentrate systems. Fluids with similar initial viscosities may possess different rates of age thickening (Lawrence, Clarke, & Augustin, 2001). Yet, single point viscosity measurement remains a popular method of investigating the effect of various processing variables on the rheological behaviour of the concentrate systems (Beeby, 1966; Newstead, Baldwin, & Hughes, 1978; Baldwin, Baucke, & Sanderson, 1980; Bloore & Boag, 1981; Vilder & Moermans, 1983; Gassem & Frank, 1991). Although such data may constitute interesting observations worth investigating, this approach shows a fundamental flaw in the understanding of rheological measurements of time-dependent systems.

Age thickening of milk systems, dilute and concentrated, has not received much attention, as evidenced by the limited number of published reports on the subject. Thixotropic behaviour of fully reversible model systems, such as clay and other colloidal suspensions, has been studied in great detail (Yziquel, Carreau, Moan, & Tanguy, 1999; Dames, Morrison, & Willenbacher, 2001; Usui, 2002). In these systems, the molecular

interactions can be controlled and measured. However, milk systems are complex with many components and interactions, including some irreversible reactions.

A popular measurement within the dairy industry is heat stability, which refers to the ability of milk to withstand high processing temperatures without visible coagulation or gelation (Singh, 2004). The measurement of heat coagulation time (HCT) is a technique for the characterisation of heat stability. HCT is defined as ‘the time taken for milk to coagulate (by visual observation) whilst being rocked or agitated in a sealed tube at a set temperature (usually between 120°C and 140°C) (Williams, 2002). Rose (1963) defined heat stability as the time required to induce coagulation at a given temperature, or the temperature required to induce coagulation in a given time. Similar definitions have been given by Kiesecker and Pearce (1978). Due to the subjective nature of HCT tests, Rose (1963) and Singh (2004) pointed out the importance of fully reporting the conditions of the test.

Heat stability tests only focus on the phase transition of the systems, from liquid to gel-solid state while age thickening refers to the continuous change in rheological behaviour of the system with time, eventually culminating in gelation. The author believes that the understanding of factors affecting heat stability can shed light on the age-thickening behaviour of dairy products, although previous authors have not drawn this parallel before. There are obvious differences between HCT and age thickening in milk systems, including temperature and solids content being the main variables. HCT is associated with less concentrated products which are subjected to higher temperature treatment. In addition, HCT is not a rheological measurement, as it does not investigate the relationship between shear stress and shear rate. It is speculated that a factor that gives rise to a lower HCT may increase the rate of age thickening, i.e. these two processes could be driven by similar mechanism/s.

This review will draw on the extensive publications in the area of HCT to shed light onto factors affecting age thickening of milk systems. However, this chapter is not a review about HCT, for which many good reviews are already available. (e.g. Singh, 2004).

The heat stability of milk is affected by the following variables (Rose, 1963; Kiesecker, 1980; Al-Tahiri, 1987; Kiesecker & Aitken, 1988; Singh, Creamer, & Newstead, 1989; Singh, 2004):

- Milk composition and concentration
- Seasonal variation
- pH
- Heat treatment prior to evaporation and drying
- Ionic strength
- Dispersion of milk fat (homogenization)
- Water characteristics (degree of hardness)
- Additives (e.g. urea)

Milk systems sometime receive severe heat treatment for a short time (140°C/4-10 sec). These are called ultra-high temperature (UHT) milk systems, which are often diluted. The severe heat treatment gives rise to a phenomenon called age gelation in UHT milk, where the viscosity increases immediately before formation of a gel (Datta & Deeth, 2001). Similarly to HCT milk systems, UHT milk differ from milk concentrates systems in terms of temperature and solids content. However, the high heat treatment received in UHT products may spark similar mechanisms to that which caused the onset of coagulation in HCT measurement and age thickening in milk concentrates. Where appropriate, some knowledge from UHT field will be borrowed for this review.

The effects of composition and processing variables on the rheological behaviour of milk concentrates will be covered first. Next modelling of the rheological behaviour of milk concentrate systems will be reviewed, including the time-dependent behaviour. Finally, postulated mechanisms of age thickening in milk systems will be briefly discussed.

### **2.1.1 Milk composition**

The force (stress) required to move a solution or suspension at a given shear rate is made up of two contributions, the force applied to the solvent and the force required to move the solute molecules or suspended particles (Einstein, 1906). The drag force exerted by the solvent on the solute or dispersed phase particles is a function of their voluminosity, shape and proximity. In milk concentrates, these factors are different for each of the many solid components including lactose, proteins, fat, minerals and other minor constituents. Thus the composition of milk has a definite effect on its viscosity.

#### **2.1.1.1 Total solids content**

It is well documented that the apparent viscosity of milk concentrates increases exponentially with total solids content for skim milk (Bloore & Boag, 1981; Snoeren, Damman, & Klok, 1982b, 1984; Vilder & Moermans, 1983) and whole milk systems (Fernandez-Martin, 1972; Vilder, Martens, & Naudts, 1979; Snoeren, Damman, & Klok, 1984; Velez-Ruiz & Barbosa-Canovas, 1997, 1998, 2000). There is also a gradual shift from Newtonian, to shear-dependent and then to time-dependent behaviour (e.g. Velez-Ruiz & Barbosa-Canovas, 2000).

The first effect of increasing the total solids content is to increase the contribution of the particles to the total force required to shear the solution because there are more of them.

The rheological properties of milk systems have often been correlated with the volume fraction of the solids (Snoeren et al., 1982b; Hinrichs, 1999). The volume fraction of milk solids can be considered as the sum of the volume fractions of the soluble components, particularly lactose, and the insoluble components both colloidal (casein, whey proteins) (Snoeren et al., 1982b) and emulsified (fat).

The importance of the volume fraction of the dispersed phase was first highlighted in the hydrodynamic theory of viscosity by Einstein (1906), shown in equation (2.1). He showed that the force required to move a dilute solution of glass beads was equal to the force required to move the solvent plus the force required to overcome the hydrodynamic resistance of the beads. The latter was described well by Stokes' formula for creeping flow past a falling sphere (Bird et al., 1960).

$$\mu = \mu_s(1 + 2.5\phi) \quad (2.1)$$

where  $\mu$  is the viscosity of the solution (Pa.s)

$\mu_s$  is the viscosity of the solvent (Pa.s)

$\phi$  is the volume fraction of the dispersed phase or solute

The constant 2.5 in Einstein's equation arises from the relation between volume and diameter of a sphere. This value has to be modified to account for the effect of shape on both the volume and hydrodynamic resistance. Numerous studies have been carried out to calculate this shape factor, notably with the next simplest shape of suspended dumbbells (Eirich, 1956). The particles investigated in this approach are called hard spheres systems as there are no chemical interactions between the particles. The movement of each particle can affect the hydrodynamic resistance of a nearby particle. Batchelor (1977) incorporated the contribution of this crowding effect for solutions up to  $\phi=0.2$  in the equation

$$\mu = \mu_s(1 + 2.5\phi + k_H\phi^2) \quad (2.2)$$

where  $k_H$  is called the Huggins coefficient which has a theoretical value of 6.2 for hard spheres (Cichocki & Felderhof, 1988).

At higher concentrations, terms in  $\phi$  of third and higher order must be incorporated into equation (2.2). The theoretical derivation of this infinite series is challenging and a

number of empirical and semi-empirical formulas have been proposed. Snoeren et al. (1984) used Eilers' correlation (Eilers, 1941)

$$\mu = \mu_s \left( 1 + \frac{1.25\phi}{1 - \phi/\phi_{\max}} \right)^2 \quad (2.3)$$

where  $\phi_{\max}$  is the maximum volume fraction of the dispersed phase. Another useful correlation is Krieger and Dougherty's (1959)

$$\mu = \mu_s \left( 1 - \frac{\phi}{\phi_{\max}} \right)^{-[\mu]\phi_{\max}} \quad (2.4)$$

where  $[\mu]$  is the intrinsic viscosity.

In the derivations reviewed so far, the dispersed particles have been treated as non-deformable particles, i.e. hard spheres. In real food systems, these particles can be deformable and have mutually attractive surface forces. When the mutually attractive forces are not very strong, clustering of particles is not permanent but will increase the viscosity because of the energy required to break up these clusters. Russel (1984) included the effect of particle surface interaction into the Batchelor formula by modifying the Huggins coefficient in his theory of so-called adhesive hard spheres

$$k_H = 5.913 + 1.9/\tau_B \quad (2.5)$$

where the Baxter interaction parameter,  $\tau_B$ , is infinite for hard spheres and decreases in value as the attraction increases. It is important to note that the adhesive hard sphere model only looks at the physical interaction at the surface, and not the chemical interactions. The adhesive hard sphere model essentially describes a system where two

particles are attracted to each other over long range, but experience a steep repulsive force at very short distance due to the steric repulsion caused by the overlapping of an adsorbed layer of active material on the surface. This model can be used to describe the behaviour of casein micelles, where the micelle core is surrounded the hairy layer of  $\kappa$ -casein which provide steric repulsion at close distance.

Luckham and Ukeje (1999) showed that at high volume fraction, significant compression and interpenetration of the stabilising polymeric layer can take place and this contributes significantly to the elasticity of a system. This brings in an additional variable that must be taken account when working with highly concentrated products.

The correlations reviewed so far are only based on interactions between separate particles. They do not take account of floc size and strength and therefore cannot describe the shear thinning behaviour often observed with colloidal solutions. Even in model systems made up from latex particles manufactured to known particle sizes and stabilised with an outer layer of surfactants (Luckham and Ukeje, 1999), the predictions of the Krieger-Dougherty equations could only be correlated with the viscosity “at high shear rate” and no attempt was made to explain the shear thinning behaviour. While the kinetics of coagulation and flocculation are well researched (e.g. Dobias, 1993), the assessment of floc size and density in concentrated opaque solutions is not available. The floc stability and therefore its size is a function of the shear rate applied (Muhle, 1993) and the volume fraction should therefore be measured at the concentration and in the shear environment applicable to the viscosity measurement. There is no method for doing this at the moment and therefore all discussions relating volume fraction to viscosity during age-thickening can only be qualitative at the time being.

Upon concentration, an increase in ionic strength and a drop in pH are always encountered (Walstra & Jenness, 1984; Upadhyay, 1998; Walstra et. al., 1999; Bienvenue et al., 2003). A decrease in pH can result in a decrease in the electrostatic repulsions of micelles, and weak flocs may form that give rise to an increase in viscosity (Bienvenue et

al., 2003). Casein micelles may increase in size during concentration due to coalescence between the micelles (Walstra & Jenness, 1984; Walstra et al., 1999).

Non-Newtonian behaviour is caused by the formation of secondary structure due to reversible interactions between particles. The state of the structure is highly dependent on shear rate, being more broken down under the influence of high shear. Time-dependent arises when these structures take a finite time to undergo changes.

Age thickening occurs at high concentrations above 42% to 45% TS. The rate of age thickening increases with solid-non-fat (SNF) concentration in milk systems (Snoeren et al., 1984; Upadhyay, 1998). Similarly, HCT decreases with an increase in SNF (Metwally et al., 1978; Kelly, 1982a; Singh, 2004). This was attributed to the decrease in pH and amount of water bound to casein, as well as an increase in concentration of the soluble milk constituents (Dahle & Pyenson, 1938).

In whole milk, the dynamic interactions can deform the stabilising layer on the surface of the fat globules and change their contributions to the viscosity (Mewis et al., 1989; Hinrichs, 1999).

#### **2.1.1.2 Protein**

Jeurnink & Dekruif (1993) demonstrated that the rate of increase in viscosity during storage at rest at 90°C increased with  $\beta$ -lactoglobulin concentration (Figure 2.1). Rohm (1988) observed higher rates of age thickening with an increase in protein. Trinh & Schraekenrad (2002) found that milk concentrates with 40% of whey proteins removed had much lower viscosity and rate of thickening than normal milk concentrates. Similarly, Newstead, Sanderson and Conaghan (1977) showed that the presence of native  $\beta$ -lactoglobulin decreased the HCT of recombined concentrated milk. White and Davies (1958b) noted that a minimum concentration of 0.9% of whey protein is required to have any effect on the heat stability of milk.

Ma et al. (2002) added a proteolytic enzyme to reconstituted whole milk at 50%TS and showed that the viscosity and rate of thickening increased significantly. More interestingly, there was a clear shift of the temperature at which age-thickening begins from about 65°C in normal milk concentrates to about 45-50°C in enzyme treated milk. The action of the enzyme, Neutrase, was shown by gel electrophoresis and high performance liquid chromatography to destabilise the casein micelles by turning the  $\kappa$ -casein into para- $\kappa$ -casein, i.e. lost of negative charge on the micelles.

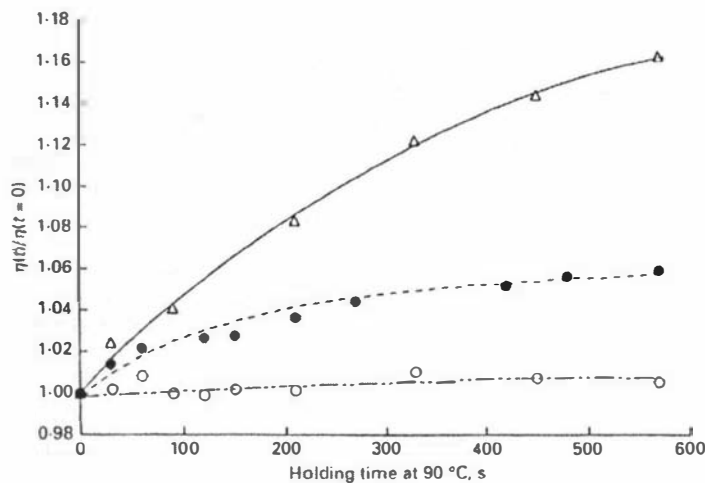


Figure 2.1: Relative change in viscosity  $\frac{\eta_t}{\eta(t=0)}$  of whey protein free milk with various concentrations of  $\beta$ -lactoglobulin ( $\beta$ -lg) as a function of the holding time at 90°C: o,  $\beta$ -lg = 0.2g/L; ●,  $\beta$ -lg = 3.3g/L;  $\Delta$ ,  $\beta$ -lg = 6.6g/L. (Jeurnink & Dekruif, 1993)

The importance of whey proteins rests on their ability to denature during heating, where the free thiol group (-SH-) at Cys<sup>121</sup> becomes available for strong disulphide bond formation (Papiz et al., 1986; Iametti et al., 1996). Interestingly, Gallagher et al. (1996) showed that heating a solution of porcine  $\beta$ -lactoglobulin did not result in gelation due to the absence of a free thiol group (Papiz et al., 1986).

During denaturation, the denatured whey proteins can associate with themselves (Alizadehfard & Wiley, 1996; Gallagher et al., 1996), casein micelles (Cho, Singh, & Creamer (2003) and the fat globule membrane (Velez-Ruiz & Barbosa-Canovas, 2000).

The formation of whey protein aggregates involves two processes: the aggregation of denatured  $\beta$ -lactoglobulin into intermediate oligomers, and secondly the use of these oligomers as building blocks for aggregate formation (Croguennec, O'Kennedy, & Mehra, 2004). These authors also noted that both  $\beta$ -lactoglobulin A and  $\beta$ -lactoglobulin B variants show similar behaviour in forming intermediates and/or soluble aggregates during heat-induced denaturation/aggregation processes.

The association between denatured whey protein and casein micelles is significantly affected by the heating conditions, including the rate of heating (Smits & van Brouwershaven, 1980), whether direct or indirect (Corredig & Dalgleish, 1996; 1999), and time (Anema & Klostermeyer, 1997).

Cho et al. (2003) showed that a concentration ratio of 1:1 denatured  $\beta$ -lactoglobulin to  $\kappa$ -casein generates the maximum quantity of disulphide bonded complexes. It is important to point out that their study was carried out on a model system, where purified  $\beta$ -lactoglobulin was heated with purified  $\kappa$ -casein solutions.

Anema and Li (2003a) showed that the rate of denaturation of whey proteins was much faster than the rate of association between the whey proteins and the casein micelles. They attributed this to the difficulty the denatured whey protein have in accessing the cysteine residues on the *para*- $\kappa$ -casein in the core of the casein micelles.

Denatured whey proteins on the micelle surface have been observed visually to act as linking bridges for micelle network formation (Sawyer, 1969; Carroll, Thompson, & Melnychyn, 1970; Kocak & Zadow, 1985; Defelipe, Melcon, & Zapico, 1991). Lucey et al. (1997) and Lucey, Munro, & Singh (1998) suggested that the denatured whey proteins

complex with the casein micelle surface, and the whey proteins can then form bridges between the casein micelles and promote the formation of a gel network.

Schorsch et al. (2001) showed that formation of a gel network in acidified milk systems was significantly different when whey protein was heated alone and with casein micelles, shown in Figure 2.2. When heated alone, the whey proteins denatured and aggregated among themselves to form a particulate gel which was weak. Some casein micelles might be entrapped within the gel network. When heated with casein micelles, the gel network was more firm and continuous, with the casein micelles incorporated within the network structure.

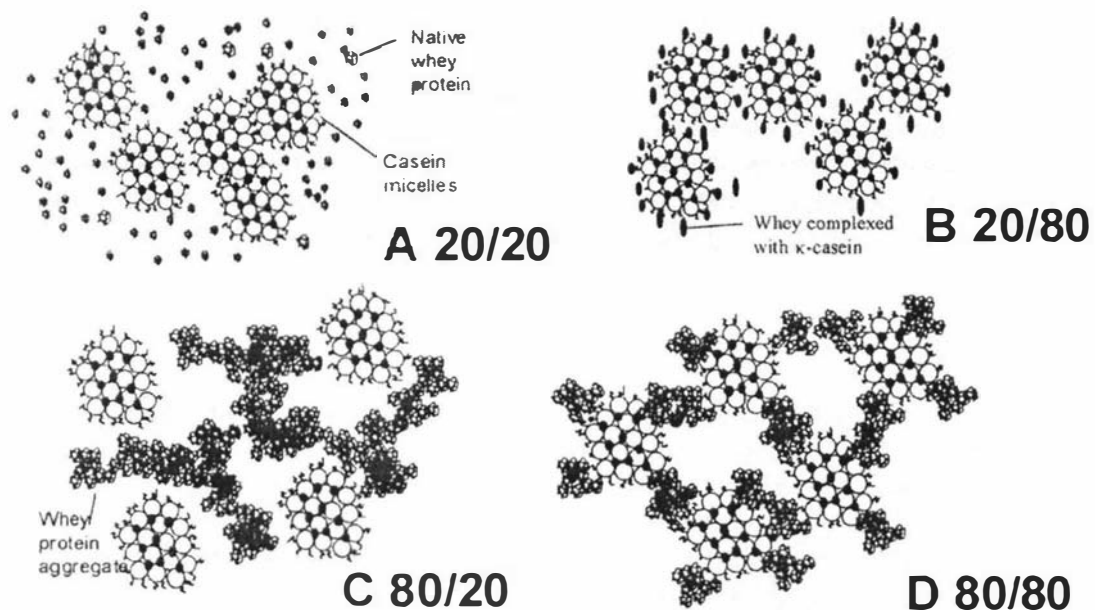


Figure 2.2: Schematic representation of the casein/whey protein acid gels. (A) casein/native whey protein heated to 20°C, (B) casein/native whey protein heated to 80°C, (C) casein/pre-denatured whey protein, which has been heated to 80°C, heated to 20°C, (D) casein-pre-denatured whey protein, which has been heated to 80°C, heated to 80°C. (Schorsch et al. 2001)

Interestingly, Schorsch et al. (2001) also showed that addition of denatured whey proteins to casein micelles does not result in the association between whey proteins and casein

micelles unless further heating is encountered. System D would yield a more porous gel system, as the denatured proteins already formed aggregates which then act as bridges. In systems where undenatured whey proteins were heated with casein micelles (B), the whey proteins would coat the casein micelles in thinner layers, which then help them to bind to other coated casein micelles. This will result in a more compact gel structure.

Similarly, Rohm (1988) and Newstead et al. (1977) showed that the addition of denatured whey protein did not have a significant effect on the viscosity and HCT of heated milk solutions.

The binding of denatured whey proteins onto the casein micelles, via disulphide bonds with the  $\kappa$ -caseins, increases the particle size and volume fraction of the casein micelles, which in turn increases the viscosity contribution of the suspended phase (Anema et al., 2004). In fact, Anema et al. (2004) found a linear relationship between particle size and viscosity during heating of diluted reconstituted skim milk systems at pH 6.5 and 6.7. Heat treatment of whey protein free milk showed no significant changes in either particle size (Anema & Li, 2003a) or viscosity (Journink & Dekruif, 1993).

Snoeren et al. (1984) argued that the age thickening behaviour of milk concentrates could be explained in terms of the hairs on the casein micelles extending out at low shear rates and being forced closer to the micelle surface at high shear. Trinh and Schraekenrad (2002) argued that the movement of hairs on the micelles cannot account for the significant increase in viscosity and particle size, and believe that the caseins must be involved in the formation of aggregates or flocs.

Numerous publications have attempted to correlate the concentration of  $\beta$ -lactoglobulin with the HCT of dilute milk systems but no relationship was established. Kieseker and Pearce (1978) attributed the difficulty to the poor analytical methods available for the determination of  $\beta$ -lactoglobulin.

Addition of  $\beta$ -lactoglobulin to whey-protein free dilute milk (less than 20%TS) gives rise to maximum and minimum heat stability on a pH-HCT curve. In concentrated milk, addition of  $\beta$ -lactoglobulin has a destabilising effect (i.e. decrease the HCT) over the entire pH range (Singh, 2004). In another word, the addition of  $\beta$ -lactoglobulin has different effect on diluted and concentrated milk systems. More importantly, the presence of  $\beta$ -lactoglobulin in milk plays a significant role in the HCT profile.

### 2.1.1.3 Fat

The fat globules in whole milk are protected by a native fat globule membrane (NFGM). The NFGM is derived mainly from the apical plasma membrane of mammary secretory cells at the time of milk fat secretion (Kim & Jimenez-Flores, 1995). It has a unique composition of mainly proteins and phospholipids that stabilise the emulsion by shielding the fat globules from the plasma and serum proteins and protect them from natural milk enzymes. In their native state the fat globules contribute to the Newtonian milk viscosity only as inert but deformable suspended particles. When the NFGM is disrupted by homogenisation, proteins from the plasma coat the surface of the uncovered fat globules to give the damaged fat globule membrane (DFGM) (Mulder & Walstra, 1974; Houlihan et al., 1992). These surface proteins can be activated to interact with other proteins and bring the fat globules into aggregates and networks of the milk solids. The interaction between damaged fat globule membrane and casein during age thickening has been regularly observed under microscope (Defelipe et al., 1991; Velez-Ruiz & Barbosa-Canovas, 2000). Since the fat globules are comparatively large (1-10  $\mu\text{m}$  compared to 50-500  $\eta\text{m}$  for the casein micelles (de Kruif, 1998; Schorsch, Jones, & Norton, 2002), aggregates in whole milk are always larger than those in skim milk.

Heat treatment allows the denatured whey proteins, mainly  $\beta$ -lactoglobulin, to interact with the membrane components via disulphide bonds, as well as causing a loss of original membrane components, such as phospholipids and membrane proteins (Lee & Sherbon, 2002). Ye et al. (2004) showed that the association of  $\beta$ -lactoglobulin and  $\alpha$ -lactalbumin

with the fat membrane could be described by a first order reaction in the low temperature range (65°C-85°C) and a second order reaction in the high temperature range (85°C-95°C).

Homogenisation causes a massive disruption of the native fat globules membrane and creates a large amount of new interface between the fat and plasma phases (Noda, Endo, & Takahashi, 1978; Keenan, Moon, & Pyloruski, 1983; Snoeren et al., 1984; McCrae, 1999; Hayes & Kelly, 2003). Lee and Sherbon (2002) showed that homogenisation without heating will only result in the incorporation of casein micelles onto the fat globule membrane.

The protein coatings of the fat globules increase the apparent volume fraction of the dispersed particles and thus increase the apparent viscosity of fresh milk concentrates (Vilder et al., 1979; Lawrence et al., 2001) and sweetened condensed milk (SCM) (Lawrence et al., 2001).

An increase in homogenisation pressure would create more fat globules (Hayes & Kelly, 2003) that can be incorporated into the evolving structure during storage, and in turn result in an increase in the rate of age thickening and a decrease in HCT for SCM and recombined sweetened condensed milk (RSCM) (Lawrence, Muller, & Rogers, 1963; Noda et al., 1978; Kieseker & Aitken, 1988). During the production of recombined sweetened condensed milk (RSCM), the use of recombined cream makes it possible to exclude the use of homogenisation and thus achieve lower viscosity and rates of age thickening (Noda et al., 1978).

Vilder et al. (1979) also noted that one-stage homogenisation resulted in a higher viscosity than a two-stage homogenisation system, for a given homogenisation pressure. During a two stage homogenisation, “the fat clusters were largely broken down in the second stage” (Vilder et al., 1979), resulting in lower viscosity values.

Snoeren et al. (1984) made a contrary observation that there was a decrease in the rates of age thickening at higher homogenization pressures. They argued that the casein adsorbed on to the newly created fat/plasma interface would “be within the sphere of the apparent volume and hence will not contribute to the size of the volume”, as shown in Figure 2.3. A higher homogenization pressure would generate a greater fat surface area and more casein micelles would be part of the apparent volume-sphere.

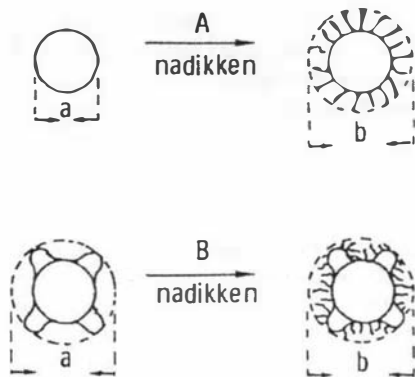


Figure 2.3: Schematic representation of the thickening of non-homogenised concentrate (A) and of homogenized concentrate (B). The filamentous structure represents the casein, while the circles represent the fat globules. (Snoeren et al., 1984)

On the other hand, Lawrence et al. (2001) noticed that an increase in homogenisation pressure during the manufacture of SCM had little effect on the age thickening profile, i.e. rate of age thickening, during storage.

More work is required to explain these contradictory observations on the effect of homogenisation of fats on the rheological behaviour of whole milk concentrates.

#### 2.1.1.4 Salts and minerals

The milk salts exist in equilibrium between diffusible and colloidal phase (de la Fuente, 1998; Udabage, McKinnon, & Augustin, 2000). The addition of salts and minerals can have a dramatic effect on the rheological behaviour and heat stability of milk concentrate

systems (Rose, 1963; Newstead, 1977; Kieseker & Pearce, 1978; Noda, Endo, & Takahashi, 1986; Pouliot & Boulet, 1995; Upadhyay, 1998; Vyas & Tong, 2003).

The addition of calcium can result in an increase in viscosity (Noda et al., 1986) and a decrease in HCT (Nieuwenhuijse et al., 1988; Vyas & Tong, 2003). Fluoride, on the other hand, combines with calcium and prevents formation of bridges between the micelles, and thus retards the rate of age thickening (Upadhyay, 1998). Addition of phosphate enhances heat stability (Nieuwenhuijse et al., 1988).

It is important to analyse the effect of both individual ions, as well as the ratio of one ion to another, on the stability of milk systems (Rose, 1963). Rose (1963) also suggested that any effects of salt compounds on HCT can only exist in the presence of  $\beta$ -lactoglobulin.

#### **2.1.1.5 Urea**

Urea is a natural component of milk and it is one of the main components of the non-protein nitrogen (NPN). There has been no study done on the effect of urea on the viscosity or rate of age thickening in milk concentrates. However, the amount of literature on the effect of urea on HCT of milk system is more abundant.

The effect of urea on HCT is well documented, where its addition increases HCT of diluted milk systems (Muir & Sweetsur, 1976, 1977; Holt, Muir, & Sweetsur, 1978; Muir, Abbot, & Sweetsur, 1978; Kelly, 1982a, 1982b; Shalabi & Fox, 1982). The effect of urea on heat stability is highly dependent on seasonal effect (White & Davies, 1958b; Newstead et al., 1977; Kelly, 1982a).

The addition of urea either before or after preheating had no significant effect on the heat stability of the reconstituted powder products (Kelly, 1982a). Kieseker and Pearce (1978) suggested that urea affects the casein coagulation process, but not the interaction between casein and whey protein, which predominantly takes place during preheating.

The addition of urea increases the sensitivity of HCT profile to changes in pH (Kelly, 1982a). The presence of urea also shifted the pH of maximum stability to the acid side of the natural pH (Kelly, 1982a).

#### **2.1.1.6 Seasonal variation and stage of lactation**

It is important firstly to distinguish between seasonal variation and stage of lactation. Seasonal variation deals with varying external factors, such as environment, feeds and farming practice. Stage of lactation is concerned with the physical state of the cow after calving and its effect on the composition of the milk.

In New Zealand, the general farming practice is to concentrate calving in spring, late July/ early August. Thus, most of the cows calve at the same time. Immediately after calving, due to the lactation effect, milk yield increases during the subsequent several weeks. During spring, the pasture is often nutritious and abundant. By concentrating the calving in spring, the farmers maximize pasture utilization during the maximum milk yield period from the cows (Auldish, Walsh, & Thomson, 1998; Nicholas et al., 2002). Thus, seasonal and lactation effects can coincide.

However, the milk yield will eventually drop. This will coincide with a drop in pasture quality and yield. The overall quantity of milk supply will drop due to the drop in concentration of key components such as protein. Thus, this farming practice results in irregularities in the supply and composition of the milk during a dairy production season.

In Europe, calving is spread across the year, and thus the interaction between stage of lactation and seasonal variation is more complex. This practice tends to minimise the seasonal variation in the supply and composition of milk (Kieseker & Pearce, 1978; Auldish et al., 1998).

Seasonal variation and stage of lactation have significant effects on milk composition, which in turn affects the viscosity of the milk system. A substantial amount of work has been carried out to analyse the variation in composition of milk systems with production season and stage of lactation.

Bloore and Boag (1981) published a thorough study of the variation in the content of various milk components over two dairy seasons. Skim milk was concentrated and then dried in a pilot plant and the resultant powder analysed. The protein content, which has a significant impact on the rheological behaviour, was found to peak in February and March, which coincides with the end of the production season.

Kiesecker and Healey (1996) found a similar seasonal variation pattern of protein content in skim milk powder from three manufacturing plants in Australia over one year of production. In this work, there were no matching viscosity measurements. For all plants, the maximum protein content was observed in the period of March-May (autumn), in agreement with Bloore and Boag (1981). A reverse trend was observed with lactose concentration, with a minimum in the period of March-May and a maximum in September-December. A similar trend in protein content was observed by Underwood and Augustin (1997) and Newstead et al. (1977). Calcium content also showed peak periods in the months of March-May (Underwood & Augustin, 1997).

O'Brien et al. (1999a, 1999b) carried out a detailed investigation into the seasonal variation in composition of manufactured and retail (of the shelf) Irish milk. Total protein, casein, whey, urea and fat showed similar trends in seasonal variation with maxima and minima observed in October-November and February-April respectively. It is important to note that October-November is the end of the milking season where indoor feeding takes place. In addition, late lactation takes place in October-November. Therefore, the trend in the fluctuation of protein with seasonal variation observed by O'Brien et al. (1999a, 1999b) agreed with the findings from Bloore and Boag (1981) and Kiesecker and Healey (1996). Vitamins and minerals showed complex relationships with lactation period. Rennet coagulation time did not show significant correlation with the

trend in protein, urea and fat. Manufacturing conditions, which could have had significant effects on the rheological behaviour of the milk systems, were not discussed in detail.

Coulon et al. (1998) carried out a thorough investigation into factors affecting the casein-whey protein ratio in milk. Genetic variation and stage of lactation had the most significant effect on the protein concentration and the casein-whey protein ratio. Breeds and dietary factors had little or no effect on the ratio.

Factors including environmental (Connolly & O'Brien, 1994), farm and herd management (Dillon et al., 1995), cow diets (Murphy & O'mara, 1993), milking practices (Stadhouders, 1972; Coulon et al., 1998) have a significant effect on the composition and the behaviour of milk systems. A combination and/or interaction of these factors could give rise to significant variability in the expected seasonal variation in the composition of milk (Barber et al., 2001).

There are many more published papers which deal with the variation of individual milk components, such as plasmin (Benslimane et al., 1990; Nicholas et al., 2002), urea (Kelly, 1982b), casein/true protein ratio (Berg & Berg, 1996; Ostersen, Foldager, & Hermansen, 1997), free fatty acids (Evers & Palfreyman, 2001; Fitzpatrick, Rogers et al., 2001), and size of casein micelles in bovine milk (Holt & Muir, 1978) during a production season.

In the literature, only Bloore and Boag (1981) have compared the variation in viscosity and protein contents, as well as other milk components. No published literature has been found on the relationship between age thickening and seasonal variation.

A significant amount of work has been published with regard to seasonal variation of HCT of milk systems (White & Davies, 1958a; Newstead, Sanderson, & Baucke, 1975; Muir & Sweetsur, 1976; Newstead & Baldwin, 1977; Holt et al., 1978; Kelly, 1982a, 1982b; Dalgleish, Pouliot, & Paquin, 1987; Singh & Tokley, 1990; Mil & Koning, 1992;

Underwood & Augustin, 1997). Maximum heat stability is often observed in mid-lactation and minimum HCT during the early and late stages of lactation with New Zealand milk.

The literature clearly showed the effects of seasonal variation, stage of lactation, as well as many other factors on the composition variation in milk system. Yet, publications on rheological behaviour and HCT of milk systems often do not include data and discussion on the composition, seasonal variation and lactation. It is apparent that there is a significant gap in communication between the two fields of dairy processing and dairying. Discrepancies in published rheology data are widely observed and not understood. The author believes that the variation in milk composition may play a crucial role in accounting for these discrepancies. In many pieces of work on rheology or HCT, compositional analysis of the raw material was of little interest. Without this information, it is difficult to identify the causes for the discrepancies between the published rheological data of milk systems (Nicholas et al., 2002). The gap in the understanding of these complex interactions may be bridged by a fusion of knowledge between the two fields.

### **2.1.2 pH**

pH of milk changes with processing steps. Venkatachalam et al. (1993) showed that when raw milk at pH 6.83 was processed, the pH dropped to 6.80 after pasteurisation, 6.77 after filtration and concentration, and 6.71-6.73 after UHT processing. Griffin et al. (1976) noted that preheating causes a reduction in pH of milk, particularly with higher preheating temperatures and longer holding times. The drop in pH of milk during heating is attributed to several causes: release of CO<sub>2</sub>, precipitation of calcium phosphate, release of H<sup>+</sup>, formation of organic acids from thermal breakdown of lactose (Walstra & Jenness, 1984; Singh & Creamer, 1997).

pH has a significant influence on the rheological properties of milk concentrate systems due to the loss of electrostatic repulsion near the isoelectric points of the casein and whey proteins. pH also has a significant effect on CCP, which dissolves as the pH decreases (de la Fuente, 1998; de Kruijff, 1999), thus causing dissociation of caseins, particularly of  $\beta$ - and  $\kappa$ -CN (Singh et al., 1996). Decrease in pH also causes an increase in calcium ion activity (de la Fuente, 1998; Singh, 2004).

Despite the importance of pH, no work on the effect of pH on the viscosity and rate of age thickening of milk systems has been found in the literature. However, there is fair number of literature on the effect of pH on the HCT profile.

The HCT of milk can show one of two types of profiles, as shown in Figures 2.4-2.5. Most milks show so called Type A behaviour, where the HCT-pH curve shows maximum heat stability in the pH range of 6.5-6.7, then declines abruptly to a minimum in the range of pH 6.7-6.9, as shown in Figure 2.4.

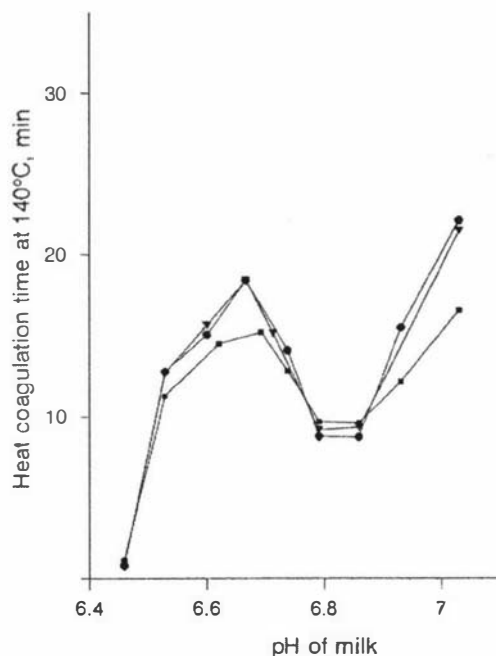


Figure 2.4: pH-HCT profile of a Type A milk. (McCrae, 1999)

The relative position of the natural pH of the milk solution in relation to the pH of maximum heat stability also plays an important part in controlling the heat stability of the system. For example, if the natural pH lies on the right of the pH at maximum HCT, then a decrease in pH of the system would shift the HCT towards the maximum on the HCT-pH scale.

In Type B milk milks as shown in Figure 2.5, the pH-HCT curves increases gradually without a maximum. Interestingly, when whey protein is removed from the milk system, the pH-HCT curve shifts from a normal type A to a type B behaviour (Kieseker & Pearce, 1978; Tan-Kintia & Fox, 1999). Conversely, the addition of  $\beta$ -lactoglobulin to serum protein-free milk (SMPF) shifts the pH-HCT profile from Type B to Type A (O'Connell & Fox, 2001). Table 2.1 lists several methods for converting the pH-HCT profile from Type A to Type B.

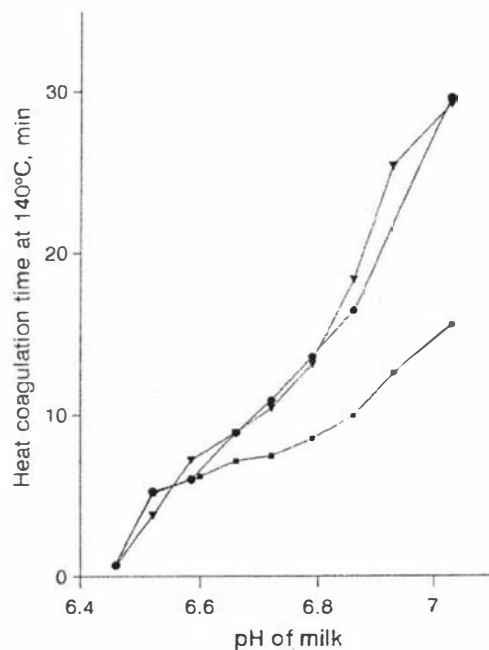


Figure 2.5: pH-HCT profile of a Type B milk. (McCrae, 1999)

Table 2.1: Methods for eliminating the minimum from the HCT-pH profiles of Type A milks (Singh, 2004)

---

Conversion of Type A to Type B
Decrease in the assay temperature (150°C to 120°C)
Addition of $\kappa$ -casein
Removal of whey protein
Reduction in the levels of soluble salts
Several additives (e.g. aldehydes, oxidising agents, polyphenols)
Treatment with transglutaminase

---

Even small changes in the acidity of the fresh milk (0.05 pH units) have a significant effect on the tendency to age thickening (Kieseker & Pearce, 1978; Upadhyay, 1998) and heat stability (Rose, 1963; Newstead et al., 1975; Griffin et al., 1976). Manipulation of composition and structural properties of the system will have an effect on the HCT-pH relationship. Griffin et al. (1976) showed that preheating increases the sensitivity of the heat coagulation time profile with pH, thus causing the maximum heat stability to occur within a smaller pH range.

### 2.1.3 Temperature during processing

There are two groups of work on this topic. One deals with the relatively diluted milk solutions (up to 20%TS), where dairy chemistry gives good insights into the chemical interaction of proteins during heating and holding. There are some viscosity measurements in this group of work, although most employed the HCT technique.

The second group of publications, which is much smaller in number, focuses on the effect of temperature on the rheology of concentrated milk solutions, and deals less with protein chemistry.

The rate of increase in viscosity of dilute milk is dependent on the temperature and duration of heating, as well as pH (Cayot et al., 2003). This increase in viscosity was found to correlate well with an increase in particle size. Below 80°C, the change in particle size is linearly dependent on heating time. Above 80°C, the particle size increases rapidly, before reaching a plateau, which is dependent on the pH (Anema & Li, 2003a).

During heating, the pH has a significant effect on the interaction between denatured whey proteins and casein micelles. At pH 6.5, a maximum of 70% of the denatured  $\beta$ -lactoglobulin and  $\alpha$ -lactalbumin proteins associate with the casein micelles, compared to just 30% when heating was carried out at pH 6.7 (Anema & Li, 2003a, 2003b, 2004). This is in agreement with the findings from Smits and van Brouwershaven (1980), Dalgleish et al., (1997), Lucey et al., (1998), Vasbinder and de Kruif (2003).

Vasbinder and de Kruif (2003) showed that below pH 6.6, all denatured whey proteins attach to the casein micelles, but the coverage is less homogeneous as the pH is decreased. At pH values above 6.6, more whey protein aggregates are formed in the serum and not bound to the casein micelles, shown in Figure 2.6. This could explain the effect of pH during heating on the particle size, where lower pH resulted in larger increase in particle size as observed by Anema and Li (2003a, 2004).

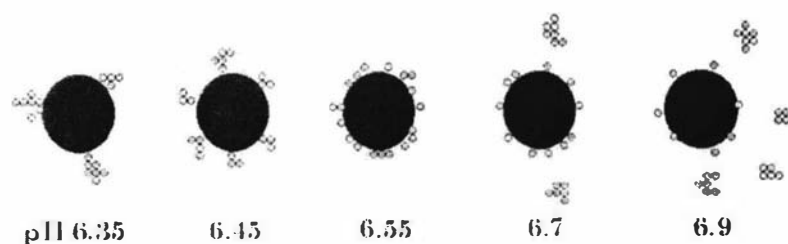


Figure 2.6: A schematic representation of the interactions between casein micelles and whey proteins occurring in milk during heat treatment for 10 minutes at 80°C at pH values ranging from 6.35 to 6.9. The small circles represent denatured whey proteins, the large circles the casein micelles. The whey proteins are either present in aggregates or covalently associated with the casein micelle. Native whey proteins are not included in the figure. (Vasbinder & de Kruif, 2003)

Heat treatment of dilute milk systems also causes a shift in gelation pH towards higher pH values (Lucey et al., 1997; Lucey et al., 1998; Vasbinder, van Mil, Bot, & de Kruif, 2001). This is because whey proteins coagulate at higher isoelectric pH than caseins. Hence, the surface coated casein micelles will flocculate at higher pH than native casein micelles (Lucey et al., 1997; Schorsch et al., 2001; Vasbinder et al., 2001; Vasbinder, van de Vilde, & de Kruif, 2004). Lucey et al. (1998) showed that serum protein-free milk had a gelation time and pH of gelation similar to unheated reconstituted milk during acidification.

Heating also causes dissociation of casein components from the micelles (Ono et al., 1999; Anema & Li, 2003a). Heating at 120°C results in 4% dissociation, while heating at 140°C yields 20% of the micellar proteins (Ono et al., 1999). An increase in pH during heating also gives rise to significant increase in the dissociation of the casein micelles, particularly the  $\kappa$ -casein above pH 6.7 (Anema & Klostermeyer, 1997).

Beaulieu et al. (1999) suggested that the maximum amount of association between denatured whey proteins and casein micelles was due to the saturation of  $\kappa$ -casein on the micelle surface. The remaining denatured whey proteins form soluble aggregates among themselves, as well as with some  $\kappa$ -casein in the serum. Interactions of  $\alpha$ -lactalbumin

with casein micelles can only occur once denatured  $\beta$ -lactoglobulin has formed complexes with the micelle surface (Dalglish et al., 1997; Fairise & Cayot, 1999).

The effect of temperature is also dependent on seasonal variation and stages of lactation. During the periods of minimum HCT in early and late lactation, heat treatment was found to have little effect (Kelly, 1982a). Newstead et al. (1977) however, observed that high preheat temperature produced satisfactory heat stable (long HCT) skim powder during late lactation.

Anema et al. (2004) attributed the increase in viscosity with temperature above 70°C to the increase in size of the casein micelles during heating. This increase in size has been linked to the association between casein micelles and denatured whey proteins (de Kruif, 1998; Beaulieu et al., 1999; Fairise & Cayot, 1999). The maximum amount of association between denatured whey proteins and casein micelles decreases with an increase in pH (Anema & Li, 2003a). Heating of whey-depleted milk showed little change in particle size (Anema & Li, 2003a) or viscosity (Journink & Dekruif, 1993). Anema et al. (2004) postulated that the adsorbed whey proteins could act as interspaced filamentous appendages extending from the micelle surface, and increase the occlusion of milk serum and thus extend the hydrodynamic radius of the micelles. This in turn increases the volume fraction of the milk system, and consequently, viscosity.

Ono et al. (1999) suggested that the increase in casein size is the result of association between small size micelles to form larger ones upon heating, and whey proteins are an important stimulator of micellar association.

In concentrated milk solution (>40%TS), many authors observed a decrease in viscosity with temperature until a minimum is reached in the temperature range of 60-70°C, before the viscosity increases again (Bloore & Boag, 1981; Snoeren et al., 1982b; Journink & Dekruif, 1993; Velez-Ruiz & Barbosa-Canovas, 1997; Trinh & Schraekenrad, 2002). Interestingly, Trinh and Schraekenrad (2002) (Figure 2.7) and Snoeren et al. (1984) showed that age thickening was significant only when reconstituted whole milk

concentrate was heated at above the critical temperature of 65°C. Below this critical temperature, no age thickening was observed in the samples. Tang et al. (1993) made the same observations with a whey protein concentrate (WPC) system, where the apparent viscosity increased sharply after the critical temperature region of 60-70°C. Below this critical range, the viscosity follows the Arrhenius model, where the logarithm of viscosity is a linear function of the reciprocal absolute temperature (Markovitz, 1985). Tang et al. (1993) argued that this behaviour may be the net result of three effects. An increase in temperature would increase the intermolecular distance and thus results in a decrease in viscosity. The second effect involve the shear-induced disruption of the protein aggregates formed by intermolecular interactions. Thirdly, irreversible physicochemical changes take place at high temperature, in particular above 60°C where denaturation of whey proteins take place. The first two effects would dominate at lower temperatures, whereas the third effect dominates at higher temperatures resulting in a viscosity minimum (Tang et al., 1993).

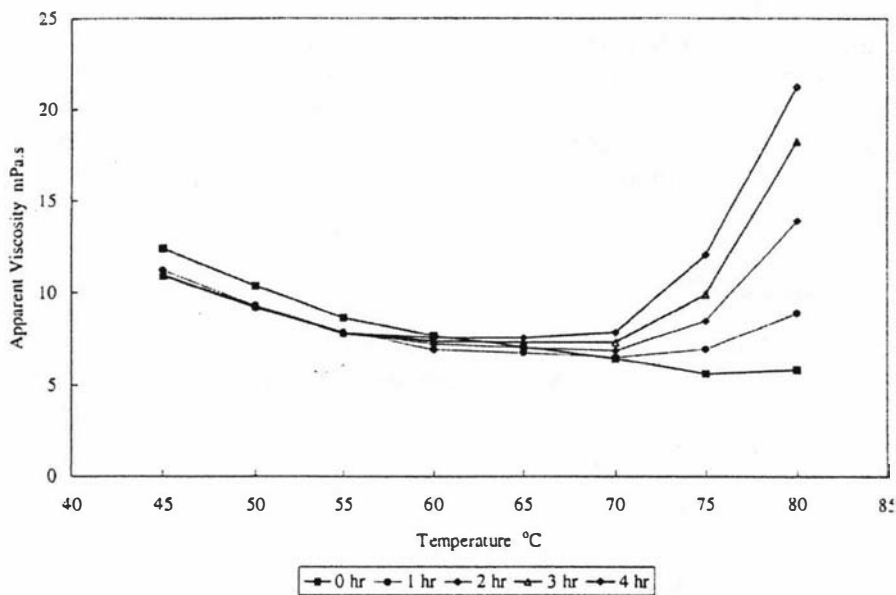


Figure 2.7: Variation of apparent viscosity with temperature and storage time. (Trinh and Shrakeenrad, 2002)

In SCM, age thickening occurs with storage at low temperature (Samel & Muers, 1962). Gelation was observed after 2 weeks of storage at room temperature, but took longer at lower temperature (Samel & Muers, 1962). Samel and Muers (1962) and Zavarin, Chekulaeva and Chekulaev (1978) suggested that at the higher end of this storage temperature range, the viscosity of the aqueous phase is low, and reactions can proceed more quickly in comparison to a more viscous medium at lower temperature. The increase in temperature also results in an increase in the strength of hydrophobic effect, and thus an increase in protein-protein interactions (Bonomi & Lametti, 1991; Lametti et al., 1993).

#### **2.1.4 Preheat treatment**

There is no work on the effect of preheat treatment of milk during powder manufacture on the age-thickening of fresh milk concentrates. However, there is information on the effect of preheat treatment on the in-line viscosity and the HCT of concentrated milk.

Preheat treatment has a significant effect on the flow behaviour of whole milk concentrate, as well as its sensory and physical properties (Baldwin, Cooper, & Palmer, 1991; Baldwin & Ackland, 1991). Higher heat treatment resulted in higher viscosity values.

Vilder and Moermans (1983) and Lawrence et al. (2001) made similar observations with in-line viscosity measurements on fresh skim milk concentrate where high preheat treatment resulted in higher viscosity values.

Severe preheat treatment was found to generally increase the heat stability (high HCT) of diluted (Vyas & Tong, 2003) and concentrated (Griffin et al., 1976; Newstead et al., 1977; Metwally et al., 1978; Kelly, 1982a; Singh & Tokley, 1990; McKenna & Singh 1991; Mil & Koning, 1992) milk systems. Bloore and Boag (1981) reported that a high temperature-short time preheat treatment yielded lower concentrate viscosity when

compared to a low temperature-long time treatment which gave a similar extent of protein denaturation.

Mil and Koning (1992) noted that an increase in heating temperature resulted in greater improvement in HCT (more heat stable) than an increase in heating time. However, there apparently appears to be an upper limit to the extent of preheat treatment where there is no further increase in HCT, and the HCT may actually decrease (Kieseker & Pearce, 1978).

In UHT milk systems, higher preheating temperature also results in more stable products which take longer storage time to exhibit age gelation (Datta & Deeth, 2001).

High preheat treatment results in a greater amount of whey protein denaturation (Metwally et al., 1978). Preheat treatment also reduces the amount of ionized calcium and magnesium, which in turns increases the stability of casein (Ismael & Grimbleby, 1958). In UHT milk, heating at 147°C for 10 seconds will deactivate all plasmin activity (Rollema & Poll, 1986).

The effect of preheat treatment on heat stability is markedly dependent on the total solids content of milk (Rose, 1963) and seasonal variation (Newstead et al., 1977). Preheat treatment was found to have minimum effect on heat stability during the periods of minimum HCT in early and late stages of lactation (Newstead et al., 1977).

An increase in preheat treatment would also trigger other reactions in milk that will have a detrimental effect on the shelf life of the products, such as additional milk deposition on heating surfaces (Kelly, 1982a).

### **2.1.5 Reconstituted versus fresh milk**

The heat stability of reconstituted skim milk was found to be dependent on the heat stability of original milk and the process treatments applied (Kieseker & Pearce, 1978; Muir et al., 1978). However, heat stability of reconstituted systems was found to have a complex relationship with the HCT of the original fresh concentrates from which the powder was manufactured (Kieseker & Pearce, 1978; Newstead & Baucke, 1983; Singh & Tokley, 1990; Singh & Creamer, 1991; Mil & Koning, 1992).

The reported viscosity of reconstituted milk concentrates varies greatly between different authors. Vilder et al. (1979) reported a viscosity of 2500 mPa.s for 50% total solids (TS) reconstituted milk concentrate compared to 70 mPa.s for fresh concentrates from which the powders were made. Buckingham (1978) reported viscosities of the order of 100 mPa.s for 40%TS reconstituted skim milk powder at 20°C. The viscosity reported by Vilder et al. (1979) is more comparable to values obtained for recombined sweetened condensed milk which are known to be age thickening. Fitzpatrick et al. (2001) noted that after reconstitution, an agitated 50% solids milk concentrate solution exhibited a dramatic increase in viscosity over 60 minutes at 20°C. Trinh and Schraekenrad (2002) suggested that the results of Vilder et al. (1979) were affected by age-thickening during recombination.

### **2.1.6 Influence of rheological behaviour of concentrate systems on processing conditions and milk powder properties**

The solubility limits imposed by the end users restrict the operating efficiency of powder manufacturing plants (King, Sanderson, & Woodhams, 1974).

It is desirable to remove as much water as possible by evaporation because it is much more energy and cost effective than spray drying (Beeby, 1966; Baldwin et al., 1980;

Vilder & Moermans, 1983). During drying, high concentrate viscosity results in larger concentrate droplets inside the drying chamber (Snoeren, Damman, & Klok, 1981, 1982a, 1983). It is more difficult for the larger droplets to dry. Thus the particles spend a longer time passing through a critical moisture range for casein denaturation, giving rise to a decreased solubility index (Baldwin et al., 1980). An increase in concentrate viscosity will also hinder the rate of movement of water to the surface of the milk droplets and thus retard the rate of moisture loss during the drying process (Baldwin et al., 1980). Moreover, the heavy drops are insufficiently deflected by the drying air immediately after atomisation, leading to deposits against the chamber wall.

High concentrate viscosity has a negative effect on several physical properties of the resultant milk powder, including average diameter, moisture content, vacuole volume, bulk and particle density (Baldwin et al., 1980; Snoeren et al., 1981, 1983).

Baldwin et al. (1980) showed that temporary storage of skim milk concentrates resulted in an increase in concentrate viscosity, and subsequently an undesirable decrease in solubility index. Thus, storage of concentrate systems should be kept to the minimum (Beeby, 1966; Baldwin et al., 1980).

### **2.1.7 Rheological Modelling**

Rheological modelling requires shear stress versus shear rate data. As HCT and single point viscosity measurements have been the preferred method of experiment, there has been little modelling work done on fresh and reconstituted milk concentrate systems. The Herschel-Bulkley model is a popular choice for rheological modelling of milk concentrates (Kristensen et al., 1997; Hinrichs, 1999; Velez-Ruiz & Barbosa-Canovas, 2000; Trinh & Schraekenrad, 2002)

$$\tau = \tau_y + K(\dot{\gamma})^n \quad (2.6)$$

where  $\tau$  is the shear stress (Pa),  $\tau_y$  yield stress (Pa),  $K$  consistency coefficient (Pa.s<sup>n</sup>),  $\dot{\gamma}$  shear rate (s<sup>-1</sup>),  $n$  behaviour index.

Velez-Ruiz and Barbosa-Canovas (1997, 1998, 2000) studied the rheological behaviour of pasteurised and homogenised whole milk concentrates and its interactions with solids content and temperature. Model parameters were fitted using Statistix and Excel 5.0 software. Essentially, the parameters were simultaneously modified to achieve minimum differential error between actual and predicted data. It is important to point out that all three Herschel-Bulkley parameters are inter-dependent. If a change in composition or structure results in an increase in viscosity at a given shear rate, the consistency coefficient and the yield stress would likely to increase, and the behaviour index would decrease (indicating more non-Newtonian behaviour). Obviously this would only apply to a shear thinning Herschel-Bulkley fluids.

They showed that below a 20.2% solid content, stored milk concentrates behaved as Newtonian fluids. Above this concentration level, the concentrates could be modelled with the power law model, and yield stress was observed in concentrate samples with solid content over 40%TS. The Herschel-Bulkley model was used to fit the data of high solid concentrates. 48%TS milk concentrate solutions exhibited a significantly lower flow behaviour index, and higher consistency coefficient and yield stress than other solutions with lower solids content. This anomalous jump was attributed to the milk behaving as a concentrated suspension (Velez-Ruiz & Barbosa-Canovas, 1998) but is more likely to have been due to the beginning of time-dependency. The effect of temperature was found to have a more pronounced effect on the consistency coefficient than the flow behaviour index.

The effect of temperature on the apparent viscosity and consistency coefficient followed the Arrhenius equation (Velez-Ruiz & Barbosa-Canovas, 1998). The changes in activation energy with solids content and temperature were also monitored. Velez-Ruiz and Barbosa-Canovas (1998) suggested activation energy could be used as a reflection of the changes in structural formation during age thickening.

Velez-Ruiz and Barbosa-Canovas (1998) also monitored the changes in the Herschel-Bulkley parameters with storage time at various temperatures. The consistency coefficient was the only parameter that displayed a clear and consistent trend, showing an exponential increase with storage time at a given temperature.

In their concentration-temperature model, there was a decrease in  $R^2$ , the coefficient of determination, with storage time. This indicated that physicochemical changes other than the effects of solid content and temperature changes take place during storage (Velez-Ruiz & Barbosa-Canovas, 1998).

The poor trends observed with the other two Herschel-Bulkley parameters illustrated the difficulty in rheological modelling using a computer-based program that operated on the basis of least square error between the predicted and the actual results. This could lead to erratic trend in the variation of individual parameters with time (Trinh & Schraekenrad, 2002).

Trinh and Schraekenrad (2002) utilised a different approach to modelling. A rough value of the flow behaviour index,  $n$ , was determined, and a  $\pm 10\%$  constraint was placed on  $n$  during modelling. Hough et al. (1988) employed similar approach in their studies of Dulce de Leche, a typical Argentine dairy product.

For each hourly measurement, Trinh and Schraekenrad (2002) showed that the rheological data was well fitted with the Herschel-Bulkley model. The yield stress ( $\tau_y$ ) and the consistency coefficient ( $K$ ) increased with storage time, heating and storage temperature, and solids content. The reverse trend was observed for the flow behaviour index ( $n$ ). They found that the effect of time on the yield stress and the consistency coefficient was adequately modelled with a sigmoid model, especially at high temperature. Trinh and Leslie (1997) and Trinh and Schraekenrad (2002) noted that models that did separate the shear and time coefficients, such as the Moore model

(Moore, 1959), were more efficient at capturing the evolution of structure with age-thickening than models that did not (e.g. Weltman, 1943; Tiu and Boger, 1974).

### **2.1.8 Postulated Mechanisms of Age Thickening, coagulation and age gelation**

Kocak and Zadow (1985) and de Koning, de Wit and Driessen (1992) believed that rheological change during storage is a two-stage process. In the first stage, an induction period, an increase in viscosity takes place while the system still behaves as a fluid. Gelation follows in the second stage where an irreversible coagulation takes place, accompanied by syneresis at rest.

Almost all the work performed on age-thickening has focused only on the first stage. Snoeren et al. (1982b, 1984) believed that the effect of age thickening on the apparent viscosity can be mostly reversed by infinite shear but on the other hand, Samel and Muers (1962) and Trinh (1994) argued that age thickening is irreversible involving two effects. The first includes the thixotropic changes that relate to a viscosity increase with time when the fluid is moved from process lines to a region of lower shear. This effect is reversible. In addition, there is also an irreversible reaction, which involves chemical changes that relate to the aggregation of solids.

There is an abundance of information on the effect of heat on the viscosity as well as composition and interactions between the milk components. Velez-Ruiz and Barbosa-Canovas (1997, 1998, 2000) measured the change in viscosity during storage of whole milk concentrates. However, they did not describe the increase in viscosity during storage as an age thickening process. There are other literature publications that discuss separately the mechanism of heat-induced gelation and thermal coagulation but do not link it to the age thickening process. Therefore, there are only a small number of references that actually do propose a mechanism on age thickening.

Snoeren et al. (1984) believed that age thickening is caused by the folding and unfolding of the hairy  $\kappa$ -casein layer during shear and storage at rest respectively. Pouliot et al. (1990), Venkatachalam et al. (1993) and Bienvenue et al. (2003a, 2003b) believed that age thickening is caused mainly by the aggregation of casein micelles during storage. Pouliot et al. (1990) thought that age thickening of sterilised infant products is caused by aggregation of casein micelles through hydrogen bonds and calcium bridges. Venkatachalam et al. (1993) believed that age gelation “involves the dissociation of proteins from the casein micelles and their formation on the micelle surface as protuberances and tendrils. Aggregation of the protein particles occurs through these appendages, not through the original micelle surface...”. Bienvenue et al. (2003a, 2003b) argued a decrease in pH during concentration affects the equilibrium state of the colloidal calcium phosphate which has a significant effect on the integrity of the casein micelles. They hypothesized that calcium phosphate may be deposited on the micelle surface decreasing both electrostatic and steric repulsion.

Many authors believe that the denaturation of whey protein upon heating at high temperature and its interaction with  $\kappa$ -casein plays a significant role in the age thickening (Rohm, 1988; Jeurink & deKruif, 1993; Trinh & Shrakeenrad, 2002), coagulation (Newstead et al., 1977; Singh, 2004), age gelation (McMahon, 1996; Datta & Deeth, 2001) and acid gelation (Schorsch et al., 2001; Vasbinder & de Kruif, 2003) processes. It is unclear on how these denatured  $\beta$ -lactoglobulin- $\kappa$ -casein complexes contribute to structure build-up process. McMahon (1996) suggested that in UHT milk, the complexes dissociate from the casein micelles and involve in cross-linking between themselves and associated proteins. Therefore, any treatments or conditions that can reduce the rate of whey protein denaturation or inhibits the release of the  $\beta$ -lactoglobulin- $\kappa$ -casein complex from the casein micelles would retard age gelation.

Linking bridges between micelles upon heating have been observed in diluted and concentrated milk (Sawyer, 1969; Carroll, Thompson, & Melnychyn, 1970; Kocak & Zadow, 1985; Defelipe, Melcon, & Zapico, 1991; Velez-Ruiz & Barbosa-Canovas,

2000). It is possible that these bridges are formed in similar manner as that in UHT system and followed the principle of McMahon (1996).

### **2.1.9 Summary**

The field of milk concentrate rheology is difficult and confusing. The number of published works in this field is adequate, but not extensive. There are many conflicting results and theories on the rheological behaviour of milk concentrate systems and the underlying causes. These discrepancies can be attributed to four factors: effect of season and stage of lactation, milk composition, sample preparation and measurement techniques.

Many published reports have investigated the effects of processing variables on a variety of milk systems, including skim and whole milk, infant and whey depleted systems. In milk systems, there are a vast number of active components, including casein micelles, whey proteins and fat globules. Complex interactions between these species are to be expected. The use of dissimilar milk systems, which differ in both composition and process treatments, was bound to generate conflicting results due to diverse interactions arising from the different mix of active components in the milk systems. Without the inclusion of detailed analyses of composition to complement the rheological data, it is difficult to account for the discrepancies in the published data, and to obtain a clear understanding of the relationship between composition and rheological behaviour.

With time-dependent systems, any application of shear or thermal or other process treatments that may affect the interactions between the components responsible for the change in rheological behaviour should be controlled and accounted for. This is imperative during sample preparation and measurement. Failure to standardize experimental procedures will result in differences in rheological behaviour, even with the same initial raw samples. There has not been an international push for some form of

standardized or agreed experimental protocol to minimize the discrepancies and variations between published results.

The study of rheology in milk systems is further complicated by the choice of raw materials for analysis. These include diluted and concentrated, fresh and reconstituted, UHT and acidified gel systems. Each of these systems employs different heating and mixing regimes, as well as additional processing steps such as pH modification, that are bound to give rise to different mechanisms of interactions between the components.

The author believes that a standardised experiment protocol is a sorely needed, and should include choice of raw material, methods of sampling, sample preparation and handling, techniques of measurement, and reporting of time-shear-temperature history of the samples as well as the composition of key milk components. This would allow international results to be compared, and collaborative work can be set up around the world in order to gain a clear understanding into the field of concentrate rheology.

None the less, the results published so far revealed several important findings:

1. An increase in solids content results in an increase in viscosity and rate of age thickening
2. Temperature has a complex interaction with the rheological behaviour
3. Below 60-65°C, an increase in temperature would lower the viscosity of milk concentrate systems due to the decrease in the viscosity of the aqueous phase
4. Above this critical region, an increase in temperature results in an increase in viscosity and tendency to age thicken
5. Preheat treatment tends to increase the viscosity of milk concentrate, but also increases HCT (more heat stable products)
6. The effect of preheat treatment was found to depend on solids content. No clear correlation was established between the effect of heat treatment on diluted and concentrated milks

7. pH affects the heat stability of the system through the modification of the electrical charge on ionic components
8. Variations in composition play an important part in the determining of rheological behaviour
9. The combined effect of seasonal variation and stage of lactation needs to be considered
10. Variation in several key compositional components has a significant effect on the viscosity and HCT of milk systems, particularly urea and whey proteins
11. The interaction of denatured  $\beta$ -lactoglobulin and  $\kappa$ -casein has been identified as a potential pathway for age thickening
12. Fat and its globule membrane play a significant role in the determination of rheological behaviour. This relates to the reactivity of the newly formed globule membrane after the original membrane is damaged, e.g. by homogenization
13. Evidence of a fat-casein network has been detected during age thickening

## 2.2 Recombination

This section lists the main findings of the literature survey on recombination that are relevant to this thesis.

The (IDF) definitions for recombined and reconstituted products are as follows:

- A recombined product is the milk product resulting from the combining of milk fat and milk solids-non-fat in one or more of their various forms with or without water. This combination must be made so as to re-establish the product's specified fat to solids-non-fat ratio and solids to water ratio.
- A reconstituted product is the milk product resulting from the addition of water to the dried or condensed form of product in the amount necessary to re-establish the specified water solids ratio (Kieseker, 1981).

### **2.2.1 Raw Ingredients**

Raw ingredients used in recombination and reconstitution can be divided into several main groups: milk powder, anhydrous milk fat, vegetable oils, additives and water. In the production of recombined milk and other milk products, the quality of the raw materials is the main factor determining that of the final products. It is important to have a strict quality control program to monitor the quality of the incoming raw ingredients. Apart from the usual physical, chemical and microbiological quality specifications generally used for these materials, some special properties are required, depending on the type of final product (Gunnis, 1980; Kieseker, 1981; Sjollem, 1988).

### **2.2.2 Recombining technology**

The difficulties encountered with reconstituting whole milk powder in ordinary and cold water may be listed as follows:

- Rate of dispersion
- Loss of solubility with the age of the powder
- The formation of foam and scum on the surface of the milk
- The adhesion of undispersed powder particles to the container wall
- The formation of distinct layers at the top and bottom of the container after several hours in a refrigerator
- A stale flavour due to the reconstituted powder (Al-Tahiri, 1987)

The choice of water temperature affects the hydration time (Sanderson, 1980). A temperature of 40-50°C would only require a hydration time of 10-15 minutes (Sanderson, 1980). Temperature also has an effect on the wettability and dispersibility of the powder (Lascelles & Baldwin, 1976; Jensen & Nielsen, 1982; Al-Tahiri, 1987). The temperature range of 40-50°C is commonly employed during mixing of powder with

water (Lawrence, Muller, & Rogers, 1963; Kiesecker & Southby, 1965; Kiesecker, Clarke, & Aitken, 1984; van Mil & deKoning, 1992).

### **2.2.3 Equipment**

Recombination involves the mixing of dry ingredients with water in appropriate proportions, before further treatment with processes such as filtering, homogenizing, pasteurizing and sterilizing. The processes following mixing may be operated continuously but mixing is commonly a batch process. Good dispersion is achieved through high shear mixing in the mixing tank. The maintenance of a vortex is imperative to ensure good suction of the powder into the fluid and achieve good dispersion (Fitzpatrick et al., 2001).

The type of mixer used in the mixing vessel affects the degree of dispersion of the dry ingredients, which depends on the concentration and viscosity of the solution, as well as the batch size. A propeller or turbine mixer is adequate for small batches and a low viscous system. At higher mix concentrations and viscosity, a greater mechanical force is required to ensure the complete dispersion of the dry ingredients (Sanderson, 1980). The Cowles mixer is suitable to deal with high total solids content solutions (Newstead, 1980; Sanderson, 1980).

## **2.3 Conclusion of literature review**

Milk powder is the biggest export product from Fonterra, contributing to nearly 25% of the total revenue. During the production of milk powder, the rheological behaviour, particularly the apparent viscosity, of the fresh milk concentrates after evaporation affects the physical and functional properties of the end powder product, and thus restricts the plant operating efficiency. It is desirable to characterise and understand the interactions between the rheological behaviour of the fresh milk concentrate system with operating conditions, as well as the physical and functional properties of the end powder.

Milk concentrate systems tend to show time-dependent rheological behaviour, where the shear stress changes with time at a constant shear rate. At rest, the increase in viscosity with storage time is commonly known as age thickening. Some authors have argued that some structural changes in milk during age thickening concentrates may be irreversible.

Rheometry and data analysis techniques for the study of time-dependent rheology are well developed for systems where structural changes are fully reversible. Models can even account for inter-particle forces, as well as structural re-arrangement during breakdown and build-up.

Rheological study on dairy systems, on the other hand, has been restricted to basic techniques. For example, the use of single point measurement has been widely applied for quality assurance purposes to systems that are really non-Newtonian. Such tests do not offer any useful insight in to the rheological behaviour of the milk system.

More comprehensive tests to investigate the time-dependent nature of the milk systems are often limited to the study of breakdown under constant shear rate. Model fitting has been carried out to describe the changes in the apparent viscosity, as well as the structure and its rate of change, with time. However, these data do not provide useful information on the age thickening process where structural build-up takes place at rest.

There are only a few authors who have attempted to measure the rheological behaviour of fresh milk concentrates during age thickening. The techniques for sample preparation, measurement and data analysis are still inadequate and require significant improvement. The issue of reproducibility needs to be resolved promptly to ensure good agreement in trends between future published works from different authors. Failure to do so would create confusion to an already difficult field of study.

The present work attempts to provide the next building block by developing new experimental tools to allow the collection of more comprehensive data to describe the age thickening phenomenon.

---

# **CHAPTER 3**

# **MATERIALS**

# **AND METHODS**

---

## CHAPTER 3: MATERIALS AND METHODS

### 3.1 Introduction

The study of the time-dependent rheology of food systems is difficult because the rheological properties are a function of the system's evolving structure, which depends on many factors.

An adequate description of time-dependent foods requires the determination of the breakdown coefficient and the build up coefficient of the structure, (Cheng, 1987, 2003; Barnes, 1997). Various authors have attempted to develop suitable methodologies for experimental measurements of these coefficients. However, these are still approximate, and based on the assumption of a fully reversible structure.

It was decided in this work to focus on the reproducible measurement of one aspect of the rheology, the build-up of the food structure. This is relevant to the topic at hand, as age thickening mainly involves the structural build up process, and the phenomenon is important in many time-dependent dairy products.

In fluid systems where some of the structural changes are irreversible, such as milk concentrates, protocols for sample preparation described in the current literature do not overcome the problem of replication. The difficulty is in controlling and achieving identical shear/temperature histories for the replicate samples, particularly in the case of milks reconstituted from powders.

Thus, the first task in this project was to design a recombination system, which would ensure repeatable replicate rheological profiles and hence structures. This was achieved by using the principle of an equilibrium structure at high (ideally infinite) shear rates where the structure is effectively broken down into its individual elements (Moore, 1959). This design essentially removes the effect of any previous shear history on the time-dependent system. However, it is only possible by this approach to investigate the

rate of build-up of structure from an initial point of a fully broken down system. The method also allows comparison between different systems from a well defined common starting point on the structural-time scale for all age-thickening time-dependent structures.

The second task was to develop a suitable protocol for measuring the rheology of time dependent systems. Every step has an impact on the structure and its rate of change with time, including the simple introduction of a measuring probe into the sample. When a shear sweep is attempted, the structure begins changing after the first application of shear. Thus, subsequent data do not reflect the same initial structure but the evolving structure over the period of measurement (Barnes, 1997).

An ideal experiment would involve the preparation of, for example, a batch of 100 samples with identical initial rheological profiles. A single shear step experiment would be conducted on each sample, with a different increment in shear rate so that the sum of all 100 experiments would cover the desired range of shear rates, starting at a reference level. For example, the first sample would be subjected to a  $0-1 \text{ s}^{-1}$  shear step test, while the second sample would receive a  $0-2 \text{ s}^{-1}$  test, and so on, to cover a  $0-100 \text{ s}^{-1}$  range. Most importantly, all samples would need to be tested simultaneously on 100 identical rheometers, in an identical manner. Obviously, such an experiment is not practical in most situations.

During the development of a protocol for rheological measurement, it also became apparent that the current method of calibrating and characterizing the constant shear stress mode rheometer was not adequate, and a new method was investigated. This exercise was imperative to prevent the collection of misleading data.

Once these issues were resolved, industrial surveys were carried out to analyse the relationship between product composition, plant design and operating conditions, and the rheological properties of dairy products under various manufacturing conditions. The main problem associated with this exercise was the difficulty in monitoring the

processing conditions in the commercial plants which had a significant influence on the rheological behaviour of the milk concentrate. Another issue was the identification of the time at which a milk sample was withdrawn from the pipe line. Techniques were developed to address and overcome some of these issues.

The industrial surveys were carried out on fresh milk concentrates. In addition, milk powder samples were collected from the industrial runs where online samples had been monitored and then reconstituted and tested at Massey University in a more controlled environment with more accurate measuring instruments. This allowed for the comparison of rheological behaviour between fresh and reconstituted concentrates.

Data analysis must ensure that correct information is extracted from the collected data and no artifacts are introduced. Truncation and correction of the raw data must be carried out where applicable. For this work, modelling techniques were developed to summarise the vast amount of data gathered.

This chapter is divided into five sections as follows.

1. Design and commissioning of a reconstitution rig, and development of a reconstitution protocol
2. Rheological measurement protocol and rheometer characterisation
3. Objectives and methodology for industrial survey
4. Methodology for controlled experiments to analyse the effect of processing variables on rheology
5. Method of data analysis

## **3.2 Recombination Rig**

The complete rheological characterisation of a time-dependent system is time consuming and is not possible with in-line samples. For this reason, data collected from in-line sampling at industrial milk powder plants could only provide a partial picture of the rheological characteristics of the fresh milk system. Further testing of reconstituted milk concentrate systems made from powder taken from the same production run allowed a more rigorous definition of the rheological profile to be carried out. However, it was first necessary to establish that the trends between in-line and reconstituted samples were similar.

Reproducible reconstitution of milk powders thus became a crucial requirement for the progress of this work. The reported viscosity of reconstituted milk concentrates varies greatly between different authors, as discussed in section 2.1.5.

### **3.2.1 Principle of Design**

The main aim of the recombination rig design was to control the age-thickening process during recombination. The recombination process can involve mixing, shearing and heating steps. In previously published studies, these steps were not separated. When designing the recombination rig for this work, these key steps were separated so that high shear and heat treatment could be applied independently of the dissolution and hydration processes. A schematic layout of the recombination rig is shown in Figure 3.1.

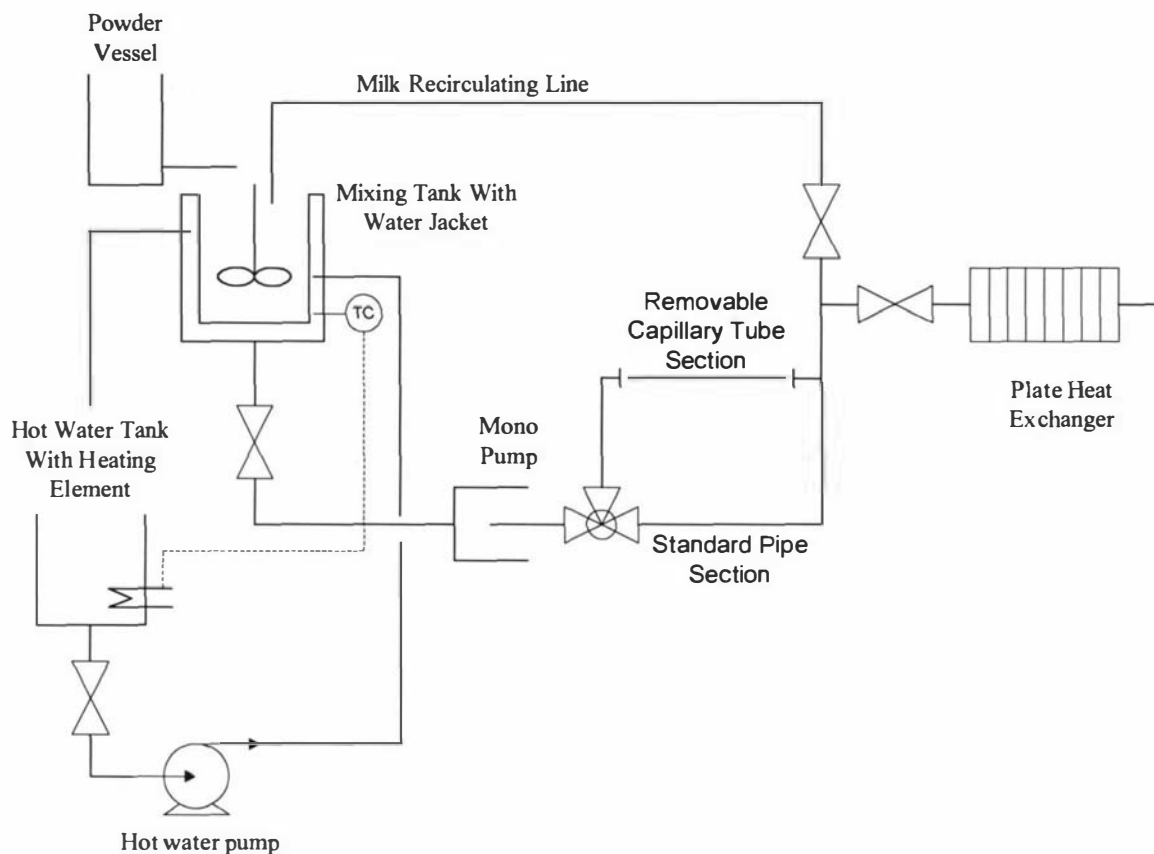


Figure 3.1: Schematic layout of the recombination rig

The milk powder was added to distilled water in the mixing tank (Figure 3.3) via a screw feed system (maximum 4kg/hour feed rate, Accurate Dry Material Feeders, Whitewater, USA) (Figure 3.2).

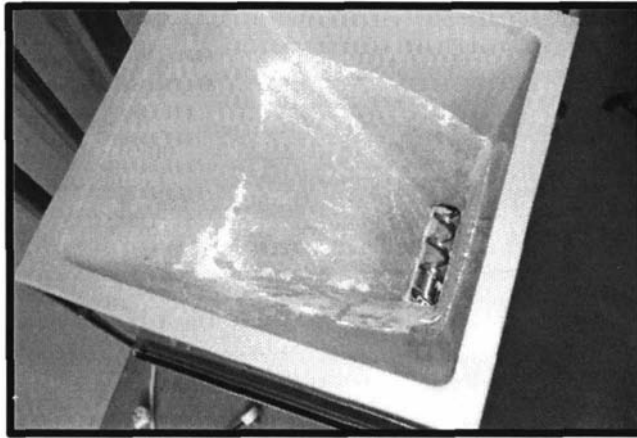


Figure 3.2: Accurate Dry Material Feeder.

The solution was mixed using a four-bladed propeller 20W mixer (model RW20.n, Werke GMBH & Co, Malaysia). A horizontal central baffle disc was attached to the impeller shaft above the propeller to prevent the formation of a vortex during high speed mixing, as shown in Figure 3.3.

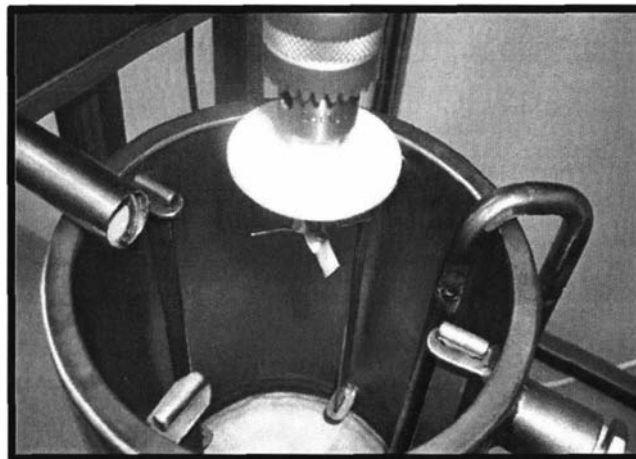


Figure 3.3: Mixing tank equipped with four baffles and a central baffle disc.

During mixing, the temperature of the milk was controlled using a water heating system connected to the water jacket of the mixing tank. The temperature was normally set at 35°C, as explained in section 3.2.2. The hot water system consisted of a 45L water tank equipped with a small heating element. A GCS300 temperature controller (Shinko North

America Ltd. Toronto, Canada) regulated the water temperature as desired. The hot water was circulated around the water jacket with a 3.5 m<sup>3</sup>/hour StarRS25/6 centrifugal pump (Wilo AG, Germany).



Figure 3.4: Powder mixing system

At all times, the concentrate solution was recirculated through a piping network, via a removable capillary tube section using a 0.5 kW mono pump (Mono Pump NZ Ltd, New Zealand), as shown in Figure 3.5. The pump speed was controlled by a Picodrive AC Motor Speed Controller (PDL Electronics LTd, New Zealand). Capillary tubes of different diameters were used to apply different nominal shear rates up to 40,000 s<sup>-1</sup>. While the application of an infinite shear rate would be ideal, a shear rate in the upper Newtonian region was considered sufficient to ensure complete breakdown of the structure to its fundamental elements.

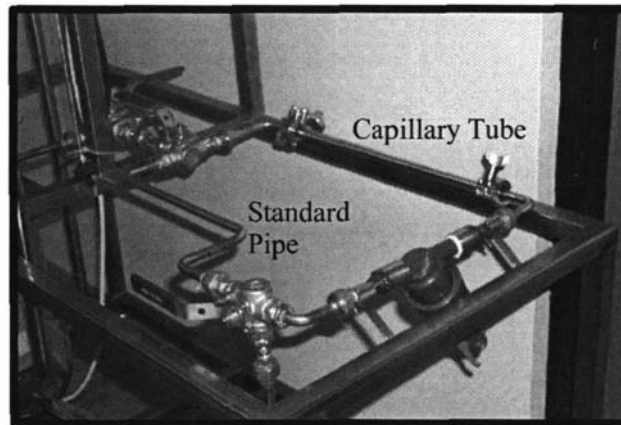


Figure 3.5: Capillary tubes system

After recirculation at high shear for a defined period of hydration, the recombined product was pumped to a plate heat exchanger (Alfa-Lava, P20-HB, Sweden) with short residence time, where it was heated or cooled to the desired temperature, independently of the mixing and recirculation temperature.

### 3.2.2 Commissioning experiments

Experimental results are not usually reported within the materials and methods chapter. However, the commissioning experiments presented here were not part of the rheological experiments in this body of work. The rig commissioning exercise is required to ensure that the equipment built has satisfied adequately the objectives of the design. Without this validation, and the results of the commissioning experiments, the reader would have difficulty understanding the rationale of the recombination protocol presented later in this chapter.

#### 3.2.2.1 Viscosity data during recombination

In experiment A1, a medium heat whole milk powder was reconstituted to a total solids content of 47%TS at a water temperature of 35°C using the recombination rig. At all times, the sample was recirculated via the capillary section at a nominal shear rate of

$40,000\text{ s}^{-1}$ . Once all the powder had been added, milk samples were taken from the rig every 15 minutes and subjected to a shear sweep test at  $35^{\circ}\text{C}$  using the Paar Physica MC1 described in more detail in section 3.3. The shear sweep curve at time zero, just after the completion of mixing, is shown in Figure 3.6.

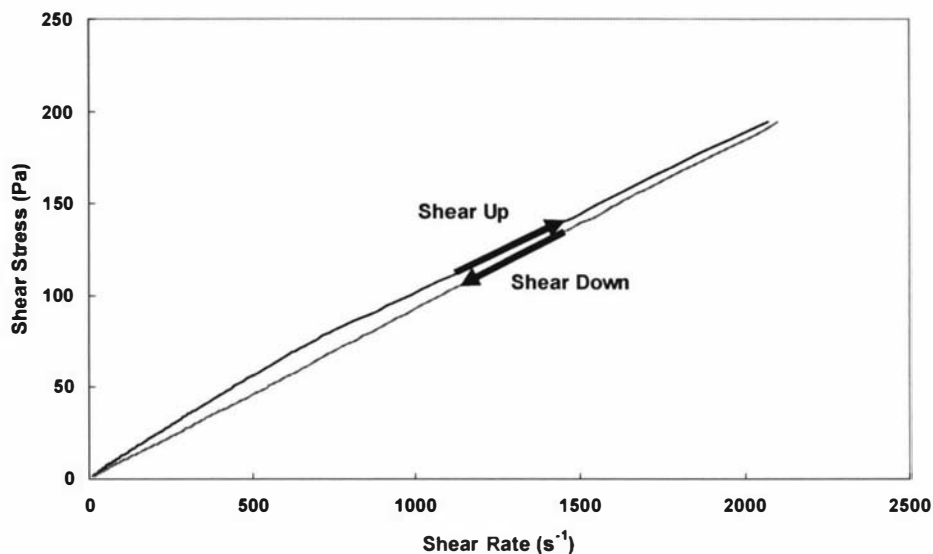


Figure 3.6: Shear sweep curve for a 47%TS reconstituted sample of medium heat whole powder just after complete mixing. Experiment A1, Paar Physica MC1, Z2.1, CSS,  $35^{\circ}\text{C}$ .

The shear down curve is lower than the shear up curve, indicating thixotropic behaviour. This means that immediately after the completion of mixing, the milk concentrate at 47%TS was already displaying time-dependent rheological behaviour. It is important to note that this thixotropic behaviour was observed during measurement in the Paar Physica MC1. Upon withdrawal from the rig, the sample would have experienced a change from the high shear in the capillary section to a lower shear in the sample container for a short time while being moved to the rheometer. Structural recovery would have taken place, and may have given rise to the thixotropic behaviour. Thus it is important to measure the samples as quickly as possible.

The viscosity at one chosen shear stress, 105.3 Pa, was calculated for each sample during recirculation. The exercise was also repeated in experiment A2 where the powder was

reconstituted to 45.8 %TS. The apparent viscosities at 105.3 Pa against recirculation time for two batches of samples at 47.1%TS and 45.8%TS are plotted in Figure 3.7. Conventionally, the apparent viscosity is quoted as a function of shear rate, and not of shear stress. However, this rheometer was operated in controlled shear stress mode and for each applied shear stress, the measured shear rate will be different for different fluids. Figure 3.7 also shows the replicate data at both concentrations.

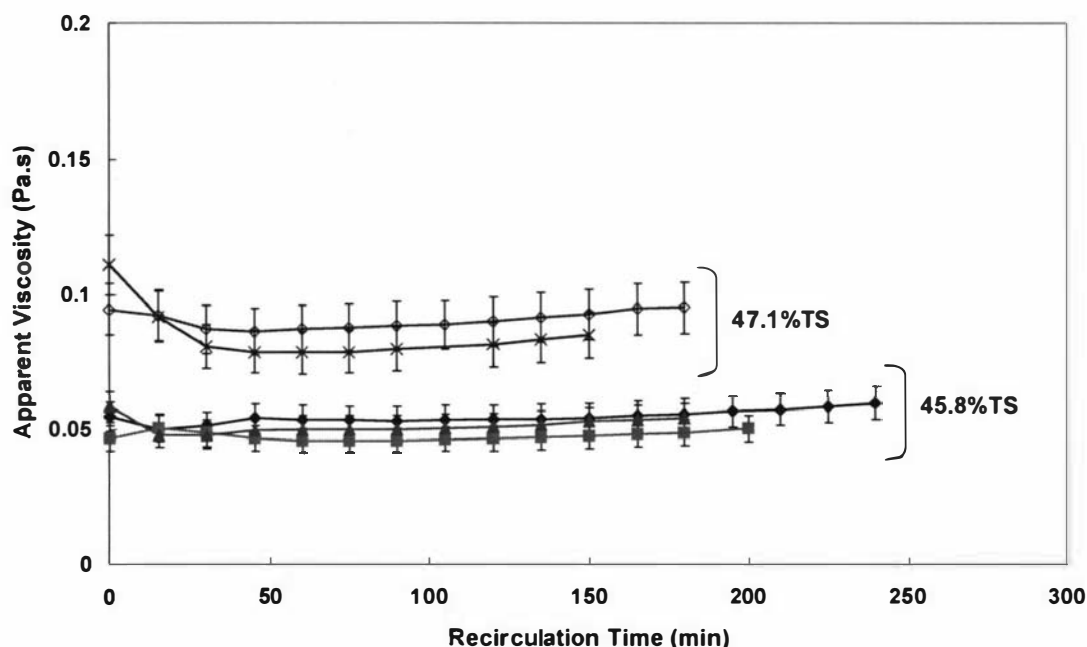


Figure 3.7: Viscosity at 105.3 Pa against recirculation time for reconstituted samples of medium whole milk powder at 47.1 %TS (A1) and 45.8 %TS (A2). Paar Physica MC1, Z2.1, CSS, 35 °C.

For both curves, the viscosity during recirculation decreased during the first 30-45 minutes of recirculation. The viscosity curve then levelled out temporarily before showing a small steady increase with time. The average percentage increase in apparent viscosity between the storage period of 60-150 minutes was similar at the two concentration levels, with 9% increase at 45.8%TS and 8.5% at 47.1%TS. However, the absolute increase in apparent viscosity was higher at 47.1%TS.

The replicate error from 60 minutes of storage time onwards was simply determined as the biggest difference between the averaged data and either the largest or the smallest data point in the replicate series. This difference was expressed as a percentage of the average value. This method would yield very large error if there were any extreme outliers in the results. However, such a case was not observed in any sets of data. The error range is essentially the maximum error one can expect from the replicate experiments. Analysis of variance would yield a lower error range as this technique would consider the variation of the entire set of data about the mean. Nonetheless, the technique used provided an adequate description of the error of repeatability. It was found that in the vast majority of experiments, the error of repeatability was less than 10% between replicate sets of data. Thus, an assumed 10% repeatability error was imposed on the rest of the data.

The original decrease in viscosity with recirculation time was attributed to the gradual escape of air bubbles from the milk concentrates. The presence of these bubbles was shown by quickly gelling the fresh milk samples with agar and observing with a light transmission microscope. The central baffle attached to the impeller axle reduced the amount of air inclusion during recombining by inhibiting the vortex but did not eliminate it completely.

It is unlikely that the initial decrease in viscosity could be attributed to break down in structure, which would only occur when the fluid is moved from a low shear to a high shear region. This is because the reconstituted solution was recirculated via the high shear capillary tube section at  $40,000 \text{ s}^{-1}$  throughout the mixing process before being taken to storage at rest.

### **3.2.2.2 Viscosity data during storage at 65°C**

Heating of milk concentrates to 65°C is an important processing step during milk powder manufacture. A study of the flow behaviour under these conditions is beneficial to the

understanding of the relationship between processing conditions, rheological properties and product functionality.

In experiment A3, the same batch of powder (that was used in experiment A2) was used to make a 48%TS reconstituted solution. Milk samples were withdrawn after recirculating at 35°C in the rig for 30, 45, 60 and 75 minutes, and then were heated to 65°C using a plate heat exchanger. The samples were then stored at rest in a water bath at 65°C, and tested every hour using the Paar Physica MC1. Figure 3.8 shows the change in viscosity during the shear up test at the shear stress of 105.3 Pa with time.

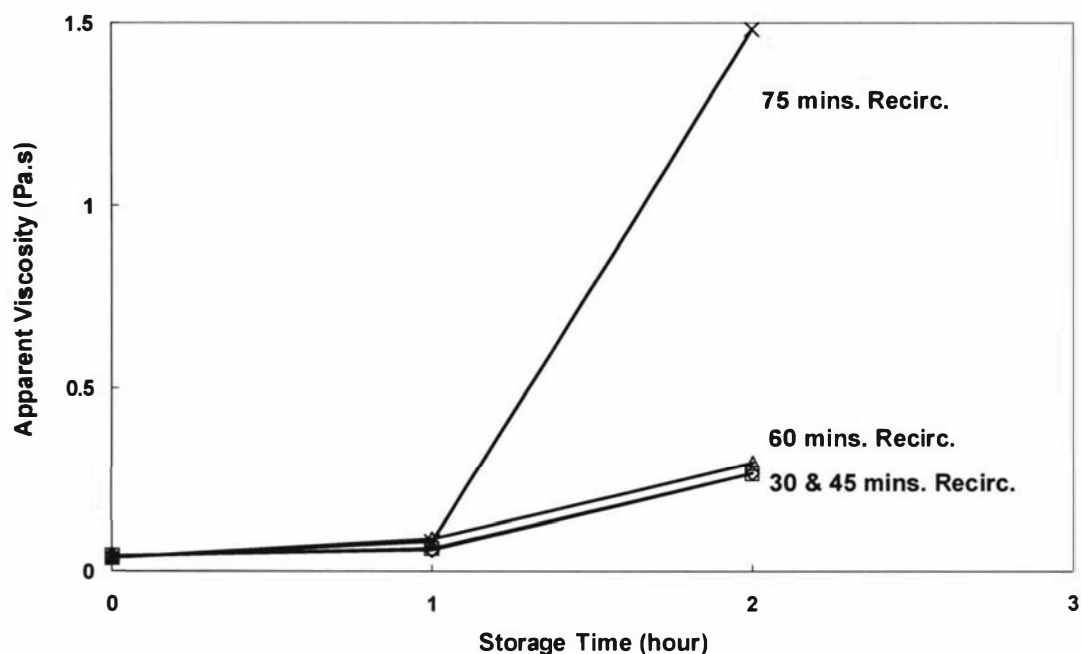


Figure 3.8: Effect of recirculation time at 35°C on the viscosity during storage for a heated reconstituted whole milk concentrate solution. Experiment A3, Paar Physica MC1, Z2.1, CSS, 48%TS, 65°C.

Figure 3.8 shows that the rates of age thickening for the two samples taken after 30 and 45 minutes recirculation were similar, within a 5% error. The curve for the 60 minutes recirculation showed a slightly higher rate of increase in viscosity in comparison with the

30 and the 45 minutes recirculation curves. The 75 minutes curve showed a dramatic increase in viscosity over two hours storage at 65°C.

The initial viscosity values after sampling for the four curves were similar, within 7% error. This indicated that there was no appreciable age thickening during recirculation in the rig but clearly the tendency to age thicken had changed. Thus measurement of the initial viscosity alone, as often reported in recombination publications, does not fully characterize the rheological profile of the recombined products, which are time-dependent.

### **3.2.2.3 Effect of bacteria**

After each run, the recombination rig was cleaned with a cleaning-in-place (CIP) cycle of water rinse, 1% (v/v) sodium hydroxide caustic wash, hot water rinse, 1% (v/v) nitric acid wash and finished with another hot water rinse. Both the caustic and acid washes involved recirculating each chemical around the system for at least 30 minutes..CIP cycles in this order are commonly carried out in the industry. The slight increase in in-line viscosity after 45 minutes of recirculation (Figure 3.7) could very well be due to enzymatic action from bacterial contamination. In experiment A4, a plate count of mesophilic bacteria was carried out before and during a recombination experiment (47%TS) to study this possibility. The results are shown in Table 3.1.

Table 3.1: Mesophilic bacteria count during a recombination experiment A4.

Test	Description	Mesophilic Count (cfu/mL)
Distilled water	Obtained from the tap	0
Rig count	Distilled water passed through the rig	5,100,000
Milk solution 0 hr		2,360,000
Milk solution 1 hr		1,870,000
Milk solution 2 hr		1,990,000
Milk solution 3 hr		2,020,000

The results show a high level of contamination in the rig prior to recombination. The growth of mesophilic bacteria count is expected due to the suitable temperature of 35°C during recombination (Spreer, 1998; Robinson & Itsaranuwat, 2002).

In run A5, the rig was carefully cleaned with caustic and acid solutions immediately before recombination. Sodium azide (0.1g/100g) was added to the milk solution during recombination to control bacterial growth (Anema & Klostermeyer, 1996; Anema, 1998). Thermophilic and mesophilic bacterial counts were taken during both the pre-cleaning CIP and the recombination run. The results are tabulated in Table 3.2.

The bacterial count for the un-cleaned rig was four times higher than that obtained from experiment A4 in Table 3.1. This result confirmed bacterial regrowth between CIP runs. The higher initial bacterial count in this run was probably because this particular experiment was conducted after a four day break, rather than a one day break between runs as in table 3.1. These results show that bacterial regrowth during equipment storage between breaks is a significant hazard, probably because of incomplete drying out of the plant. Thus, the plant must always be cleaned immediately before a recombination run. In this plant all piping was drained after each CIP. However, the water hold up inside the mono pump could not be removed without damaging the pump that must not run dry. The results in Table 3.2 show that the addition of sodium azide did not significantly reduce the number of bacteria in the milk concentrate solution.

Table 3.2: Effect of cleaning and addition of sodium azide on bacterial count during a recombination experiment A5.

Test	Description	Mesophilic Count (cfu/mL)	Thermophilic Count (cfu/mL)
Plant before recombination	Distilled water was flushed through the rig before recleaning	2,000,000	100,000
Caustic cycle	Recirculation of 60 mL of 50% sodium hydroxide in 5L of distilled water	1,330	10
Hot water rinse	Hot water at 80°C	-	-
Acid	Recirculation of 60 mL of 68% nitric acid in 5L of distilled water	0	0
Hot water rinse	Hot water at 80°C	89	-
Milk solution	Without sodium azide	32,000	10,000
Milk solution 0 hour	5.23 g of sodium azide was added per litre of reconstituted milk concentrates	24,500	100
Milk solution 1 hour		26,800	100
Milk solution 2 hour		26,400	1000

Recontamination of previously CIPed equipment by biofilm is possible, and a “quick acid or hot water flush just before beginning of the production run will restore the hygienic quality of the plant” (Trinh, 2003). Further experimental runs, A6 (45.1%TS), A7 (46.5%TS), A8(47%TS) were conducted following an improved hygiene protocol, where the rig was cleaned with caustic and acid before the runs and sodium azide was added to the reconstituted solutions. During recirculation, milk samples were taken from the rig and the viscosity was measured.

Figure 3.9 shows the change in viscosity with time during 120 minutes of recirculation at 35°C for experiments A6-A8. In the figure, all three curves showed an initial decrease in viscosity as expected and attributed to the escape of entrapped air bubbles.

After the initial drop, the viscosity values of the three curves remained constant with time. Thus, the addition of sodium azide and thorough cleaning of the rig immediately before reconstitution appeared to have eliminated age thickening during recirculation.

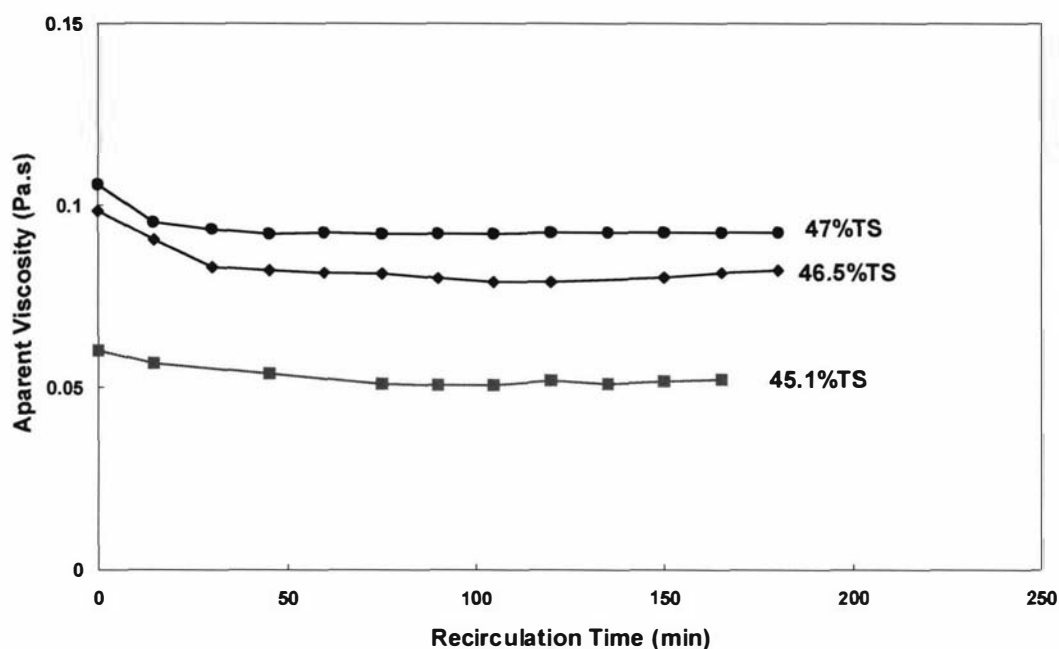


Figure 3.9: Change in in-line viscosity with recirculation time at 35°C for three reconstituted solutions at three concentrations, 45.1%TS (A6), 46.5%TS (A7), 47%TS (A8). Paar Physica MC1, Z2.1, CSS, 35°C.

Another run, experiment A9, was performed in the rig under the new hygiene protocol with a concentrate solution of 47.5%TS. After recirculation for 30, 45, 60 and 75 minutes through the capillary section at  $40,000\text{ s}^{-1}$  and 35°C, the solution was heated to 65°C in the plate heat exchanger. The samples were stored in a water bath at 65°C and the rheological flow curves measured at hourly intervals. The results are shown in Figure 3.10.

All four curves showed good agreement with one another. The initial viscosity values for the four curves in Figure 3.10 showed a 1% error, which is significantly smaller than the 7% error observed in Figure 3.8, indicating little or no age thickening in the system during recirculation.

It is interesting to note that the 45 minutes recirculation curve was situated slightly higher than the 60 and 75 minutes curves. Thus, after 45 minutes of recirculation, air bubbles may have continued to escape. The error between the 45, 60 and 75 minutes curves was within 10%. The good agreement between the 30, 45, 60 and 75 minutes curves suggested that both the initial viscosity value and the tendency to age thicken were identical for the samples taken after 30, 45, 60 and 75 minutes recirculation. In other words, if two samples were taken from the rig between 30-75 minutes of recirculation, they will have the same rheological profile.

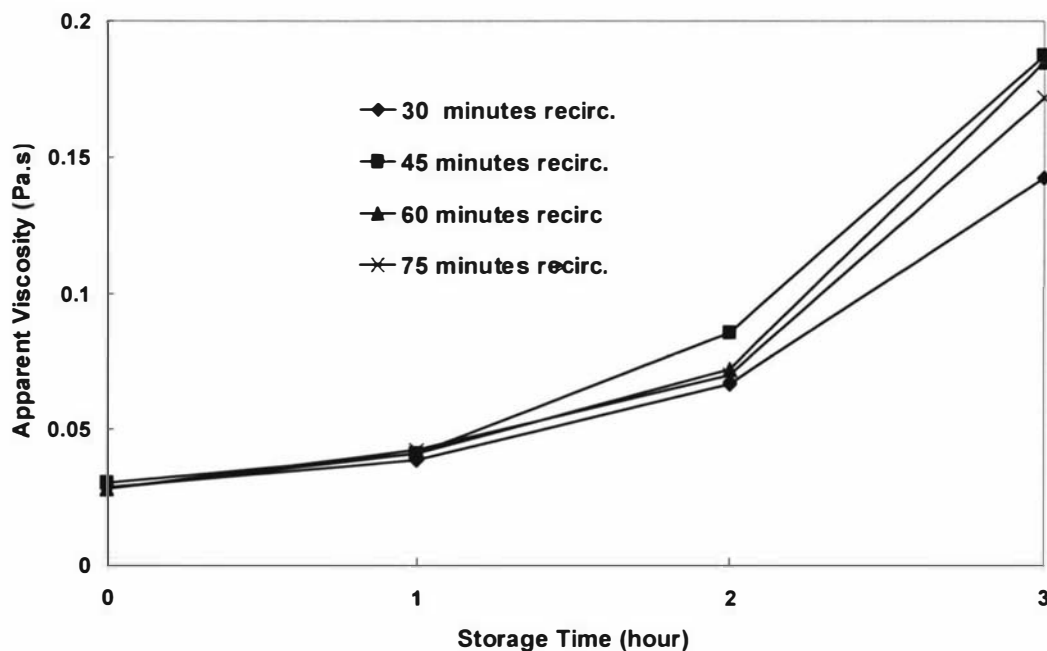


Figure 3.10: Effect of recirculation time at 35°C on the viscosity during storage for heated reconstituted whole milk concentrates. Experiment A9, Paar Physica MC1, Z2.1, CSS, 47.5%TS, 65°C.

#### **3.2.2.4 Replicate error**

Many runs were conducted to check the repeatability error of 10%. It is important to point out that this error represents the repeatability of measurements of age thickening, i.e. both the initial viscosity as well as its rate of change with storage time. Replicate experiments were conducted in runs A10-A31 which confirmed the 10% error. In heating and storage runs, the rates of change in apparent viscosity were similar between the replicate samples. For example in runs A30-A31 with powder B concentrates at 50%TS, even the gelling times were similar between two replicate samples after 10 hours of storage at 75°C.

#### **3.2.3 Recombination protocol**

The recombination rig and any plate heat exchangers (PHE) to be used in a trial received CIP treatment before any experiment was conducted. Hot water of 80°C was used for all wash cycles. Maximum flow rate achievable of 80 L/hour was used at all times. The rig and PHEs were first rinsed with hot water, followed by a caustic wash where 100mL of 50% caustic soda (Orica Chemnet, New Zealand) was added to hot water to achieve 1% v/v concentration. After 30 minutes, the equipment was rinsed with hot water before receiving an acid wash at 1% concentration using 68% nitric acid (Orica Chemnet, New Zealand) for 30 minutes. A final rinse with hot water was carried out to remove any traces of acid or caustic solutions in the equipment.

Distilled water was added to the rig, and recirculated throughout the piping network to remove any entrapped air in the system. Distilled water and powder were weighed to achieve the desired solids content. Powder was added via the Accurate Dry Materials Feeder and mixed with the water. Throughout the mixing process, the solutions were constantly being recirculated via the capillary tube section at the maximum flow rate of 80 L/hour, unless otherwise stated. The jacket water temperature was set at the desired value.

During mixing, it was important to ensure that no excess movement of water surface took place to minimize the inclusion of air into the milk systems. This was achieved by manipulation of the mixing speed, the distance between the propeller and the surface, and the height of the central baffle disc on the propeller shaft. Addition of powder was done with care to prevent formation of powder lumps if the rate of powder feed was faster than the rate of powder dissolution.

Sodium azide (0.01% w/v) was added to the reconstituted milk concentrate to prevent bacterial growth (Fairise & Cayot, 1999; Anema & Li, 2003, Vasbinder, Alting, Visschers, & de Kruif, 2003).

After mixing, the reconstituted milk concentrates could either be withdrawn from the rig directly, or be pumped to one or several plate heat exchangers for heating or cooling.

Once the experiment was terminated, the rig and the PHEs received a second CIP treatment to remove traces of milk solutions. The procedures were similar to the pre-experiment CIP cycles listed above. Upon completion, water inside the rig was flushed out, and the rig was shut down with the emergency stop button.

### **3.3 Performance Characterisation of the Paar Physica MC1**

The Paar Physica MC1 rheometer (Anton Paar, Graz, Austria) was used in all controlled experiments at Massey University. When appropriate and available, the rheometer was also used in industrial surveys.

The rheometer is a rotational controlled shear stress and creep rheometer (Physica Messtechnik, 1993). The rheometer uses a ball bearing system. Temperature control is achieved with the use of a Julabo F25 water bath (Julabo Labortechnik, GbmH, Germany), which is connected to the water jacket of the chamber where the spindle and the cup are inserted. Measurements were controlled using the Rheosolve v2.11 software

which was later upgraded to version 3.08. The software upgrade, which occurred mid way through the project, did not affect the accuracy and precision of the instrument.

There are three modes of measurements available, controlled shear rate (CSR), controlled shear stress (CSS) and creep mode. The creep mode was not used in this work. In the CSS mode, a torque is set and the shear rate is measured. The system supplies a current to the motor to achieve a desired torque through a current torque transducer. The natural mode of operation of the Paar Physica MC1 is the CSS mode. In order to achieve the CSR mode, the desired shear rate is set, but the rheometer then applies a current to the current torque transducer, measures the corresponding shear rate, and compares it to the set point through a control loop until the desired shear rate is achieved.

A number of spindle geometries were supplied with the MC1. Most were of a cup and bob design (Z2.1 and Z3), but the most sensitive spindle, Z1, is a double gap concentric cylinder design, suitable for products with low viscosity values. The operating conditions of the Paar Physica MC1 and the dimensions of the spindles as specified by the manufacturer are listed in Tables 3.3 and 3.4 respectively.

Table 3.3: Background data on the Paar Physica MC1 (quoted from Physica Messtechnik GmbH, 1993)

Accuracy	+ 1% of maximum value or + 1 digit
Torque range (mains power)	0.05 to 50 mNm
Torque resolution	0.01 mNm
Speed range	0.3 to 1200 min <sup>-1</sup>
Angle range	0.8 mrad
Shear rate range (dependent on the temperature control system used)	0.9 to 4000 s <sup>-1</sup>
Shear stress range (dependent on the temperature control system used) (mains power)	0.7 to 34,000 Pa
Viscosity range (dependent on the temperature control system used) (mains power)	1 mPa.s to 3000 Pa.s

Table 3.4: Dimensions for several spindle geometries for the Paar Physica MC1 (Physica Messtechnik GmbH, 1993)

	Z1	Z2.1	Z3
Shear rate range ( $s^{-1}$ )	0-4031	Not available	0-1032
Shear stress range (Pa)	0-67	Not available	0-1141
Viscosity range (Pa.s)	0.001-1.3	Not available	0.118-100
Sample volume (mL)	22.5	69.76	17
Bob Radius (mm)	Not available	23.9	12.5
Cup Radius (mm)	Not available	24.4	13.56
Ratio of radii	1.021	1.0209	1.0847
Inner bob radius (mm)	22.75	Not available	Not available
Outer bob radius (mm)	23.5	Not available	Not available
Inner cup radius (mm)	22.25	Not available	Not available
Outer cup radius (mm)	24	Not available	Not available



Figure 3.11: Paar Physica MC1 and Julabo water bath



Figure 3.12: Paar Physica MC1 spindles Z2,1 (left bob and cup) and Z3 (right bob and cup)

Conventionally, Newtonian oils with known viscosity have been used to calibrate a wide range of rheometers (Lewis et al., 1994; Shi & NapierMunn, 1996; Shorey et al., 1999; Ascanio et al., 2002; Houchin & Hanley, 2004). Obviously, measurement of any given Newtonian oil should yield a constant viscosity across any chosen shear rate range at a given temperature. Any deviation from a straight line would indicate performance weaknesses of the instrument.

A typical set of results could be displayed on a flow curve, where a best fit straight line could be drawn, as shown in Figure 3.13. The data came from a calibration experiment A32 with a S60 Cannon standard oil, which was standardised by the National Institute of Standards and Technology in America. Measurements were carried out at 20°C where the viscosity was expected to be 0.1425 Pa.s, according to the Cannon Instrument Company (USA). At first impression, the data could be correlated well with a straight line, with a correlation coefficient  $R^2$  of 1. The fitted straight line indicated Newtonian behaviour and the accuracy and reliability of the data were acceptable.

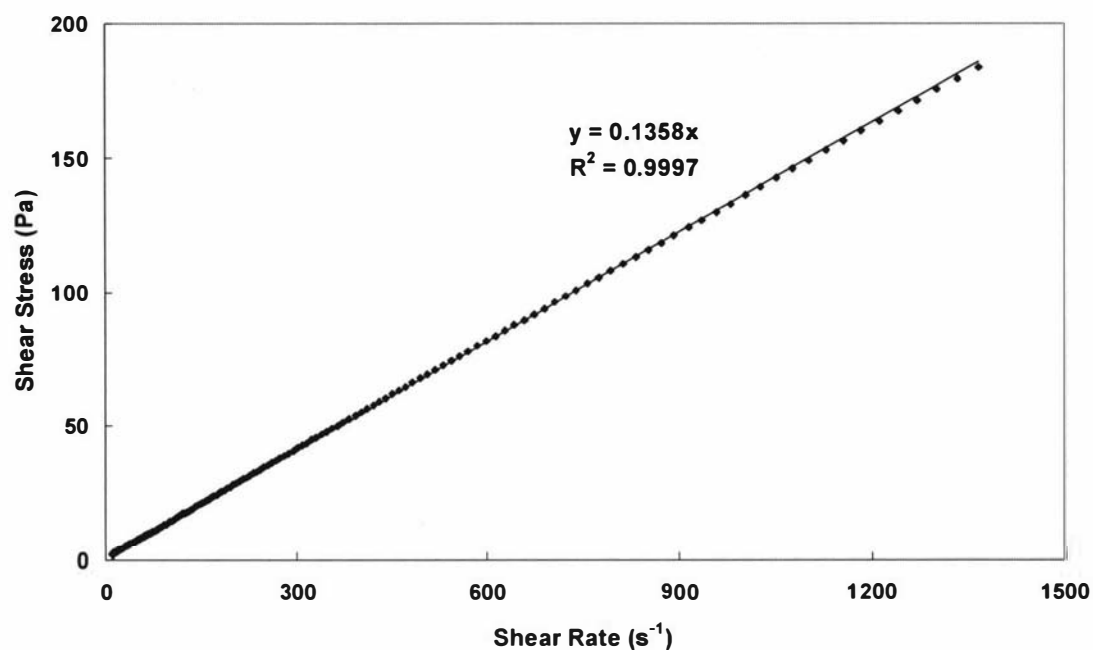


Figure 3.13: Flow curve of a S60 oil at 20°C using a Z2.1 spindle in CSS mode. Experiment A32.

However, when the same data was re-plotted as viscosity versus shear rate, new information emerged, as shown in Figure 3.14. The straight line shows the expected viscosity profile for the Newtonian solution. At low shear rates, the reported viscosity deviated significantly from the expected straight line, and at higher shear rates, the viscosity fell below the expected value. This introduced a false non-Newtonian artefact into the data.

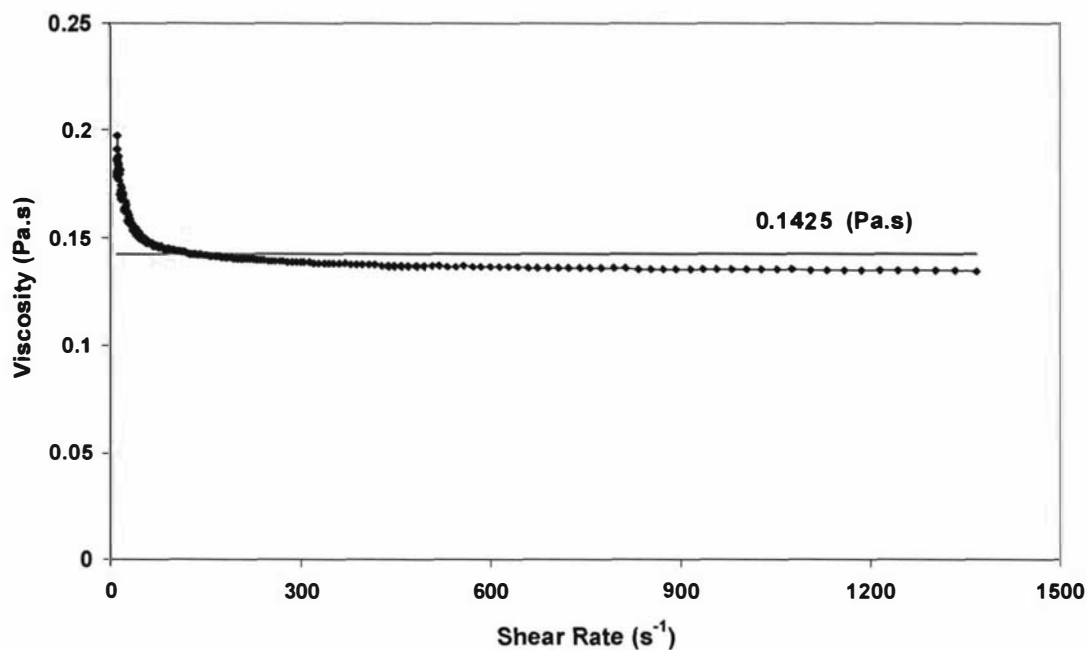


Figure 3.14: Viscosity against shear rate for an S60 oil at 20°C using a Z2.1 spindle in CSS mode. Experiment A32.

The calibration exercise revealed the presence of minimum reliable operating conditions, below which the accuracy of the collected data was severely jeopardised. Numerous experiments were conducted in both CSS and CSR modes and similar observations were made. Thus, the issues with non-linearity and reliable operating conditions were primarily caused by the design and operating mechanisms of the instrument, not by the mode of operation or the tested medium.

It was evident that new correction and calibration protocols had to be developed.

### 3.3.1 Minimum reliable operating spindle speed

The shear rate is related to the geometry of the spindle and the spindle speed. Thus, for a given spindle speed, the calculated shear rate at the bob surface will be different for different spindles. The same situation exists with measured torque and calculated shear

stress. Because torque and speed are the primary parameters measured in a rheometer, the performance of the MCI was analysed against spindle speed and torque rather than shear stress and shear rate.

The viscosity-temperature data given by the manufacturer of three Newtonian oil solutions are listed in Table 3.5. The viscosities for all standards are based on the National Institute of Standards and Technology value of 1.0016 mPa.s for water at 20°C. The S60 solution listed in Table 3.5 is different to that for which results are shown in Figures 3.13-3.14.

Table 3.5: Viscosity-temperature data for three Cannon Instrument Company's Newtonian standard oils (Cannon Instrument Company, USA).

Temp. (°C)	Viscosity (mPa.s)		
	S60	S200	S2000
20	138.4	586.4	8437
25	101.9	406.3	5324
37.78	51.14	177.7	1838
40	45.94	156	1552
50	29.42	79.9	659
70	9.98	21.38	112

In experiment A33-A36, the Canon S200 oil was subjected to shear sweep experiments at various temperatures using the Z1 spindle in CSR mode. According to Table 3.4, at 20°C, the viscosity value of 586.4 mPa.s lies well within the range of the Z1 spindle, as recommended by Paar Physica Ltd. The same data were plotted in Figure 3.15a and 3.15b below showing the effects of spindle speed and torque respectively in the two graphs.

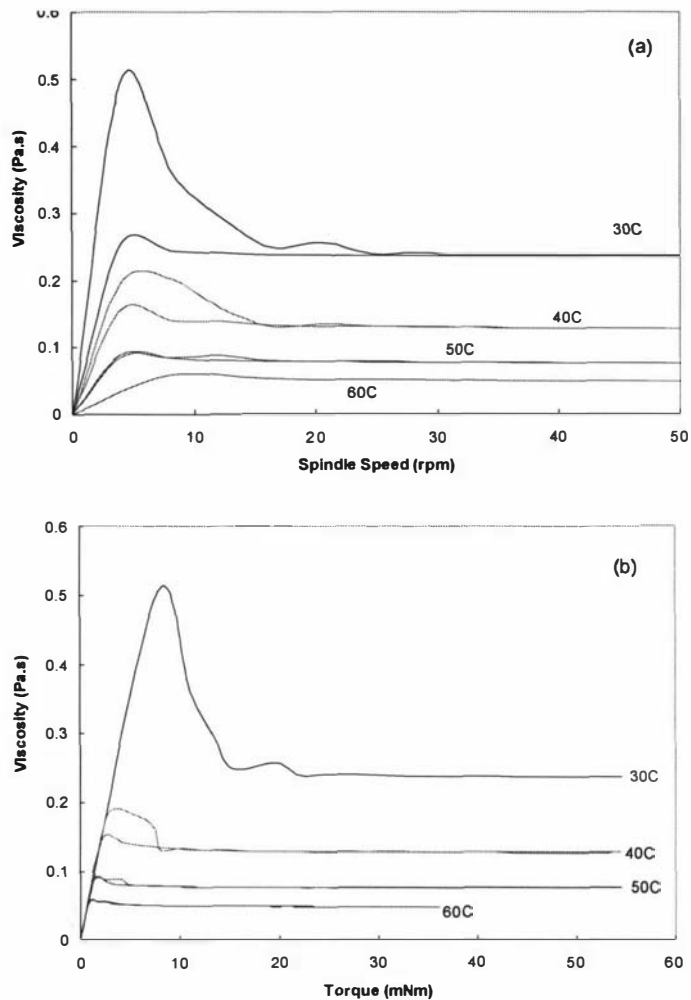


Figure 3.15: Shear sweep curves for S200 oil at several temperatures. (a) viscosity versus spindle speed, (b) viscosity versus torque. Experiment A33-A36, Paar Physica MC1, Z1, CSR.

The standard oil is a Newtonian fluid and the viscosity is theoretically a function of temperature only, not spindle speed (shear rate) or torque (shear stress). Hence all lines in Figures 3.15 (a) and (b) should be horizontal.

The curves in Figure 3.15 (a) and (b) departed from those expectations and exhibited some peculiar characteristics. The viscosity increased dramatically and overshoot the expected viscosity at low spindle speeds. The overshoot was more significant at lower

temperatures (higher viscosities). For all four temperatures, the curves levelled out at the same spindle speed, approximately 20 rpm, but at different torque values. The 30°C curve levelled out at 20+ mNm, in comparison with just 3 mNm for the 60°C curve.

The same S200 oil was subjected to a shear sweep (A37) and three shear step tests (A38-A40) at 40°C. In the shear step test, the spindle speed was held at a constant speed for 60 second intervals with data being collected at 3 second intervals before the speed was increased. Thus, the shear step test was essentially a shear sweep test, where each spindle speed was held for a longer time to collect more data points and to allow additional statistical analysis on the precision of measurement at each shear rate. However, the shear step test only involved the shearing up portion. The result is shown in Figure 3.16. The continuous line represents the shear sweep test data where the shear up and shear down curves are shown. The data points are the triplicate shear step test data. For each spindle speed, the data come from three replicate experiments.

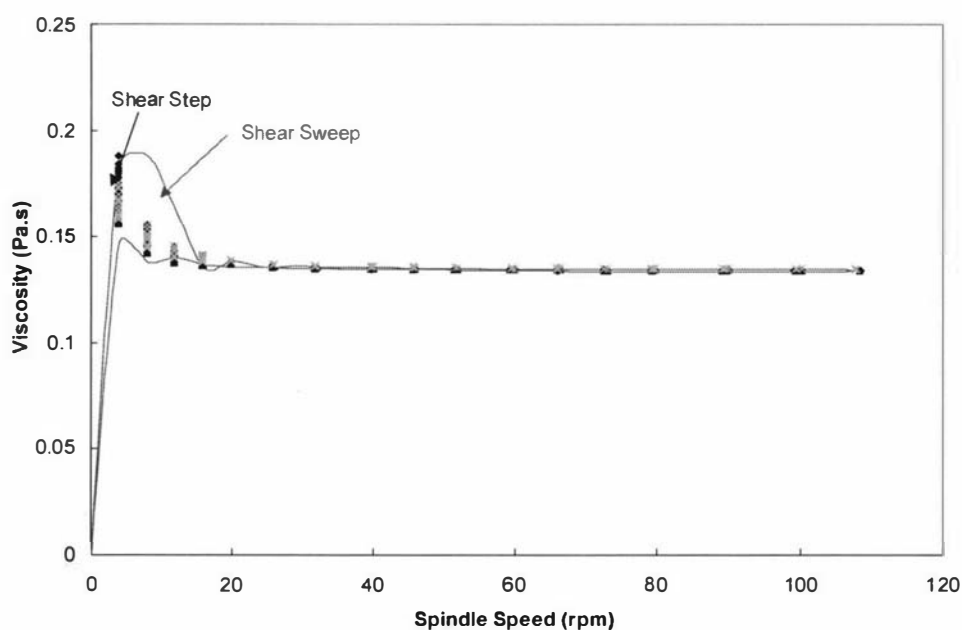


Figure 3.16: Comparison between shear sweep and shear step tests for S200 oil using the Z1 spindle at 40°C in CSR mode. Experiment A37-A40, Paar Physica MC1, Z1,

CSR. Solid line represents the data from a single shear sweep test. The data points represent the data from three replicate shear step tests.

In the three shear step tests (A38-A40), there was significant scatter in the data at low spindle speeds. The scatter quickly diminished and disappeared at 20 rpm and above. The presence and disappearance of the scatter also coincided with the overshoot in viscosity values in both the shear step and shear sweep tests.

The cause of the scatter in rheological data, particularly at low shear levels will be discussed in section 3.3.1.1.

The scatter in the shear step test could be calculated and normalised. The standard deviation,  $\sigma$ , and the average viscosity,  $\bar{\mu}$  were determined for each spindle speed. The coefficient of variation was calculated using equation 3.1.

$$\text{Coefficient of variation (COV)} = \frac{\sigma}{\bar{\mu}} \quad (3.1)$$

where  $\sigma$  is the standard deviation

$\bar{\mu}$  is the viscosity (Pa.s)

The COV for the S200 oil in experiments A41-44 at different temperatures were plotted against spindle speed shown in Figures 3.17.

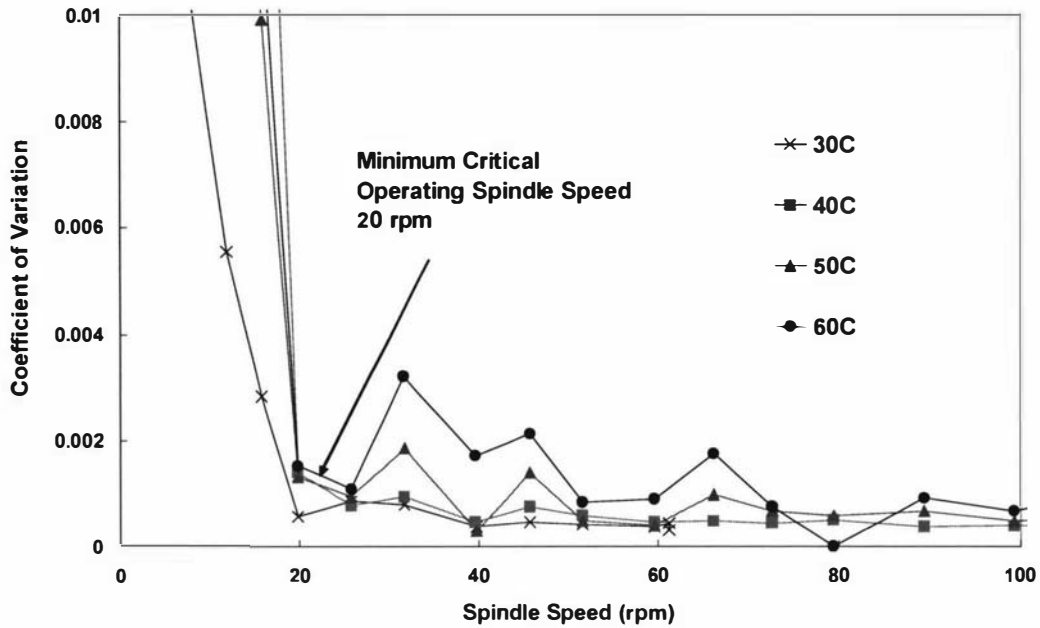


Figure 3.17: Coefficient of variation (COV) against spindle speed at different temperatures for S200 oil. Experiments A41-A44, Paar Physica MC1, Z1, CSR.

In Figure 3.17, the COV curves for all temperatures dropped to a minimum of 0.001 at 20 rpm, and after this point the fluctuation was negligible. The data shown suggests that a critical minimum operating spindle speed for the MC1 was 20 rpm.

The shear step experiment was repeated with more viscous S2000 oil with the Z3 spindle in experiments A45-A49. The plot of COV versus spindle speed is shown in Figure 3.18. A minimum critical spindle speed of 20 rpm was again observed.

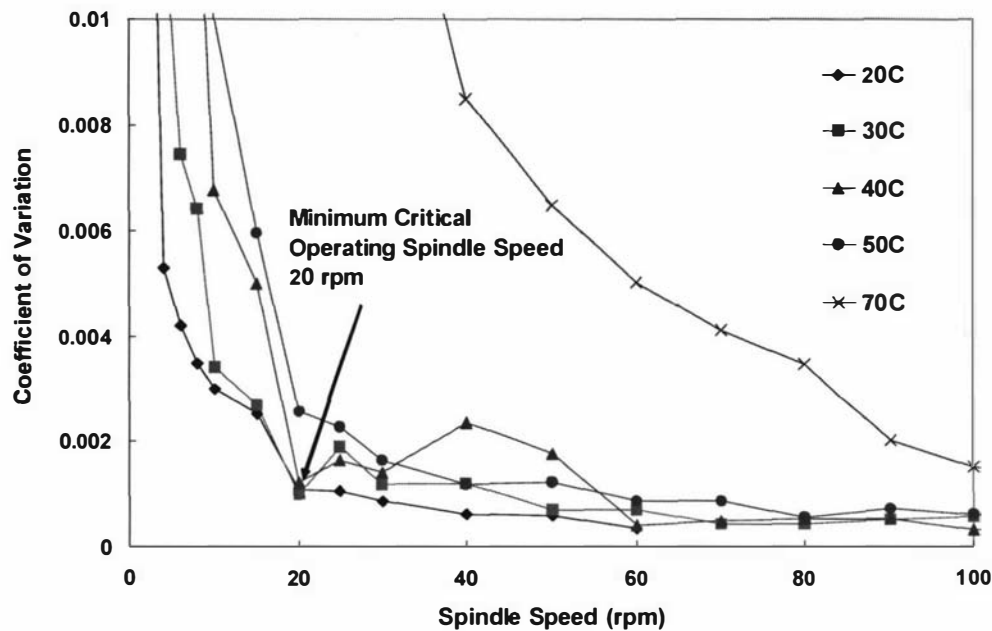


Figure 3.18: Coefficient of variation (COV) against spindle speed at different temperatures for S2000 oil. Experiments A45-A49, Paar Physica MC1, Z3, CSR.

The 70°C curve was anomalous due to its low viscosity at high temperature. The curve eventually reached a low coefficient of variation, but at a much higher spindle speed. The reason for this anomaly will be explained in section 3.3.2 where the minimum reliable torque will be discussed.

The S200 oil was tested with the Z2.1 spindle in experiments A50-A59. The Z2.1 spindle covered a larger range of spindle speeds than that of Z1 spindle for a given torque range. The shear step test was conducted in both CSS (experiments A50-A54) and CSR (experiments A55-A59) modes. Similar to Figure 3.18, the COV for both the CSS and CSR tests reached the minimum at 20 rpm. The results suggested that the mode of operation, either CSR or CSS, had no significant effect on the coefficient of variation, and more importantly, the minimum reliable operating spindle speed of the instrument.

The 70°C curves in the CSR and CSS tests once again showed peculiar trends compared to the other curves at lower temperatures. This is in agreement with the observation made in Figure 3.18.

Similar exercises were carried out at numerous other spindle geometries and standard oil solutions using both CSS and CSR tests in experiments A60-A73. Significant scattering and offsets in the measured viscosity were observed in speeds below 20 rpm as expected. Both the scale of oscillation and the offset diminished with an increase in spindle speed.

Interestingly, close inspection of some of the data published in the literature does reveal overshoot of apparent viscosity at low shear rate, similar to that observed during the Paar Physica MC1 calibration exercise e.g. (Tang et al., 1993; Schmidt & Munstedt, 2002). In their work with polyisobutylene fluids, Schmidt & Munstedt (2002) argued that the “increase of the shear viscosity at small stresses ... can be attributed to a formation of a particle network due to particle diffusion during preshearing”.

### **3.3.1.1 Cause of scattering error**

The scattering effect observed in the shear step tests was not a random event. A plot of viscosity against time for S200 oil at two constant speeds of 4 and 90 rpm in experiment A74, shown in Figure 3.19, shows that:

1. At 4 rpm, the average viscosity was 0.15 Pa.s which was significantly higher than 0.132 pa.s obtained at 90 rpm
2. The magnitude of periodic oscillations in viscosity at 4 rpm was larger than that observed at 90 rpm
3. The magnitude of periodic oscillations did not diminish with shearing time at constant speeds of 4 and 90 rpm.

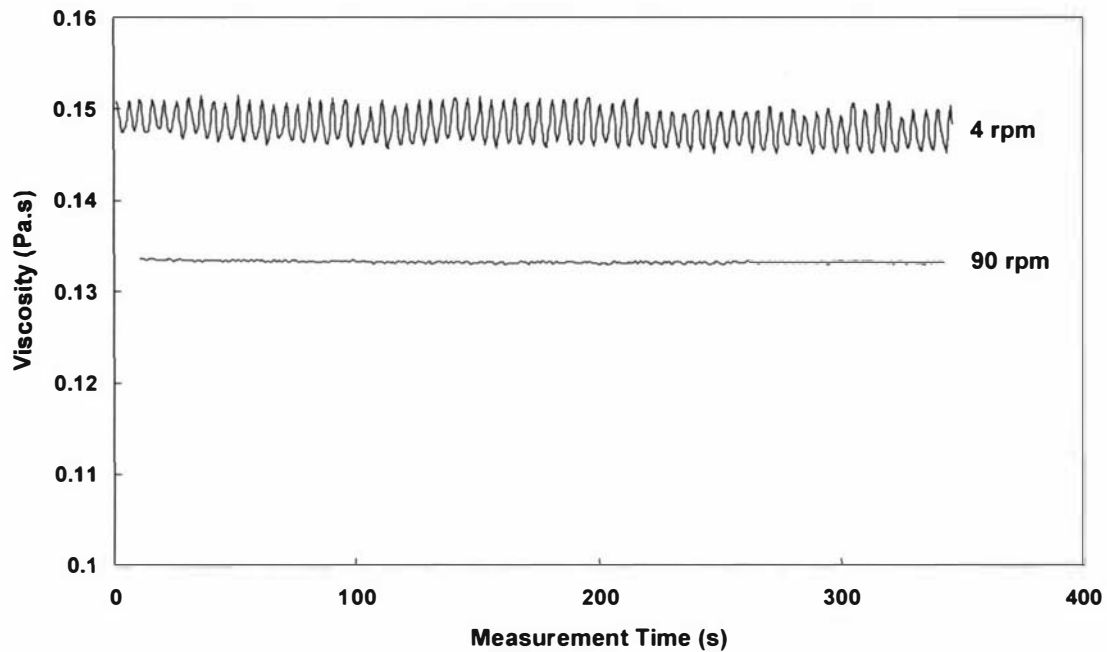


Figure 3.19: Variation in viscosity over 5 minutes of constant shear of 4rpm and 90 rpm for an S200 oil at 40°C. Experiment A74, Paar Physica MC1, Z1, CSR.

The regular pattern of the oscillations and their dependence on spindle speed suggested that they were related to the positions of the spindle as the spindle moved through a complete 360° rotation. The Paar Physica MC1 is a ball-bearing based rheometer. Any imperfection in alignment or manufacture would give rise to variable frictional resistances during a complete rotation.

The time taken for a complete rotation can easily be calculated from the spindle speed. Thus the relative position of the spindle from 0 to 360° can be mapped on the time axis together with the variations of measured viscosity. This was carried out on the data obtained in experiment A74, and the resulting graph of viscosity and relative position against spindle speed is plotted in Figure 3.20. It shows clearly that the periodic oscillation in the viscosity reading followed a pattern similar to the relative position of the spindle (change position from 0-100% to 0-360 degrees)

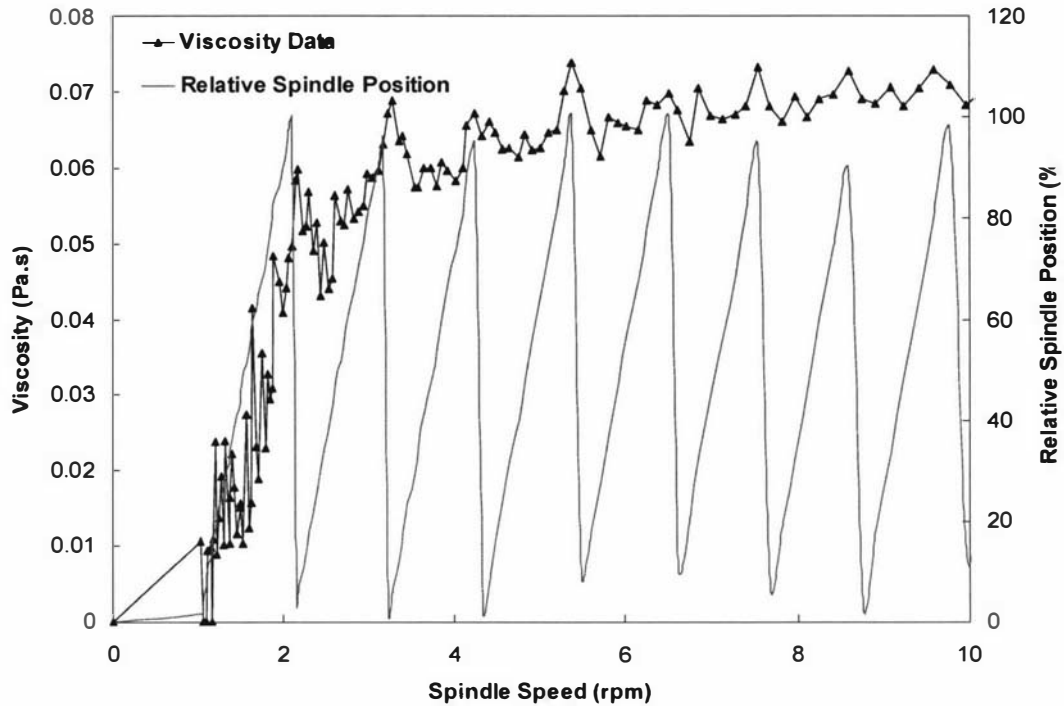


Figure 3.20: Viscosity and relative position versus spindle speed for an S200 oil at 40°C. Experiment A74, Paar Physica MC1, Z1, CSR.

Taking the data in Figure 3.20, it was possible to plot the relationship between viscosity and relative spindle position for both spindle speeds of 4 rpm and 90 rpm for the first 5 minutes of shear, as shown in Figure 3.21. During the constant shear test at 4 rpm, measurements were taken at 3 seconds intervals. This resulted in the movement of the bob by 20% of a complete revolution for every measurement. This explains the discrete groups of data at every 20% along the x-axis in Figure 3.21. At 90 rpm, the shear step test was conducted at 1 second measurement intervals, which gave rise to a constant scatter of data points along the entire x-axis.

In Figure 3.21, there was a clear correlation between viscosity and rotational position at 4 rpm, with maximum viscosity at 20% and minimum at 60%. Within experimental error, no correlation was observed between viscosity measurement and rotational position at 90 rpm.

Similar observations were made when the exercise was carried out at various spindle speeds and geometries, experiments A75-A80. The data illustrated the existence of a friction-positional dependence in the rotation system. Similar findings were made by Giles & Denn (1990) in their analysis with a Rheometrics Stress Rheometer (RSR).

In operating the Paar Physica MC1, for a given test, a measurement time interval input is required from the user with a minimum of 1 second. This variable specifies the time period for a measurement output by the MC1, i.e. 1 set of rheological data for every second. During the specified measurement interval, numerous values are recorded and then averaged. Thus, a longer measurement interval would yield more accurate data as the averaged value would be evaluated from more data points. The same would apply at high spindle speeds, where more rotations are achieved for a given measurement interval. This could explain the low scattering error observed at high spindle speeds.

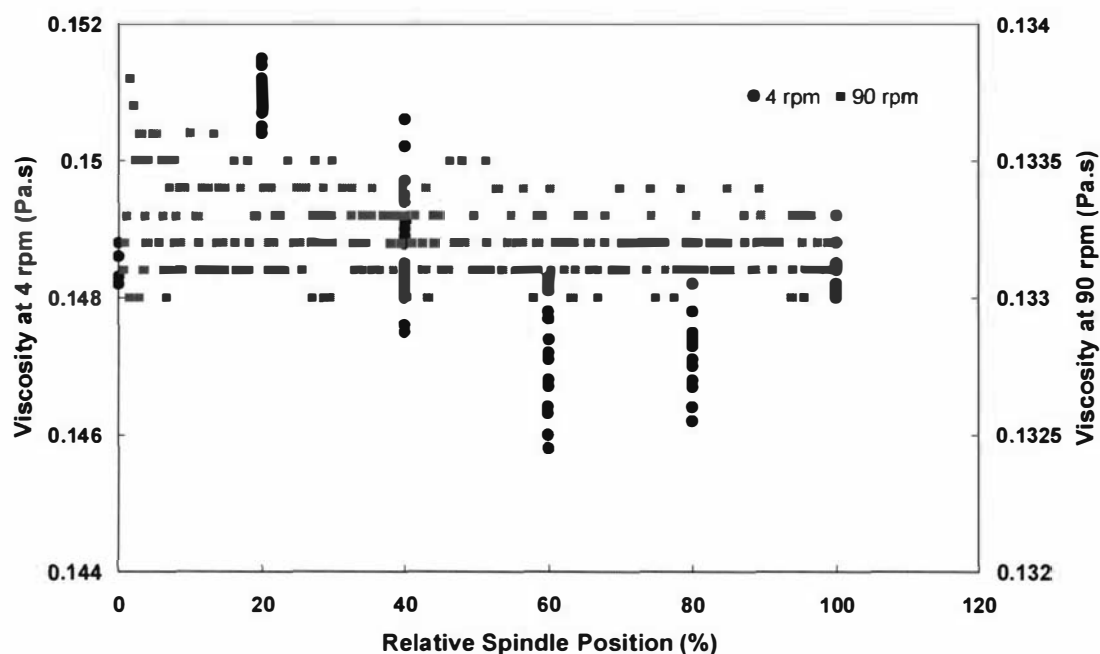


Figure 3.21: Viscosity versus rotational position at 4rpm and 90 rpm, for an S200 oil at 40°C. Experiment A74, Paar Physica MC1, Z1, CSR.

As shown, the effect of friction forces was more prominent at low shear level. Yet, it is interesting to note that the viscosity values obtained at low torque values were in fact lower than the viscosity values in the high shear range, which represented a more true value. The presence of additional friction forces during measurement at a given shear rate would in theory increase the total torque and hence viscosity values obtained due to the definition of apparent viscosity

$$\mu_{app} = \frac{\tau}{\dot{\gamma}} \quad (3.2)$$

where  $\mu_{app}$  is the apparent viscosity (Pa.s)

$\tau$  is the shear stress (Pa)

$\dot{\gamma}$  is the shear rate ( $s^{-1}$ )

Thus, the drop in viscosity at low shear levels cannot be explained by increased friction but reflects another shortcoming in the design of the rheometer and the importance of characterization exercise.

It is also clear that the measurement of yield stress cannot be performed by increasing the shear level in small increments starting from zero because the scatter of results in that range would be overwhelming.

### **3.3.1.2 Effect of measurement time on the performance of the MC1**

The effect of measurement interval time on the performance of the Paar Physica MC1 was investigated in experiments A81-A85. Three measurement interval time values were tested, 1, 3 and 5 seconds. An S60 oil was used with the Z2.1 spindle at 20°C. The oil solution was subjected to a shear step test using CSR mode. The COV was analysed and plotted against spindle speed and measured torque, as shown in Figures 3.22 and 3.23 respectively.

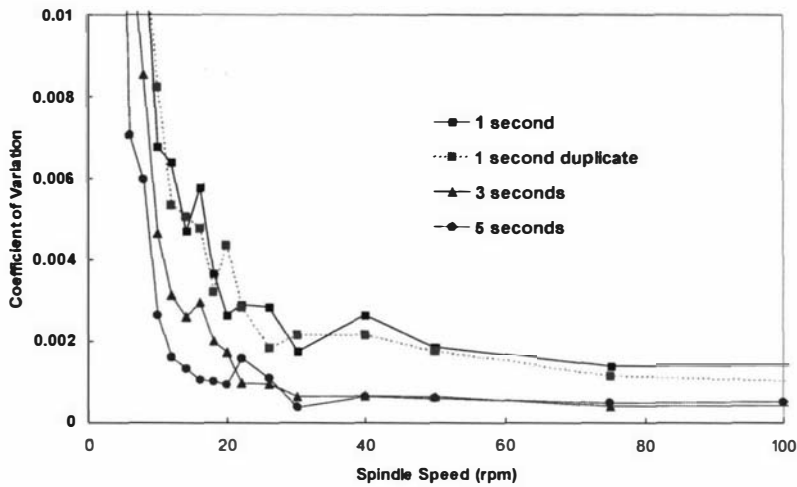


Figure 3.22: Effect of measurement time on the COV versus spindle speed plot of a S60 oil at 20°C. Experiments A73-A77, Paar Physica MC1, Z2.1, CSR.

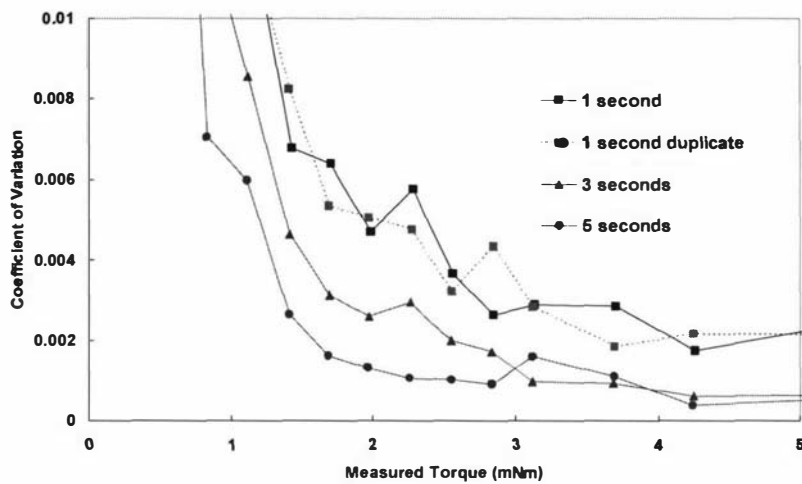


Figure 3.23: Effect of measurement time on the COV versus torque plot of a S60 oil at 20°C. Experiments A81-A85, Paar Physica MC1, Z2.1, CSR.

For a given spindle speed or measured torque, an increase in measurement time interval improved the COV value as shown in Figures 3.22 and 3.23. Similar observations were made when the exercise was repeated using different oil solutions, spindle geometries and operating modes, in experiments A86-101.

As explained in section 3.3.1.1, any given output set of data is an average of a number of measured data points recorded by the instrument for the duration of measurement. Thus, a longer measurement time would generate more data points and subsequently yield more accurate average values, and thus lower COV.

### 3.3.2 Minimum reliable torque

It will be recalled that the curve for the S2000 oil at 70°C in Figure 3.18, was significantly different from those at lower temperatures. The critical spindle speed and critical torque at which the COV curves decreased to 0.001 for the data in Figure 3.18 are tabulated in Table 3.6.

Table 3.6: Spindle speeds and measured torques at critical COV of 0.001 for Z3 spindle with S2000 oil at various temperatures. Experiments A45-A49.

Temperature	Spindle speed (rpm) at critical COV	Torque (mNm) at critical COV
20	20	8.5
30	20	3.5
40	20	1.5
50	55	1.5
70	130	1.5

A constant critical speed of 20 rpm was observed for S2000 oil at 20°C, 30°C and 40°C for Z3 spindle. For these three lower temperatures, the torque values were higher than 1.5 mNm. At 50°C and 70°C, the required spindle speed at the critical COV value of 0.001 increased sharply to 55 rpm and 130 rpm respectively, whereas the critical measured torque reached down to 1.5 mNm and it remained at that value.

Similar observations were made when the exercise was repeated with different oil solutions and spindle geometries, in experiments A50-A59. The COV results

demonstrated that the precision of the data collected is affected by both the spindle speed and the measured torque. Thus, any given set of data must not fall below either of these two limits of 20 rpm and 1.5 mNm. These limits are conservative and represent worst case scenarios. There will be some fluids that achieve a low COV even when the speed and torque are lower than 20 rpm and 1.5 mNm, depending on the viscosity of the sample and the spindle used. Data collected above these limits will almost always possess a small coefficient of variation.

The analysis of COV can only discuss the precision of data collected. A different analysis must be made to discuss measurement accuracy. The measured torque was found to have a significant effect on the accuracy of the data, as well as the precision of the data. The viscosity values at different shear rates can be normalised against the relatively constant viscosity readings achieved at higher shear rates in a shear sweep.

$$\mu_{normalised} = \frac{\mu}{\mu_{highshear}} \quad (3.3)$$

$\mu_{normalised}$  reflected the percentage deviation of the reading from the correct viscosity readings achieved at higher shear rate. Thus if  $\mu_{normalised}$  is 0.97, it means the current viscosity reading is 97% of the correct viscosity, or 3% error.

In experiments A102-A106, S2000 oil was subjected to a shear sweep test at different temperatures in CSR mode using the Z3 spindle. The normalised viscosity was plotted against spindle speed and measured torque for the S2000 oil using the Z3 spindle at various temperatures in Figure 3.24 (a) and 3.24 (b) respectively.

The normalised viscosity in Figure 3.24 (a) reached 0.97 at different spindle speeds. By contrast, the curves in Figure 3.24 (b) possessed similar shape and consistently reached 0.97 around the torque of 1.5 mNm.

Similar observations were made in other experiments with different oil solutions using different spindle geometry and operating modes. The results showed that the critical torque limit affected both the precision and the accuracy of the rheology data obtained from the Paar Physica MC1. This relationship is independent of the fluid rheological behaviour, or the spindle geometry or operating modes. The effect of torque is related to the physical design of the rheometer itself.

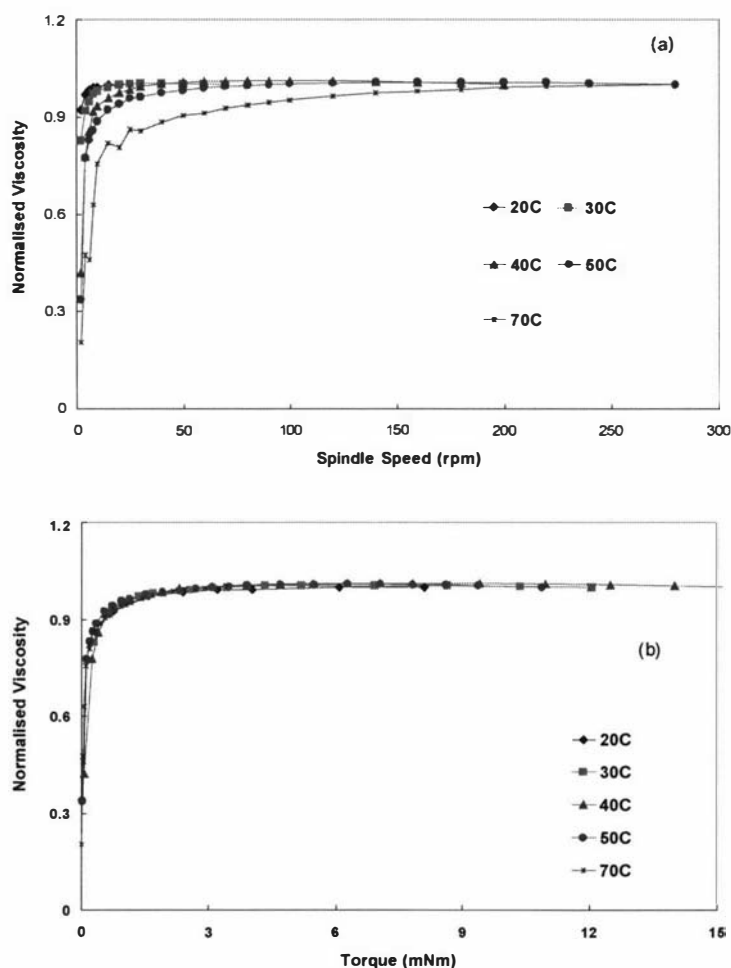


Figure 3.24: Normalised viscosity for S2000 oil at different temperatures. (a) normalised viscosity versus spindle speed (b) normalised viscosity versus torque. Experiments A102-A106, Paar Physica MC1, Z3, CSR.

These user defined limits of reliability are much more restrictive than the minimum torque of 0.05 mPa and speed of 0.3 rpm quoted by the manufacturer (Table 3.3). These equipment limitations are important in experiments where changes in viscosity with time cover a wide range of shear rates, such as in the study of age thickening of milk concentrates. As the milk ages, the viscosity increases with time, the spindle speed decreases for a set torque and the rheological data will eventually fall below the critical operating limits of the Paar Physica MC1. Thus, more and more of the data collected in shear sweeps would need to be truncated as age thickening progressed.

### **3.3.2.1 Accuracy and stress correction protocol**

Z1, Z2.1 and Z3 spindles were calibrated with the Cannon Instrument Company's Newtonian oil, and the measured viscosity values were compared to the expected values given in Table 3.5. The Z1 and Z3 spindles were found to record accurate data within an acceptable level of uncertainty. However, the Z2.1 spindle consistently displayed lower viscosity values than expected, by 50%. Consultation with Physica Messtechnik revealed that the original shear rate conversion factor supplied, which is required to determine shear rate from spindle speed, was incorrect. A new shear rate conversion factor was applied to rectify the situation.

In experiments A107-A118, triplicate runs of shear sweep tests were conducted using a new batch of S60 oil at four different temperatures, 20°C, 25°C, 37.8°C and 40°C using the Z2.1 spindle. The expected viscosity values for the new S60 oil as specified by Cannon Instrument Company (2003) are listed in Table 3.7. Care was taken to ensure that the temperature of the oil solution was close to the desired setting. This was achieved through the use of a calibrated thermocouple to measure the temperature of the oil in the cup prior to measurement, rather than relying on the temperature reading of the temperature sensor in the Jubalo water bath (which reflects the temperature of the water in the spindle jacket). The uncorrected viscosity profiles against shear stress for the S60

oil at all four temperatures are shown in Figure 3.25. The dashed straight lines represent the expected viscosity as given by Canon Instrument Company (2003).

Table 3.7: Viscosity values for the S60 Newtonian oil (lot 03201) (Cannon Instrument Company, USA), manufactured in 24 February 2003, expires on 08 February 2005.

Temperature (°C)	Viscosity (mPa.s)
20	142.5
25	104.4
37.8	52.01
40	46.64

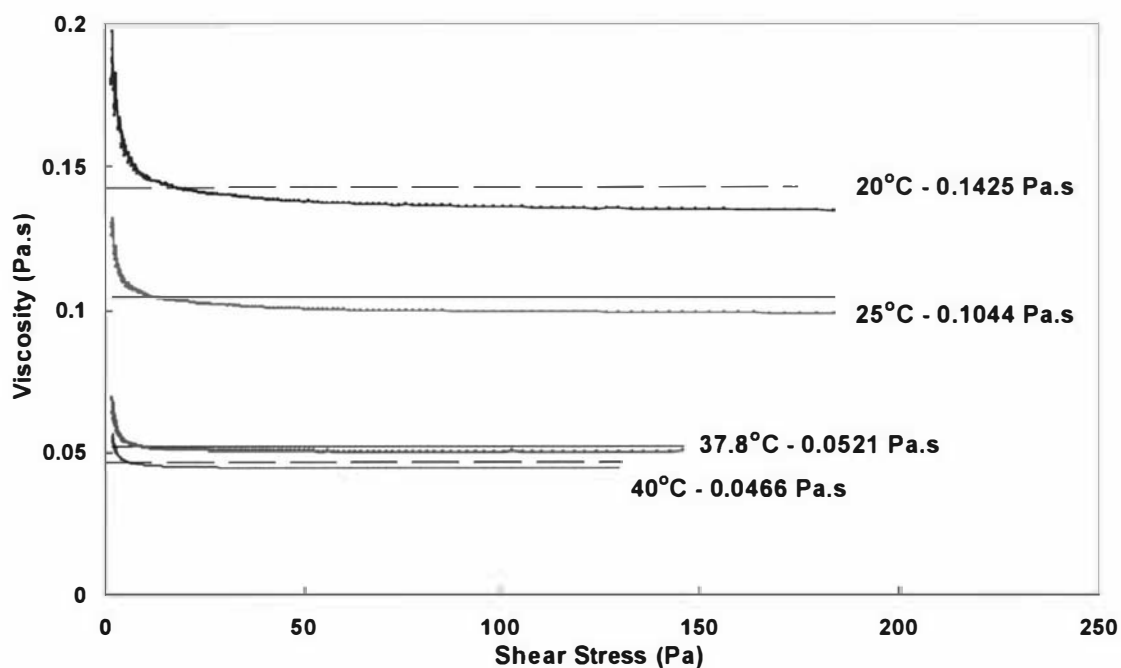


Figure 3.25: Viscosity against shear stress for the S60 oil at different temperatures without stress correction. Experiments A107-A118, Paar Physica MC1, Z2.1, CSS.

A departure from the correct viscosity was found at all nominal shear stresses reported by the viscometer software, especially at low shear stresses. For any given shear stress value, a correction coefficient was determined using equation 3.4.

$$\text{stress correction coefficient} = \frac{\text{MC1 reported viscosity}}{\text{actual viscosity}} \quad (3.4)$$

The change in the stress correction coefficient (SCC) with shear stress in the range of 1.4-194 Pa was calculated for all tests and the results are shown in Figure 3.26. At the higher temperatures (lower viscosity), the maximum spindle speed of 750 rpm was reached before the maximum shear stress of 194 Pa. In such cases the software does not stop measurements but keeps calculating the shear rate, which is clearly in error since the speed cannot change. The data in that range were discarded, and thus are not shown in Figure 3.26.

The SCC profiles for all curves at different viscosities were similar across the whole range of shear stress. The SCC results clearly showed that the spurious report of non-Newtonian behaviour at low shear rate is attributed to the operating mechanism of the Paar Physica MC1.

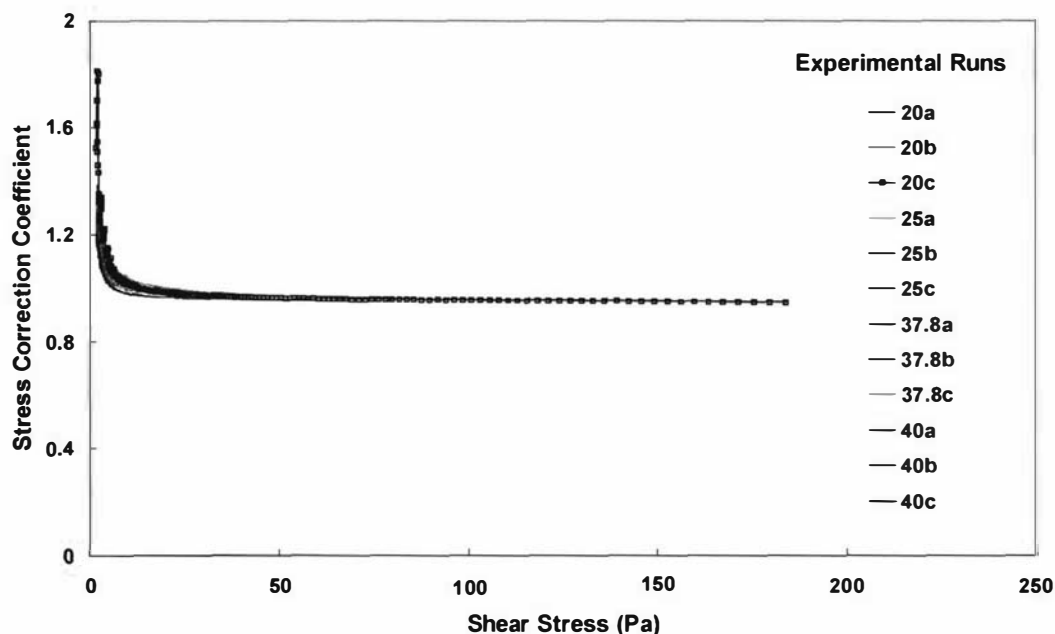


Figure 3.26: Stress correction coefficient versus spindle speed for S60 oil at different temperatures. Experiments A107-A118, Paar Physica MC1, Z2.1, CSS.

For each shear stress, an average SCC can be determined. An average SCC profile across the shear stress range was determined from the replicate runs (12 altogether) and was applied to all subsequent rheological measurements. The corrected shear stress value is determined as follows

$$\text{corrected shear stress} = \frac{\text{MC1 reported shear stress}}{\text{average SCC}} \quad (3.5)$$

The graph of viscosity versus the corrected shear stress for the S60 oil more closely resembled that for a Newtonian fluid, as shown in Figure 3.27. However, at low shear stress levels, significant deviation from Newtonian behaviour was still apparent. For all curves, the corrected viscosity data above the minimum reliable torque and spindle speed of 1.5 mNm and 20 rpm was within 3% of the expected viscosity value.

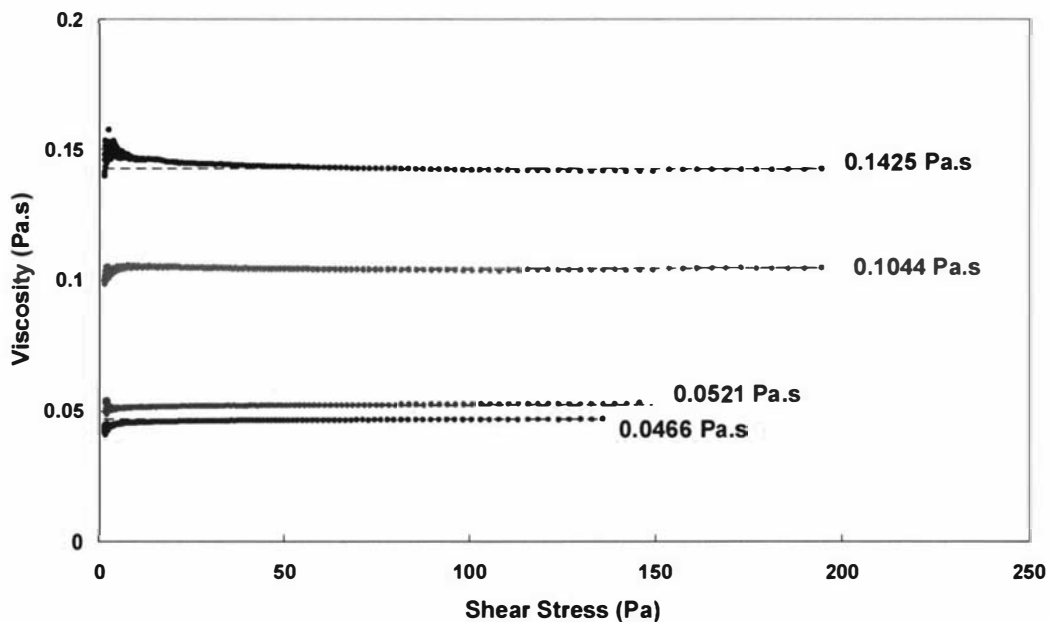


Figure 3.27: Corrected viscosity against shear stress for the S60 oil at different temperatures with stress correction. Experiments A107-A118, Paar Physica MC1, Z2.1, CSS.

### 3.3.3 Rheological measurement protocol for the Paar Physica MC1

In view of the results of the characterisation work discussed in the preceding sections, a measurement protocol was devised, and applied in further laboratory work and industrial surveys.

The water bath of the Paar Physica MC1 (Julabo Labortechnik, GbmH, Germany) was set to the appropriate temperature. 69.5mL of sample was loaded into the cup of the Z2.1 spindle. Each test comprised of three steps with details listed in Table 3.8. The test takes just over 8 minutes to complete.

Table 3.8: Measuring protocol for shear sweep test using the Paar Physica MC1.

Step #	Mode	Type	Torque (mNm)	Temp. equilibration time (s)	Measurement time (s)	Number of points
1	CSS	Sweep	0.5-50	60	1	200
2	CSS	Step	50	3	1	15
3	CSS	Sweep	50-0.5	3	1	200

In time-dependent fluids, the structure continuously changes with time unless the system is in equilibrium state. In order to minimize the effect of shear history during measurement, it was essential to complete the test in as short time duration as possible. A measurement time of only 1 second was used. Before commencing each test, a 60 second waiting time was allowed for temperature equilibrium. The inclusion of step two, where the torque was held at 50 mNm for a period of 18 seconds, was to minimize the effect of spindle inertia during rotation at high speed (Krieger, 1990).

The use of the Z2.1 spindle, which covered the highest range of viscosity values of all three spindles available, was found to be adequate to capture the age thickening trends in milk concentrates in this work. No other spindle was used. It was considered preferable

to use only one spindle because milk concentrates are known to be non-Newtonian and a correction to the reported nominal shear rate calculated by the Rheosolve software was necessary (as reported in section 3.6.2.2). This correction is dependent both on the fluid rheological properties and the spindle geometry. Since the geometries of commercial rheometer spindles are usually complex, the theoretical correction, which is based on simple geometries, is not perfect and it is difficult to dovetail completely the results using several spindles. In addition the rate of structure breakdown of time-dependent fluids also depends on the spindle used and the problem is exacerbated by the unnecessary use of several spindles.

### **3.4 Industrial survey**

The objective of the industrial surveys was to understand and record the effect of product composition, manufacturing conditions and plant design on the rheological behaviour of various concentrates encountered in dairy powder manufacture in the New Zealand dairy industry.

Figure 3.28 shows a schematic diagram of the processing steps involved during the manufacturing of milk powder at the three milk powder plants surveyed, Te Awamutu, Waitoa and Pahiatua. Raw milk was collected and stored in silos at 7°C. The milk was separated into cream and skim portions. Obviously, the skim portion was used for skim milk powder processing. The protein content was standardized to the level required by the product specification by adding lactose or whey permeate. The product was then pasteurized, preheated to achieve the desired whey protein nitrogen index before being evaporated to reach approximately 45-50%TS. In most plants, several evaporation systems operated in parallel. After evaporation, the concentrate was heated in the concentrate heater before being transported to the spray drier. After spray drying, the powder was packed and stored away.

At the Waitoa plant, there are three parallel processing lines. After the evaporators, density meters are situated to measure the density of the concentrates, from which the

solids content can be determined. The concentrate is then stored in the concentrate balance tanks, before it is pumped through the concentrate filters, then through to the concentrate heaters and subsequently the spray drier.

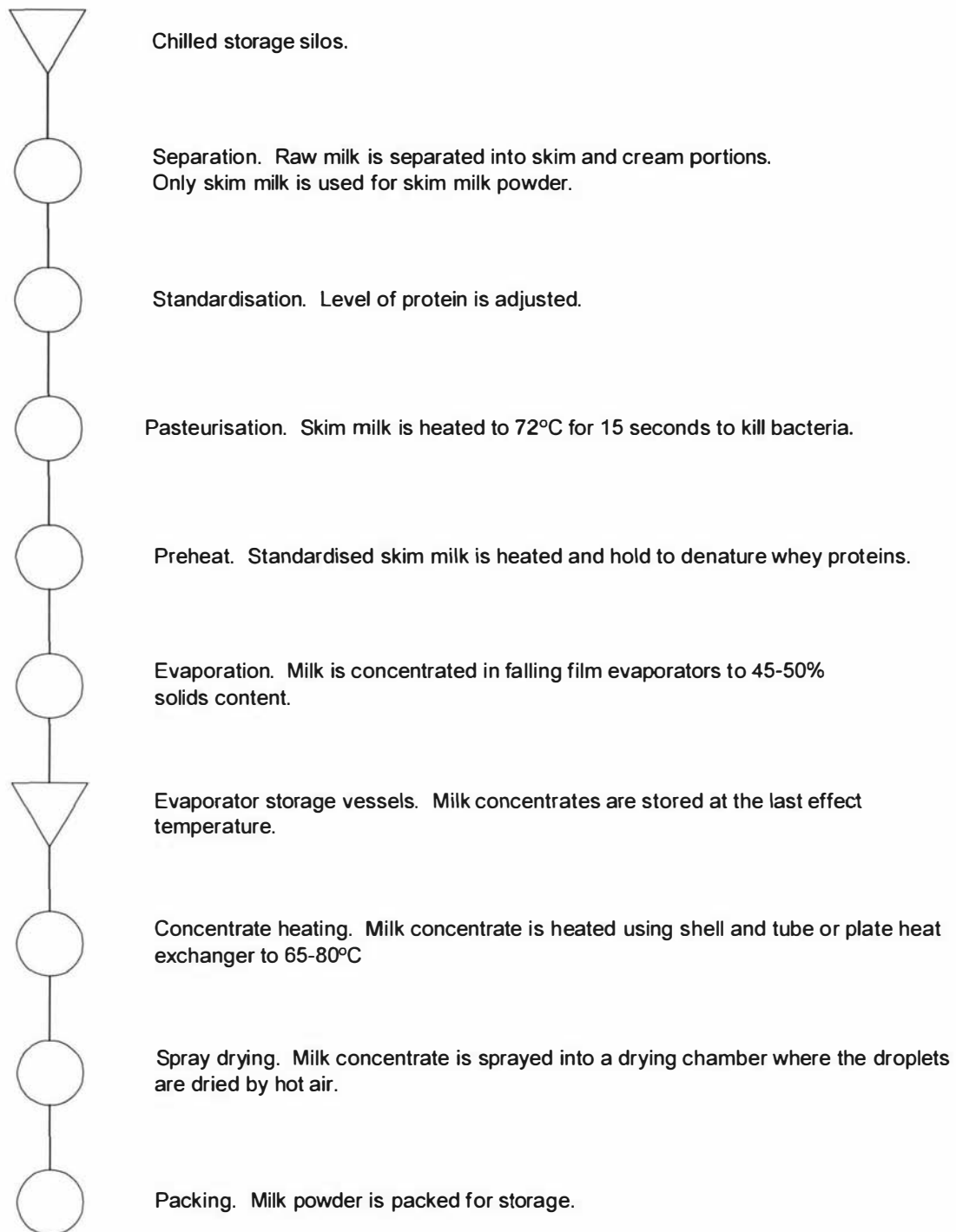


Figure 3.28: General process flow chart during skim milk powder processing.

The frequency of the industrial surveys was constrained by the manufacturing schedules of the three plants, which all have different designs and operating conditions. As a guest researcher, it was difficult to have any control over the processing conditions, which were changed from day to day, and fluctuated from sample to sample. Besides these production changes, there were random fluctuations and drifts in the conditions of manufacture. Thus, during industrial measurements, it was important to record information that may affect the rheological data. These included the following:

- Flow rate of milk through the evaporator
- Preheat temperature and holding time (where applicable)
- Evaporator first and final effect temperature
- Concentrate heater temperature

While other information such as temperature and residence time at each evaporator effect would have an effect on the rheological behaviour of the concentrate, the relationship is complex and not understood. In addition this information is much more difficult to obtain and was therefore not recorded.

Milk concentrate samples were withdrawn from taps, which were only situated after the evaporator and concentrate heater in most plants. The use of septa was avoided due to the high pressure in the line and the long period of time required to collect the desired sample volume.

During most industrial surveys, a simple manual Brookfield LVTD viscometer was the only available piece of equipment for rheological measurements on site. It was not possible to conduct fast shear sweep tests on the Brookfield, and measurements of age thickening were tedious. In many cases, samples of powder were also taken from the run and subsequently reconstituted at Massey University to provide more detailed information with a more accurate rheometer. However, the rheology of the reconstituted systems may be different to that from fresh, it is a rheological measurement of the final product, and not the in-process concentrates.

There was no attempt to correlate fluctuations in the plant processing conditions with changes in rheological behaviour. The information was used only to account for any unusual observations or drastic discrepancies in trends.

### **3.4.1 Sampling method**

A thermally insulated vessel with a constant internal diameter was used as a sample container to minimize heat loss. A plastic lid was placed on top to further minimize heat loss and evaporation. If available, the container was placed in a water bath to maintain temperature.

A stopwatch was started the instant the tap was opened. This was considered 'time zero'. When sufficient sample had been collected, the tap was closed and the time was noted. The sample was then carried back to the rheometer and set up for measurement. The time of measurement was also recorded. Thus, there were three time scales in total to account for the three stages of sampling and measurement: time zero for the opening of tap, sampling time for the duration of the sample collection period, and the measurement time at which the first measurement was recorded.

The container was carefully carried to the laboratory and gently placed onto the bench. A calibrated thermocouple was placed inside the thermally insulated container to monitor the change in temperature during measurement. Rheological measurement was carried out with a Brookfield viscometer, which is shown in Figure 3.29 along with a LV1 spindle.

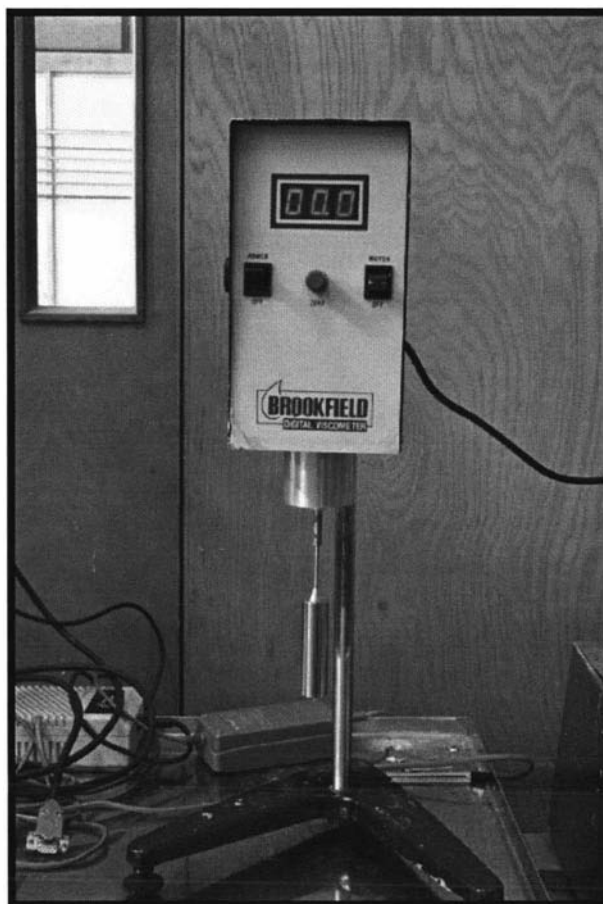


Figure 3.29: Brookfield LVTD viscometer and LV1 spindle

A Paar Physica MC1 rheometer was also used on a few occasions, when it was made available, to obtain rheological data in the industrial environment. The sampling procedure was modified to utilize the full potential of the equipment. The sample was collected in a large 3 litre container, which was then stored at the temperature of collection. Aluminium foil was used to cover the container to minimise water loss through evaporation. The milk sample was allowed to equilibrate in the hot water bath. Rheological measurements were carried out at periodic intervals to monitor the rate of thickening during storage, as described in section 3.3.3.

### 3.4.2 Rheological measurement protocol for Brookfield viscometer

The Brookfield viscometer was zeroed at 12 rpm without a spindle before each measurement, as specified by the manufacturer.

For any given spindle speed and spindle geometry, the Brookfield viscometer provides a percentage torque value as the only output variable, which had to be converted into apparent viscosity. It was recommended by the manufacturer that the output percentage value should exceed 10% of maximum range to avoid large friction errors.

The choice of spindle was dependent on the viscosity and the rate of age thickening in the product. For samples that possessed low initial viscosity values and rates of age thickening, the LV1 spindle was used. The LV4 spindle was sometimes used with infant formula products, which thickened quickly. Technical data for the various Brookfield spindles are listed in Table 3.9.

Table 3.9: Technical data for several Brookfield spindles (Brookfield Engineering Labs).

Spindle	Diameter (mm)	Cylindrical Length (mm)
LV1	18.84	65.1
LV2	10.25	53.95
LV3	5.88	42.86
LV4	3.2	31.01

Four spindle speeds were used: 6, 12, 30 and 60 rpm. For each sampling location, such as the evaporator and concentrate heater, fresh samples were collected for measurement at each of the four spindle speeds.

The attached spindle was slowly lowered into the centre of the sample container until the groove in the spindle was submerged in the solution. A specially designed circular

plastic disc with a hole in the centre to accommodate the spindle shank was placed on top of the flask to minimize heat loss. The spindle speed was set to the desired value. The change in percentage output, i.e. viscosity, was recorded with time over a period of 20 minutes at a given spindle speed. The change in temperature during this time was also monitored.

### 3.4.3 Brookfield versus Paar Physica MCI

An exercise was carried out to compare the data obtained from the Brookfield LVTD viscometer and the Paar Physica MCI rheometer. The aim of the exercise was to determine the adequacy of the Brookfield LVTD to generate accurate, reliable and meaningful data for industrial surveys, in comparison with the Paar Physica MCI rheometer.

A production run, A119, was monitored at the Waitoa milk powder plant. The general composition of the product (an infant milk formula) and operating conditions are listed in Tables 3.10 and 3.11 respectively. Fresh milk concentrate samples were collected after the density meter, concentrate filter and the concentrate heater described in section 3.4.

Table 3.10: General composition of the infant milk concentrates in experiment A119 at the Waitoa milk powder plant.

Component	%
Ash	4
Lactose	55.5
Moisture	2.5
Protein	18
Fat	20

Table 3.11: Plant operating conditions in experiment A119 at the Waitoa milk powder plant.

<b>Run #</b>	<b>B1</b>
<b>Process Variables</b>	<b>Evap. #2</b>
DSI temperature (°C)	96
Evaporator feed flow rate (m <sup>3</sup> /hr)	53
Evaporator concentrate flow rate (m <sup>3</sup> /hr)	12
1 <sup>st</sup> effect temperature (°C)	70
Evaporator concentrate temperature (°C)	53
Evaporator concentrate total solids (%TS)	47
Concentrate heater milk temperature (°C)	75
Concentrate balance tank level (%)	18

Measurements with the Brookfield viscometer were analysed through the change in viscosity with the spindle rotating at four constant speeds over a 20 minute period as described in section 3.4.2. Samples used for the Paar Physica MC1 were stored at rest at the temperature of the process line and shear sweeps were performed at regular storage intervals. The fundamental difference between the sample handling procedures between the two viscometers was that the Brookfield LVTD viscometer measured the data when the sample was stored under shear, whereas for the Paar Physica MC1, the sample was stored at rest, before conducting a shear sweep test at periodic intervals.

### 3.4.3.1 Comparison of Brookfield and Paar Physica MC1 measurements

The viscosity of the concentrates after the evaporator and concentrate heater measured with the Brookfield viscometer is plotted against shearing time at four constant spindle speeds in Figures 3.30 and 3.31 respectively. The concentrate heater samples were taken directly from the high pressure concentrate line.

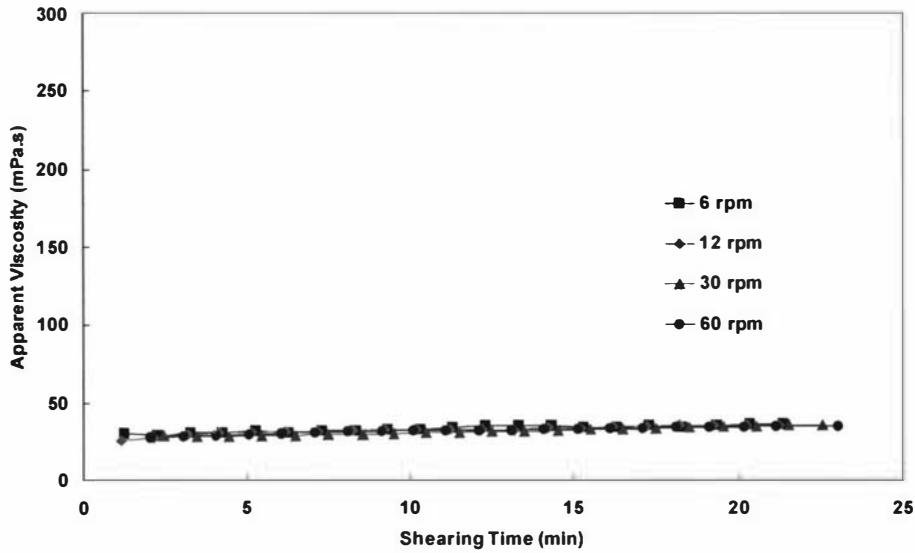


Figure 3.30: Change in viscosity with shearing time for fresh infant milk concentrate samples taken after the evaporator (47.4%TS, 52°C) at the Waitoa milk powder plant with the Brookfield LVTD viscometer. Experiment A119.

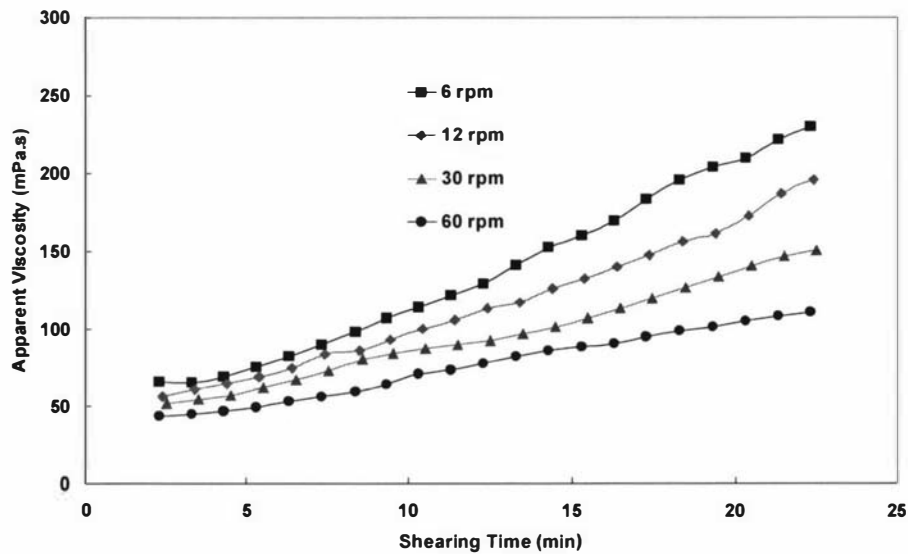


Figure 3.31: Change in viscosity with shearing time for fresh infant milk concentrate samples taken after the concentrate heater (47.12%TS, 72°C) at the Waitoa milk powder plant with the Brookfield LVTD viscometer. Experiment A119.

Figure 3.30 shows that the viscosity of the four evaporator samples remained fairly constant during the 20 minutes of constant shear at the four spindle speeds. On the other hand, the four curves in Figure 3.31 showed significant increases in viscosity with shear time, indicating age thickening of the samples after the concentrate heater.

The changes in apparent viscosity at 105.3 Pa with time from data collected and measured with the Paar Physica MCI were plotted in Figure 3.32 for samples collected at both the evaporator and the concentrate heater.

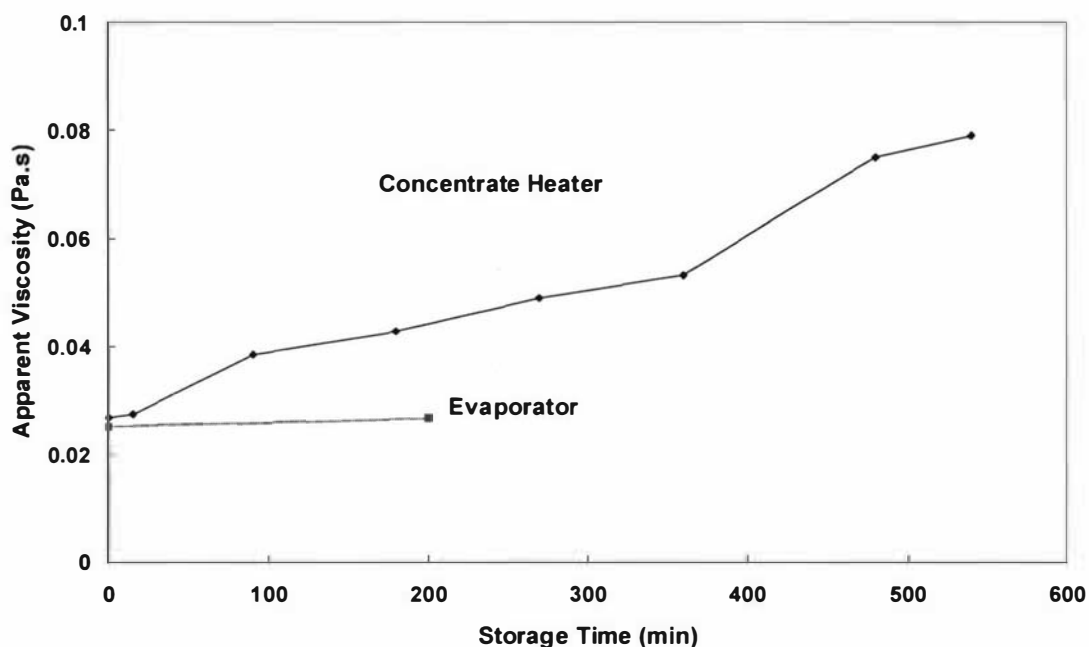


Figure 3.32: Change in viscosity at 105.3 Pa with storage time for fresh infant milk concentrate samples taken after the evaporator (47.4 %TS, 52°C) and concentrate heater (47.4%TS, 74°C) at the Waitoa milk powder plant. Experiment A119, Paar Physica MCI.

The viscosity of the evaporator sample again remained constant with time while the concentrate heater samples showed significant age-thickening. Thus similar trends in the data were observed with the Paar Physica MCI and Brookfield viscometers.

Comparing the absolute apparent viscosity values from the two instruments revealed the Paar Physica MC1 yielded lower values. The initial apparent viscosity value for the evaporator curve in Figure 3.32 was 25 mPa.s compared to 28 mPa.s obtained from the Brookfield viscometer in Figure 3.30.

This was attributed to several reasons. The first is simply the difference in shear stress at which the viscosity values were reported for the two different instruments. At 60 rpm, the shear stress at LV1 spindle is approximately 1 Pa with the Brookfield viscometer. This is well below the 105.3 Pa at which the viscosity values were measured with the Paar Physica MC1. However, it is not possible to report viscosity values at 1 Pa with the Paar Physica MC1 as this would fall into the truncated region as discussed in section 3.3. Therefore, the two instruments operate in two different shear regions.

The Paar Physica MC1 uses narrow gap geometry, where the gap between the cup and the bob is kept to a minimum. This was not the case with the Brookfield LVTD viscometer, where only fluid layers adjacent to the spindle surface were sheared. Thus, the shear distribution profile inside the fluids during measurement is different with the two instruments.

Because of Couette flow and the narrow gap design, the data obtained from the Paar Physica MC1 gives a more accurate picture of the rheology. However, the trends in age thickening profiles were similar between the two instruments. The data shows the adequacy of the Brookfield LVTD to monitor the age thickening trends in industrial surveys.

#### **3.4.3.2 Time-dependent analysis**

The Weltman model (Weltman, 1943) was developed to describe an exponential relationship between the rates of breakdown or build up of the structure with shearing time ( $t$ ).

$$\tau = A - B \ln(t) \quad (3.6)$$

where A and B are constant parameters which are dependent on the shear rate at which the test was conducted. The model can be easily re-arranged to monitor the change in viscosity with time, instead of shear stress, by simply replacing the subject of the equation.

The model describes an exponential relationship between shear stress and shear time at a constant shear rate. However, Figure 3.31 clearly shows a linear increase in viscosity over 20 minutes of constant shear at several spindle speeds. Therefore, the Weltman model did not fit the data collected from the Brookfield LVTD viscometer.

It is important to point out that an exponential curve essentially consists of three parts, a lower linear region, an exponential section, and then an upper linear region. Thus, a full exponential curve would need to cover all three regions. If data is only collected over the linear region, then a linear relationship would be apparent, but the exponential portion would not be detected.

It is possible that the rheological data recorded over the first 20 minutes of constant shear with the Brookfield LVTD viscometer only covered the linear section of a full age thickening profile. If given longer time, an exponential curve might be detected. However, with the data available, the Weltman did not give a good fit to the rheological data collected with the Brookfield LVDT viscometer. The rates of age thickening of the fresh concentrate samples at each shear rate were simply calculated as the rate of increase in viscosity with the change in shearing time.

The Weltman model could not be easily applied to the data collected with the Paar Physica MC1. The model was designed to study the changes in rheological behaviour under constant shear, i.e. shear step test, but the Paar Physica MC1 was operated in shear sweep test mode. Cross plotting between different sets of shear step data to yield a set of

shear sweep data would be required if the Weltman model was to be applied to the Paar Physica MC1 data.

There is a significant difference between the two modes of time-dependent analysis that were used with the Brookfield LVTD viscometer and the Paar Physica MC1. With the Brookfield, the samples were stored at a constant shear rate, and the changes in the time-dependent rheology were monitored. The exercise was then repeated at different shear rates. Analysis of shear stress versus shear rate would require cross plotting between different sets of shear step data at several shear rates.

Measurements made with the Paar Physica MC1 were carried out on samples that were allowed to rest for different lengths of time. The samples were subjected to shear sweep tests where the shear stress versus shear rate relationship was monitored. Analysis of the change in rheological behaviour with time at a constant shear stress requires cross plotting between different sets of shear sweep data at different storage time. Figure 3.32 is an example of such cross plotting. The results from Figures 3.30-3.32 showed that the rheological measurements from the two rheometers produced similar trends in rheological behaviour.

The shear sweep data collected with the Paar Physica MC1 can be fitted to a phenomenological model. The Herschel-Bulkley model was chosen and the changes in the model parameters,  $\tau_y$ ,  $K$  and  $n$ , with time were used to monitor the time-dependent behaviour of the systems. For example, the changes in the Herschel-Bulkley parameters for the concentrate heater sample in experiment A119 are plotted in Figures 3.33-3.35.

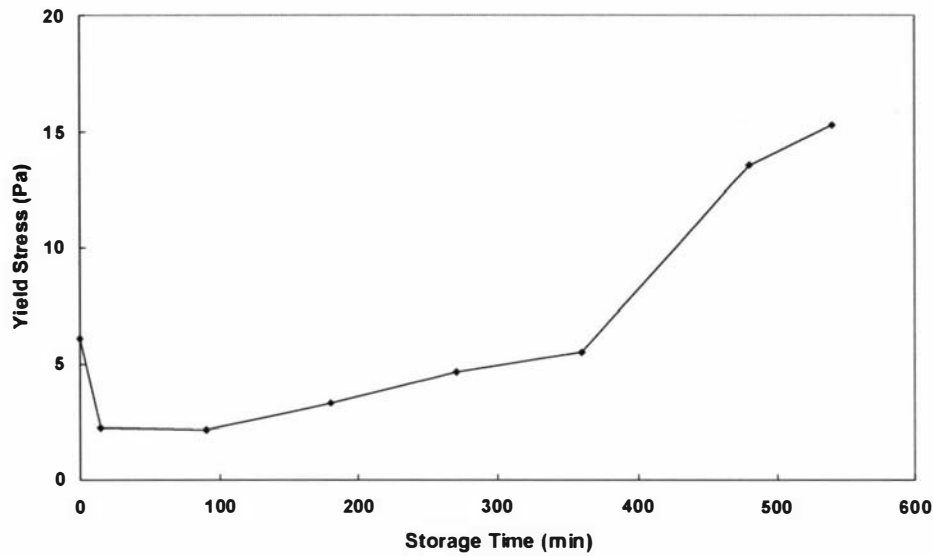


Figure 3.33: Change in  $\tau_y$  with storage time for fresh infant milk concentrate samples collected after the concentrate heater at the Waitoa milk powder plant. Experiment A119, Paar Physica MC1, 47.5%TS, 75°C.

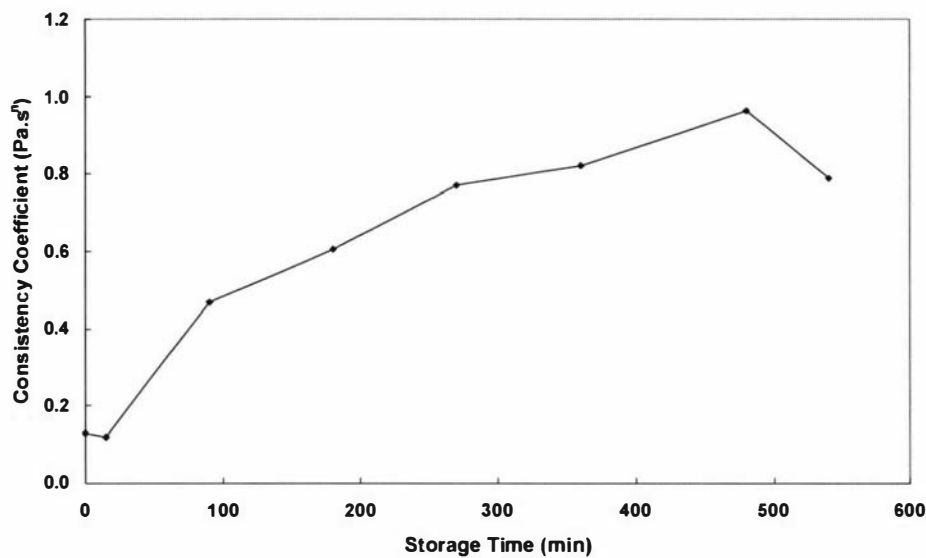


Figure 3.34: Change in  $K$  with storage time for fresh infant milk concentrate samples collected after the concentrate heater at the Waitoa milk powder plant. Experiment A119, Paar Physica MC1, 47.5%TS, 75°C.

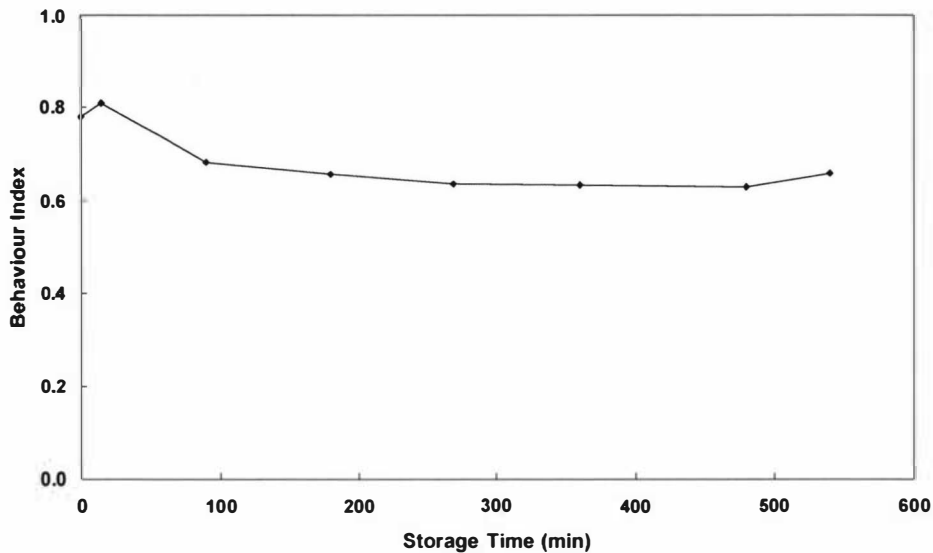


Figure 3.35: Change in  $n$  with storage time for fresh infant milk concentrate samples collected after the concentrate heater at the Waitoa milk powder plant. Experiment A119, Paar Physica MC1, 47.5%TS, 75°C.

Figures 3.33-3.35 show that the milk concentrate systems became more viscous (increase in  $\tau_y$  and  $K$ ) and displayed more non-Newtonian behaviour (decrease in  $n$ ) with storage time.

This analysis demonstrates that more information can be derived from data collected with the Paar Physica MC1 compared to the Brookfield LVTD, but the data from both viscometers exhibited similar trends.

### 3.5 Controlled rheology experiments protocols

A series of experiments were conducted in the pilot plant facilities at Massey University using the recombination rig discussed in section 3.2. The main objective of the controlled rheology experiments was to understand the relationship between processing conditions and the resultant rheological behaviour of reconstituted milk concentrate systems, in a controlled environment. By using powder, which is stable during storage,

the variation in the functional and physical properties of the raw materials was minimized, which improved the reproducibility of the rheological profiles of the reconstituted samples.

A number of procedures were used for the experiments with reconstituted milk concentrates, depending on the purpose of the experiment. The details are discussed in the results chapter 5 under the appropriate section. A generalized experimental protocol is given here, as well as several measurement and structural analysis techniques that were employed in conjunction with reconstitution and rheological protocols.

### 3.5.1 Materials

Several skim and whole milk powders were obtained from Fonterra Co-operative Group Ltd. Composition specifications are given Tables 3.12.

Table 3.12: General compositional specifications for several tested powder used in the controlled rheology experiments.

	<b>A</b>	<b>B</b>	<b>C</b>
<b>Powder</b>	Whole	Whole	Skim
<b>Heat Treatment</b>	Medium	Medium	Medium
<b>Protein</b>	24.34%	25.61%	36.4%
<b>Fat</b>	23.68%	24.26%	0.11%
<b>Lactose</b>	42.3%	40.76%	51.74%
<b>Ash</b>	5.78%	5.44%	7.86%
<b>Moisture</b>	3.9%	3.93%	3.89%

The majority of the controlled rheology experiments were carried out on whole milk powders A and B. The two powders were obtained from two different manufacturing plants. The general compositional specifications for the two powders were similar, with

powder B possessing slightly higher protein content. The preheat treatment during processing was similar in both powders also, with powder A heated to 101°C for 20 seconds while powder B was heated to 100°C for 40 seconds. The operating conditions during evaporation, concentrate heating and spray drying were unknown. These operating conditions, as well as the plant design and layout, will contribute to the shear and temperature history of the fluid that are expected to significantly affect the rheological behaviour of the two reconstituted powders.

### **3.5.2 Generalised experimental procedures for reconstituted samples**

Only distilled water was used for reconstitution experiments. Powder and water were weighed to achieve the desired solids content in the final reconstituted products. However, the quantities required had to take into account the water that was trapped inside the rig within the mono pump section from the post-CIP pre-rinse. This quantity of water was determined to be approximately 650 mL.

The moisture content of the powder must also be taken into account during the weighing process. Moisture analysis was conducted on several batches of powder. The average moisture content was 4% w/w, this value was used for calculating the powder requirements for all experiments.

The powder and the water were reconstituted according to the protocol listed in 3.2.3. The reconstitution temperature was usually set at 35°C to minimize age thickening during reconstitution. However, this temperature was increased in several sets of experiments where age thickening was purposely promoted to study the effect of recombination conditions.

Two standard types of experiments were conducted: in-line and storage. For in-line investigations, samples were withdrawn from the rig at 15 minute intervals and immediately subjected to a shear sweep test in the Paar Physica MC1, using the

measurement protocol in 3.3.3. At all times, the reconstituted solutions were recirculated around the rig via the capillary tube at  $40,000 \text{ s}^{-1}$ .

In storage experiments, the reconstituted milk concentrate system was allowed to recirculate via the high shear capillary tube for 60 minutes, after which samples were withdrawn from the rig and heated using a plate heat exchanger (Alfa Laval, P20-HB, Sweden). The samples were collected in a 3 L container then stored in a water bath at the temperature of the final heating step. Approximately 70 mL of milk concentrate was extracted periodically from the container and subjected to a shear sweep test using the Paar Physica MCI.

### **3.5.3 TEM protocol**

Electron microscopy is the science and technology of using an electron beam to form magnified images of specimens (Flegler, Heckman, & Klomparens, 1993).

A negative staining technique was employed to prepare milk samples for TEM analysis. These techniques are thoroughly described in several books (Harris & Horne, 1991; Bozzola & Russell, 1992; Flegler et al., 1993), as well as journal articles. Essentially, milk samples were fixed with glutaraldehyde and washed overnight with cacodylate-HCl buffer. The mixture of milk and glutaraldehyde was inverted several times. The samples were handled gently in order to prevent the destruction of the internal structure of the milk system, which is an important requirement during the fixing step (Harris & Horne, 1991; Bozzola & Russell, 1992; Hunter, 1993, Flegler et al., 1993). The fixed samples were further treated with a series of washes in buffer solution and rinses in distilled water, before being dehydrated in a series of acetone-water mixtures. The samples were stained in a mixture of acetone and uranyl acetate, washed and then treated with acetone-copper sulphate solution. After a few rinses with acetone, the samples were embedded in

Araldite resin mixture. The resin blocks were cut into thin slices and examined using a Phillips 201C Transmission Electron Microscope (Phillips, Eindhoven, Holland).

#### **3.5.4 Particle size distribution (PSD) analysis**

Particle size distribution (PSD) analysis was carried out on a Malvern Mastersizer Sizer E (Malvern Instrument, Worcestershire, UK).

In some experiments, several samples were set aside during rheological measurement for particle size analysis. The sample was diluted in distilled water at approximately three parts water to one part milk concentrate to minimize the age thickening process during storage at 4°C. The samples were held for no longer than a 24 hour period.

The solids content of the diluted milk solution was approximately 10%TS. The dilution and storage steps were found to have no adverse effect on the PSD results of the Mastersizer. However, without the inclusion of these steps, the milk samples would age thicken during storage, forming aggregates and flocs that would affect the PSD.

#### **3.5.5 Total solids content measurement**

The solids contents for all reconstituted samples were measured by using the AOAC official method 990.20 (AOAC International, 2002), with an experimental error of  $\pm 0.5$  %TS.

## 3.6 Data analysis

### 3.6.1 Brookfield LVTD data

#### 3.6.1.1 Shear stress and shear rate calculations

The gap between the bob (spindle) and the cup during measurement with the Brookfield LVTD viscometer is large, and the system is effectively one with a cup radius of infinity. The shear stress at the spindle surface can be calculated as follow.

Shear stress at the bob surface is given as (Bird, Dai, & Yarusso, 1983; Darby, 1985; MacSporran, 1986; Princen, 1986; Nguyen & Boger, 1992),

$$\tau_b = \frac{M}{2\pi R_b^2 L} \quad (3.7)$$

where:

- $\tau_b$  shear stress at the surface of the spindle (Pa)
- $M$  torque applied (Nm)
- $R_b$  radius of the bob (m)
- $L$  length of bob (m)

As the equation implies, the shear stress does not depend on the rheological behaviour of the tested solutions.

The maximum torque range for the Brookfield LVTD viscometer is 673.7 dyne.centimeters, as given by Brookfield Engineering Labs., Inc. where

$$1 \text{ dyne.centimeter} = 10^{-7} \text{ Newton.meter} \quad (3.8)$$

For any given percentage value output from the Brookfield viscometer, the equivalent torque value can be calculated from

$$\text{Torque} = M = \frac{\text{reading}}{100} \times 673.7 \times 10^{-7} \quad (3.9)$$

The torque value can be substituted into equation (3.7) to determine the shear stress.

The shear rate can be expressed in terms of the derivative of the rotation velocity (Darby, 1985; Princen, 1986; Nguyen & Boger, 1992),

$$\dot{\gamma} = -r \frac{d\omega}{dr} \quad (3.10)$$

where  $r$  radius at which shear rate is measured (m)

$\omega$  angular velocity (rad/sec)

For the infinite cup radius situation, Van Wazer et al. (1963) derived a simpler approximation to equation (3.10)

$$\dot{\gamma}_b = -2 \frac{dN}{d \ln(\tau_b)} \quad (3.11)$$

Where  $N$  is the spindle speed (rpm)

$\dot{\gamma}_b$  is the shear rate at the surface of the spindle ( $s^{-1}$ )

However, the solution cannot be applied to any fluid that has a yield stress value.

Cheremisinoff (1993) provided a generalized alternative equation, which can be used for any time-independent non-Newtonian fluid.

$$\dot{\gamma}_b = \frac{4\pi N}{n''} \quad (3.12)$$

where  $n''$  is the slope of a logarithmic plot of torque versus rotational speed.

To calculate the slope  $n''$  in equation (3.12) , a relationship between spindle speed and either torque or shear stress is required (Nguyen & Boger, 1992). In the case of the Brookfield LVTD viscometer, only shear step tests were conducted (as described in section 3.1.2) where the change in viscosity with time was monitored at a constant speed for four different spindle speeds. In order to obtain a relationship between spindle speed and torque or stress, cross plotting between data sets with different spindle speeds is required. As cross plotting can only be carried out on four sets of data from four different samples, experimental error was significant.

When using the Brookfield viscometer, the spindle geometry was sometimes switched between measurements. Thus, for a given spindle speed, different torque values were obtained for different spindle geometries. This makes it difficult to obtain a relationship between torque and spindle speed suitable for use in equation (3.12), as the calculated stress for a given spindle speed would change with a change in spindle geometry. Thus, the data from the same spindle geometry must be used during shear rate calculations.

Due to the significant error arising from cross plotting and the need to use different spindles during measurement, detailed non-Newtonian shear rate calculations were not carried out on data obtained from the Brookfield LVTD viscometer. Non-Newtonian corrections were not attempted due to the significant inherent uncertainties in the data.

### **3.6.2 Paar Physica MC1 data**

#### **3.6.2.1 Shear stress and shear rate calculations**

The shear stress equation is given by the manufacturer as,

$$\tau = \frac{1 + \varepsilon^2}{2 \cdot \varepsilon^2} \cdot \frac{M}{2\pi L \cdot R_b^2 \cdot C_L} \quad (3.13)$$

where  $C_L$  = End effect correction factor = 1.1 (given by Paar Physica)

$\varepsilon$  is the ratio of  $\frac{R_b}{R_c}$

The end effect correction factor  $C_L$  varies depending on the test fluid.

A shear stress constant,  $f_{ss}$ , can be derived from the above equation,

$$f_{ss} = \frac{1 + \varepsilon^2}{2 \cdot \varepsilon^2} \cdot \frac{1}{2\pi L \cdot R_b^2 \cdot C_L} \quad (3.14)$$

And,

$$\tau = M \cdot f_{ss} \quad (3.15)$$

Equation (3.13) is specific to the Z2.1 spindle while equation (3.15) can be applied to other spindle geometries, provided the shear stress constants are obtained from the manufacturer.

The shear rate equation for spindle Z2.1 is given by the manufacturer as follows

$$\dot{\gamma}_b = \frac{2\pi \cdot N}{60} \cdot \frac{1 + \varepsilon^2}{\varepsilon^2 - 1} \quad (3.16)$$

where  $N$  spindle speed (rpm)

$\varepsilon$  the ratio of the cup radius  $R_c$  to the bob radius  $R_b$ ,  $\varepsilon = \frac{R_c}{R_b}$

From equation (3.16), a shear rate constant,  $f_{sr}$ , can be derived:

$$f_{sr} = \frac{2\pi}{60} \cdot \frac{1 + \varepsilon^2}{\varepsilon^2 - 1} \quad (3.17)$$

Substitution equation (3.17) back into equation (3.16)

$$\dot{\gamma}_b = f_{sr} \cdot N \quad (3.18)$$

Examination of equation (3.17) clearly indicates that it can only be applied to Newtonian fluids since it does not involve the slope of the logarithmic plot of torque versus speed. As with the shear stress calculations, equation (3.16) holds specifically for spindle Z2.1, but equation (3.18) was true for other spindle geometries, provided the test fluid was Newtonian.

It was interesting to note that during the calibration exercise with Canon standard oils with the Z2.1 spindle, the apparent viscosity values were consistently higher than the expected values by 1.4 times. Communication with Anton Paar revealed that the value of  $f_{sr}$  (5.085) supplied for use in equations (3.16) and (3.17) was incorrect due to some false assumptions about the geometry of the Z2.1 spindle. A new value for the  $f_{sr}$  (was supplied by the company and proved adequate for the determination of the Newtonian shear rate.

The exercise illustrates the need to carry out independent testing of the equipment.

### 3.6.2.2 Non-Newtonian correction

Rao et al. (1975) and Chilton et al. (1996) noted that during the rheological analysis of non-Newtonian systems, the assumption of Newtonian behaviour can yield significant errors, ranging from 20-50%.

Equation (3.11) can be integrated between the spindle and cup surfaces using the Euler-MacLaurin theorem (Krieger & Maron, 1952; Krieger & Elrod, 1953; Yang & Krieger, 1978) giving the following relationship for concentric cylinder geometry.

$$\dot{\gamma}_b = \frac{N}{\ln \varepsilon} \left[ 1 + \left( \ln \varepsilon \cdot \frac{d(\ln N)}{d(\ln \tau_b)} \right) + \frac{(\ln \varepsilon)^2}{3N} \cdot \frac{d^2 \ln(N)}{(d \ln(\tau_b))^2} - \frac{(\ln \varepsilon)^4}{45} \cdot \frac{d^4 \ln(N)}{(d \ln(\tau_b))^4} + \dots \right] \quad (3.19)$$

Van Wazer et al. (1963) listed 7 assumptions made during the development of fundamental equation:

1. the liquid is incompressible
2. the system is isothermal
3. laminar flow during measurement
4. the streamlines of flow are circles on the horizontal plane perpendicular to the axis of rotation
5. the motion is steady
6. the motion is two-dimensional
7. there is no slippage

Equation (3.19) represents the formal relationship between the spindle speed and the shear rate for any fluid system and spindle size when measurements are carried out using concentric cylinder rheometers.

Van Wazer et al. (1963) noted that from equation (3.19),  $\frac{d \ln N}{d \ln \tau_b}$  is unity for Newtonian

fluids and thus the equation can be simplified to

$$\dot{\gamma}_b = \frac{N}{\ln \varepsilon} \quad (3.20)$$

For non-Newtonian fluids,  $\frac{d \ln N}{d \ln \tau_b}$  needs to be determined, and thus the second and higher order terms in the power series of equation (3.19) must be evaluated.  $\frac{d \ln N}{d \ln \tau_b}$  is simply the slope  $m$  of the logarithmic plot of  $\ln N$  versus  $\ln \tau_b$ .

Krieger and Maron (1952) noted that if  $(m \ln \varepsilon)$ , is less than 0.2, the third and higher terms can be discarded with an error of less than 1%. This is likely to be encountered in the Paar Physica MC1 due to the small gap between the spindle and the cup. Thus equation (3.19) is simplified to

$$\dot{\gamma}_b = \frac{N}{\ln \varepsilon} (1 + m \ln \varepsilon) \quad (3.21)$$

where  $(m \ln \varepsilon)$  accounts for the non-Newtonian behaviour of the system.

Taking a similar approach to the concentric cylinder geometry, an approximate non-Newtonian correction can be applied to the Paar Physica MC1 data with the use of the  $(m \ln \varepsilon)$  parameter by ignoring the effect of the cone at the bottom of the cylindrical bob. Thus, equation (3.21) becomes

$$\dot{\gamma}_b = f_{sr} \cdot N(1 + m \ln \varepsilon) \quad (3.22)$$

If  $m$  yields a straight line, then the fluid exhibits power law behaviour. However, when a graph of  $d \ln N$  versus  $d \ln \tau_b$  yields a curve, then the slope  $m$  must be determined for every spindle speed value on the graph.

The effect of non-Newtonian correction is demonstrated on the data from run A119, as discussed previously in section 3.4.3. The results are shown in Figure 3.36 for the measurement made after 540 minutes of storage. The graph shows viscosity against shear stress, with and without non-Newtonian correction on the left axis and the percentage error between the two lines on the right axis. An additional curve, which labelled “apparent viscosity with stress correction only”, shows the data which have taken account of the stress correction factor, as outlined in section 3.3.2.1. However, no non-Newtonian correction was carried out on this line.

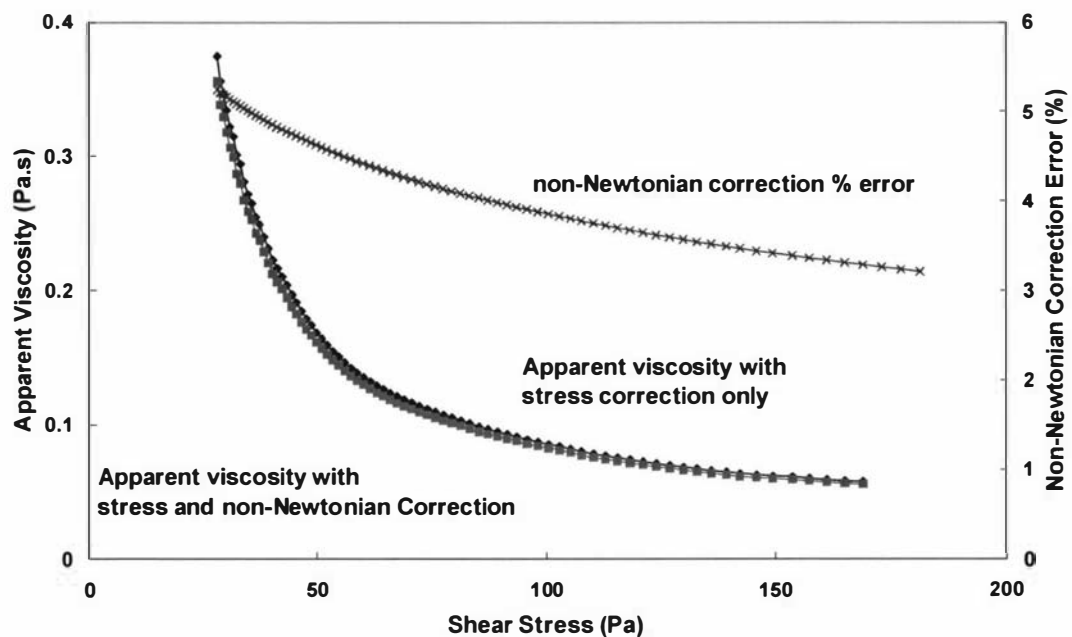


Figure 3.36: Effect of non-Newtonian correction on the rheological data measured in fresh milk concentrates collected after the concentrate heater (47.6%TS, 75°C) at the Waitoa milk powder plant with the Paar Physica MC1 rheometer. Experiment A119.

The apparent viscosity data with the non-Newtonian correction were lower than the nominal uncorrected values. This is expected as the non-Newtonian correction increases the value of the shear rate, as shown in equation (3.22). In Figure 3.36, the effect of the non-Newtonian correction decreases with an increase in shear stress.

The non-Newtonian correction had a small effect on the viscosity data, as seen by the 3-5% correction error observed in Figure 3.36. However, larger corrections were sometimes encountered in samples that were close to the gelling point where non-Newtonian behaviour is significant. In these samples, the non-Newtonian corrections could result in an apparent viscosity shift of 10% or more, depending on the shear stress level. As an example, Figure 3.37 shows the effect of the non-Newtonian correction as well as the percentage error for a reconstituted whole milk concentrate sample (powder A, 48%TS, 75°C). The rheological data were taken at the point of gelation.

Gelation was only encountered in a small proportion of samples. In these cases, the non-Newtonian correction error is larger than 10%. In most other samples, the non-Newtonian correction error was less than 5%, particularly at the shear stress of 105.3Pa where the apparent viscosity data are reported in age thickening experiments. Nonetheless, the non-Newtonian correction was applied on all truncated rheological data for analysis.

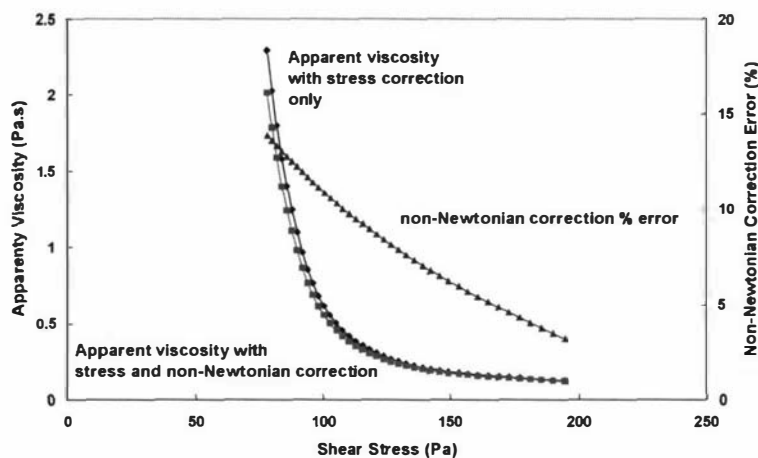


Figure 3.37: Effect of non-Newtonian correction on rheological data measured in a reconstituted whole milk concentrate sample (48%TS, 75°C) with the Paar Physica MCI rheometer.

### 3.6.2.3 Model fitting and data analysis

Mathematical modelling was used to summarize the time-dependent data collected from the Paar Physica MC1. This step was only carried out once truncation, shear stress and non-Newtonian corrections had been applied on the data.

Matlab 5.3.0.10183 (R11) was used to conduct the modelling exercise. Attempts were made to fit three models, Herschel-Bulkley, Sisko and Cross models to each set of data. One constraint was placed on all the models, which required all parameters to be larger than zero since negative values had no physical meaning. The model parameters were transferred to Microsoft Excel 2002 for further analysis. The data fitted to the Sisko and Cross models had poor correlation coefficients, in comparison with the Herschel-Bulkley model, and will not be presented.

The values obtained for the model parameters are highly dependent on the data available. The truncation and correction protocols carried out on the collected rheological data had a significant effect during the modeling exercise. From the 48%TS and 65°C experiments, Table 3.13 compares the three Herschel-Bulkley parameters obtained from the original set of data, as well as those from the truncated and corrected data. The table shows that the use of non-Newtonian and shear stress corrections had small effects on the model parameters. However, the application of truncation significantly changed the values of the three Herschel-Bulkley model parameters, as seen in the last three columns in Table 3.13. More importantly, the rates of age thickening suggested by the three sets of data were significantly different. Thus, it was important that the same data analysis procedure was carried out on all sets of data.

Table 3.13: Effects of data corrections and truncation during rheological modeling.

Storage Time (min)	Raw Data			Non-Newtonian and shear stress corrections			Non-Newtonian and shear stress corrections and truncation		
	$K$	$n$	$\tau_y$	$K$	$n$	$\tau_y$	$K$	$n$	$\tau_y$
0	0.13	0.87	1.32	0.13	0.88	0.88	0.10	0.91	2.44
30	0.20	0.84	3.34	0.20	0.85	3.06	0.15	0.88	5.51
60	0.38	0.77	3.10	0.37	0.78	2.84	0.24	0.83	7.08
90	1.30	0.64	4.68	1.25	0.65	4.50	0.57	0.74	13.51
105	3.17	0.53	5.73	3.07	0.54	5.63	0.71	0.72	24.38
120	12.41	0.36	3.59	12.18	0.37	3.45	0.79	0.72	46.40
150	26.22	0.28	0.00	25.47	0.29	0.00	1.75	0.63	66.29

---

# **CHAPTER 4**

# **INDUSTRIAL SURVEYS**

---

## CHAPTER 4: INDUSTRIAL SURVEYS

This chapter presents the results of an industrial survey of rheological behaviour of fresh milk concentrates in several manufacturing plants within New Zealand. The survey investigated the relationship between the rheology of concentrated milk taken after the evaporator and concentrate heater and processing conditions particular to each individual plant. The purpose of the survey was to develop a database of rheological behaviour of milk concentrates during processing in New Zealand milk powder plants.

The methodology of the survey has already been described in Chapter 3. Section 4.1 compares the rheological behaviour of fresh milk concentrates after the evaporator and concentrate heater. Section 4.2 discusses the effect of plant design. The subsequent three sections of 4.3-4.5 discuss the effect of solids content and preheat treatment and protein content on concentrate rheology. Section 4.6 investigates the effect of shear rate during sampling on the rheological behaviour of collected milk concentrate samples and the care needed to avoid artefacts that excessive shear rate can impart.

### 4.1 Effect of plant operation on the rheology of fresh milk concentrate systems

The rheological behaviour of medium heat skim milk was analysed at the Te Awamutu skim milk powder plant in experiment B1. The general composition of the product at this plant is listed in Table 4.1. The results are shown in Figure 4.1 and clearly showed the rate of age thickening was more prominent after the concentrate heater. This agrees with the results obtained by Trinh (1994).

The extrapolated time-zero viscosity values, determined by fitting a linear regression on each data set, for the four spindle speeds were higher after the concentrate heater than the evaporator. For both sets of data from the evaporator and the concentrate heater in Figure 4.1, shear thinning was observed where the viscosity decreases with an increase in shear rate, i.e. spindle speed. Previous publications (Snoeren, Damman, & Klok, 1982; Velez-

Ruiz & Barbosa-Canovas, 1998) have also noted that fresh skim milk concentrates display shear thinning behaviour.

Table 4.1: General composition of the skim milk concentrates in experiment B1 at the Te Awamutu skim milk powder plant.

Component	%
Ash and Lactose	62.7
Moisture	3.65
Protein	33.0
Fat	0.65

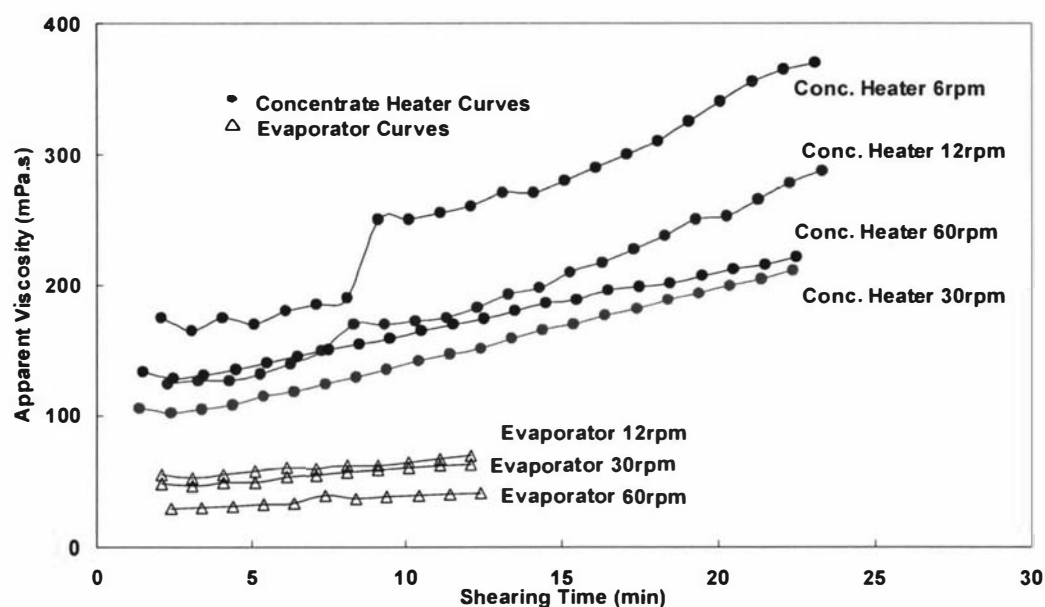


Figure 4.1: Change in viscosity with shearing time for fresh skim milk concentrate samples (46.5%TS) taken after the evaporator #4 (64°C) and concentrate heater (65°C) at the Te Awamutu skim milk powder plant. Experiment B1, Brookfield LVTD.

The reliability of the industrial measurements was verified by repeating this monitoring exercise a number of times. An example is shown in Figure 4.2, which compares the

tendency to age thicken after the evaporator (at 30 rpm) and the concentrate heater (at 6 rpm) for two sets of experiments, B1 and B2, taken one week apart. The results showed less than 10% error between the curves within each set of data. A maximum error of 10% was observed between replicate measurements. It is important to note that this error is not replicate error of the measurement in a true sense, as variation in the plant operating conditions significantly affects the results. This error incorporates both the repeatability of measurement techniques as well as variation in the plant processing conditions.

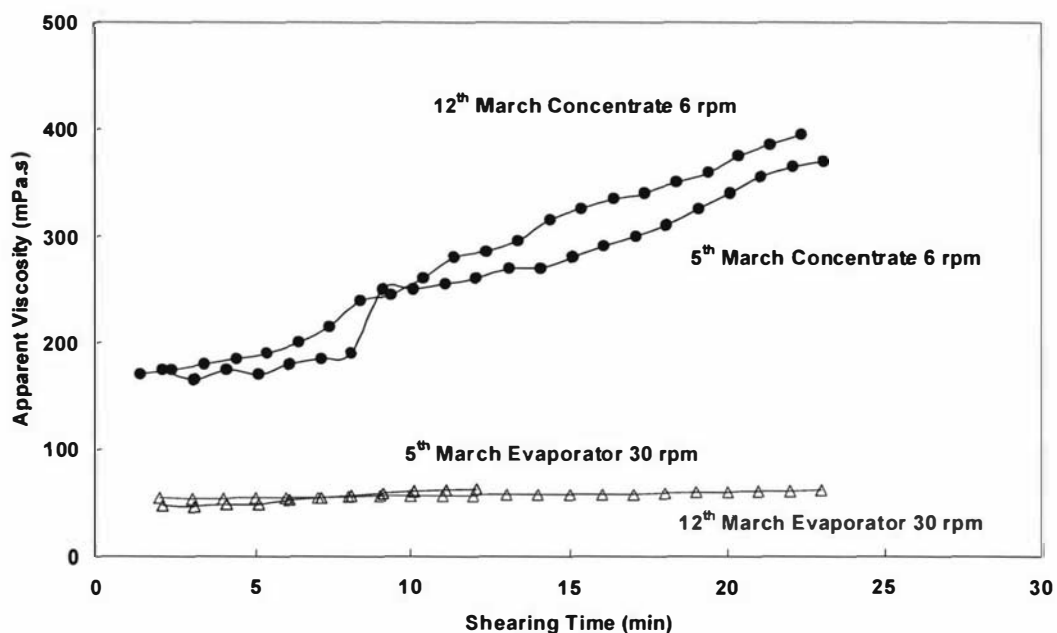


Figure 4.2: Comparison of replicate values in the age thickening profiles after the evaporator at 30 rpm and the concentrate heater at 6 rpm for experiments B1 and B2 at the Te Awamutu skim milk plant.

Table 4.2 lists in line values for solids content and sample temperatures in runs B1 and B2 later. The solids content values were evaluated from various plant records including density readings, fat content etc. However, as there was no density meter after the concentrate heater, it was not possible to evaluate the solids content in-line. In subsequent surveys, samples were collected after the concentrate heater for determination of solids content by oven drying.

Table 4.2: Solids contents and temperatures of milk concentrate samples from the Te Awamutu skim milk powder plant for experiments B1 and B2.

<b>B1</b>						
Locations	Evap. #4			Conc. Heater #3		
Spindle Speed	Time of sample	%TS	Temp	Time of sample	%TS	Temp
6				20:19		65.98
12	20:58	47.0	64.25	18:15		65.97
30	21:35	46.94	64.27	19:30		66.12
60	21:20		64.13	18:49		65.82
<b>B2</b>						
Locations	Evap. #4			Conc. Heater #3		
Spindle Speed	Time of sample	%TS	Temp	Time of sample	%TS	Temp
6	11:11	46.67	63.22	15:40		66.20
12	11:48		63.3	14:04		65.99
30	12:21	46.54	63.27	14:39		65.45
60	13:01	46.49	63.15	15:13		66.07

The plant records of the solids content and temperature of the milk concentrates upon exiting the evaporator for two production dates are plotted in figures 4.3 and 4.4. The solids content curves in Figure 4.3 show significant fluctuations while the temperature curves in Figure 4.4 exhibit greater stability. Since the viscosity of the samples is a strong function of both temperature and total solids, the data illustrates why it is not possible to get consistent results in the plant survey and highlights the need to monitor the processing variables at the time of sample collection.

The solids content values for milk concentrate samples after the evaporator over each production date showed a 7% scatter, which is within the maximum 10% variation observed in the viscosity-time data.

In all subsequent experiments a 10% experimental variation was assumed for rheological measurements. During the survey, replicate samples were taken periodically to ensure that the experimental uncertainty still fell within this 10% margin of variation.

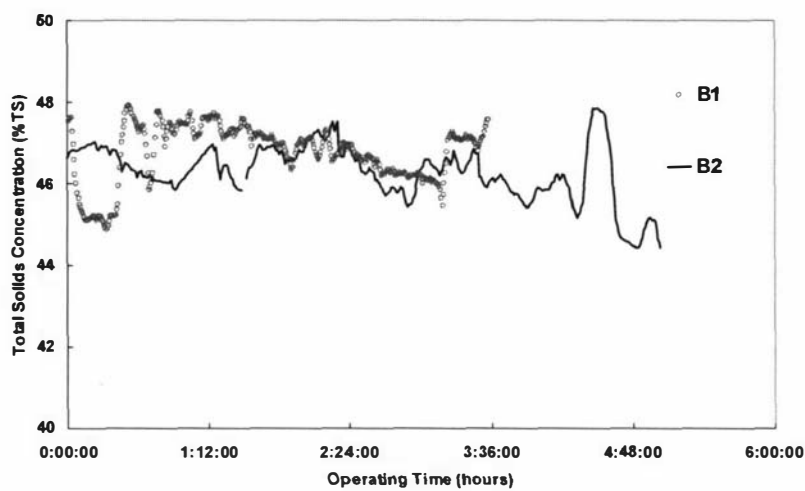


Figure 4.3: Variation in total solids content of milk concentrate samples after the evaporator for experiments B1 and B2 at the Te Awamutu skim milk powder plant.

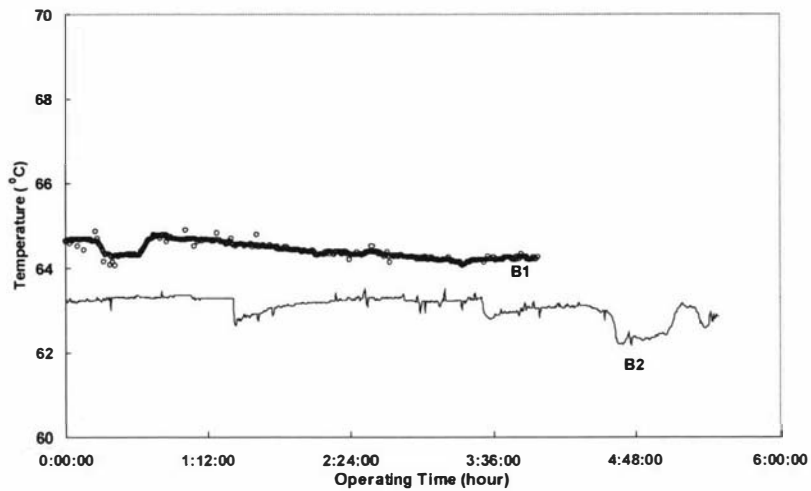


Figure 4.4: Variation in milk concentrates temperature after the evaporator for experiments B1 and B2 at the Te Awamutu skim milk powder plant.

Experiments B3 and B4 were carried out at the Te Awamutu skim milk plant with a slightly different skim milk product, but with a similar composition to that listed in Table 4.1. The experiments were carried out on consecutive days of production. The rheological data after the evaporator and the concentrate heater are plotted in Figures 4.5 and 4.6 for experiment B3.

The evaporator curves in Figure 4.5 were mainly flat, with insignificant rise in viscosity with time. Any rise in viscosity was probably due to a fall in temperature in the thermos flask during measurement.

Figure 4.6 shows that age thickening was more significant after the concentrate heater. The 6 rpm curve showed over 200% increase in viscosity after 20 minutes of constant shear. Shear thinning was observed as the spindle speed (shear rate) was increased. There was a lag period in the viscosity-time curves in Figure 4.6 for the concentrate heater samples. The extrapolated time-zero average viscosity value was higher for concentrate heater samples than those after the evaporator. Similar observations were made in Experiment B4.

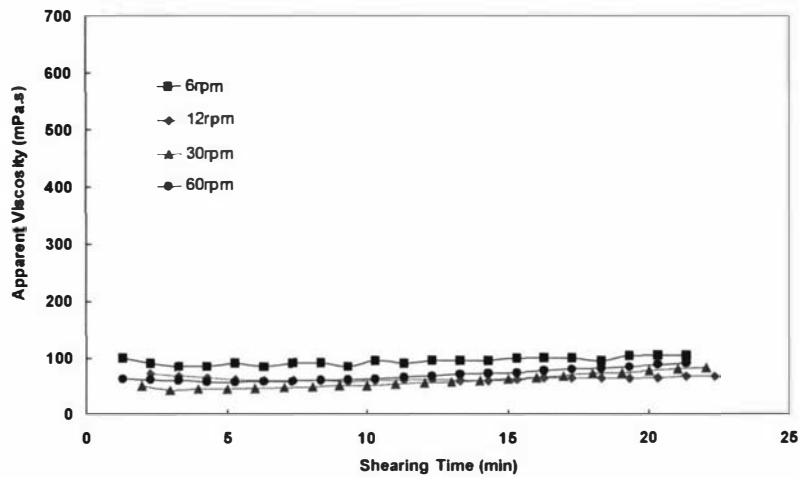


Figure 4.5: Change in viscosity with shearing time for fresh skim milk concentrate samples taken after the evaporator #1 at the Te Awamutu skim milk powder plant. Experiment B3, Brookfield LVTD, 50%TS, 48°C.

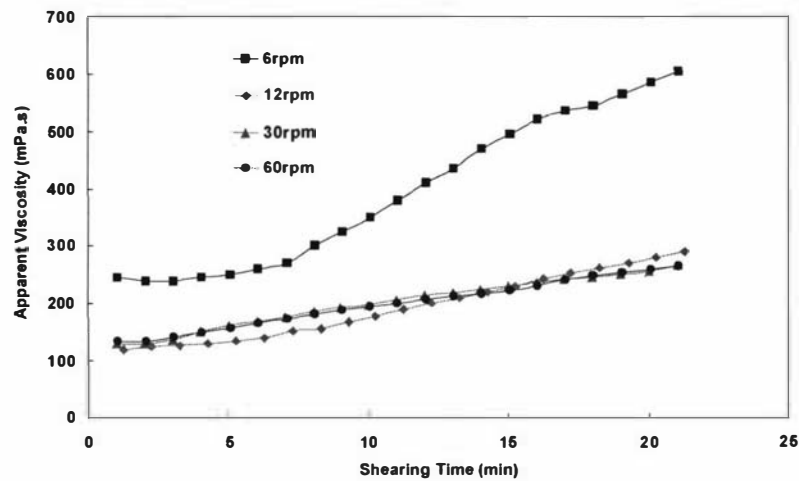


Figure 4.6: Change in viscosity with shearing time for fresh skim milk concentrate samples taken after the concentrate heater at the Te Awamutu skim milk powder plant. Experiment B3, Brookfield LVTD, 50%TS, 62°C.

Table 4.4 tabulates the total solids concentration and the inline temperature values for all samples over the two production dates. The solids concentration was determined by

drying the concentrate samples in a hot air oven. The temperature values were obtained from an inline temperature probe.

The temperatures of the concentrate heater samples were consistently over 61-66°C, while the temperature for the evaporator samples averaged in the 50-51°C range. The solids content values showed small differences between the samples. This suggests that high heat treatment at the concentrate heater was responsible for the observed age thickening behaviour observed. This agrees with the observations made by Trinh & Schraekenrad (2002) where age thickening was only observed above 65°C for a whey depleted reconstituted milk concentrate system.

In Table 4.3, the average and the COV values of temperature and solids content for the evaporator and concentrate heater data were determined for experiments B3 and B4. Higher COV were obtained for solids content data than temperature. This confirms the trends in Figures 4.3 (run B1) and 4.4 (run B2), where larger fluctuations were observed in the solids content data during processing.

Table 4.3: Variation in temperature and total solids content for experiments B3 and B4 at the Te Awamutu skim milk powder plant.

<b>B4</b>						
	<b>Evap #1</b>	<b>%TS</b>	<b>Temp</b>	<b>Conc. Heater</b>	<b>%TS</b>	<b>Temp</b>
<b>Speed</b>	<b>Time</b>			<b>Time</b>		
<b>6</b>	19:33	50.16	51.23	18:03	49.71	62.28
<b>12</b>	18:57	49.94	51.21	16:43	50.58	62.39
<b>30</b>	19:45	50.05	51.06	17:10	49.43	62.11
<b>60</b>	18:30	49.7	51.28	17:38	50.34	61.64
<b>Average</b>		49.96	51.2		50.015	62.105
<b>COV</b>		$3.9 \times 10^{-3}$	$1.8 \times 10^{-3}$		$10.7 \times 10^{-3}$	$4.9 \times 10^{-3}$
<b>B5</b>						
	<b>Evap #2</b>	<b>%TS</b>	<b>Temp</b>	<b>Conc. Heater</b>	<b>%TS</b>	<b>Temp</b>
<b>Speed</b>	<b>Time</b>			<b>Time</b>		
<b>6</b>	08:41	50.41	50.3	10:06	50.47	65.97
<b>6</b>	09:03	50.79	50.2			
<b>12</b>	10:35	50	50.74	07:22	50.61	66.03
<b>30</b>	10:10	50.5	50.13	08:13	49.98	65.92
<b>60</b>	11:50	50.01	50.18	08:37	50.4	65.9
<b>Average</b>		50.342	50.31		50.365	65.955
<b>COV</b>		$6.7 \times 10^{-3}$	$4.9 \times 10^{-3}$		$5.4 \times 10^{-3}$	$0.9 \times 10^{-3}$

Experiments B1-B4 illustrate the effect of processing on the rheological behaviour of fresh milk concentrates. Age thickening was more prominent after the concentrate heater than the evaporator.

The evaporated milk concentrates are temporarily stored in the concentrates balance tanks prior to the concentrates heater. At this point, the concentrate is held for a variable residence time at low shear rate, and age thickening can occur. This was evidenced by

the increase in extrapolated time-zero average viscosity value at the concentrate heater in comparison to that after the evaporator. In other words, the initial viscosity values of milk concentrate samples taken after the concentrate heater would be higher than those taken after the evaporator.

If milk concentrate samples were to be taken from other parts in the process, such as before and during evaporation, they would likely yield different rheological behaviour to those observed so far. For example, during evaporation, the solids content of the concentrate changes as it moves through the system. One would expect the rheological behaviour to change with the change in solids content and heat treatment during the various stages of evaporation.

#### **4.2 Effect of plant design on the rheology of fresh milk concentrate systems**

In November 2001, due to the large milk supply during the peak period, several evaporators were used to cope with the milk influx at the Te Awamutu milk powder plant. Two evaporators, evaporator #1 and a smaller evaporator #4, were used in the skim milk powder plant to handle the large volume of milk. Different milk concentrates from these two evaporators had been evaluated in previous experiments, with evaporator #4 in experiments B1 and B2, and evaporator #1 in experiment B3.

Experiment B5 was conducted in this period of November 2001 when both evaporators 1 and 4 processed the same batch of milk. The general composition of the milk system was similar to that in Table 4.1. The plant operating conditions in experiment B5 are listed in Tables 4.4. The viscosity-time curves of the milk concentrate samples collected from evaporator #1 and #4 are shown in Figures 4.7 and 4.8.

Table 4.4: Plant processing conditions in experiment B5 at the Te Awamutu skim milk powder plant.

Date	B5	B5
<b>Process Variables</b>	<b>Evap. #1</b>	<b>Evap. #4</b>
Milk feed temperature (°C)	14.4	14.4
DSI temperature (°C)	86	92
Evaporator's milk flow rate (m <sup>3</sup> /hr)	35	30
Evaporator feed balance tank level (%)	70	55
1 <sup>st</sup> effect temperature (°C)	66.8	71.6
1 <sup>st</sup> effect TVR steam pressure	720	620
Evaporator concentrate temperature (°C)	47.5	55.6
Evaporator concentrate total solids (%TS)	50	49
Concentrate heater milk temperature (°C)	64	64

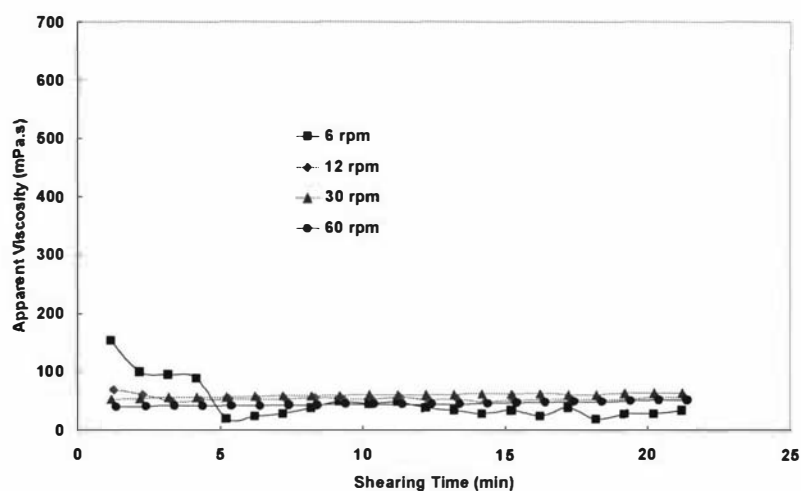


Figure 4.7: Change in viscosity with shearing time for fresh skim milk concentrate samples taken after the evaporator #1 at the Te Awamutu skim milk powder plant. Experiment B5, Brookfield LVTD, 50%TS, 47.5°C.

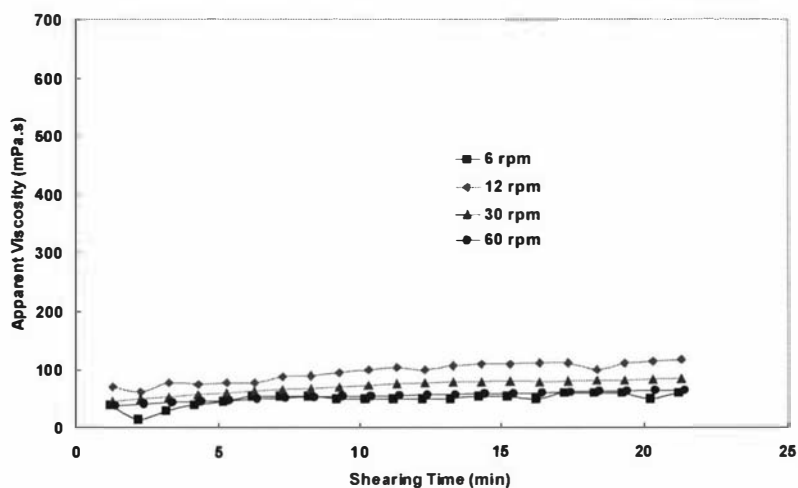


Figure 4.8: Change in viscosity with shearing time for fresh skim milk concentrate samples taken after the evaporator #4 at the Te Awamutu skim milk powder plant. Experiment B5, Brookfield LVTD, 50%TS, 55.5°C.

The viscosity data for the milk from the evaporators #1 in Figure 4.7 remained flat over 20 minutes of constant shear at various spindle speeds. The average viscosity value for all data collected from evaporator #1 in Figure 4.7 was 53mPa.s, compared to 68mPa.s obtained from evaporator #4 in Figure 4.8.

Figure 4.8 shows a more distinct separation between the four curves than that seen in Figure 4.7. The curves in Figure 4.8 also displayed a small, but noticeable increase in apparent viscosity with time, which was not seen in Figure 4.7.

The solids content of the concentrates from the two evaporators were similar as shown in Table 4.6, but the temperatures and the temperature history during evaporation differed significantly between the two configurations. The flow rate of the milk concentrate was higher in evaporator #1. The DSI temperature during preheat was also lower in evaporator #1 than #4. Unfortunately, no whey protein nitrogen index (WPNI) data, which measures the degree of whey protein denaturation during preheating, were available for comment. The combination of these differences in the operating variables

may have caused the discrepancies in rheological behaviour between the two evaporator systems.

The exercise was repeated in experiment B6 where evaporators #1 and #4 were utilised to handle the large volume of daily milk in December 2001. The product composition and plant operating conditions in experiment B6 were comparable to that in experiment B5. Similar observations were made in experiment B6, where the viscosity-time curves were flat from evaporator #1, but showed a slight increasing trend from evaporator #4.

Experiment B7 monitored the rheological behaviour of a skim milk concentrate system at the Waitoa milk powder plant where three evaporators fed into the same balance tank. Milk samples were collected at three points at the Waitoa plant, at the density meter, the filter after the concentrate balance tank, and the concentrate heater. The density meter was located immediately after the evaporator. The milk concentrate was then pumped to the concentrate balance tank. Filters were located at the exit of the concentrate balance tank to remove large particles before the milk is passed to the homogeniser, concentrate heater and the spray drier.

Table 4.5 lists the general composition of the milk product, and Table 4.6 lists the operating conditions during processing. Age thickening profiles after the density meter and filters were obtained for evaporator systems #1 and #3. Figures 4.9 and 4.10 plotted the evaporator data for systems #1 and #3 respectively, while Figures 4.11 and 4.12 plotted the filter data.

Table 4.5: General composition of the skim milk concentrates in experiment B7 at the Waitoa milk powder plant.

Component	%
Ash	7.9
Lactose	54.1
Moisture	3.8
Protein	33.4
Fat	0.8

Table 4.6: Plant processing conditions in experiment B7 at the Waitoa milk powder plant.

Experiment	B7	B7
Process Variables	Evap. #1	Evap. #3
DSI temperature (°C)	77	77
Evaporator feed flow rate (m <sup>3</sup> /hr)	59	59
Evaporator concentrate flow rate (m <sup>3</sup> /hr)	12	12
Evaporator feed balance tank level (%)	60	70
1 <sup>st</sup> effect temperature (°C)	70	71
Evaporator concentrate temperature (°C)	54	54
Evaporator concentrate total solids (%TS)	48	48
Concentrate heater milk temperature (°C)	63	63
Concentrate balance tank level (%)	20	25

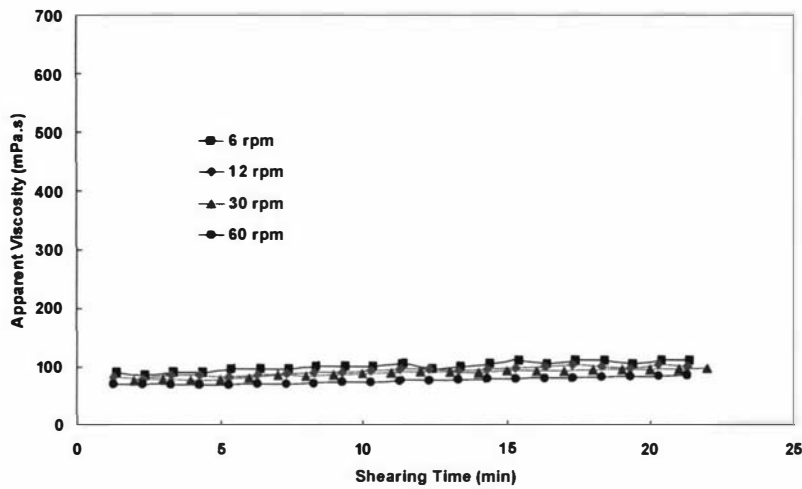


Figure 4.9: Change in viscosity with shearing time for fresh skim milk concentrate samples taken after the density meter #1 at the Waitoa milk powder plant. Experiment B7, Brookfield LVTD, 48%TS, 54°C.

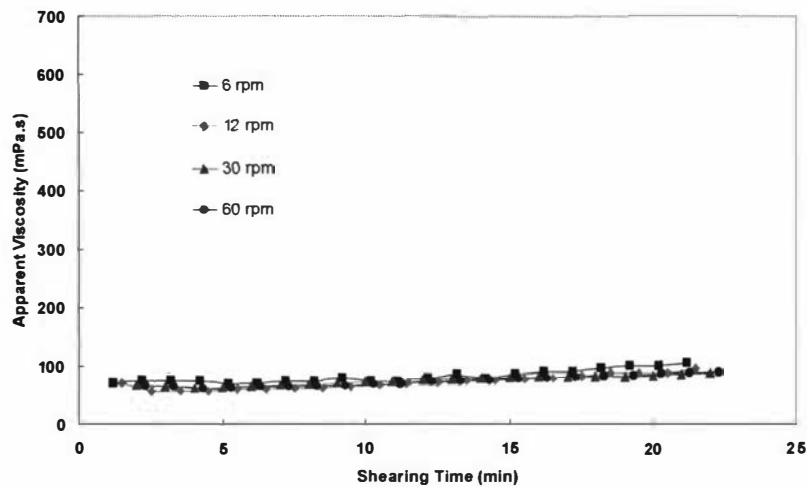


Figure 4.10: Change in viscosity with shearing time for fresh skim milk concentrate samples taken after the density meter #3 at the Waitoa milk powder plant. Experiment B7, Brookfield LVTD, 48%TS, 54°C.

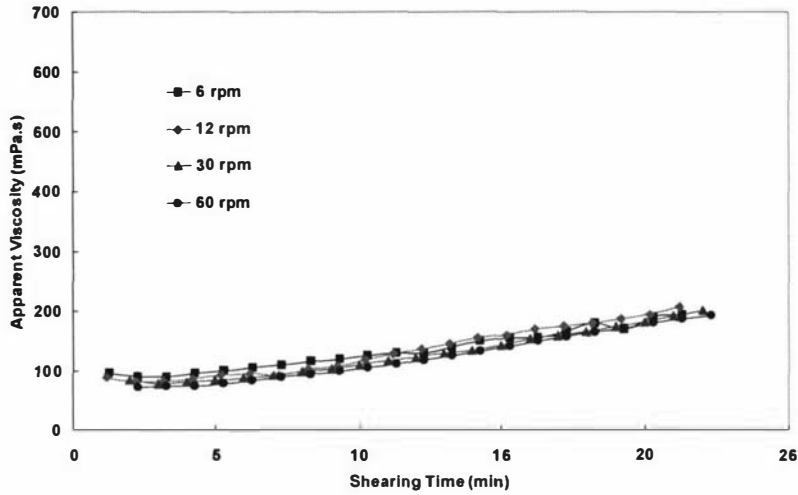


Figure 4.11: Change in viscosity with shearing time for fresh skim milk concentrate samples taken after the filter #1 at the Waitoa milk powder plant. Experiment B7, Brookfield LVTD, 48%TS, 54°C.

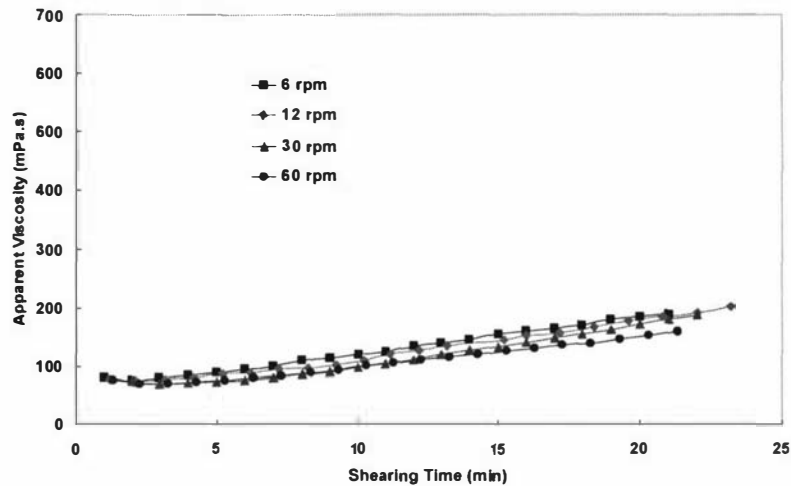


Figure 4.12: Change in viscosity with shearing time for fresh skim milk concentrate samples taken after the filter #3 at the Waitoa milk powder plant. Experiment B7, Brookfield LVTD, 48%TS, 54°C.

The data for samples taken at the density meter showed flat curves, with no significant increase in viscosity over time in Figures 4.9 and 4.10. Age thickening was seen in Figures 4.11 and 4.12, with samples from the filters where the apparent viscosity was

found to increase approximately two-fold in all curves. The trends between the two graphs were similar, within 10% error, reflecting the similar operating conditions between the two evaporator systems

There were no heating steps between the density meter and the filters, so both the temperature and the solids concentration were similar in all samples at the two processing steps. The cause for the onset of age thickening in the filter samples could thus not be attributed to a temperature effect but must be related to the residence time between the density meter and the filter.

Rheological data was only collected at one concentrate heater due to logistical constraints. Thus, it was not possible to compare the age thickening profile between the two concentrate heater lines.

The results from experiments B5-B7 showed that there is a strong correlation between processing conditions and plant design on the one hand and the rheological behaviour of the heated milk concentrates on the other.

An additional experiment was carried out at the Te Awamutu skim milk plant to complement the results obtained so far. In experiment B8, high heat skim milk concentrate samples were obtained at the filter for both evaporators, as well as from two concentrate heaters. The evaporators were operated under different conditions, while the concentrate heaters were similar in design and operating conditions. The general composition specification of the milk system was similar to that in Table 4.1. Table 4.7 lists the plant operating conditions in run B8.

Table 4.7: Plant processing conditions in experiment B8 at the Te Awamutu skim milk powder plant.

<b>Experiment</b>	<b>B9</b>	<b>B9</b>
<b>Process Variables</b>	<b>Evap. #2</b>	<b>Evap. #4</b>
DSI temperature (°C)	110	110
Evaporator feed flow rate (m <sup>3</sup> /hr)	36	30
Evaporator concentrate flow rate (m <sup>3</sup> /hr)	6.4	5
1 <sup>st</sup> effect temperature (°C)	67	76
Evaporator concentrate temperature (°C)	47	60
Evaporator concentrate total solids (%TS)	46	46
Concentrate heater milk temperature (°C)	66	66
Concentrate balance tank level (%)	50	70

The viscosity-time plots for the evaporators #2 and #4 are shown in Figures 4.13 and 4.14 respectively, while those data for concentrate heaters #2 and #4 are shown in Figures 4.15 and 4.16. The trends in the two evaporator graphs in Figures 4.13 and 4.14 showed a small but noticeable difference in the tendency to age thicken, which is more prominent in Figure 4.14 (for the evaporator #4 with a two fold increase in viscosity) than in Figure 4.22 (roughly 1.5 fold increase).

The viscosity-time data for the two different concentrate heaters in Figures 4.15 and 4.16 showed similar rates of age thickening within 10% error. Thus, the discrepancies in rheological profile after the evaporators were removed during concentrate heating under similar conditions.

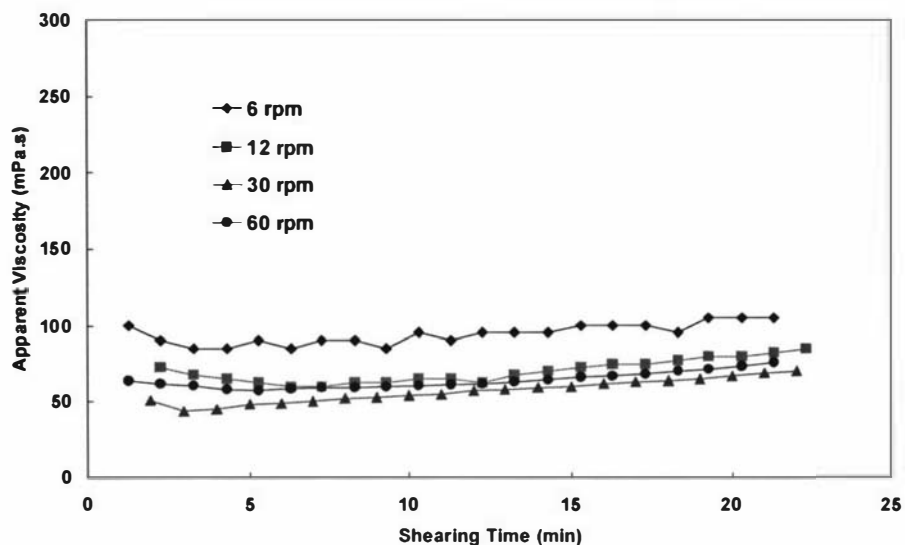


Figure 4.13: Change in viscosity with shearing time for fresh skim milk concentrate samples taken after the evaporator #2 at the Te Awamutu skim milk powder plant. Experiment B8, Brookfield LVTD, 46.2%TS, 47.5°C.

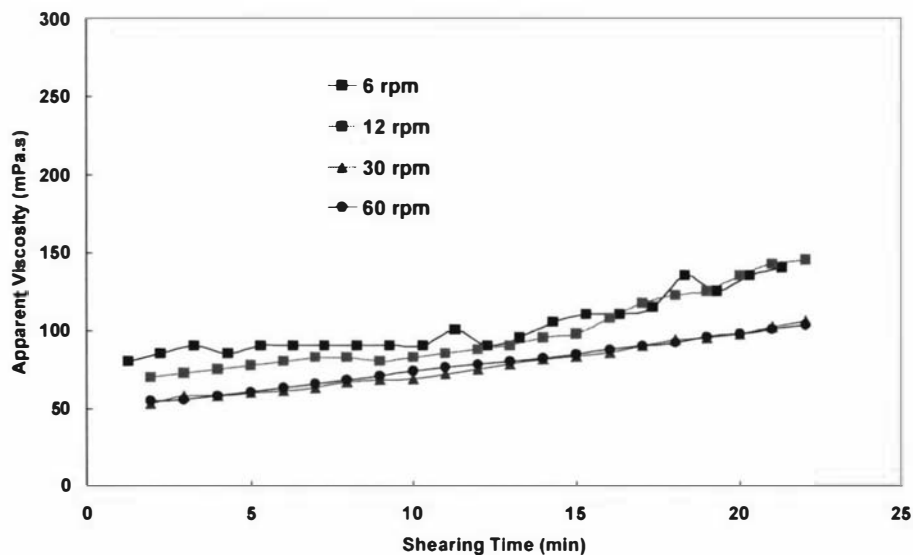


Figure 4.14: Change in viscosity with shearing time for fresh skim milk concentrate samples taken after the evaporator #4 at the Te Awamutu skim milk powder plant. Experiment B8, Brookfield LVTD, 46.4%TS, 60°C.

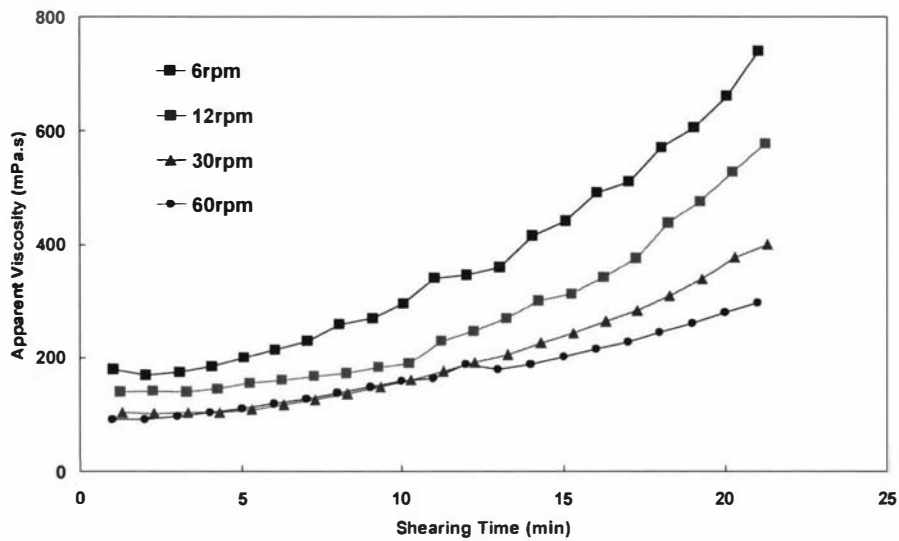


Figure 4.15: Change in viscosity with shearing time for fresh skim milk concentrate samples taken after the concentrate heater #2 at the Te Awamutu skim milk powder plant. Experiment B8, Brookfield LVTD, 46%TS, 66°C.

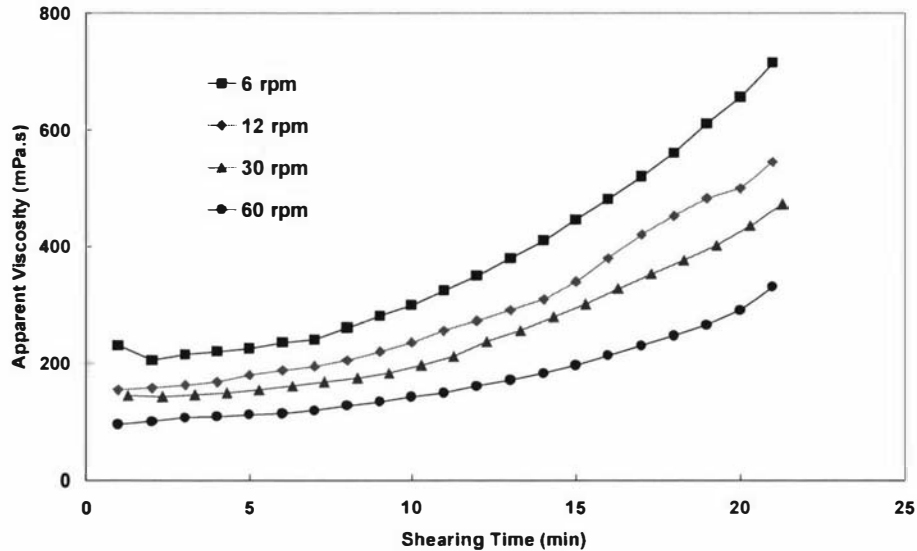


Figure 4.16: Change in viscosity with shearing time for fresh skim milk concentrate samples taken after the concentrate heater #3 at the Te Awamutu skim milk powder plant. Experiment B8, Brookfield LVTD, 46%TS, 66°C.

The operating conditions were significantly different between the two evaporation systems, as shown in Table 4.7. During evaporation, milk in evaporator #4 was subjected to consistently higher temperatures than that in evaporator #2. Lower flow rate was also encountered in evaporator #4. The combination of high temperature and low shear may have contributed to the age thickening observed in evaporator #4.

The results illustrated the effect of equipment design, plant configuration and operating conditions on the rheological behaviour of milk concentrate systems. Where the configuration and operating conditions of the evaporation and concentrate heating systems are significantly different, such as found at the Te Awamutu plant, visible discrepancies in the tendency to age thickening in the evaporator milk concentrates were observed. However, such discrepancies in the rate of age thickening of fresh milk concentrates were not observed when the plant design and operating conditions were similar between process lines, such as that encountered at the Waitoa milk powder plant.

### **4.3 Effect of solids content on the rheology of fresh milk concentrate systems**

Figures 4.17 and 4.18 compare the tendency to age thicken of samples after the concentrate heater for experiments B5 and B6. These experiments were conducted on the same skim milk supply at the same Te Awamutu skim milk plant with similar operating conditions and plant configuration. However, experiment B6 was conducted shortly after the plant was started up, when there were significant fluctuations in operating conditions. This resulted in a considerable temporary increase in solids content, from 50%TS in B5, to 52%TS in B6. To capture the full extent of age-thickening in both experiments the y-axis scale on the two graphs was extended to 6000 mPa.s.

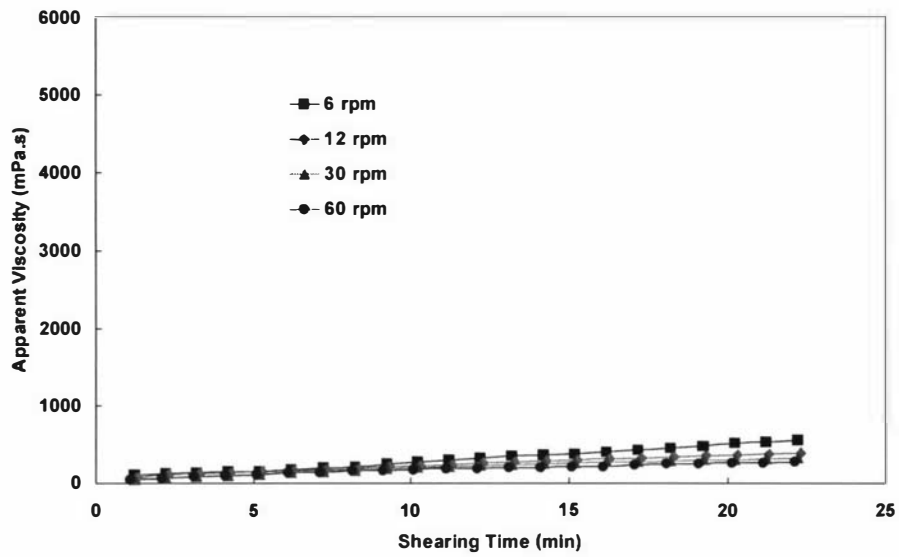


Figure 4.17: Change in viscosity with shearing time for fresh skim milk concentrate samples (50%TS, 66°C) taken after the concentrate heater at the Te Awamutu skim milk powder plant. Experiment B5, Brookfield LVTD.

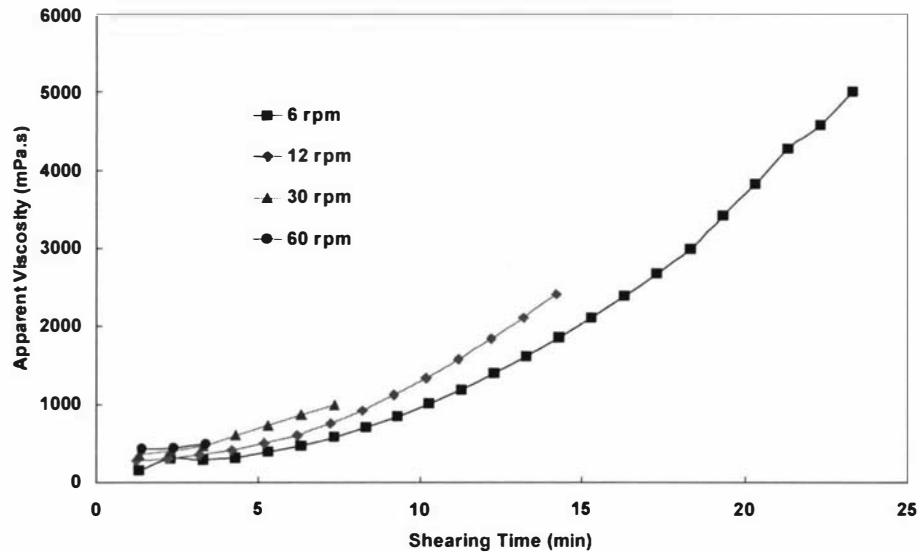


Figure 4.18: Change in viscosity with shearing time for fresh skim milk concentrate samples taken (52%TS, 66°C) after the concentrate heater at the Te Awamutu skim milk powder plant. Experiment B6, Brookfield LVTD.

An increase in 2%TS resulted in a significant increase in the rate of age thickening. In Figure 4.17, an average four fold increase over about 29 minutes was observed in all four viscosity-time curves. In Figure 4.18, the 6 rpm curve showed a remarkable 32 times increase in viscosity over 20 minutes of constant shear. Thus the control of concentrate total solids is very important for the control of concentrate rheology.

It is also interesting to note that the data in Figure 4.18 may suggest shear thickening behaviour in the milk concentrates. It is unclear why such a peculiar behaviour is observed. The 60 rpm curve only contained 3 data points and this was due to the limitation of measurement range of the Brookfield viscometer.

#### **4.4 Effect of preheat treatment on the rheology of fresh milk concentrate systems**

The effect of preheat treatment intensity on the rheological behaviour of concentrates after evaporation and concentrate heating was analysed by following production runs for low, medium and high heat skim milk powders. The product compositions and operating conditions for four skim milk systems are shown in Tables 4.8 and 4.9 respectively. Experiments B1, B8 and B10 were conducted at the Te Awamutu skim milk plant. Experiment B9 with low heat skim milk was carried out at the Te Awamutu whole milk plant, due to its capability to process low heat products. Table 4.9 also shows the rate of age thickening in concentrate heater samples. The rates of age thickening were determined simply from the ratio of final to the initial viscosity.

Table 4.8: General composition of skim milk concentrates in experiments B9, B1, B8 and B10 at the Te Awamutu skim milk and whole milk powder plants.

Component	B9	B1	B8 & B10
Heat treatment	Low	Medium	High
Ash and Lactose	61	62.7	62.7
Moisture	4	3.65	3.65
Protein	34	33.0	33.0
Fat	1	0.65	0.65

Table 4.9: Plant processing conditions in experiments B9, B1, B8 and B10 at the Te Awamutu skim and whole milk powder plants.

Experiment	B9	B1	B8	B10
<b>Process Variables</b>				
Plant	TAWMP	TASMP	TASMP	TASMP
Evaporator	N/A	#1	#2	#1
Heat intensity	Low	Medium	High	High
DSI temperature (°C)	92	94	110	120
Holding time (s)	0	0	120	120
Evaporator feed flow rate (m <sup>3</sup> /hr)	53	27	34	36
1 <sup>st</sup> effect temperature (°C)	69		67	71
Evaporator concentrate temperature (°C)	40	64	48	48
Evaporator concentrate total solids (%TS)	47	46	46	46
Concentrate heater milk temperature (°C)	55	66	66	66
Rate of age thickening after concentrate heating	1	1.6	3.5	5

The rate of age thickening increased with the heat treatment intensity. No age thickening was observed in low heat skim milk concentrates at the Te Awamutu whole milk plant.

The data agreed with the observations made by Vilder and Moermans (1983) where the inline viscosity of fresh whole milk concentrates increased with preheat treatment. This

highlights the importance of temperature history in determining the rheological behaviour of milk concentrates during processing.

Similar observations were made in experiments B11 and B12 at the Waitoa milk power plant. The two sets of experiments were conducted on consecutive dates of production on the same instant infant powder products. The product compositions and production conditions for the two sets of experiments are listed in Tables 4.10 and 4.11.

Table 4.10: General composition of the infant milk concentrates in experiments B11 and B12 at the Waitoa milk powder plant.

Component	B11 & B12
Ash	5.6
Lactose	53.4
Moisture	2.5
Protein	21.5
Fat	17

Table 4.11: Plant processing conditions in experiments B11 and B12 at the Waitoa powder plant.

Date	B11	B12
<b>Process Variables</b>	<b>Evap. #1</b>	<b>Evap. #1</b>
DSI temperature (°C)	96	90
Holding time (s)	20	20
Evaporator feed flow rate (m <sup>3</sup> /hr)	62	58
Evaporator concentrate flow rate (m <sup>3</sup> /hr)	15	13
1 <sup>st</sup> effect temperature (°C)	69	70
Evaporator concentrate temperature (°C)	53	53
Evaporator concentrate total solids (%TS)	47.8	47.5
Concentrate heater milk temperature (°C)	72	78
Concentrate balance tank level (%)	18	18

The operating conditions for experiments B11 and B12 were similar, except for the higher DSI temperature encountered in B11. The holding time during preheat treatment was similar in both experiments. Thus, the higher DSI temperature in experiment B11 would have resulted in harsher preheat treatment on the milk products. Figures 4.19 and 4.20 plot the change in apparent viscosity with time for the concentrate heater samples from the two sets of experiments.

As the two experiments were conducted on the milk products with similar composition and plant configuration, the discrepancy in the age thickening profiles must be attributed to the operating conditions.

It is interesting to note that the concentrate heater temperature was higher in experiment B12, which should have resulted in a higher rate of age thickening. This was obviously not the case, as the rates of age thickening were more prominent in experiment B11, seen in Figure 4.19, than those in experiment B12 in Figure 4.20. It is possible that the harsher preheat treatment in experiment B11 played a more dominant role in the determination of the rheological profile of milk concentrates than that of the heating temperature at the concentrate heater.

Thus temperature history, especially preheat treatment, has a significant influence on the rate of age thickening in milk concentrates after concentrate heater.

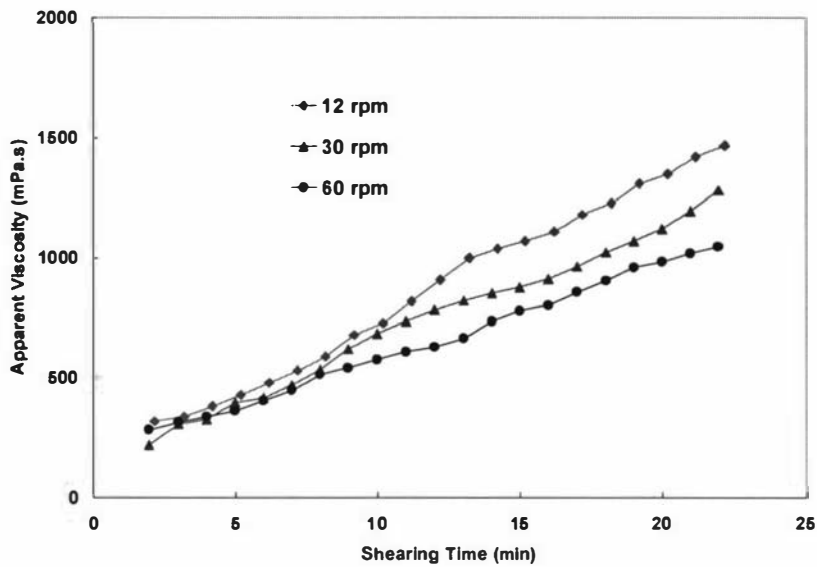


Figure 4.19: Change in viscosity with shearing time for fresh infant milk concentrate samples taken after the concentrate heater at the Waitoa milk powder plant. Experiment B11, Brookfield LVTD, 48%TS, 72°C.

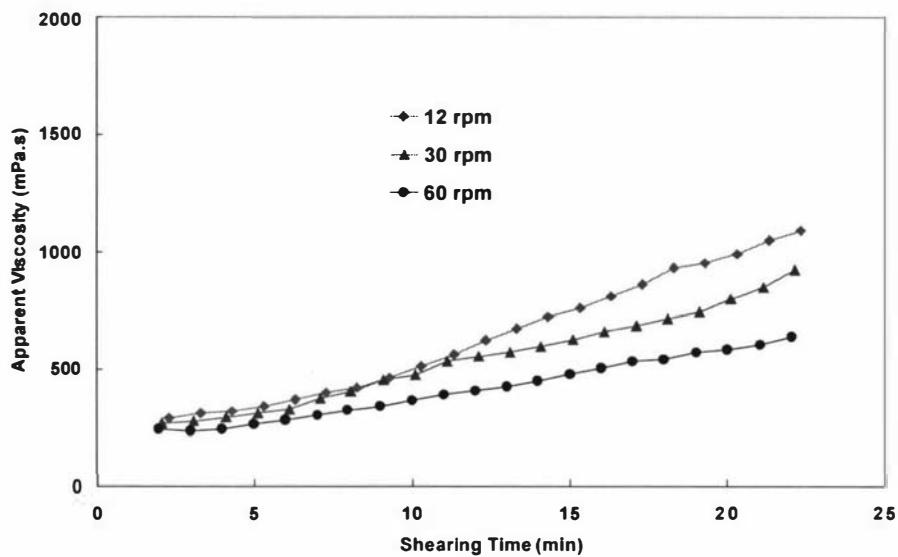


Figure 4.20: Change in viscosity with shearing time for fresh infant milk concentrate samples taken after the concentrate heater at the Waitoa milk powder plant. Experiment B12, Brookfield LVTD, 48%TS, 78°C.

#### 4.5 Effect of protein content on the rheology of fresh milk concentrate systems

Experiment B13 was performed at the Te Awamutu whole milk plant by monitoring the manufacture of a low heat skim milk product with high protein content. This was then compared with the data from experiment B9, another low heat skim milk product from the same plant, to study the effect of protein content on the rheological behaviour of milk concentrates. The product composition and operating conditions for experiments B9 and B13 are listed in Tables 4.12 and 4.13 and the age thickening profiles for the concentrate heater samples are plotted in Figures 4.21 and 4.22.

Table 4.12: General composition of the skim milk concentrates in experiments B9 and B13 at the Te Awamutu whole milk powder plant.

Component	B9	B13
Ash	7.5	7.8
Lactose	53.5	49.8
Moisture	4.0	3.8
Protein	34	37.8
Fat	1	0.8

Table 4.13: Plant operating conditions in experiments B9 and B13 at the Te Awamutu skim milk and whole milk powder plants.

<b>Experiment</b>	<b>B9</b>	<b>B13</b>
<b>Process Variables</b>		
Plant	TAWMP	TASMP
Heat intensity	Low	Low
DSI temperature (°C)	92	70
Holding time (s)	0	0
Evaporator feed flow rate (m <sup>3</sup> /hr)	53	55
1 <sup>st</sup> effect temperature (°C)	69	69
Evaporator concentrate temperature (°C)	40	37
Evaporator concentrate total solids (%TS)	47	46
Concentrate heater milk temperature (°C)	55	55
Rate of age thickening	1	2

The operating conditions listed in Table 4.13 showed that the skim milk products in run B9 received a harsher preheat treatment, and had a higher solids content than the product in run B13. With higher preheat and total solids, the concentrates in run B9 should show a higher rate of age thickening than in experiment B13, provided all other factors being the same in the two experiments. However, the opposite was observed in Figures 4.21 and 4.22.

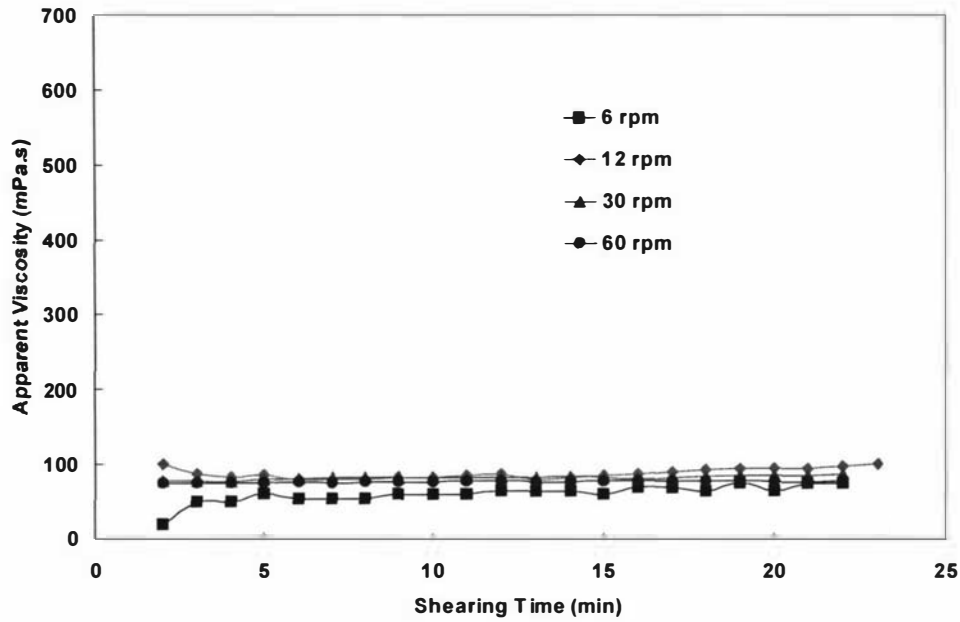


Figure 4.21: Change in viscosity with shearing time for fresh skim milk concentrate samples taken after the concentrate heater at the Te Awamutu whole milk powder plant. Experiment B9, Brookfield LVTD, 47.5%TS, 55°C.

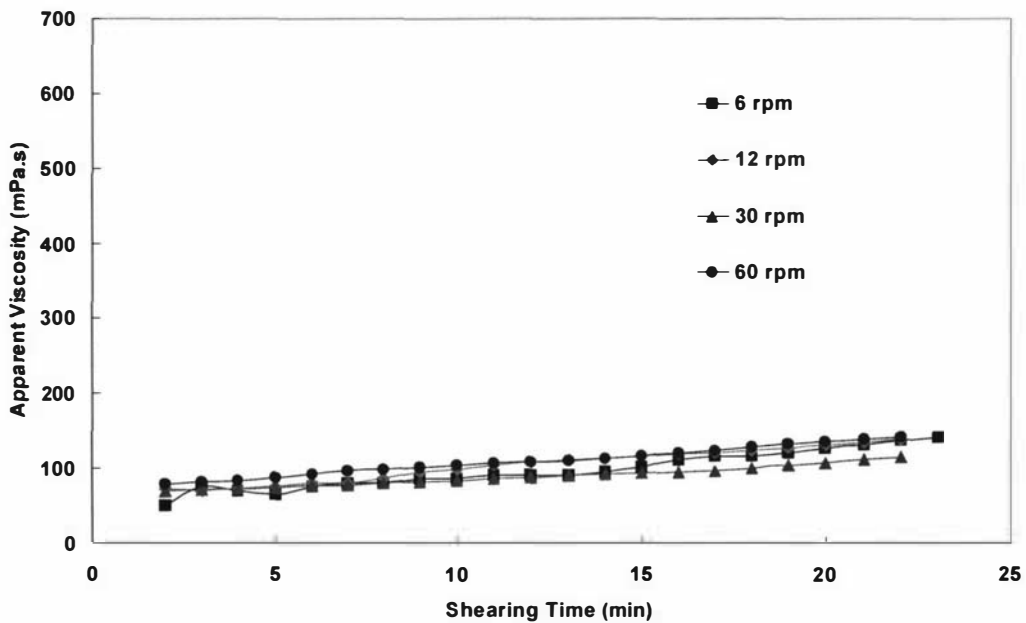


Figure 4.22: Change in viscosity with shearing time for fresh skim milk concentrate samples taken after the concentrate heater at the Te Awamutu whole milk powder plant. Experiment B13, Brookfield LVTD, 46%TS, 55°C.

In Figure 4.21, the viscosity remained unchanged with time when subjected to constant shear at various spindle speed. The concentrate heater data in Figure 4.22 clearly showed an increase in viscosity over 20 minutes of constant shear for all four spindle speeds. There was a two fold increase for most curves.

The noticeable age thickening observed in Figure 4.22 was likely to be caused by the increase in protein content. Future experiments would need to keep processing conditions constant, and only change the protein content in the milk concentrates to illustrate this point more clearly and definitely.

#### **4.6 Effect of shear rate during sampling on the rheology of fresh milk concentrate systems**

The rate of age thickening has been shown to be dependent on shear rate (Snoeren, Brinkhuis, Damman, & Klok, 1984). The shear rate applied is also widely known to have a significant influence on the subsequent rheological behaviour of time-dependent systems. However, there are no data in the literature that describe the effect of shear rate during sampling on the rheological behaviour of the milk concentrates (or time-dependent fluids).

At the Te Awamutu skim milk and whole milk plants, the concentrate heaters were situated before the homogeniser so that samples could be taken via taps from a low pressure line. However, this was not the case at the Waitoa powder plant where the concentrate heater was situated after the homogeniser. The samples were extracted via taps located in a high pressure line, at approximately 250 bar. In addition, the sampling taps at Waitoa were small and can only be slightly opened to prevent excess splashing of the hot milk concentrates during sampling. This resulted in an excessively high shear level being imposed on the fluids during sampling. This system gave rise to a de facto additional homogenization step for the concentrate samples collected. Two-stage

homogenization has been found to increase the viscosity values of whole milk concentrates (de Vilder et. al, 1979).

A low shear sampling module was put in place at the Waitoa milk powder plant. The module consisted of a chamber which could be isolated from both the high pressure line and atmospheric pressure. The system was first attached to the line and isolated from the atmosphere to allow the chamber pressure to almost equilibrate with the line pressure during sampling. The chamber was isolated from the line and the pressure in the chamber released before the sample was withdrawn. A schematic diagram of the low shear sampler is shown in Figure 4.23.

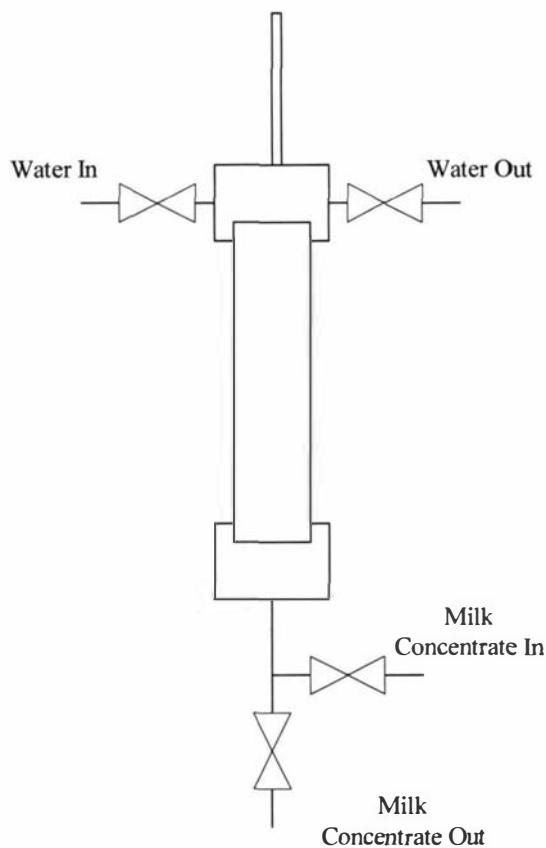


Figure 4.23: Schematic diagram of the low shear sampler at the Waitoa milk powder plant.

For both methods of sampling, fresh milk concentrate samples were withdrawn from the high pressure concentrate line. The difference between the two methods lay in the shear level enforced on the fluids during the actual withdrawal stage.

Experiment B14 was carried out at the Waitoa plant using both the high and low shear sampling techniques. Rheological measurements were made with both the Brookfield LVTD and the Paar Physica MCI rheometers. The general compositional specification of the powder and the operating conditions for experiment B14 are listed in Tables 4.14 and 4.15 respectively.

Table 4.14: General composition of the infant milk concentrates in experiment B14 at the Waitoa milk powder plant.

Component	B14
Ash	4
Lactose	55.5
Moisture	2.5
Protein	18
Fat	20

Table 4.15: Plant operating conditions in experiment B14 at the Waitoa milk powder plant.

Experiment	B14
<b>Process Variables</b>	
DSI temperature (°C)	96
Holding time (s)	20
Evaporator feed flow rate (m <sup>3</sup> /hr)	53
1 <sup>st</sup> effect temperature (°C)	70
Evaporator concentrate temperature (°C)	52
Evaporator concentrate total solids (%TS)	47
Concentrate heater milk temperature (°C)	74

With the use of the Brookfield LVTD, samples collected directly from the high pressure concentrate lines showed higher rates of age thickening at constant viscometer spindle speed than samples taken through the low-shear sampler (results not shown). At 12 rpm the high-shear concentrate samples showed a five fold increase in viscosity after 20 minutes of constant shear compared to just a two fold increase the low-shear sampled concentrate.

The data from the Paar Physica MC1 is shown in Figure 4.24. The samples were collected from the concentrate lines and stored in a water bath at 74°C. Rheological measurements were then made at regular intervals. The changes in apparent viscosity with storage time were plotted. Age thickening was more prominent in samples which were taken via the high shear taps. This was in good agreement with the observations made with the Brookfield LVTD viscometer.

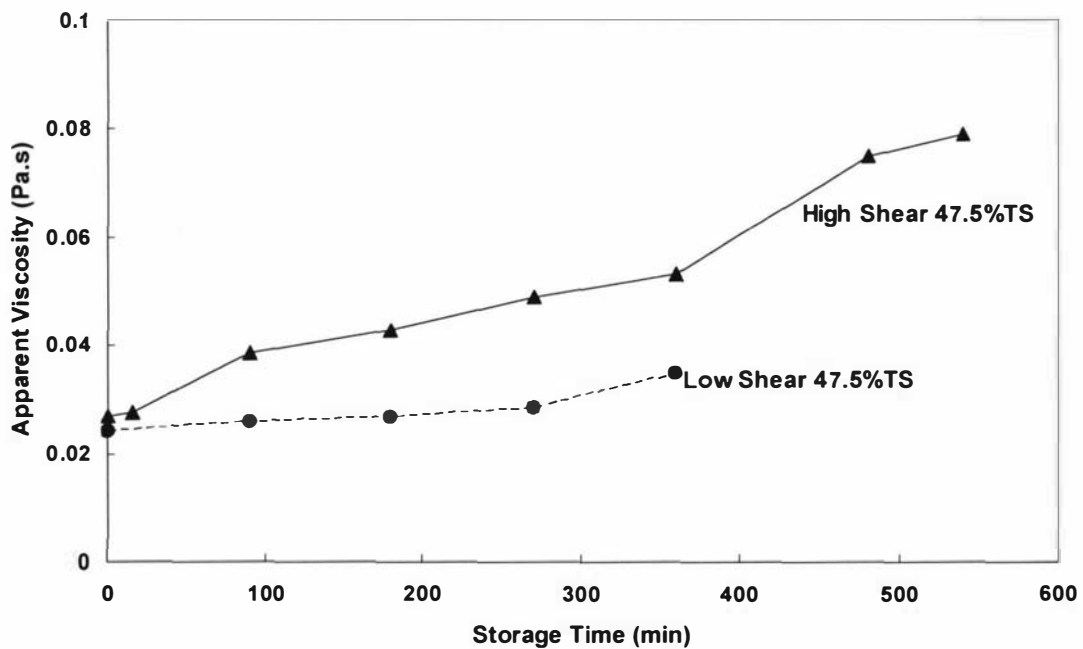


Figure 4.24: Effect of shear level during sampling on the rate of age thickening of fresh infant milk concentrate samples taken after the concentrate heater at the Waitoa milk powder plant. Experiment B14, Paar Physica MC1, 47.2%TS, 72°C, apparent viscosity at 105.3 Pa.

The flow curves for the high shear and lower shear sampling data were fitted with the Herschel-Bulkley model, and the results are shown in Figure 4.25. For both sets of data,  $\tau_y$  and  $K$  increased while  $n$  decreased with storage time at 75°C.

Sampling using the low shear sampling module significantly reduced the values of  $\tau_y$  and  $K$  during age thickening at 75°C. The quasi lack of build up in structure in this sample when stored at rest is evident in the smallness of the increase in apparent viscosity at a given shear stress with storage time seen in Figure 4.24.

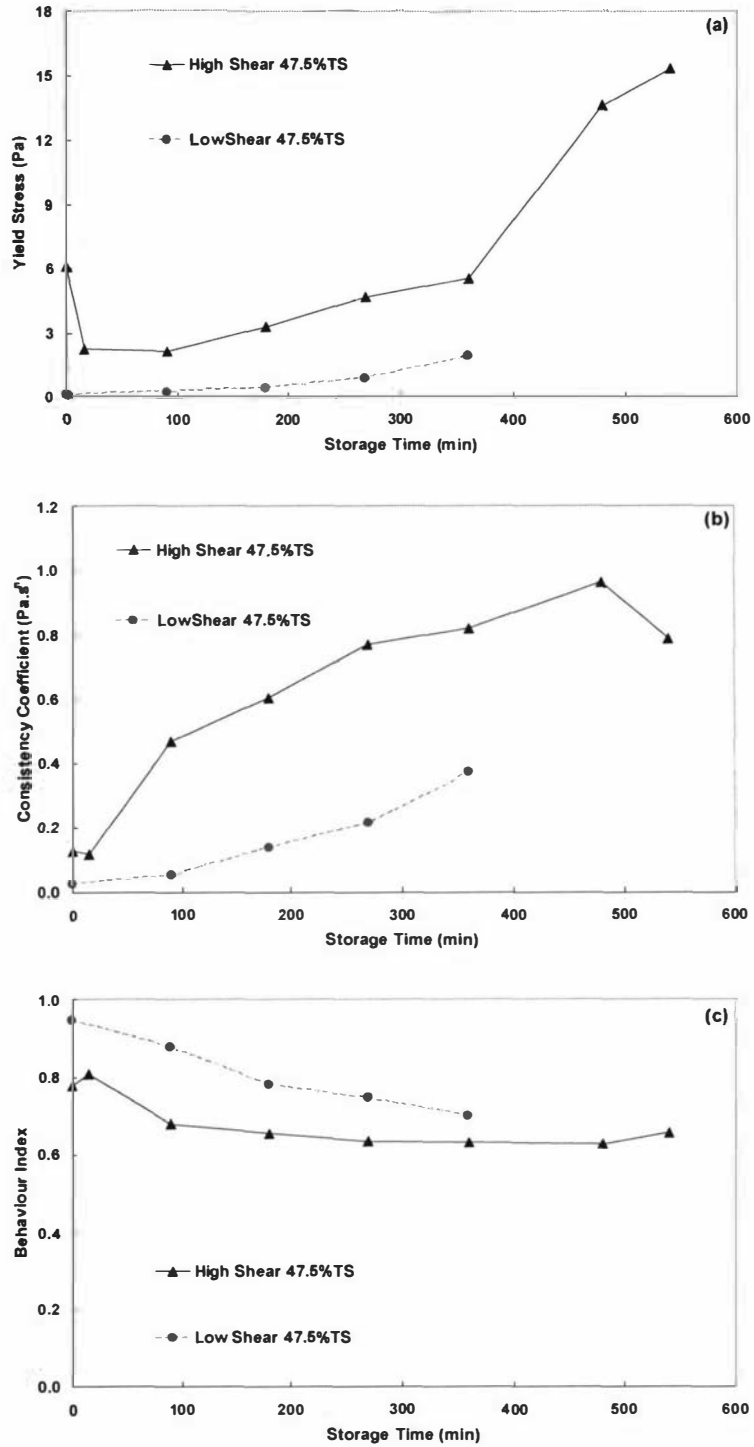


Figure 4.25: Changes in the Herschel Bulkley model parameters for 47.5%TS with storage time at 75°C. (a) yield stress  $\tau_y$ ; (b) consistency coefficient  $K$ ; (c) behaviour index  $n$ .

The effect of shear level during sampling was also analysed in experiments B11 (Figure 4.19) and B12 (Figure 4.20), which were also conducted at the Waitoa milk powder plant with the Brookfield LVTD viscometer. In these two experiments, samples collected from the high pressure concentrate lines showed a 4 fold increase in viscosity over 20 minutes of constant shear, compared to just a twofold increase observed in samples from the low shear module. This is in good agreement with observations made in experiment B14.

The results showed the importance of shear level during sampling and its effect on the rheological profile of the time-dependent systems. The choice of a suitable shear level during sampling in time-dependent systems is not widely known, has not been discussed in the literature and remains an unanswered question. The results from experiments B11, B12 and B14 indicated that high shear sampling results in a significant increase in viscosity and age thickening. Sampling after the concentrate heater at low shear yielded initial viscosity values that were similar to those after the density meter and the filter systems. More experimental work is required to obtain a better understanding of the relationship between sampling shear level and the resultant rheological behaviour of time-dependent systems.

---

**CHAPTER 5**

**CONTROLLED**

**RHEOLOGY**

**EXPERIMENTS**

---

# CHAPTER 5: CONTROLLED RHEOLOGY EXPERIMENTS

This chapter presents the controlled experimental results obtained mainly at Massey University, Palmerston North, New Zealand.

There were four main aims of the exercise:

1. To develop a new methodology for analysing the rheology of time-dependent systems
2. To understand the effect of several processing variables on the rheology of milk concentrates upon heating and subsequent storage
3. To obtain structural measurements of milk concentrates during age-thickening
4. To provide a better understanding of the age-thickening process.

Section 5.1 presents new methods of data analysis to provide a more comprehensive picture of the age thickening process. Such techniques have been not available in the past and thus restricted the amount of information that could be extracted from the raw flow curve data.

The majority of the experimental runs in this chapter were carried out on reconstituted milk concentrates. Section 5.2 compares the rheological behaviours of fresh and reconstituted systems. In doing so, the section investigates the legitimacy of using reconstituted systems to study the rheological behaviour of fresh concentrates.

The effect of processing variables during reconstitution is shown in sections 5.3-5.7. The results show that when working with time-dependent systems, such as milk concentrates, any processing steps that contribute to the shear and temperature history profiles have a significant effect on the rheological behaviour of the end product.

Section 5.8 investigates the change in structure of reconstituted whole and skim milk concentrates during age thickening. The section also compares the changes in structure with the changes in rheological behaviour during age thickening in a single

run. Such data is rarely available in the literature. Section 5.9 presents data from a novel experimental technique which examines the reversibility of the age thickening process.

## 5.1 Rheological characterisation of whole milk concentrate systems

The rheological behaviour of time-dependent fluids has been often studied with measurement of both viscoelasticity and thixotropy. Viscoelasticity is mainly measured with an oscillatory test that monitors the material's response to small reversible deformations. The present study is aimed at rheological behaviour during transport and processing which involve much larger deformations. Therefore shear sweep and shear step tests (where high shear rates can be applied) are more appropriate.

Many studies of time-dependent behaviour in multiphase systems have been based on the assumption that structural changes are fully reversible and structural recovery after the removal of the shear stress is complete (Cheng, 1987; Barnes, 1997). This assumption implies that there is a unique equilibrium shear stress- shear rate curve. At equilibrium point, the rate of break down is equal to the rate of build-up, and thus there is a zero net change in structure. In other words, for a given shear stress, there is only one equilibrium shear rate, and thus one equilibrium apparent viscosity, provided that the samples is allowed to be sheared for a sufficient period of time to reach the equilibrium state. The use of this equilibrium flow curve removes the influence of shear history. Obtaining the equilibrium flow condition can be time consuming in systems where the structural changes are slow.

Shear sweep tests are quick and simple. The shear stress - shear rate data are fitted with phenomenological models, and the changes in the model parameters can be followed with time to analyse the time-dependent behaviour (Velez-Ruiz & Barbosa-Canovas, 1997, 2000; Trinh & Schraekenrad, 2002; Ma et al., 2002). Sometimes, the rheological measurement can be further simplified to just a single point measurement, which is commonly used for quality control but provides little information about the rheology of the products (Beeby, 1966; Newstead et al., 1978; Baldwin et al., 1980; Bloore & Boag, 1981; Vilder & Moermans, 1983; Gasseem & Frank, 1991).

In many real systems, particularly food systems, the complex nature of the composition and interactions between the components can give rise to irreversible

reactions. Age thickening is a well known phenomenon in many dairy products where the viscosity increases during storage at rest. The phenomenon is accompanied by physical and chemical changes that are irreversible (Samel & Muers, 1962) and culminate in gelation with possible syneresis, such as in yoghurt (Steventon et al., 1990). Such irreversible changes invalidate the assumption of an equilibrium flow curve, the basis for many analyses of reversible thixotropy.

This section discusses the procedure developed in this work for rheological characterisation of time-dependent fluids, whether reversible or not. The procedure uses the shear sweep data at different periods of storage to capture the instantaneous snapshots of rheological behaviour. The technique can only work if the time scale of the shear sweep experiments is much shorter than the period of storage. The shear sweep data can be supplemented with oscillatory tests to provide complementary data on linear viscoelasticity. However, oscillatory tests were not attempted in the present work, which concentrated the effort on high shear deformations.

### **5.1.1 Materials and Methods**

Medium heat whole milk powder A was used in this section. In run C1, the powder A was reconstituted to 48%TS at 35°C and 40,000s<sup>-1</sup>, and then heated to 65°C before being stored in a 65°C hot water bath.

### **5.1.2 Results**

#### **5.1.2.1 Basic flow Curve**

Figure 5.1 shows the flow curve as well as change in the apparent viscosity with shear rate for the heated 48%TS reconstituted concentrate sample after 150 minutes of storage at 65°C. The decrease in the apparent viscosity with shear rate showed shear thinning behaviour, which is often observed in milk concentrates (Velez-Ruiz & Barbosa-Canovas, 1997, 1998, 2000; Bienvenue, Jimenez-Flores, & Singh, 2003a, 2003b). The shear up and shear down flow curves showed that the heated concentrate

sample was time-dependent exhibiting a well defined hysteresis effect between the shear up and shear down legs.

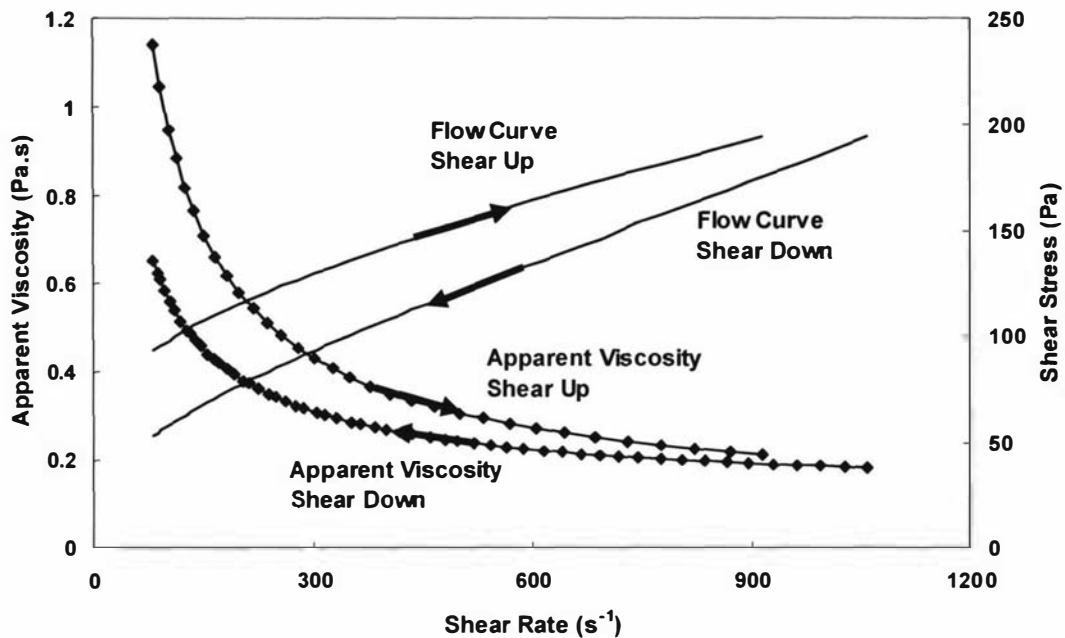


Figure 5.1: Shear sweep curves and change in apparent viscosity with time for 48%TS heated reconstituted whole milk concentrates after 150 minutes of storage at 65°C. Run C1.

### 5.1.2.2 Rheological descriptors of time-dependent fluids

Much more information could be extracted from the basic flow curve in Figure 5.1 but the total information contained in all the instantaneous snapshots was so large that it must be broken down into several separate descriptors.

#### 5.1.2.2.1 Apparent viscosity

The change in rheological behaviour during age thickening is sometimes illustrated by plotting apparent viscosity against shear rate for different storage times (Bienvenue et al., 2003a, 2003b). In this work, it was found that the age thickening process could be more easily visualised by following the evolution of the apparent viscosity with time. This apparent viscosity must always be determined at a constant reference shear rate

or shear stress depending on the operating mode of the rheometer. Figure 5.2 plots the change in apparent viscosities for the 48%TS sample at three different reference shear stresses from the shear-up leg of the flow curves. As expected for a non-Newtonian fluid, there are differences between the viscosities at different reference shear stresses. There is also a difference between the trends calculated from the shear-up and shear-down legs, as shown in Figure 5.3 for the reference shear stress of 105.3 Pa. The viscosities calculated from the shear-down leg are lower. This is because the shear-up sweep was performed first and has already broken down the original structure to some degree before the shear-down sweep. The behaviour of the shear down leg is very dependent on the history of the shear-up sweep and does not provide an accurate picture of the original structure of the stored sample. Thus, in subsequent analyses only data from the shear-up leg will be presented.

The shapes of all the curves in Figures 5.2 and 5.3 are similar. The apparent viscosity showed a region of slow but steady initial increase, followed by a region of rapid rise. The point at which the viscosity showed a rapid increase with time can be used to identify the onset of gelation (Clark, 1992). This point is determined by visual inspection. According to Clark (1992), gelation involves firstly the slow formation of individual clusters that are randomly dispersed throughout the aqueous phase. As the number and size of the clusters grow, the viscosity increases, reflecting the increase in resistance to flow. At the point of gelation, one particular cluster reaches a critical size and shape, so that future associations between components and clusters take place via this one cluster. These associations will quickly lead to the development of a three-dimensional solid network throughout the system.

The rate of age thickening up to the point of gelation, illustrated by the change in apparent viscosity with time, decreased with an increase in shear stress, as shown in Figure 5.2. This is in agreement with the observations of Snoeren et al. (1982), even though they plotted the apparent viscosity against shear rate. However, the same gelling time is indicated by all curves in Figures 5.2 and 5.3.

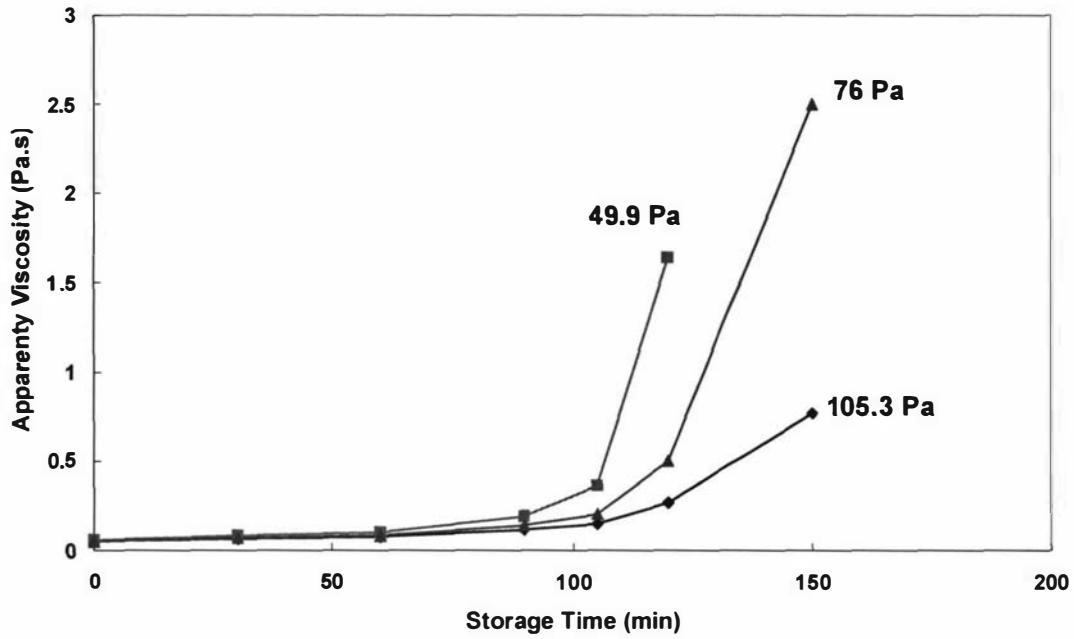


Figure 5.2: Apparent viscosity of 48%TS reconstituted whole milk concentrate sample during storage at 65°C at three different shear stress values. Calculated from the shear-up legs.

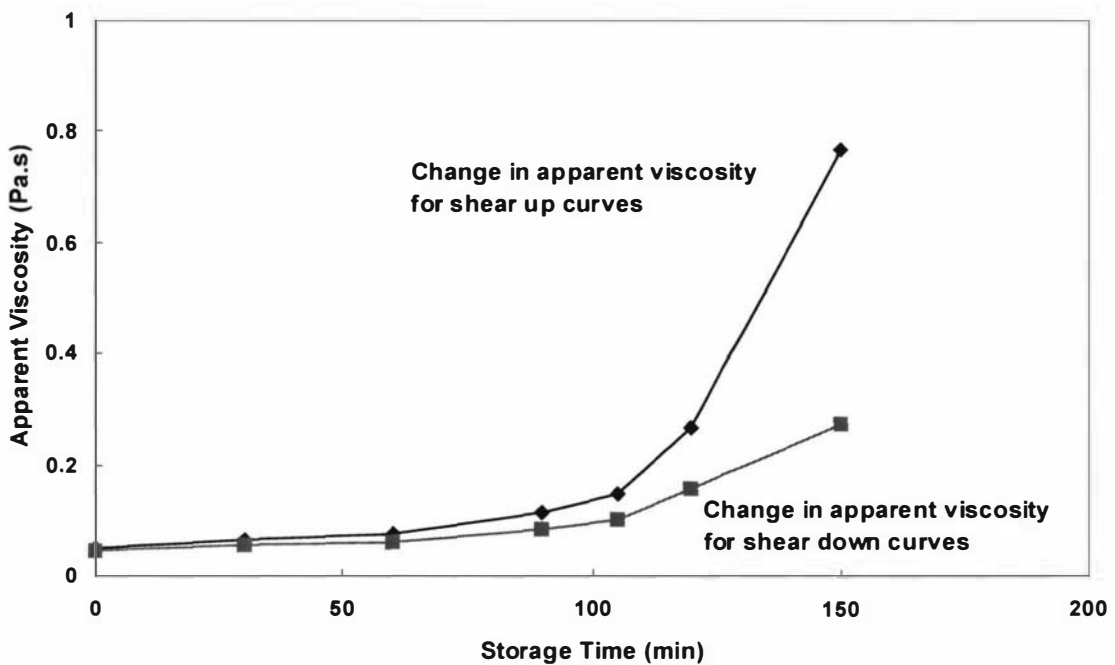


Figure 5.3: Apparent viscosities of 48%TS reconstituted whole milk concentrate sample calculated for shear up and shear down legs of the flow curves at the reference shear stress of 105.3 Pa. Run C1.

The presence of the gelling point during age thickening has never been reported in the literature. This provides a new powerful tool to characterise the age thickening process for milk concentrates, as well as other time-dependent systems where gelation occurs if adequate measurement time is allowed.

#### **5.1.2.2.2 Extrapolated viscosity at infinite shear rate**

In principle, when a non-Newtonian fluid is subjected to infinite shear rate, the structure breaks down to the basic particles. This is shown by the existence of an upper Newtonian region in the viscosity-shear rate curve (Steffe, 1992). In the view of the candidate and his supervisors, the changes of this viscosity at infinite shear with time should reflect permanent physical and chemical changes observed during age thickening.

It is extremely difficult to build rheometers that can provide the required shear rate to reach the second upper Newtonian region. Commercial rotary rheometers only achieve shear rates in the range of thousands of  $s^{-1}$ . However, the apparent viscosity at infinite shear rate,  $\mu_{\infty}$ , can be obtained by extrapolating the changes in apparent viscosity with the reciprocal of the shear rate using linear regression. The advantage of using this method of plotting is that the reciprocal of shear rate diminishes quickly to zero as the shear rate is increased, thus a y-axis intercept can be obtained by extrapolation. This technique has been used by Snoeren et al. (1982) for fresh skim milk concentrates. This technique should be compared with the conventional extrapolation technique used to determine the yield stress (Chapter 2) and should have the same advantage, mainly convenience, and the same weaknesses. In particular, since the range of shear rate attainable during measurement for a solution diminishes as it age-thickens, the extrapolated viscosity value at infinite shear rate may actually be affected by the gradual decrease in the shear rate range. A possible way of counteracting this bias is to normalise the viscosity at infinite shear with the shear rate range of the flow curve being extrapolated. This variable will be called “adjusted extrapolated viscosity”,  $\mu_{\infty ad}$  at infinite shear.

The shear rate range (the difference between the largest and smallest shear rates) at time zero was taken as the reference range. For subsequent storage times, a ratio of shear rate range was determined by simply dividing the new shear rate range over the reference, which would yield a value less than one, as expected from Figure 5.4.  $\mu_{\infty ad}$  was calculated by dividing the extrapolated viscosity at infinite shear by this ratio.

Figures 5.4 (a) and (b) plot the apparent viscosity values against shear rate and  $\frac{1}{Shear\ rate}$  respectively for the 48%TS milk concentrate samples during storage at 65°C. The decrease in the shear rate range during measurement due to age thickening was more apparent in Figure 5.4 (a) than in Figure 5.4 (b).

Figure 5.5 plots the changes in the extrapolated and adjusted extrapolated apparent viscosity at infinite shear with storage time, and compares them with the change in apparent viscosity at 105.3 Pa.s. The increase in both the adjusted and non-adjusted extrapolated apparent viscosity values at infinite shear with storage time did not follow the exponential curve of the apparent viscosity at 105.3 Pa. The 2.5 fold increase in  $\mu_{\infty ad}$  with storage time indicates the formation of strong aggregates that can withstand the destructive effect of infinite shear rate. In addition, Figures 5.4 and 5.5 showed little differences between  $\mu_{\infty}$  and  $\mu_{\infty ad}$ .

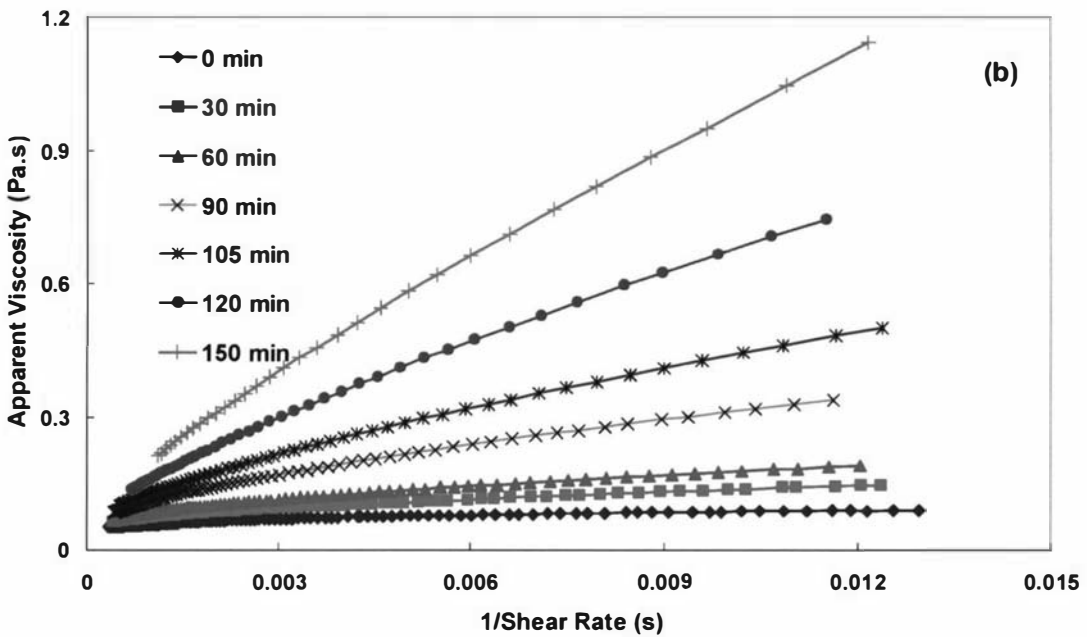
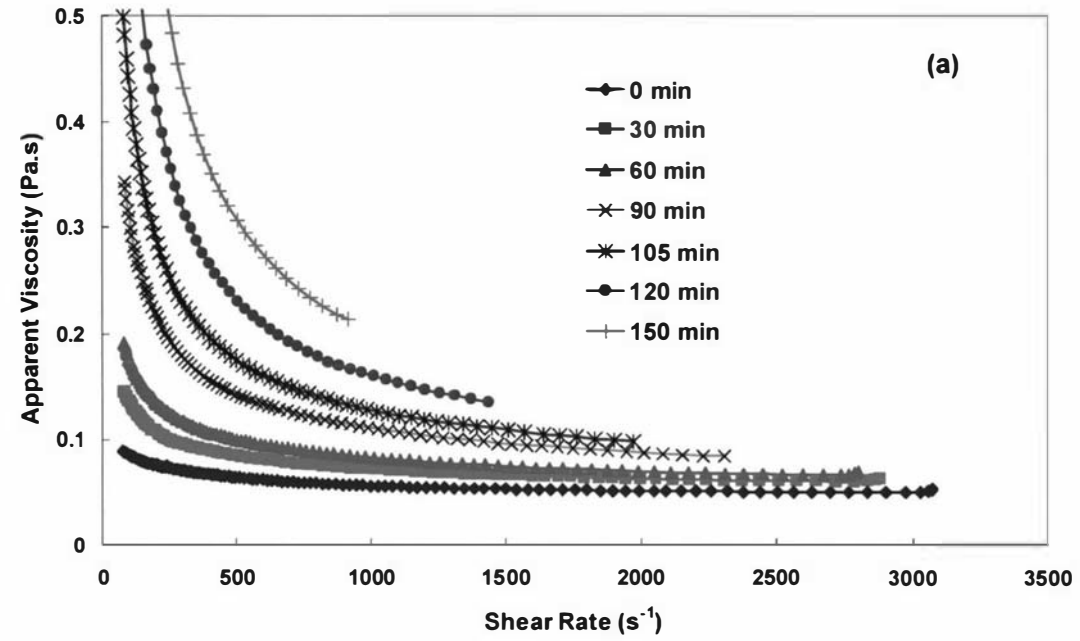


Figure 5.4: Changes in apparent viscosity with (a) shear rate and (b)  $\frac{1}{\text{Shear Rate}}$  for a 48%TS reconstituted whole milk concentrate sample during 148 minutes of storage at 65°C. Run C1.

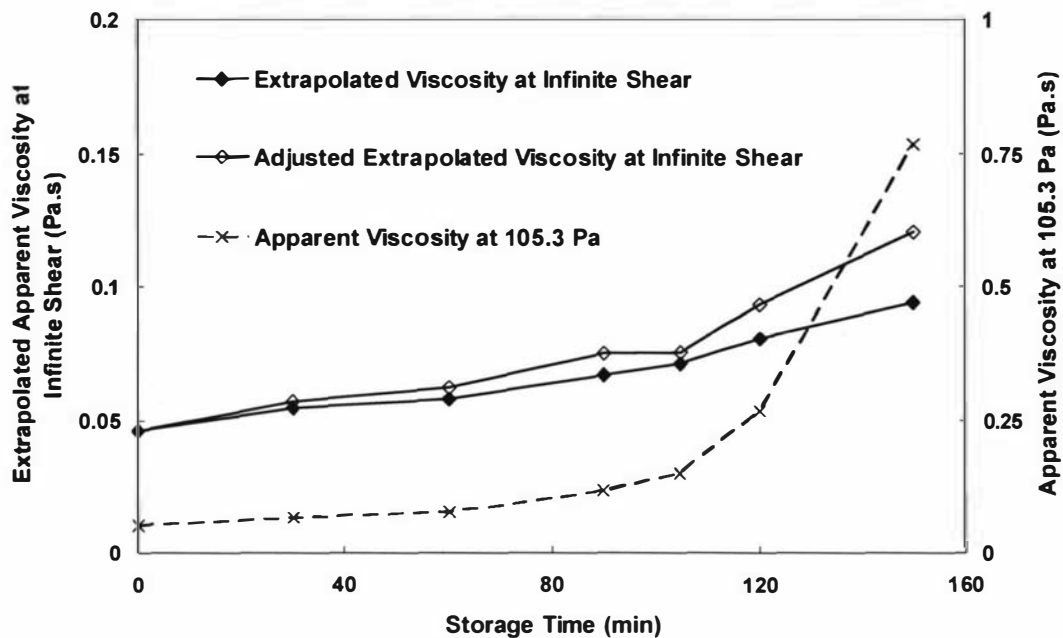


Figure 5.5: Comparison between the extrapolated infinite apparent viscosity and apparent viscosity at 105.3 Pa of a 48%TS reconstituted whole milk concentrate sample during 150 minutes of storage at 65°C. Run C1.

### 5.1.2.2.3 Hysteresis loop area

The hysteresis loop area (HLA) is the area between the shear up and shear down legs of the flow curve in Figure 5.1 and can be easily estimated. It is often used as a qualitative indication of thixotropy (Barnes, 1997) but there is no record of its use for quantitative analysis. The literature does not describe very clearly the physical significance of this hysteresis area but it can be interpreted as an indication of the scale of structural breakdown after a shear sweep. The hysteresis loop area is affected by the sensitivity of the structure to break down during shearing, and the time scale of the recovery process.

During the determination of HLA, it was important to ensure that the final shear rate value of the shear up curve matched the beginning shear rate value of the shear down curve. Because the shear sweep test was conducted in CSS mode and the milk concentrate system was time-dependent, the beginning shear rate of the shear down

curve was often larger than the final shear rate of the shear up curve even though both points were measured at 50 mNm, as seen in Figure 5.6. This is because there is an additional shearing step between the two curves where the torque was held constant at 50 mNm for 15 measurements at 1 second intervals. This shearing step results in an additional break down in structure, and thus a decrease in apparent viscosity. As the apparent viscosity can be determined from

$$\mu_{app} = \frac{\tau}{\dot{\gamma}} \quad (5.1)$$

for a constant shear stress  $\tau$ , a decrease in the apparent viscosity  $\mu_{app}$  would result in an increase in shear rate  $\dot{\gamma}$ , as observed in Figure 5.6. Therefore, the initial shear rate of the shear down curve is often truncated to the value of the maximum shear rate of the shear up curve.

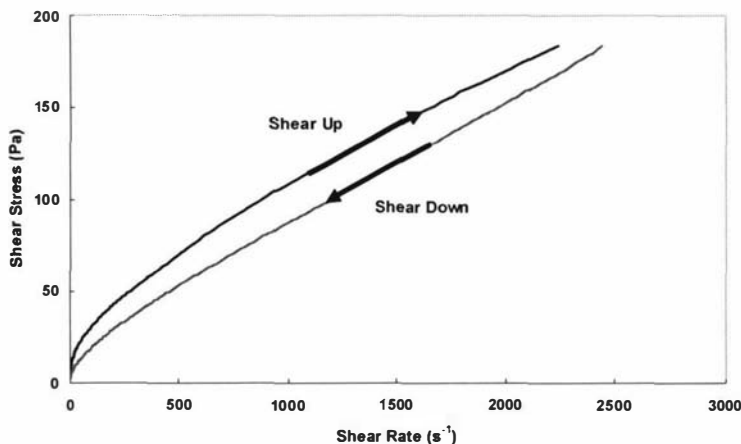


Figure 5.6: Flow curve of the reconstituted milk concentrate sample after 90 minutes of storage. C1, powder A, 48%TS, 65°C.

The HLA is determined by splitting the shear rate range into segments using two adjacent data points. For each segment, the HLA is the area underneath the curve, which is approximated by summing together the areas of a rectangle and a triangle. This approximation will always yield a lower HLA value than the actual one.

The initial calculation of HLA for each flow curve was carried out over the truncated shear rate range at which the flow curve was obtained reliably. Figure 5.7 plots the (HLA) and the apparent viscosity against storage time for the 48%TS sample during storage at 75°C. It is interesting to note that the breakdown area increases during the initial rate of age thickening but decreases abruptly after the gelling point. The two curves in Figure 5.7 give powerful complementary tools for the determination of the sol-gel transition in thixotropic and other time-dependent systems. As far as the author knows this method of using of the HLA for the characterisation of time-dependent systems is unique to the present work.

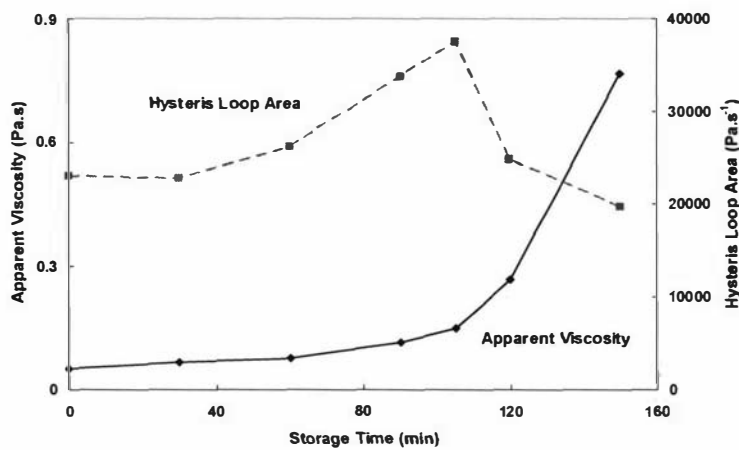


Figure 5.7: Changes in thixotropy hysteresis area and apparent viscosity of the 48%TS reconstituted whole milk concentrate sample during storage at 65°C. Run C1.

The value of the HLA depended on the spacing between the shear up and down curves, as well as the shear rate range over which the HLA was determined. During storage, the milk concentrate samples thickened and the maximum shear rate attainable decreased. The changes in the maximum shear rate with storage time of the milk concentrate samples in run C1 are plotted in Figure 5.8 together with the HLA. The maximum shear rate decreased continuously with storage time. For the same shear sweep range with the same upper shear stress value, this reduction in the range of shear rate resulted in a smaller value of HLA.

The shapes of the two curves in Figure 5.8 were completely different. There was no dramatic decrease in the maximum shear rate after 105 minutes of storage time to coincide with the sudden drop in the HLA. It was interesting to observe that the HLA

continued to increase with storage time up to the gelling point despite the decrease in the maximum shear rate.

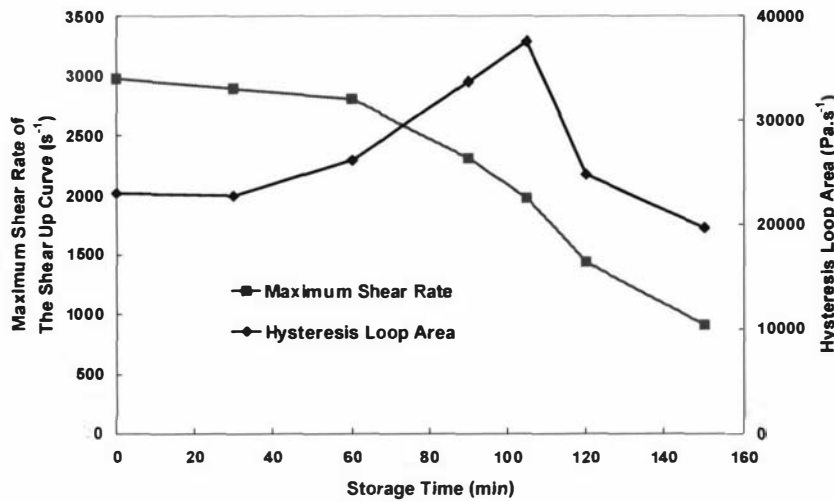


Figure 5.8: Changes in the maximum shear rate of the shear up curve and the HLA with storage time in the reconstituted milk concentrate sample. Run C1, powder A, 48%TS, 65°C.

A better understanding of the significance of the HLA is given by examining the changes in the flow curves of the milk concentrate samples before and after gelation as shown in Figure 5.9 for 90 minutes and 120 minutes of storage.

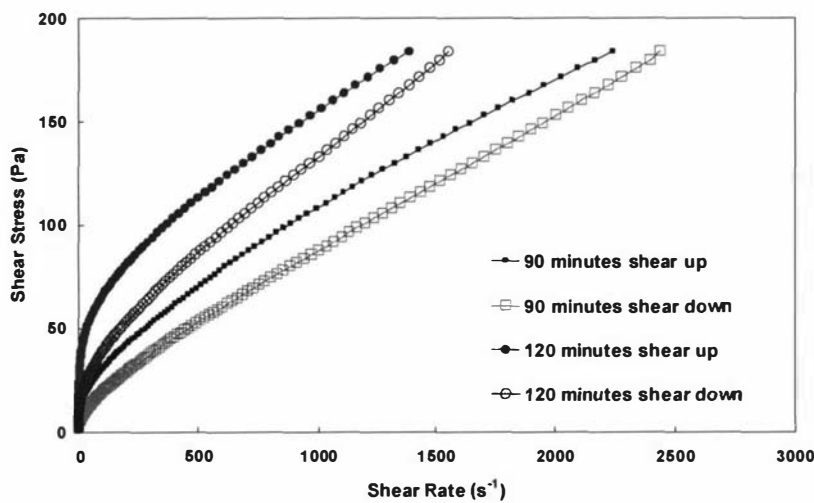


Figure 5.9: Changes in the flow curves of the shear up and down tests of the reconstituted milk concentrate samples after 90 and 120 minutes of storage. Run C1, powder A, 48%TS, 65°C.

To better obtain an idea of the spacing between the up and down curves, we can use one of two techniques:

1. Calculate the HLA of different samples in a set for a fixed range of shear rates. By necessity, this will be the smallest of range of shear rates found with the thickest sample. For convenience this will be called standardised HLA. It must be understood that the smallest range of shear rate differs with each set of data taken with different products and that the method is only useful for comparison of samples within a set. There is no absolute standard.
2. Calculate the HLA per unit interval of shear rate by using equation (5.2). Again, for convenience, this is called the intrinsic HLA.

$$\text{Intrinsic HLA} = \frac{\text{HLA}}{(\text{Maximum Shear Rate} - \text{Minimum Shear Rate})} \quad (5.2)$$

The standardised and intrinsic HLAs were calculated for data in run C1, for a range of shear rates from about 80 to 870 s<sup>-1</sup> which was the maximum shear rate in the sample after 150 minutes. Figure 5.10 plots the changes in the standardised and intrinsic HLAs with storage time during age thickening. The two trends were similar and either method can be used to identify trends.

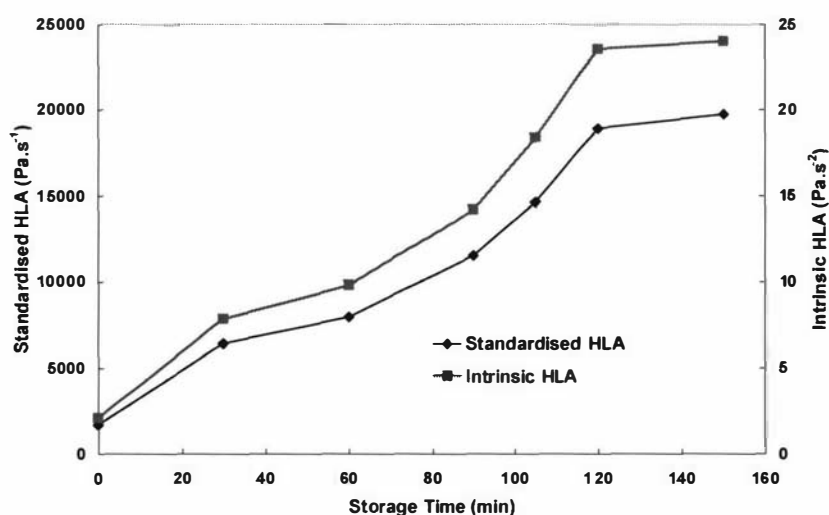


Figure 5.10: Changes in the standardised and intrinsic HLA with storage time. Run C1, powder A, 48%TS, 65°C.

Both the intrinsic and standardised HLA showed that the degree of thixotropy of the concentrate increased with storage time, even after gelation and did not drop as shown by the non-standardised HLA as observed in Figure 5.7. The reason the non-standardised HLA decreased sharply after gelation in Figure 5.7 was caused by the dominating effect of the decrease in the maximum shear rate range over the continuous increase in the degree of thixotropy during age thickening. The sudden drop in the HLA curve gives a convenient method of identifying the onset of gelation. This is a practical observation, not a theoretical postulation.

#### 5.1.2.2.4 Rheological modelling

The previous information must be complemented by some indication of the evolution of shear dependence of the viscosity with storage time. This requires an analysis of the basic flow curves like the one presented in Figure 5.1. The massive amount of information available in the instantaneous flow curves can be summarised by fitting a rheological model to the data. The model of choice was the Herschel-Bulkley model because it can degenerate to the simpler Newtonian and power law models under different operating conditions such as low total solids or low temperatures as shown later in this chapter. The model has been used by others to describe the rheological behaviour of dairy products, including milk concentrate systems (Velez-Ruiz & Barbosa-Canovas, 1997, 1998, 2000; Trinh & Schraekenrad, 2002; Ma et al., 2002).

Model fitting was carried out using Matlab V11, where the three parameters were varied simultaneously until the lowest residual squares error between the predicted and the actual data was achieved.

The three parameters of the Herschel-Bulkley model, yield stress  $\tau_v$ , consistency coefficient  $K$  and the behaviour index  $n$  were plotted in Figure 5.11 against storage time for the 48%TS reconstituted milk concentrate samples. The decrease in the behaviour index indicated that the viscosity became more shear dependent with storage time. The consistency coefficient  $K$  increased almost exponentially with storage time indicating that the material becomes thicker. The yield stress  $\tau_v$  also

increased exponentially indicating that the rested structure was more difficult to deform initially. In the author's view, the yield stress could also be interpreted as the limiting stress for elastic deformation of the rested structure.

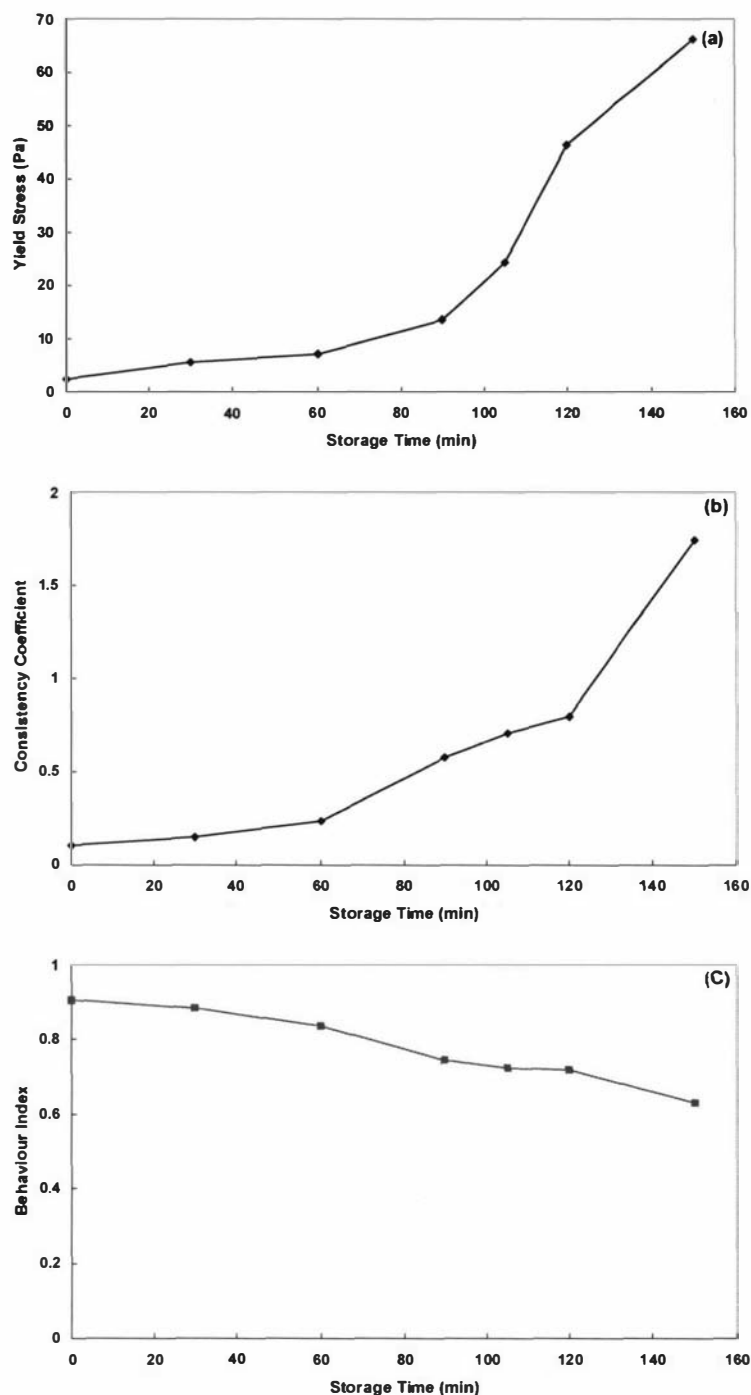


Figure 5.11: Changes in the Herschel Bulkley model parameters for 48%TS with storage time at 65°C. (a) yield stress  $\tau_y$ ; (b) consistency coefficient  $K$ ; (c) behaviour index  $n$ . Run C1.

### 5.1.2.3 Limitations

The use of the shear sweep tests for characterisation of time dependent fluids is not without serious drawbacks. The first problem arises from the fact that the structure of the fluid changes upon the first shear disturbance applied and the successive points on a shear sweep actually deal with different structures, not the original one at the beginning of the test as explained in Appendix 2.

The shape of the hysteresis loop area is a function of many parameters that the experimenter can set for the test: for example the values of the maximum and minimum shear stresses in the loop, the delay time between successive readings, the measuring time for each point and the number of points monitored within the chosen range of shear stresses. The derived parameters such as the apparent viscosity, the hysteresis loop area, the yield stress, the consistency and the behaviour index are in turn all affected.

These effects have been studied with yoghurt, a well known time-dependent dairy product (Rohm, 1992, Fangary, Barigou, & Seville, 1999). Two sets of experiments were conducted in this work on two commercial yoghurt samples that were bought from a local supermarket (Mainland Products Limited, Naturelea Acidophilus, Plain Unsweetened; Yoplait New Zealand Limited, Yoplait Lite vanilla). No non-Newtonian corrections were carried out for the calculation of the nominal shear rate on these two sets of data. In the first set of experiments with the Mainland products, the shear stress range was kept constant at 1.94-194 Pa. The number of data points collected at 1 second intervals was varied, from 20 to 200 data points in a shear sweep. The test was conducted in CSS mode with the Z2.1 spindle at 10°C. In total 11 runs (C2-C12) were carried out including replicate runs which confirmed the maximum experimental error of 10% for rheological measurements in this work. The results are shown in Figures 5.12 and Table 5.1. Figure 5.12 shows the change in the apparent viscosity at 105.3 Pa with the number of data points, while Table 5.1 lists the changes in the Herschel-Bulkley parameters. An increase in the number of data points resulted in a decrease in the apparent viscosity. This is expected because the structure of the yoghurt sample would be subjected to a greater amount of destruction

during measurement. An increase in the number of data points would mean the sample is sheared for a longer time period before the shear stress of 105.3 is reached. The change in apparent viscosity also led to the changes in the Herschel-Bulkley model parameters, seen in Table 5.1.  $K$  increased while  $n$  decreased with an increase in the number of data points.

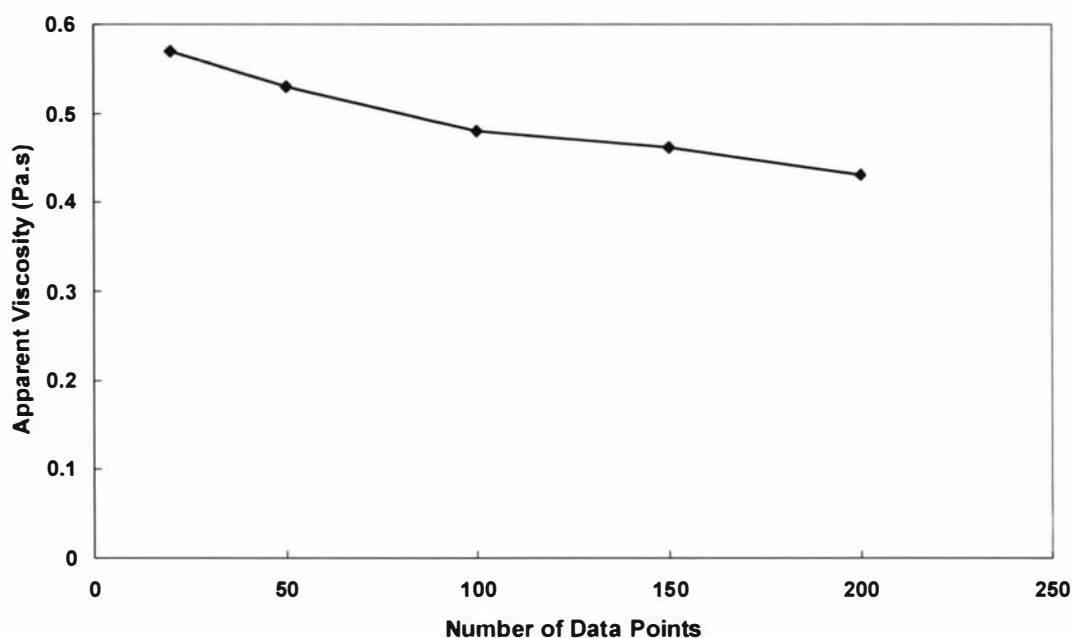


Figure 5.12: The effect of the number of data points on the apparent viscosity when conducting a shear sweep test on Mainland yoghurt samples at 10°C in CSS mode using the Paar Physica MC1. Runs C2-C12.

Table 5.1: The effect of the number of data points on the Herschel-Bulkley model parameters when conducting a shear sweep test on Mainland yoghurt samples at 10°C in CSS mode using the Paar Physica MC1. Runs C2-C12.

Number of data points	$K$ (Pa.s <sup><math>n</math></sup> )	$n$	$\tau_y$ (Pa)
20	12.02	0.42	3.00E-07
50	14.53	0.38	8.02E-08
100	16.23	0.35	3.16E-08
150	16.32	0.35	1.35E-07
200	16.71	0.34	6.50E-08

The second set of experiments with the Yoplait yoghurt measured 50 measurement points at 1 second intervals. Nine runs (C13-C21) were carried out where the minimum torque in a shear sweep test was varied from 0.5 to 25 mNm. The results are shown in Table 5.2 which lists the changes in the apparent viscosity and the Herschel-Bulkley model parameters. An increase in the minimum torque while keeping the number of data points constant resulted in a decrease in apparent viscosity and  $K$  and an increase in  $\tau_y$ .

Table 5.2: The effect of the minimum torque on the Herschel-Bulkley model parameters when conducting a shear sweep test on Yoplait yoghurt samples at 10°C in CSS mode using the Paar Physica MC1. Runs C13-C21.

Minimum Torque (Pa)	Apparent Viscosity (Pa.s)	$K$ (Pa.s <sup>n</sup> )	$n$	$\tau_y$ (Pa)
0.5	0.154	2.40	0.55	18.12
10	0.124	1.34	0.60	30.61
25	0.114	0.05	0.94	76.65

The results from runs C2-C21 showed that it is not possible to compare the results of tests on different time-dependent samples unless the protocol of experimentation is clearly defined and followed rigorously. If this is done, then the method presented here can provide useful trends.

## 5.2 Comparative rheology of fresh and reconstituted whole milk concentrates

The use of fresh milk concentrate systems poses two issues, variation in the raw materials and in processing conditions during concentration.

A fresh milk system has a shelf life in the order of several weeks. Thus, if the number of experiments is extensive and requires a lengthy period of time, more than one batch of milk is required. This brings in the problem of variation in composition of the raw material. Daily fluctuation in protein and fat contents will be unavoidable. Even if the same raw material is used, storage under chilled conditions to prolong the shelf life is required. However, chill storage would still give rise to chemical and physical changes to the raw milk system. On top of this, the processing conditions during preheating and concentration would need to be carried out in the exactly the same manner for all samples in order to ensure that the shear and temperature histories are similar between sets of concentrated samples.

Powder is stable and does not deteriorate quickly. A large batch can be obtained and serves as the common raw material for many experiments. Composition variation is minimal. Recombination involves a smaller number of processing variables than preheating and evaporation. Shear and temperature histories can be more strictly controlled with reconstituted systems. Cost is significantly reduced, and time-management for experimentation is more flexible with the use of powder as the source of raw material.

The rheological behaviour of reconstituted milk concentrates has been reported to be different from the corresponding fresh milk concentrates obtained during the manufacture of the powders. Vilder et al. (1979) reported that the viscosity of reconstituted whole milk concentrates was six to fifty times higher than fresh concentrated systems from which the milk powder was produced. Similarly, work on HCT also showed that it was not possible to predict the HCT of reconstituted systems from the data obtained for fresh

systems (Kiesecker & Pearce, 1978; Newstead & Baucke, 1983; Singh & Tokley, 1990; Singh & Creamer, 1991; Mil & Koning, 1992). It is possible that physical and chemical changes during reconstitution have not been considered carefully as an explanation for the discrepancies both in rheological behaviour and heat stability between fresh and reconstituted systems.

Commissioning trials on the recombination rig showed that the reconstitution of powder to yield concentrated systems should be done with care as rheological changes are inevitable. Particularly, age thickening can take place during reconstitution which alters the rheological behaviour of the final heated solutions.

In the commissioning trial, the storage experiment A3, the 48%TS reconstituted milk concentrate was heated to 65°C and stored at 65°C. The averaged initial apparent viscosity value was 0.03 Pa.s. This value is substantially lower than the viscosity value of 1.2 Pa.s for a 45.6 %TS reconstituted non-homogenised whole milk concentrates reported by Vilder et al. (1979). In fact, this value is more comparable to the apparent viscosity values of 0.022 Pa.s obtained for fresh milk concentrate as measured in experiment A119. Bienvenue et al. (2003a, 2003b) carried out a study on 45%TS fresh skim milk concentrates which were stored at 50°C for rheological measurements. The initial apparent viscosity at 50°C was approximately 0.025-0.03 Pa.s, which is similar to that obtained in experiment A3.

This section analyses the rheological behaviour of fresh and reconstituted systems in more detail. The section will also discuss the feasibility of the use of powder as an alternative raw material to fresh milk systems for rheological studies. The comparative analysis between the flow behaviours of fresh and reconstituted milk concentrate systems was done under three different conditions:

1. Different shear histories during sampling and preparation, and measured using two different rheometers, the Brookfield LVTD on the fresh and the Paar Physica MC1 on the reconstituted concentrates.

2. Different shear histories during sampling and preparation, but measured on the same piece of equipment, the Paar Physica MC1.
3. Similar shear history during sampling and preparation, as well as being measured on the same rheometer, the Paar Physica MC1.

## 5.2.1 Materials and methods

### 5.2.1.1 Fresh versus reconstituted milk with different shear history using the Brookfield LVTD and the Paar Physica MC1

During industrial surveys, powder was collected for further experimentation at Massey University. The powder was reconstituted using the custom-built recombination rig at 35°C and 40,000 s<sup>-1</sup>. After recirculation for 60 minutes, the reconstituted solutions were heated and stored at the heated temperature in a water bath. For each type of powder, the solids content and the heating and storage temperatures were kept identical to those encountered in the plant. Thus, during milk powder processing in industrial plants, if the milk concentrates were evaporated to 47%TS and heated to 75°C in the concentrate heater, the powder would be mixed to 47%TS and heated and stored at 75°C.

It is important to point out that during industrial surveys, rheological measurements of the fresh concentrates were made with the Brookfield LVTD viscometer. The shear step test was used where the sample was sheared at a constant spindle speed for 20 minutes. At Massey University, all rheological measurements were carried out using the Paar Physica MC1, where the reconstituted samples were stored in a water bath and subjected to a shear sweep test at regular intervals.

Aside from using different instruments, the reconstituted and fresh systems possessed different shear history profiles prior to sampling. Reconstituted systems were sheared at a constant shear rate of 40,000 s<sup>-1</sup> during recirculation. The shear history in the industrial environment is more complicated and difficult to assess. Also the shear history varies

between plant configurations. Thus, it is not possible to analyse the difference in the shear history between fresh and reconstituted systems.

The exercise was carried out on 4 industrial surveys, where the powder was collected in experiments B8, B9, B10 and B11, and reconstituted experiments C22-C25.

#### **5.2.1.2 Fresh versus reconstituted with different shear history using the Paar Physica MC1**

In industrial survey B14, the fresh milk concentrates were measured using the Paar Physica MC1. The 47%TS fresh concentrates were heated to 75°C in the concentrate heater. Samples were collected just before the spray drier and were stored at 75°C in a hot water bath. Samples were obtained from both the high shear concentrate drier line via a tap, and a low shear sampling module, as explained in section 4.6.

In run C26, the powder collected from the survey B14 was reconstituted to 47%TS at 35°C and 40,000 s<sup>-1</sup>. The concentrates were recirculated for 60 minutes, heated to 75°C and stored at 75°C to achieve similar solids content and temperature settings as encountered in the industrial survey. A replicate experiment was also carried out in run C27.

#### **5.2.1.3 Fresh versus reconstituted with the same shear history using the Paar Physica MC1.**

A more carefully planned experiment than the standard industrial surveys presented in chapter 4 was conducted at the Fonterra Cooperative Ltd. Pahiatua milk powder plant. In order to achieve similar shear histories in the fresh and in the reconstituted systems before measurement, the recombination rig was transported to the Pahiatua plant. In run C28, the fresh whole milk system was evaporated to 47%TS and heated to 75°C in the

Pahiatua milk powder plant. The composition specification and operating conditions are listed in Tables 5.3 and 5.4.

Fresh milk concentrates were collected after the concentrate heater and recirculated through the recombination rig at  $40,000\text{ s}^{-1}$  and  $75^{\circ}\text{C}$  for 60 minutes. The solutions were withdrawn from the rig and stored in a  $75^{\circ}\text{C}$  water bath while rheological measurements were carried out at regular intervals using the Paar Physica MC1.

Ideally, the fresh concentrates should have been cooled to  $35^{\circ}\text{C}$  before recirculation in the recombination rig, and then heated to  $75^{\circ}\text{C}$  for rheological measurements to match exactly the procedure used for reconstituted samples. However, the unavailability of a plate heat exchanger and a hot water source at the plant did not allow this.

The powder obtained from industrial survey C28 was reconstituted at a later date in experiment C29 to 47%TS at  $35^{\circ}\text{C}$  and  $40,000\text{ s}^{-1}$  in the recombination rig. The solution was then heated to  $75^{\circ}\text{C}$  and stored at  $75^{\circ}\text{C}$ . The reconstituted milk concentrates were not recirculated at  $75^{\circ}\text{C}$  as was done in run C28 with fresh concentrates. Instead, it was recirculated at  $35^{\circ}\text{C}$  to prevent age thickening during recirculation. Rheological measurements were made with the Paar Physica MC1.

Table 5.3: General composition of the infant milk concentrates in experiments C28 & C29 at the Pahiatua milk powder plant.

Component	C28 & C29
Protein	25
Fat	26.6

Table 5.4: Plant operating conditions in experiments C28 & C29 at the Pahiatua milk powder plant.

<b>Experiment</b>	<b>C28 &amp; C29</b>
<b>Process Variables</b>	
DSI temperature (°C)	98
Holding time (s)	45
Evaporator concentrate total solids (%TS)	47-48
Concentrate heater milk temperature (°C)	76

## 5.2.2 Results

### 5.2.2.1 Fresh versus reconstituted milk with different shear history using the Brookfield LVTD and the Paar Physica MC1

Figure 5.13 plots the changes in apparent viscosity with measurement time for the fresh concentrate (B8), and storage time for the reconstituted concentrate (C22). The apparent viscosity values of the reconstituted samples were determined at the shear stress of 105.3 Pa, which was considerably higher than the shear stress that would be encountered at 60 rpm in the Brookfield LVTD viscometer.

The initial viscosity for the reconstituted concentrate was higher than the fresh concentrate by approximately twofold. However, the rate of increase in viscosity with time was higher in the Brookfield data. The sudden decrease in apparent viscosity after 70 minutes of storage in the reconstituted concentrate data cannot be explained and is considered an outlier due to some unknown disturbance to the experiment.

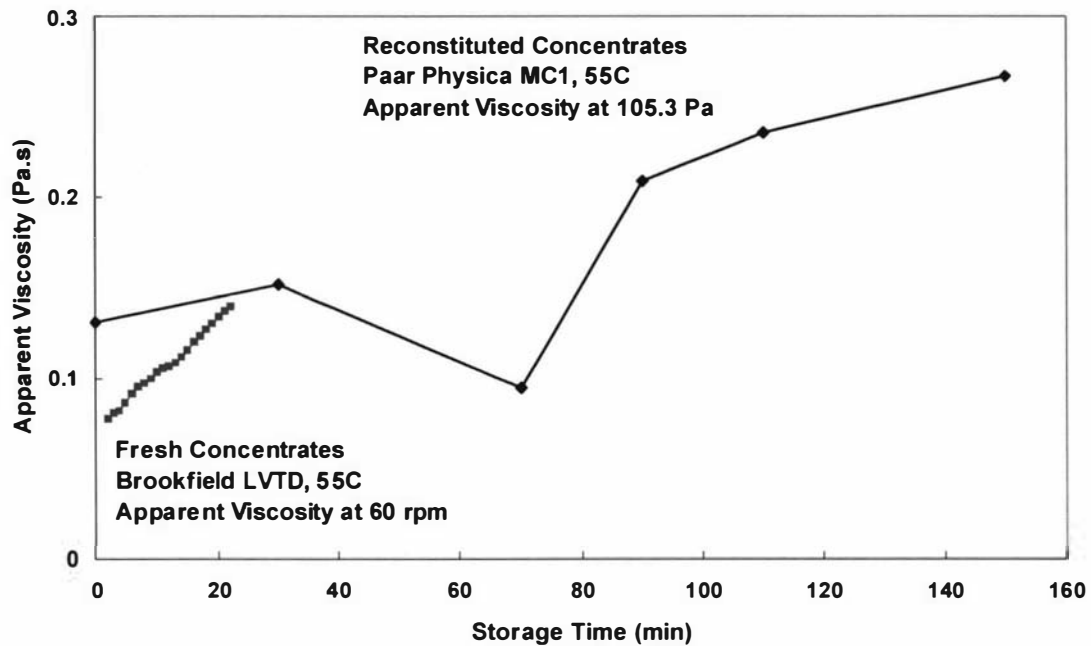


Figure 5.13: Apparent viscosity against storage time for the reconstituted concentrate with the Paar Physica MC1 and measurement time for the fresh concentrate with the Brookfield LVTD. 47.5%TS and 75°C. C22.

The higher apparent viscosity data for the reconstituted system agreed with Vilder et al. (1979), but obviously not in the same ratio. This is due to the several factors:

1. different shear history during sampling and measurement between fresh and reconstituted systems
2. different shear rate at which the apparent viscosity values were determined

Thus, the data obtained from the Brookfield LVTD and the Paar Physica MC1 should not be compared in terms of absolute values, but only in trends.

Similar observations were made in runs C23-C25.

### 5.2.2.2 Fresh versus reconstituted milk with different shear history using the Paar Physica MC1

Figure 5.14 plots the change in apparent viscosity during storage time for the fresh concentrate (B14) and reconstituted concentrate (C26) that was made from the powder collected in run B14. The solids contents for both systems were 47.5%TS and the final temperatures were 75°C. Figure 5.15 plots the changes in the Herschel-Bulkley model parameters with storage time for the fresh and reconstituted systems. For the fresh systems, the data obtained from the high shear concentrate line and the low shear sampling module are presented.

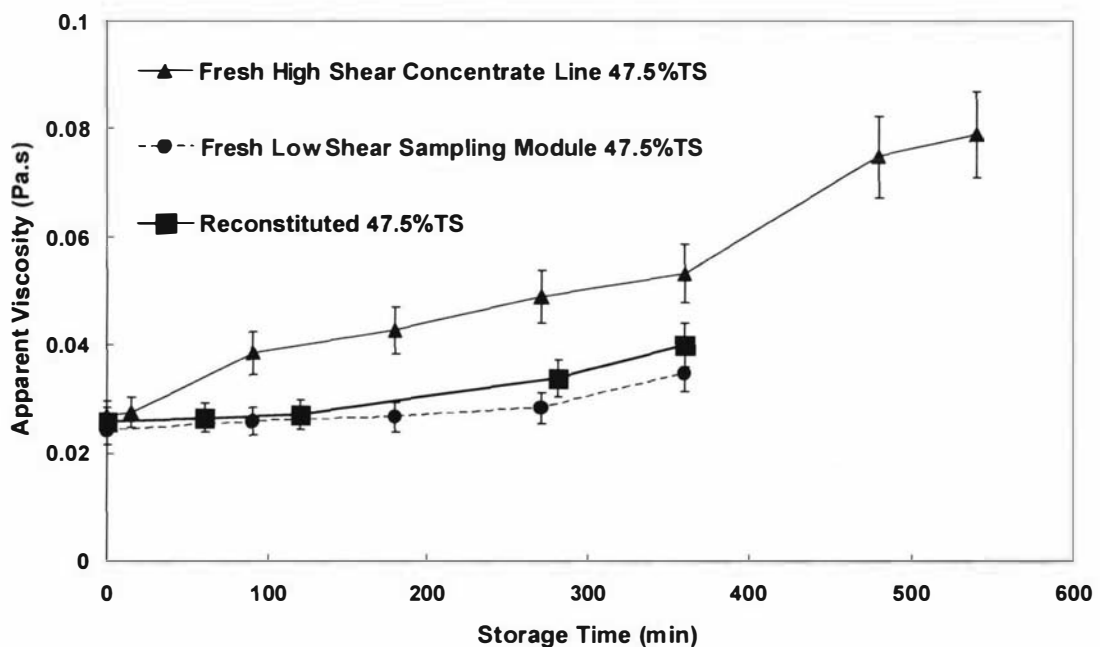


Figure 5.14: Apparent viscosity against storage time for fresh (B14) and reconstituted (C26) concentrates using the Paar Physica MC1. 47.5%TS and 75°C.

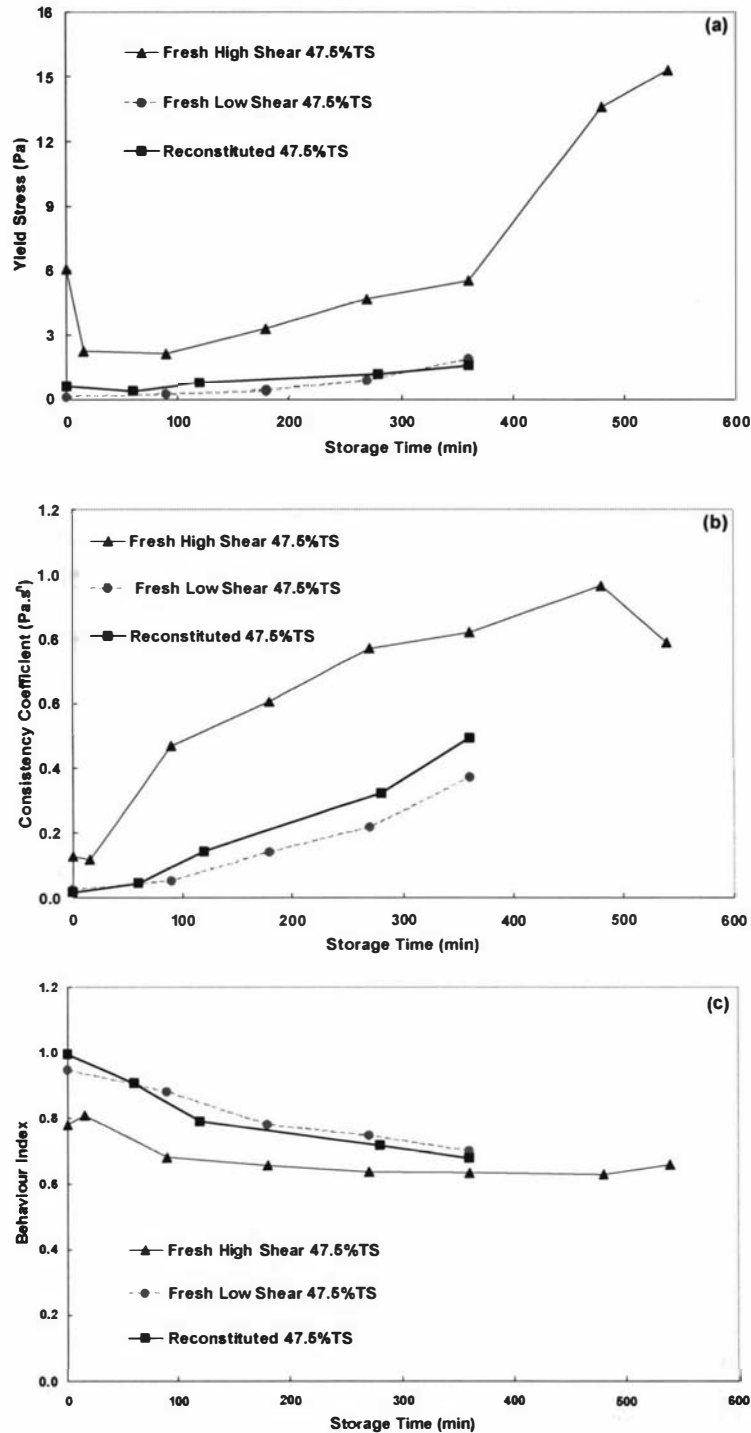


Figure 5.15: Changes in the Herschel-Bulkley model parameters with storage time for fresh (B14) and reconstituted concentrates (C26) using the Paar Physica MC1. 47.5%TS and 75°C. (a)  $\tau_y$ ; (b)  $K$ ; (c)  $n$ .

Figures 5.14 and 5.15 showed that the rheological behaviour of the reconstituted concentrate was similar to the fresh samples within 10% experimental error, but only when the fresh sample was collected via the low shear sampling module. Section 5.5 discusses in more detail the effect of shear level during sampling.

The reconstituted milk concentrate possessed a slightly higher apparent viscosity,  $\tau_y$ ,  $K$  and lower  $n$  in comparison to those of the fresh system when sampled at low shear rate. However, these differences were small and fell within the 10% experimental error band.

Duplicate run C27 showed similar results to that observed in run C26 and agreed within the 10% experimental error uncertainty.

### **5.2.2.3 Fresh versus reconstituted milk with the same shear history using the Paar Physica MC1.**

The changes in rate of age thickening during storage at 75°C for runs C28 and C29 are shown in Figure 5.16. The y-axis error bars are also plotted in Figure 5.16 with a 10% uncertainty range. The initial apparent viscosity values for the fresh and reconstituted systems were 0.0278 Pa.s and 0.0299 Pa.s respectively, less than 10% difference. The literature review showed that there has never been a comparison between fresh and reconstituted system within one study that has achieved this close agreement in initial apparent viscosity values.

The changes in apparent viscosity during age thickening were also similar in both systems. The fresh concentrates consistently showed slightly higher viscosity values than the reconstituted system. It was possible that in run C28 with fresh concentrate, recirculation at high temperature resulted in an increase in the initial apparent viscosity and rate of age thickening. The effect of temperature during recirculation is dealt with in detail in section 5.6.

In Figure 5.16, 10% y-axis error bars were drawn for each data point to provide a qualitative analysis of the agreement between the two lines. A more appropriate test would be to assume a hypothesis that the two sets of data could be drawn by a common line, where the y-axis intercept and the slope of the graph are identical. The hypothesis could then be tested to see whether it is significant or not at a particular level of probability.

$$F_{value} = \frac{(RSS_{com} - RSS_{sep})(df_{com} - df_{sep})}{RSS_{sep}/df_{sep}} \quad (5.3)$$

where  $RSS_{com}$  is the residual sums of squares of the common line model

$RSS_{sep}$  is the sum of residual sums of squares of each separately fitted line

$df_{com}$  is the degrees of freedom for error of the common line model

$df_{sep}$  is the sum of the degrees of freedom for error of each separately fitted line

Using equation (5.3), an F value of 5.79 was obtained, which was not significant at  $p < 0.01$ , therefore the original hypothesis was accepted and the two sets of data could be represented by a common line. Thus, the two sets of data do agree with each other at  $p < 0.01$ .

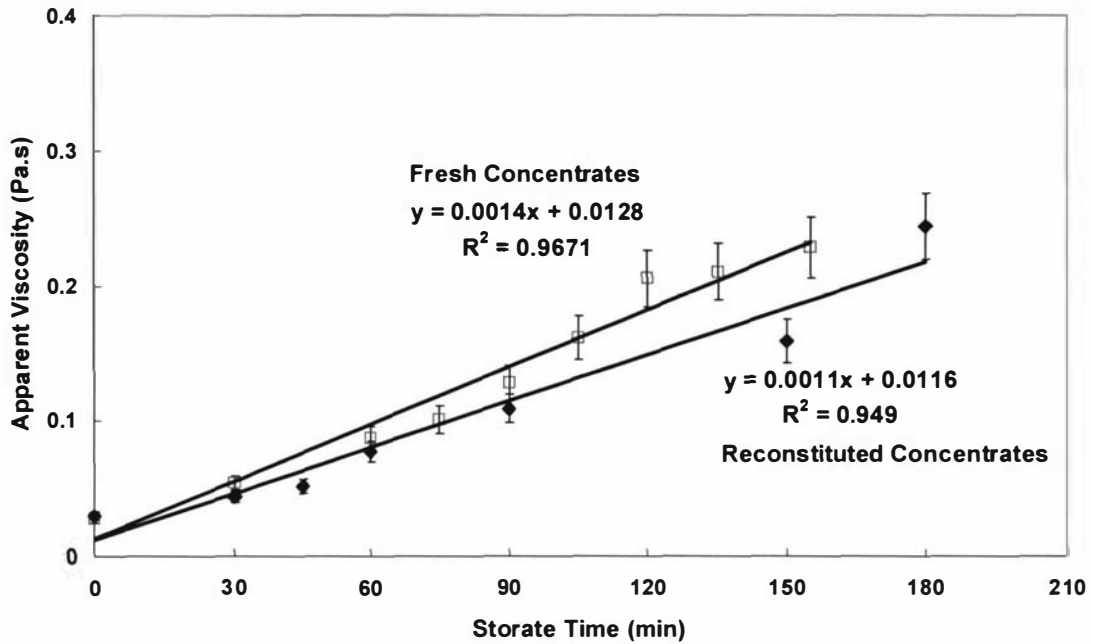


Figure 5.16: Apparent viscosity against storage time for fresh (C28) and reconstituted (C29) concentrates using the Paar Physica MC1. 47.5%TS and 75°C. Paar Physica MC1.

The flow curves were fitted with the Herschel-Bulkley model and the changes in the model parameters with storage time for fresh and reconstituted systems are plotted in Figure 5.17. The model parameters provide a clearer picture of the instantaneous rheological behaviour at each measurement time, as well as the evolution of the changes in the flow curve.

The most obvious observation in Figure 5.17 is the similarity in trends of the Herschel-Bulkley three model parameters with storage time for both fresh and reconstituted systems. The yield stress and the consistency coefficient increased while the behaviour index decreased with storage time. During age thickening, the fluid is getting thicker (increase in  $K$ ) and requires stronger force to initiate flow (increase in  $\tau_y$ ). The material also shows a greater degree of shear thinning during age thickening (decrease in  $n$ ). The similar trends in all three parameters between the fresh and reconstituted systems clearly showed that both systems build up in a similar manner during age thickening, and break

down in similar manner during shearing. This is clear evidence that fresh and reconstituted systems possess similar rheological behaviour when proper care is exercised in the reconstitution and pre-shearing steps.

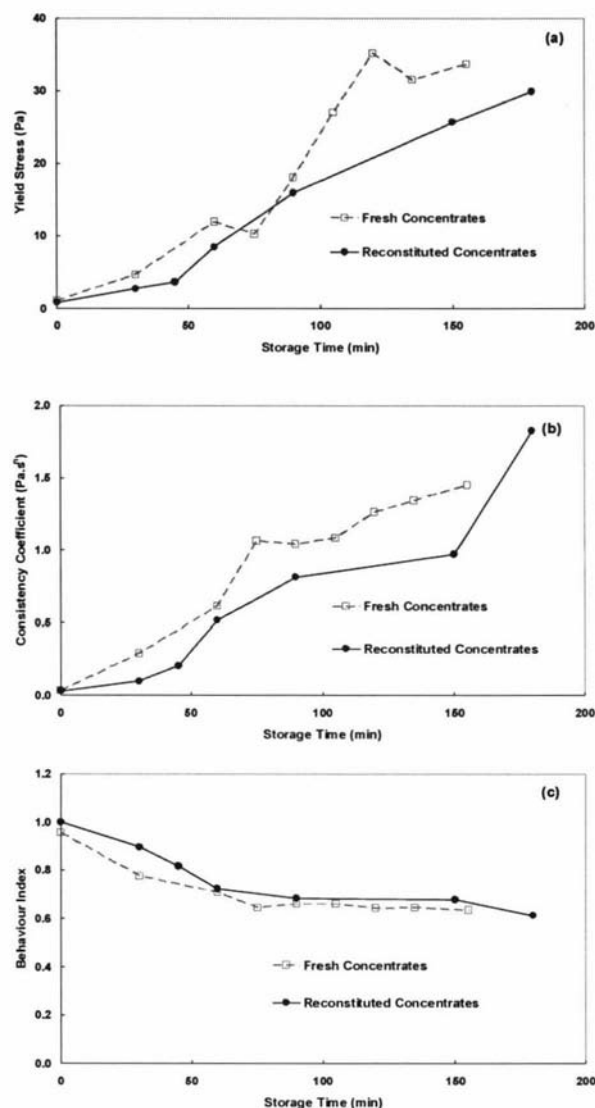


Figure 5.17: Changes in the Herschel Bulkley model parameters with storage time for fresh (C28) and reconstituted milk concentrates (C29) with storage time. 47.5%TS and 75°C. Paar Physica MCI. (a) yield stress  $\tau_y$ ; (b) consistency coefficient  $K$ ; (c) behaviour index  $n$ .

### **5.3 Effect of solids content on the rheology, pH and PSD of the reconstituted whole milk concentrates**

An increase in solids content has an effect on apparent viscosity and rate of age thickening (Snoeren et al., 1984), pH and ionic activities (Walstra & Jenness, 1984; Walstra et al., 1999; Bienvenue et al., 2003a, 2003b), and particle size (Walstra & Jenness, 1984; Walstra et al., 1999). However, quantitative data analysis has only been found for the relationship between solids content and apparent viscosity. Changes in particle size with solids content have been studied by Anema (2000) and Bienvenue et al. (2003a). However, in these experiments, the fresh milk concentrates were heated prior to particle size measurement. The effect of solids content on pH in milk systems has only been noted and acknowledged. No data has been found in the literature on this interaction.

In this set of experiments, whole milk powder B (documented in section 3.5.1) was mixed to various solids contents at 35°C. No heating was carried out. The changes in rheology, pH, and PSD were measured.

#### **5.3.1 Materials and methods**

Whole milk powder B was used in this experiment. In run C30, the powder was reconstituted at 35°C and 40,000s<sup>-1</sup>. The powder and distilled water were initially added to achieve 10%TS. Samples were withdrawn after 60 minutes of recirculation for rheological, pH and particle size distribution measurements. More powder was then added to achieve 20%TS. The exercise was repeated for different solids content, up to 52%TS ± 0.5%TS. Rheological measurements were carried out at 35°C, and no heating took place. The milk samples were allowed to equilibrate to room temperature for 30 minutes before pH measurements were carried out.

### 5.3.2 Results

Figure 5.18 plots the change in apparent viscosity at the shear stress of 105.3 Pa with solids content of the reconstituted whole milk solutions at 35°C. An exponential relationship was observed between apparent viscosity and solid content, which agreed with previous work (Fernandez-Martin, 1972; Bloore & Boag, 1981; Snoeren et al., 1982, 1984; Vilder & Moermans, 1983; Velez-Ruiz & Barbosa-Canovas, 1997, 1998). Above 45%TS, the apparent viscosity increased sharply with an increase in solids content.

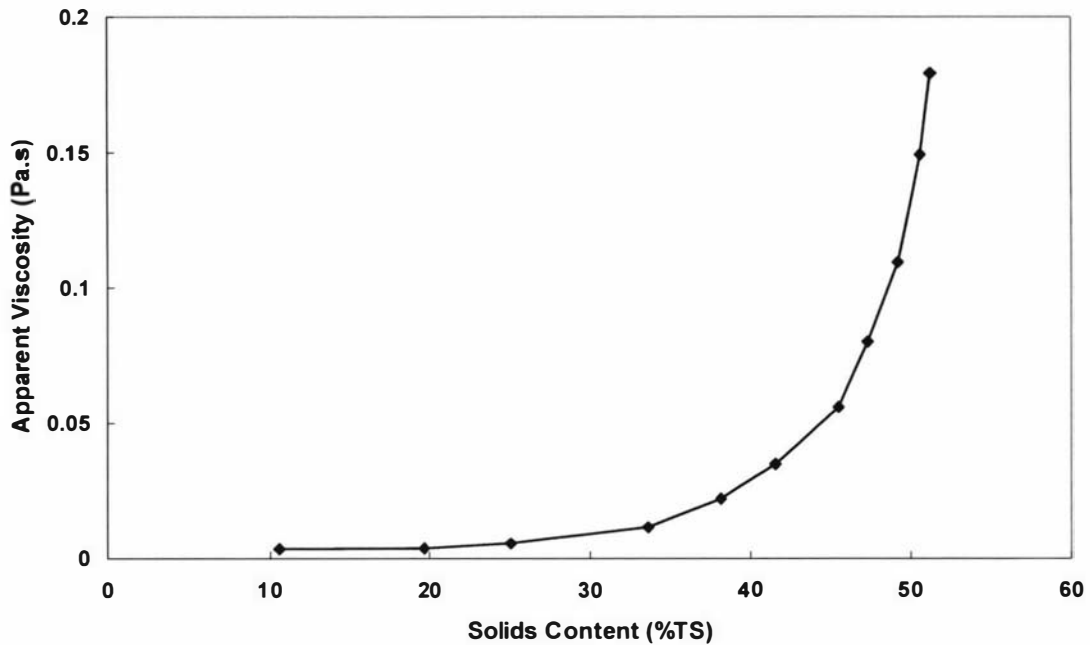


Figure 5.18: Effect of solids content on the apparent viscosity at 105.3 Pa of the reconstituted whole milk solutions. Powder B. 35°C.

The flow curves for each solids content were fitted with the Herschel-Bulkley model and the results are shown in Figure 5.19. The yield stress did not exist below 35%TS. Above this critical mark, the yield stress showed a proportionate increase with solids content.

The consistency coefficient,  $K$ , increased exponentially with solids content, in a trend similar to that of the apparent viscosity. This agreed with findings of Velez-Ruiz and Barbosa-Canovas (1998). The increase in  $K$  is due to the increase in the interaction effects between the individual milk components suspended in an aqueous phase with a decrease in water content (Tung, 1978).

The behaviour index did not deviate significantly from the Newtonian value of 1. The first deviation from the value of 1 was observed at 45%TS. However, at solids content of 50.6%TS and 51.3%TS, the behaviour index values were 1. Thus, the reconstituted whole milk solutions prepared from powder B at 35°C and 40,000 s<sup>-1</sup> showed Newtonian behaviour up to 35%TS, above which Bingham plastic behaviour was observed where only the yield stress and the consistency coefficients varied with solids content.

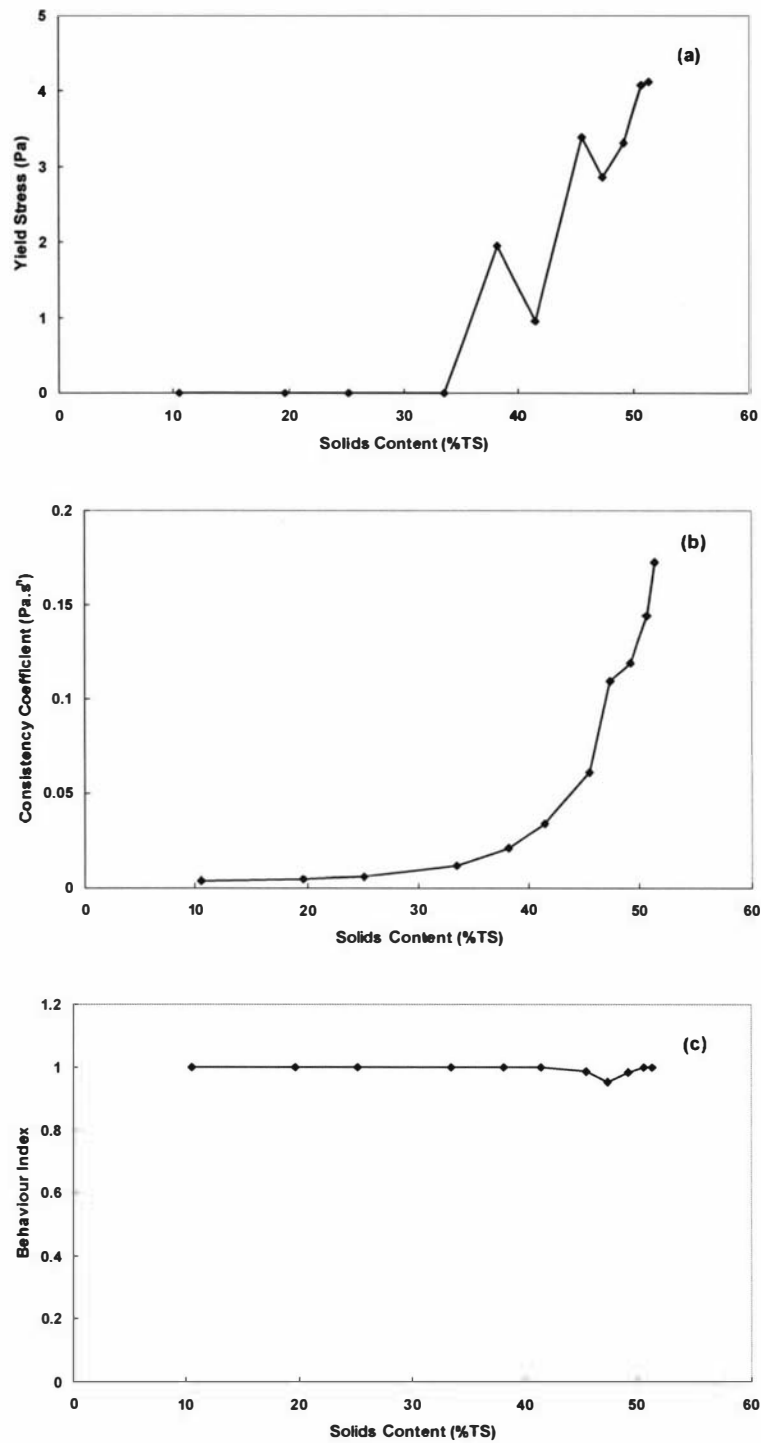


Figure 5.19: Effect of solids content on the Herschel-Bulkley model parameters of the reconstituted whole milk solutions. (a)  $\tau_y$ ; (b)  $K$ ; (c)  $n$

The change in pH with solids content is shown in Figure 5.20. The pH at the solids content of 10%TS is 6.68, which closely resembles the pH of 6.7-6.8 of fresh raw milk at 10-12%TS (Venkatachalam et al.,1993). An increase in solids content resulted in a gradual decrease in pH up to the value of 47%TS. Above this concentration, the pH appeared to have reached a minimum plateau of 6.22. The inversely proportional relationship between pH and solids content has been discussed by previous authors (Upadhyay, 1998; Bienvenue et al., 2003a). However no detailed data covering a wide solids content range has been found in the literature.

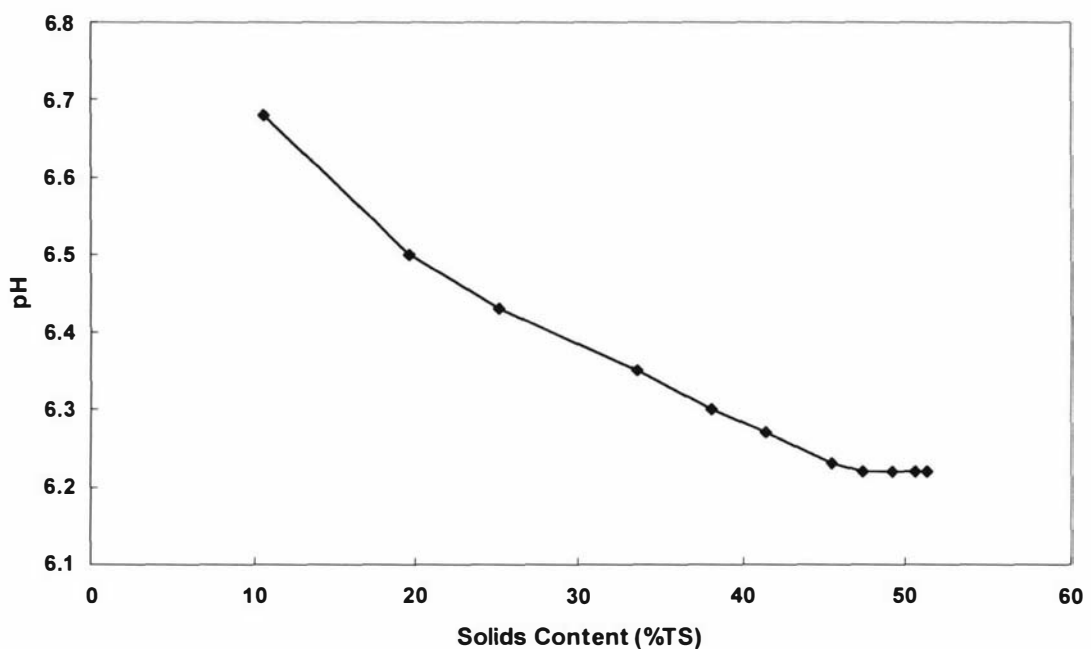


Figure 5.20: Effect of solids content on the pH of the reconstituted whole milk solutions at 35°C. Powder B, 50%TS.

Figure 5.21 shows that the particle size distribution did not change with an increase in solids content. A mono-modal distribution shape was observed for all curves. Particles larger than 2  $\mu\text{m}$  were considered as aggregated particles formed during the powder manufacturing and recombination processes and were not present in raw milk at 10%TS. Thus, the PSD could be subdivided into two zones,  $< 2\mu\text{m}$  and  $> 2\mu\text{m}$  which can be regarded as an aggregation zone. Figure 5.22 plots the changes in aggregation zone with solids content. Approximately 5% of the particles were larger than 2  $\mu\text{m}$ . No significant

changes were observed in the aggregation zone, indicating no aggregation process with an increase in solids content.

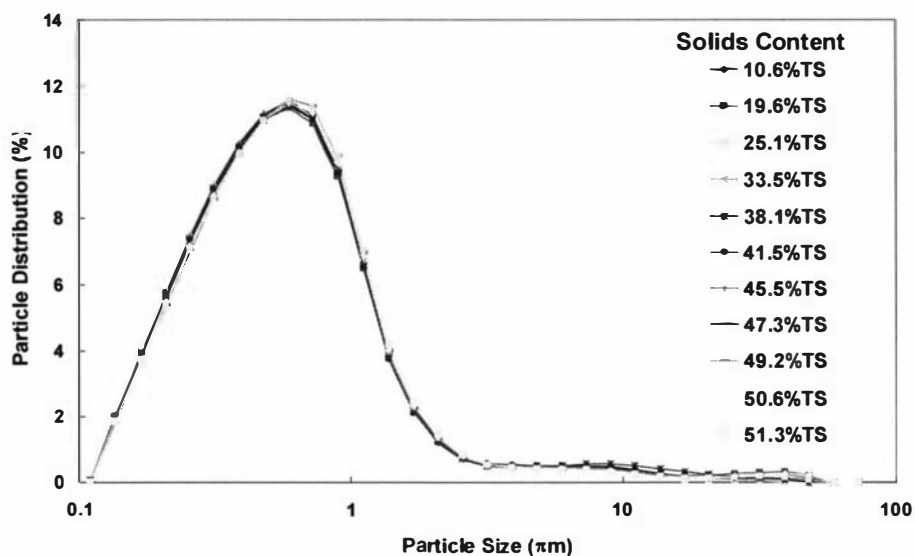


Figure 5.21: Effect of solids content on the particle size distribution of the reconstituted whole milk solutions at 35°C.

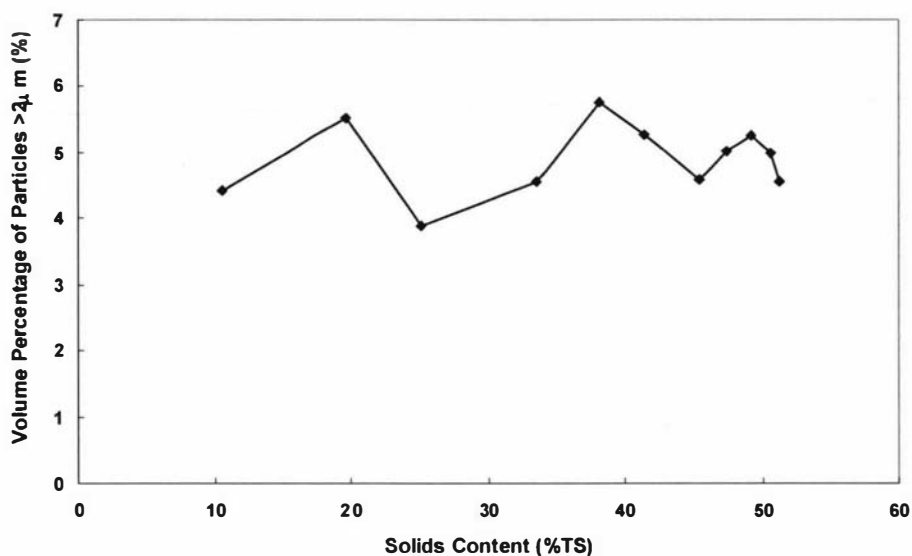


Figure 5.22: Effect of solids content on the volume percentage of particles > 2 μm at 35°C.

## **5.4 Effects of solids content and temperature on the rheology of reconstituted whole milk concentrates**

The picture of milk concentrate rheology painted in the literature is still patchy. Most authors working with fresh concentrates did not have access to full pilot plant facilities with adequate preheating systems and evaporators of suitable design. More important, many previous experiments only covered solids content of 20% and below (e.g. Fernandez-Martin, 1972, Anema, Lowe, & Li, 2004). Snoeren et al. (1984), Velez-Ruiz and Barbosa-Canovas (1997, 1998, 2000) and Bienvenue et al. (2003a, 2003b) are among the few authors who experimented with milk concentrates above 25%TS.

A comprehensive set of data describing the effects of temperature, total solids content, protein content, milk quality, preheat treatment, equipment configuration and storage time on milk concentrate rheology is still some time away. Rheological measurements of reconstituted milk concentrates are also very incomplete. The problem here lies in the inadequate control of age-thickening during the reconstitution process. When this is not done widely, variable results are obtained (Trinh et al., 2002).

The current work investigated the combined effect of solids content and storage temperature on the rheological behaviour for two different reconstituted medium heat whole milk concentrate systems.

### **5.4.1 Materials and methods**

Medium heat whole milk powders A and B were used in this exercise. However, the number of experiments and the experimental conditions varied between the concentrates made from the two different powders.

As stated in chapter 3, section 3.5.1, the two powders were obtained from two different manufacturing plants in New Zealand. The two powders possessed similar compositional

specifications, with powder B possessing a slightly higher protein content at 25.6% compared to 24.3% in powder A. Powder B also received slightly harsher preheat treatment at 100°C for 40 seconds, compared to 101°C for 20 seconds in powder B.

Powder A was reconstituted to different solids contents (10-48%TS  $\pm$  0.5%TS). The reconstituted milk solutions were recirculated for 60 minutes at 40,000 s<sup>-1</sup> before being heated to different temperatures (45-85°C  $\pm$  2°C) in a PHE. The heated solutions were then stored in a water bath at the temperature of the final heating step. The experimental runs and their associated solids content and temperature values are listed in Table 5.5.

Table 5.5: Experimental conditions to study the effect of solids content and temperature on the rheology of reconstituted whole milk concentrates made from powder A.

<b>Temp. (°C)</b> <b>Solids Content (%TS)</b>	<b>45</b>	<b>55</b>	<b>65</b>	<b>75</b>	<b>85</b>
<b>10</b>	C31				C32
<b>20</b>	C33				C34
<b>30</b>	C35				C36
<b>35</b>	C37				C38
<b>40</b>			C39	C40	C41
<b>44</b>			C42	C43	C44
<b>46</b>	C45	C46	C47	C48	C49
<b>48</b>	C50	C51	C52	C53	C54

Powder B was reconstituted to 50%TS  $\pm$ 0.5%TS at 35°C and 40,000s<sup>-1</sup>. The reconstituted concentrates were then heated to four different temperatures, 35°C, 65°C, 71°C and 75°C. Thus, only the effect of temperature on the rheological behaviour of the reconstituted concentrates made from this powder was investigated. The purpose of the

exercise was to provide some preliminary data to allow comparison be made on the rheological behaviour of concentrates made from two batches of powder. The experimental runs and their associated temperature values are listed in Table 5.6.

Table 5.6: Experimental run conditions to study the effect of solids content and temperature on the rheology of reconstituted whole milk concentrates made from powder B.

<b>Temp (°C)</b>	35	65	71	75
<b>Runs</b>	C55	C56	C57	C58

PSD analysis was carried out on runs C55 and C57.

## 5.4.2 Powder A results

### 5.4.2.1 Effect of solids content and temperature on the initial apparent viscosity

The initial (0 hr) apparent viscosities of reconstituted milk solutions at 45°C are shown in Figure 5.23.

The apparent viscosity increased exponentially with an increase in solids content. This type of correlation has also been observed in other studies with skim milk (Bloore & Boag, 1981; Snoeren et al., 1982; Snoeren et al., 1984; Vilder & Moermans, 1983); and whole milk systems (Femandez-Martin, 1972; Vilder et al., 1979; Snoeren, Brinkhuis et al., 1984; Velez-Ruiz & Barbosa-Canovas, 1997, 1998, 2000; Hinrichs, 1999). Note that the 45°C curve was obtained from cross plotting between 5 different reconstitution experiments.

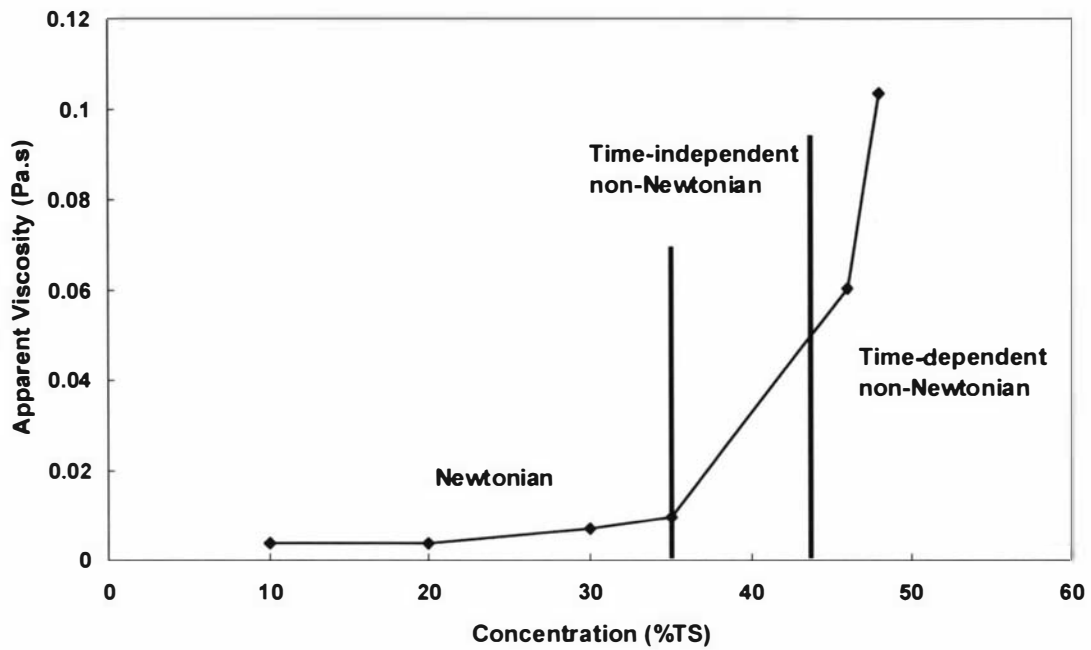


Figure 5.23: Effect of solids content on the initial (0 hr) viscosity of reconstituted whole milk concentrates at 45°C (runs C31, C33, C35, C37, C45, C50).

Reconstituted milk samples below 35%TS at 45°C exhibited Newtonian behaviour and no age-thickening was observed after 4 hours of storage, as shown in Figure 5.24.

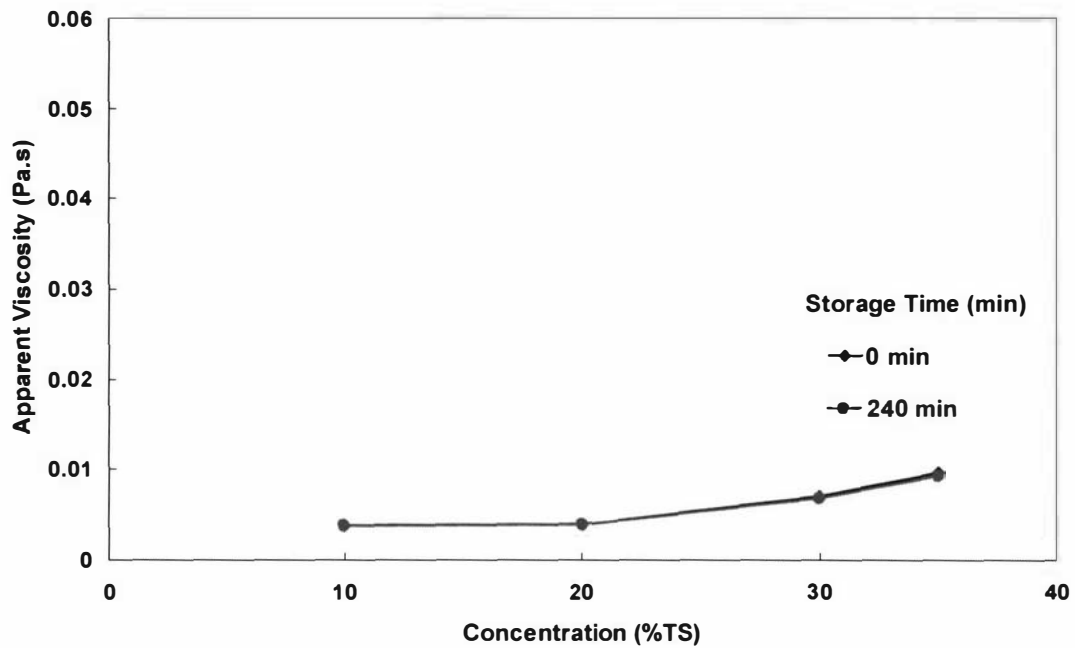


Figure 5.24: Effect of concentration and storage time on the viscosity of reconstituted whole milk concentrates during storage at 45°C. Runs C31 (10%TS), C33 (20%TS), C35 (30%TS), C37 (35%TS), powder A, 45°C.

When the reconstituted milk concentrates were heated and stored at the higher temperature of 85°C, the results were different as shown in Figure 5.25. During storage at 85°C, age thickening was observed after 7 hours of storage at solids contents of 30%TS and 35%TS. Storage at 85°C triggered the onset of age thickening in the 35%TS system.

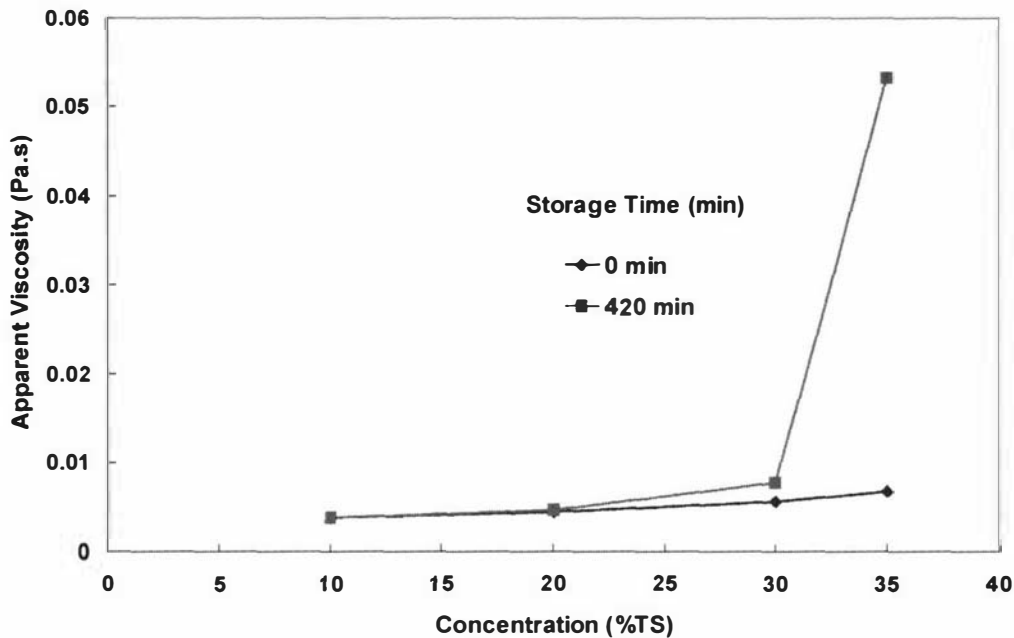


Figure 5.25: Effect of concentration and storage time on the viscosity of reconstituted whole milk concentrates during storage at 85°C. Runs C31 (10%TS), C33 (20%TS), C35 (30%TS), C37 (35%TS), powder A, 85°C.

Velez-Ruiz and Barbosa-Canovas (1997, 1998, 2000) observed power law behaviour at solids content as low as 22% for freshly evaporated milk concentrates. In this work, non-Newtonian behaviour was only observed above 40%TS at 45°C and 30%TS at 85°C. The difference may be due to the much higher shear rate used during reconstitution in this work ( $40,000\text{s}^{-1}$ ), which may delay the onset of age-thickening as discussed in section 3.2 and by Trinh et al. (2004).

The effect of temperature on samples at four nominal concentrations 40%, 44%, 46% and 48% TS is shown in Figure 5.26 (immediately after heating) and Figure 5.27 (after 60 minutes of storage at the heating temperature). The time dependence effect was more visible in Figure 5.27 after 60 minutes of storage. In both graphs, the two higher concentration curves showed a clear minimum viscosity at 65-75°C region. Within experimental error a minimum was not observed at the two lower concentrations (40% and 44% TS).

The general shape of the curve is in qualitative agreement with previous work and the value of the minimum viscosity is also of the same order of magnitude (Bloore & Boag, 1981; Velez-Ruiz & Barbosa-Canovas, 1997; Trinh & Schraekenrad, 2002). Tang et al. (1993) also observed similar minima with whey protein concentrates from 15-30%TS. Interestingly, Anema and Klostermeyer (1997) and Anema (1998) observed a minimum turbidity in heated dilute reconstituted skim milk at 65-70°C.

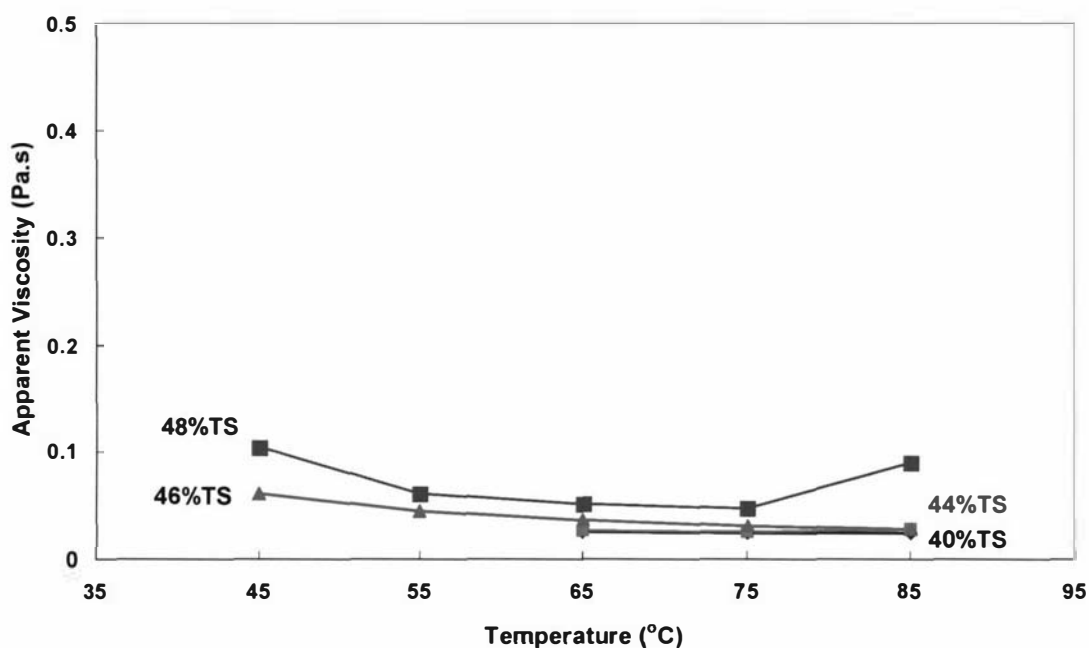


Figure 5.26: Initial apparent viscosity values of various reconstituted whole milk concentrates as a function of temperature. Powder A.

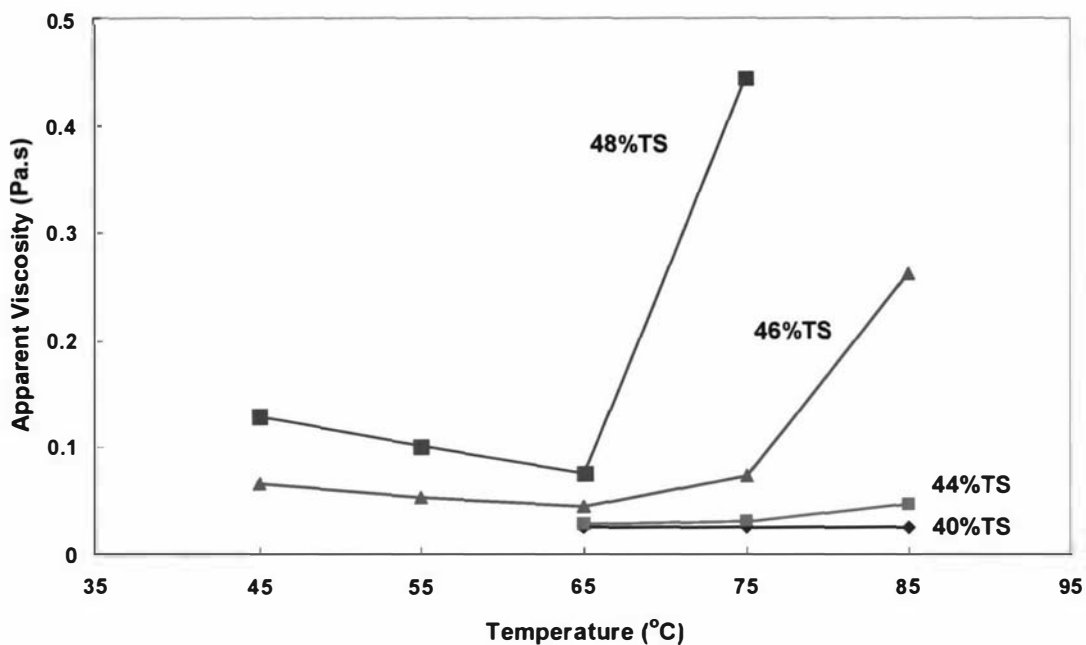


Figure 5.27: Apparent viscosities of various reconstituted whole milk concentrates as a function of temperature after 60 minutes of storage. Powder A.

#### 5.4.2.2 Effect of solids content and temperature on age thickening

Figure 5.28 plots the changes in the apparent viscosity with shear rate at three different storage times in run C52 with 48%TS concentrates heated to 65°C. The data in both the shear up and down legs for each storage time was plotted. Shear thinning behaviour is observed in all samples, where the apparent viscosity decreased with shear rate. This agreed with previously published results (Snoeren et al., 1984; Bienvenue et. al., 2003a, 2003b).

Time dependent behaviour was evidenced by the existence of the hysteresis loop area between the shear up and shear down legs. For this particular run at 48%TS and 65°C, time-dependent behaviour was observed at all times during storage.

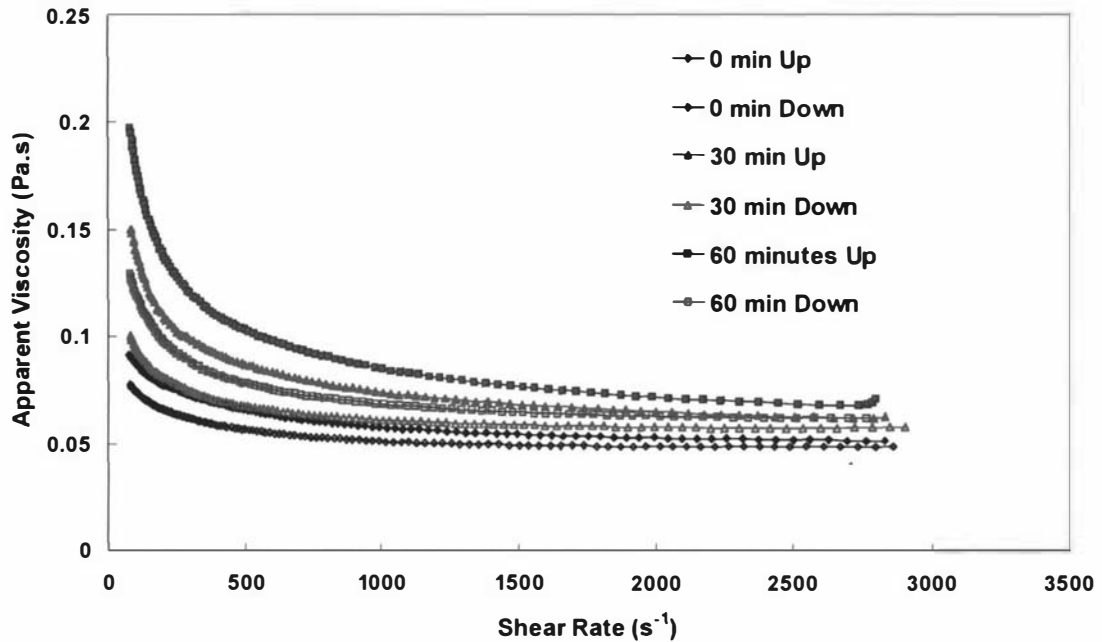


Figure 5.28: Changes in the apparent viscosity with shear rate at different storage times. Run C52, powder A, 48%TS, 65°C.

The age thickening process can be easier to visualise with a plot of the change in apparent viscosity at a given shear stress of 105.3 Pa with storage time. The effects of heating and storage temperature on the rate of age thickening of milk concentrate solutions were analysed at three solids content of 44%TS, 46%TS and 48%TS, and the data are plotted in Figures 5.29, 5.30 and 5.31 respectively.

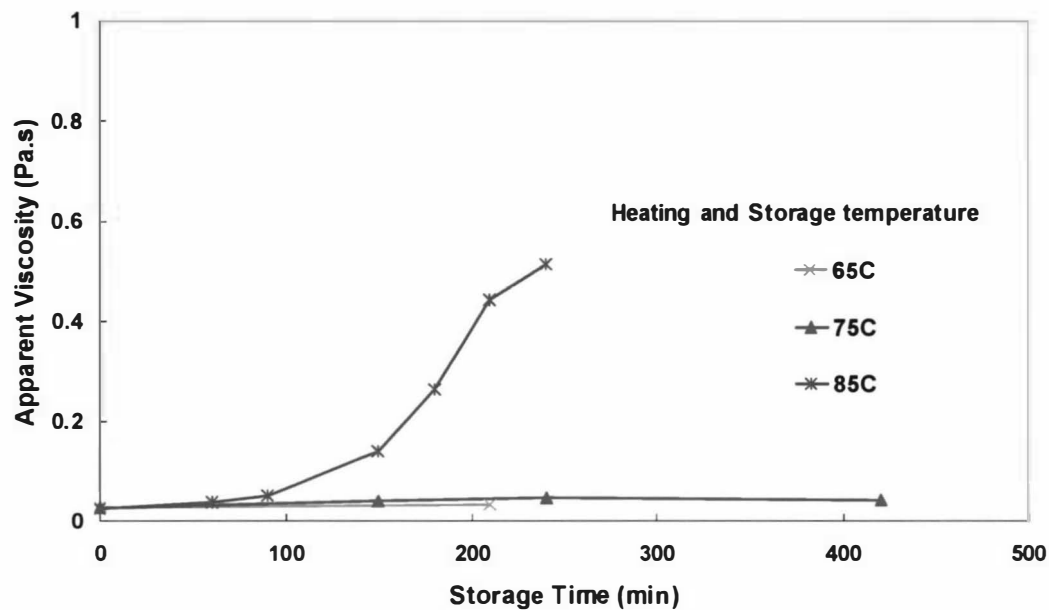


Figure 5.29: Effect of heating and storage temperature on the changes in apparent viscosity with storage time of 44%TS reconstituted milk concentrates. Powder A.

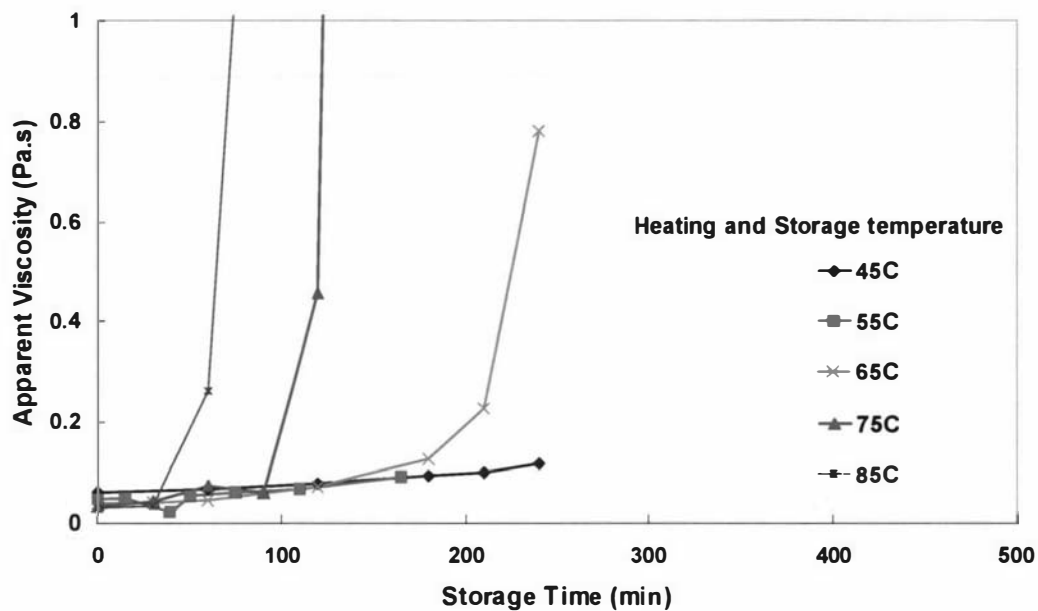


Figure 5.30: Effect of heating and storage temperature on the changes in apparent viscosity with storage time of 46%TS reconstituted milk concentrates. Powder A.

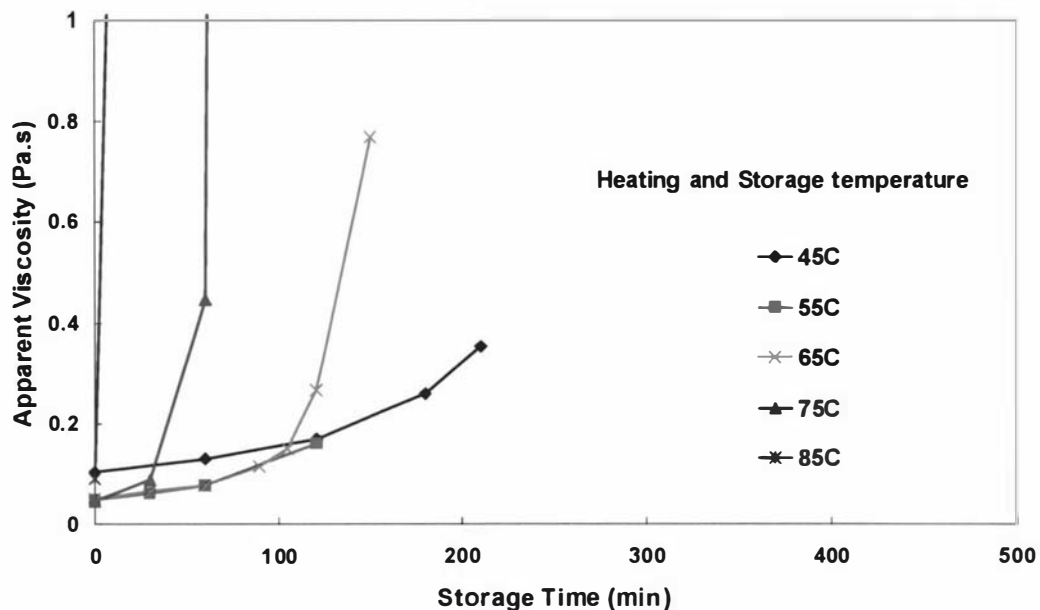


Figure 5.31: Effect of heating and storage temperature on the changes in apparent viscosity with storage time of 48%TS reconstituted milk concentrates. Powder A.

Age thickening was visible in many samples, as evidenced by the slow initial increase in apparent viscosity, followed by a rapid rise which marked the gelling point.

The onset of age thickening depended on both temperature and solids content. At 44%TS in Figure 5.29, age thickening was only observed when the concentrate was heated to 85°C. The increase in apparent viscosity at the two lower heating temperatures of 65°C and 75°C could be accounted for by the 10% error.

In Figures 5.30 for 46%TS, and 5.31 for 48%TS concentrates, the increase in apparent viscosity with storage time in all samples could not be accounted for by the 10% error. An increase in solid content to 46%TS and 48%TS lowered the minimum temperature required for the onset of age thickening to 65°C and 45°C respectively.

In Figures 5.30 and 5.31, as the temperature was increased, the gelling time decreased. This indicated that the formation of a network structure takes place faster at higher

temperatures. However, the viscosity values at the gelling point were roughly similar at 0.1 Pa.s. If the viscosity value represents an indication of the state of the structure, the results suggest that the critical structure at which gelation occurs was independent of temperature and solids content.

It is interesting to observe that in Figure 5.31, at 48%TS, the concentrates heated to 45°C and 55°C did not show any sign of gelation (sharp rise in viscosity with time) even though the apparent viscosity reached the value of 0.1 Pa.s and beyond. It is possible that more than one mechanism is responsible for the onset of gelation at different temperatures, in particular above and below 65°C.

The changes in the apparent viscosity with storage time up to the gelling point could be fitted with an exponential curve. Figure 5.32 plots the changes in the apparent viscosity with storage time for runs C46 (46%TS, 55°C) and C47 (46%TS, 65°C). The fitted correlation coefficients obtained were 0.98 for run C46 and 0.96 for run C47. The exponential relationship could not account for the dramatic increase in the apparent viscosity after gelation. Thus, a multi-component model is required if post-gelation behaviour is to be monitored.

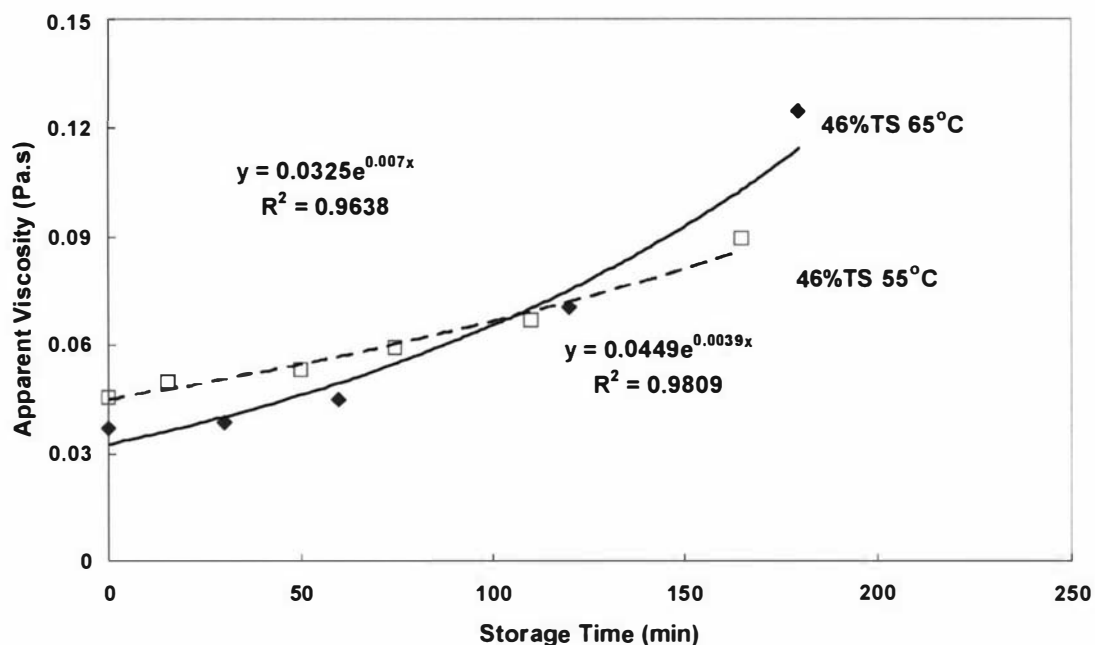


Figure 5.32: Changes in the apparent viscosity with storage time up to the gelling point at two heating and storage temperatures. Runs C46 (55°C) and C47 (65°C), powder A, 46%TS.

For simplicity, the rate of age thickening (RAT) up to the gelling point is determined as

$$\text{Rate of age thickening (RAT)} = \frac{\Delta\mu}{\Delta t} = \frac{\mu_b - \mu_a}{t_b - t_a} \quad (5.4)$$

where the subscripts  $a$  and  $b$  define the start and end points.

Thus the change in apparent viscosity with storage time is simplified to a straight line formula.

The effect of concentration on age-thickening is illustrated in Figures 5.33-5.35 for solutions that were heated and stored at 65°C, 75°C and 85°C respectively. As expected, the results clearly showed that age thickening took place at lower solids content as the heating temperature was increased. For example, the 46%TS gelled after 200 minutes of

storage at 65°C, 100 minutes at 75°C and 60 minutes at 85°C. The 44%TS curve only exhibited significant age thickening behaviour when heated to 85°C.

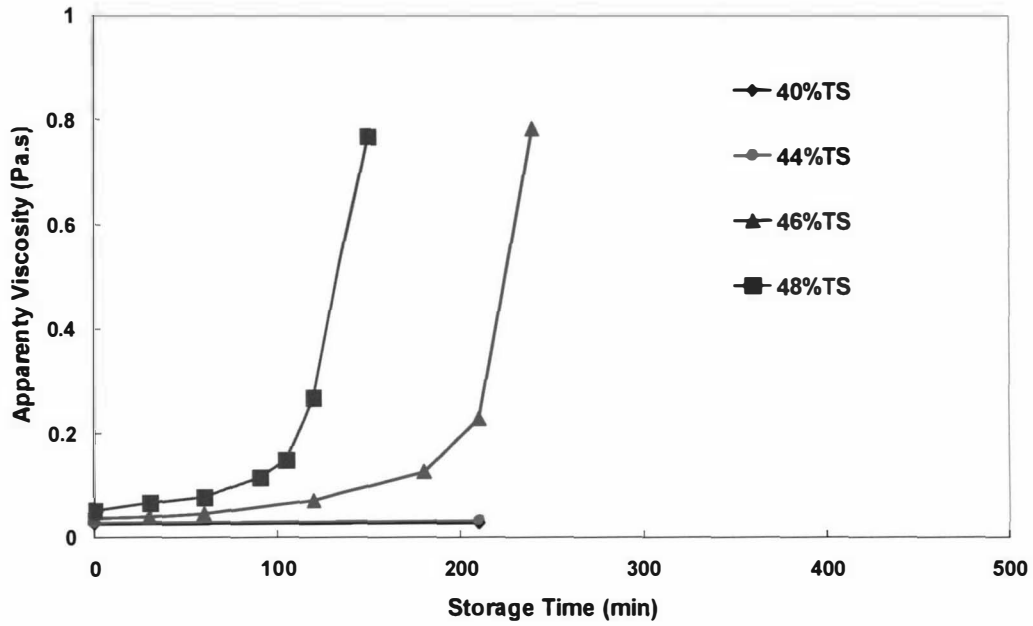


Figure 5.33: Effect of solids content on the changes in apparent viscosity with storage time in reconstituted milk concentrate solutions that were heated and stored at 65°C. Powder A.

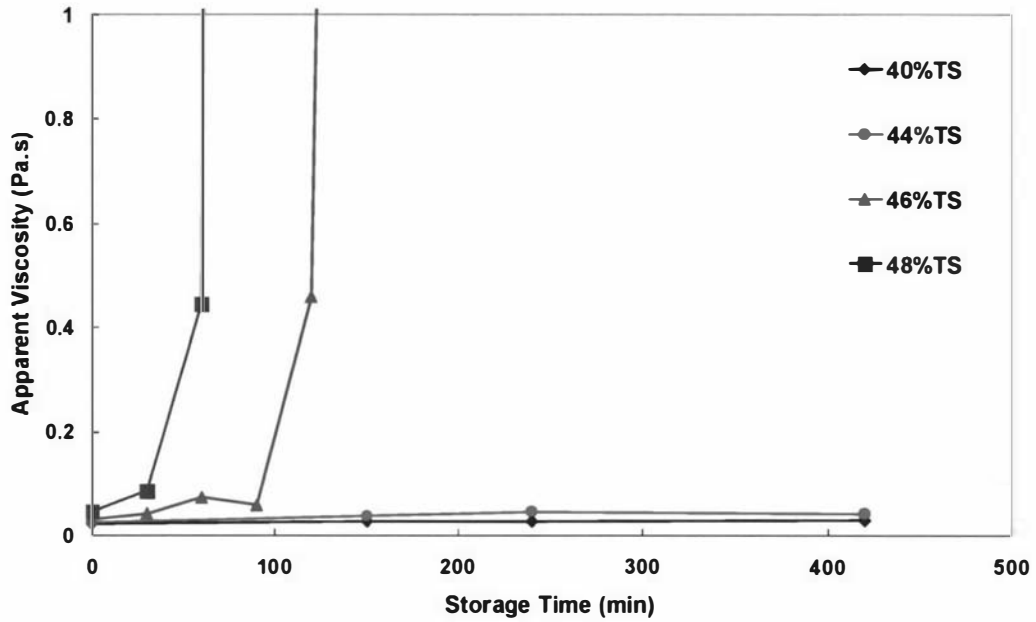


Figure 5.34: Effect of solids content on the changes in apparent viscosity with storage time in reconstituted milk concentrate solutions that were heated and stored at 75°C. Powder A.

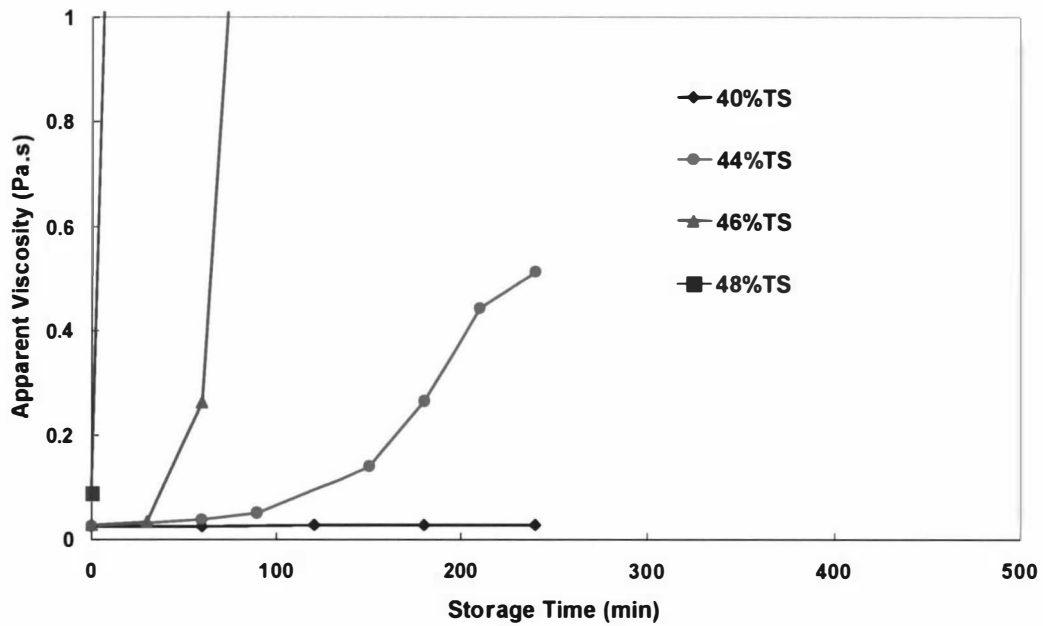


Figure 5.35: Effect of solids content on the changes in apparent viscosity with storage time in reconstituted milk concentrate solutions that were heated and stored at 85°C. Powder A.

The effects of solids content and heating and storage temperature on the gelling time are plotted in Figure 5.36. For a given temperature, the gelling time decreased with an increase in solids content (Figure 5.36 (a)). While for a given solids content, the gelling time decreased with an increase in heating and storage temperature (Figure 5.36 (b)). For the 46%TS concentrates, the gelling time decreased with an increase in heating temperature.

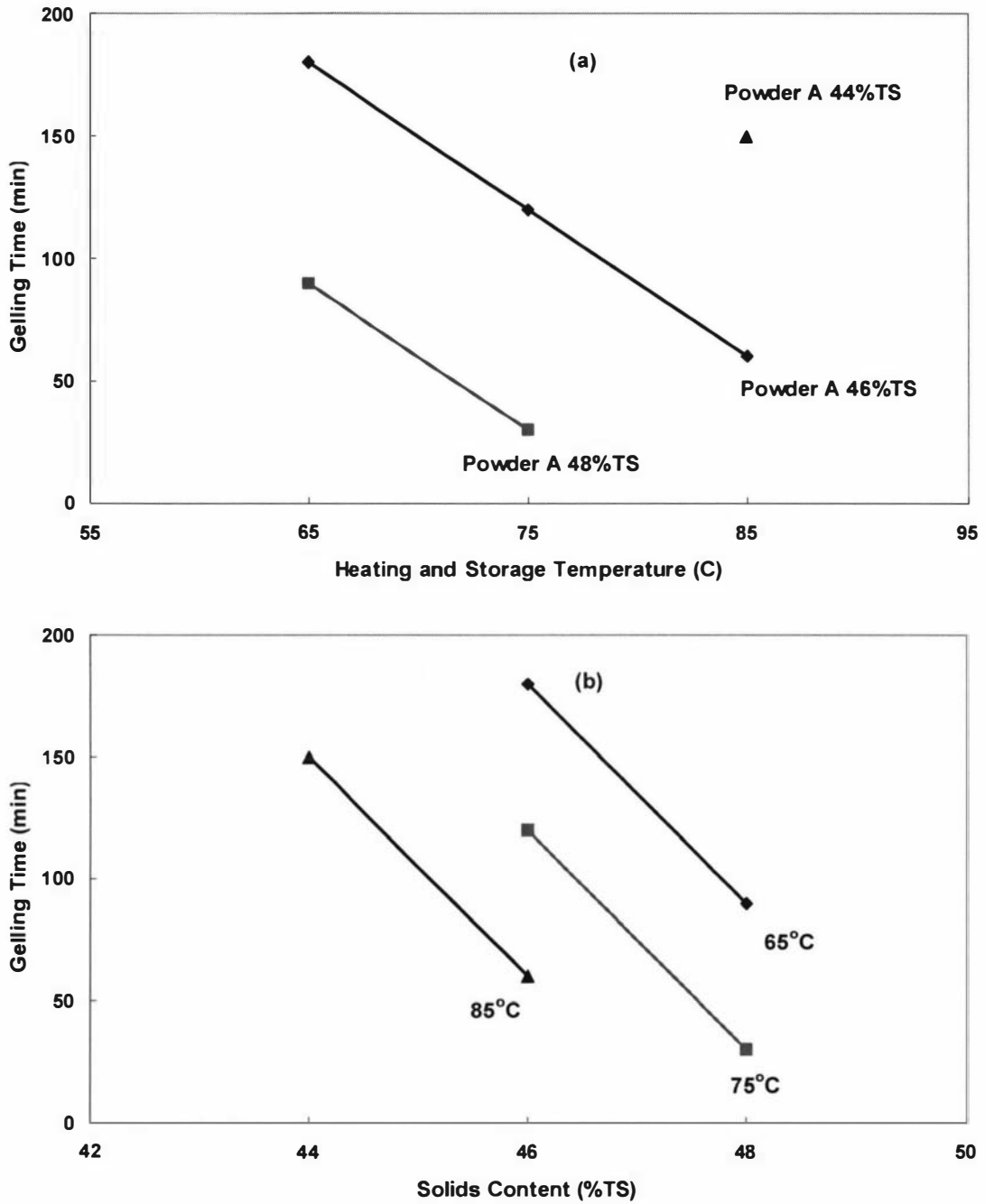


Figure 5.36: Effects of solids content and temperature on the gelling time of the reconstituted concentrates made from powder A. (a) gelling time versus heating and storage temperature at different solids contents, (b) gelling time versus solids content at different heating and storage temperatures.

### 5.4.2.3 Rheological modelling

Solutions at concentrations above 40%TS showed non-Newtonian behaviour. The flow curves for these solutions were fitted with a Herschel-Buckley model to capture snapshots of the age thickening process.

$$\tau = \tau_y + K\dot{\gamma}^n \quad (5.5)$$

A better overall picture is obtained from three-dimensional plots of the yield stress  $\tau_y$ , the consistency coefficient  $K$  and the behaviour index  $n$ . For clarity, separate plots are presented of rheological parameters against temperature-time for one concentration of 48%TS (Figures 5.37-5.39) and against concentration-time for one temperature at 75°C (Figures 5.40-5.42). Because of restricted space, the full data base spanning 5 temperatures, four concentrations and an average of 5 storage times will not be presented here. The trends in the graphs were observed in other sets of data, and provide a true general view of the relationship between solids content, storage temperature and rheological behaviour.

As a requirement for 3D plots, equal number of data points are required along the two horizontal, x and y axes. This was not possible as some samples gelled faster than others. Using the “smooth” function in SigmaPlot 2002 (v9.0), the vacant spots for fast gelling samples were filled with predicted values, and artificial plateaus can be observed. The “inverse distance” smooth function was employed, where the weighted average of the values at neighbouring points is computed using inverse distance.

In Figures 5.37-5.39, as the temperature and storage time increased, there was an increase in the yield stress (5.38) and consistency coefficient (5.37), as well as a decrease in the behaviour index (5.39). This agreed with the observations made by Velez-Ruiz and Barbosa-Canovas (1997).

The data confirms the argument forwarded by Trinh and Yoo (1997) that time-dependent rheological models that attempt to separate the rheological parameters  $\tau_y$ ,  $K$  and  $n$  from a time-dependent “structure” coefficient cannot adequately describe the rheological data of time-dependent systems. Models where the apparent viscosity or rheological parameters all change with time are more successful.

It is also important to point out that the values for the three parameters are fitted values. In particular the yield stress is a fitted yield stress and not a measured yield stress. Whether or not the yield stress has any physical significance is still debatable. A more detailed discussion of yield stress is documented in the appendix, A.2.3.2.

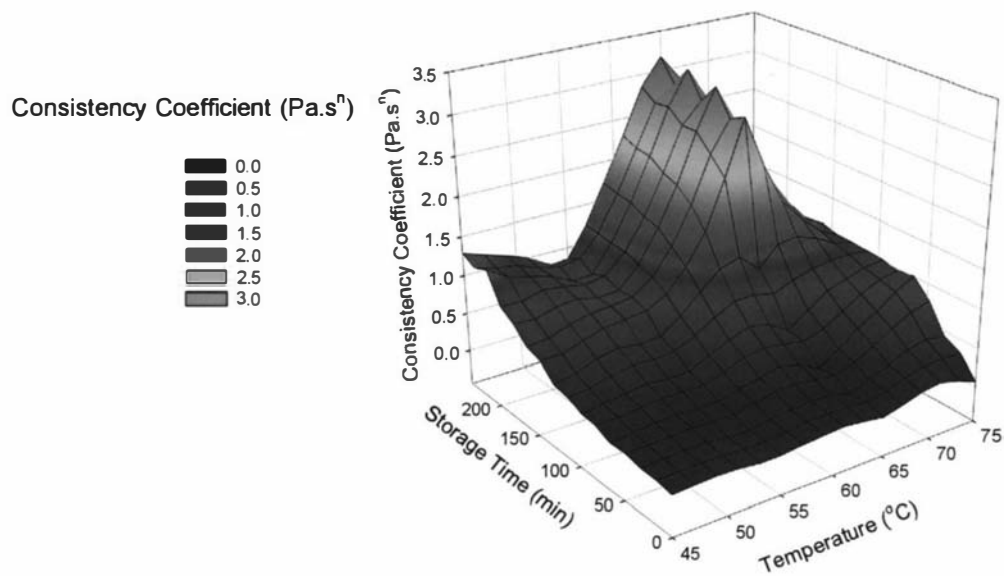


Figure 5.37: Variation of consistency coefficient  $K$  with time-temperature for 48%TS reconstituted whole milk concentrates. Powder A.

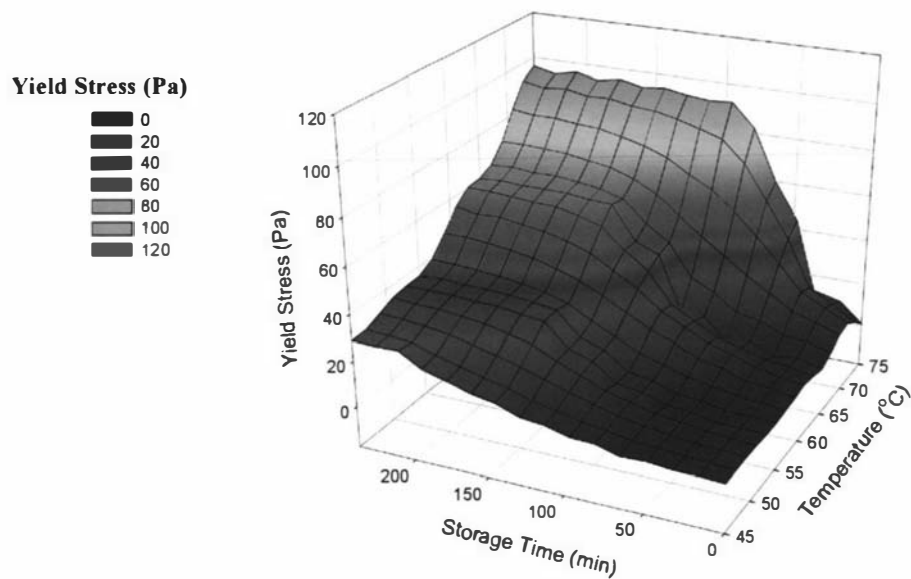


Figure 5.38: Variation of yield stress  $\tau_y$  with time-temperature for a 48%TS solution reconstituted whole milk concentrates. Powder A.

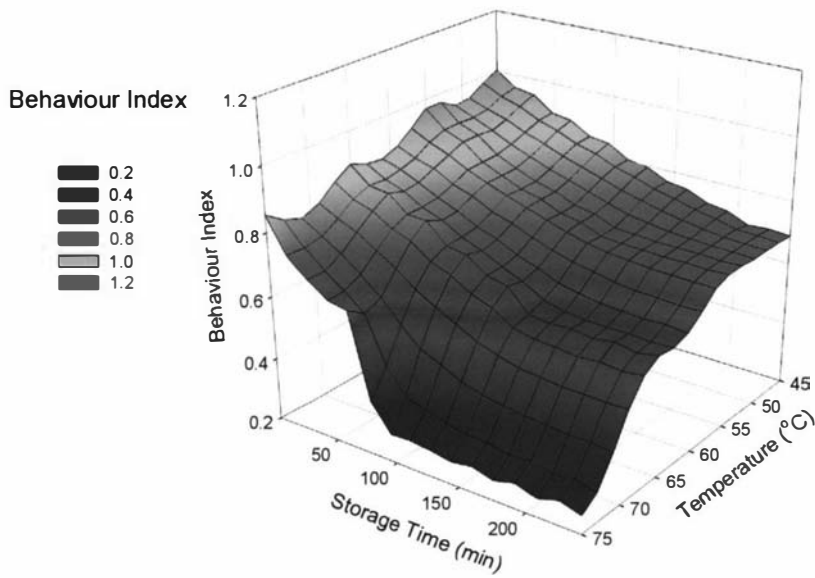


Figure 5.39: Variation of behaviour index  $n$  with time-temperature. 48%TS reconstituted whole milk concentrates. Powder A.

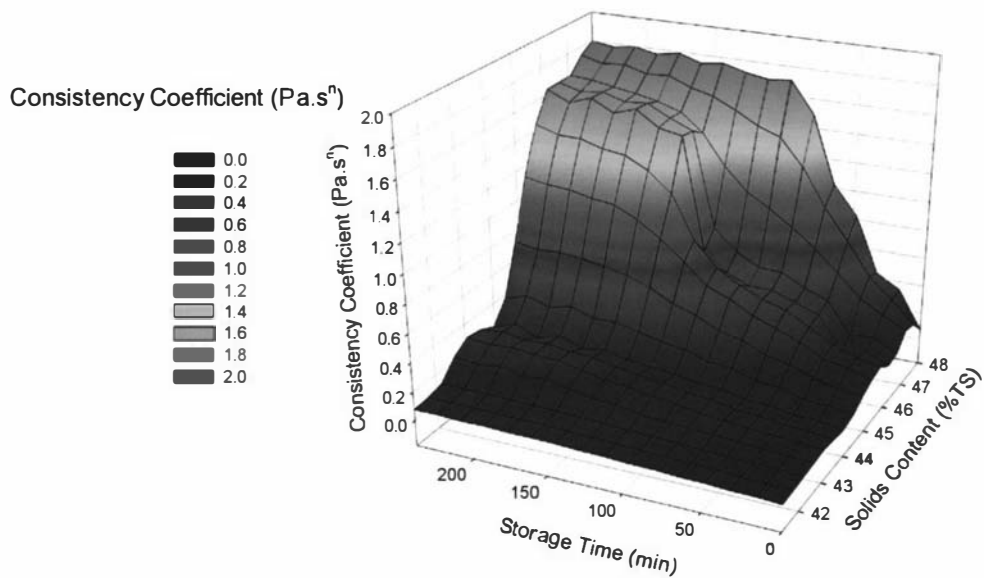


Figure 5.40: Variation of consistency coefficient  $K$  with time-concentration at 75°C for powder A reconstituted whole milk concentrates.

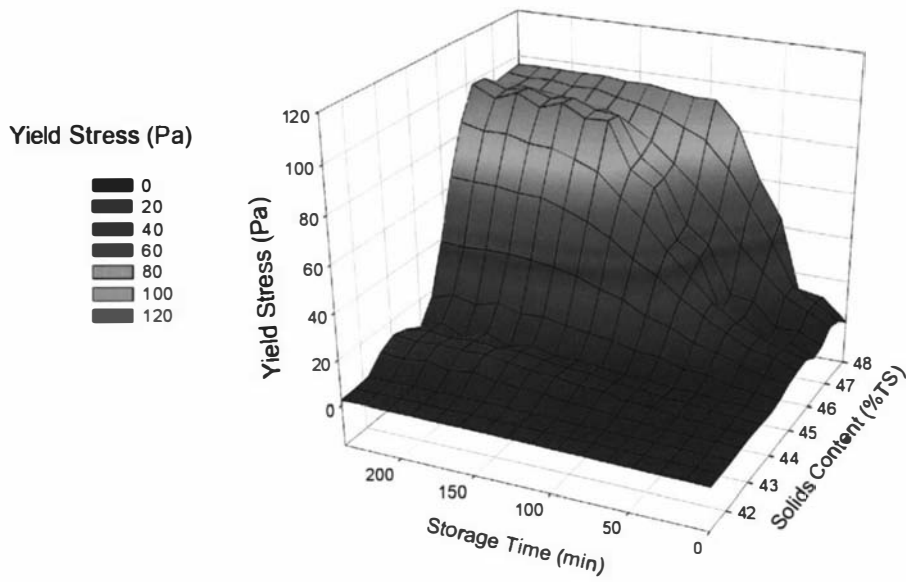


Figure 5.41: Variation of yield stress  $\tau_y$  with time-concentration at 75 °C for powder A reconstituted whole milk concentrates.

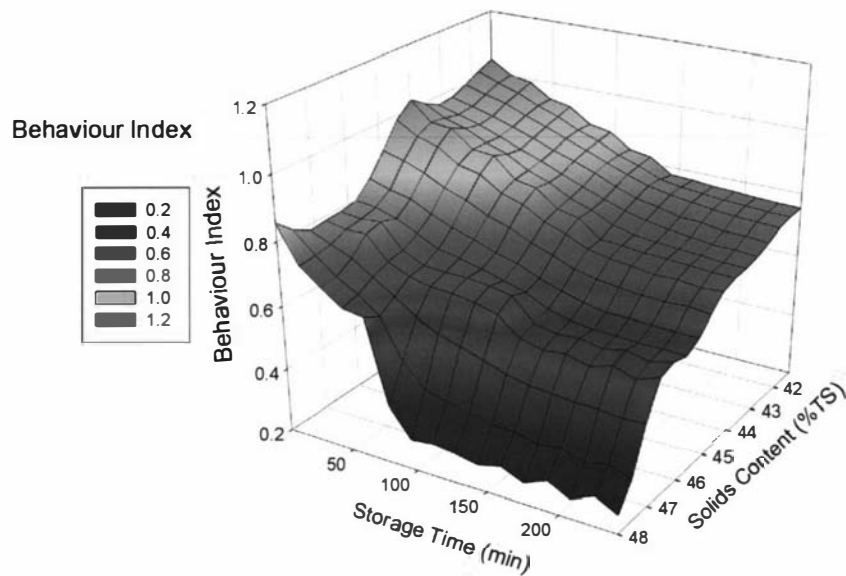


Figure 5.42: Variation of behaviour index with time-concentration at 75 °C for powder A reconstituted whole milk concentrates.

Figures 5.37-5.42 showed that as the milk concentrates age thickened, the systems moved away from Newtonian behaviour as evidenced by the decrease in the behaviour index,  $n$ , with storage time. The accompanying increases in consistency index  $K$  and yield stress  $\tau_y$ , suggested a build up of structure.

The effects of temperature, solids content and storage time on the flow behaviour index were more complex. An increase in solids content and storage time resulted in a decrease in behaviour index. The effect of temperature on behaviour index is similar to that of apparent viscosity, where a minimum is observed in the 65-75°C range, as seen in Figure 5.39.

In Figures 5.39 and 5.42, the behaviour index values obtained at the lower concentrations slightly exceeded the value of 1. This should not be interpreted as an indication of dilatancy but must be seen as a consequence of the uncertainties in curve fitting of three parameter models.

It is difficult to provide a clear trend for the changes in the Herschel-Bulkley parameters at the gelling point with solids content and heating temperature. The concentrates made from powder A exhibited significant changes in rheological behaviour near the gelling point, even within 15 minutes between two measurements. For concentrates made from powder A, the typical ranges of values for the Herschel-Bulkley parameters are given in Table 5.7.

Table 5.7: Typical values for the Herschel-Bulkley parameters at the gelling points in reconstituted concentrates made from powder A.

Herschel-Bulkley parameters	Yield Stress $\tau_y$ (Pa)	Consistency Coefficient (Pa.s <sup>n</sup> )	Behaviour Index $n$
	0-60	0.5-1.5	0.6-0.7

### 5.4.3 Powder B results

#### 5.4.3.1 Effect of solids content and temperature on age thickening

The effect of heating temperature on the rheological behaviour of 50%TS reconstituted milk concentrates samples made from powder B during storage is shown in Figure 5.43. The changes in the apparent viscosity with storage time during age thickening in powder B concentrates showed similar trends to those observed in Figures 5.29-5.31 and 5.33-5.35 for reconstituted concentrates made from powder A. A steady initial increase in apparent viscosity was observed with time, followed by a sudden sharp increase which marked the gelling point. The apparent viscosity at the gelling point for the three heated solutions (65°C, 71°C and 75°C curves) in Figure 5.43 averaged at approximately 0.6 Pa.s. This was significantly higher than the value of 0.1 Pa.s observed in concentrates made from powder A.

In Figure 5.43, age thickening was apparent even at 35°C where no additional heating was carried out after reconstitution. In addition, the apparent viscosity at 35°C did not show any significant sharp rise with storage time to mark the onset of gelation. The result is similar to that observed in 48%TS reconstituted concentrates made from powder A where heating to 45°C and 55°C did not show a sharp rise in viscosity with storage time. For the analysis sake, the gelling time in the 35°C curve was taken as the time required for the apparent viscosity to pass the 0.6 Pa.s mark.

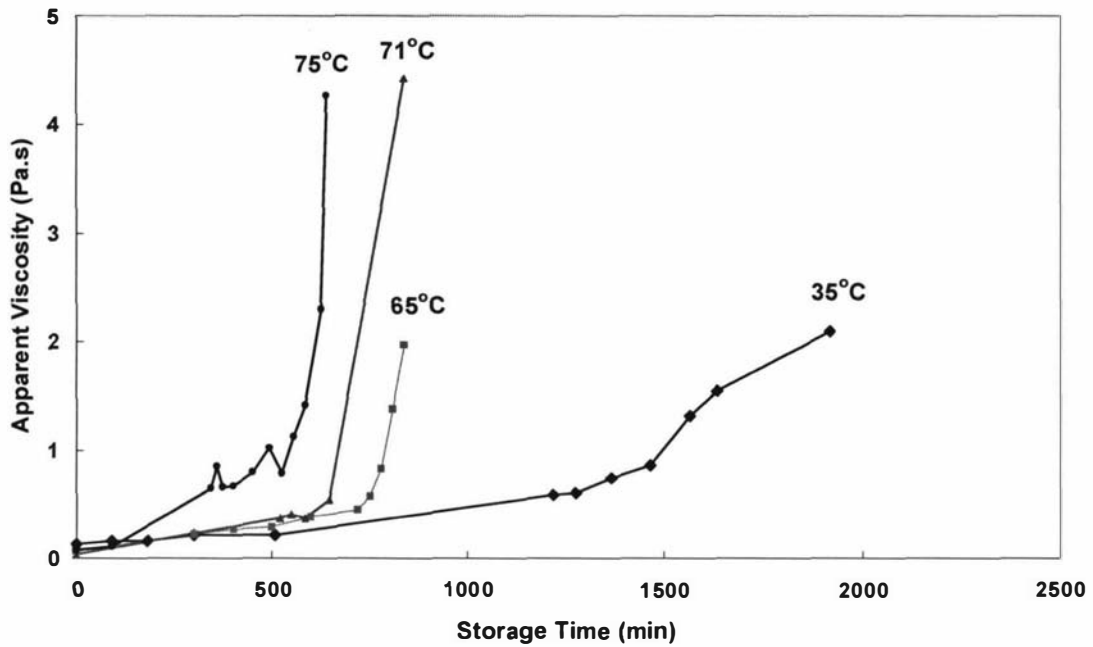


Figure 5.43: Effect of heating and storage temperature on the changes in apparent viscosity with storage time in 50%TS reconstituted milk concentrate solutions. Runs C55-C58, powder B.

Figure 5.44 plots the gelling times at different combinations of solids content and heating temperatures for reconstituted concentrates made from powders A and B. An increase in heating temperature resulted in a decrease in gelling time for concentrates made from the two powders. However, concentrates made from powder B had significantly higher gelling times than those made from powder A.

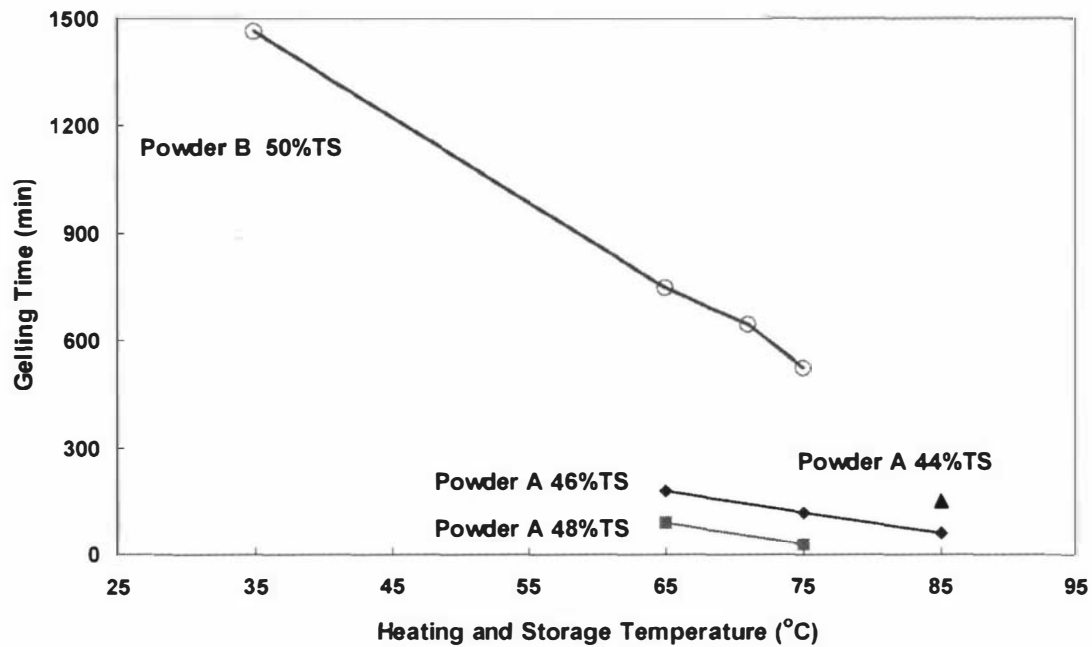


Figure 5.44: Effects of solids content and temperature on the gelling time of the reconstituted concentrates made from powders A and B.

The RAT up to the gelling point for the reconstituted concentrates made from powder B was determined using equation (5.4) and the results are plotted in Figure 5.45. The figure also plots the RAT for the concentrates made from powder A at 44%TS, 46%TS and 48%TS.

Figure 5.45 showed that RAT increased exponentially with temperature for concentrates made from powders A and B. Given that the apparent viscosity at the gelling point does not vary significantly within a concentrate system, a high RAT would result in a shorter gelling time. This agreed with the trends in the gelling time observed in Figures 5.36 for powder A and Figure 5.44 for powder B. Figure 5.45 also showed that the 48%TS concentrates from powder A and the 50%TS concentrates from powder B possessed similar RAT.

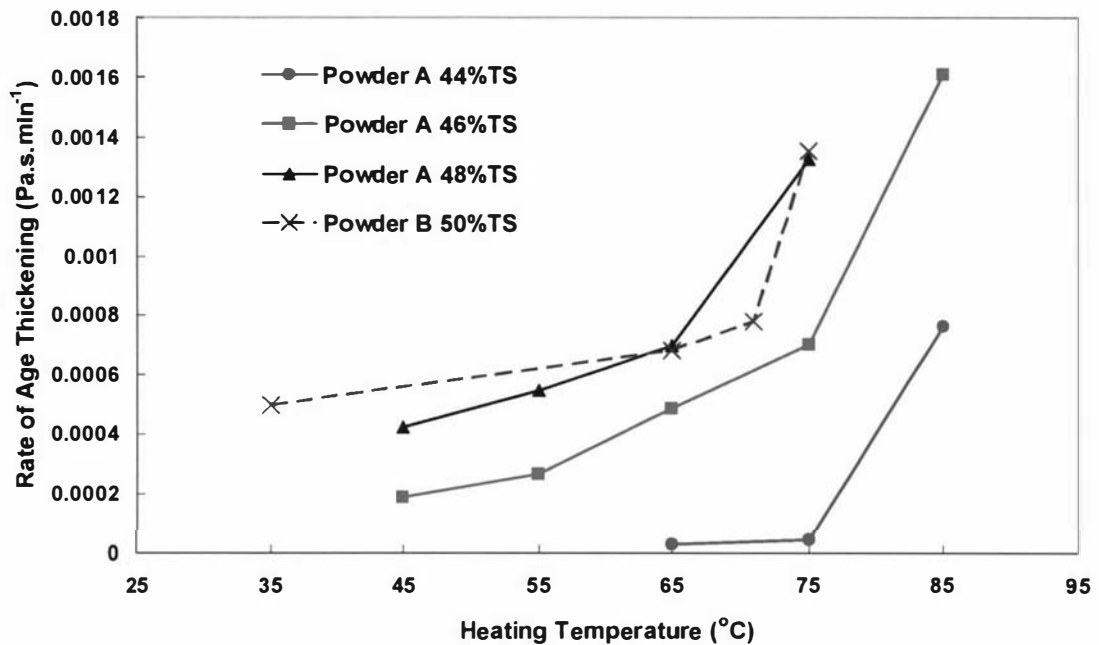


Figure 5.45: The effect of powder type on the rate of age thickening (RAT) up to the gelling point of reconstituted concentrate samples made from powders A and B.

### 5.4.3.2 Rheological modelling

The changes in the Herschel-Bulkley model parameters with storage time for the concentrates made from powder B in runs C55-C58 are shown in Figure 5.46. Similar to that observed in section 5.4.2 with concentrates made from powder A, Figure 5.4.5 showed that during age thickening,  $\tau_y$  and  $K$  increased while  $n$  decreased with storage time. This trend was more prominent at higher heating temperatures.

Table 5.8 lists the apparent viscosities and the Herschel-Bulkley parameters at the gelling point at three different heating temperatures in concentrates made from powder B. Compared to Table 5.7 that listed the typical values of the Herschel-Bulkley parameters at gelation for powder A concentrates,  $K$  is generally higher while  $n$  is lower for concentrates made from powder B.

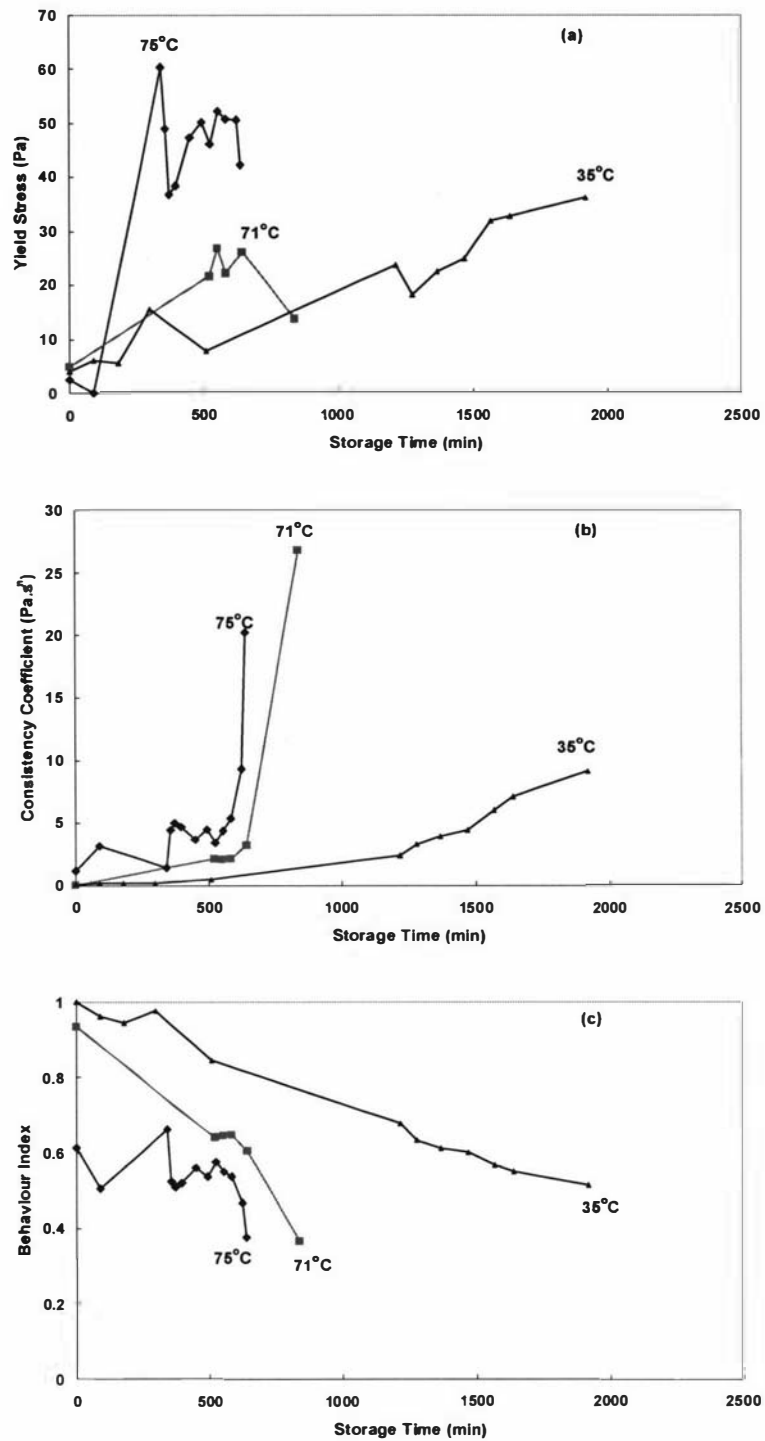


Figure 5.46: Effect of heating and storage temperature on the changes in the Herschel-Bulkley model parameters with storage time in reconstituted whole milk concentrates made from powder B. (a)  $\tau_y$ ; (b)  $K$ ; (c)  $n$ . Runs C55-C58, powder B, 50%TS.

Table 5.8: Changes in the apparent viscosity and the Herschel-Bulkley parameters at the gelling points in reconstituted concentrates made from powder B at different heating temperatures.

Temperature (°C)	$\mu_{app}$ (Pa.s)	$\tau_y$ (Pa)	$K$ (Pa.s <sup>n</sup> )	$n$
35	0.85	24.98	4.42	0.60
71	0.54	26.12	3.21	0.61
75	0.78	46.19	3.44	0.58

In comparing the data in Table 5.9 for concentrates made from B and Table 5.8 for concentrates made from powder A, it is clear that the rheological behaviour at the gelling point differed significantly between the two concentrate systems. The reconstituted concentrates made from powder B possessed higher apparent viscosity, consistency coefficient and lower behaviour index at the gelling point, as well as longer gelling time.

#### 5.4.3.3 Changes in PSD of powder A reconstituted concentrates during age thickening

The changes in the PSD in runs C55 and C58 are shown in Figures 5.47 and 5.48 respectively. At 35°C, the PSD did not change significantly with storage time, and thus did not agree with the trend in apparent viscosity which increased during age thickening. At 75°C, the PSD changed from a mono-modal to a bi-modal distribution during age thickening. This agreed with the observations made by Bienvenue et al. (2003a, 2003b) in their studies with 45%TS fresh skim milk concentrates.

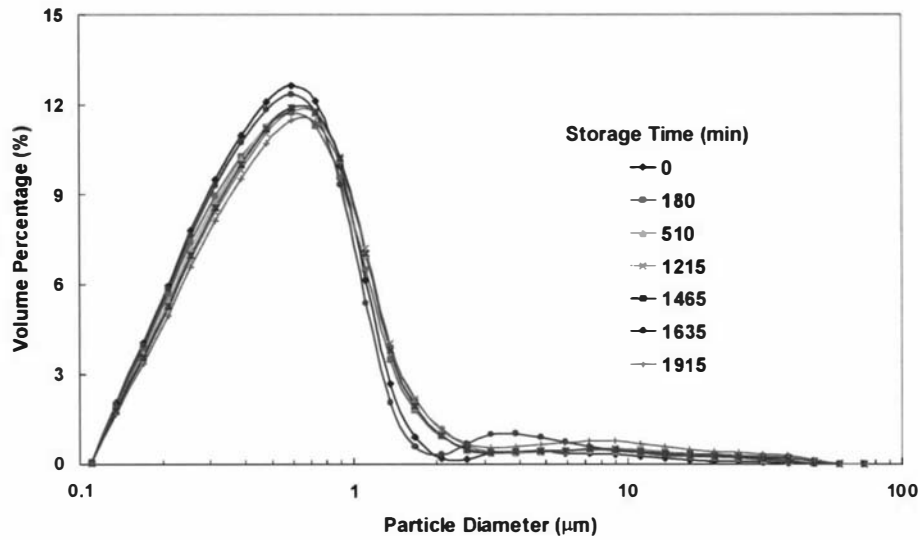


Figure 5.47: Changes in particle size distribution with storage time. Run C55, powder B, 50%TS, 35°C.

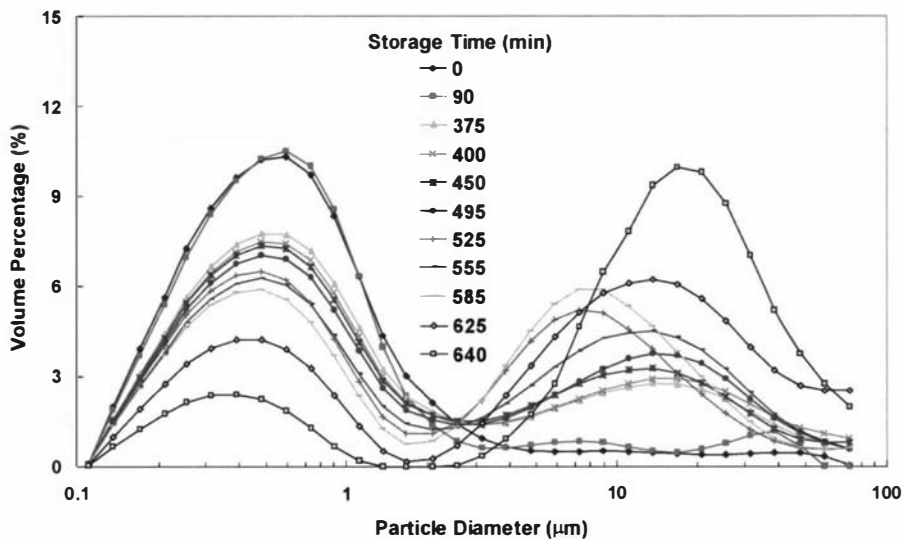


Figure 5.48: Changes in particle size distribution with storage time. Run C58, powder B, 50%TS, 75°C.

The newly formed particles that are larger than 2 $\mu\text{m}$  can be considered as aggregates formed during age thickening. Therefore, the change in the volume percentage of

particles larger than  $2\mu\text{m}$  with storage time was considered as the aggregation profile. Figures 5.49 and 5.50 compare the changes in the aggregation profile and apparent viscosity in runs C55 and C58.

Figure 5.49 in run C55, where the concentrates did not receive a high heat treatment, showed no significant change in the aggregation profile with storage time. The aggregation profile did increase from 3% to 8%. However, the small increase in volume percentage of particles larger than  $2\mu\text{m}$  did not agree with a seventeen times increase in apparent viscosity with storage time during age thickening.

In Figure 5.50, the general trend in the aggregation profile and apparent viscosity showed similar behaviour with storage time. The volume percentage of particles  $>2\mu\text{m}$  increased significantly after 525 minutes of storage time, which coincided with the gelling time.

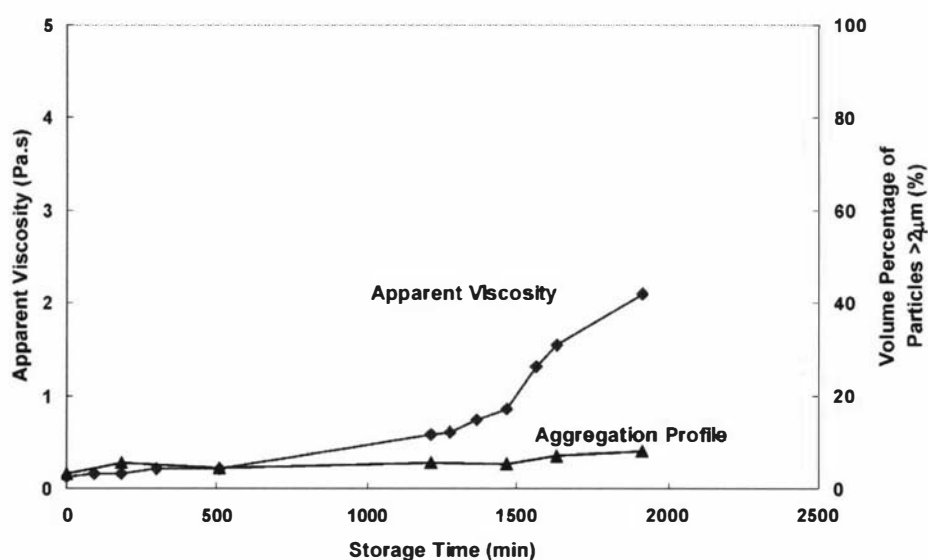


Figure 5.49: Comparison of the change in apparent viscosity and aggregation profile with storage time. Run C55, powder B, 50%TS,  $35^{\circ}\text{C}$ .

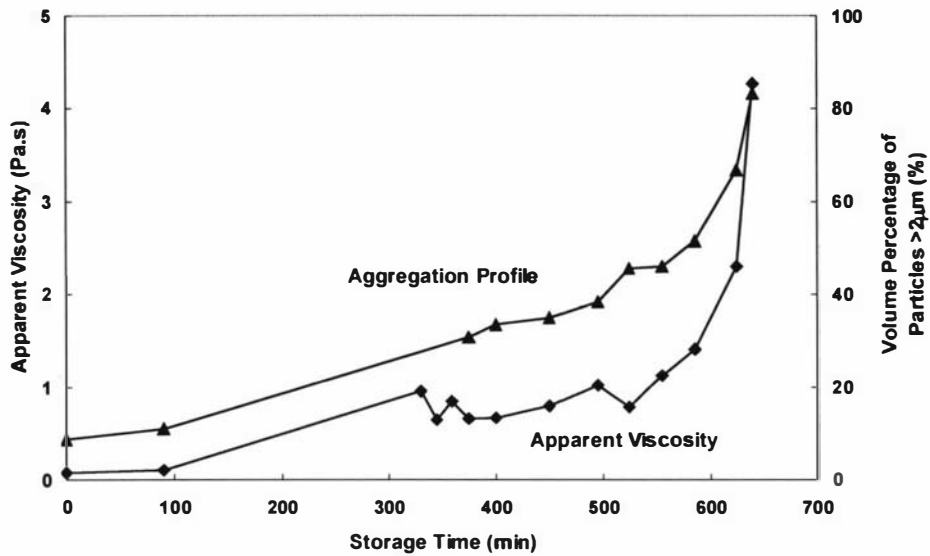


Figure 5.50: Comparison of the change in apparent viscosity and aggregation profile with storage time. Run C58, powder B, 50%TS, 75°C.

#### 5.4.4 Data summary

The results showed the combined effects of temperature and solids content on the time-dependent rheological behaviour of reconstituted milk concentrates. Higher solids content and temperature tended to give rise to faster rate of age thickening and subsequently shorter gelling time. Rheological modelling showed that the concentrates shifted away from Newtonian behaviour as age thickening progresses, as indicated by a decrease in  $n$ . An increase in  $\tau_y$  and  $K$  with storage time indicated structural build-up during age thickening, which agreed with the PSD results.

It should be noted that the reconstituted concentrates from powder A never exceeded 48%TS due to the rapid rate of age thickening upon heating. For example, at 85°C, the 48%TS samples gelled almost instantly.

## **5.5 Effect of shear rate during recirculation on the rheological behaviour of reconstituted milk concentrates during reconstitution and subsequent heating and storage**

It is often argued that the rheology of time-dependent systems is dependent on their shear history (e.g. Cheng, 1987; Barnes, 1997; Bienvenue et al., 2003a). Unfortunately most publications on recombined and reconstituted products provide little information about the shear history. In fact, there has been no work to study the effect of shear history during recombination on the rheology of reconstituted time-dependent food systems.

During the commission work of the recombination rig, it was shown that age thickening could be suppressed through the use of high shear, moderate temperature, sodium azide and thorough cleaning procedures, as documented in chapter 3. The effect of shear level during recirculation on the rheological behaviour of time-dependent systems was investigated in more detail.

### **5.5.1 Materials and methods**

Medium heat whole milk powder A was mixed to 48%TS for the recirculation experiment and 47%TS & 48%TS for the two sets of storage experiments. Whole milk powder B was mixed to 50%TS at 35°C. As explained in section 5.4, concentrates made from powder A were only reconstituted to 48%TS and 47%TS as the concentrates at 50%TS would gel too quickly to be monitored.

Three sets of experiments were performed to explore three different aspects of the effect of shear during mixing.

- The first set of experiments analysed the effect of recirculating shear rate on the line viscosity of the milk samples measured off line.
- The second set analysed the effect of these recirculating shear rates over a fixed shearing time on the subsequent rheological behaviour of heated milk products.

- The third experiment investigated in more detail the combined effect of shear level and shearing time during recirculation on the resultant rheological behaviour of the heated time-dependent milk systems.

As shown in section 5.4, powder B possessed a longer gelling time as well as different rheological behaviour during age thickening. Thus the results also compared the effect of recirculation shear rate on the rheological behaviour of reconstituted concentrates made from two different types of whole milk medium heat powder.

The first set consisted of five experiments, C55-C59, where the reconstituted concentrate was recirculated through the rig at 35°C and samples withdrawn from the rig every 15 minutes over a period of 180 minutes for rheology measurement. Recirculation was carried out with five capillary tubes with different internal diameters to modify the shear level applied to the reconstituted milk concentrate systems. The nominal shear rate values at the wall of the tube could be estimated assuming the concentrates behaved as Newtonian fluids as follows

$$\dot{\gamma}_{Newtonian} = \frac{8V}{D} \quad (5.6)$$

where  $V$  is the velocity flow rate (m/s)

$D$  is the inner diameter of the capillary tube (m)

Powders A and B were used in the first set of experiments as shown in Table 5.9.

Table 5.9: Experimental conditions to study the effect of shear rate on the rheology of reconstituted whole milk concentrates during recirculation at 35°C

Tube ID (mm)	1.76	2.56	3.76	5.74	7.06
Recirc. Shear Rate (s <sup>-1</sup> )	40000	1000	4400	1200	600
Powder B	C59	C60	C61		C62
Powder A	C63	C64	C65	C66	C67

In addition, 5 replicate experiments were carried out on both powders A and B to confirm the experimental error was within 10% (C68-72).

In the second set of experiments, the whole milk powder A was reconstituted to 48%TS and recirculated for 60 minutes at five different shear rates (C73-C77). The reconstituted milk solutions were then pumped to a plate heat exchanger with an 18 seconds residence time to achieve 65°C. The heated solutions were divided into a number of samples and stored in a 65°C water bath. The exercise was repeated with powder B 50%TS reconstituted concentrates. However, only two recirculation shear rates were tested, 600 s<sup>-1</sup> in run C78 and 40,000 s<sup>-1</sup> in run C79. The reconstituted concentrates were heated to 75°C, instead of 65°C as carried out on concentrates prepared from powder A.

In the third set of experiments, the whole milk powder A was reconstituted to 47%TS and recirculated at two nominal shear rates of 40,000 s<sup>-1</sup> (C80) and 600 s<sup>-1</sup> (C81). Portions of the products were withdrawn at intervals of 30, 45, 60 and 75 minutes of recirculation and pumped through the plate heat exchanger with 18 seconds residence time to achieve a temperature of 65°C. The heated solutions were stored as before and subjected to rheological measurement.

Particle size distribution (PSD) was measured in runs C67, C80 and C81.

## **5.5.2 Results**

### **5.5.2.1 Effect of recirculation shear rate on the inline rheological behaviour**

The effect of recirculation shear rate on the inline rheological behaviour of reconstituted whole milk concentrates made from powder B is shown in Figure 5.51. A decrease in the recirculation shear rate resulted in an increase in the initial apparent viscosity. At 40,000 s<sup>-1</sup>, the apparent viscosity levelled out after 60 minutes of recirculation. At the two lower shear rates, the apparent viscosity increased with recirculation time after 60 minutes of

recirculation. In fact, the rate of increase in apparent viscosity after 60 minutes of recirculation increased as the shear rate decreased.

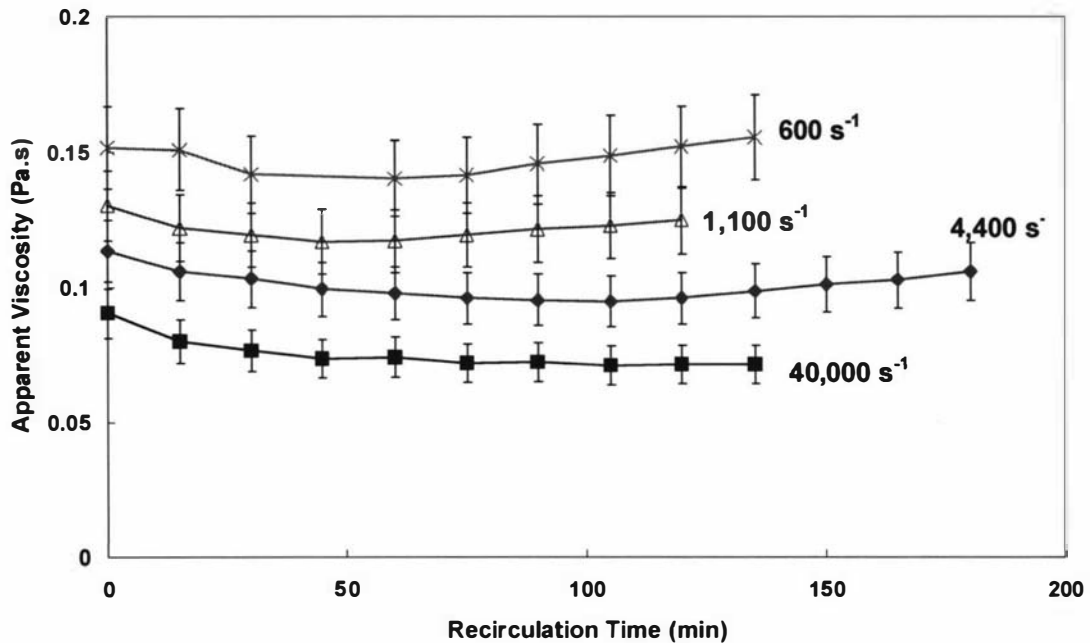


Figure 5.51: Effect of recirculation shear rate on the in-line apparent viscosity at 105.3Pa with recirculation time of the reconstituted milk concentrates. C59-C62, powder B, 50%TS, 35°C.

The flow curves for the data in Figure 5.51 were fitted to the Herschel-Bulkley model, and the changes in the parameters with recirculation time and shear rate are shown in Figure 5.52.

The yield stress trend in Figure 5.52 (a) was anomalous and did not show any consistent trend. The yield stress values during recirculation at 4,400 s<sup>-1</sup> were higher than the values obtained at three other recirculation shear rates. The discrepancy was not significant, and could have been due to experimental error or shortcomings in the model fitting.

The trend for the consistency coefficients against recirculation time in Figure 5.52 (b) resembled that of the apparent viscosity against recirculation time in Figure 5.51. As the consistency coefficient reflects the thickness of the systems, it is likely to match the trends shown by the apparent viscosity data. Similarity between the trends of consistency coefficient and apparent viscosity during age thickening was observed in many cases, as will be shown in the data in subsequent sections. The significance of this observation will be discussed in section 6.3.2.3.

The behaviour index for the four curves in Figure 5.52 (c) initially started below 1, and then quickly reached the value of 1. The results showed that after 60 minutes of recirculation, the reconstituted systems do not show shear thinning behaviour, even at the recirculation shear rate of  $600 \text{ s}^{-1}$ . Thus, the reconstituted systems essentially behaved as Bingham plastic fluids, showing the flexibility of the Herschel-Bulkley model.

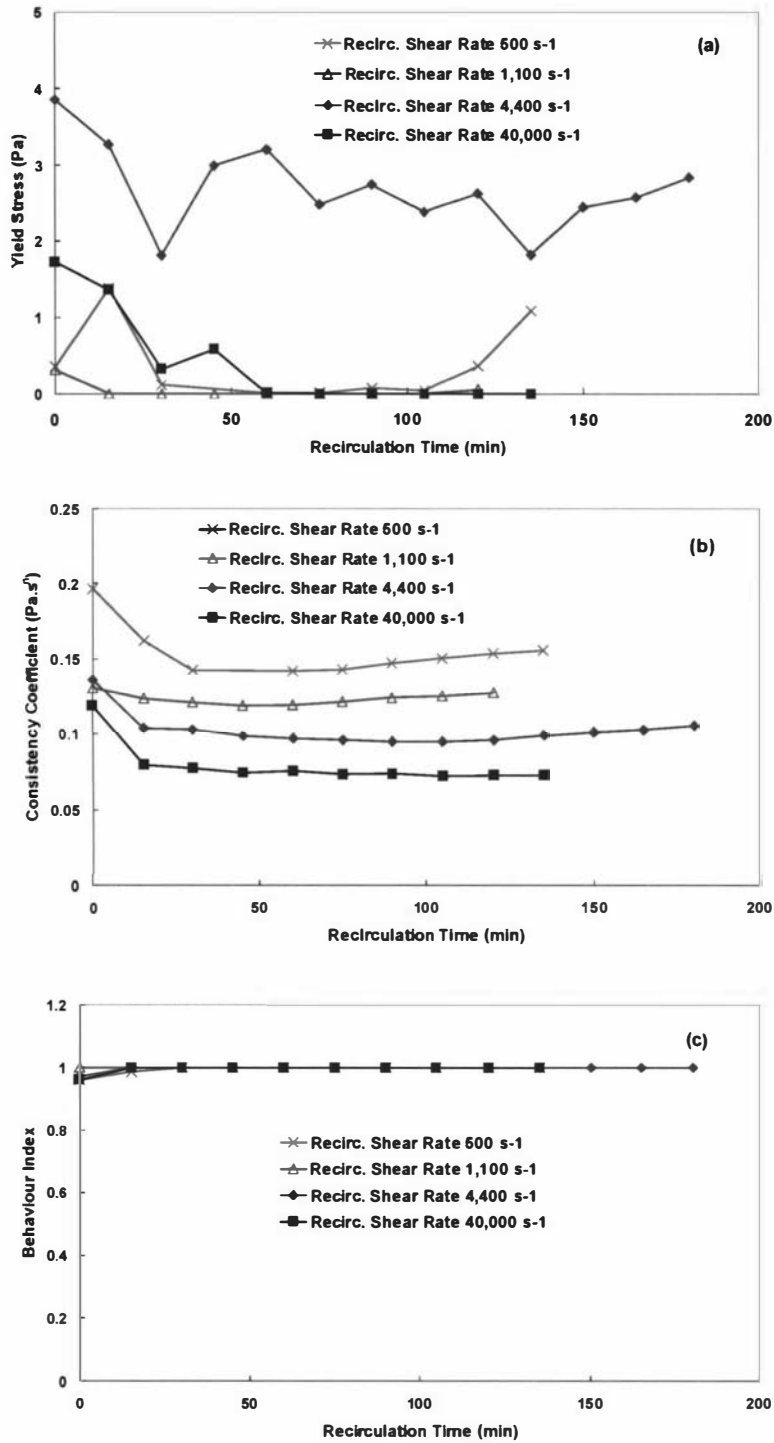


Figure 5.52: Changes in the in-line Herschel-Bulkley model parameters during recirculation at different shear rate for reconstituted whole milk concentrates. (a)  $\tau_y$ ; (b)  $K$ ; (c)  $n$ . C59-C62, powder B, 48%TS, 35°C.

Quite different results were obtained when this experiment was repeated with powder A as shown in Figure 5.53, which plots the effect of recirculation shear rate on the changes in the inline apparent viscosity with recirculation time.

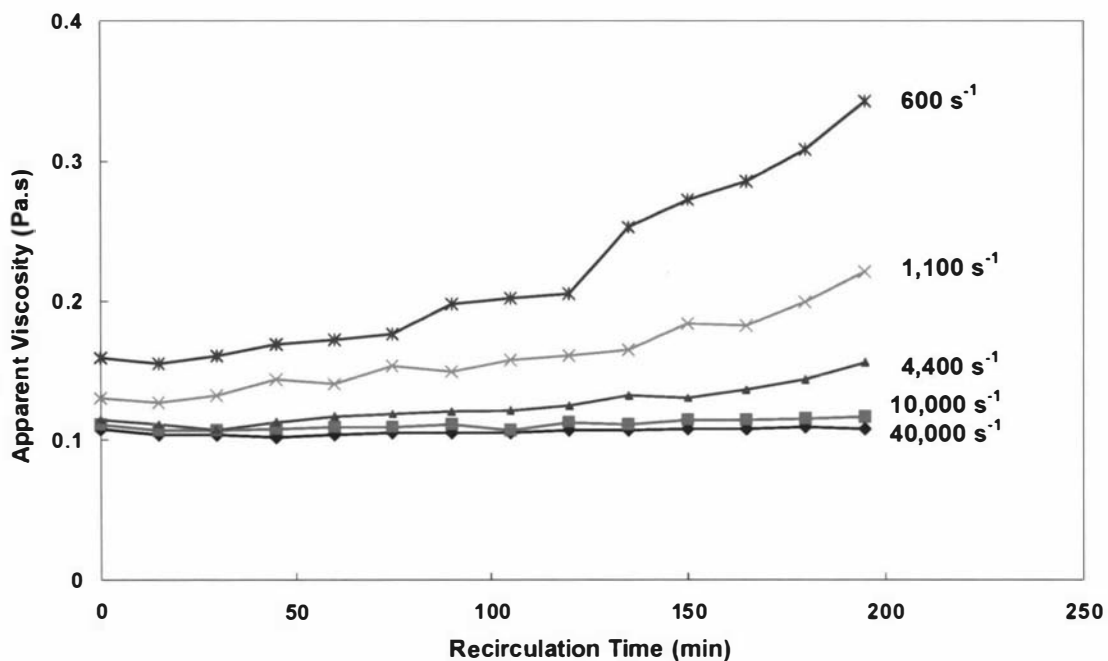


Figure 5.53: Effect of recirculation shear rate on the inline apparent viscosity during recirculation at 35°C. C63-C67, powder A, 48%TS, 35°C.

At the two higher shear levels (40,000 s<sup>-1</sup> and 10,000 s<sup>-1</sup>), the apparent viscosity remained fairly constant over 180 minutes of recirculation indicating no age thickening within 10% experimental uncertainty. Duplicate experiments confirmed this experimental error range. The 40,000 s<sup>-1</sup> data agreed with the earlier experiments observed during the rig commissioning exercise (Chapter 3) within 10% experimental error.

For the three lower shear levels, 600 s<sup>-1</sup> to 4400 s<sup>-1</sup>, age thickening increased with a decrease in shear level. This agreed with the trends reported by Snoeren et al. (1982, 1984) where the rate of age thickening of skim milk concentrate was inversely proportional to shear rate during 4 hours measurement at constant shear rate.

Comparison between powders A and B showed that the initial apparent viscosity values were similar within the 10% error for both powders at the recirculation shear rate of  $40,000 \text{ s}^{-1}$  despite the difference in the solids content, with powder A concentrates at 48%TS and powder B concentrates at 50%TS.

The rate of in-line age thickening was defined as the rate of change in apparent viscosity per minute from when the inline apparent viscosity was lowest (usually after 60 minutes of recirculation) to the final data point on the time scale. Figure 5.54 plots the rates of in-line age thickening with recirculation shear level for reconstituted milk concentrates made from powder A and B. For both powders, below a shear level of  $10,000 \text{ s}^{-1}$ , there is an inverse exponential relationship between nominal shear level and rates of age thickening during recirculation. Above  $10,000 \text{ s}^{-1}$ , the rates of age thickening do not change significantly with recirculating shear rate. The rate of age thickening was significantly higher in powder A concentrates, particularly at low recirculation shear rates.

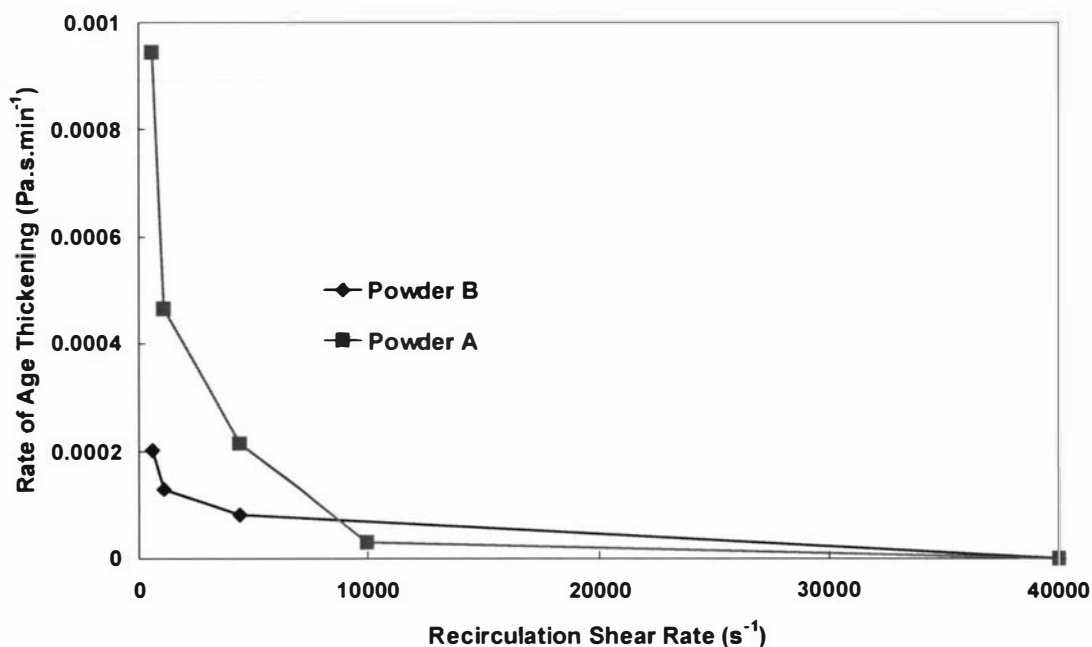


Figure 5.54: Changes in rates of age thickening with nominal shear rates during recirculation in reconstituted milk concentrates made from powders A and B.

### **5.5.2.2 Effect of recirculation shear rate on the rheological behaviour of heated reconstituted milk concentrates during storage at 75°C for powder B concentrates at 50%TS and 65°C for powder A concentrates at 48%TS**

The effect of shear rate during recirculation on the rheology of heated and stored reconstituted whole milk concentrates made from powder B in runs C78-C79 is shown in Figure 5.55. A lower recirculation shear rate resulted in a faster gelling time.

The gelling time can be determined from a plot of the change in the non-standardised HLA with storage time, as shown in Figure 5.56. The time at which the non-standardised HLA suddenly decreased was used to indicate the gelling time. Recirculation at  $600\text{ s}^{-1}$  resulted in a gelling time of 400 minutes, compared to 530 minutes when recirculation was carried out at  $40,000\text{ s}^{-1}$ . The gelling time of 530 minutes observed at  $40,000\text{ s}^{-1}$  agreed well with the 525 minutes of gelling time in run C57 observed in Figure 5.43 for 50%TS concentrates made from powder B.

The averaged apparent viscosity value at the gelling points in Figure 5.55 was 0.5 Pa.s. This is slightly lower than the 0.6 Pa.s observed for concentrates made from powder B in section 5.4. As discussed, the apparent viscosity at the gelling point can vary considerably as significant changes in the rheological behaviour are observed over a short time frame near the gelling point.

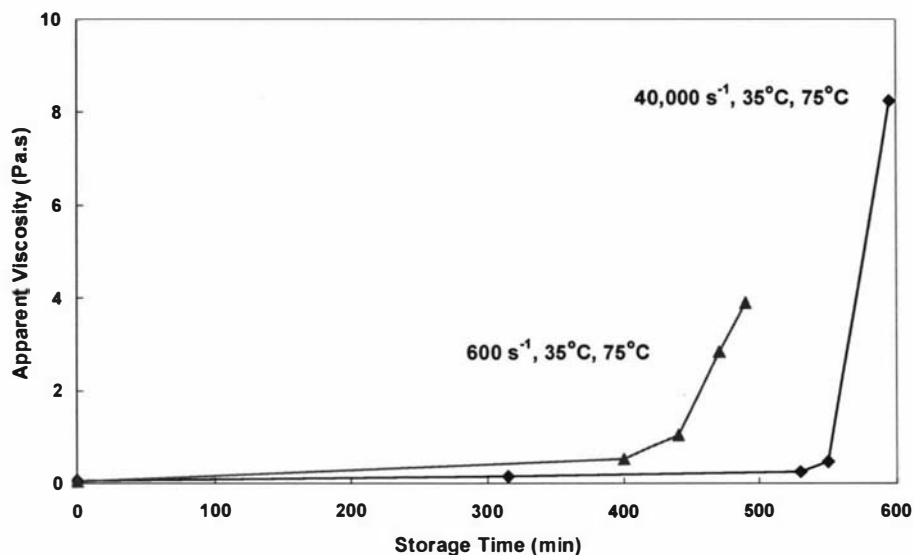


Figure 5.55: Effect of shear rate during recirculation at 35°C on the rheology of heated reconstituted whole milk concentrates during storage at 75°C. C78-C79, powder B, 50%TS, 75°C.

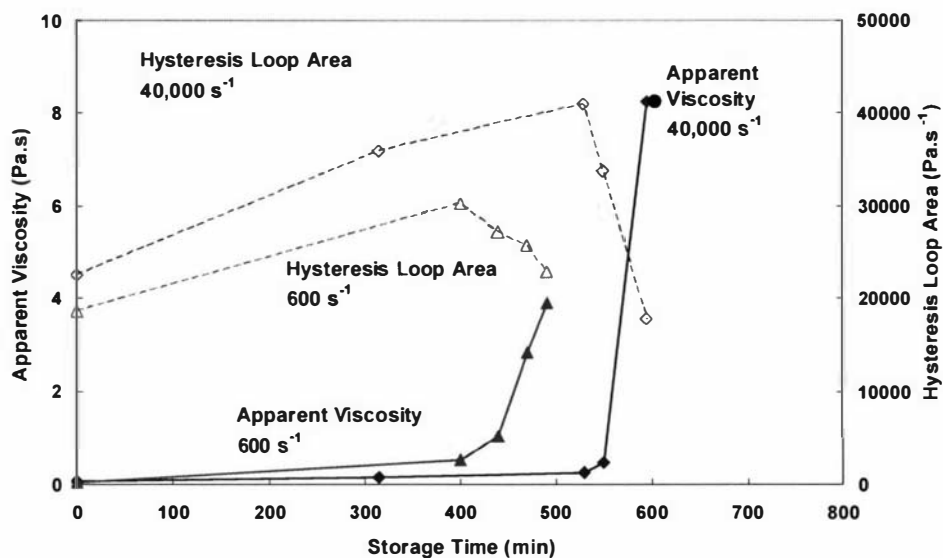


Figure 5.56: Effect of recirculation shear rate on the hysteresis loop area of the reconstituted whole milk concentrates during storage at 75°C. C78-C79, powder B, 50%TS, 75°C.

Changes in the Herschel-Bulkley model parameters with storage time for runs C78-C79 are shown in Figure 5.57.  $\tau_y$  and  $K$  increased while  $n$  decreased with storage time as expected. The respective degree of increase and decrease of the three parameters was more significant when recirculation was carried out at lower shear rates.

There were again anomalies in the yield stress results. The yield stress  $\tau_y$  dropped after the gelling point for both curves in Figure 5.57 (a). The results point to a short coming of rheological modelling process used here rather than the changes in the real physical behaviour of the reconstituted milk concentrates systems during age thickening. This issue will be discussed in greater detail in chapter 6.

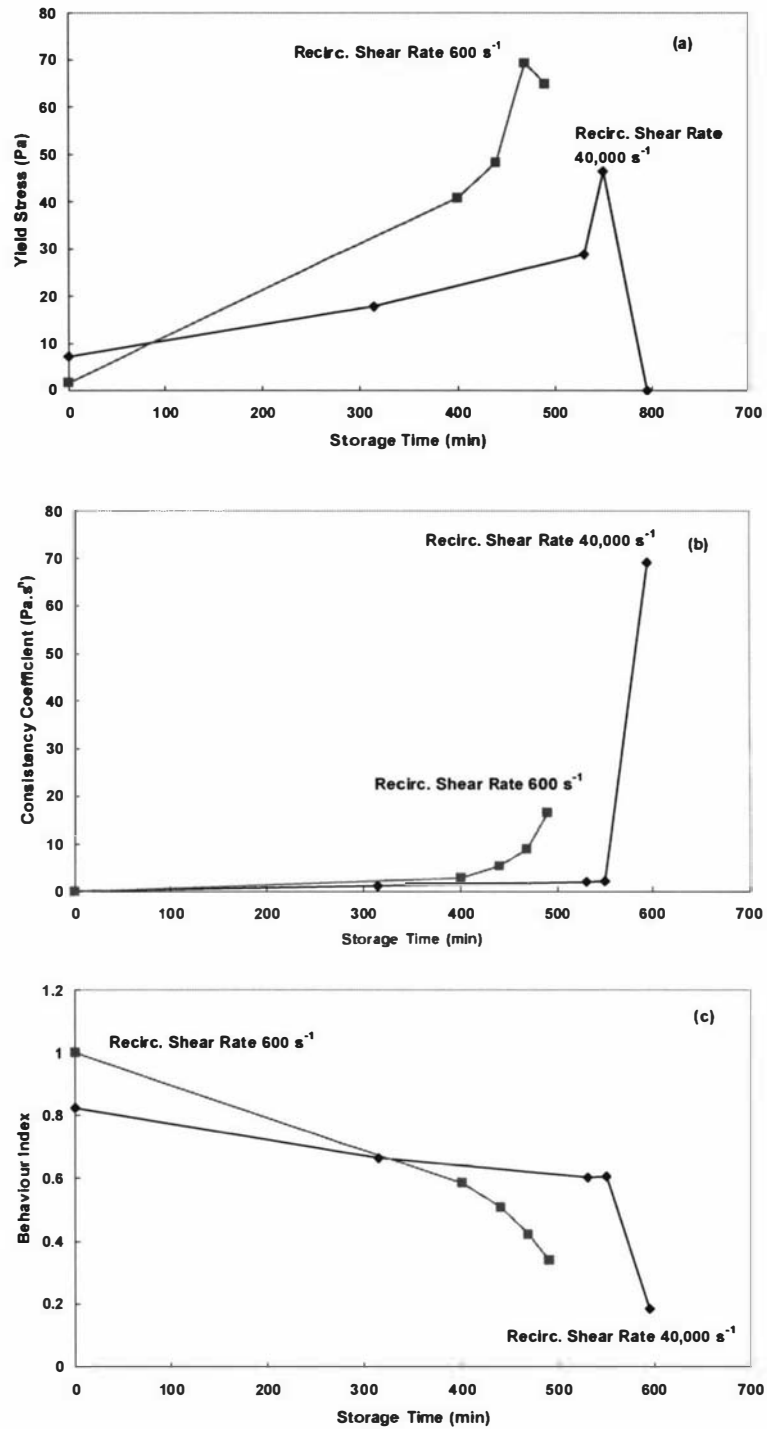


Figure 5.57: Effect of recirculation shear rate on the Herschel-Bulkley model parameters during storage at 75°C. (a)  $\tau_y$ ; (b)  $K$ ; (c)  $n$ . C78-C79, powder B, 50%TS, 75°C.

The effect of recirculation shear rate on the rheology of heated 48%TS reconstituted milk concentrates made from powder A in runs C73-C77 is shown in Figure 5.58. The  $40,000\text{s}^{-1}$  curve agreed with the data in Figure 5.31 in section 5.4 within 10% error.

In Figure 5.58, higher recirculation shear rates resulted in longer gelling times, similar to the observations made with Powder B concentrates. The relationship between recirculation shear rate and gelling time during storage at  $65^{\circ}\text{C}$  is shown in Figure 5.59. The gelling time significantly increased with an increase in recirculation shear rate. Above  $10,000\text{ s}^{-1}$ , this effect is less prominent.

The results agreed in principle with those observed with powder B. However, comparison between the data in Figure 5.58 (powder A) and Figure 5.55 (powder B) showed that the reconstituted concentrates made from powder A gelled at a significantly lower apparent viscosity at 0.1 Pa.s, compared to 0.5 Pa.s for powder B concentrates. The gelling times were also significantly shorter for powder A concentrates. This agreed with the results in section 5.4.

It is interesting to note that the powder B concentrates were heated to  $75^{\circ}\text{C}$ , while powder A concentrates were only heated to  $65^{\circ}\text{C}$ . It was shown in section 5.4 that for a given powder, the gelling times at higher temperatures usually decreased as the temperature increased. When recirculation was carried out at  $40,000\text{ s}^{-1}$ , the gelling time for powder A concentrate was 90 minutes, compared to 530 minutes in powder B. Thus, powder A concentrates had a faster gelling time even though they were reconstituted at 2%TS lower and heated at  $10^{\circ}\text{C}$  lower than those made from powder B.

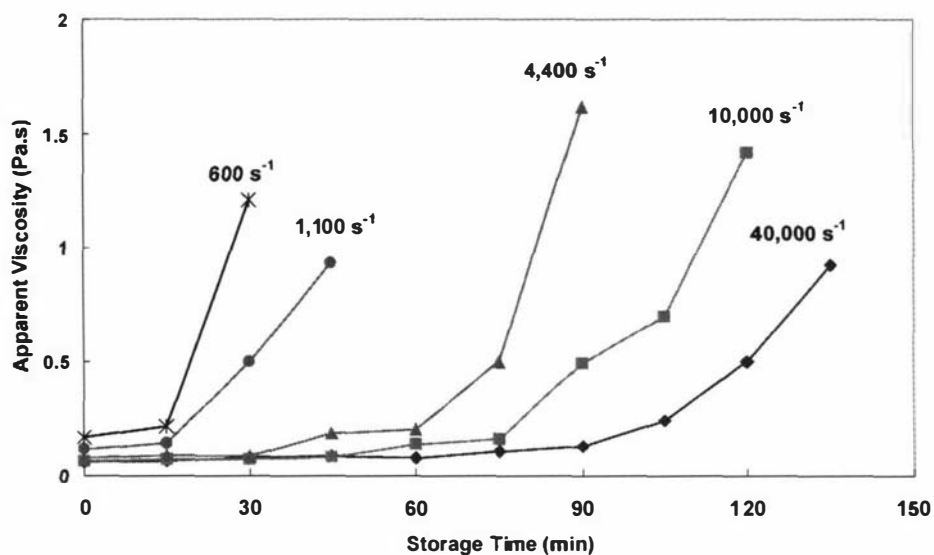


Figure 5.58: Effect of shear rate during recirculation on the rheology of heated reconstituted whole milk concentrates during storage at 65°C. C73-C77, powder A, 48%TS, 65°C.

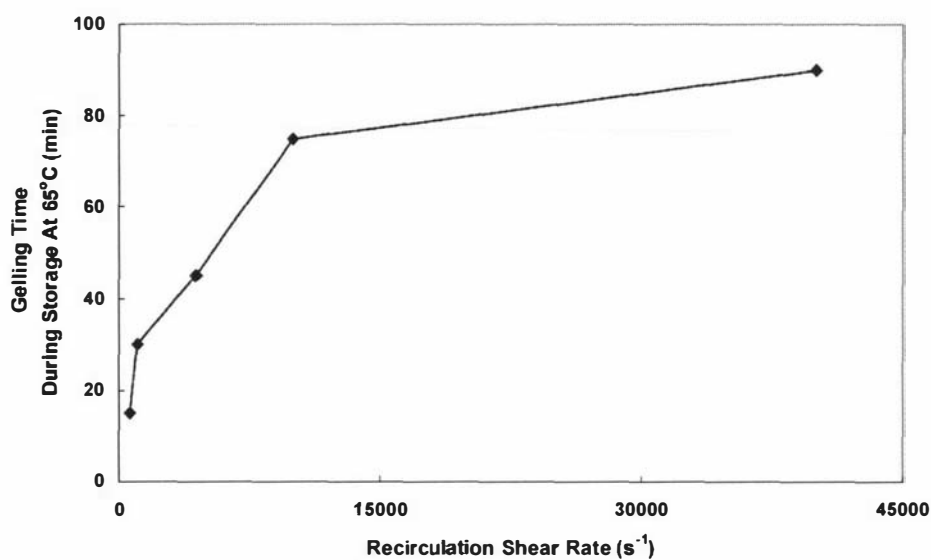


Figure 5.59: Effect of recirculating shear rate on the gelling time of heated reconstituted whole milk concentrates during storage at 65°C. C73-C77, powder A, 48%TS, 65°C.

### 5.5.2.3 Effect of recirculation time and shear rate on the rheology of 47%TS heated reconstituted milk concentrates made from powder A during storage at 65°C

The results from the third set of experiments, C80 and C81, are shown in Figures 5.60 and 5.61 respectively. Experiment C80 was conducted at  $40,000\text{s}^{-1}$  and C81 at  $600\text{s}^{-1}$ .

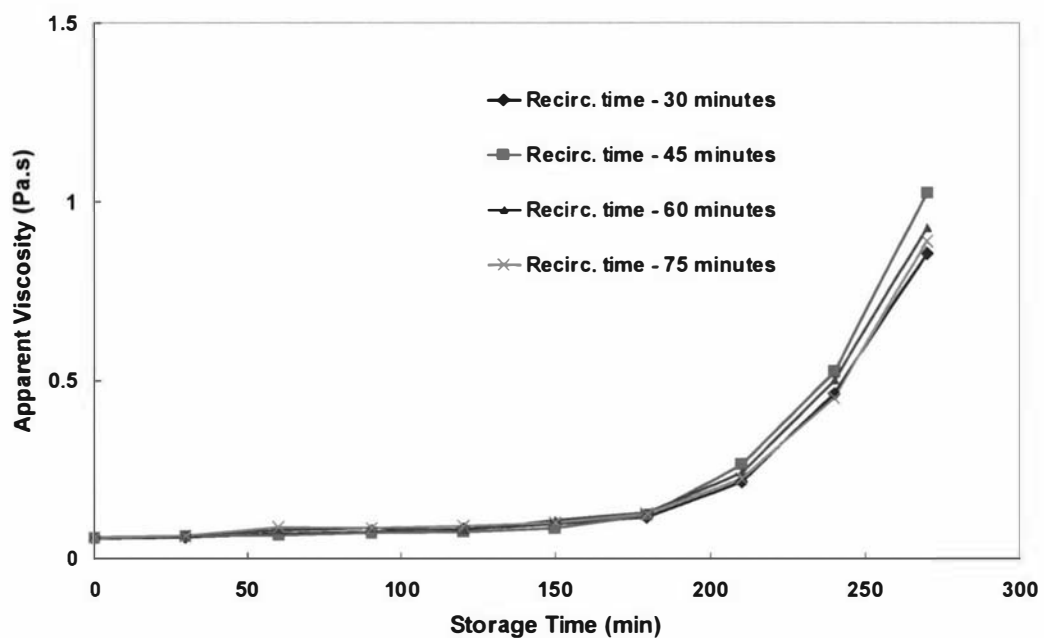


Figure 5.60: Effects of recirculation time on the apparent viscosity with storage time at 65°C for 47%TS reconstituted milk concentrates that had been sheared at  $40,000\text{s}^{-1}$  during recirculation at 35°C. C80, powder A, 47%TS.

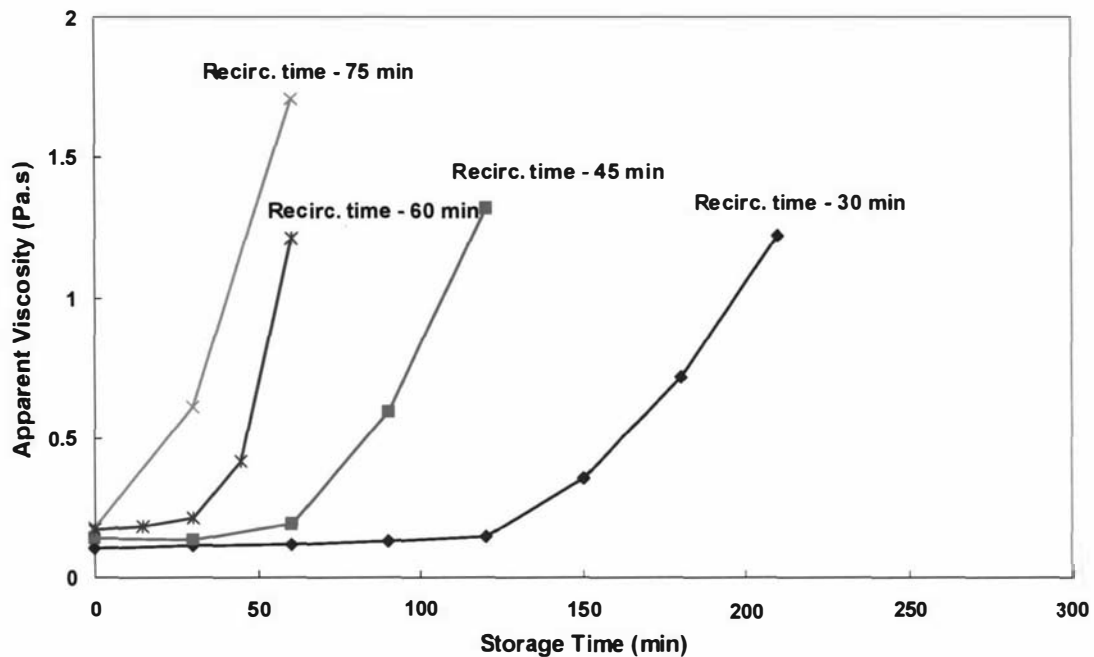


Figure 5.61: Effects of recirculation time on the apparent viscosity with storage time at 65°C of 47%TS reconstituted milk concentrates that had been sheared at 600s<sup>-1</sup> during recirculation at 35°C. C81, powder A, 47%TS.

In Figure 5.60, when the solution was recirculated at 40,000s<sup>-1</sup>, the gelling time during storage was independent of the recirculation time. This complemented the data obtained in Figure 5.53 where the reconstituted concentrates sheared at 40,000s<sup>-1</sup> showed no signs of age thickening during recirculation. In other words, when the concentrates were recirculated at a high shear rate, the inline viscosity did not change with time, and the rate of age thickening and gelling time were similar regardless of the recirculation time. This agreed with the results obtained in experiment A9 during the commissioning trials with the recombination rig, as discussed in section 3.2.2.3.

Figure 5.61 clearly showed that when recirculation took place at 600s<sup>-1</sup>, recirculation time had a significant influence on the rates of age thickening during storage. Longer

recirculation times at  $600\text{s}^{-1}$  resulted in higher initial viscosity and subsequently shorter gelling time when the concentrates were heated and stored at  $65^\circ\text{C}$ .

#### 5.5.2.4 Changes in PSD of powder A reconstituted concentrates during recirculation and storage

The PSD was analysed only in reconstitution experiments with powder A. The PSD of the reconstituted concentrates in runs C67 (recirculation at  $600\text{ s}^{-1}$ ), C80 (recirculated at  $40,000\text{ s}^{-1}$  for 60 minutes and then heated) and C81 (recirculated at  $600\text{ s}^{-1}$  for 60 minutes and then heated), and these are plotted in Figures 5.62, 5.63 and 5.64 respectively. The concentrates were allowed to recirculate

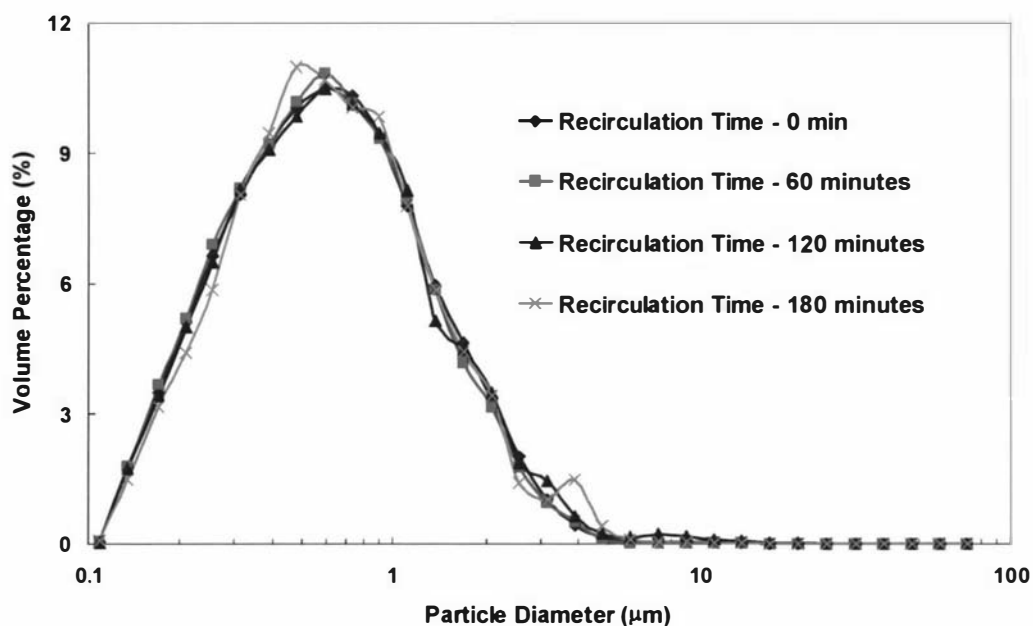


Figure 5.62: Changes in particle size distribution with recirculation time during recirculation at  $600\text{s}^{-1}$  at  $35^\circ\text{C}$ . Run C67, powder A, 48%TS,  $35^\circ\text{C}$ .

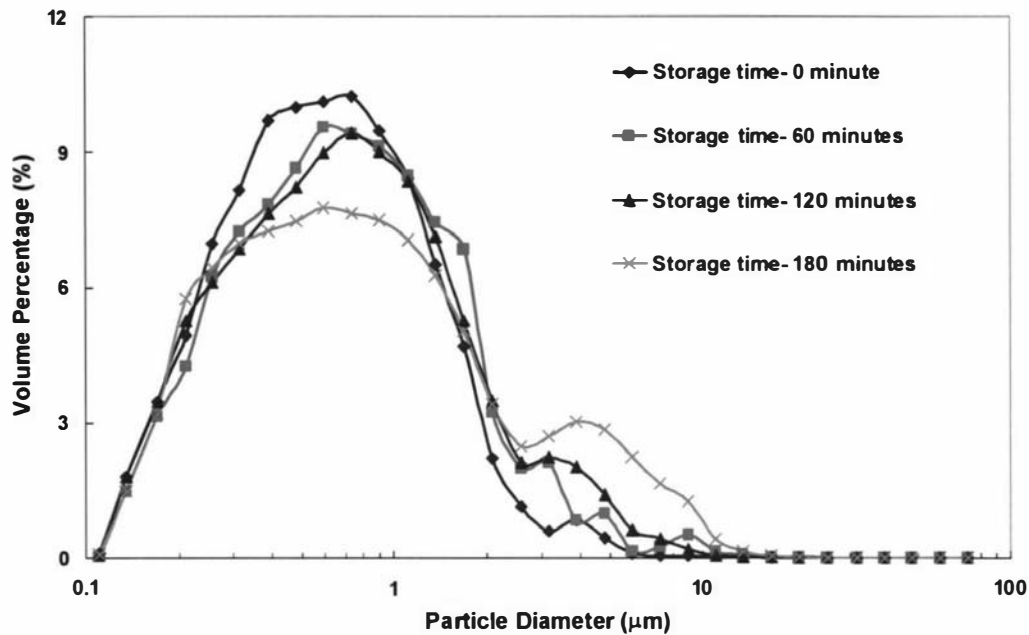


Figure 5.63: Changes in particle size distribution with storage time at 65°C when the milk concentrates were sheared at  $40,000\text{s}^{-1}$  at 35°C. Run C80, powder A, 47%TS, 65°C

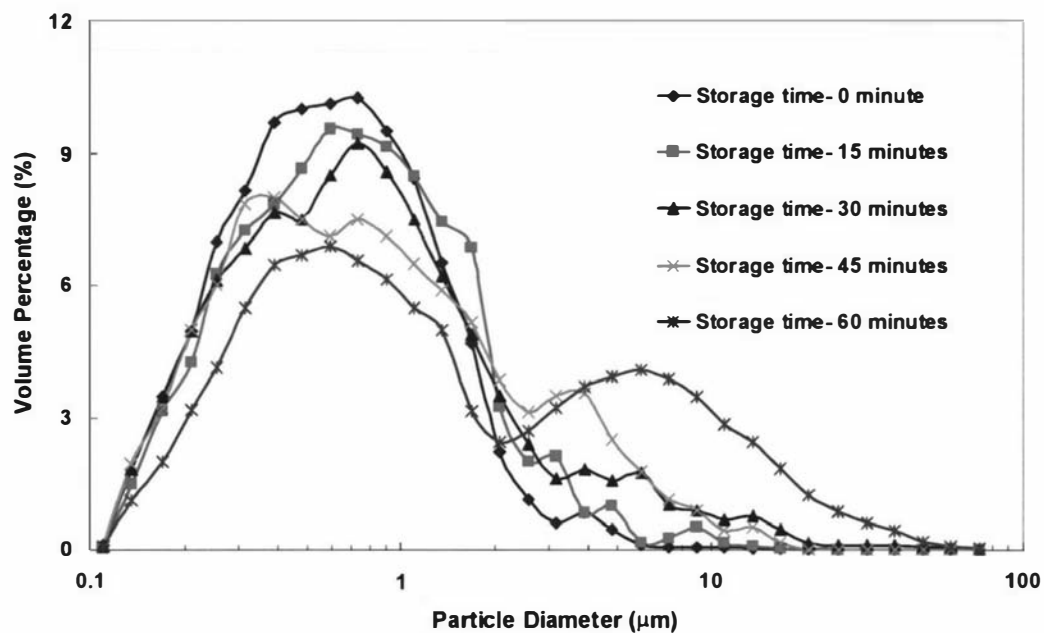


Figure 5.64: Changes in particle size distribution with storage time at 65°C when the milk concentrates were sheared at  $600\text{s}^{-1}$  at 35°C. Run C81, powder A, 47%TS, 65°C.

During recirculation, little change was observed in the particle distribution profile (Figure 5.62 with run C67), but more significant shifts were noticed when the reconstituted systems were heated and stored at 65°C. Figures 5.63 and 5.64 showed an obvious shift from a mono-modal to a bimodal particle size distribution with storage time at 65°C. Similar changes in the PSD during age thickening were observed by Bienvenue et al. (2003a, 2003b) in 45%TS fresh skim milk concentrates stored at 50°C.

The appearance of the second peak occurred at a faster rate in Figure 5.64 compared to Figure 5.63, indicating that the rate of aggregation during storage occurred faster when the system was reconstituted at a lower shear rate.

The aggregation profile was determined from the PSD curves in Figures 5.62-5.64. The changes in the aggregation profile were compared against the changes in apparent viscosity during recirculation in run C67 (Figure 5.65) and storage in runs C80 (Figure 5.66) and C81 (Figure 5.67).

During recirculation at  $600 \text{ s}^{-1}$  and 35°C there was a 1% increase in the volume percentage of particles larger than  $2 \mu\text{m}$ , compared to a 100% increase in apparent viscosity. In agreement with the PSD results obtained below 65°C shown in section 5.4, the volume percentage of particles  $> 2 \mu\text{m}$  in run C67 did not increase with an increase in apparent viscosity.

Upon heating to and storage at 65°C, the PSD increased with storage time during age thickening. The trend was more prominent at lower recirculation shear rate. The increase in PSD with storage time followed a similar trend to that of the apparent viscosity.

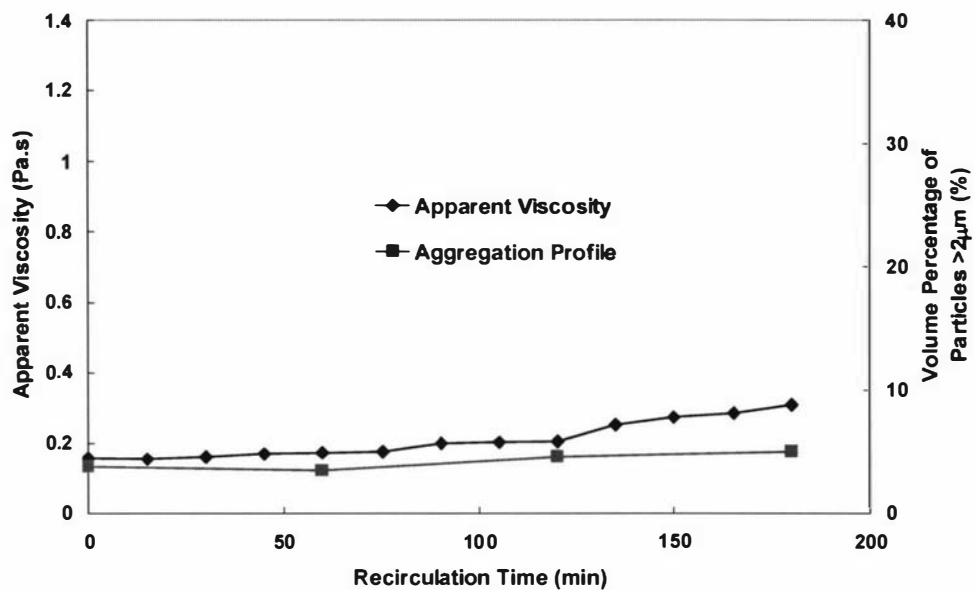


Figure 5.65: Comparison of the changes in apparent viscosity with the aggregation profile during recirculation at  $600 \text{ s}^{-1}$  at  $35^\circ\text{C}$ . Run C67, powder A, 48%TS,  $35^\circ\text{C}$ .

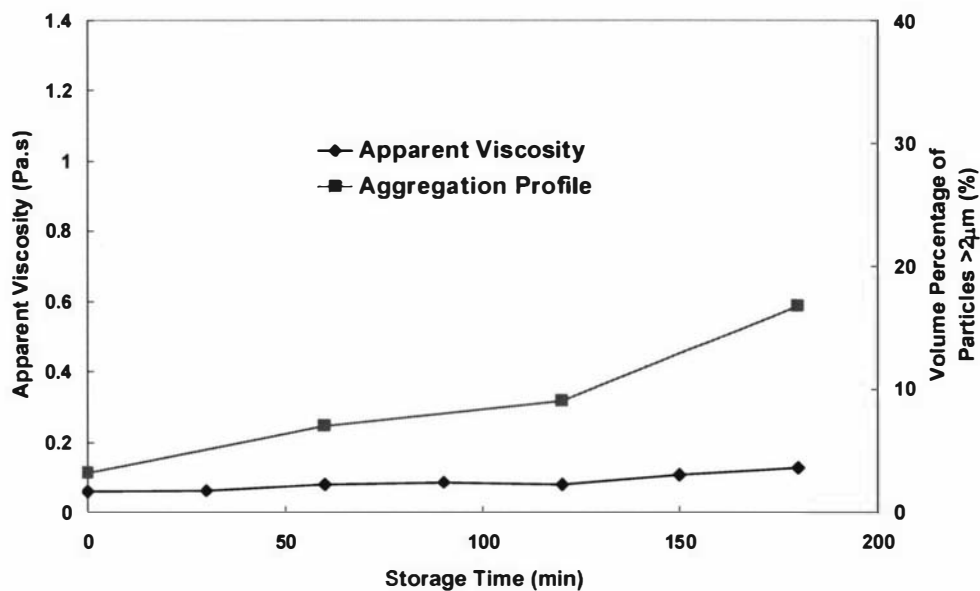


Figure 5.66: Comparison of the changes in apparent viscosity with the aggregation profile during storage at  $65^\circ\text{C}$ . Recirculation was carried out at  $40,000 \text{ s}^{-1}$  for 60 minutes. C80, powder A, 47%TS,  $65^\circ\text{C}$ .

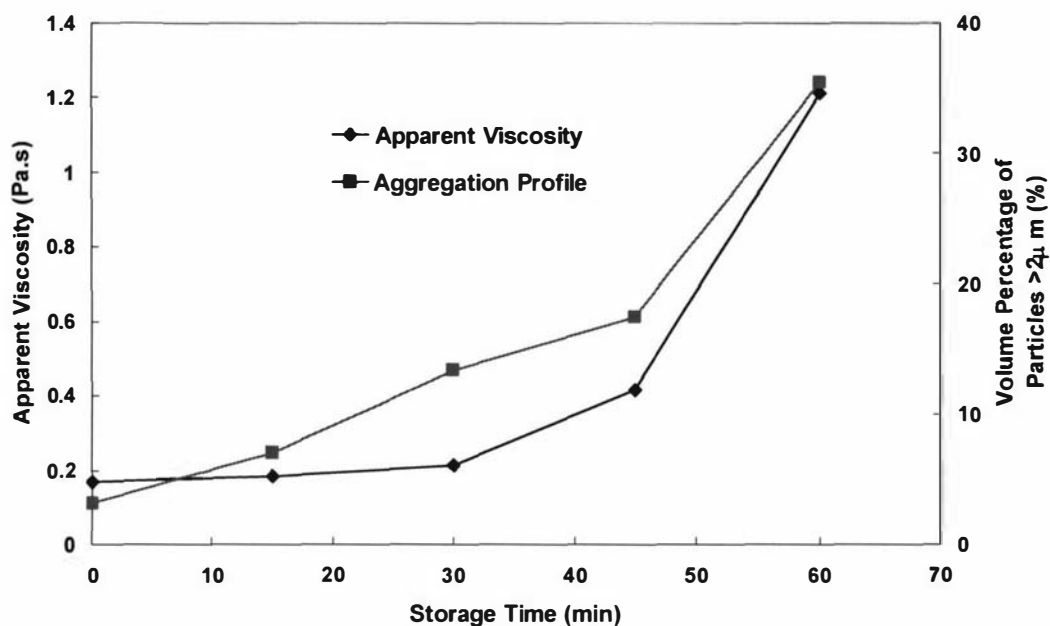


Figure 5.67: Comparison of the changes in apparent viscosity with the aggregation profile during storage at 65°C. Recirculation was carried out at 600s<sup>-1</sup> for 60 minutes. C81, powder A, 47%TS, 65°C.

### 5.5.3 Data summary

The results showed that the shear history during recirculation has a significant effect on the rheological behaviour of the reconstituted milk concentrates. Higher recirculation shear rates decreased the rate of age thickening during recirculation and during subsequent heating and storage. At shear rates above 10,000s<sup>-1</sup>, no age thickening was observed during recirculation at 35°C for reconstituted milk concentrates made from powder B.

## **5.6 Effect of temperature during recirculation on the rheological behaviour of reconstituted whole milk concentrates during reconstitution and subsequent heating and storage**

The dependence of viscosity of fresh and reconstituted milk concentrate systems on temperature has been studied by many authors (Beeby, 1966; Bloore & Boag, 1981; Snoeren et al., 1982; Snoeren, Brinkhuis et al., 1984; Trinh & Schraekenrad, 2002). The viscosity decreases with an increase in temperature, shows a minimum in the temperature range of 60-70°C, and then increases at higher temperatures.

Another aspect of the rheological behaviour of milk concentrate systems is age thickening, which occurs at a faster rate at high temperature (Snoeren, Brinkhuis et al., 1984).

This work analyses the effect of temperature during recirculation on the rheological behaviour of reconstituted whole milk concentrates.

### **5.6.1 Materials and method**

Whole milk powder A was reconstituted to 48%TS + 0.5%TS and powder B was reconstituted to 50%TS  $\pm$  0.5 %TS at 40,000 s<sup>-1</sup>.

Two sets of experiments were performed. The first set of experiments investigated the effect of recirculating temperature on the changes in inline viscosity with time. Reconstituted concentrates made from powder A were mixed at 35°C (run C82) and 45°C (run C83) at 40,000 s<sup>-1</sup>. Powder B concentrates were recirculated through the rig at three different temperatures, 35°C (run C84), 45°C (run C85) and 65°C (run C86) at the shear rate of 40,000s<sup>-1</sup>. Samples were withdrawn from the rig every 15 minutes over a period of 120 minutes for rheological measurement.

In the second set of experiments, the powder was again reconstituted and recirculated at  $40,000\text{s}^{-1}$  for 60 minutes at four temperatures. For powder A concentrates, the solutions were made to 48%TS and the runs at different recirculation temperatures were as follows; 35°C-C87, 45°C-C88, 55°C-C89 and 65°C-C90. The solutions were heated and stored at 65°C. For powder B 50%TS reconstituted concentrates, two recirculation temperatures were tested, 55°C in run C91 and 65°C in run C92. However, the reconstituted concentrates in these two runs were heated to 75°C, instead of 65°C as carried out in the runs C87-C90.

An additional 3 further replicate experiments (runs C93-C95) were carried out to ensure that the data were within the 10% error as suggested in the previous recombination rig commissioning trials. Table 5.10 lists the run numbers.

Table 5.10: Reconstitution conditions for experiments C82-C92.

Run #	Powder	Experiment	Recir. Temp. (°C)	PHE Heating Temp. (°C)	Recirc. Shear (s <sup>-1</sup> )
C82	A	Recirc.	35	N/A	40,000
C83	A	Recirc.	45	N/A	40,000
C84	B	Recirc.	35	N/A	40,000
C85	B	Recirc.	45	N/A	40,000
C86	B	Recirc.	65	N/A	40,000
C87	A	Heating	35	65°C	40,000
C88	A	Heating	45	65°C	40,000
C89	A	Heating	55	65°C	40,000
C90	A	Heating	65	65°C	40,000
C91	B	Heating	55	75°C	40,000
C92	B	Heating	65	75°C	40,000

## 5.6.2 Powder A results

### 5.6.2.1 Effect of recirculation temperature on the inline rheological behaviour

Figure 5.68 plots the changes in the inline apparent viscosity during recirculation in 47%TS reconstituted concentrates made from powder A. Recirculation at 35°C resulted in no increase in apparent viscosity during recirculation. This agreed with the results obtained from the recombination rig commissioning trial discussed in chapter 3. Recirculation at 45°C, however, resulted in a significant increase in apparent viscosity after 45 minutes of recirculation. The gap between the 35°C and 45°C results was greater than the nominal 10% experimental error.

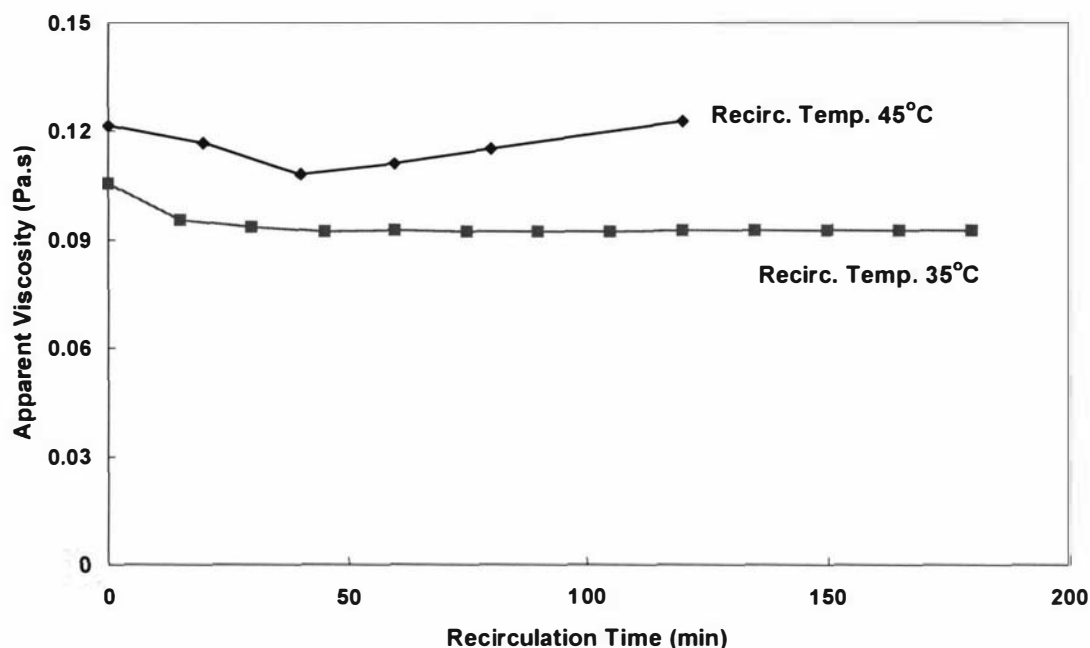


Figure 5.68: Effect of recirculation temperature on the inline apparent viscosity with recirculation time at shear level of  $40,000\text{s}^{-1}$ . C82-C83, powder A, 48%TS.

### 5.6.2.2 Effect of recirculation temperature on the rheological behaviour of stored samples at 65°C

Figure 5.69 plots the change in apparent viscosity with storage time at 65°C. The 35°C curve agreed well with the data in Figure 5.31 where the solution was mixed at 35°C and heated to 65°C.

Figure 5.69 clearly shows all four curves displayed similar two-stage age thickening-gelation characteristics. However, an increase in mixing temperature from 35°C-65°C resulted in a decrease in the gelling time, with a particularly strong influence when mixing was carried out at 65°C.

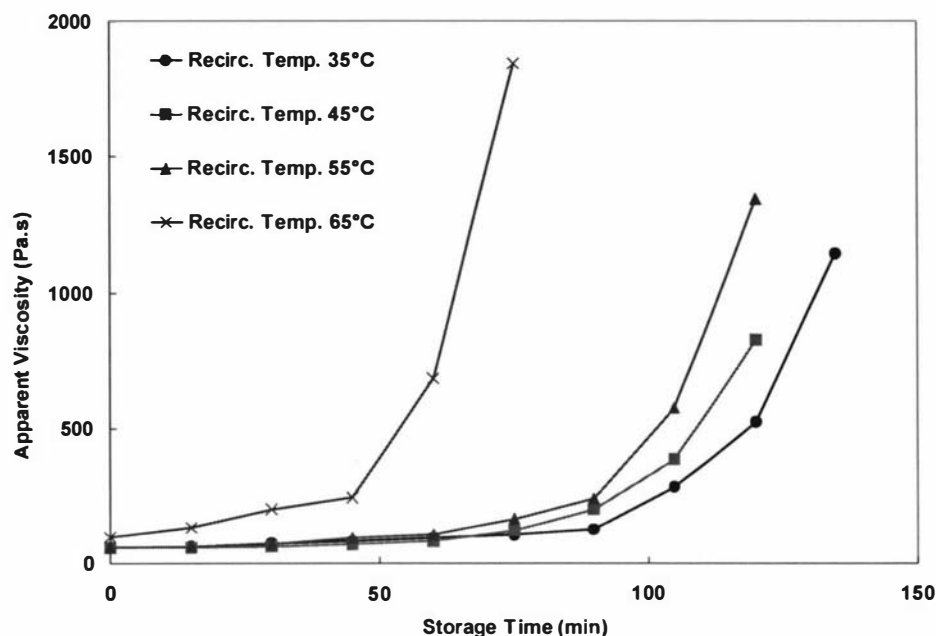


Figure 5.69: Effect of recirculation temperature on the apparent viscosity during storage at 65°C. C87-C90, powder A, 48%TS.

### 5.6.3 Powder B results

#### 5.6.3.1 Effect of recirculation temperature on the inline rheological behaviour

Figure 5.70 plots the inline apparent viscosity at the shear stress of 105.3 Pa against recirculation time at three temperatures. The initial apparent viscosity decreased with an increase in recirculation temperature. This is expected as viscosity is widely known to have an inversely proportional relationship with temperature (Steffe, 1992).

After 60 minutes of recirculation, the viscosity-time curve for reconstitution temperatures of 35°C and 45°C levelled out and showed no signs of increase in viscosity. The slight increase in the 65°C curve was within 10% error with the other two curves at lower recirculation temperatures. Therefore, it was difficult to analyse the effect of heating to 65°C during recirculation on the inline viscosity.

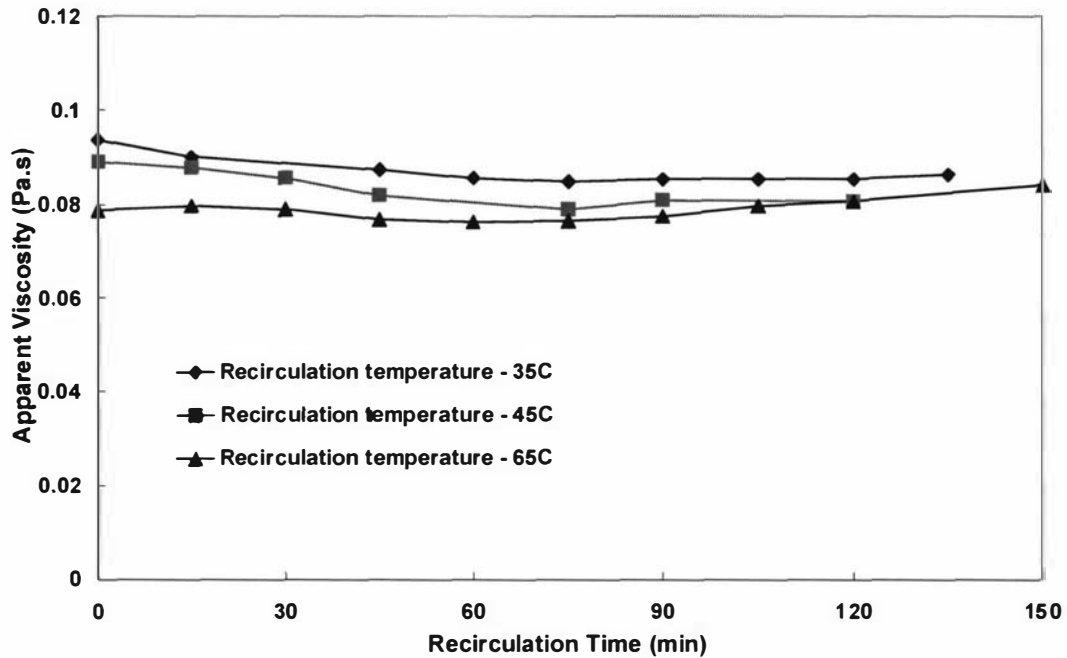


Figure 5.70: Effect of recirculation temperature on the inline apparent viscosity with recirculation time at shear level of  $40,000\text{s}^{-1}$ . C84-C86, powder B, 50%TS.

### 5.6.3.2 Effect of recirculation temperature on the rheological behaviour of stored samples at 75°C

Figure 5.71 plots the effect of recirculation temperature on the apparent viscosity during storage at 75°C in 50%TS reconstituted concentrates made from powder B. The 35°C data was from run C79 in section 5.5. The 35°C essentially represented the control experiment.

An increase in the recirculation temperature to 55°C had little effect on the gelling time. However, recirculation at 65°C resulted in a significant decrease in the gelling time. This agreed with the data shown in Figure 5.70. Obviously, the effect of heating during recirculation on rheological behaviour was more prominent when the milk solutions were heated and stored at elevated temperature.

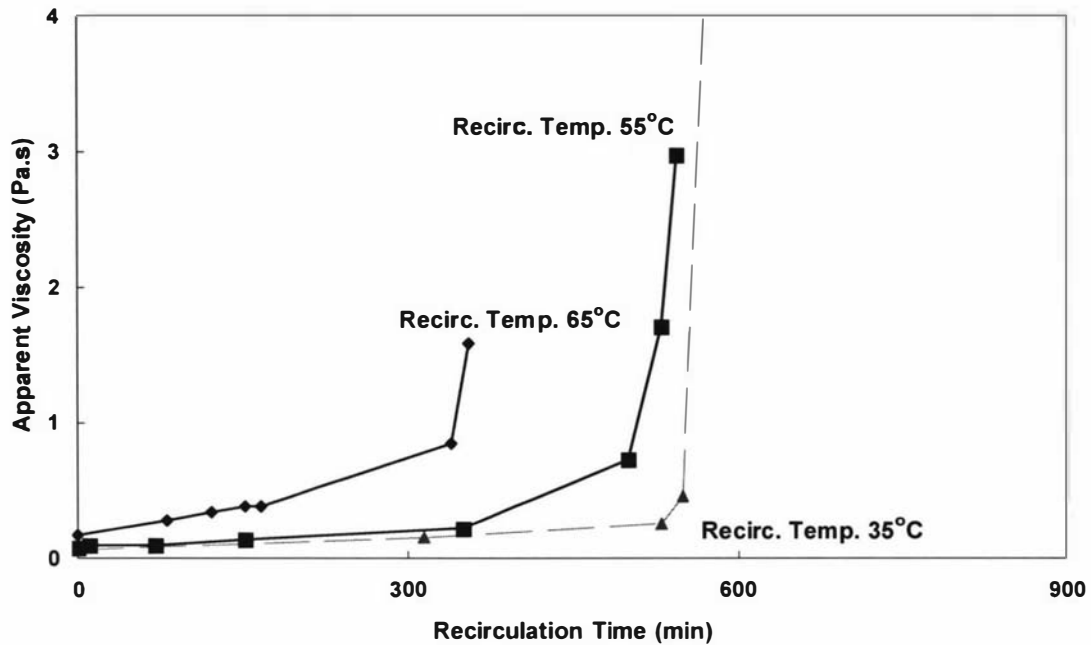


Figure 5.71: Effect of recirculation temperature on the apparent viscosity during storage at 75°C. C91-C92, powder B, 50%TS.

#### 5.6.4 Data summary

Recirculation temperature during reconstitution has a significant effect on the rheological behaviour of downstream time-dependent products. Even at shear rates above  $10,000\text{s}^{-1}$ , a high temperature can still give rise to age thickening during recirculation. This critical temperature is dependent on product specification.

## **5.7 Effect of shear and residence time during heating on the rheology of reconstituted whole milk concentrates**

Heating is important in the food industry as it is used for cooking, pasteurisation and sterilisation. Heat exchangers come in a wide range of designs, such as parallel plate, shell and tube, scraped surface and direct steam injection.

The design and operation of heaters are generally geared to the flow rate of the products and the required heating temperature. The shear and temperature history profiles during heating are often overlooked, and their effects on the rheology of heated or cooled time-dependent systems are thus unknown.

As shown in sections 5.5 and 5.6, shear and temperature histories during recirculation have a significant effect on the rheology of heated products. Even though the residence time inside the heater during heating may be relatively short (less than one minute), the history of processing conditions may significantly affect the rheological profile of the heated products.

This section investigates the effect of shear level and residence time (i.e. the duration of shear applied) during heating on the rheology of reconstituted whole milk concentrate systems.

### **5.7.1 Materials and methods**

Whole milk powder B was mixed to  $50\%TS \pm 0.5\%TS$ . After 60 minutes of recirculation, reconstituted milk concentrates were heated and stored at  $75^{\circ}\text{C}$ . The flow rate and the residence time of the milk concentrates inside the plate heat exchanger (PHE) were controlled by varying the speed of the mono pump and the number of plates of the PHE respectively. Two flow rates of 80L/hour and 40L/hour and three different numbers of plates, 6, 10 and 20 plates were used. The milk products only make one pass through

the PHE and the plates are in series, i.e. one plate after another. The flow rate affects the shear rate and the residence time, while the number of plates only affects the residence time of the milk concentrates during heating. It is important to note that the flow rate of 80 L/hour was maintained during recirculation to achieve the desired shear rate of  $40,000\text{s}^{-1}$ . The flow rate was modified to the appropriate setting only when the reconstituted concentrates were ready to be heated.

The temperature and flow rate of the hot water were recorded for all experiments. The testing variables during experimentation are listed in Table 5.11.

Table 5.11: Operating parameters during heating experiments.

<b>Run</b>	<b>C96</b>	<b>C97</b>	<b>C98</b>	<b>C99</b>	<b>C100</b>	<b>C101</b>
<b>Plates</b>	6	6	10	10	20	20
<b>Flow rate (L/hour)</b>	80	40	80	40	80	40
<b>Solids Content (%TS)</b>	51.07	50.5	50.12	49.7	50.5	50.8
<b>Residence time (s)</b>	10.17	14.03	13.5	17.89	18	22
<b>Milk temperature (°C)</b>	77	76.8	76.2	76.5	77.5	77
<b>Hot water flow (kg/hour)</b>	247.1	225.7	228.4	205.8	221.3	249.1
<b>Hot water inlet (°C)</b>	84.6	82	83.4	82.7	84	81.6
<b>Hot water outlet (°C)</b>	82.8	79.04	82.1	81.7	83.1	78.9

One replicate run (C102) was carried out as a duplicate to run C100 with 20 plates and 80 L/hour.

## 5.7.2 Results

### 5.7.2.1 Age thickening during storage

Figures 5.72-5.74 plot the change in apparent viscosity during storage at 75°C when heating was carried out with 20, 10 and 6 plates respectively. In each figure, two curves

were plotted for each flow rate of 80L/hour and 40L/hour. The axis scales on all three graphs were identical.

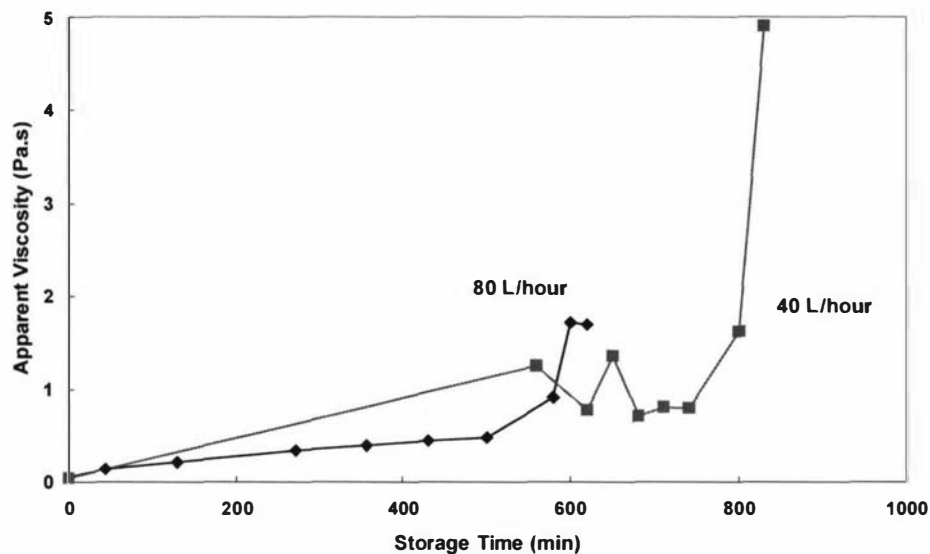


Figure 5.72: Effect of flow rate during heating on the rheology of reconstituted milk concentrates during storage at 75°C. C96-97, powder B, 50%TS, 6 plates.

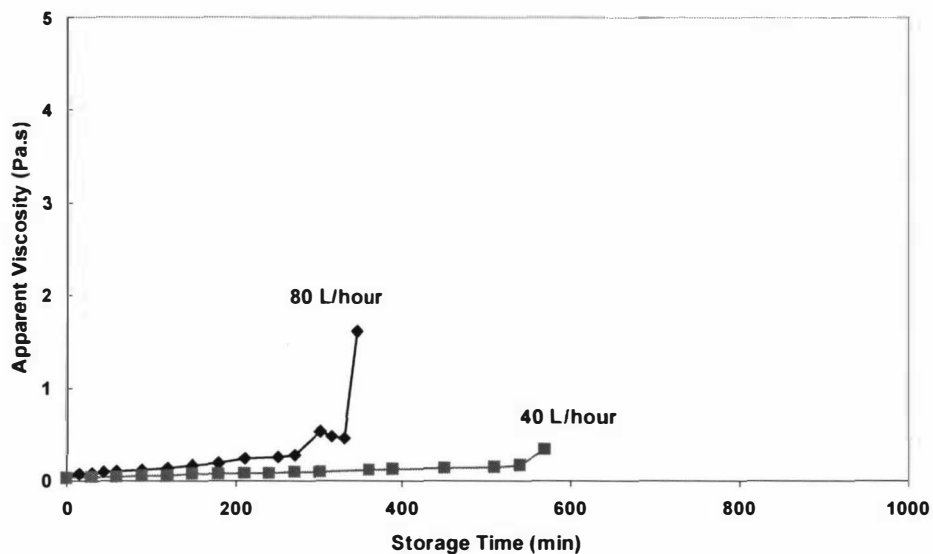


Figure 5.73: Effect of flow rate during heating on the rheology of reconstituted milk concentrates during storage at 75°C. C98-99, powder B, 50%TS, 10 plates.

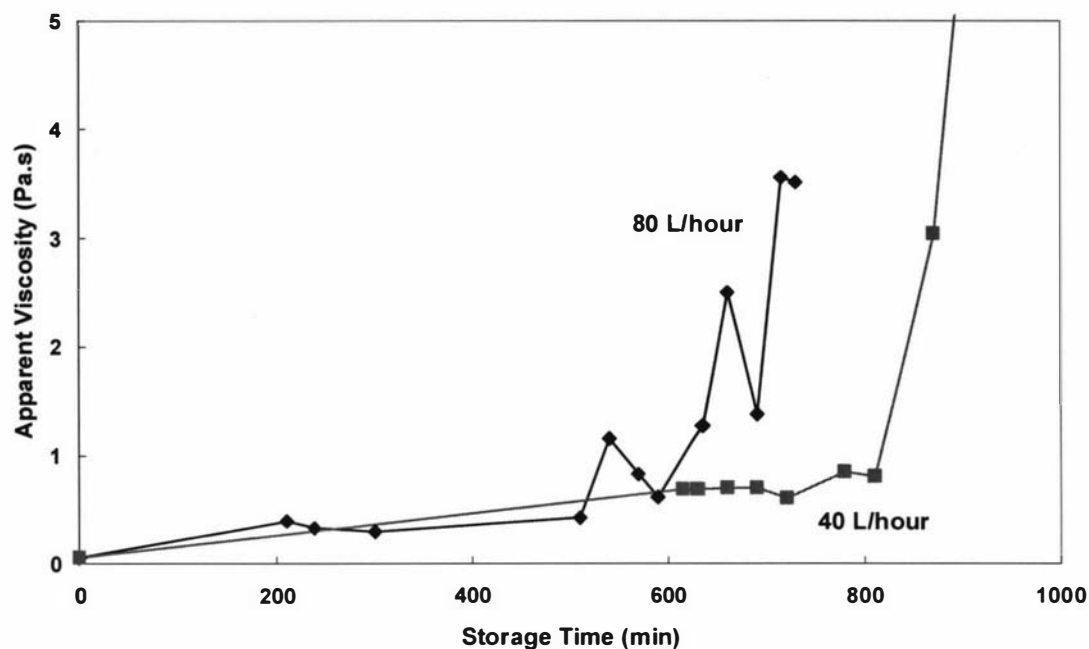


Figure 5.74: Effect of flow rate during heating on rheology of reconstituted milk concentrates during storage at 75°C. C100-101, powder B, 50%TS, 20 plates.

All curves in Figures 5.72-5.74 displayed similar characteristics, where a gradual increase in viscosity with storage time was first observed, followed by a sudden break point and a significant increase in viscosity thereafter.

From the flow curves, the non-standardised HLA were determined and used to determine the gelling points. The effects of flow rate and number of plates during heating on the gelling time of the 50% reconstituted whole milk solutions are shown in Figure 5.75.

Figure 5.75 showed that a decrease in the flow rate during heating resulted in a longer gelling time. Secondly, a minimum gelling time was observed at 10 plates for both flow rates. There is no apparent explanation for this minimum and it is unclear whether it is the 6 plates or the 10 plates data that are anomalous.

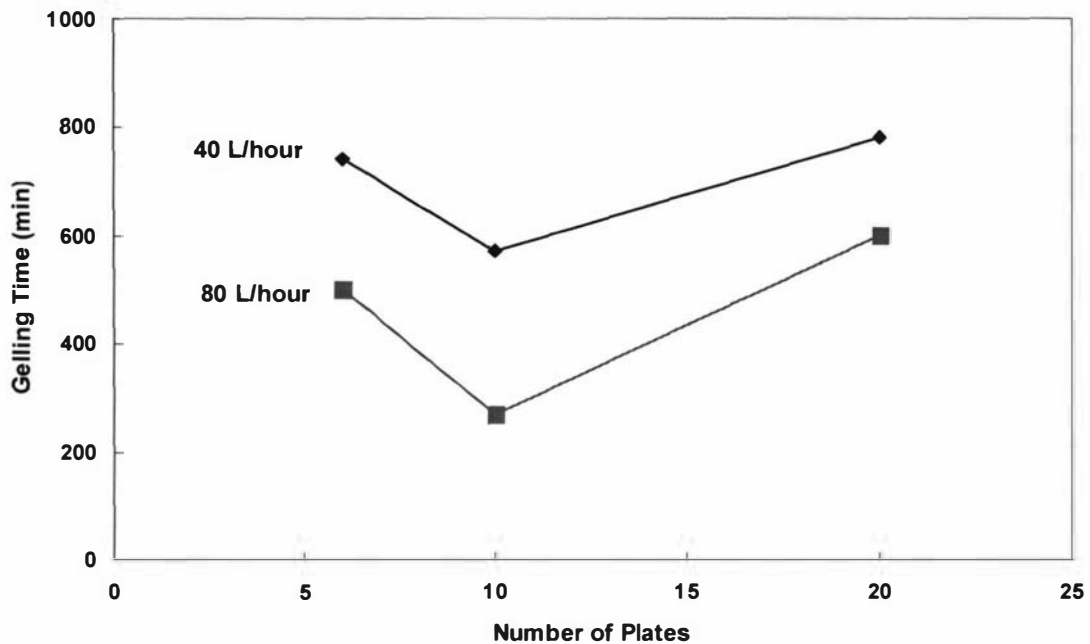


Figure 5.75: Effect of shear rate and number of plates during heating on the gelling time of heated products during storage.

Another set of experiments was conducted under the same conditions, but using a different batch of reconstituted whole milk concentrates (results not shown). The gelling time again showed a minimum at 10 plates. Thus the observed trend is reproducible. However, there were insufficient data to identify the underlying mechanism that gave the 6 plates result.

It is also interesting to note the variation in the apparent viscosity at the gelling points in Figures 5.72-5.74. For the 6 and 20 plates experiments in Figures 5.72 and 5.74 respectively, the gelling point occurred at a viscosity around 0.5 Pa.s, which agreed with previous results in sections 5.4, 5.5 and 5.6. In Figure 5.73 with the 10 plates experiment, gelling occurred at approximately 0.3 Pa.s, which was considerably lower than that observed for the other two experiments and previous results.

### 5.7.2.2 Rheological modelling

The changes in the Herschel-Bulkley model parameters with storage time in runs C90-C91 with 20 plates are shown in Figure 5.76. The trends in the values of  $K$  and  $n$  were similar to those previously observed, where  $K$  increases and  $n$  decreases with storage time during age thickening.  $\tau_y$  on the hand displayed some unusual behaviour, as seen in Figure 5.76 (a).

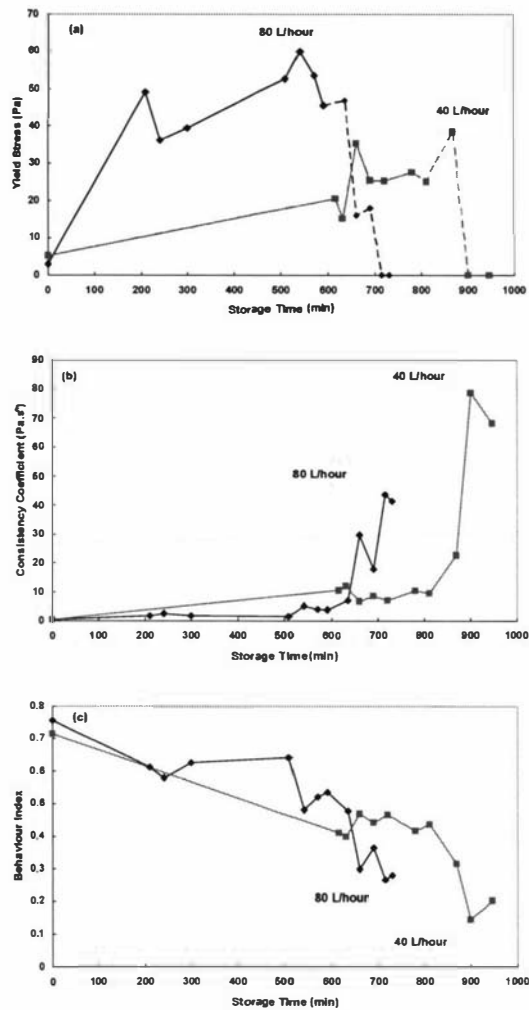


Figure 5.76: Effect of flow rate during heating on the Herschel-Bulkley model parameters during storage at 75°C in a hot water bath. (a)  $\tau_y$ ; (b)  $K$ ; (c)  $n$ . C90-C91, powder B, 50%TS, 20 plates.

$\tau_y$  initially increased with storage time during age thickening, indicating an increase in the initial resistance to deformation upon an application of shear. Thus, the structure was building into a stronger network that had a higher initial resistance to deformation. However,  $\tau_y$  then suddenly dropped significantly after gelation. This was observed in other runs in this series of experiments. Similar observations in the yield stress trends were also made in section 5.6. The estimates of yield stress obtained after gelation were distorted by the modelling process which will be discussed in more detail in chapter 6. The drop in yield stress after gelation should be ignored for the time being.

The changes in the consistency coefficient,  $K$ , with storage time once again showed similar trends to that of the apparent viscosity.

### **5.7.2.3 Changes in PSD during age thickening**

Figure 5.77 plots typical changes in PSD curves obtained during storage in run C97 with 6 plates at 40 L/hour. The curves shifted from a mono-modal to a bimodal mode, indicating an aggregation process during age thickening.

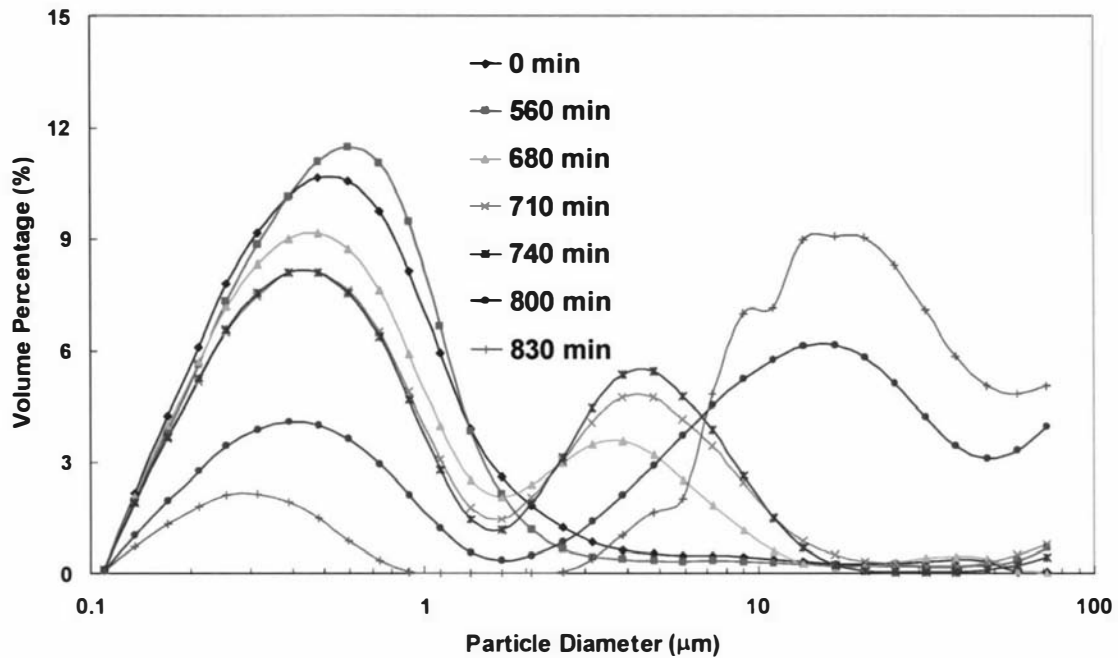


Figure 5.77: Change in particle size distribution during storage of heated reconstituted whole milk concentrates. C97, powder B, 50%TS, 75°C, 6 plates, 40 L/hour.

The aggregation profile was determined from the changes in the volume percentage of particles larger than 2 μm. The aggregation profile was compared with the changes in the apparent viscosity during age thickening (Figure 5.78). The two curves showed similar trends, where a significant increase in apparent viscosity and aggregation profile were observed after 740 minutes of storage which was the gelling point.

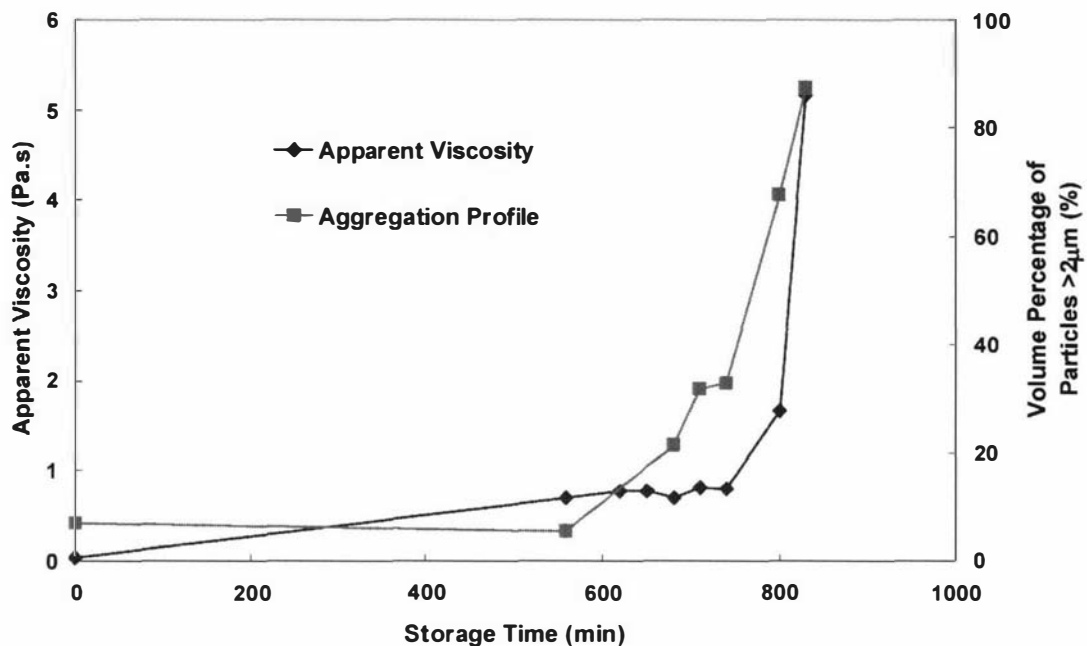


Figure 5.78: Comparison of the changes in the apparent viscosity and the aggregation profile with storage time during age thickening at 75°C. C97, powder B, 50%TS, 75°C, 6 plates, 40 L/hour.

### 5.7.3 Summary

During heating, the residence time (seconds) inside the PHE is very short in comparison to the age thickening time during storage (hours). However, the shear history profile during this critical short period has a significant effect on the rheological behaviour of the heated time-dependent milk concentrates during storage. The effects of residence time and shear history during heating on the rheological behaviour of the heated time-dependent products still require more detailed investigation before a solid conclusion can be drawn.

## **5.8 Age thickening of skim and whole milk concentrates- TEM, rheology, PSD**

The mechanism of age thickening of reconstituted milk concentrates at high temperature is still largely unknown. Information with regard to different aspects of age thickening has been discovered independently. Temperature is known to have an effect on apparent viscosity (Bloore & Boag, 1981; Tang et al., 1998; Trinh & Schraekenrad, 2002) and age thickening (Velez-Ruiz & Barbosa-Canovas, 1998, 2000). Anema and Klostermeyer (1997), Anema (1998, 2000), Anema and Li (2003), and Anema et al. (2004) studied the effect of temperature on the compositional changes, in particular the dissociation kinetics of casein and its interaction with denatured whey proteins. No age thickening study was carried out. Velez-Ruiz and Barbosa-Canovas (1997, 1998) used a rheological approach to study age thickening of fresh milk concentrates, and Velez-Ruiz and Barbosa-Canovas (2000) also used TEM techniques to reveal some insights into the structural changes of the fat globules. TEM has also been used by others to show the interaction between casein via whey protein bridges (Sawyer, 1969), as well as participation of fat (Defelipe et al., 1991) during heating.

This section utilises several methods of rheological and structural measurements to provide a comprehensive picture of the age thickening process. These techniques include shear sweep measurements, particle size analysis, as well as TEM.

### **5.8.1 Materials and methods**

Whole milk powder B and skim milk powder C were used in this experiment. Whole milk powder B was reconstituted to 50%TS in run C103, while skim milk powder C was mixed to 47%TS in run C104.

Reconstitution was carried out at 35°C and 40,000s<sup>-1</sup>. After 60 minutes of recirculation, reconstituted milk concentrates were heated to 75°C, and subsequently stored in a water bath.

In run C103 with whole milk concentrates, rheological measurement, particle size distribution and TEM analysis were carried out. In run C104 with skim milk powder C, only TEM was conducted.

## 5.8.2 Results

### 5.8.2.1 Age thickening in reconstituted whole milk concentrates

#### 5.8.2.1.1 Rheological measurement

The apparent viscosity at the reference shear stress of 105.3 Pa was plotted against storage time, shown in Figure 5.79. The apparent viscosity curve increased steadily with storage time. No gelling point was detected. This was expected as the apparent viscosity only reached 0.3 Pa.s after 350 minutes of storage, whereas previously, gelation in powder B concentrates at 50%TS and 75°C occurred at the apparent viscosity of 0.5 Pa.s and 550 minutes, as observed in sections 5.4, 5.5 and 5.7.

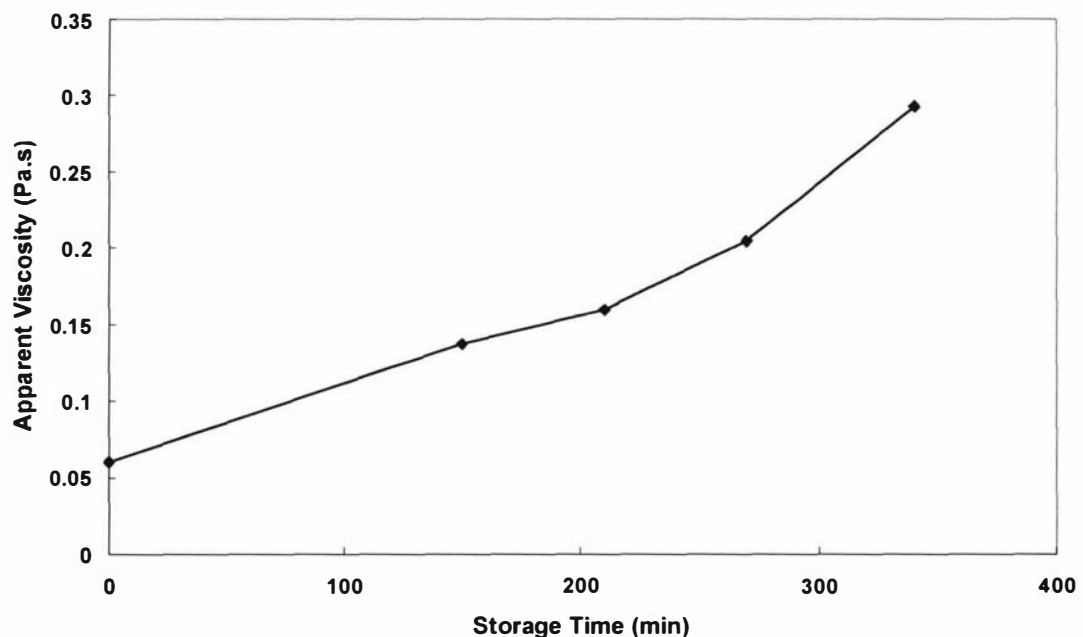


Figure 5.79: Changes in the apparent viscosity at 105.3 Pa with storage time during age thickening at 75°C. Run C103, whole milk powder B, 50%TS.

The flow curves were fitted to the Herschel-Bulkley model, and the changes in the model parameters with storage time are plotted in Figure 5.80. As expected,  $K$  and  $\tau_y$  increased while  $n$  decreased with storage time during age thickening. Even though the trends for  $K$  and  $n$  followed smoothly with storage time,  $\tau_y$  however displayed an unusual drop after 270 minutes of storage as shown in Figure 5.80 (a). It was expected that  $\tau_y$  would continue to increase with time due to the development in structure during age thickening. This unusual data point for the yield stress curve can either be attributed to experimental error during sampling and measurement, or to the weakness of model fitting as discussed in chapter 6.

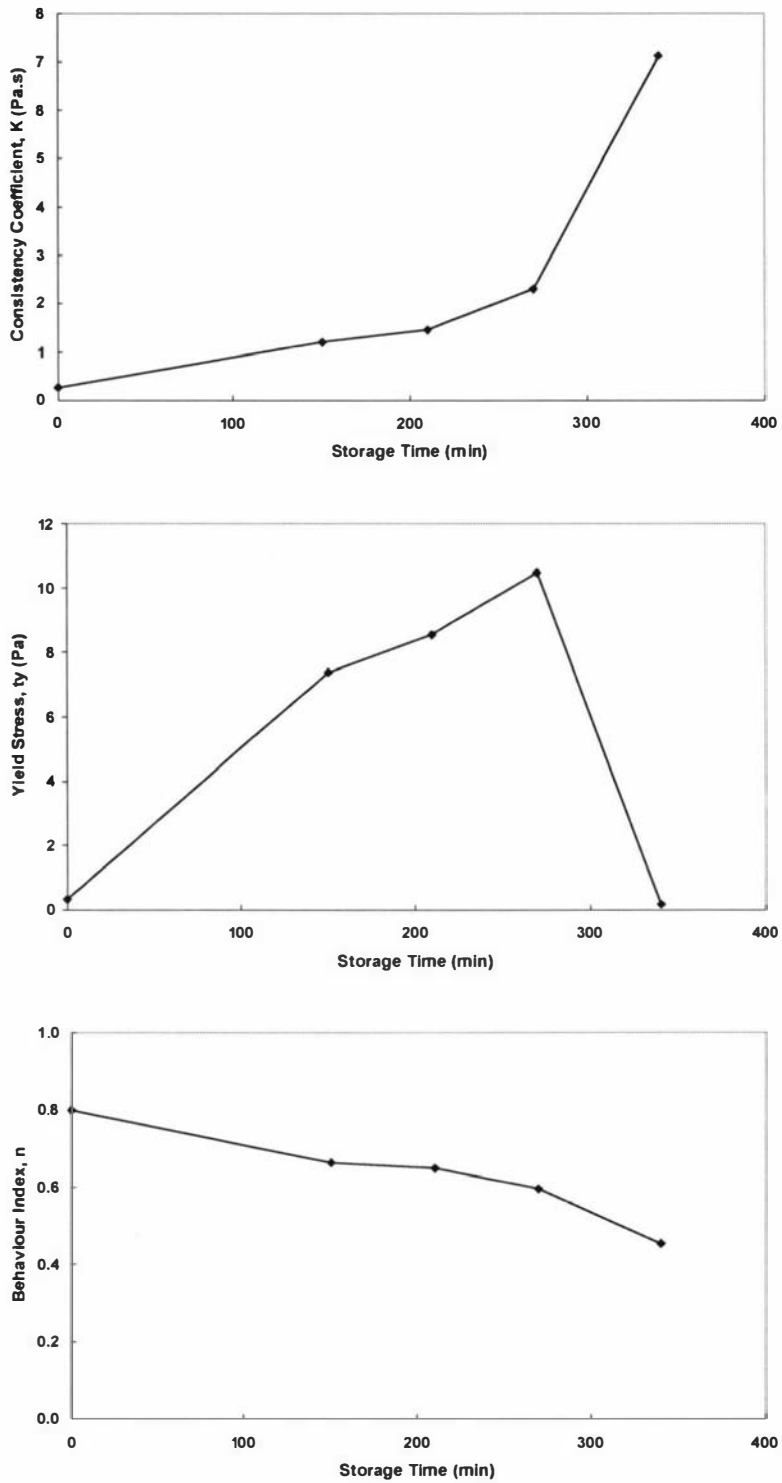


Figure 5.80: Changes in the behaviour index,  $n$ , of the Herschel-Bulkley model with time for a 50%TS reconstituted whole milk concentrate during storage at 75°C. Run C103, whole milk powder B, 50%TS.

### 5.8.2.1.2 PSD

The PSD for the 50%TS whole milk concentrate during storage is shown in Figure 5.81. The particle size distribution shifted from a mono-modal to a bi-modal mode, indicating aggregation between particles. The change in the percentage of particles bigger than 2  $\mu\text{m}$  was determined and plotted against the change in apparent viscosity with storage time, shown in Figure 5.82. The two curves displayed similar trends indicating the close relationship between particle size distribution and apparent viscosity.

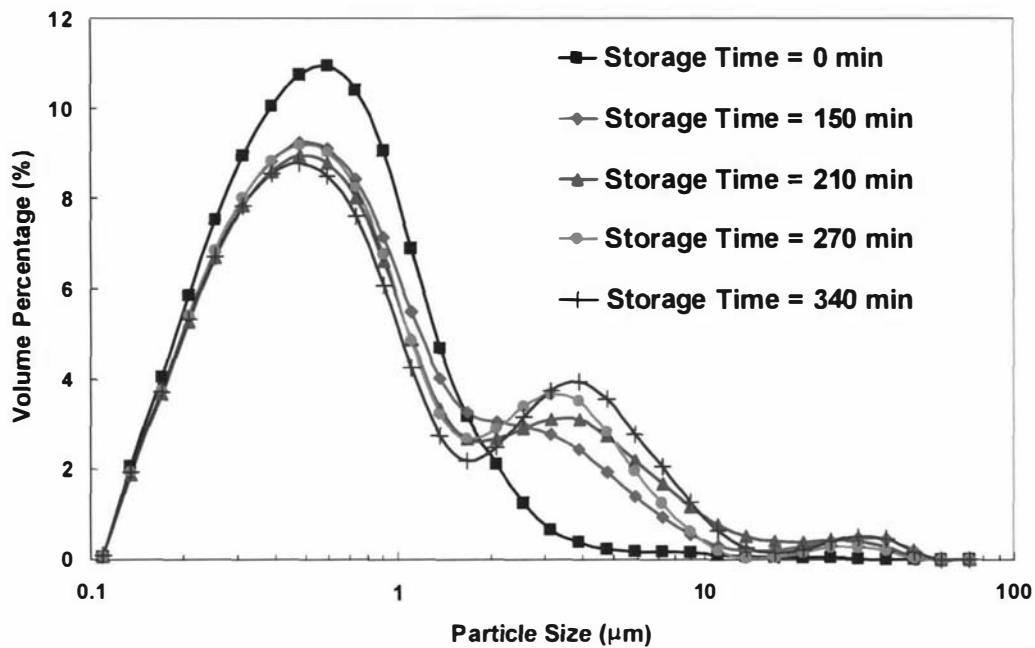


Figure 5.81: Change in particle size distribution of the 50%TS reconstituted whole milk concentrates during storage at 75°C. Run C103, whole milk powder B.

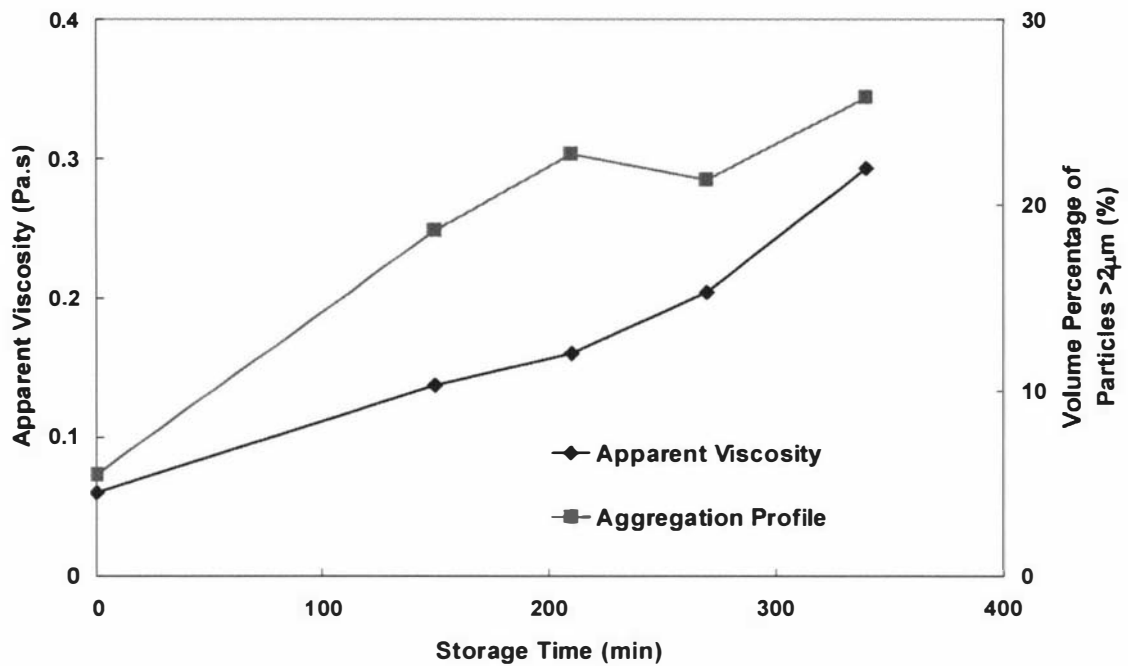


Figure 5.82: Comparison of the changes in the aggregation profile and apparent viscosity with storage time at 75°C during age thickening for the 50%TS reconstituted whole milk concentrates. Run C103, whole milk powder B.

### 5.8.2.1.3 TEM

Figures 5.83-5.85 show the changes in structure during age thickening in reconstituted whole milk concentrates over 340 minutes of storage at 75°C at three different magnifications, 3200x in Figure 5.83, 9100x in Figure 5.84 and 20600x in Figure 5.85. The large oval shaped particles represent the fat globules, while the dark circles are the casein micelles. Denatured whey protein can sometimes be seen as filamentous appendages.

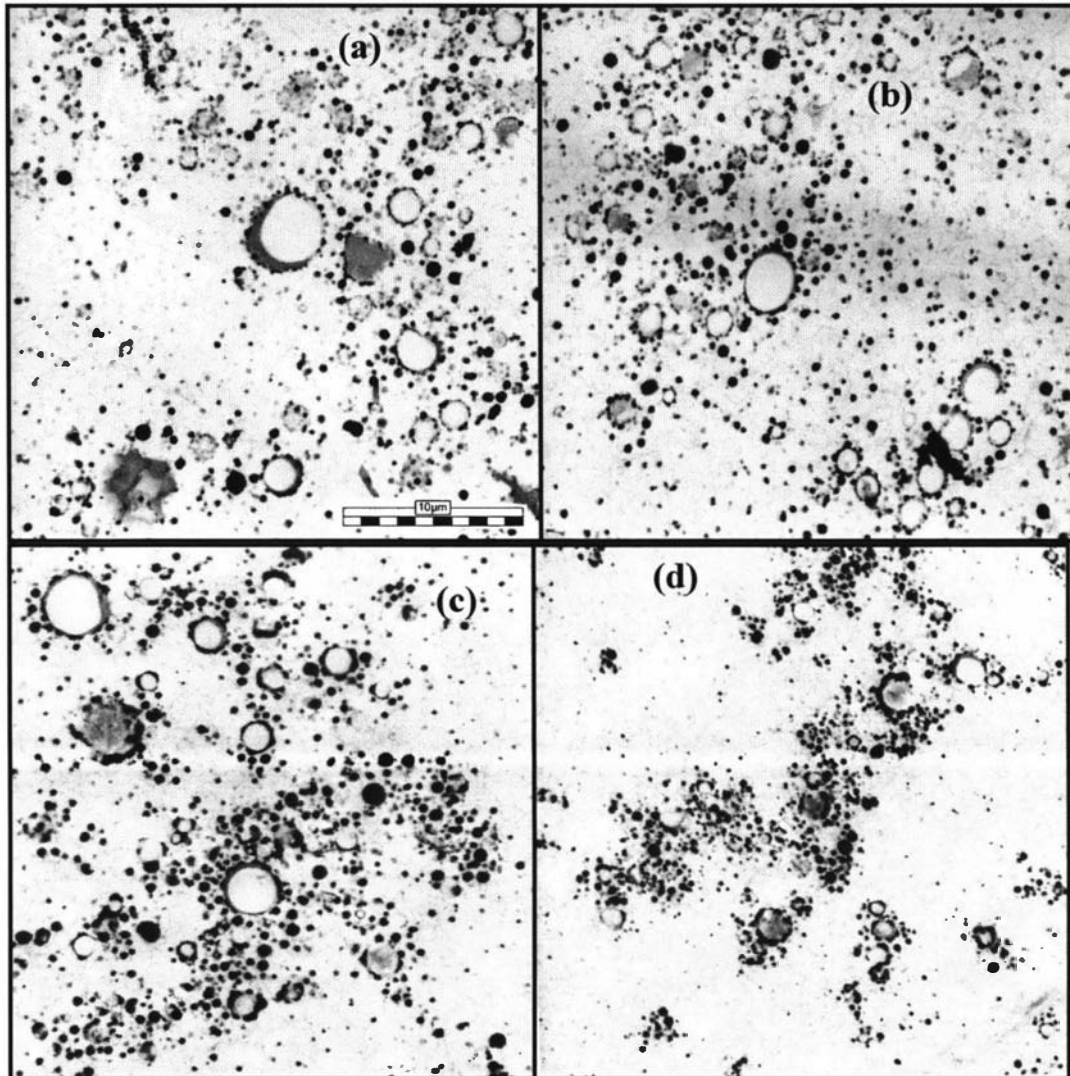


Figure 5.83: Age thickening in reconstituted whole milk concentrates during storage at 75°C. Magnification 3200x. Storage time: (a) 0 min, (b) 150 min, (c) 270 min, (d) 340 min. Run C103, whole milk powder B, 50%TS, 75°C.

In Figure 5.83 (a), during the initial stage of age thickening, the fat globules and the casein micelles are scattered randomly through the dispersed phase. As age thickening progressed, clusters are formed, where the fat globules are buried within the casein network (Figure 5.83 (b)-(d)).

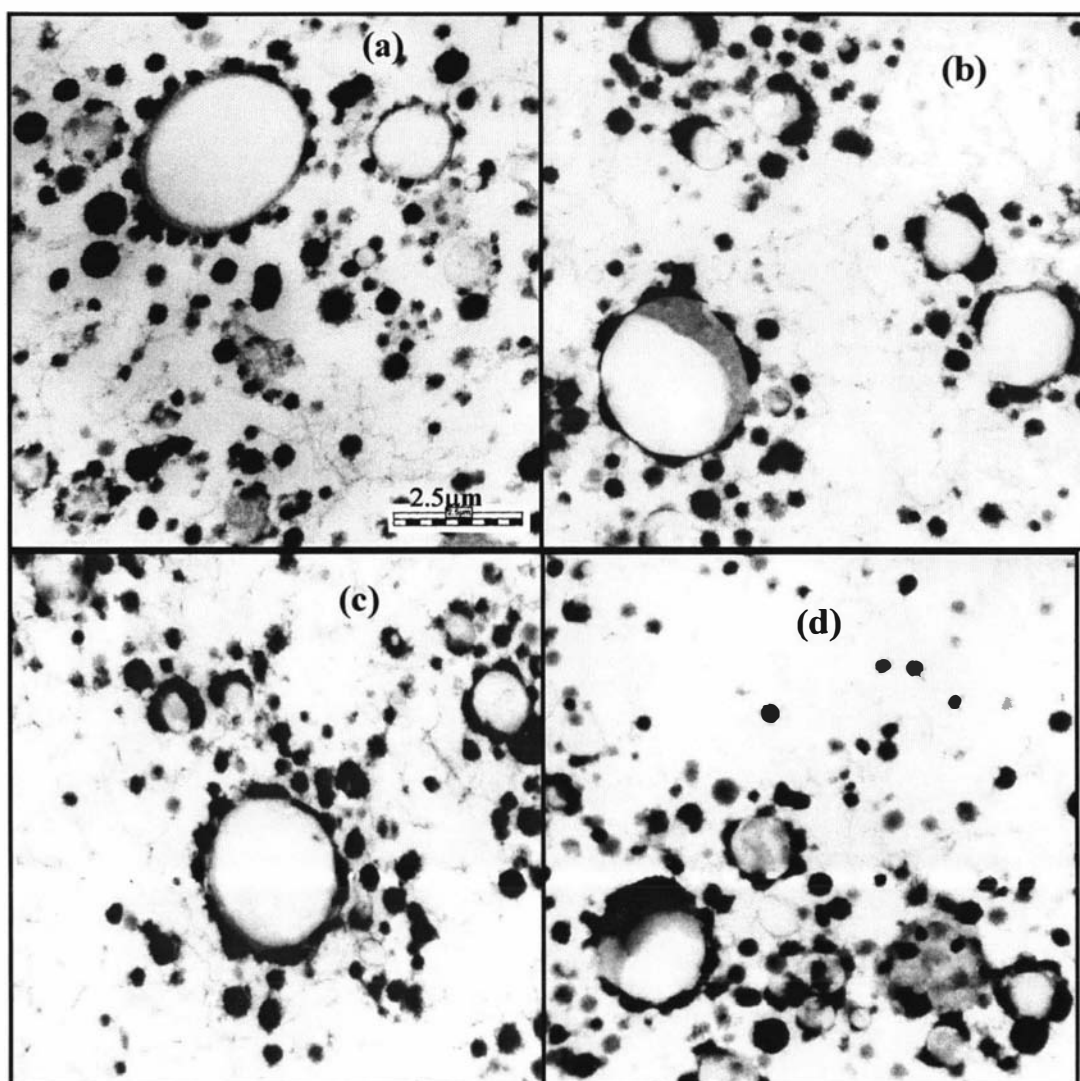


Figure 5.84: Age thickening in reconstituted whole milk concentrates during storage at 75°C. Magnification 9100x. Storage time: (a) 0 min, (b) 150 min, (c) 270 min, (d) 340 min. Run C103, whole milk powder B, 50%TS, 75°C.

Under higher magnification (Figure 5.84), the association of the casein micelles with the fat globules membrane is better discerned. Initially, caseins occupy random sites on the membrane and are individually attached, as evidenced by distinct humps on the perimeter of the fat globules (Figure 5.84 (a) and (b)). During age thickening, the adsorbed caseins fuse and form a continuous layer which eventually covers most or all of the available fat globule membrane (Figure 5.84 (c) and (d)).

Aggregation between casein micelles can be readily seen at 20600x magnification (Figure 5.85 (a)). Fusion of globular casein micelles is shown by the large dark formations, often of an oval shape. The progressive casein aggregation on the surface

of the fat globules with storage time is evident in the growth of the dark bands that suggest direct casein-casein interactions.

Figure 5.85 also shows a light shaded area surrounding the free casein micelles as well as the adsorbed caseins on the fat globules. The light shaded area has been observed by others authors and could represent the hairy  $\kappa$ -casein layers (Beaulieu et al., 1999; McKenna, Lloyd, & Munro, 1999; Velez-Ruiz & Barbosa-Canovas, 2000).

In Figure 5.85 (a)-(d), faint filamentous connections between the casein micelles can be seen. These filaments have been observed previously (Harwalkar & Vreeman, 1978; Koning et al., 1985; Kalab, 1993) and are thought to represent the presence of denatured whey proteins, acting as cross-linking bridges between casein micelles (Carroll et al., 1970; Davies et al., 1978; Kocak & Zadow, 1985; Defelipe et al., 1991).

Figure 5.85 (d) also shows that the fat globules interact with one another and with the casein network through the adsorbed casein micelles. This implies that the fat globules can only participate in the protein network via the adsorbed protein layers on the membrane.

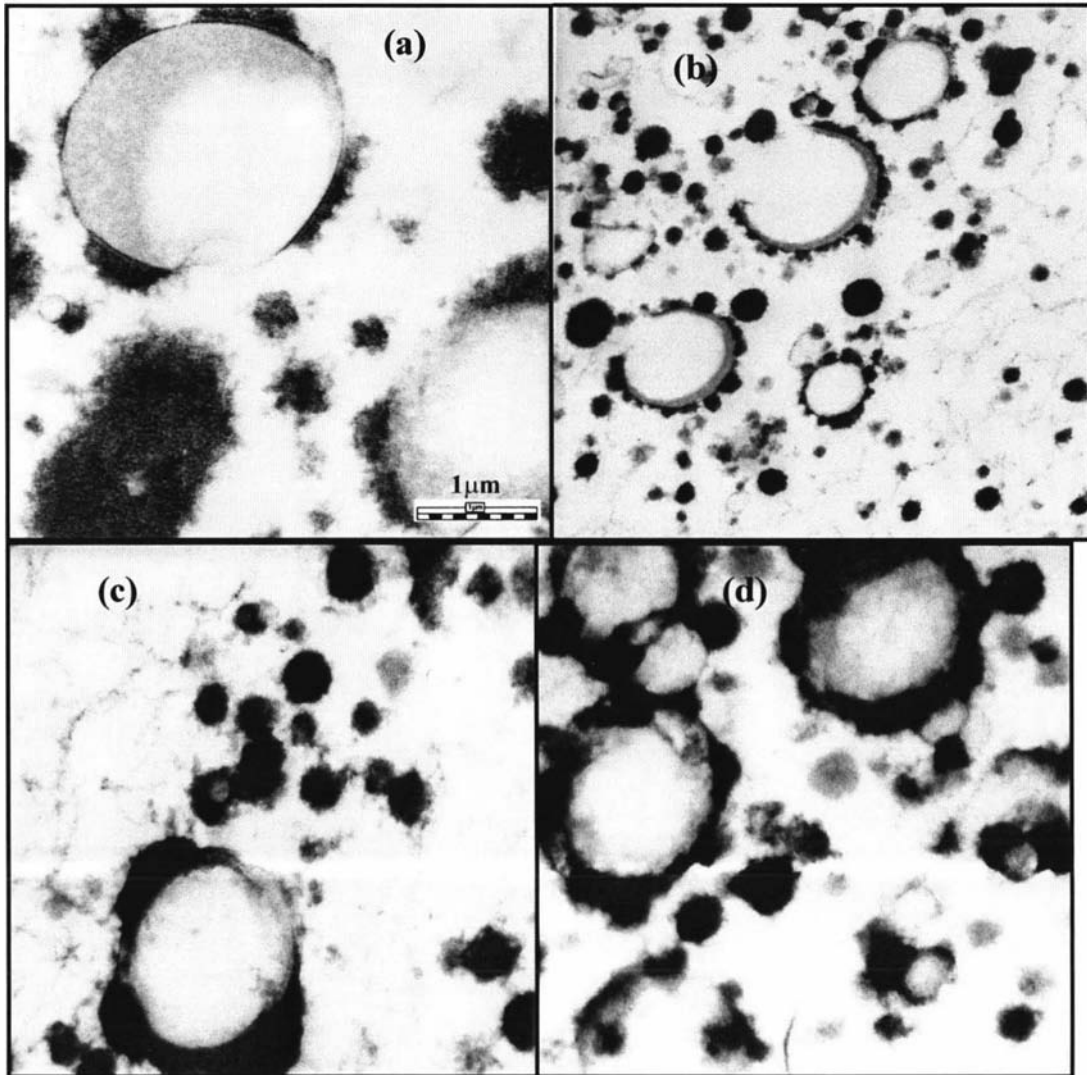


Figure 5.85: Age thickening in reconstituted whole milk concentrates during storage at 75°C. Magnification 20600x. Storage time: (a) 0 min, (b) 150 min, (c) 270 min, (d) 340 min. Run C103, whole milk powder B, 50%TS, 75°C.

### 5.8.2.2 Age thickening in reconstituted skim milk concentrates

Figures 5.86 and 5.87 show the changes in structures during age thickening in the reconstituted skim milk concentrate samples over 4 hours of storage at 75°C at two different magnifications, 3200x in Figure 5.86 and 20600x in Figure 5.87.

The first obvious observation in the Figures 5.86 and 5.87 is the absence of opaque circles which represent fat globules in TEM images. The dark black circles and

blotches represent casein micelles and aggregates. The background area is the serum protein.

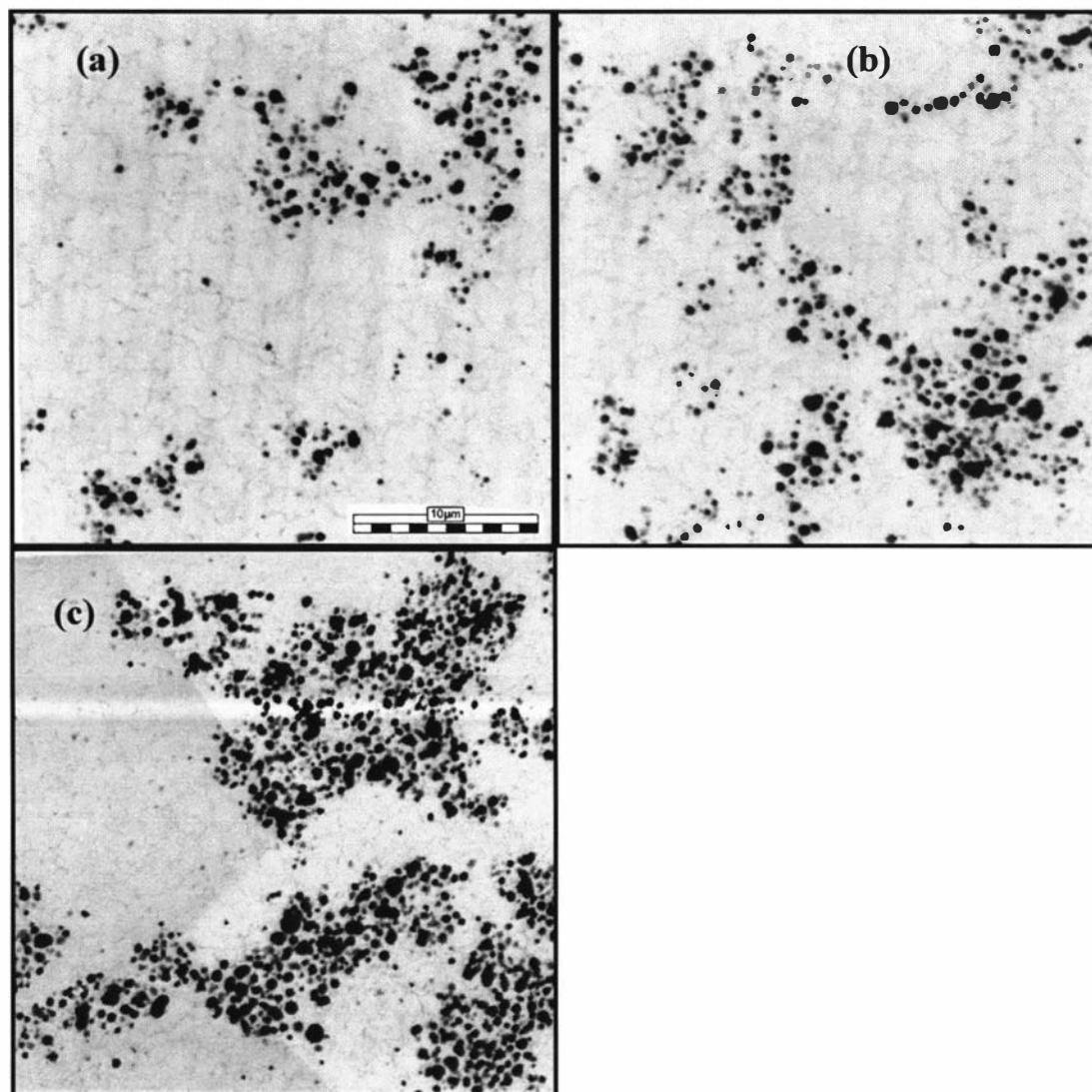


Figure 5.86: Age thickening in reconstituted skim milk concentrates during storage at 65°C. Magnification 3200x. Storage time: (a) 1 hour, (b) 2 hours, (c) 4 hours. Run C104, skim milk powder C, 50%TS, 75°C.

In Figure 5.86 (a)-(c), there is an increase in the number of observable casein particles per given area of image during age thickening. As all samples were made with the same dilution ratio, a given area of image presents the same portion of milk sample being examined. Therefore during age thickening, the caseins organise into some form of distinct cluster network.

At the initial stage of age thickening seen in Figure 5.86 (a), the casein micelles are already in loose cluster network..Most casein micelles retain the globular shapes. As age thickening progresses, the caseins associate with one other and form clusters. Figure 5.86 (c) clearly show formation of distinct groups of caseins, which are closely associated.

The size of the casein micelles increases with age thickening. This is more readily seen at high magnification shown in Figure 5.87. Initially, the casein micelles are globular, ranging in size between 01-0.3  $\mu\text{m}$ , which agreed with others, (e.g. Kalab, 1993; Lucey, 2002). It is important to remember that the solution is a reconstituted system made from powder which has received both heat and shear treatments during the manufacturing process. After 2 hours of storage, visible indications of aggregation between two or more casein micelles are apparent. This results in formation of casein aggregates (Figure 5.87 (c)), which are more than 3 times larger than the individual casein micelles (Figure 5.87 (a)). It is unclear whether the increase in size of the casein micelles is caused by the increase in size of the micelles themselves or due to the aggregation process between micelles or both.

In Figure 5.87, there is a light shaded area surrounding the casein micelles and aggregates. It is uncertain whether or not these light shaded areas represent layers of  $\kappa$ -casein as depicted in the casein models by Walstra et al. (1999). Careful observations of Figure 5.87 suggest the presence of denatured whey protein to provide cross-linkages between casein micelles and aggregates. This has been observed by Sawyer (1969) for skim milk concentrates.

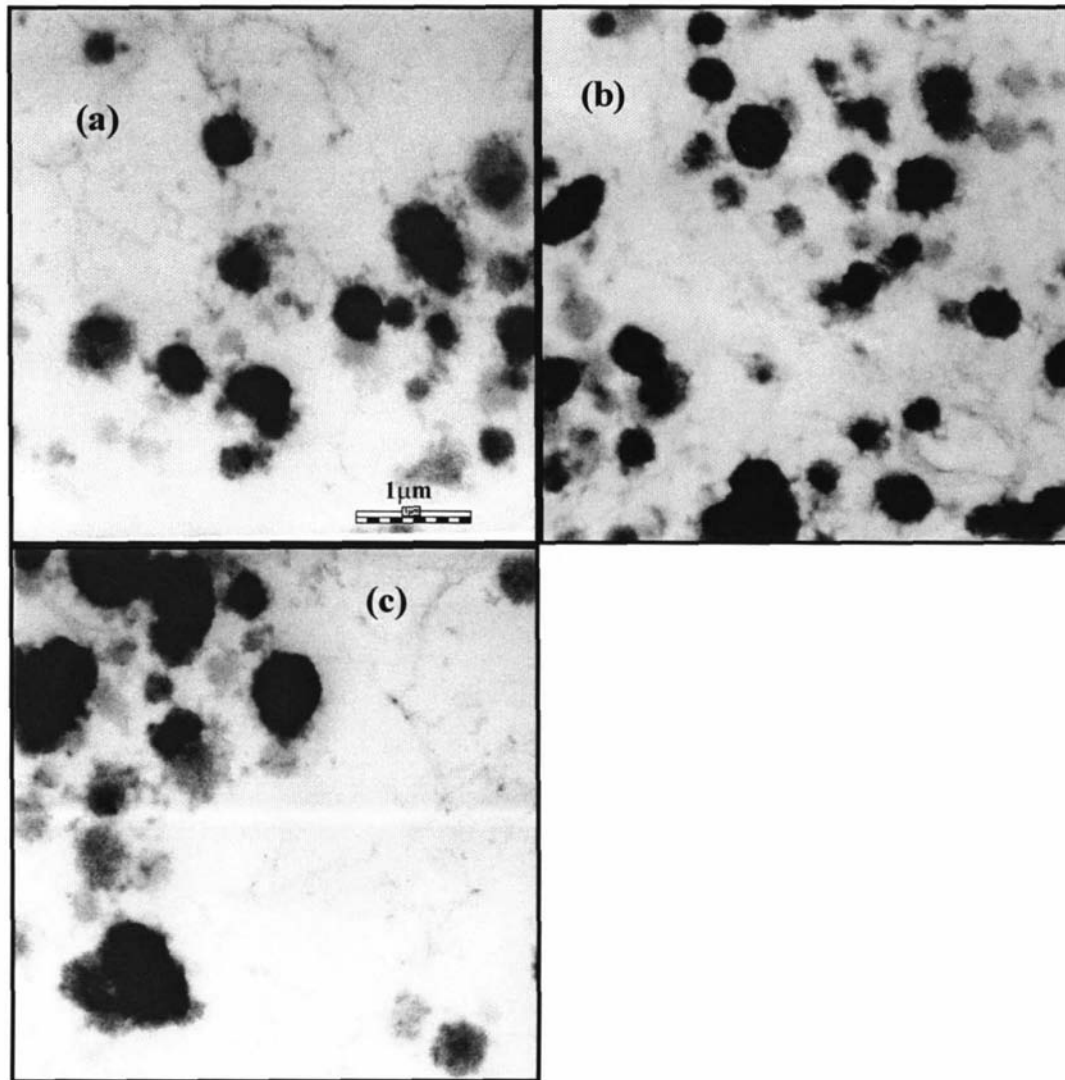


Figure 5.87: Age thickening in reconstituted skim milk concentrates during storage at 65°C. Magnification 20600x. Storage time: (a) 1 hour, (b) 2 hours, (c) 4 hours. Run C104, skim milk powder C, 50%TS, 75°C.

### 5.8.3 Data summary

TEM images showed that casein micelles play a crucial role in the formation of aggregates and eventually a gel network during age thickening. In whole milk, the fat globules could only take place in the build-up structure via the adsorbed protein layer on the DFGM. While in skim milk, the casein micelles grew bigger during age thickening and even fused together to form larger aggregates. Linking bridges were observed in both systems, which may represent the denatured whey proteins.

## 5.9 Direct experimental proof of irreversible changes during age thickening

The irreversibility of the age thickening and gelation processes has often been linked to the denaturation of whey proteins and their interactions with other whey proteins as well as casein micelles to form permanent aggregates (e.g. Jeumink & Dekruif, 1993; Schorsch et al., 2001). Denaturation of whey proteins is an irreversible process that results in exposed free thiol groups that can form covalent disulfide bonds.

Proof of the irreversibility of the changes in structure and rheological behaviour during age thickening comes in several forms. SDS PAGE (polyacrylamide gel electrophoresis using sodium dodecyl sulfate) has been used to show irreversible changes in the concentration of each individual protein during heating (e.g. Dalgleish, 1990; Anema & Li, 2003). Changes in PSD during age thickening have been associated with irreversible changes in the structure (Bienvenue et al., 2003a, 2003b). An increase in viscosity at high shear rate has also been taken as an indication of a permanent structural change. Bienvenue et al. (2003a, 2003b) noted that the apparent viscosity at  $1000 \text{ s}^{-1}$  during measurement increased with storage time. They considered this as sufficient evidence to prove irreversibility by high shear.

Snoeren et al. (1982) utilised extrapolated viscosity at infinite shear as a measure of the basic viscosity, while the increase in viscosity during age thickening constitutes the structural viscosity. Snoeren et al. (1982) argued that the changes in structural viscosity during age thickening were “almost completely” disrupted by maximum agitation, as evidenced by the mild increase in the extrapolated viscosity at infinite shear rate with storage time. However, they did not provide direct experimental proof that the structure formation during age-thickening could be dismantled completely by shear.

This section proposes a novel experimental method to investigate the irreversibility by high shear of the age thickening process. As shown in section 5.5, a shear rate of  $40,000 \text{ s}^{-1}$  can minimise the onset of age thickening during recirculation. At this high

shear rate, the apparent viscosity approaches the upper Newtonian region, and one can assume that the structure is substantially broken down to its individual elements, and any further break down is not possible. Therefore, an increase in viscosity at  $40,000 \text{ s}^{-1}$  indicates that these individual elements have either increased in size (which may increase the volume fraction) or formed strong bonds that cannot be destroyed by high shear processes. This is a strong evidence that some irreversible changes have taken place in the system during age thickening.

Adopting this principle, we set out to measure the apparent viscosity, standardised HLA, Herschel-Bulkley parameters and PSD of milk concentrates after alternate age thickening and high-shear disruption cycles. The reconstituted milk concentrates were prepared as normal with mixing carried out at  $35^\circ\text{C}$  and  $40,000 \text{ s}^{-1}$ . The concentrates were allowed to age thicken at different temperatures for a predetermined period, re-sheared at  $40,000 \text{ s}^{-1}$  for 60 minutes, and then age thickened under similar storage conditions as before. If the application of the second high shear recirculation step returned the system to its original state, it could be taken that the observed changes were fully reversible. On the other hand, if the system could not be fully returned to its original condition, this would be proof that there had been some irreversible changes.

### **5.9.1 Materials and methods**

Whole milk powder B was reconstituted to  $49.5 \text{ \%TS} \pm 0.5 \text{ \%TS}$  at  $35^\circ\text{C}$  and  $40,000 \text{ s}^{-1}$  for one hour in run C105. No additional heating was carried out and the reconstituted concentrates were stored at  $35^\circ\text{C}$  for 23 hours. Rheological measurements, pH and PSD analysis were carried out at regular intervals. One hour cycle of recirculation is the standard reconstitution protocol that has been applied to all previous reconstituted concentrates.

After the first 23 hours of storage, the remaining volume of sample was put back in the rig to be recirculated at  $40,000 \text{ s}^{-1}$  for 60 minutes. Note that the rig received a CIP wash before the second recirculation run. The twice-recirculated concentrates were then stored

at 35°C in a water bath for an additional 23 hours after which rheological measurement and PSD analysis were carried out.

Solids content measurements were carried out after the first and second cycle of recirculation. The change in pH during age thickening was also monitored.

The exercise was repeated in run C106 with a 47.5%TS concentrates made from powder B. The reconstituted concentrates were heated to 75°C. After the first storage step which lasted just over 1300 minutes, the concentrates were recirculated for 60 minutes at 40,000 s<sup>-1</sup> and 75°C before being stored again at 75°C. However, there was only enough sample for two measurements. PSD and rheological measurements were carried out. The change in pH was not monitored for this run at 75°C.

## 5.9.2 Results

### 5.9.2.1 Irreversibility at 35°C

The solids content measurements for the two sets of data are shown in Table 5.12. It was difficult to completely empty out the recombination rig after the CIP run because of water hold up in the mono pump. Table 5.12 clearly showed that some dilution occurred during the second recirculation cycle, where the solids content dropped from 49.4 %TS to 48%TS.

Table 5.12: Changes in solids content after recirculation

	<b>After first recirculation</b>	<b>After second recirculation</b>
<b>%TS</b>	49.4	48
	49.5	48
	49.4	47.9
<b>Average</b>	49.4	48

Figure 5.88 plots the change in apparent viscosity with storage time during age thickening in the concentrates after one and two cycles of recirculation at  $40,000 \text{ s}^{-1}$ .

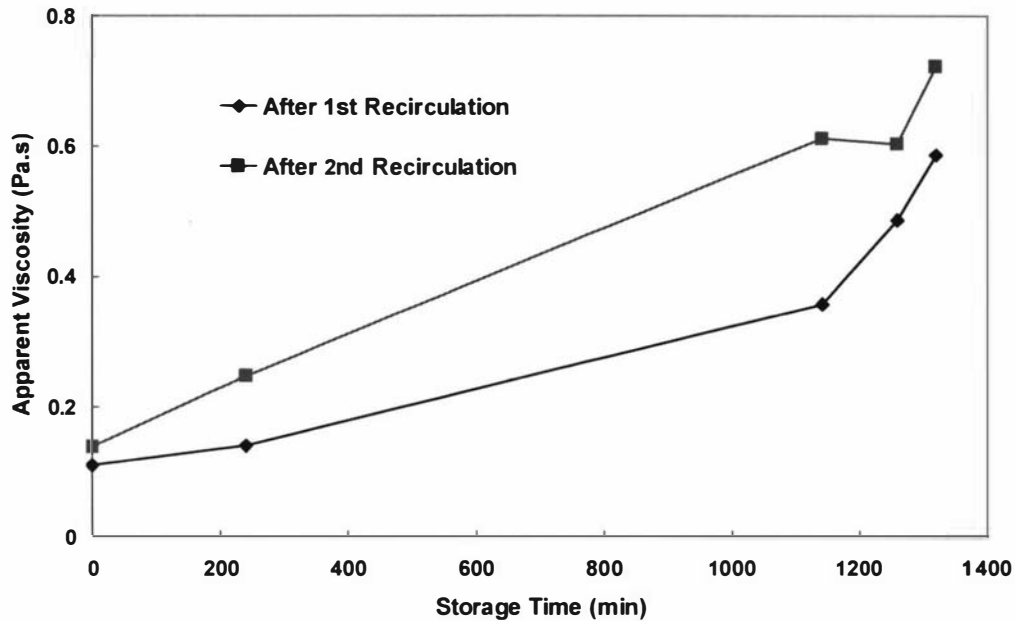


Figure 5.88: Change in apparent viscosity with storage time during age thickening at  $35^\circ\text{C}$ . Run C105, powder B, 49.4%TS,  $35^\circ\text{C}$ .

After one cycle of recirculation, the initial and the rate of change in viscosity with storage time were slightly lower than that observed in Figure 5.43 in section 5.4.3.1 where a 50%TS concentrates made from powder B was stored at  $35^\circ\text{C}$ . The slightly lower solids content of 49.4 %TS may have contributed to these discrepancies.

The application of the second cycle of recirculation reduced the apparent viscosity significantly, from 0.59 Pa.s (the last point on the “after first recirculation” curve) down to 0.14 Pa.s (the first point on the “after second recirculation” curve). Comparison of the initial apparent viscosity between the two curves showed a 25% increase. The RAT was determined from equation 5.4, and a 22% increase was observed after the second recirculation step.

Given the reduction in solids content by dilution after the second recirculation step, it is reasonable to suggest that the initial apparent viscosity and RAT after the second recirculation step would have been even higher if the solids content had been maintained at 49.4%TS. None the less, the higher initial apparent viscosity and RAT after the second recirculation step showed that it was not possible to completely reverse the changes in structure and rheological behaviour by applying a shear rate of  $40,000\text{ s}^{-1}$ .

The change in pH was monitored and shown in Figure 5.89. For both sets of sample, the initial pH value was 6.17 after one recirculation and 6.18 after the second recirculation. This agreed with the pH 6.2 plateau that was observed in Figure 5.20 in section 5.3.2. The pH fluctuated slightly throughout the 23 hours of storage, and no significant change was observed.

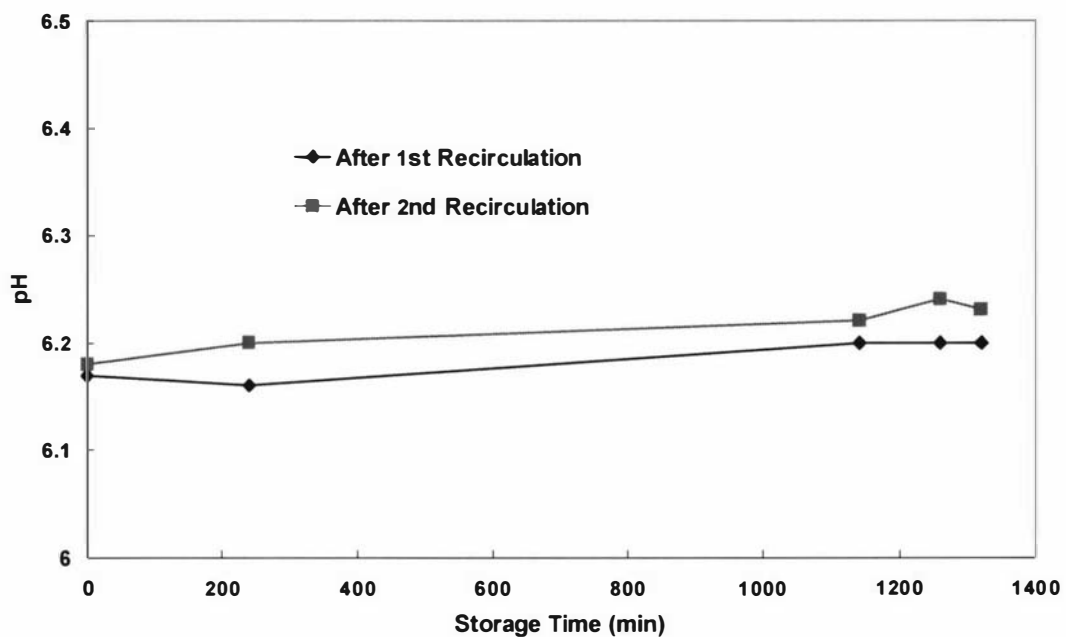


Figure 5.89: Change in pH with storage time during age thickening at  $35^{\circ}\text{C}$ . Run C105, powder B, 49.4%TS,  $35^{\circ}\text{C}$ .

The standardised HLA was determined to analyse the degree of thixotropy of the concentrates after one and two cycles of recirculation. The standardised HLA was

determined over the measurement shear rate range of  $80 \text{ s}^{-1}$  -  $410 \text{ s}^{-1}$ , and the results are shown in Figure 5.90. The standardised HLA was consistently higher after the second recirculation step at  $40,000 \text{ s}^{-1}$ .

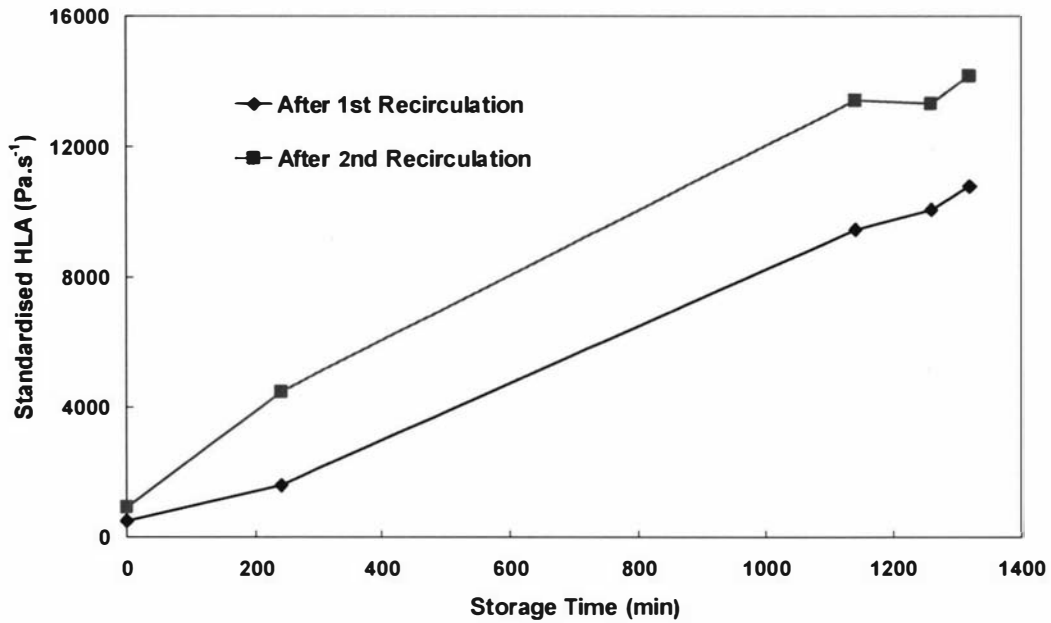


Figure 5.90: Change in standardised HLA with storage time during age thickening at  $35^\circ\text{C}$ . Run C105, powder B, 49.4%TS,  $35^\circ\text{C}$ .

The rheological data was fitted to the Herschel-Bulkley model and the results are shown in Figure 5.91.  $K$  was consistently higher and  $n$  was lower in the samples that have received two recirculation steps. This means that the samples were thicker as well as more shear thinning.

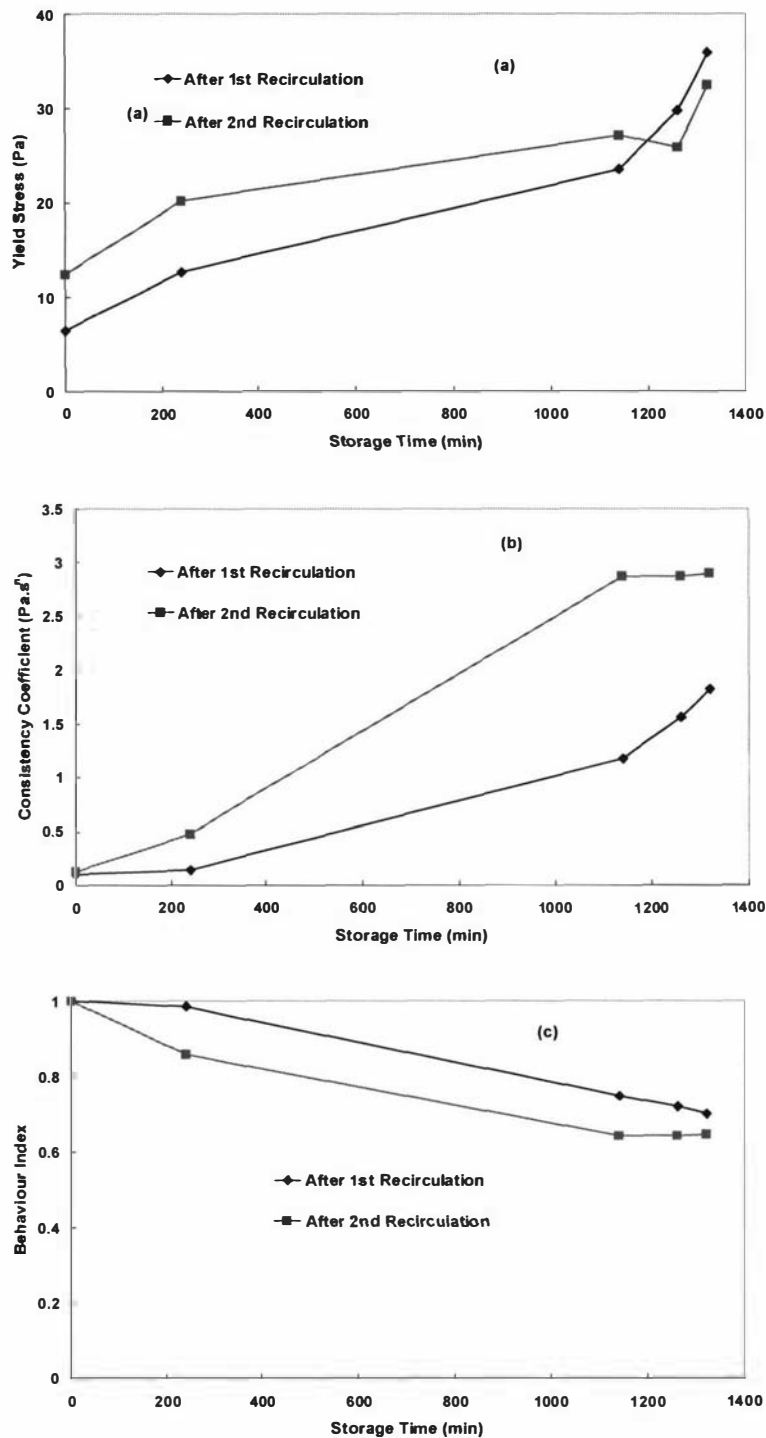


Figure 5.91: Effect of heating and storage temperature on the Herschel-Bulkley model parameters with storage time in concentrates made from powder B. (a)  $\tau_y$ ; (b)  $K$ ; (c)  $n$ . Run C105, powder B, 49.4%TS, 35°C.

The changes in PSD with storage time during age thickening at 35°C are shown in Figures 5.92-5.93.

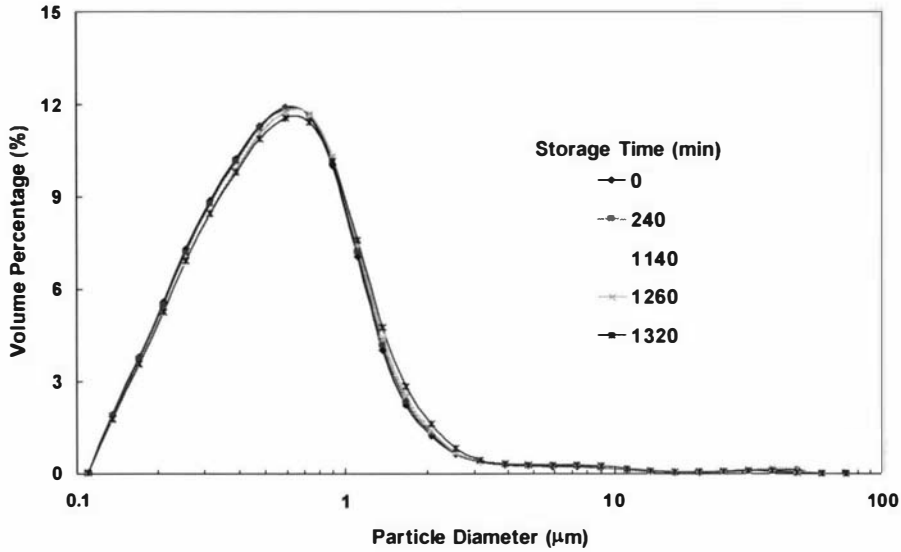


Figure 5.92: Changes in PSD with storage time after the first recirculation step. Run C105, powder B, 49.4%TS, 35°C.

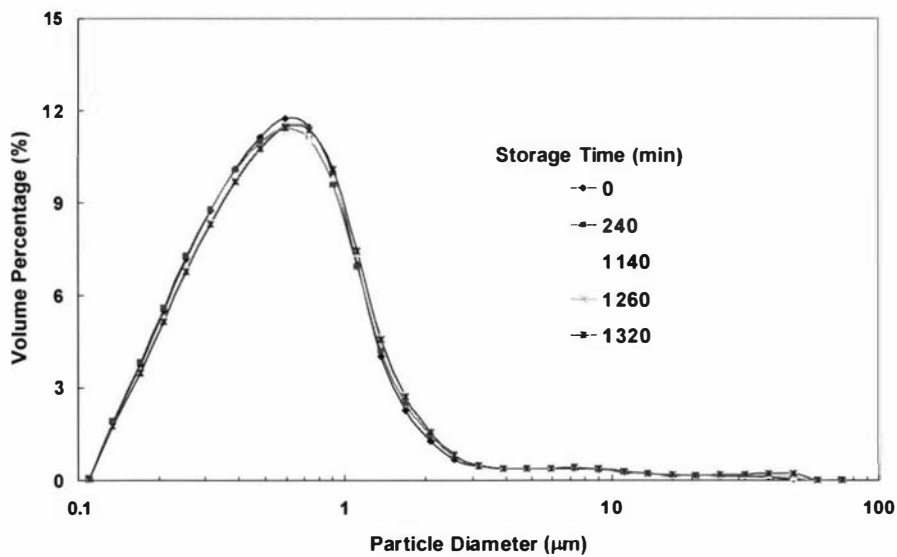


Figure 5.93: Changes in PSD with storage time after the second recirculation step. Run C105, powder B, 49.4%TS, 35°C.

In Figures 5.92-5.93, the mono-modal distribution curve did not change with storage time. This is in agreement with the PSD results obtained at 35°C for a 50%TS concentrates made from powder B, as shown in Figure 5.47 in section 5.4.3.3. The results indicated no significant difference in the PSD after one or two cycles of recirculation at 40,000 s<sup>-1</sup>.

The aggregation profiles were determined for both sets of data and compared as shown in Figure 5.94. No significant increase in the aggregation profile with storage time was observed in either curve. The two curves were similar in values, with average aggregation profile of 4% after the first recirculation and 3% after the second recirculation step.

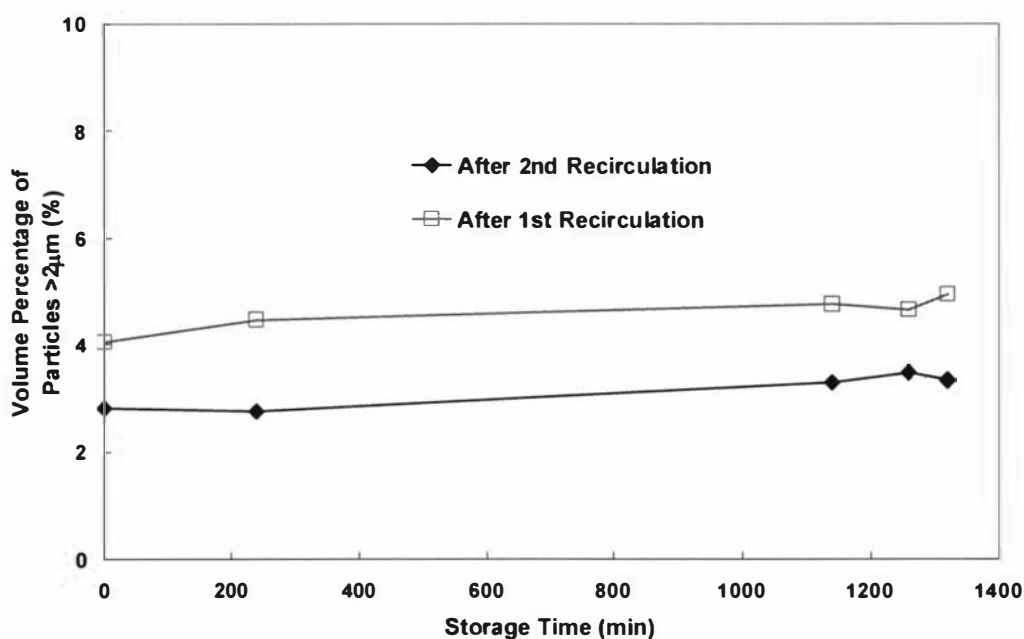


Figure 5.94: Changes in volume percentage of particles >2µm with storage time. Run C105, powder B, 49.4%TS, 35°C.

### 5.9.2.2 Irreversibility at 75°C

The solids contents after the first and second recirculation step were 47.5%TS and 47%TS respectively.

The changes in apparent viscosity with storage time during age thickening are shown in Figure 5.95. The initial apparent viscosity value after one cycle of recirculation was 0.026 Pa.s. This value is lower than 0.06-0.07 Pa.s observed previously in 50%TS reconstituted concentrates made from powder B that were heated to 75°C. The lower solids content of 2.5%TS would have contributed to the lower apparent viscosity in Figure 5.95.

The second recirculation step at  $40,000\text{ s}^{-1}$  reduced the apparent viscosity from 0.12 Pa.s (last point on the “after 1<sup>st</sup> recirculation” curve) to 0.03 Pa.s. This is a 15% increase in the initial apparent viscosity between the two curves. This increase is obviously smaller than the 25% increase in apparent viscosity observed in run C105 at 35°C. Once again, this can be attributed to the lower solids content in this run.

As there were only two data points available in the “after 2<sup>nd</sup> recirculation” curve in Figure 5.95, the RAT could not be reliably estimated.

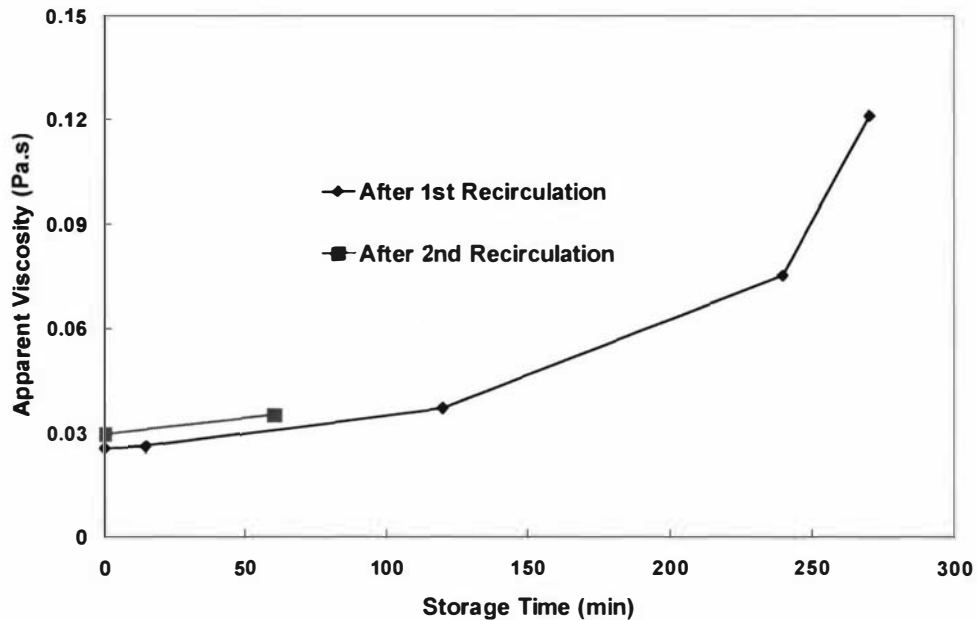


Figure 5.95: Change in apparent viscosity with storage time during age thickening at 35°C. Run C106, powder B, 47.5%TS, 75°C.

The standardised HLA was determined over the range of 80-410 s<sup>-1</sup> (the same as run C105 at 35°C) and the results are shown in Figure 5.96. The initial standardised HLA values were similar between the two curves. After 60 minutes of storage, the standardised HLA after the second recirculation step was slightly lower than after just one recirculation step, obviously against the apparent viscosity trend in Figure 5.95.

The results of standardised HLA between runs C105 at 35°C and C106 at 75°C are plotted together in Figure 5.97. The initial standardised HLA were lower in the two 75°C curves. However, the standardised HLA after the first recirculation step increased dramatically at 75°C and surpassed the 35°C after 120 minutes of storage. Therefore, even though the apparent viscosity values were lower at 75°C, the standardised HLA was higher, indicating a greater degree of thixotropy.

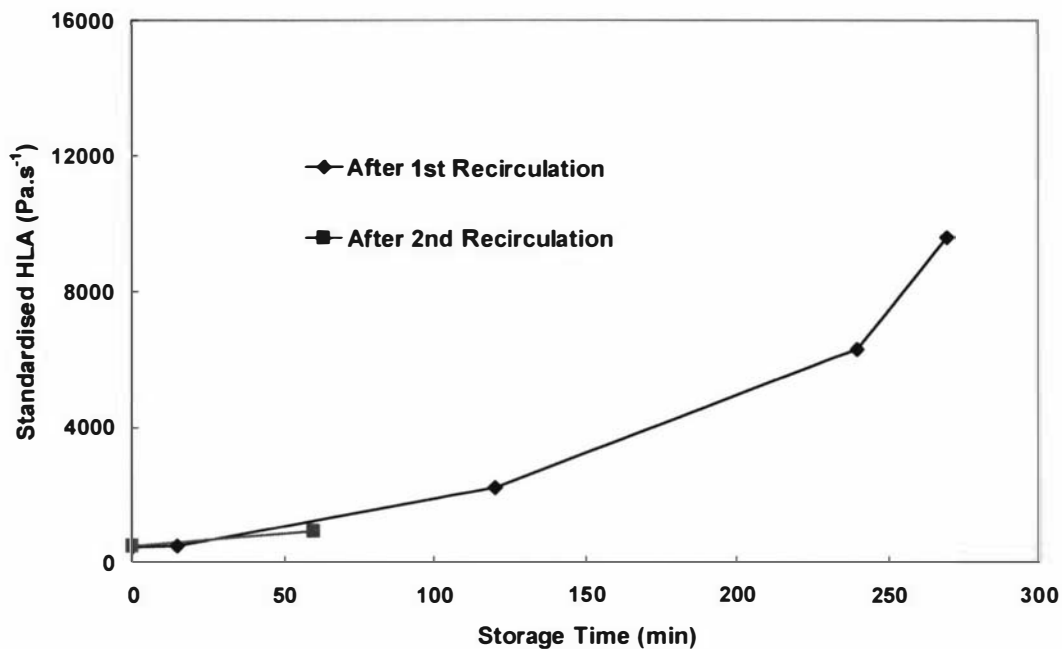


Figure 5.96: Change in standardised HLA with storage time during age thickening at 35°C. Run C106, powder B, 47.5%TS, 75°C.

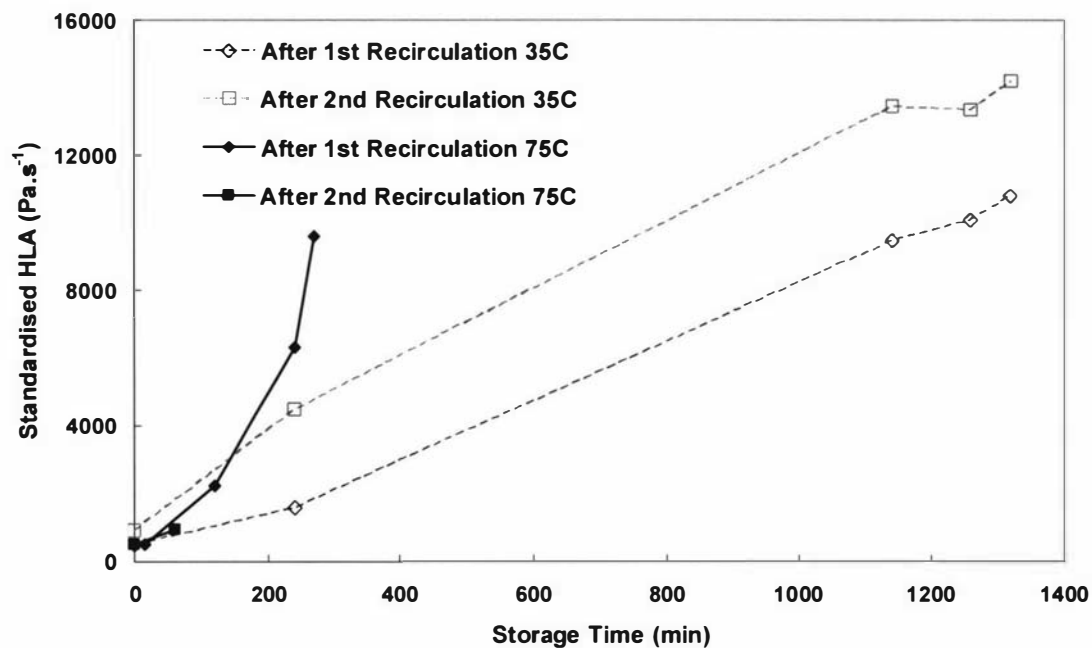


Figure 5.97: Comparison of standardised HLA between runs C105 at 35°C and C106 at 75°C.

The flow curve data in run C106 were fitted to the Herschel-Bulkley model and the results are shown in Figure 5.98. There was little difference between the two curves. However,  $K$  was consistently higher and  $n$  was lower in the samples that have received two recirculation steps. This agreed with the observations made in run C105 in Figure 5.91.

The changes in PSD with storage time during age thickening are plotted in Figure 5.99 for one recirculation cycle, and Figure 5.100 for two recirculation cycles. In both figures, the PSD changes from a mono-modal to a bi-modal shape during age thickening. This is in contrast with the data in run C105 where no change in PSD was observed during age thickening at 35°C despite a significant increase in apparent viscosity.

It was interesting to observe that the structure was almost broken down back to its original state upon recirculation at 40,000 s<sup>-1</sup>. Thus, the aggregates that contributed to the second peak in Figure 5.103 (one cycle of recirculation) were broken down upon high shear.

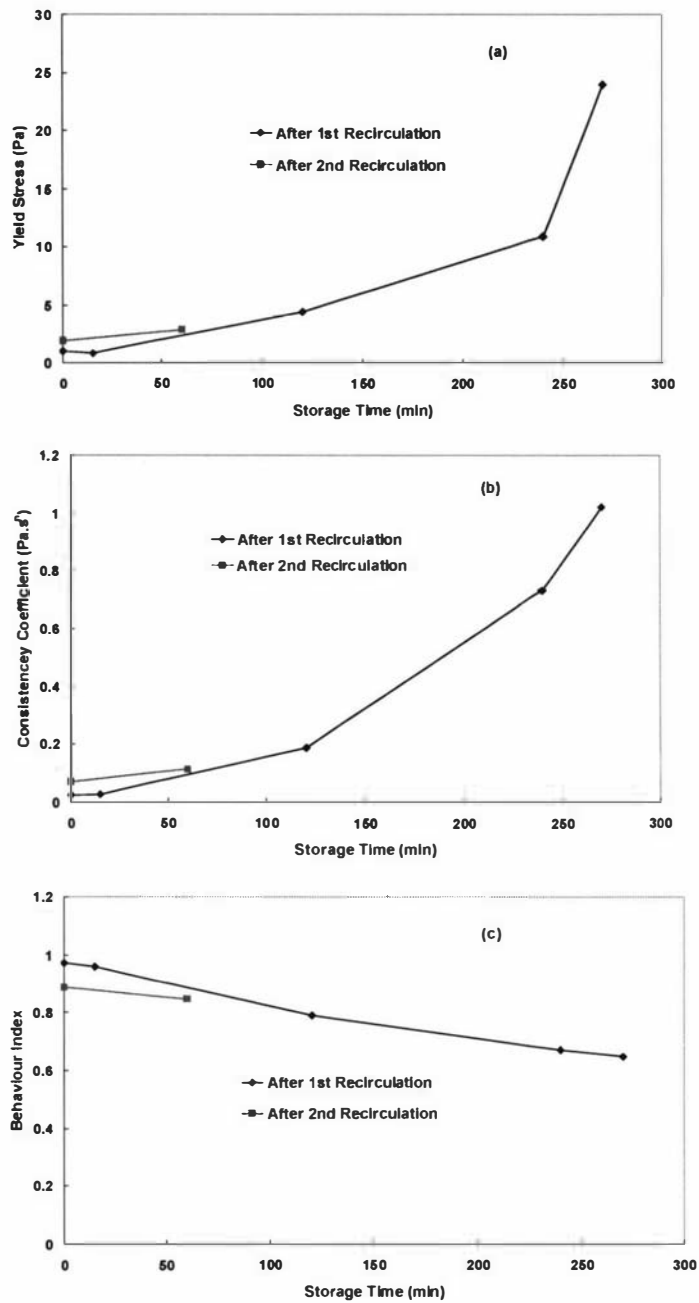


Figure 5.98: Effect of heating and storage temperature on the Herschel-Bulkley model parameters with storage time in reconstituted milk concentrates made from powder B. (a)  $\tau_y$ ; (b)  $K$ ; (c)  $n$ . Run C106, powder B, 47.5%TS, 75°C.

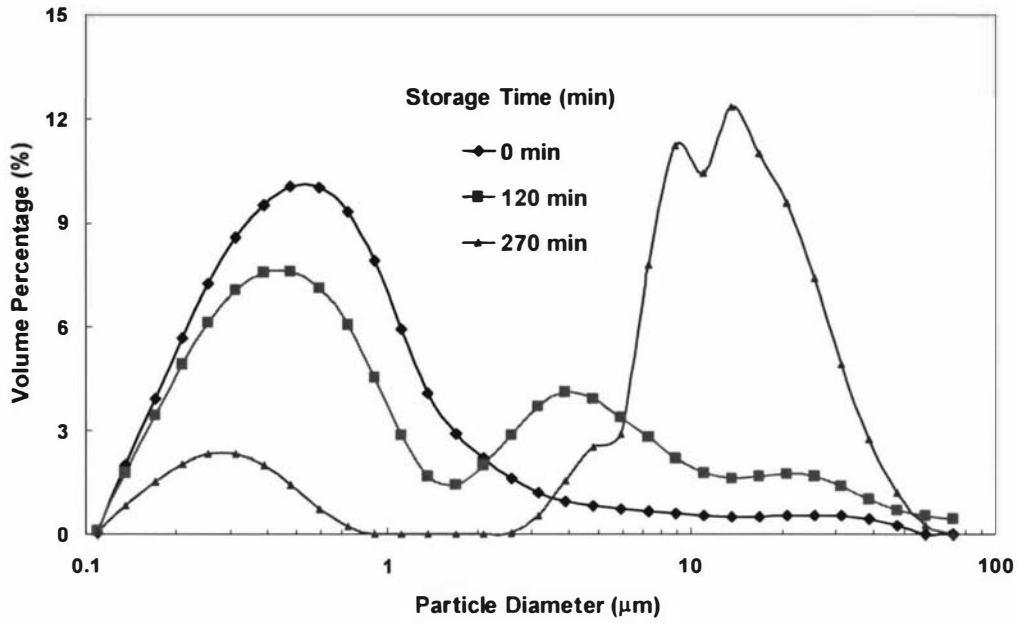


Figure 5.99: Changes in PSD with storage time after the first recirculation step. Run C106, powder B, 47.5%TS, 75°C.

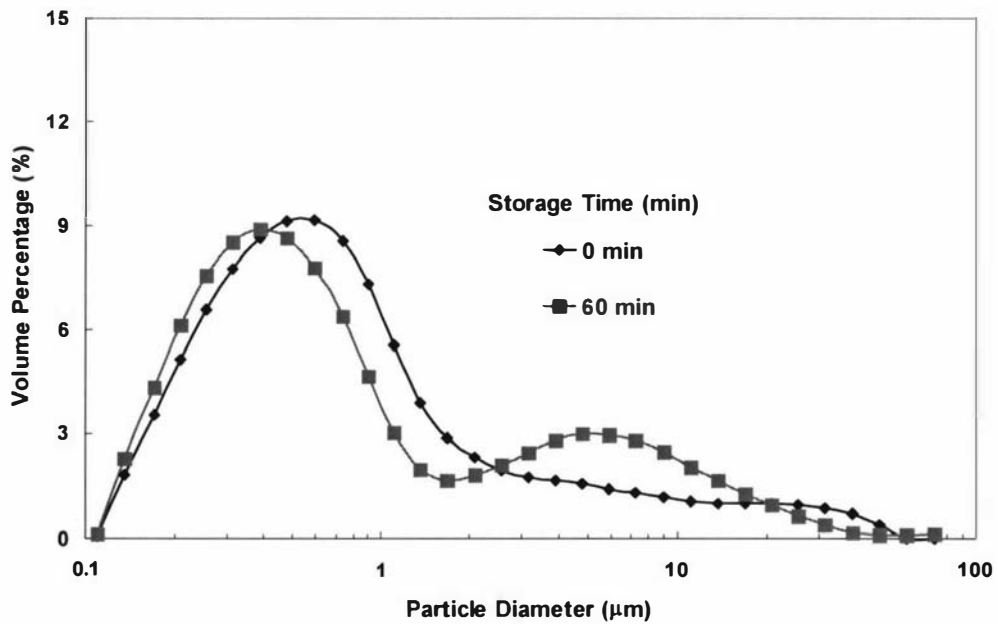


Figure 5.100: Changes in PSD with storage time after the second recirculation step. Run C106, powder B, 47.5%TS, 75°C.

The aggregation profile was determined for the two sets of data in run C106 and the results are plotted in Figure 5.101. The initial volume percentage of particles  $>2\mu\text{m}$  after one cycle of recirculation was 10.5%, which was significantly higher than the 3% observed in run C105 at  $35^\circ\text{C}$ , as shown in Figure 5.94. The volume percentage increased to over 80% during age thickening at  $75^\circ\text{C}$ .

After the second recirculation step, the volume percentage decreased to 18%. This is a significant increase from the initial volume percentage of 10% in the samples that received one cycle of recirculation. Similar to the determination of RAT, it is not possible to compare the rate of change in the volume percentage of particles  $>2\mu\text{m}$  from only 2 data points.

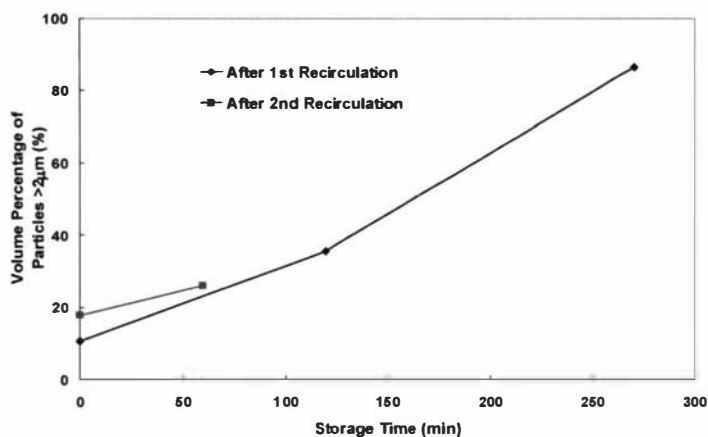


Figure 5.101: Changes in volume percentage of particles  $>2\mu\text{m}$  with storage time. Run C106, powder B, 47.5%TS,  $75^\circ\text{C}$ .

### 5.9.3 Data summary

Using an innovative testing method, it was possible to show that when the reconstituted milk concentrates were heated to  $75^\circ\text{C}$ , age thickening during storage was partly irreversible as indicated by the increase in apparent viscosity when the age thickened samples were sheared to  $40,000\text{ s}^{-1}$ .

---

# **CHAPTER 6**

# **DISCUSSION**

---

## CHAPTER 6: DISCUSSION

Throughout the course of the project, many new techniques were developed and interesting results were obtained. This chapter summarises the techniques developed and the results collected, discusses their significance in comparison to other published work in the literature and their contribution toward the fields of time-dependent rheology and milk concentrate rheology.

The chapter is divided into four main sections as followed

1. Data analysis methods: the techniques that have been developed to collect and analyse the data are discussed for their strength and limitations
2. Method of reconstitution: the importance of the new recombination rig is discussed in terms of design, operation and application
3. Results: the results are summarized and reviewed
4. Age thickening: a mechanism of age thickening is proposed using the results obtained here and those available in the literature.

### 6.1 Data analysis methods

The accuracy and reproducibility of results in the study of time-dependent rheological behaviour are affected by the techniques of sample preparation and collection, of rheological measurement and of data analysis.

#### 6.1.1 Data collection and measurement procedures

##### 6.1.1.1 Oscillatory versus flow curve tests

Non-Newtonian fluids should always be measured in a shear rate range that encompasses the shear rate of their intended application. However, this is not always possible with available commercial rheometers.

Many works in the literature have studied the rheology of gel and semi-solid systems with oscillatory tests (low shear deformation) to obtain  $G'$  and  $G''$  (e.g. Ozer et al., 1998; Kelly & O'Kennedy, 2001; Trckova et al., 2004). These tests give no indication about the flow behaviour in process applications that involve much greater deformations at higher shear rates, such as during homogenisation and atomisation

These considerations led to the determination of the flow behaviour at high shear rates as the most relevant method of rheological measurement for the study of thixotropy in this work. No oscillatory test was performed.

#### **6.1.1.2 Structure breakdown and build-up**

Time-dependent systems exhibit both structural build-up and breakdown at any given time and shear rate. Characterisation of these systems must involve the analysis of these two processes. However, many published experiments and models have only attempted to characterize the breakdown process. In these experiments, the fluids are sheared at a constant shear rate, and the decrease in shear stress with measuring time is monitored (e.g. Tiu & Boger, 1974; Ramaswamy & Basak, 1991).

Age thickening is a phenomenon where the apparent viscosity increases during storage at rest. Thus, the phenomenon is mainly caused by a build-up of structure with time. In order to study the age thickening process, the structural build-up process must be monitored.

The snapshot technique utilised by Velez-Ruiz and Barbosa-Canovas (1997, 2000) and Trinh and co-workers (Trinh & Yoo, 1997; Trinh & Leslie, 1997; Trinh & Schraekenrad, 2002; Ma et al., 2002) for rheological modelling was more appropriate in the study of age thickening where no assumption is made on the reversibility of structural recovery. The protocol consists of shear sweep tests of samples stored at rest for various lengths of time under different conditions. However, unlike these previous studies, this work included

three phases in the shear sweep test: a shear up, a constant shear and a shear down leg. The technique allows several important pieces of information to be collected:

- The flow curves show the shear dependent flow behaviour of the systems for each storage time
- The changes in the flow curve with storage time give insight into the changes in flow behaviour during age thickening and hence a measure of the build-up of structure
- The difference between the shear up and shear down legs gives a relative indication of the level of thixotropic breakdown due to shear

### **6.1.2 Measurement with the Brookfield LVTD viscometer and the Paar Physica MC1 rheometer**

The Brookfield LVTD viscometer was mainly used in the industrial surveys due to its portable design. Age thickening occurred during measurement because the shear rates during measurement were smaller than those in the process lines. Due to the limited capability of the Brookfield LVTD, shear sweep tests were not possible.

The Paar Physica MC1 rheometer was mainly used in controlled rheology experiments in the more stable environment of the pilot plant. The ability to record data automatically via a computer made it possible to conduct more extensive shear sweep tests.

The two instruments were found to provide complementary trends, but the absolute values obtained were different. This is due to both the difference in the modes of operation and in the operating shear rate ranges.

The measurement parameters, including the minimum and maximum shear rates, the number of data points and the measurement intervals were found to have a significant effect on the rheological behaviour during measurement of time-dependent systems (runs C2-C21). This agreed with the findings from Rohm (1992). Without the full knowledge of the measurement parameters, it is not possible to compare absolute values between

different experiments. Thus, the measurement conditions must always be, and were always, recorded and noted for each set of data. Unfortunately, this practice has only been carried out by a small number of workers (e.g. Buttler & McNulty, 1995).

### **6.1.3 Techniques for rheology characterization of time dependent milk concentrates**

Several new methods of data analysis were developed in this work to follow the changes in the rheological behaviour with storage time during age thickening. The first method involved tracking the changes in the apparent viscosity with storage time during age thickening.

Any given rheometer is limited by both a maximum torque (shear stress) and speed (shear rate). Measurements of a fluid as it thickens with time involve steadily decreasing the maximum attainable shear stresses and shear rates. This issue can be visualised by plotting torque versus spindle speed for two Newtonian fluids A and B with two different viscosities as shown in Figure 6.1. Fluid B is significantly thicker than fluid A as indicated by the slope of the two straight lines. The maximum spindle speed (750 rpm) and torque (50 mNm) of the Paar Physica MC1 are also indicated on the graph. The thinner solution (fluid A) reaches the maximum spindle speed before it reaches the maximum torque. The thicker fluid (fluid B) reaches the maximum torque before it reaches the maximum spindle speed. Thus during age thickening, the maximum shear rate attainable at the instrument's maximum shear stress of 50 mNm would decrease with storage time.

For consistency, the apparent viscosity was determined at a reference shear stress of 105.3 Pa (27.4 mN.m). This reference shear stress value was chosen because it was included in most of the flow curve data obtained in this work. The change in apparent viscosity with time describes the rate of age thickening.

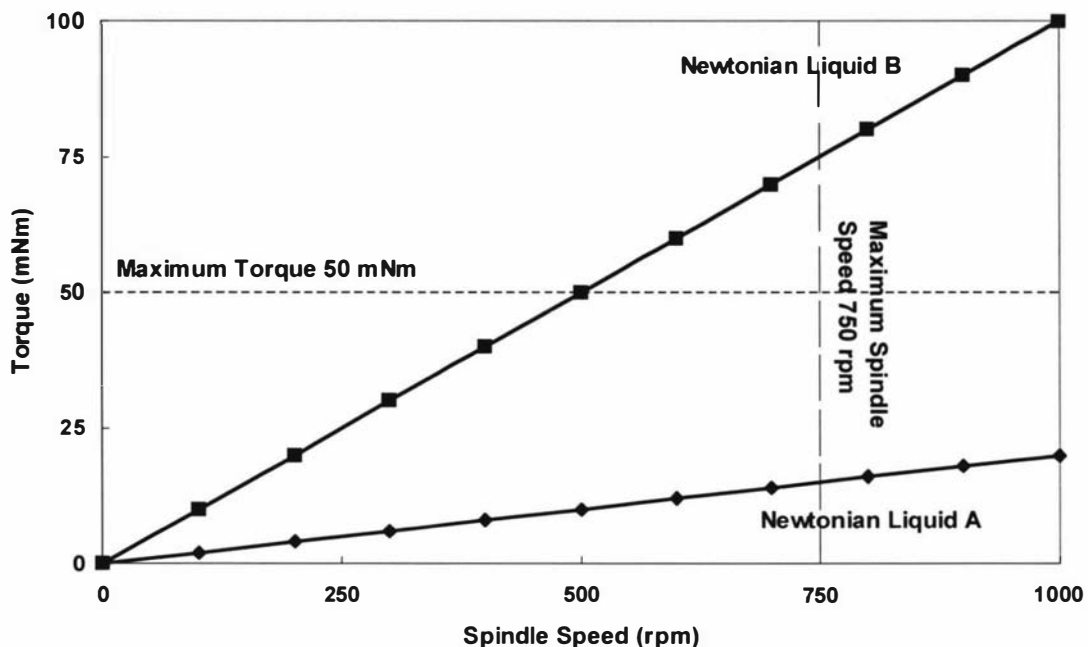


Figure 6.1: Typical flow curves drawn as torque versus spindle speed for two typical Newtonian solutions.

During storage, the rate of age thickening at 105.3 Pa was higher in the shear up than the shear down curve data. This is because the shear down curve data would have already been affected by the additional structural breakdown during the shear up portion of the test. Therefore the rate of age thickening was analysed with the shear up curve only.

The extrapolated apparent viscosity at infinite shear rate,  $\mu_{\infty}$ , was estimated by using the method of Snoeren et al. (1982) where the plot of apparent viscosity against  $\frac{1}{\dot{\gamma}}$  is extrapolated to the y-axis intercept. Using linear regression  $\mu_{\infty}$  was the y-axis interception. The change in  $\mu_{\infty}$  with storage time can be used to analyse the irreversibility of the age thickening process.

The hysteresis loop area (HLA) has been linked to time-dependent behaviour (Barnes, 1997) as an indication of the degree of thixotropy. However, it is rarely used in the literature to quantify the time-dependent behaviour. The determination of HLA, used as

a descriptor of age thickening in this work, is highly dependent on the shear rate range over which it is calculated. Therefore the determination of the HLA must be standardised to a particular shear rate range.

Even though the standardised HLA provided a more accurate description of the change in the degree of thixotropy, the non-standardised HLA still provided a useful tool to be used in conjunction with apparent viscosity-time curve to identify the gelling point. The HLA was found to increase up to the gelling point where it suddenly decreased sharply.

Modelling is a useful tool to summarise the vast amount of data available. Structural models are most desirable because they are evolved from fundamental concepts as discussed in Appendix 2. They are capable of describing both the breakdown and build-up coefficients (Cheng, 1987; Barnes, 1997). However, many authors who have used the structural models restricted their study to the structural breakdown process only (e.g. Tiu & Boger, 1974; Baravian et al., 1996) and thus provided no information on the structural build-up coefficient. As a further restriction, these techniques required the structural changes to be fully reversible, which is not applicable to concentrated milks. Finally, the use of structural models has yet to be applied to the analysis of process applications, such as spray drying and homogenization, where breakdown in structure is encountered.

The preferred modelling method here was to fit a phenomenological model, the Herschel Bulkley model, to the instantaneous flow curves and to follow the evolution of its parameters with storage time. While it is not the most rigorous modelling technique, it is simple to apply and does not require a postulate of reversible structure changes. The technique has been used by others (e.g. Velez-Ruiz & Barbosa-Canovas, 1997, 1998, 2000; Trinh & Schraekenrad, 2002; Ma et al., 2002).

#### **6.1.4 Bias and short comings of the modelling technique**

The modelling technique used in this work has many draw backs and shortcomings that the reader needs to be aware of. The steadily decreasing range of shear rates of the flow

curves measured during age-thickening as discussed in section 6.1.3 affects both the HLA (section 5.1.2.2) and the estimates of the Herschel-Bulkley parameters.

Figure 6.2 plots actual changes in nominal shear rate and shear stress for the 50%TS milk concentrate samples made from powder B in run C100 after three storage times of 0, 570 (gelling time) and 730 (after gelation) minutes. The maximum attainable shear rate decreased with storage time, from 2950 s<sup>-1</sup> at 0 minute, to 890 s<sup>-1</sup> at 570 minutes, and 245 s<sup>-1</sup> at 730 minutes. If the maximum shear rates for the 0 and 570 minutes samples were restricted to 245 s<sup>-1</sup> to match the 730 minutes sample, rheological modelling would return different results, as shown in Table 6.1.

Table 6.1: Changes in the HLA and the Herschel-Bulkley parameters with shear rate range in three concentrate samples. Run C100, powder B, 50%TS, 75°C.

Storage Time (min)	$\mu_{app}$ at 105.3 Pa (Pa.s)	Max. $\dot{\gamma}$ (s <sup>-1</sup> )	$\tau_y$ (Pa)	$K$ (Pa.s <sup>n</sup> )	$n$	HLA (Pa.s <sup>-1</sup> )	Intrinsic HLA (Pa.s <sup>-2</sup> )
No truncation in the maximum shear rate range							
0	0.06	2950	2.93	0.34	0.76	11290	
570	0.83	890	53.56	4.06	0.52	37881	
730	3.51	245	0.00	41.29	0.28	12512	
Truncation of the maximum shear rate to 245 s <sup>-1</sup>							
0	0.06	245	3.15	0.35	0.75	655	3.97
570	0.83	245	20.66	16.16	0.34	10381	62.91
730	3.51	245	0.00	41.22	0.28	12512	75.83

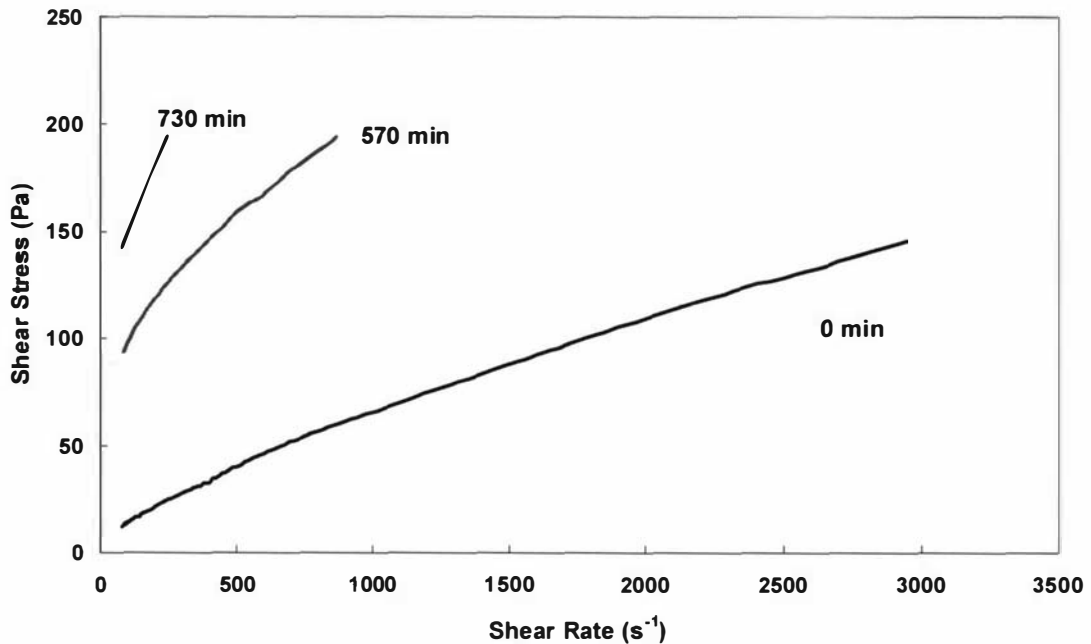


Figure 6.2: Changes in the flow curve during age thickening in run C100. Powder B, 50%TS, 75°C.

As shown in Table 6.1, a decrease in the shear rate range had the most impact on the estimate of the yield stress, particularly in the 570 minutes data. The problem cannot always be circumvented by truncating the maximum shear rates and shear stresses to the same level in all data sets. As shown in Table 6.1, the maximum shear rate achieved in the 730 minutes sample was only 245 s<sup>-1</sup>. The data for this sample was now completely devoid of data points in the quasi linear region between 245 s<sup>-1</sup> and 890 s<sup>-1</sup> as observed in the 570 min sample in Figure 6.2. Consequently the extrapolated line obtained by curve fitting with the Herschel-Bulkley model had a very steep slope and estimated a zero yield stress. This result was of course counter intuitive as one would expect the gelled samples to show a much higher yield stress. The only recourse was to ignore the modelling results for the gelled samples because of the artefacts created by the torque limitation of the Paar Physica MCI.

## 6.2 Methods of recombination

Many authors have pointed out that the samples must be conditioned prior to rheological measurement to improve reproducibility in the measurements of time-dependent fluids (e.g. Tiu & Boger, 1974). In these fluids, the structure and thus the rheological behaviour changes with time. This makes it difficult to identify the time zero throughout the sample preparation, handling and measurement steps. It is important that all replicates samples prior to rheological measurement have the same initial structure as well as the rate of change with time, since these will affect the subsequent rheological behaviour.

A popular method of conditioning is to store the samples at rest and at low temperature prior to measurement. The resting period ranged from 1 hour (Lawrence et al., 2001) to 1 day (Schelhass & Morris, 1985) to 5 days (Velez-Ruiz & Barbosa-Canovas, 1998). There is no published argument that explains exactly how this conditioning ensures good reproducibility. One may assume that the storage step would allow the system to fully rebuild its structure to reach an equilibrium state. This will remove the effect of shear history, and thus produce replicate samples with reproducible rheological behaviour. However no proof, buttressed by data, has been given in the literature that this conditioning by storage has removed the effect of shear history or ensured that the initial rheological behaviours of the replicate samples are similar. There is no theoretical guidance in the literature as to what conditions should be employed, particularly the storage time and temperature required, to ensure good reproducibility between replicate samples.

The author and his supervisors propose a new method of conditioning samples, as described in section 3.2, which subjects samples to shear rate of  $40,000\text{s}^{-1}$  or any other shear rate able to reach the upper Newtonian plateau of colloid systems. This effectively removes most of the effect of prior shear history and can contribute to a more systematic study of time dependent fluid rheology. The biggest advantage of the technique is the ability to obtain the same reference point on the structure-time scale for all samples.

The effect of recirculation shear rate on the changes in the inline apparent viscosity was investigated in section 5.5. The data in Figure 5.53 are replotted in Figure 6.3 to show the exponential decrease in apparent viscosity with recirculation shear rate at different recirculation times. It is clear that the apparent viscosity reached a minimum plateau between 10,000 and 40,000  $s^{-1}$ . This is characteristic of the upper Newtonian plateau where the viscosity is no longer dependent on shear rate or on time. Rheological modelling of all the data gathered showed that the flow behaviour index was 1 throughout the recirculation process at 40,000  $s^{-1}$ , indicating Newtonian behaviour. When recirculation took place at 40,000  $s^{-1}$ , the rheology of samples withdrawn after 60 minutes of recirculation was constant. Under these conditions, there was no time-dependent behaviour. This made it possible to produce replicate reconstituted milk concentrate samples with rheological profiles within 10% error, an important requirement in the rheological study of age-thickening or any time-dependent phenomenon.

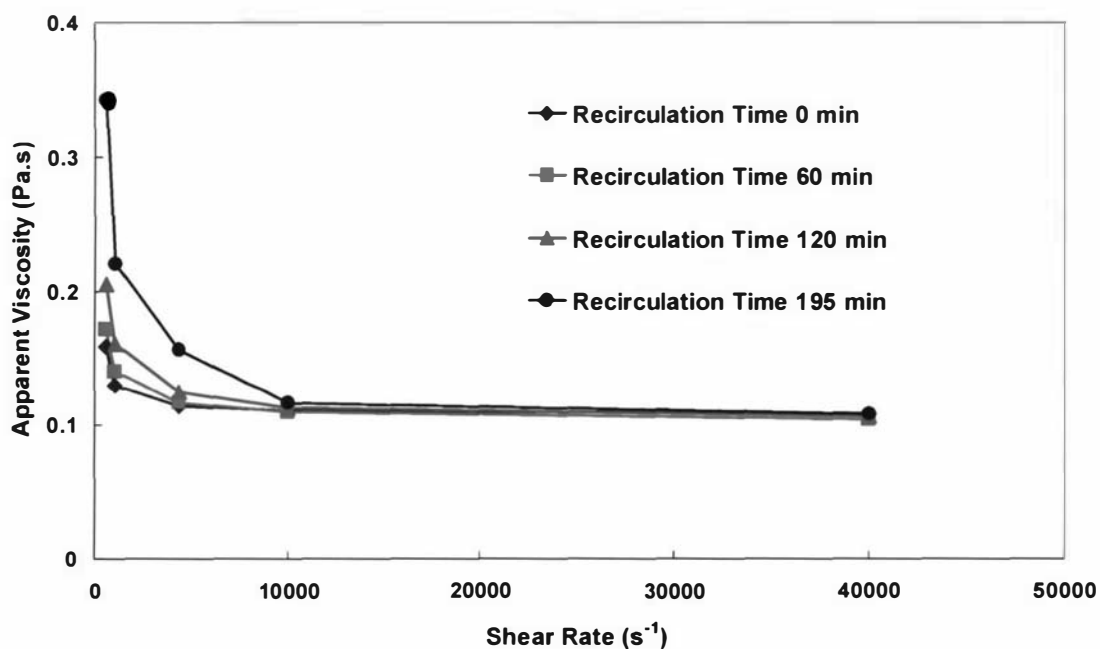


Figure 6.3: The changes in apparent viscosity with shear rate after different duration of recirculation. Runs C63-C67, powder A, 48%TS, 35°C.

Several authors have acknowledged good reproducibility between replicate samples can be achieved by breaking down the aggregates to the primary particles through the application of high shear rates (Wolthers et al., 1996; Corvisier et al., 2001). Yet, the methods they applied to achieve this degree of breakdown were restricted to relatively low shear rates compared to the  $40,000 \text{ s}^{-1}$  carried out in this work (e.g. solutions mixed for three minutes with a “whirl mixer” (no shear rate given) by Wolthers et al. (1996) and sheared at  $500 \text{ s}^{-1}$  by Corvisier et al.(2001)). More importantly, the results in section 5 showed that age thickening can still occur at  $4,400 \text{ s}^{-1}$ , which is significantly higher than the shear rates achieved by these authors. It is fair to argue that the critical minimum shear rate required to reach the upper Newtonian plateau varies between systems. However, it should be demonstrated that what ever the choice of shear rate, it is sufficient to reach the upper Newtonian region.

The rheological behaviour of the reconstituted milk concentrates, a time-dependent system, was defined here by:

- The initial apparent viscosity and flow curve after recirculation and heating
- Changes in the apparent viscosity and flow curve with storage time during age thickening.

Samples with the same apparent viscosity at one shear rate do not necessarily have similar flow curves or a similar rate of change in viscosity with time. Thus, a full description of the rheological behaviour of a time-dependent system must include both the initial flow curve and its rate of change with time under specified test conditions. Thus, the reproducibility data presented in section 3.2.2 is much stronger than any that was previously available in the literature.

### **6.3 Controlled rheology experiments**

#### **6.3.1 Use of reconstituted powder solutions versus fresh milk concentrates**

Milk powder was used as an alternative raw material to fresh raw milk to avoid the lack of uniformity in fresh milk supply.

There is evidence in the literature which shows that the apparent viscosity of reconstituted milk differs significantly from fresh milk (e.g. Vilder et al., 1979). The author believes that the lack of control of the age thickening process during reconstitution was the main reason for the difference in the rheological behaviour between fresh and reconstituted systems in previous work. The use of the new recombination system overcomes this problem with the use of high shear rate and low temperature during recirculation.

In order to compare the rheology of fresh and reconstituted milk concentrates, the shear history of the two systems must be similar. To achieve this, the fresh concentrates were recirculated in the recombination rig at  $40,000 \text{ s}^{-1}$ . The results in section 5.2 showed that the rheology of the fresh and reconstituted concentrates were similar (significant at  $p < 0.01$ ) when care is taken during the reconstitution process to minimise age thickening. This validates the use of powder and reconstituted milk concentrates system as an alternative source of raw material in this work.

The controlled rheology experiments were mainly carried out on two medium heat whole milk powders A and B which had similar compositional specifications.

#### **6.3.2 Effects of solids content and temperature on the transition of rheological behaviour in reconstituted whole milk concentrates**

Much has been made of the importance of controlling concentrate viscosity in the manufacture of powders of good quality (Bloore & Boag, 1981; Snoeren et al., 1983;

Vilder & Moermans, 1983; Snoeren et al., 1984). Since these concentrates normally range between 48% and 50%TS, correlations of viscosity to powder characteristics such as particle diameter and solubility are at best only indicative because these viscosity numbers are point values of much more complex rheological profiles. Atomisation in dairy plants should be designed for non-Newtonian time-dependent fluids, not simple Newtonian fluids.

It is essential therefore to define the transition regions between the different rheological behaviours, in other words the temperatures and concentrations when the milk concentrates change from Newtonian to time-independent non-Newtonian and time-dependent non-Newtonian behaviours. Simple analysis of apparent viscosity against concentration and temperature without modelling the time-dependency (Velez-Ruiz & Barbosa-Canovas, 1997) can be misleading.

The results from section 5.4 showed that reconstituted concentrates made from powder A exhibited Newtonian behaviour below 30%TS. Between 30%TS-40%TS, the behaviour was time-independent non-Newtonian (shear thinning), the level of non-Newtonian behaviour depending on the temperature of the fluid. At even higher solids content, above 40%TS, the rheology is time-dependent, i.e. age thickening.

The onset of non-Newtonian behaviour in powder A concentrates occurred above 30%TS, with the exact value depending on the temperature. The critical 30%TS mark is a much greater value than found previously (Velez-Ruiz & Barbosa-Canovas, 1997, 1998, 2000). A key difference appears to be the shear rate used in the research. In the current work, recombination was carried out at  $40,000\text{s}^{-1}$  which may have resulted in lower rates of age thickening during storage and thus delayed the onset of non-Newtonian behaviour. Velez-Ruiz and Barbosa-Canovas (1997) prepared their concentrates in a small rotary bench top evaporator, which implies very low shear rates. Even while acknowledging that fresh and reconstituted concentrates cannot have exactly the same rheological profile, it can still be argued that the higher shear rates in the present

recombination rig were responsible for the onset of non-Newtonian behaviour occurring at a much higher concentration.

For a given solids content, the onset of time-dependent behaviour is dependent on the heating temperature. For example, the 30%TS concentrates exhibited shear thinning behaviour but were still time-independent at 35°C (Figures 5.24-5.25). However, heating to 85°C triggered time-dependent behaviour in milk concentrates of 30-35%TS. In more diluted solutions (10-20%TS), heating above 65°C did not trigger the age thickening process.

### 6.3.3 Behaviour of milk concentrates observed during age thickening

There are four distinctive features of the age thickening phenomenon.

1. Initial rate of increase in apparent viscosity (or model parameters) and HLA with time
2. Gelling time
3. Apparent viscosity at the gelling point
4. Changes in the apparent viscosity with time after gelation

In the literature, only the first of the four features has been acknowledged previously. This is because the experimentation times were not sufficiently long for the system to reach gelation.

Rheological modelling showed that  $\tau_y$  and  $K$  increased while  $n$  decreased with storage time at temperatures between 35°C and 85°C. This is in qualitative agreement with the results from Velez-Ruiz and Barbosa-Canovas (1998) where the fresh milk concentrates were stored between 5°C and 25°C. These results indicated that during age thickening, there was a build-up in structure that resulted in an increase in the initial resistance to flow deformation (increase in  $\tau_y$ ) and the overall resistance to shear deformation (increase in  $K$ ). The degree of shear thinning increased with time (decrease in  $n$ ).

Since the onset of gelation can be considered the natural end point of age thickening (Walstra et al., 1999), the gelling time and the flow curve at gelation are as relevant to the issue as the rate of age-thickening itself. The physical characteristics of gels have been studied with solid rheology, particularly with oscillatory tests (e.g. Zoon et al., 1988; Ozer et al., 1998) but they have also been studied by liquefying the gel with shear (Ma et al., 2002), the method used in this work.

During age thickening, the apparent viscosity showed first a steady increase with time. At high temperature (above 65°C in the present work), a second phase showed a sharp increase in viscosity with storage time. Clark (1992) suggested that the gelling point is marked by this sudden sharp rise in the viscosity. Kieseker and Pearce (1978) proposed similar kinetics for the heat coagulation process. Kieseker and Pearce (1978) believed that coagulation is a two-step process consisting of an induction period of variable length, during which the milk remains fluid but increases steadily in viscosity, followed by a rapid coagulation stage.

In this work, the gelling point was determined from the sharp rise in apparent viscosity at the start of the second phase, and also from the sudden decrease in the HLA that often occurs at the same time.

The adjusted extrapolated apparent viscosity at infinite shear rate was found to increase with storage time during age thickening. Such increase indicated that there was a growth of the basic structure at infinite shear with storage time indicating some permanent linkage between the individual elements of the products.

### **6.3.4 Effect of solids content and temperature on the rheology of reconstituted milk concentrates**

#### **6.3.4.1 Solids content**

For a given temperature, the initial apparent viscosity increased exponentially with solids content in powder A concentrates, as shown in section 5.3. This was observed at temperatures between 35°C-85°C, which agreed with results from (Bloore and Boag 1981; Snoeren et al., 1982; Snoeren et al., 1984; Velez-Ruiz and Barbosa-Canovas, 1997, 1998, 2000).

The first effect of concentration on viscosity is through the increase in volume fraction of the suspended solids. The second effect is due to crowding that brings the particles closer together. It is known that particles in close proximity experience a higher hydrodynamic resistance to motion than when they are alone in an infinite fluid medium (Richardson & Zaki, 1954). Beeby (1966), Prentice (1992) and Caric (1994) suggested that the increase in viscosity with total solids content indicates that the casein micelles are physically interacting as they are forced closer together.

In milk systems, the size of the individual particles can also increase upon concentration. This third effect is illustrated for example by changes in casein micelle size during concentration (Walstra et al., 1999). This phenomenon is often linked to the changes in the balance between the colloidal and soluble calcium with an increase in solids content (Walstra & Jenness, 1984; Walstra et al., 1999). This shift in calcium balance between the colloidal and soluble states causes a drop in pH, leading to a reduction in the electrostatic repulsion between casein micelles, as well as an increase in the solubility of  $\beta$ -casein (Bienvenue et al., 2003a).

It is well known that the pH of a system falls when a neutral salt is added. An increase in solids content would increase the concentration of all associated electrolytes (Galster, 1991). Therefore a decrease in pH is expected.

The results in section 5.3 showed that the pH of milk decreases with concentration up to 47%TS and then plateaus. Such a quantitative relationship between pH and solids content, in particular the plateau at pH 6.2 above 47%TS, has not been found in the literature. It may be due to some saturation effect such as insufficient water to further affect the ionic balance of the calcium or increased buffering effect in the system. These possible mechanisms are only conjectures that can be best investigated by dairy protein chemists. What is clear in this work is that any further increase in apparent viscosity with solids content above 47.5% TS cannot be caused by pH changes.

Upon concentration, the particles are forced closer together and the chances of association to form flocs and aggregates increase. Flocs have three basic physical effects:

1. an increase in apparent volume of the dispersed phase because of the occlusion of continuous phase trapped inside the flocs (Cheng, 1987),
2. formation of particles with irregular shape that also tend to increase the hydrodynamic resistance to motion (Walstra et al., 1999) and
3. induction of shear dependence of the viscosity profile because the floc structure can be disrupted by high shear and the irregular shaped particles tend to align in the direction of flow (Steffe, 1992).

#### **6.3.4.2 Temperature**

Above 40%TS, the apparent viscosity decreased with temperature to a minimum at 65°C-75°C, and then increased significantly (Figures 5.26, 5.27 in section 5.4). This phenomenon was more apparent at higher solids content and longer storage times. This has also been observed by Bloore and Boag (1981), Snoeren et al. (1982) and Snoeren et al. (1984) for skim milk concentrates, Snoeren et al. (1983) on whole milk concentrates Trinh and Schraekenrad (2002) on whey depleted whole milk concentrates.

The apparent viscosity-temperature relationship is driven by two opposing effects: a reduction in the viscosity of the aqueous substrate with increasing temperature (Steffe, 1992; Walstra et al, 1999) and an increase in milk protein interactions, in particular the

activation of whey proteins above 65°C (Dalglish, 1990; Beaulieu et al., 1999). The interactions of denatured whey proteins with either other denatured whey proteins or casein micelles are well documented, and would be expected to contribute significantly to the increase in apparent viscosity above 65°C. Tang et al. (1993) made a similar argument to explain the temperature dependence of the viscosity of WPC solutions.

At 40-50%TS, age thickening occurs at a slow rate at low temperatures, 35-55°C. Upon heating above 65°C, gelation was observed during age thickening in reconstituted concentrates made from powders A and B. An increase in heating temperature and solids content resulted in faster rates of age thickening and subsequently shorter gelling times.

The results showed a complex relationship between solids content, temperature and rheology of milk concentrates. There is likely to be more than one mechanism that contributes to the age thickening process, with different dominating effects at different temperatures. The effect of temperature above 65°C-75°C may be linked to the denaturation of whey proteins and the formation of complexes with other proteins. However, the particles are still required to collide for interaction to take place. This is less likely at low solids contents where the particles too far apart. An increase in solids contents increases the proximity of the particles, and thus promotes and increases the rate of interaction.

The apparent viscosity at the point of gelation did not change significantly with solids content and temperature (Table 5.8, section 5.4). For all concentrate samples made from powder A, it was 0.1 Pa.s, compared to 0.5 Pa.s for powder B. These results suggest that the apparent viscosity at the gelling point is a characteristic property of the powder.

As explained by Clarke (1992), gelation marks the time when a critical structure has been reached where future associations between components are centralized via one group of aggregates. The fact that for a particular powder, the apparent viscosity at gelation was the same for all temperatures and concentrations suggests that the critical structure does not change with solids content or temperature, and is only a function of the chemistry of

the reconstituted milk protein. It is not known how this critical structure is affected by powder composition or processing variables.

### **6.3.5 Effect of sample preparation techniques on the rheology of reconstituted milk concentrates**

The importance of shear and temperature histories on the rheology of time-dependent systems has been discussed in reviews and published articles (e.g. Cheng, 1987; Barnes, 1997; Corvisier et al., 2001). Yet, the methods of sample preparation and measurement protocols are not often reported in detail in the literature.

The results presented in sections 5.5 to 5.7 clearly demonstrated that the shear and temperature histories of a time-dependent material, in this case concentrated milk, significantly affect their rheological behaviour, not only right after preparation but also in subsequent processing steps such as heating and storage at different temperatures. The importance of age-thickening during sample preparation has not been recognised or analysed previously.

#### **6.3.5.1 Effect of recombination shear rate**

In traditional recombination processes, the shear is applied during mixing to improve the sinkability of the powder (Fitzpatrick et al., 2001). It has long been recognised that a high shear rate helps the dissolution process, especially through the maintenance of a vortex at the liquid surface (Fitzpatrick et al., 2000). Thus high shear mixers like the Cowles mixer are preferred when recombining to a high solids content (Yziquel et al., 1999; Hou et al., 2000; Lawrence et al., 2001; O'Donnell and Butler, 2002). One constraint on high speed mixing is the amount of entrained air that cannot easily be expelled from concentrated milk solutions.

In the current design of the new recombination rig, the recirculation shear rate was separated from the mixing shear rate. The recirculation shear rate was manipulated via

the interchangeable capillary tubes and the recirculation flow rate. Since the structure of a time-dependent fluid is defined by the highest shear rate it is subjected to, the shear rate in the recirculation line was always kept much higher than the shear rate in the mixing vessel. In addition, the impeller speed in the mixing vessel was kept low to minimise air inclusion and a centre baffle was fitted to minimise vortex formation.

In a normal tank mixing with an impeller, the shear rate achieved is in the order of hundreds. This can be estimated using the Metzner and Otto (1957) equation, which gives a shear rate of  $433 \text{ s}^{-1}$  inside the tank during mixing. This simple estimation of the shear rate in the tank is well short of the  $40,000 \text{ s}^{-1}$  achieved with the capillary system and the minimum  $10,000 \text{ s}^{-1}$  required to control the rate of age-thickening during reconstitution (section 5.5.2.1).

The effect of recirculation shear rate can be better illustrated using the extrapolated apparent viscosity at infinite shear. The  $\mu_{\infty}$  after 60 minutes was used as the reference point. All subsequent  $\mu_{\infty}$  divided against this  $\mu_{\infty}$  (at 60 minutes) to give a ratio. The change in the ratio of  $\mu_{\infty}$  during storage at rest to the viscosity value after 60 minutes of recirculation was calculated and plotted for runs C59-C62, as shown in Figure 6.4. At  $40,000 \text{ s}^{-1}$ , the extrapolated apparent viscosity at infinite shear rate did not increase with recirculation time. This suggests that the fully broken down structure does not change with time. When the powder was reconstituted at  $600 \text{ s}^{-1}$  (shear rate similar to that encountered in the mixing tank), the extrapolated viscosity at infinite shear increased with time. This suggests that the elementary particles were interacting with one another to form flocs resulting in an increase in apparent viscosity.

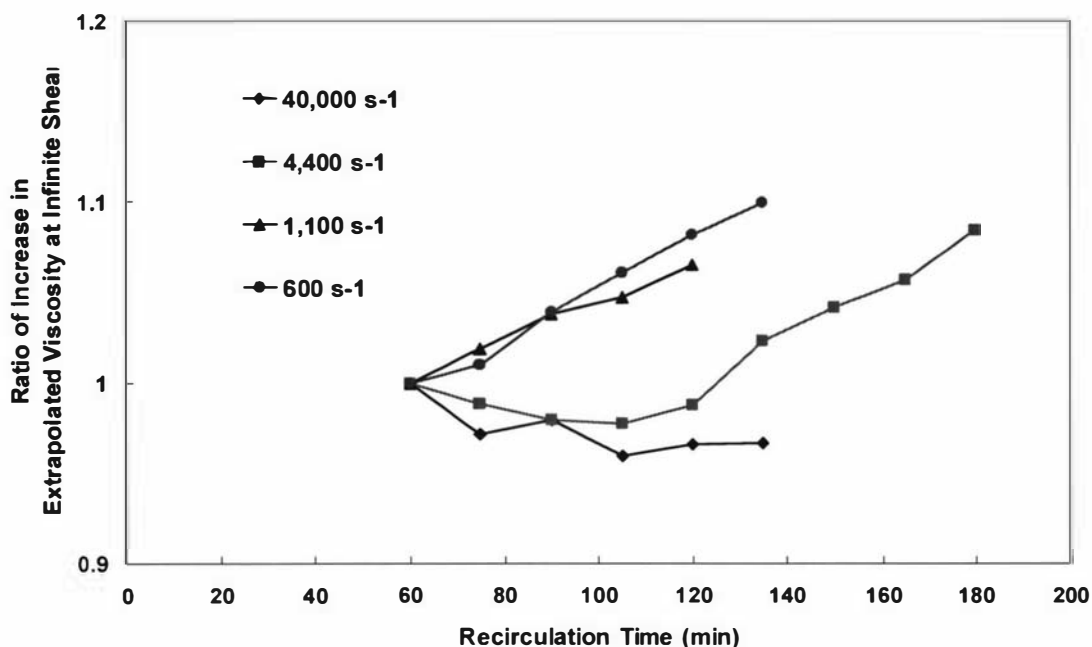


Figure 6.4: Effect of shear rate on the ratio of increase in the extrapolated apparent viscosity at infinite shear rate during recirculation.

When the recombination shear rate is high, the solutions are disaggregated: the structure is broken down to its elementary particles containing a very large amount of kinetic energy. This essentially forces the particles to move past one another very fast so that contact times are very short making bond formation difficult. When the shear rate is dropped, the particles have a greater chance to collide and interact with one another to form flocs during circulation that can result in an increase in apparent viscosity.

A consequence of age-thickening, whether occurring in a system undergoing some shear, or at rest, is that the flocs become larger with time and move increasingly closer. The rate of collision is consequently increased with age-thickening time. This is seen both in the industrial surveys (e.g. Figures 4.15 and 4.16) and the controlled rheology experiments (e.g. Figure 5.2). Consequently, when the recirculation shear rate is low enough and age thickening occurs, the time duration of the recombination process is also an important factor in the history of the product. This is clearly shown in Figure 5.58 where longer

recirculation time at  $600\text{ s}^{-1}$  resulted in an increase in the rate of age thickening and a decrease in gelling time.

#### **6.3.5.2 Effect of recombination temperature**

Recombination is commonly carried out at 40-50°C to ensure good solubility and short hydration time (Harper, 1960; Samel and Muers, 1962). However, 40-50°C is an ideal temperature range for the growth of thermophilic bacteria (Spreer, 1998; Robinson and Itsaranuwat, 2002). A few authors such as Fitzpatrick et al. (2001) reconstitute at low temperatures, but even at 20°C, Fitzpatrick et al. (2001) noticed that immediately after reconstitution, a 50%TS skim milk concentrate showed a 3.5 times increase in apparent viscosity within 1 hour of storage at that temperature.

The results in section 5.6 showed that age thickening occurred during reconstitution if the mixing temperature was too high even during recirculation at  $40,000\text{ s}^{-1}$ . This critical temperature was 65°C for powder B concentrates and 45°C for powder A concentrates.

#### **6.3.6 Effect of powder origin**

All of the above effects of recombination variables on the rheology of milk concentrates are highly dependent on the place and date of production of the powders. For this project, the majority of the work was carried out on two medium heat whole milk powders, A and B. The general compositional specifications for the two powders are listed in Table 6.2. The two powders shared similar compositional specifications. Powder B had slightly higher fractions of protein and fat.

Table 6.2: General composition of the two whole milk powders used in the controlled rheology experiments.

	<b>A</b>	<b>B</b>
<b>Powder</b>	Whole	Whole
<b>Heat treatment</b>	Medium	Medium
<b>Protein</b>	24.34	25.61
<b>Fat</b>	23.68	24.26
<b>Lactose</b>	42.3	40.76
<b>Ash</b>	5.78	5.44
<b>Moisture</b>	3.9	3.93

The reconstituted concentrates made from the two powders behaved distinctly differently from each other. Firstly, powder A concentrates gelled much faster, at around 4 hours at 48%TS and 75°C, compared to 10 hours for powder B at 50%TS at 75°C. The apparent viscosity at which gelation took place was only 0.1 Pa.s for powder A concentrates, and a much higher value of 0.5-0.6 Pa.s for powder B concentrates. The rate of age thickening up to gelation was similar between the concentrates made from the two powders. The significantly shorter gelling time in powder A concentrates is mainly caused by the lower apparent viscosity at the gelling point.

The reconstituted concentrates made from powder A were more sensitive to process treatments than that from powder B. For example, during recirculation, powder A showed signs of age thickening at 45°C, while powder B concentrates did not age thicken until the recirculation temperature was increased to 65°C. The effect of recirculation shear rate was more pronounced on concentrates made from powder A.

The results suggested that powder A is more prone to gelation, and thus more sensitive to process treatments that can affect its tendency to age thicken and ultimately gel.

Currently, there is not enough data to understand the difference in the structure and rheological behaviour between the two reconstituted powders during age thickening.

However, the results clearly showed that the rheological behaviour can be significantly different between two time-dependent systems, even though the composition specifications are similar. Thus, it is important to document as much information as possible on the raw material, such as time-temperature history, to provide the reader the necessary background to understand the rheological behaviour of the tested fluid.

#### **6.4 Industrial surveys**

The main purpose of the industrial surveys was to capture trends in rheological behaviour of fresh milk concentrates in industrial processing environments. Despite the number of variables that could not be controlled to the same level as during the controlled rheology experiments, the trends obtained during the industrial surveys agreed surprisingly well with those from the controlled rheology experiments.

After the evaporation process, the fresh milk concentrates showed time-independent shear thinning behaviour. After the concentrate heater, time-dependent behaviour was prominent. After evaporation, the milk concentrates are stored in the concentrate balance tank for at least 10-15 minutes and up to 30 minutes before being pumped to the concentrate heater, homogeniser and spray drier. The tank serves as a buffer point in the process line to damp out fluctuations in the milk flow rate in the upstream processes. During storage in the buffer tank, age thickening can take place, which may contribute to the greater age thickening observed downstream at the concentrate heater.

The effect of solids content, temperature, preheat treatment, equipment design and operating conditions, variation in composition all have significant effect on the rheology of fresh concentrates. These results agreed with other published results in regard to the effect of processing variables on the rheology of milk concentrates (de Vilder et al., 1979; Bloore & Boag, 1981; Vilder & Moermans, 1983; Snoeren et al., 1984; Lawrence et al., 2001). However, these previous authors only measured the apparent viscosity and not the

rate of age-thickening of the fresh concentrates. The present work shows that age thickening can be significant during processing.

One could argue that it is unnecessary to study the rheology of fresh concentrates over time periods that are much longer than any residence times in milk processing lines. For example, after the concentrate heater, the milk concentrates spend less than a few minutes in transportation before being spray dried into powder. During this short time frame, the change in the rheological behaviour is small and unlikely to have any significant effect on the rheological behaviour of the products.

However, this line of reasoning is obviously proven incorrect by the results presented in section 5.7. The shear rate and residence time during heating (which is only in the order of seconds) in a plate heat exchanger had significant effects on the rheological behaviour of the heated reconstituted milk concentrates. Similar effects of shear rate and residence time on the rheology are likely to exist in the industrial environment, possibly extending as far back as the preheat treatment, in addition to the evaporation, concentrate heating and spray drying processes.

There are data available in the literature on the effect of viscosity of milk concentrates on the physical and functional properties of the powder. However, there are no data on the effect of age thickening on the powder properties. It is recommended that extensive experimentation should be carried out to study this relationship between processing variables, time-dependent rheological behaviour of the milk concentrates, and the powder properties.

## **6.5 Mechanism for age thickening**

Previous discussions of the mechanisms of age-thickening can be roughly grouped into two categories: those that focus on the change in volume of individual particles (Snoeren et al., 1984) and those based on the chemical causes of flocculation in concentrated milk (e.g. Bienvenue et al., 2003a). Others (e.g. Velez-Ruiz & Barbosa-Canovas, 1997, 1998,

2000) simply provided phenomenological models of age-thickening without attempting to discuss the mechanism.

The following discussion can be divided into four issues:

1. What physical changes are involved?
2. Are these changes reversible?
3. What milk components are involved?
4. What kind of reactions are taking place?

### **6.5.1 Physical changes during concentration and heating**

The changes in viscosity during age-thickening are linked to several factors:

1. Changes in the hydrodynamic resistance to flow of the dispersed solids. These involve changes in shapes and apparent volume of the individual colloidal particles.
2. Flocculation, coagulation and aggregation modify the volume fraction of the dispersed phase and the PSD. In cases of extensive age-thickening, the PSD can change from monomodal to bimodal distributions. These factors necessarily involve interactive forces between particles that must therefore be surface forces, not those involved in internal cohesion.

Coagulation phenomena can be divided into two types depending on the nature of particle movement: orthokinetic phenomena i.e. those originating from fluid flow, and perikinetic phenomena i.e. those originating from Brownian motion of the dispersed particles (Muhle, 1993). Therefore, floc formation during evaporation (Croy et al, 2002), recombination (section 5.5) and in shear step tests (section 4.1) follows orthokinetic coagulation principles, while age-thickening of samples stored at rest is perikinetic coagulation. This difference has not been mentioned in the literature of age-thickening presumably because this work is the first to have measured the former mechanism of coagulation during flow.

The Massey University research group, to which this project is affiliated, believes that it is more fruitful to first analyse the physical phenomena that contribute to the shear stress and therefore the apparent viscosity (Trinh, personal communication, 2005) before attempting to analyse the chemical interactions underlying these phenomena. This strategy allows a more systematic and detailed examination of all the elements involved.

#### **6.5.1.1 Volume fraction**

The models that described the relationship between volume fraction and rheology reviewed in Appendix 2 are based on interactions between separate particles. They do not take into account the floc size and strength and therefore cannot describe the shear thinning behaviour often observed with colloidal solutions. Even in model systems made up from latex particles manufactured to known particle sizes and stabilised with an outer layer of surfactants (Luckham and Ukeje, 1999), the predictions of the Krieger-Dougherty equations could only be correlated with the viscosity “at high shear rate” and no attempt was made to explain the shear thinning behaviour. While the kinetics of coagulation and flocculation are well researched (Dobias, 1993) the assessment of floc size and density in concentrated opaque solutions cannot be easily measured as discussed in more detail in the next section. The floc stability and therefore its size is a function of the applied shear rate (Muhle, 1993) and the volume fraction should therefore be measured at the concentration and in the shear environment applicable to the viscosity measurement. There is no easy method for doing this at the moment and therefore all discussions relating volume fraction to viscosity during age-thickening can only be qualitative.

#### **6.5.1.2 PSD**

The volume fraction is affected by the degree of packing of the dispersed particles throughout the continuous phase, but it does not provide information on the size, or

shape, or formation of any flocs or aggregates. This is where PSD is useful to some extent.

Direct measurements of PSD have been made on fresh and reconstituted skim and whole milk concentrates by Yoo et al. (1996), Ma et al. (2002), Croy et al. (2002), Bienvenue et al. (2003a, 2003b) and in this work. However, it must be pointed out that the measurement of PSD with the Malvern Mastersizer, and indeed other systems based on microscopic observation, light scattering or coulter counting require the samples to be diluted (Anema and Li, 2003b; Bienvenue et al., 2003a).

In this work, the milk concentrates were diluted with distilled water to achieve an opacity range of 15-20% prior to measurement. The dilution step may break up any weak flocs or loose networks that contribute to the viscosity.

Milk concentrates reconstituted at 35°C showed no change in PSD with concentration between 10% and 52%TS, despite the exponential increase in apparent viscosity with solids content. Similar trends were observed when concentrates made from powder B age thickened during storage at 35°C. No change in PSD was observed even though the apparent viscosity increased significantly with storage time.

These results lead to the paradox that while the volume fraction does not increase during age-thickening, since both the solids content and PSD remain constant with storage time, the change in viscosity indicates that particle flocculation or aggregation has taken place. Since this would normally be reflected by a change in PSD, it is suggested that the flocs formed during this age-thickening are weak and destroyed by the dilution process.

In contrast, when the concentrates were heated above the temperature for minimum viscosity, gelation was observed and a change in PSD from a monomodal to a bimodal distribution took place. The aggregation profile paralleled the changes in apparent viscosity during age thickening (section 5.4). The onset of aggregation is caused by heating and not by the high solids content since no change in PSD was observed at 35°C.

Therefore, heating above the temperature at minimum viscosity triggered new reactions that resulted in stronger bonds which are not readily reversed upon dilution during PSD measurement.

Other researchers have maintained that an increase in solids content results in an increase in particle size due to association between the casein micelles (Croy et al., 2002; Anema & Li, 2003a, 2003b; Bienvenue et al., 2003a, 2003b). However, in all these works the milk was pre-heated above 65°C either before or after concentration.

A comparison of changes in age thickening and PSD above and below the temperature at minimum viscosity has not been shown before. The results here clearly show that a change in viscosity does not necessarily equate to a change in PSD, as measured by laser diffraction.

## **6.5.2 Reversible and irreversible changes during age thickening**

Irreversible changes during age-thickening can be classified into two categories:

1. Not reversible by dilution
2. Not reversible by shear

### **6.5.2.1 Changes not reversed by dilution**

The PSD results suggest that any changes in PSD at low temperatures are reversible by dilution. However, after heating the concentrates, changes in PSD in the diluted samples are apparent. This indicates that some irreversible aggregation has occurred. However, it cannot be assumed that all the aggregates are resistant to breakdown.

### 6.5.2.2 Changes not reversed by shearing

Bienvenue et al. (2003a) claimed that the exponential increase in viscosity at  $1000\text{ s}^{-1}$  with storage time during shear sweep tests in 45%TS skim milk samples (that had been preheated to  $90^{\circ}\text{C}$  and then stored for eight hours at  $50^{\circ}\text{C}$ ) was direct evidence of irreversible (by shear) interactions.

It was shown in section 5.5 that concentrates reconstituted at  $4,400\text{ s}^{-1}$  could still age thicken during recirculation. Therefore, a shear rate of  $1000\text{ s}^{-1}$  is not sufficiently high to prove the irreversibility of age thickening as proposed by Bienvenue et al. (2003a). One may argue that the critical shear rate to reach the upper Newtonian plateau during recirculation is different for different fluids. However, the critical shear rate for the 45%TS milk concentrates was not determined in Bienvenue's et al. (2003a) work.

The results in section 5.9 indicated that the large aggregates (between 2 and  $100\text{ }\mu\text{m}$ ) in concentrates stored at  $75^{\circ}\text{C}$  are largely disrupted by re-shearing at  $40,000\text{ s}^{-1}$  and only a very small fraction remains. The rheological behaviour after re-shearing of the concentrate samples, that have already been age thickened, was also different from freshly reconstituted concentrates. This has significant practical implications since Bienvenue et al. (2003a, 2003b) suggested that their results showed that homogenisation and atomisation would reverse any age thickening which occurred during processing. There are no published measurements of shear rates in homogenisation and atomisation processes although preliminary estimates, due to be consolidated in upcoming projects at Massey University, put them at least within the range of maximum shear developed in the recombination rig.

The evidence presented in this section indicates that the forces involved in the formation of flocs during age-thickening have at least three levels of cohesive strengths. The weakest forces are likely to be the van de Waals forces. Upon dilution, the flocs held only by van der Waals forces are the most likely to be disrupted. At the other end of the spectrum, the irreversible aggregates that can withstand shear levels in the upper

Newtonian region probably involve extremely strong bonds. These are more likely to be of a chemical (covalent bonds) rather than electrical nature. A discussion of likely chemical reactions in age-thickening is presented in a later section (6.5.5)

### **6.5.3 Milk components and chemical changes involved in the age-thickening process**

It is well known that when milk proteins are heated above 65-70°C, denaturation of whey proteins takes place. The combination of high temperature and solids content and a decrease in pH gives rise to a series of interactions between the denatured whey proteins, in particular  $\beta$ -lactoglobulin with  $\kappa$ -casein. Fat globules can participate in the build-up structure but can only do so via the adsorbed protein layer on the DFGM.

During the initial stage of age thickening, the fat globules and the casein micelles are randomly dispersed in the continuous phase, as shown in Figure 5.87. The fat globules are at least ten times larger than the casein micelles (Walstra et al., 1999) and therefore must make a significant contribution to the size of any aggregates. Their participation in the gel network has been shown to increase  $G'$  during gelation, in comparison to gels made from skim milk only (Underwood & Augustin, 1997).

Black “lumps” on the fat globule membrane are often observed during age thickening. These are casein micelles associating with the fat globule surface (Pouliot et al., 1990; Velez-Ruiz & Barbosa-Canovas, 2000). It is possible that denatured whey proteins also associate with the fat globules (Brun & Dalgleish, 1999).

During age thickening, the amount of plasma proteins adsorbed on the fat globules increases until the caseins appear to have fused together into a continuous layer. The layer also increases in thickness during age thickening, as shown in Figure 5.86. Similar observations were made by Velez-Ruiz & Barbosa-Canovas (2000).

The participation of the fat globules, caseins and possibly denatured whey proteins in the continuous network is clearly seen in the TEM images in section 5.8. There are an increasing number of aggregates of fat globules and casein micelles with storage time during age thickening (Figures 5.84-5.86). The incorporation of the fat globules into this network most likely takes place through the interactions of the surface plasma proteins and the serum proteins. Sharma and Singh (1999) shared a similar view during their analysis of HCT of recombined milk.

The participation of casein micelles and denatured whey proteins can readily be seen in skim milk concentrates (Figures 5.87-5.88). Caseins can either interact with themselves or with denatured whey proteins. Filamentous appendages from the casein micelles can sometimes be seen acting as cross linking bridges. These have been identified as denatured whey proteins (Carroll et al., 1970; Davies et al., 1978; Kocak & Zadow, 1985; Defelipe et al., 1991; de Koning et al., 1992). It is also possible that these linking bridges are the  $\beta$ -lactoglobulin- $\kappa$ -casein complex that have been formed, released from the micelles and then attached themselves between micelles, as suggested by McMahon (1996).

Casein micelles interact with one another to form clumps that grow in size. Again there is evidence of direct fusion of casein micelles or sub-micelles into large non-spherical particles suspended in the continuous phase. A decrease in pH at high concentration results in the solubilisation of the CCP, with complete solubilisation at pH 5.3 (de la Fuente, 1998). This results in an increase in the  $\text{Ca}^{2+}$  activity, which can decrease the electrostatic repulsion between the casein micelles and consequently increase the aggregation rate.

The possibility that casein micelles can affect age-thickening without the help of whey proteins was illustrated by Ma et al. (2002) who added a proteolytic enzyme, Neutrase, to attack the para- $\kappa$ -caseins. This action destabilised the casein micelles which became much more heat sensitive. The viscosity and rate of thickening increased with the level of addition of the enzyme and more importantly the point of minimum viscosity (which

coincides with the first significant evidence of age-thickening) fell to 40°C from the 60-65°C range.

#### **6.5.4 Types of age thickening**

When heating and storage were carried out at temperatures below the temperature for minimum viscosity, age thickening proceeded slowly, and no gelation and changes in PSD took place. On the other hand with heating above 65°C, age thickening was rapid, gelation took place, and changes in PSD were observed.

The results suggest that the rate of development, structure and strength of the flocs are significantly different in the two temperature regions, implying different mechanisms of structure formation. A typical industrial example of viscosity change with time in the low temperature region is the age-thickening of RSCM during storage at room temperature. Well-known examples of viscosity changes with time in the high temperature range are concentrate heating during milk powder manufacture and recombined evaporated milk manufacture. To simplify further references to these two situations, the writer proposes to call low temperature age-thickening type I and high temperature age-thickening type II.

Authors who have worked with acid gelation of diluted milk systems have also observed two mechanisms of gelation in two temperature ranges resulting from different pre-heat treatments (Lucey, Tamehana et al., 1998; Lucey et al., 1999; Steffl et al., 1999; Schorsch et al., 2001; Vasbinder et al, 2003a, 2003b; Famelart et al., 2004).

Walstra et al. (1999) noted that there is a fundamental difference in the phenomena of age-gelation (of say RSCM) and the viscosity changes in the measurement of HCT, normally conducted at very high temperatures (above 120°C). They did not quote direct evidence to illustrate their statement nor differentiate between type I and type II.

The writer agrees with Walstra et al. (1999) and further argues that since proteins are activated at all temperatures above the temperature of minimum viscosity, the difference between type II age-thickening and heat stability measurements is only one of extent and not fundamental mechanism. While the HCT is not a rheological measurement, changes in viscosity have been used to measure the HCT (van Mil and de Koning, 1992). Coagulation marks the change in phase of the system from liquid to semi-solid. Thus one may argue that the formation of aggregates in HCT measurement is equivalent to the first sign of phase change during age thickening that could eventuate in the formation of a full gel network. Therefore, the knowledge from the very extensive studies of HCT in the literature may give clues to the mechanism of type II age thickening. Obviously, the difference in solids content (low solids content for HCT measurement in comparison to the high solids content in milk concentrates) would play an intricate role. However, that knowledge cannot be used to explain type I age-thickening.

The preheat treatment contributes to the temperature history. Data from Trinh and Leslie (1996), and Bienvenue et al. (2003b) showed that preheating above 65°C gave rise to changes in PSD and age thickening during storage. Thus it appears that both type I and type II should be further divided into two sub-types A and B to take into account the effect of preheating, as shown in Figure 6.6.

Under types Ia and IIb, the important characteristics of the rheological behaviour of the milk concentrates are deduced from the experimental data obtained in this thesis. However, no such information is predicted for types Ib and IIa due to insufficient data and knowledge on age thickening and gelation under those conditions.

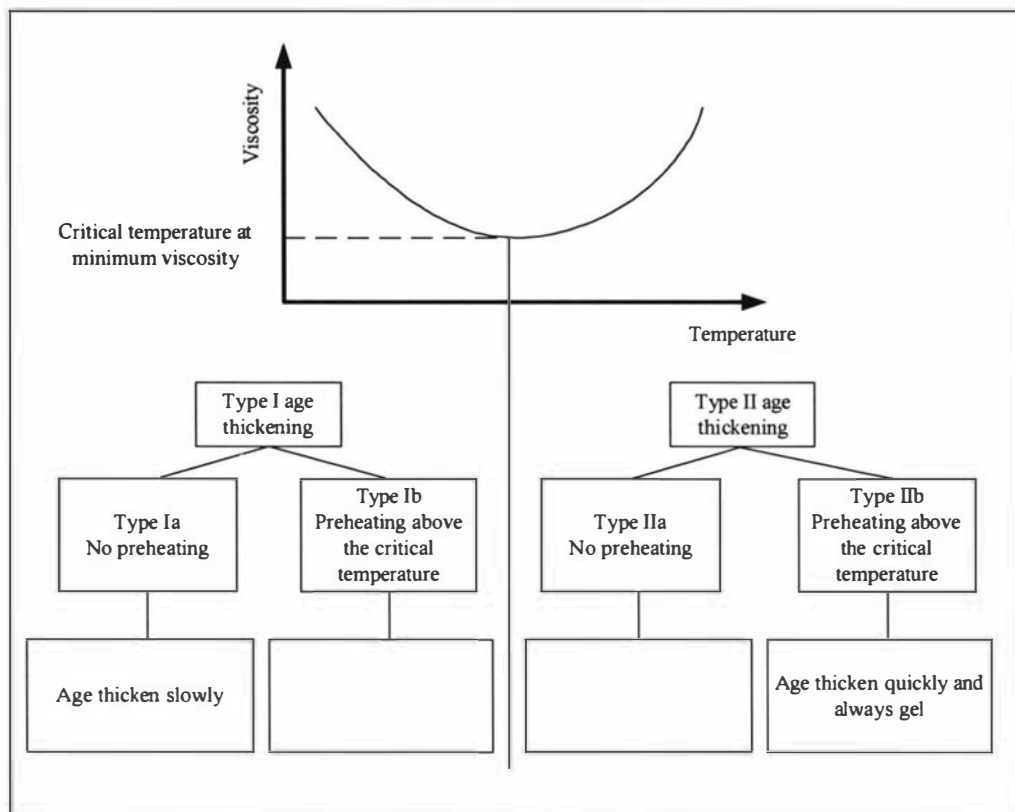


Figure 6.5: Proposed types of age-thickening

## 6.5.5 Proposed mechanisms of age-thickening

### 6.5.5.1 Physical interactions in type I mechanism

A large body of literature is available on the rheology of concentrated colloidal suspensions (e.g. Batchelor, 1977; Le and Bhattacharya, 1990; Luckham and Ukeje, 1999). The consensus indicates that these solutions are shear thinning with a yield stress and can be described adequately with the Herschel-Bulkley model as found in this work. Much of the rheological behaviour of these colloidal systems may be explained in terms of primary particles consisting of a core and an outer layer (Luckham & Ukeje, 1999). The kinetics of aggregation and disaggregation of particles can also be analysed in terms of the relative strengths of the surface interactions defined by this outer layer and the

motion of the particles (Muhle, 1993). These analyses are made in terms of physical behaviour and can be applied to all colloid systems, not just milk.

The rheology of skim milk and its concentrates below the temperature of minimum viscosity is dominated by the contribution of the casein micelles which can be pictured as an inert core with an outer layer made up of  $\kappa$ -casein hairs. The complication in characterising the behaviour of the milk system in terms of volume fraction lies in the way the hairs are distributed on the micelle surface and the manner in which the layer interacts with other milk components.

The solids content affects the volume fraction of the individual particles, hydrodynamic interactions between the particles in a flow field, and more importantly the proximity of the particles. At low solids content, the colloidal particles can be considered as individual spheres with no interactions. An increase in solids content promotes physical interactions between particles. At sufficiently high solids content, the close proximity allows bonding to take place that results in the formation of weak flocs. The bonds at this stage are likely to be weak ionic, hydrogen, and possibly hydrophobic bonds.

In highly concentrated milk, when the casein micelle domains can overlap, one should not discount the possibility of steric entanglement of the hairs in the outer layer. Luckham and Ukeje (1999) have postulated that this entanglement and compression of the steric layer may explain the strong viscoelastic properties of highly concentrated colloid solutions.

At 35°C, age thickening does take place, but only at high solids content, i.e. 50%TS in powder B concentrates. The  $\kappa$ -casein casein layer may be destabilised to some extent during powder manufacture resulting in a reduction in the steric and electrostatic repulsion. Casein-casein aggregates are expected to primarily contribute to the formation of weak flocs. A decrease in pH upon concentration and its effect on the CCP may also contribute to the unstable micelles.

### **6.5.5.2 Aggregation in type II mechanism**

Upon heating above the temperature of minimum viscosity, additional interactions take place due to the denaturation of whey proteins that exposes free thiol groups. Heating also affects the interactions between the serum and plasma proteins with the fat globules. Even though heating chemically modifies the components and makes them more reactive, collisions are still required for interactions to take place. Thus, the effect of temperature is dependent on solids content, where high value brings particles closer together and thus increases the rate of reaction.

The formation of aggregates between casein micelles, denatured whey proteins and fat globules via covalent bonds give rise to strong flocs and extended network structures. This affects the PSD, and in turn the volume fraction and the rheological behaviour. . Unfortunately, PSD cannot differentiate between the increase in size of individual particles and the size of the aggregates and flocs.

Luchkham and Ukeje (1999) have demonstrated that the maximum volume fraction of a polydispersed colloidal suspension of latex particles increases with the polydispersibility of the dispersed phase. Thus the effect of PSD is not restricted to an increase in apparent volume fraction of the solid phase but also reflected in the maximum packing efficiency of the flocs. This manipulation of PSD to affect the viscosity of food systems has been previously carried out, as reviewed by Servais et al. (2002).

### 6.5.5.3 Particle interactions

The results obtained in this project suggest that there are at least three levels of the strength of linkages between the particles in an aggregate:

1. weak bonds that are disrupted by dilution
2. stronger interactions which are not reversible by dilution, but reversible by high shear
3. very strong bonds that cannot be broken up by high shear

The RAT of samples stored at rest increased with storage time indicating clearly that either the rate of collisions of particles increased or the bonding effectiveness of each encounter was increased, or both, during storage. Similarly the PSDs of type II age-thickening show increasingly large flocs with time indicating more bonds that cannot be affected by dilution.

Brownian motion only applies to particles smaller than 1  $\mu\text{m}$  and in a shear field of less than  $10 \text{ s}^{-1}$  (Muhle, 1993). During storage at rest, small particles move towards each other under the influence of Brownian motion and interact to form flocs through van der Waals forces. As the flocs get bigger during age thickening, the influence of the Brownian motion is less prominent and certainly cannot affect the movement of large flocs, only unattached small particles. In addition, the distance between free particles and established flocs diminishes with time, since the apparent volume occupied by the flocs increases, resulting in a higher adsorption rate (Muhle, 1993). Using the gelation theory by Clark (1992), one can speculate that one floc eventually reached a critical size where future association takes place primarily through this main floc.

There is little agreement on the mechanism of age thickening of milk concentrates in the literature. However, the literature on acid gelation observed a multi-stage gelation process that depended on the range of gelation temperature as well as preheat treatment. This is remarkably similar to observations here on types I and II age-thickening. Some insight into the mechanisms of age-thickening can be gathered from the large amount of

work published on acid milk gelation, although the work on acid milk gelation often involved only dilute systems, 10-15%TS. In addition, electrostatic and possibly steric repulsion are minimal due to the low pH.

Vasbinder et al. (2003a, 2003b) showed that gels made by acidification between 20°C and 40°C without preheating were much weaker than those made from milk preheated to 90°C for 10 min. When the milk was preheated before acid gelation, there was an increase in gel hardness and storage modulus ( $G'$ ) (Lucey et al, 1997, 1998; Parnell-Clunies et al., 1998) and the gels were less susceptible to syneresis (Dannenberg and Kessler, 1988). The effect of preheat treatment on acid gelation has been linked with whey protein coating of casein micelles creating a shift in the gelation pH from 4.6 (isoelectric point of caseins) to 5.2 (isoelectric point of whey proteins) (Lucey et al., 1997; Vasbinder et al. 2001).

Vasbinder et al. (2003a) used N-ethylmaleimide (NEM) and SDS-agarose gel electrophoresis to show that the disulphide bonding only takes place when the solutions were heated at high temperatures. This presence of the covalent disulphide bonds at high temperature has also been observed by others (Jang & Swaisgood, 1989; Schorsch et al., 2001; Famelart et al., 2004). While the covalent bonding of  $\beta$ -lactoglobulin to  $\kappa$ -casein is the principal heat induced change (Jang & Swaisgood, 1990; Singh, 1993; Corredig & Dalgleish, 1996), significant amounts of  $\alpha$ -lactalbumin and other minor whey proteins also interact with the casein micelles (Corredig and Dalgleish, 1996, Oldfield et al., 2000).

Vasbinder et al. (2003) summarised their views into two different mechanisms of acid gel formation. In acid gels made from unheated milk, the structure is formed by direct aggregation of casein micelles through physical, and therefore weaker, interactions (hydrogen, hydrophobic and electrostatic bonds). In acid gels made from preheated milk, casein micelles network through the intermediary of disulfide linked complexes of whey and casein.

It is proposed that during age-thickening, the effect of floc formation outweighs the contribution of the volume changes of the individual particles especially in the later stages close to the gelation point. Two mechanisms of coagulation are distinguished: one involving direct interaction between casein micelles and the other involving disulfide linkages, particularly but not exclusively through the  $\beta$ -lactoglobulin- $\kappa$ -casein complex, as shown in Figure 6.6.

The first mechanism applies to age-thickening of milk concentrates made with whey-protein free milk, milk with addition of blocking agents for the thiol groups, by evaporation of fresh but not preheated milk, or by reconstituting milk powders at temperatures below the critical point of the viscosity minimum (Type Ia). The second mechanism applies to milk concentrates made from fresh preheated milk, reconstituted milk concentrates heated above the temperature of the viscosity minimum and then cooled back (Type Ib) and milk concentrates age-thickened at temperatures above this critical point (Type II).

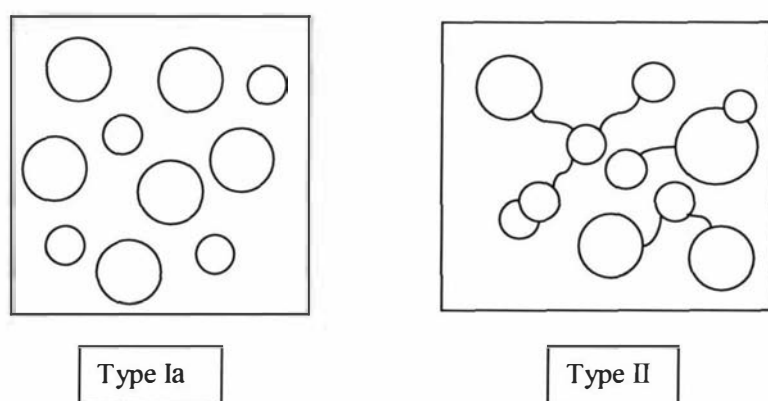


Figure 6.6: Proposed mechanisms of age thickening.

Upon cooling the milk back to ambient temperature after heating, a number of thiol groups remain active (Hashizume & Sato, 1988; Guincamp et al., 1993). The difference between types Ib and II is that in Type Ib there are only a fixed number of activated thiol groups able to participate in the gelation process whereas new thiol groups are

continuously activated in type II age-thickening until the reserve of thiol groups is exhausted.

The weak physical particle interactions in casein-casein aggregates, in particular the electrostatic and hydrogen bonds, are easily disrupted by dilution. This explains why the diluted milk samples show no change in PSD during age-thickening in type Ia. Addition of a proteolytic enzyme, like Neutrase (Ma et al, 2002) cuts the glycomacropeptide from the  $\kappa$ -caseins thus providing more destabilised casein micelles for the aggregation reaction. Hydrophobic interactions can also take place during casein aggregation.

The greater strength of Type II age-thickening structure arises from the presence of disulfide bonds associated with the hair like linkages between casein micelles. When part of the whey proteins is removed, both the viscosity and age-thickening rate decrease significantly as found by Trinh and Schrackenraad (2002).

The nature of association between the denatured whey proteins and casein micelles is not yet clear, but it has been suggested that this takes place via the  $\kappa$ -casein (Anema & Li, 2003a; Cho et al., 2003). Since the dissociation rate of  $\kappa$ -caseins is strongly pH dependent, the author predicts that the rate of type II age-thickening is also pH sensitive by analogy with well documented observations of heat coagulation time (HCT) behaviour (Singh, 2004). Obviously, extensive experimentation is required to prove this hypothesis.

It is also not known whether the denatured  $\beta$ -lactoglobulin first attaches to the  $\kappa$ -casein on the micelle surface and then the complex dissociates from the micelle or whether the  $\beta$ -lactoglobulin attaches to the already dissociated  $\kappa$ -casein. Obviously, direct casein-casein and denatured whey protein aggregation can also take place and contribute to the gel network. Thus at any stage, several mechanisms can co-exist in type II age-thickening.

### 6.5.6 Modelling of the age thickening process

There is currently no mathematical model available to monitor the age thickening process in milk concentrates, or any other dairy system. There is no attempt to develop one here, but the author wishes to point out a few issues that need to be addressed in the development and/or choice of a suitable time-dependent rheological model.

A suitable model will involve both time-dependent structural viscosity and elasticity, as proposed by Mujumdar et al. (2002)

$$\tau_t = \tau_e + \tau_v \quad (6.1)$$

where  $\tau_t$  is the total stress (Pa)

$\tau_e$  is the elastic stress (Pa)

$\tau_v$  is the viscous stress (Pa)

The viscous stress is likely to dominate the first phase called hereafter age-thickening phase and the elastic stress to dominate the second phase called gelation phase. A number of such models exist (e.g. Fang and Tiu, 1990; Mujumdar et al., 2002) but have not been applied to milk concentrates. For example, Mujumdar et al. (2002) developed a model which summed the elastic and viscous contribution to the total stress. They found that the model gave better prediction of the variation of the  $G'/G''$  ratio with oscillation frequency of concentrated suspensions of silicon particles and silicon carbide whiskers in polyethylene than the Rutgers-Delaware model (Doraiswamy et al., 1991). This is because the Rutgers-Delaware model was found to apply only to the linear viscoelastic region, while the Mujumdar et al. (2002) model could be applied in the non-linear region i.e. at large deformations encountered in process operations. These models should be considered for contributing elements into rheological models of milk concentrates and other dairy products.

Mujumdar et al. (2002) and Fang and Tiu (1990) did not indicate how their models could be applied to the sol-gel transition.

The structural modelling can either follow direct (monitoring the bonds directly) or indirect microstructural approach (structural parameter).

In direct structural modelling, the bonds involved between the milk components can be modelled to some extent, as shown by Tuinier and de Kruif (2002). They calculated the strength of the attractive and repulsive forces on the surface of casein micelles to estimate the viscosity of milk during renneting. Their analysis was quite accurate up to 40% of  $\kappa$ -casein cleaved off by rennet (destabilisation of casein micelles) and qualitatively described the shape of the viscosity-rennet addition curve but predicted gelation at too low cleaved-off levels. This approach may be adapted to estimate the viscosity at gelation and possibly the gelation time. The difficulty here is that direct casein-casein interactions are only one of three types of bonds, which would result in at least three different types of structures. A substantial amount of work will be needed to identify the kinetics and mechanisms of these protein interactions and will hopefully give an estimate of the success rate of particle collisions to be employed in coagulation kinetics (Dobias, 1993).

Indirect structure models use the lumped structural parameter to monitor the change in structure, and thus change in viscosity (e.g. Moore, 1959; Tiu and Boger, 1974; Nguyen and Boger, 1985; Cheng 1987; Baravian et al., 1996). In most of these models, the structural viscosity at infinite shear is constant. The results from section 5.9 showed that during age thickening, this value changes with storage time. The structural viscosity at infinite shear must be a function of time to account for irreversible changes during age-thickening. For example the Cross (Cross, 1965) model should be rewritten as

$$\frac{\mu - \mu_{\infty}(t)}{\mu_o - \mu_{\infty}(t)} = \frac{1}{1 + \frac{k_1}{k_o} \dot{\gamma}^m} \quad (6.2)$$

Of course the relationship between  $\mu_\infty$  and time must be defined through careful and extensive experimentation. It is likely that it will be a function of the composition and quality of the raw milk used to make the concentrate and as such will also exhibit a dependence on seasonality, stage of lactation and feed quality.

The age thickening process is mainly governed by the rate of structural build-up. It must be noted that even in sheared systems, age thickening can still take place. In such cases, the structural breakdown will also affect the age thickening process, but obviously, structural build-up still dominates.

The build-up coefficient can be analysed through the change in the Herschel-Bulkley parameters with storage time during age thickening, where structural build-up dominates. The same structural parameter can be used to determine all three Herschel-Bulkley parameters, with three separate time functions.

$$\tau = f_1(\lambda)\tau_y + (f_2(\lambda)K\dot{\gamma}^{f_3(n)}) \quad (6.3)$$

The model proposed by Mujumdar et al. (2002) to take into account both the elastic and viscous stresses is as follows

$$\tau_t = \tau_e + \tau_v = \lambda(G\gamma_e) + (1 - \lambda)K\dot{\gamma}^n \quad (6.4)$$

where  $\gamma_e$  is the elastic strain associated with the flowing structure

The yield stress term  $\tau_y$  from the Herschel-Bulkley model is essentially replaced by the elastic stress term  $\lambda(G\gamma_e)$ . Equation 6.4 can be modified in a similar manner to equation 6.3 to give

$$\tau_t = (f_1\lambda)(G\gamma_e) + (1 - f_2(\lambda))K\dot{\gamma}^{f_3(n)} \quad (6.5)$$

The effect of other variables in the processing history, such as temperature and solids content, seasonality, lactation, lactose and permeate addition are too complex to be modelled at the present time.

---

# **CHAPTER 7**

## **CONCLUSIONS AND RECOMMENDATIONS**

---

## CHAPTER 7: CONCLUSIONS AND RECOMMENDATIONS

The literature survey in chapter 2 indicated that the rheological characterisation of time dependent fluids is extremely difficult and time consuming. The understanding of this phenomenon in concentrated milk solutions is still very incomplete and the experimental techniques currently available in the literature were either inadequate or inappropriate for this project.

### 7.1 Calibration of the Paar Physica MC1

Calibration of the Paar Physica MC1 rheometer ensured that the collection of data was accurate and reliable. The calibration exercise showed that there were strict limits to the operating spindle speed and torque of the Paar Physica MC1. Therefore, the reliable operating ranges were smaller than claimed in the operating manual. Shear stress corrections were applied to correct for non-linearity in the rheometer response, and a non-Newtonian correction was also required.

### 7.2 Controlled rheology experiments

The rheological behaviour of reconstituted milk concentrate systems was highly dependent on the reconstitution process. Milk concentrates reconstituted in a purpose-built recombination rig, where they were recirculated at  $40,000\text{ s}^{-1}$  and  $35^{\circ}\text{C}$  for 60 minutes were similar in rheological behaviour to fresh concentrates (correlation significant at  $p < 0.01$ ). In addition, under these conditions, both the rates of build up and breakdown of the dispersed phase structures were zero: the fluid was in structural equilibrium, and replicate samples showed excellent reproducibility with a maximum experimental error range of 10%.

#### 7.2.1 The rheology of milk concentrates

The rheology was mainly affected by solids content and heating and storage temperatures. The rheology of the reconstituted milk concentrates at  $35^{\circ}\text{C}$  shifted

from Newtonian (below 30%TS) to time-independent non-Newtonian (30-40%TS) to time-dependent non-Newtonian (above 40%TS) behaviours.

Below 20%TS, Newtonian behaviour existed at 35°C and 85°C. At 30-35%TS, heating to 85°C triggered the onset of time-dependent behaviour. At 40%TS and above, the degree of thixotropy and age thickening increased with an increase in heating and storage temperature.

#### **7.2.1.1 Effect of solids content and temperature on the viscosity of reconstituted milk concentrates**

An increase in solids content resulted in an exponential increase in viscosity and a decrease in pH from 6.7 to 6.2 at 47%TS where a plateau was reached. An increase in heating temperature resulted in a decrease in viscosity until a minimum at 65°C-75°C, above which the viscosity increased significantly.

#### **7.2.2 Age thickening behaviour**

Age thickening was characterised by:

1. Initial rate of increase in apparent viscosity (or yield stress and consistency index) and HLA with time.
2. Gelling time
3. Apparent viscosity at the gelling point

The rate of age thickening was dependent on solids content and heating and storage temperatures. The viscosity at the gelling point was independent of concentration and temperature, and appeared to be a property of the milk powder.

### **7.2.2.1 Processing conditions affecting the age thickening behaviour**

In addition to solids content and heating and storage temperature, the rate of age thickening and gelling times in the reconstituted concentrates were highly dependent on the processing conditions during the reconstitution and heating stages.

An increase in recirculating shear rate during reconstitution at 35°C, resulted in lower rates of age thickening and subsequently longer gelling times when heated and stored at high temperatures. An increase in recirculating temperature, resulted in shorter gelling times when the concentrates were heated and stored at the elevated temperature.

When heating and storage of the concentrates was carried out under industrial conditions, using plate heat exchangers with different numbers of plates, similar, but quantitatively different results, to the controlled rheology experiments were obtained. The design and operating conditions of the heat exchangers had a significant effect on the rheological behaviour.

### **7.2.2.2 Effect of powder origin**

Reconstituted concentrates made from two whole milk powders, A and B, with very similar compositions, showed different age thickening behaviour.

Powder A concentrates gelled at 0.1 Pa.s, while powder B concentrates gelled at 0.5-0.6 Pa.s. As both concentrates had similar rates of age thickening, powder B concentrates consequently took a longer time to gel during age thickening.

## **7.3 Industrial surveys**

Industrial surveys of fresh milk concentrate systems showed that many processing conditions, including the preheating level, heating temperature during evaporation and concentration, solids content and protein content affect the viscosity and age-thickening behaviour of the concentrates. The shear level during sampling also played

a significant role. The design of the plants also affected the viscosity of the concentrates, presumably through their temperature, shear and residence time histories.

#### **7.4 Mechanisms of age thickening**

A new classification of age thickening in dairy solutions is proposed:

- Type 1 age thickening taking place below the temperature at minimum viscosity,
- Type 2 occurring above this temperature.

In type 1 age thickening, the lack of change in PSD during age thickening suggested that the bonds involved are weak and readily broken up by dilution. It is proposed that these bonds resulted from direct physical interactions between casein micelles. A change in PSD in type 2 suggested heat treatment above the temperature at minimum viscosity triggered new reactions that resulted in stronger bonds, which can be attributed to the irreversible denaturation of whey proteins upon heating above 65-70°C and their interactions with other denatured whey proteins, casein micelles, dissociated caseins, or fat globules.

#### **7.5 Recommendations for future studies**

##### **7.5.1 Improvements to the recombination rig**

Despite the success achieved with the recombination rig, there are many design changes that could improve the efficiency of the rig and make the operation and data collection easier. These include:

- A more powerful mono pump to deliver higher shear rates during recirculation
- Automatic control of the heating system
- Installation of more sensors, including pressure sensors
- Automatic powder feeding system to control the solids content in short time frame.
- Larger mixing capacity from 5 L to at least 10 L.

### **7.5.2 Industrial surveys**

The database obtained from the industrial surveys needs to be expanded to include more milk products at different plants throughout several production seasons. The change in rheological behaviour during processing should also be correlated with the physical and functional properties of the end powder. This will provide valuable information to ensure the production of milk powders with the desired properties in a consistent manner.

### **7.5.3 Factors affecting the age thickening behaviour of reconstituted milk concentrates**

There is still a need to do further tests on the effect of processing variables, such as solids content, temperature, as well as operating conditions during recombination and heating. The effect of pH on age thickening should be investigated thoroughly. The relationship between age thickening and HCT should also be established. In addition, future experiments should include a wide variety of products, including skim and whole milk, RSCM, recombined evaporated milk and other time-dependent dairy products. Establishment of the critical conditions for the onset of age thickening and gelation in each product would be valuable.

TEM, SDS-page and SDS-agarose, PSD, and any other chemical analytical techniques that may prove beneficial towards the understanding of the chemical interactions and change in structure during age thickening should also be employed to support the rheological data.

## **7.6 Concluding remarks**

This project has successfully developed improved methods for the rheological study of time-dependent fluids. Even though this work is focused on the rheology of reconstituted milk concentrates, the techniques developed are applicable to the study of other time-dependent systems.

Age thickening is far more complex than previously envisaged in the literature. Age thickening is affected by many processing variables, including composition, solids content, as well as temperature and shear histories. The knowledge of the interactions between the processing variables, rheology of the milk concentrates and the properties of the end powder could provide an important quality control tool during processing. The physical and functional behaviour of the products can then be controlled systematically. This would allow the production of more consistent products, and the development of products with new texture and mouth feel characteristics.

---

# REFERENCES

---

- Abu-Jdayil, B., & Mohameed, H. (2002). Experimental and Modelling Studies of the Flow Properties of Concentrated Yogurt as Affected by the Storage Time. Journal of Food Engineering, 52(4), 359-365.
- Al-Tahiri, R. (1987). Recombined and reconstituted milk products. New Zealand Journal of Dairy Science & Technology, 22: 1, 1-23.
- Anema, S. G. (1998). Effect of milk concentration on heat-induced, pH-dependent dissociation of casein from micelles in reconstituted skim milk at temperatures between 20°C and 120°C. Journal of Agricultural and Food Chemistry, 46(6), 2299-2305.
- Anema, S. G. (2000). Effect of milk concentration on the irreversible thermal denaturation and disulfide aggregation of  $\beta$ -lactoglobulin. Journal of Agricultural and Food Chemistry, 48, 4168-4175.
- Anema, S. G., & Klostermeyer, H. (1997). Heat-induced, pH-dependent dissociation of casein micelles on heating reconstituted skim milk at temperatures below 100°C. Journal of Agricultural and Food Chemistry, 45, 1108-1115.
- Anema, S. G., & Klostermeyer, H. (1996). Zeta-potentials of casein micelles from reconstituted skim milk heated at 120°C. International Dairy Journal, 6(7), 673-687.
- Anema, S. G., & Li, Y. (2003). Association of denatured whey proteins with casein micelles in heated reconstituted skim milk and its effect on casein micelle size. Journal of Dairy Research, 70, 73-83.
- Anema, S. G., & Li, Y. (2003). Effect of pH on the association of denatured whey proteins with casein micelles in heated reconstituted skim milk. Journal of Agricultural and Food Chemistry, 51, 1640-1646.
- Anema, S. G., Lowe, E. K., & Li, Y. (2004). Effect of pH on the viscosity of heated reconstituted skim milk. International Dairy Journal, 14, 541-548.

- AOAC International. (2002). Official methods of analysis of AOAC International (17th Edition, Revision 1 ed.). (Official methods of analysis of AOAC International No. 17th ). Gaithersburg, Maryland, USA: AOAC International.
- Ascanio, G., Carreau, P. J., Brito-de la Fuente, E., & Tanguy, P. A. (2002). Orifice flowmeter for measuring extensional rheological properties. Canadian Journal of Chemical Engineering, 80(6), 1189-1196.
- Auldish, M. J., Walsh, B. J., & Thomson, N. A. (1998). Seasonal and lactational influences on bovine milk composition in New Zealand. Journal of Dairy Research, 65(3), 401-411.
- Baldwin, A. J., & Ackland, J. D. (1991). Effect of preheat treatment and storage on the properties of whole milk powder. Changes in physical and chemical properties. Netherland Milk Dairy Journal, 45, 169-181.
- Baldwin, A. J., Baucke, A. G., & Sanderson, W. B. (1980). The effect of concentrate viscosity on the properties of spray dried skim milk powder. New Zealand Journal of Dairy Science & Technology, 15(3), 289-297.
- Baldwin, A. J., Cooper, H. R., & Palmer, K. C. (1991). Effect of preheat treatment and storage on the properties of whole milk powder. Changes in sensory properties. Netherland Milk Dairy Journal, 45, 97-116.
- Baravian, C., Quemada, D., & Parker, A. (1996). Modelling thixotropy using a novel structural kinetics approach: basis and application to a solution of iota carrageenan. Journal of Texture Study, 27, 371-390.
- Barber, D. G., Gobius, N. R., Hannah, I. J. C., Poppi, D. P., & Cant, J. P. (2001). An approach to identify factors affecting milk protein concentration in dairy cattle. Australian Journal of Dairy Technology, 56(2), 155.
- Barnes, H. A. (1997). Thixotropy-a review. Journal of Non-Newtonian Fluid Mechanics, vol.69, no.2-3, pp.1-33.

- Batchelor, G. K. (1977). The effect of Brownian motion on the bulk stress in a suspension of spherical particles. Journal of Fluid Mechanics, 83, 97-117.
- Beaulieu, M., Pouliot, Y., & Pouliot, M. (1999). Thermal aggregation of whey proteins in model solutions as affected by casein/whey protein ratios. Journal of Food Science, 64(5), 776-780.
- Beeby, R. (1966). Heat-induced changes in the viscosity of concentrated skim milk. 115-121.
- Benslimane, S., Dognin-Bergeret, M. J., Berdague, J. L., & Gaudemer, Y. (1990). Variation with season and lactation of plasmin and plasminogen concentrations in montbeliard cows' milk. Journal of Dairy Research, 57(4), 423-435.
- Berg, M. G. Van Den, & Berg, G. Van Den. (1996). Seasonal variation of the casein/true protein ratio of cow's milk. Netherlands Milk and Dairy Journal, 50(4), 581-585.
- Bienvenue, A., Jimenez-Flores, R., & Singh, H. (2003). Rheological properties of concentrated skim milk: Importance of soluble minerals in the changes in viscosity during storage. Journal of Dairy Science, 86, 3813-3821.
- Bienvenue, A., Jimenez-Flores, R., & Singh, H. (2003). Rheological properties of concentrated skim milk: Influence of heat treatment and genetic variants on the changes in viscosity during storage. Journal of Agricultural and Food Chemistry, 51, 6488-6494.
- Bird, R. B., Dai, G. C., & Yarusso, B. J. (1983). The rheology and flow of viscoplastic materials. Reviews in Chemical Engineering, 1(1), 1-70.
- Bloore, C. G., & Boag, I. F. (1981). Some factors affecting the viscosity of concentrated skim milk. New Zealand Journal of Dairy Science & Technology, 16(2), 143-154.
- Bonomi, F., & Lametti, S. (1991). Real-time monitoring of the surface hydrophobicity changes associated with isothermal treatment of milk and milk protein fractions. Milchwissenschaft, 46, 71-74.

- Bozzola, J. J., & Russell, L. D. (1992). Electron microscopy. Principles and techniques for biologists. Boston, USA: Jones and Bartlett Publishers, Inc.
- Brookfield Engineering Labs., I. More solutions to sticky problems. Brookfield.
- Brun, J. M., & Dalgleish, D. G. (1999). Some effect of heat on the competitive adsorption of caseins and whey proteins in oil-in-water emulsions. International Dairy Journal, *9*, 323-327.
- Buckingham, J. H. (1978). Kinematic viscosities of New Zealand skim milk. Journal of Dairy Research, *45*, 25-35.
- Caric, M. (1994). Concentrated and dried dairy products. New York: VCH Publishers.
- Carroll, R. J., Thompson, M. P., & Melnychyn, P. (1970). Gelation of concentrated skim milk: Electron microscopic study. Journal of Dairy Science, *54*(9), 1245-1252.
- Cayot, P., Fairise, J.-F., Colas, B., Lorient, D., & Brule, G. (2003). Improvement of rheological properties of firm acid gels by skim milk heating is conserved after stirring. Journal of Dairy Research, *70*, 423-431.
- Cheng, D. C. H. (2003). Characterisation of thixotropy revisited. Rheological Acta, *42*, 372-382.
- Cheng, D. C. H. (1987). Thixotropy. International Journal of Cosmetic Science, *9*(4), 151-191.
- Cheremisinoff, N. P. (1993). An introduction to polymer rheology and processing. Florida, USA: CRC Press Inc.
- Chilton, R., Stainsby, R., & Thompson, S. (1996). The design of sewage sludge pumping systems. Journal of Hydraulic Research, *34*(3), 395-408.
- Cho, Y., Singh, H., & Creamer, L. K. (2003). Heat-induced interactions of  $\beta$ -lactoglobulin A and  $\kappa$ -casein B in a model system. Journal of Dairy Research, *70*, 61-71.

- Cichocki, B., & Felderhof, B. U. (1988). Long-time self-diffusion coefficient and zero-frequency viscosity of dilute suspensions of spherical Brownian particles. Journal of Chemical Physics, *89*, 3705-3709.
- Connolly, B., & O'Brien, B. (1994). Milk quality for processing: breeding, feeding and milking management to ensure good quality milk for manufacturing.
- Corredig, M., & Dalgleish, D. G. (1996). Effect of temperature and pH on the interactions of whey proteins with casein micelles in skim milk. Food Research International, *29*, 49-55.
- Corredig, M., & Dalgleish, D. G. (1999). The mechanisms of the heat-induced interaction of whey proteins with casein micelles in milk. International Dairy Journal, *9*, 233-236.
- Corvisier, P., Nouar, C., Devienne, R., & Lebouche, M. (2001). Development of a thixotropic fluid flow in a pipe. Experiments in Fluids, *31*, 579-587.
- Coulon, J. B., Hurtaud, C., Remond, B., & Verite, R. (1998). Factors contributing to variation in the proportion of casein in cows' milk true protein: a review of recent in vitro experiments. Journal of Dairy Research, *65*(3), 375-387.
- Croguennec, T., O'Kennedy, B. T., & Mehra, R. (2004). Heat-induced denaturation /aggregation of  $\beta$ -lactoglobulin A and B: kinetics of the first intermediates formed. International Dairy Journal, *14*, 399-409.
- Cross, M. M. (1965). Rheology of non-Newtonian fluids: a new flow equation for pseudoplastic systems. Journal of Colloid Science, *20*, 417-437.
- Croy, R. J., Trinh, K. T., Hemar, Y., & Chen, H. (2002). Time-temperature-concentration history effects on milk concentrate rheology in a falling film evaporator. Paper #398 in 9th APCChE Congress and Chemeca, Christchurch, New Zealand.
- Dahle, C. D., & Pyenson, H. (1938). Bound water and its relation to some dairy products. Journal of Dairy Science, *21*, 407.

- Dalgleish, D. G. (1990). Denaturation and aggregation of serum proteins and caseins in heated milk. Journal of Agricultural Food Chemistry, *38*, 1995-1999.
- Dalgleish, D. G., Pouliot, Y., & Paquin, P. (1987). Studies on the heat stability of milk. ii. Association and dissociation of particles and the effect of added urea. Journal of Dairy Research, *54*(1), 39-49.
- Dalgleish, D. G., Spagnuolo P. A., & Goff, H. D. (2004). A possible structure of the casein micelle based on high-resolution field-emission scanning electron microscopy. International Dairy Journal, *14*, 1025-1031.
- Dames, B., Morrison, B. R., & Willenbacher, N. (2001). An empirical model predicting the viscosity of highly concentrated, bimodal dispersions with colloidal interactions. Rheologica Acta, *40*, 434-440.
- Dannenber, F., & Kessler, H. G. (1998). Reaction kinetics of the denaturation of whey proteins in milk. Vol. *53*(1), 258-263.
- Darby, R. (1985). Couette viscometer data reduction for materials with a yield stress. Journal of Rheology, *29*(4), 369-378.
- Datta, N., & Deeth, H. C. (2001) Age gelation of UHT milk- a review. Trans. IchemE, Part C, *79*, 197-210.
- Davies, F. L., Shankar, P. A., Brooker, B. E., & Hobbs, D. G. (1978). A heat-induced change in the ultrastructure of milk and its effect on gel formation in yoghurt. Journal of Dairy Research, *45*, 53-58.
- de Koning, P. J., de Wit, J. N., & Driessen, F. M. (1992). Process conditions affecting age-thickening and gelation of sterilised canned evaporated milk. Netherland Milk Dairy Journal, *46*, 3-18.
- de Kruif, C. G. (1999). Casein micelle interactions. International Dairy Journal, *9*, 183-188.
- de Kruif, C. G. (1998). Supra-aggregates of casein micelles as a prelude to coagulation. Journal

of Dairy Science, 81, 3019-3028.

- de la Fuente, M. A. (1998). Changes in the mineral balance of milk submitted to technological treatments. Trends in Food Science and Technology, 9, 281-288.
- Defelipe, A. I. A., Melcon, B., & Zapico, J. (1991). Structural changes in sweetened condensed milk during storage - an electron microscopy study. Journal of Dairy Research, 58(3), 337-344.
- Dillon, P., Crosse, S., Stakelum, G., & Flynn, F. (1995). The effect of calving date and stocking rate on the performance of spring-calving dairy cows. Grass and Forage Science, 50(3), 286-299.
- Dobias, B. (1993). Coagulation and flocculation. Theory and applications. New York, US: Marcel Dekker, Inc.
- Doraiswamy, D., Mujumdar, A. N., Tsao, I., Beris, A. N., Danforth, S. C., & Metzner, A. B. (1991). The Cox-Merz rule extended - a rheological model for concentrated suspensions and other materials with a yield stress. Journal of Rheology, 35(4), 647-685.
- Eilers, H. (1941). Die viskositat von emulsionen hochviskoser stoffe als funktion der konzentration. 313.
- Einstein, A. (1906). Eine nenu Bestimmung der Molekul-dimensionen. Annual Physik, 19, 289-306.
- Eirich, F. R. (1956). Rheology: Theory and applications. 1956: Academic Press.
- Evers, J. M., & Palfreyman, K. R. (2001). Free fatty acid levels in New Zealand raw milk. Australian Journal of Dairy Technology, 56(3), 198-201.
- Fairise, J. F., & Cayot, P. L. D. (1999). Characterisation of the protein composition of casein micelles after heating. International Dairy Journal, 9, 249-254.
- Famelart, M.-H., Tomazerski, J., Piot, M., & Pezennec, S. (2004). Comprehensive study of acid gelation of heated milk with model protein systems. International Dairy Journal, 14, 313-

- Fang, T., & Tiu, C. (1990). A generalised rheological model for elasto-thixotropic fluids. International Journal of Engineering Fluid Mechanics, 3(2), 148-174.
- Fernandez-Martin, F. (1972). Influence of temperature and composition on some physical properties of milk and milk concentrates. II. Viscosity. Journal of Dairy Research, 39, 75-82.
- Fitzpatrick, J. J., Weidendorfer, K., Weber, M., & Teunou, E. (2001). Practical considerations for reconstituting dairy powders to high solids content in a stirred-tank. Milchwissenschaft-Milk Science International, 56(9), 512-516.
- Fitzpatrick, J. J., Weidendorfer, K., & Teunou, E. (2000). Reconstitution of dairy powders to high solids content in a stirred-tank; The effect of agitation. Milchwissenschaft, 55, 437-440.
- Fitzpatrick, K. I., Rogers, G. L., Ajlouni, S., & Roginski, H. (2001). The effect of seasonal variation, milk harvesting methods and storage on lipolysis in Australian milk. Australian Journal of Dairy Technology, 56(2), 127.
- Flegler, S. L., Heckman, J. W. Jr., & Klomparens, K. L. (1993). Scanning and transmission electron microscopy an introduction. New York: W. H. Freeman and Company.
- Gallagher, D. P., Lynch, M. G., & Mulvihill, D. M. (1996). Porcine  $\beta$ -lactoglobulin does not undergo thermally induced gelation. Journal of Dairy Research, 63, 479-482.
- Gassem, M. A., & Frank, J. F. (1991). Physical properties of yogurt made from milk treated with proteolytic enzymes. Journal of Dairy Science, 74(5), 1503-1511.
- Giles, D. W., & Denn, M. M. (1990). Strain measurement error in a constant stress rheometer. Journal of Rheology, 34(4), 603-608.
- Griffin, A. T., Hickey, M. W., Bailey, L. F., & Feagan, J. T. (1976). The significance of preheat and pH adjustment in the manufacture of recombined evaporated milk. Australian Journal

of Dairy Technology, 31, 134-137.

- Guincamp, M., Humber, G., & Linden, G. (1993). Determination of sulfhydryl groups in milk using Ellman's procedure and clarifying reagent. Journal of Dairy Science, 76, 2152-2155.
- Gunnis, L. F. (1980). Recombined dairy products- Deveopment and technology. "Milk for the millions". 12-17.
- Harris, J. R., & Horne, R. (1991). Negative Staining. J. R. Harris Electron Microscopy in Biology . Oxford: Oxford University Press.
- Harwalkar, V. R., & Vreeman, H. J. (1978). Effect of added phosphates and storage on changes in ultra-high temperature short-time sterilised concentrated skim milk. 2. Micelle structure. Netherland Milk Dairy Journal, 32, 204-216.
- Hashizume, K., & Sato, T. (1988). Gel-forming characteristics of milk proteins 1: Effect of heat treatment. Journal of Dairy Science, 71, 1439-1446.
- Hayes, M. G., & Kelly, A. L. (2003). High pressure homogenisation of raw whole bovine milk (a) effects on fat globule size and other properties. Journal of Dairy Research, 70, 297-305.
- Hinrichs, J. (1999). Influence of volume fraction of constituents on rheological properties and heat stability of concentrated milk. Milchwissenschaft, 54(8), 450-454.
- Holt, C., & Muir, D. D. (1978). Natural variations in the average size of bovine casein micelles. II. Milk samples from creamery bulk silos in south west Scotland. Journal of Dairy Research, 45(3), 347-353.
- Holt, C., Muir, D. D., & Sweetsur, A. W. M. (1978). Seasonal changes in the heat stability of milk from creamery silos in south-west Scotland. Journal of Dairy Research, 45(2), 183-190.
- Houchin, T. L., & Hanley, T. R. (2004). Measurement of rheology of distiller's grain slurries

using a helical impeller viscometer. Applied Biochemistry and Biotechnology, 113-116, 723-732.

Hough, G., Moro, O., Segura, J., & Calvo, N. (1988). Flow properties of Dulce-de-Leche, a typical Argentine dairy product. Journal of Dairy Science, 71(7), 1783-1788.

Houlihan, A. V., Goddard, P. A., Nottingham, S. M., Kitchen, B. J., & Masters, C. J. (1992). Interactions between the bovine milk fat globule membrane and skim milk components on heating whole milk. Journal of Dairy Research, 59, 187-195.

Hunter, E. (1993). Practical electron microscopy. A beginner's illustrated guide (2nd ed.). Canada: Cambridge University Press.

Huppertz, T., Fox, P. F., & Kelly, A. L. (2004). High pressure treatment of bovine milk: effects on casein micelles and whey proteins. Journal of Dairy Research, 71, 97-106.

Iametti, S., de Gregori, B., Vecchio, G., & Bonomi, F. (1996). Modifications occur at different structural levels during the heat denaturation of  $\beta$ -lactoglobulin. European Journal of Biochemistry, 237, 106-112.

Ismael, A. A., & Grimbleby, F. A. (1958). Changes occurring in certain constituents during the preparation of evaporated milk. XV International Dairy Congress, 3, 1873.

Jang, H. D., & Swaisgood, H. E. (1989). Disulfide bond formation between thermally denatured  $\beta$ -lactoglobulin and  $\kappa$ -casein in casein micelles. Journal of Dairy Science, 900-904.

Jensen, G. K., & Nielsen, P. (1982). Reviews of the progress of dairy science: milk powder and recombination of milk and milk products. Journal of Dairy Research, 49: 3, 515-544.

Jeurnink, T. J. M., & Dekruif, K. G. (1993). Changes in milk on heating - viscosity measurements. Journal of Dairy Research, 60(2), 139-150.

Keenan, T. W., Moon, T. W., & Pyleruski, D. P. (1983). Lipid globules retain globule membrane material after homogenisation. Journal of Dairy Science, 66, 196-203.

Kelly, P. M. (1982). The effect of preheat temperature and urea addition on the seasonal

- variation in the heat stability of skim-milk powder. Journal of Dairy Research, 49(2), 187-196.
- Kelly, P. M. (1982). Effect of seasonal variation, urea addition and ultrafiltration on the heat stability of skim milk powder. Journal of Dairy Research, 49(1), 119-126.
- Kelly, P. M., & O'Kennedy, B. T. (2001). The effect of casein/whey protein ratio and minerals on the rheology of fresh cheese gels using a model system. International Dairy Journal, 11, 525-532.
- Kieseker, F. G. (1980). Recombined evaporated milk. 79-88.
- Kieseker, F. G. (1981). Recombined UHT products. Technical Publication, Australian Society of Dairy Technology, 26, 57-62.
- Kieseker, F. G., & Aitken, B. (1988). An objective method for determination of heat stability of milk powders. Australian Journal of Dairy Technology, 43, 26-31.
- Kieseker, F. G., Clarke, P. T., & Aitken, B. (1984). A comparison of recombination and reconstitution processes for the preparation of dairy products. The Australian Journal of Dairy Technology, 39, 145-153.
- Kieseker, F. G., & Healey, D. (1996). Protein adjusted non fat milk powders. Australian Journal of Dairy Technology, 51(2), 83-88.
- Kieseker, F. G., & Pearce, R. J. (1978). Producing heat stable milk powder. CSIRO Food Research Quarterly, 38(2), 35-40.
- Kieseker, F. G., & Southby, P. (1965). Studies of recombined sweetened condensed milk. Australian Journal of Dairy Technology, 20, 136.
- Kim, H. H. Y., & Jimenez-Flores, R. (1995). Heat-induced interactions between the proteins of milk fat globule membrane and skim milk. Journal of Dairy Science, 78, 24-35.
- King, D. W., Sanderson, W. B., & Woodhams, D. J. (1974). Spray drying of dairy products. Dairy Industries, ; 39(1,2), 13-16.

- Kocak, H. R., & Zadow, J. G. (1985). Age gelation of UHT whole milk as influenced by storage temperature. The Australian Journal of Dairy Technology, *40*(1), 14-21.
- Koning, de. P. J., Kaper, J., Rollema, H. S., & Driessen, F. M. (1985). Age-thinning and gelation in unconcentrated and concentrated UHT-sterilised skim milk. Effect of native milk proteinase. Netherland Milk and Dairy Journal, *39*, 71-87.
- Koning, P. J. d. e., Koops, J., & Rooijen, P. J. v. a. n. (1974). Some features of the heat stability of concentrated milk. III. Seasonal effects on the amounts of casein, individual whey proteins and NPN and their relation to various in heat stability. Netherlands Milk and Dairy Journal, ; *28*(3,4), 186-202.
- Krieger, I. M. (1990). The role of instrument inertia in controlled stress rheometers. Journal of Rheology, *34*(4), 471-483.
- Krieger, I. M., & Dougherty, T. J. (1959). A mechanism for non-Newtonian flow in suspensions of rigid spheres. Transactions of the Society of Rheology, *3*, 137-152.
- Krieger, I. M., & Elrod, H. (1953). Direct determination of the flow curves of non-Newtonian fluids II. Shearing rate in the concentric cylinder viscometer. Journal of Applied Physics, *24*(134-134).
- Krieger, I. M., & Maron, S. H. (1952). Journal of Applied Physics. Journal of Applied Physics, *23*, 147.
- Kristensen, D., Jensen, P. Y., Madsen, F., & Birdi, K. S. (1997). Rheology and surface tension of selected processed dairy fluids: influence of temperature. Journal of Dairy Science, *80*, 2282-2290.
- Kudo, S. (1980). Influence of lactose and urea on the heat stability of artificial milk systems. New Zealand Journal of Dairy Science & Technology, *15*(2), 197-200.
- Lametti, S., Giagiacomio, R., Messina, G., & Bonomi, F. (1993). Influence of processing on the

- molecular modifications of milk proteins in the course of enzymic coagulation. Journal of Dairy Research, *60*, 151-159.
- Lascelles, D. R., & Baldwin, A. J. (1976). Dispersibility of whole milk powder in warm water. New Zealand Journal of Dairy Science and Technology, *11*, 283-284.
- Lawrence, A. J., Muller, L. L., & Rogers, W. O. (1963). Studies on recombined sweetened condensed milk. Vol. 18, 289-191.
- Le, D. C., & Bhattacharya, S. N. (1990). Influence of temperature on the viscous behaviour of some concentrated dispersions. Journal of Rheology, *34*(5), 637-655.
- Lee, S. J., & Sherbon, J. W. (2002). Chemical changes in bovine milk fat globule membrane caused by heat treatment and homogenisation of whole milk. Journal of Dairy Research, *69*, 555-567.
- Lewis, J. L., Burns, S. M., Samuels, S. J., Powell, R. L., & Katz, D. F. (1994). Calibration and error analysis of a new magnetic sphere microrheometer. Review of Scientific Instruments, *65*(10), 3268-3275.
- Lucey, J. A., Munro, P. A., & Singh, H. (1999). Effects of heat treatment and whey protein addition on the rheological properties and structure of acid skim milk gels. International Dairy Journal, *9*(3-6), 275-279.
- Lucey, J. A., Munro, P. A., & Singh, H. (1998). Whey separation in acid skim milk gels made with glucono-d-lactone: effect of heat treatment and gelation temperature. Journal of Textural Studies, *29*, 413-426.
- Lucey, J. A., Tamehana, M., Singh, H., & Munro, P. A. (1998). Effect of interactions between denatured whey proteins and casein micelles on the formation and rheological properties of acid skim milk gels. Journal of Dairy Research, *65*, 555-567.
- Lucey, J. A., Tet Teo, C., Munro, P. A., & Singh, H. (1997). Rheological properties at small (dynamic) and large (yield) deformation of acid gels made from heated milk. Journal of Dairy Research, *64*(4), 591-600.

- Luckham, P. F., & Ukeje, M. A. (1999). Effect of particle size distribution on the rheology of dispersed systems. Journal of Colloid and Interface Science, *220*, 347-356.
- Ma, C. C. H., Trinh, K. T., Brooks, J., Kitson, K. E., & Maddox, I. S. (2002). Effect of a commercial proteinase on the rheological properties of recombined whole milk concentrates. Paper #400 in 9th APCCChE Congress and Chemeca, Christchurch, New Zealand.
- Ma, C. H. C., Trinh, K. T., Brooks, J. D., Kitson, K. E., & Maddox, I. S. (2002). Effect of commercial proteinase on the rheological properties of recombined whole milk concentrates. Paper #400.
- MacSporran, W. C. (1986). Direct numerical evaluation of shear rates in concentric cylinder viscometry. Journal of Rheology, *30*(1), 125-132.
- Markovitz, H. (1985). Rheology: in the beginning. Journal of Rheology, *29*(6), 777-798.
- McCrae, C. H. (1999). Heat stability of milk emulsions: phospholipid-protein interactions. International Dairy Journal, *9*, 227-231.
- McKenna, A. B., Lloyd, R. J., & Munro, P. A. S. H. (1999). Microstructure of whole milk powder and of insolubles detected by powder functional testing. Scanning Volumes, *21*, 305-315.
- McKenna, A. B., & Singh, H. (1991). Age gelation in UHT-processed reconstituted concentrated skim milk. International Journal of Food Science and Technology, *26*, 27-38.
- McMahon, D. J. (1996) Age-gelation of UHT milk: Changes that occur during storage on shelf-life and the mechanism by which age-gelation occurs. Heat Treatments and Alternative Methods (International Dairy Federation – Ref. S. I. 9602, Vienna, Austria), 315-325
- Metwally, M., Abou-Dawood, A. E., Nagmouh, M. R., Hewedi, M. M., & Hamdy, A. M. (1978). Studies on the heat stability of evaporated skimmilk. I. Effect of preheating and

- concentration on the heat stability of evaporated skim milk. Egyptian Journal of Dairy Science, 6(1), 113-118.
- Mewis, J., Frith, W. J., Strivens, T. A., & Russel, W. B. (1989). The rheology of suspensions containing polymerically stabilized particles. Aiche Journal, 35(3), 415-422.
- Mil, P. J. J. M., & de Koning, J. (1992) Effect of heat treatment, stabilizing salts and seasonal variation on heat stability of reconstituted concentrated skim milk. Netherlands Milk & Dairy Journal, 46, 169-182.
- Moore F. (1959). The rheology of ceramic slips and bodies. Transactions of the British Ceramic Society, 58, 470-492.
- Muhle, K. (1993). Floc stability in laminar and turbulent flow. (pp. 355-390). New York, US: Marcel Dekker, Inc.
- Muir, D. D., Abbot, J., & Sweetsur, A. W. M. (1978). Changes in the heat stability of milk protein during the manufacture of dried skim-milk. Journal of Food Technology, 13(1), 45-53.
- Muir, D. D., & Sweetsur, A. W. M. (1977). Effect of urea on the heat coagulation of the caseinate complex in skim-milk. Journal of Dairy Research, 44, 249-257.
- Muir, D. D., & Sweetsur, A. W. M. (1976). The influence of naturally occurring levels of urea on the heat stability of bulk milk. Journal of Dairy Research, 43(3), 495-499.
- Mujumdar, A., Beris, A. N., & Metzner, A. B. (2002). Transient phenomena in thixotropic systems. Journal of Non-Newtonian Fluid Mechanics, 102(2), 157-178.
- Mulder, H., & Walstra, P. (1974). The milk fat globule. Emulsion science as applied to milk products and comparable foods. Pudoc, Wageningen, Netherlands.; Commonwealth Agricultural Bureaux, Farnham Royal, England.
- Murphy, J. J., & O'mara, F. (1993). Nutritional manipulation of milk protein concentration and its impact on the dairy industry. Livestock Production Science, 35(1-2), 117-134.

- Newstead, D. F. (1977). Effect of protein and salt concentrations on the heat stability of evaporated milk. New Zealand Journal of Dairy Science and Technology, 12, 171-175.
- Newstead, D. F. (1980). Recombined sweetened condensed milk. IDF Recombination Seminar, 59-62.
- Newstead, D. F., & Baldwin, A. J. (1977). Viscosity of recombined sweetened condensed milk. 72-73.
- Newstead, D. F., Baldwin, A. J., & Hughes, I. R. (1978). Factors affecting the viscosity of recombined sweetened condensed milk. New Zealand Journal of Dairy Science & Technology, 13(2), 65-70.
- Newstead, D. F., & Baucke, A. G. (1983). Heat stability of recombined evaporated milk and reconstituted concentrated skim milk: effects of temperature and time of preheating. New Zealand Journal of Dairy Science & Technology, 18(1), 1-11.
- Newstead, D. F., Sanderson, W. B., & Baucke, A. G. (1975). The effects of heat treatment and pH on the heat stability of recombined evaporated milk. New Zealand Journal of Dairy Science and Technology, 10, 113-118.
- Newstead, D. F., Sanderson, W. B., & Conaghan, E. F. (1977). Effects of whey protein concentrations and heat treatment on the heat stability of concentrated and unconcentrated milk. New Zealand Journal of Dairy Science & Technology, 12(1), 29-36.
- Nguyen, Q. D., & Boger, D. V. (1992). Measuring the flow properties of yield stress fluids. Annual Review in Fluid Mechanics, 24, 47-88.
- Nguyen, Q. D., & Boger, D. V. (1985). Thixotropic behaviour of concentrated bauxite residue suspensions. Rheologica Acta, 24(4), 427-37.
- Nicholas, G. D., Auld, M. J., Molan, P. C., Stelwagen, K., & Prosser, C. G. (2002). Effects of stage of lactation and time of year on plasmin- derived proteolytic activity in bovine milk in New Zealand. Journal of Dairy Research, 69(4), 533-540.

- Nieuwenhuijse, J. A., Timmermans, W., & Walstra, P. (1988). Calcium and phosphate partitions during the manufacture of sterilised concentrated milk and their relations to the heat stability. Netherlands Milk and Dairy Journal, *42*, 387-421.
- Noda, K., Endo, M., & Takahashi, T. (1986). The effect of calcium on the viscosity of sweetened condensed milk. Journal of the Japanese Society for Food Science and Technology-Nippon Shokuhin Kagaku Kogaku Kaishi, *33*( 8), 572-578.
- O'brien, B., Lennartsson, T., Mehra, R., Cogan, T. M., Connolly, J. F., Morrissey, P. A., & Harrington, D. (1999). Seasonal variation in the composition of Irish manufacturing and retail milks. 3. Vitamins. Irish Journal of Agricultural and Food Research, *38*(1), 75-85.
- O'brien, B., Mehra, R., Connolly, J. F., & Harrington, D. (1999). Seasonal variation in the composition of Irish manufacturing and retail milks. 1. Chemical composition and renneting properties. Irish Journal of Agricultural and Food Research, *38*(1), 53-64.
- O'brien, B., Mehra, R., Connolly, J. F., & Harrington, D. (1999). Seasonal variation in the composition of Irish manufacturing and retail milks. 4. Minerals and trace elements. Irish Journal of Agricultural and Food Research, *38*(1), 87-99.
- O'Connell, J. E., & Fox, P. F. (2001). Effect of  $\beta$ -lactoglobulin and precipitation of calcium phosphate on the thermal coagulation of milk. Journal of Dairy Research, *68*, 81-94.
- Ono, T., Yoshida, M., Tanaami, H., & Ohkoshi, H. (1999). Changes in casein micelle size induced by heating. International Dairy Journal, *9*, 405-406.
- Ostensen, S., Foldager, J., & Hermansen, J. E. (1997). Effects of stage of lactation, milk protein genotype and body condition at calving on protein composition and renneting properties of bovine milk. Journal of Dairy Research, *64*, 207-219.
- Ozer, B. H., Robinson, R. K., Grandison, A. S., & Bell, A. E. (1998). Gelation properties of milk concentrated by different techniques. International Dairy Journal, *8*(9), 793-799.
- Papiz, M. Z., Sawyer, L., Eliopoulos, E. E., North, A. C. T., Findlay, J. B. C., Sivaprasadarao, R., Jones, T. A., Newcomer, M. E., & Kraulis, P. J. (1986). The structure of  $\beta$ -

lactoglobulin and its similarity to plasma retinol-binding protein. Nature, **324**, 383-385.

Parnell-Clunies, E., Kakuda, Y., Mullen, K., Amott, D. R., & Deman, J. M. (1986). Physical properties of yoghurt; a comparison of vat versus continuous heating systems of milk. Journal of Dairy Science, **69**, 2593-603.

Pouliot, Y., & Boulet, M. (1991). Seasonal variations in the heat stability of concentrated milk: effect of added phosphates and pH adjustment. Journal of Dairy Science, **74**, 1157-1162.

Pouliot, Y., Britten, M., & Latereille, B. (1990). Effect of high pressure homogenisation on a sterilised infant formula: microstructure and age gelation. Food Structure, **9**, 1-8.

Prentice, J. H. (1992). Dairy rheology. A concise guide. New York: VCH Publishers.

Princen, H. M. (1986). A novel design to eliminate end effects in a concentric cylinder viscometer. Journal of Rheology, **30**(2), 271-283.

Ramaswamy, H. S., & Basak, S. (1991). Time dependent stress decay rheology of stirred yogurt. International Dairy Journal, **2**: 1, 17-31.

Rao, V. N. M., Hamann, D. D., & Humphries, E. G. (1975). Flow behaviour of sweet potato puree and its relation to mouth feel quality. Journal of Texture Studies, **6**(2), 197-209.

Richardson, J. F., & Zaki, W. N. (1954). Sedimentation and fluidisation : Part I. Transactions of the Institution of Chemical Engineers, **32**, 35-52.

Robinson, R. K., & Itsaranuwat, P. (2002). The microbiology of concentrated and dried milks. (Third Edition ed., pp. 175-212). New York, United States of America: John Wiley and Sons, Inc.

Rohm, H. (1988). Viscosity of recombined sweetened condensed milk. Milchwissenschaft-Milk Science International, **43**(5), 303-306.

Rollema, H. S., & Poll, J. K. (1986). The alkaline milk proteinase system: Kinetics and mechanism of heat-inactivation. Milchwissenschaft, **41**(9), 536-540.

- Rose, D. (1963). Heat stability of bovine milk: a review. Dairy Science Abstracts, 25, 45-52.
- Russel, W. B. (1984). The Huggins coefficient as a means for characterising suspended particles. Journal of the Chemical Society , Farady Transactions 2, 80, 31-41.
- Samel, R., & Muers M. M. (1962). The age-thickening of sweetened condensed milk. I. Rheological properties. Journal of Dairy Research, 29, 249-258.
- Sanderson, W. B. (1980). Recombination of milk and milk products- Principal processes and equipment. 18-21.
- Sawyer, W. H. (1969). Complex between  $\beta$ -lactoglobulin and  $\kappa$ -casein. Journal of Dairy Science, 52(9), 1347-1355.
- Schelhass, S. M., & Morris, H. A. (1985). Rheological and scanning electron microscopic examination of skim milk gels obtained by fermenting with ropy and non-ropy strains of lactic acid bacteria. Vol. 4, 279-87.
- Schorsch, C., Jones, M. G., & Norton, I. T. (2002). Micellar casein gelation at high sucrose content. Journal of Dairy Science, 85, 3155-3163.
- Schorsch, C., Wilkins, D. K., Jones, M. G., & Norton, I. T. (2001). Gelation of casein-whey mixtures: Effects of heating whey proteins alone or in the presence of casein micelles. Journal of Dairy Research, 68(3), 471-481.
- Servais, C., Jones, R., & Roberts, I. (2002). The Influence of Particle Size Distribution on the Processing of Food. Journal of Food Engineering, 51(3), 201-208.
- Shalabi, S. I., & Fox, P. F. (1982). Heat stability of milk - Influence of modification of Lysine and Arginine on the heat stability pH Profile. Journal of Dairy Research, 49(4), 607-617.
- Sharma, R., & Singh, H. (1999). Heat stability of recombined milk systems as influenced by the composition of fat globule surface layers. Milchwissenschaft, 54(4), 193-196.
- Shi, F. N., & NapierMunn, T. J. (1996). Measuring the rheology of slurries using an on-line viscometer. International Journal of Mineral Processing, 47(3-4), 153-176.

- Shorey, A. B., Kordonski, W. I., Gorodkin, S. R. , Jacobs, S. D., Gans, R. F., Kwong, K. M., & Famy, C. H. (1999). Design and testing of a new magnetorheometer. Review of Scientific Instruments, 70(11), 4200-4206.
- Singh, H. (2004). Heat stability of milk. International Journal of Dairy Technology, 57(2-3), 111-119.
- Singh, H., & Creamer, L. K. (1991). Denaturation, aggregation and heat stability of milk protein during the manufacture of skim milk powder. Journal of Dairy Research, 58(3), 269-283.
- Singh, H., & Creamer, L. K. (1997). Heat stability of milk. (pp. 621-656). New York: Blackie Academic & Professional Publishers.
- Singh, H., Creamer, L. K., & Newstead, D. F. (1989). Effect of heat on the proteins of concentrated milk systems. Fil-Idf, 238, 94-104.
- Singh, H., Roberts, M. S., Munro, P. A., & Teo, C. T. (1996). Acid-induced dissociation of casein micelles in milk: effects of heat treatment. Journal of Dairy Science, 79(8), 1340-1346.
- Singh, H., & Tokley, R. P. (1990). Effects of preheat treatments and buttermilk addition on the seasonal variations in the heat stability of recombined evaporated milk and reconstituted concentrated milk. Australian Journal of Dairy Technology, 45(1), 10-16.
- Sjollema, A. (1988). Specification of dairy products used as raw materials for recombining. Netherlands Milk & Dairy Journal, 42: 4, 365-374.
- Smits, P., & van Brouwershaven, J. H. (1980). Heat-induced association of  $\beta$ -lactoglobulin and casein micelles. Journal of Dairy Research, 47, 313-325.
- Snoeren, T. H. M., Brinkhuis, J. A., Damman, A. J., & Klok, H. J. (1984). Viscosity and age-thickening of skim-milk concentrate. Netherlands Milk and Dairy Journal, 38(1), 43-53.
- Snoeren, T. H. M., Damman, A. J., & Klok, H. J. (1981). Effect of concentrate viscosity on properties of dried skim milk. Voedingsmiddelentechnologie, 14(26), 27-31.

- Snoeren, T. H. M., Damman, A. J., & Klok, H. J. (1982). The effect of droplet size distribution on the properties of spray-dried skim-milk. Proceedings of the Third International Drying Symposium, Vol. 2., 290-297.
- Snoeren, T. H. M., Damman, A. J., & Klok, H. J. (1984). Effect of homogenization on the viscosity of whole milk concentrate and properties of dried whole milk. Voedingsmiddelentechnologie, 17(4), 28-30.
- Snoeren, T. H. M., Damman, A. J., & Klok, H. J. (1983). The viscosity of whole milk concentrate and its effect on the properties of whole milk powder. Voedingsmiddelentechnologie, 16(9), 68-71.
- Spreer, E. (1998). Milk and Dairy Product Technology. New York, United States of America: Marcel Dekker, Inc.
- Stadhouders, J. (1972). Technological aspects of the quality of raw milk. Netherlands Milk and Dairy Journal, 26(2), 68-90.
- Steffl, A., Schreiber, R., Hafenmair, M., & Kessler, H. (1999). Influence of whey protein aggregates on the renneting properties of milk. International Dairy Journal, 9, 403-404.
- Tan-Kintia, R. H., & Fox, P. F. (1999). Effect of various preheat treatments on the heat stability of unconcentrated milk. International Dairy Journal, 9, 219-225.
- Tang, Q., Munro, P. A., & McCarthy, O. W. (1993). Rheology of whey protein concentrate solutions as a function of concentration, temperature, pH and salt concentration. Journal of Dairy Research, 60, 349-361.
- Tiu, C., & Boger, D. V. (1974). Complete rheological characterization of time-dependent food products. Journal of Texture Studies, 5(3), 329-338.
- Trckova, J., Stetina, J., & Kinsky, J. (2004). Influence of protein concentration on the rheological properties of carrageenan gels in milk. International Dairy Journal, 14, 337-343.

- Trinh, K. T. (1994). Rheology of milk concentrates and process implications. Proceeding of the Milk Powders for the Future II. Palmerston North, New Zealand
- Trinh, K. T., & Leslie, S. M. (1997) Effect of heat exchanger operation on the properties of milk concentrates. Proceeding of the 7<sup>th</sup> International Congress on Engineering and Food, United Kingdom
- Trinh, K. T., & Schraekenrad, H. (2002). Effect of heating on the rheological properties of milk concentrates. Proceeding 6th Congress of Chemical Engineering Melbourne, Australia.
- Trinh, K. T. (2003) CIP of solids handling equipment. In Encyclopaedia of Agricultural, Food and Biological Engineering, pp. 135-138. New York: Marcel Dekker Inc.
- Trinh, B., Haisman, D., Trinh, K. T., & Pranker, B. (2004). Effect of shear during recombination of time-dependent food products. Paper #131, International Conference Engineering and Food.
- Trinh, B., Haisman, D., Trinh, K. T., & Weeks, M. (2002). Design of recombination system for time-dependent food systems. Paper #402 in 9th APCCChE Congress and Chemeca, Christchurch, New Zealand .
- Trinh, K. T., & Schraekenrad, H. (2002). Effect of heating on the rheological properties of milk concentrates. Paper #401 in 9th APCCChE Congress and Chemeca, Christchurch, New Zealand .
- Tuinier, R., & de Kruif, C. G. (2002). Stability of casein micelles in milk. Journal of Chemical Physics, 117(3), 1290-1295.
- Tumer, L. G., Swaisgood, H. E., & Hansen, A. P. (1978). Interaction of lactose and proteins of skim milk during ultra- high temperature processing. Journal of Dairy Science, 61(4), 384-392.
- Udabage, P., McKinnon, I. R., & Augustin, M. (2000). Mineral and casein equilibria in milk:

- effects of added salts and calcium chelating agents. Journal of Dairy Research, *67*, 361-370.
- Underwood, J. E., & Augustin, M. A. (1997). Rheological characteristics of acid and heat-induced gels made from reconstituted or recombined concentrated milks. The Australian Journal of Dairy Technology, *52*, 88-91.
- Underwood, J. E., & Augustin, M. A. (1997). Seasonal variation in the rheological properties of acid and heat-induced gels made from reconstituted concentrated milk. Australian Journal of Dairy Technology, *52*(2), 83-87.
- Upadhyay, K. G. (1998). Age thickening in sweetened condensed milk. Indian Dairyman, *50*(10), 27-34.
- Usui, H. (2002). Prediction of dispersion characteristics and rheology in dense slurries. Journal of Chemical Engineering of Japan, *35*( 9), 815-829.
- van Mil, P. J. J. M., & deKoning, J. (1992). Effect of heat treatment, stabilizing salts and seasonal variation on heat stability of reconstituted concentrated skim milk. Netherlands Milk & Dairy Journal, *46*(3,4), 169-182.
- Van Wazer, J. R., Lyons, J. W., Kim, K. Y., & Colwell, R. E. (1963). Viscosity and flow measurement. A laboratory handbook of rheology. New York: John Wiley & Sons, Inc.
- Vasbinder, A. J., Alting, A. C., Visschers, R., & de Kruif, C. G. (2003). Texture of acid milk gels: formation of disulfide cross-links during acidification. International Dairy Journal, *13*, 29-38.
- Vasbinder, A. J., & de Kruif, C. G. (2003). Casein-whey protein interactions in heated milk: the influence of pH. International Dairy Journal, *13*, 669-677.
- Vasbinder, A. J., Rollema, H. S., Bot, A., & de Kruif, C. G. (2003). Gelation mechanism of milk as influenced by temperature and pH; studied by the use of transglutaminase cross-linked casein micelles. Journal of Dairy Science, *86*, 1556-1563.

- Vasbinder, A. J., van de Velde, F., & de Kruif, C. G. (2004). Gelation of casein-whey protein mixtures. Journal of Dairy Science, *87*, 1167-1176.
- Vasbinder, A. J., van Mil, P. J. J. M., Bot, A., & de Kruif, C. G. (2001). Acid-induced gelation of heat-treated milk studied by diffusing wave spectroscopy. Colloids Surfaces B: Biointerfaces, *21*, 245-250.
- Velez-Ruiz, J. F., & Barbosa-Canovas, G. V. (1997). Effects of concentration and temperature on the rheology of concentrated milk. Transactions of the ASAE, *40*(4), 1113-1118.
- Velez-Ruiz, J. F., & Barbosa-Canovas, G. V. (2000). Flow and Structural Characteristics of Concentrated Milk. Journal of Texture Studies, *31*(3), 315-333.
- Velez-Ruiz, J. F., & Barbosa-Canovas, G. V. (1998). Rheological properties of concentrated milk as a function of concentration, temperature and storage time. Journal of Food Engineering, *35*(2), 177-190.
- Venkatachalam, N., McMahon, D. J., & Savello, P. A. (1993). Role of protein and lactose interactions in the age gelation of ultra-high temperature processed concentrated skim milk. Journal of Dairy Science, *76*(7), 1882-1894.
- Vilder, J. d. e., Martens, R., & Naudts, M. (1979). The influence of the dry matter content, the homogenization and the heating of concentrate on physical characteristics of whole milk powder. Milchwissenschaft, *34*(2), 78-84.
- Vilder, J. d. e., & Moermans, R. (1983). The continuous measurement of the viscosity of the concentrate during the production of milk powder. Milchwissenschaft, *38*(8), 449-452.
- Vyas, H. K., & Tong, P. S. (2003). Impact of source and level of calcium fortification on the heat stability of reconstituted skim milk powder. Journal of Dairy Science, *87*, 1177-1180.
- Walstra, P., Geurts, T. J., Noomen, A., Jellema, A., & van Boekel, M. A. J. S. (1999). Dairy technology. Principles of milk properties and processes. New York, United States: Marcel Dekker, Inc.

- Walstra, P., & Jenness, R. (1984). Dairy Chemistry and Physics. New York: John Wiley.
- White, J. C. D., & Davies, D. T. (1958). The relation between the chemical composition of milk and the stability of the caseinate complex. IV. Coagulation by heat. Journal of Dairy Research, 25, 281-296.
- Williams, R. P. W. (2002). The relationship between the composition of milk and the properties of bulk milk products. Australian Journal of Dairy Technology, 57(1), 30-44.
- Wolthers, W., Duits, M. H. G., Vandenende, D., & Mellema, J. (1996). Shear history dependence of the viscosity of aggregated colloidal dispersions. Journal of Rheology, 40(5), 799-811.
- Yang, T. M. T., & Krieger, I. M. (1978). Comparison of methods for calculating shear rates in coaxial viscometers. Journal of Rheology, 22(4), 412-421.
- Ye, A., Singh, H., Oldfield, D. J., & Anema, S. (2004). Kinetics of heat-induced association of  $\beta$ -lactoglobulin and  $\alpha$ -lactalbumin with milk fat globule membrane in whole milk. International Dairy Journal, 14, 389-398.
- Zavarin, Yu. A., Chekulaeva, L. V., & Chekulaev, N. M. (1978). Structure formation of sweetened condensed milk. XX International Dairy Congress, E736.
- Zoon, P., van Vliet, T., & Walstra, P. (1988). Rheological properties of rennet-induced skim milk gels. 1. Introduction. Netherlands Milk and Dairy Journal, 42, 249-269.

---

# APPENDICES

---

## A.1 Milk system literature review

Milk contains approximately 85% w/w water. Lactose (4.6% w/w), fat (3.9% w/w), and protein (3.25% w/w) make up the bulk of the remaining components. Other miscellaneous components, including vitamins, are present in trace amount.

The milk system is mainly aqueous, with various species of dispersed particles. Fat globules are the biggest constituents with an average diameter of 0.1-10  $\mu\text{m}$ . Casein micelles are the next largest components in the plasma, the milk solution minus the fat, averaging 10-300 nm in diameter and constitute approximately 80% of the protein in milk (Lucey, 2002). Milk without fat globules and casein micelles is called serum. The fat globules and the casein micelles are the colloids that contribute to the white appearance of milk (ten Grotenhuis et al., 2003).

The aqueous part constitutes the continuous phase, and thus the properties of milk are primarily those of an aqueous system. Polar substances dissolve well in milk. The low viscosity of milk enables it to be mixed easily.

Fresh milk varies widely in composition and properties. The variations are caused by genetic and physiological differences, arising particularly from the stage of lactation and the breeding environment. Milk from different cows behaves differently during processing (Hill et al., 1996).

The milk system is never in equilibrium. Once collected, milk undergoes significant changes. Thus the system constantly changes, even if the environment is held constant. The changes in the milk system can be divided into the following categories:

- Physical changes: e.g. separation of phases
- Chemical changes: e.g. natural oxidation of lipids
- Biochemical changes: are largely enzymatic
- Microbial changes: fermentation by lactic acid bacteria (Walstra & Jenness, 1984)

### A.1.1 Lipids

The composition of milk fat is very variable. Variations of feed, in particular both its lipid and non-lipid components, is an important factor. Consequently, the fat composition varies with time of year, region, farming practice, and so on.

The triglycerides are very non-polar and not surface active. They act as a solvent for many other non-polar substances. Fatty acids are surface-active and somewhat soluble in water. They dissolve well in fat, and tend to associate into dimers by hydrogen bonding.

The triglycerides can be attacked by milk and bacteria enzymes to yield diglycerides. These can also be subjected to further attacks to yield monoglycerides. Diglycerides do not differ much from the triglycerides in properties. Monoglycerides are much more polar and surface-active. They tend to accumulate at an oil-water or air-water interface. The attack on triglycerides can also yield free fatty acids.

The monoglycerides have hydrophilic and hydrophobic sections. This makes the molecule amphiphilic, and means that the molecule is compatible with both water and oil. The molecules form micelles with polar ends on the outside in the presence of water, and inside in the presence of oil. In milk, they are in contact with water and with proteins.

There are numerous other lipids in milk in very small quantities. These include pigments (carotenoids), vitamins (mainly A, D, and E), antioxidants and squalene. They are all predominantly dissolved in the core of the fat globules.

Milk is an oil-in-water emulsion and no emulsion is entirely stable. Some physical properties, such as the colour and viscosity of milk and its products, are influenced particularly by the dispersed state of the fat.

### **A.1.1.1 Milk Fat Globules**

A fat globule can be visualised as a coated spherical particle, ranging in size from <1 to about 10  $\mu\text{m}$ . The core consists of numerous non-polar triglycerides and other lipids with different lengths and attached groups (Jensen, 2002). The content is bounded and protected by a layer of membrane, known as the natural fat globule membrane (NFGM) (Mather, 2000; Michalski et al., 2002). The natural membrane consists mainly of bipolar materials including phospholipids, protein, as well as enzymes (Kim & Jimenez-Flores, 1995; Jensen, 2002). All interactions between fat and plasma must take place through the membrane (Lee & Sherbon, 2002). The NFGM is a natural barrier and thus protects the fat globules from deteriorative reactions such as lipolysis and autoxidation, as well as flocculation and coalescence. The NFGM also acts as an emulsion stabilizer in milk systems.

Under certain conditions, such as high shear (homogenisation) and high temperature (heating), as well as the presence of enzymes and air bubbles, the NFGM is damaged (Kim & Jimenez-Flores, 1995; Hayes & Kelly, 2003). The damaged fat globule membrane does not offer the same resistance to deteriorative reactions as its natural counterpart.

Heating results in the denaturation of whey proteins which interact with the membrane components of the fat globules via mainly but not exclusively disulphide bonds (Sharma & Dalgleish, 1994; Kim & Jimenez-Flores, 1995; Lee & Sherbon, 2002), as well as the  $\kappa$ -casein on the casein micelles (Jang & Swaisgood, 1989). Ye et al. (2004) showed that association between the whey protein and the milk fat globule membrane of fresh whole milk system follows a first-order reaction in the low temperature range (65-85°C) and a second-order reaction in the high temperature range (85-95°C). Heating also results in loss of membrane lipid components (Lee & Sherbon, 2002).

Homogenisation breaks up the fat globules into smaller ones and thus increases the total surface area. New membranes are formed via the adsorption of plasma proteins (preferentially casein micelles over whey proteins) (McCrae & Muir, 1991; Houlihan

et al., 1992). Lee and Sherbon (2002) showed that homogenization only results in the adsorption of casein onto the fat membrane. Incorporation of whey protein only takes place in heated milk, either before or after homogenization.

### **A.1.2 Proteins**

About 80% of the milk proteins consist of caseins (Hansen et al., 1996; Marchesseau et al., 2002), a group of phosphate containing milk-specific proteins that precipitate upon acidification to pH 4.6-5 (Singh et al., 2000). Almost all casein in milk is present in casein micelles. The proteins remaining in solution at pH 4.6-5 are called whey proteins (or milk serum proteins). The isoelectric pH of whey protein is around 5.2-5.5.

#### **A.1.2.1 Caseins**

Compositionally, the hallmark of the caseins is ester-bound phosphate and all of the casein polypeptide chains have at least one such group per molecule. Caseins are a family of phosphoprotein (Rasmussen et al., 1999), consisting of four types of casein proteins,  $\alpha$ ,  $\beta$ ,  $\lambda$ , and  $\kappa$  caseins (Curley et al., 1998; Lucey, Johnson, & Home, 2003; Vasbinder, Rollema, Bot, & de Kruif, 2003). Of the four caseins, only  $\alpha_{s2}$ - and  $\kappa$ -casein contain cysteine residues, which can form disulphide bonds (Rasmussen et al., 1999).

Casein micelles in milk are roughly spherical particles, ranging in size from 50-500 nm (de Kruif, 1998; Schorsch, Jones, & Norton, 2002). The micelles are highly hydrated and have large voluminosity containing 20,000-150,000 casein molecules.

Three types of models for the structure of casein micelles have been proposed.

Slattery & Evard (1973), Slattery (1976), Schmidt (1982), Walstra (1990, 1999), Hansen et al. (1996) visualized a casein micelle as a roughly spherical, swollen particle with a hairy outer layer consisting of  $\kappa$ -casein, shown in Figure A.1.

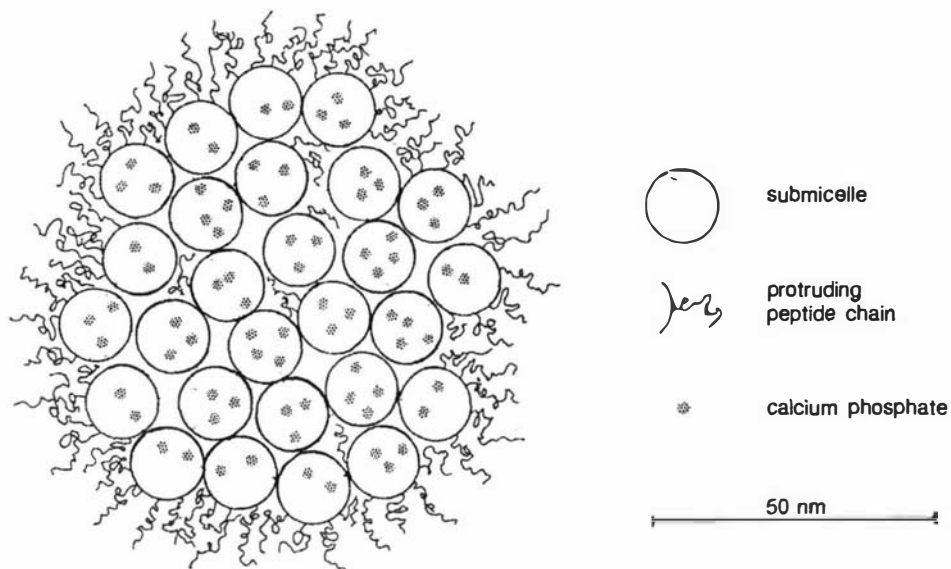


Figure A.1. Model (cross section) of a casein micelle. (Walstra, 1999)

When whole casein is in solution at a concentration, pH, and ionic strength as in milk, but at low  $\text{Ca}^{2+}$  activity, small aggregates are formed. These are 10-20  $\mu\text{m}$ , and contain between 10-100 casein molecules. These aggregates have a similar structure to globular proteins, with a dense hydrophobic core, in which most hydrophobic parts of the casein molecules are buried, and a more loosely packed, hydrophilic outer layer, containing most of the acidic (carboxylic and phosphoric) and some of the basic groups

Each of these small aggregates of whole casein is called a submicelle. On increasing the activity of  $\text{Ca}^{2+}$ , the association between the submicelles increases considerably. Under conditions as in milk, the submicelles aggregate into micelles.

The calcium phosphate acts as a cementing agent which accounts for approximately 7% of the micelle dry mass (Smyth et al., 2004), but it is not known what bonds are involved. The  $\kappa$ -casein occupies key positions at the micelle surface (Kirchmeier, 1973; Schmidt, 1982; Walstra, 1990). The molecular chains of the C-terminal end of  $\kappa$ -casein protrude from the micelle's surface into the solvent as flexible hairs (Walstra, 1979; Singh, 2004). The protruded  $\kappa$ -casein provides stabilization via electrostatic repulsion from the negative charge associated with the micelles and steric stabilisation through entropic repulsion between the protruding hairs at short range

(Slattery, 1976; de Kruif, 1999; Singh, 2004), , Interestingly, de Kruif (1999) pointed out the negative charges on  $\kappa$ -casein contribute little directly to the stability of the micelles, but do so by promoting the solvency of the  $\kappa$ -casein in the continuous phase. Removal of  $\kappa$ -casein, such as by the action of chymosin during renneting, promotes coagulation between casein micelles due to the loss of repulsion.

Holt (1998) argued against this model showing that selective removal of the colloidal calcium phosphate (CCP) did not result in a sub-micelle distribution. McMahon & McManus (1998) found no concrete proof of existence of submicelle structure using transmission electron microscopy (TEM). Holt (1992) suggested that the internal structure of casein micelles comprises a mineralized, entangled, or cross-linked web of chains of casein molecules. CCP acts as cross-linking agent responsible for holding the network together.

Home (1998) believed casein micelles are made of individual caseins in a cross-linked network through hydrophobic regions of the caseins and bridging using CCP. The stability of casein micelles is governed by the balance between attractive (localized excess of hydrophobic attraction) and repulsive forces (static repulsion) (Lucey, 2002). This theory can be supported by observations that the dissociation of CCP by acidification at low temperature does not disrupt the micelle structure (Dalgleish & Law, 1988; Lucey, Dick, Singh, & Munro, 1997).

Recently, Dalgleish et al. (2004) obtained pictures of casein micelles with much better resolution through the use of field emission scanning electron microscopy. They proposed that the caseins in the micelle are not organised into spherical sub-micelles but into tubular structures that protrude outside the micellar surface. Their images also show the micellar surfaces without a hairy coating and they suggest that the  $\kappa$  caseins may be situated on the tubular protrusions.

The importance of  $\kappa$ -caseins in retaining the globular structure of casein micelles is well documented. Structural understanding of  $\kappa$ -caseins has been attempted (Creamer, Plowman, Liddell, Smith, & Hill, 1998). At the natural pH of milk, 6.7-6.9,  $\kappa$ -casein has been widely postulated to occupy key positions on the surface of

casein micelles to prevent casein aggregation via electrostatic and steric repulsion (Holt & Home, 1996; Creamer et al., 1998; Dickinson, 1999; Vasbinder et al., 2003).

The de-stabilization of casein micelles is thought to be associated with either the dissociation of  $\kappa$ -caseins from the micelles (Anema & Li, 2003), or the collapse of the hairy  $\kappa$ -casein layers. This results in the loss of the repulsive barrier causing the micelle particles to come together under Van der Waals forces. These interactions between the casein micelles can be described by an adhesive hard sphere (AHS) model, where the inter-molecular potential is characterised by a short ranged attraction preceding a steep repulsion (de Kruif, 1998, 1999).

Aggregation of micelles can also take place. Several different treatments may lead to the aggregation of the micelles. If the cause is a change in environment, such as pH or salt content, the lack of stability usually can be explained in terms of colloid science; the aggregation can be reversed by restoring the original environment. Aggregation may also be caused by permanent chemical changes in the casein micelles, such as renneting and age gelation.

The stability of the micelles correlates well with their voluminosity, where a higher voluminosity means great stability. This is because a higher volume may correspond with a more extensive hairiness, hence a stronger steric repulsion. The stability also depends on casein composition, markedly increasing with increasing proportion of  $\kappa$ -casein. Other factors which can influence the stability of casein micelles include salt composition, pH and heat treatment.

#### **A.1.2.2 Whey proteins**

Whey proteins are highly nutritive and stable in mildly acidic conditions (Ibrahim, Kobayashi, & Kato, 1993).  $\beta$ -lactoglobulin is the most abundant whey protein in bovine milk accounting for 50% of the total whey protein (Gallagher, Lynch, & Mulvihill, 1996; Croguennec, O'Kennedy & Mehra, 2004).

$\beta$ -lactoglobulin is a small globular protein that is soluble in dilute salt solution. It occurs in two natural variants,  $\beta$ -lg A and  $\beta$ -lg B.  $\beta$ -lactoglobulin consists of 162 amino acid residues that fold up into an eight stranded, antiparallel  $\beta$ -barrel (Kontopidis, Holt, & Sawyer, 2004).  $\beta$ -lactoglobulin contains two disulphide (-SS-) and a free thiol group (-SH-) at CYS121 which become available upon denaturation of the protein (Papiz et al., 1986; Iametti, de Gregori, Vecchio, & Bonomi, 1996).

Heating above 70°C results in the denaturation of whey proteins, where the tertiary structure is broken and the globular protein is unfolded (Anema & McKenna, 1996; Dannenberg & Kessler, 1998). The rate of denaturation has been studied extensively, which can vary between a first order reaction (Reddy et al., 1999) to a 1.5 order (Dannenberg & Kessler, 1988) to a second order reaction (Lyser, 1969) depending on the system and the heating conditions.

The denaturation process is often irreversible due to permanent chemical interactions between the exposed thiol groups to form strong covalent disulfide bonds (Hill et al., 1996; Vasbinder et al., 2004), which can form soluble whey protein aggregates or be associated with the casein micelles via  $\kappa$ -casein to yield whey protein coated casein micelles (Singh & Fox, 1987; Jang & Swaisgood, 1989; Oldfield, Singh, & Taylor, 1998; Anema, Lowe, & Li, 2004). Interestingly, denaturation of porcine  $\beta$ -lactoglobulin, which does not contain free thiol groups, is fully reversible (Burova, Grinberg, Visschers, Grinberg, & de Kruif, 2002).

### **A.1.3 References**

1. Anema, S. G., & Li, Y. (2003). Association of denatured whey proteins with casein micelles in heated reconstituted skim milk and its effect on casein micelle size. Journal of Dairy Research, 70, 73-83.
2. Anema, S. G., Lowe, E. K., & Li, Y. (2004). Effect of pH on the viscosity of heated reconstituted skim milk. International Dairy Journal, 14, 541-548.
3. Burova, T. V., Grinberg, N. V., Visschers, R. W., Grinberg, V. Ya., & de Kruif, W. H. (2002). Denaturation of porcine  $\beta$ -lactoglobulin: effect of pH and heating conditions. Journal of Dairy Science, 85, 100-106.

- C. G. (2002). Calorimetric study of porcine  $\beta$ -lactoglobulin at different pH. European Journal of Biochemistry, *269*, 3958-3968.
4. Creamer, L. K., Plowman, J. E., Liddell, M. J., Smith, M. H., & Hill, J. P. (1998). Micelle stability:  $\kappa$ -casein structure and function. Journal of Dairy Science, *81*, 3004-3012.
  5. Curley, D. M. , Kumosinski, T. F., Unruh, J. J., & Farrell, H. M. Jr. (1998). Changes in the secondary structure of bovine casein by Fourier transform infrared spectroscopy: Effects of calcium and temperature. Journal of Dairy Science, *81*, 3154-3162.
  6. Dalgleish, D. G., & Law, J. R. (1988). pH induced dissociation of casein micelles. 1. Analysis of liberated caseins. Journal of Dairy Research, *55*, 529-538.
  7. Dalgleish, D. G., Spagnuolo, P. A., & Goff, H. D. (2004). A possible structure of the casein micelle based on high-resolution field-emission scanning electron microscopy. International Dairy Journal, *14*, 1025-1031.
  8. Dannenberg, F., & Kessler, H. G. (1998). Reaction kinetics of the denaturation of whey proteins in milk. Vol. 53(1), 258-263.
  9. de Kruif, C. G. (1998). Supra-aggregates of casein micelles as a prelude to coagulation. Journal of Dairy Science, *81*, 3019-3028.
  10. de Kruif, C. G. (1999). Casein micelle interactions. International Dairy Journal, *9*, 183-188.
  11. Dickinson, E. (1999). Caseins in emulsion: interfacial properties and interactions. International Dairy Journal, *9*, 305-312.
  12. Gallagher, D. P., Lynch, M. G., & Mulvihill, D. M. (1996). Porcine beta-lactoglobulin does not undergo thermally induced gelation. Journal of Dairy Research, *63*, 479-482.
  13. Hansen, S., Bauer, R., Lomholt, S. B., Quist, K. B., Pedersen, J. S., & Mortensen, K. (1996). Structure of casein micelles studied by small-

- angle neutron scattering. European Biophysics Journal, 24, 143-147.
14. Hayes, M. G. , & Kelly, A. L. (2003). High pressure homogenisation of raw whole bovine milk (a) effects on fat globule size and other properties. Journal of Dairy Research, 70, 297-305.
  15. Hill, J. P., Boland, M. J., Creamer, L. K., Anema, S. G., Otter, D. E., Paterson, G. R., Lowe, R., Motion, R. L., & Thresher, W. C. (1996). Effect of the Bovine b-lactoglobulin phenotype on the properties of b-lactoglobulin, milk composition and dairy products. 281-294.
  16. Holt, C. (1992). Structure and stability of bovine casein micelles. Advance Protein Chemistry, 43, 63-151.
  17. Holt, C. (1998). Casein micelle substructure and calcium phosphate interactions studied . Journal of Dairy Science, 81, 2994-3003.
  18. Holt, C., & Home, D. (1996). The hairy casein micelle: evolution of the concept and its implications for dairy technology. Netherland Milk Dairy Journal, 50, 85-111.
  19. Home, D. S. (1998). Casein interactions: Casting light on the Black Boxes, the structure in dairy products. International Dairy Journal, 8, 171-177.
  20. Houlihan, A. V., Goddard, P. A., Nottingham, S. M., Kitchen, B. J., & Masters, C. J. (1992). Interactions between the bovine milk fat globule membrane and skim milk components on heating whole milk. Journal of Dairy Research, 59, 187-195.
  21. Iametti, S., de Gregori, B., Vecchio, G., & Bonomi, F. (1996). Modifications occur at different structural levels during the heat denaturation of  $\beta$ -lactoglobulin. European Journal of Biochemistry, 237, 106-112.
  22. Ibramhim, H. R., Kobayashi, K. K., & Kato, A. (1993). Improvement of the surface functional properties of b-lactoglobulin and a-lactalbumin by heating in a dry state. Bioscience Biotechnology and Biochemistry. 57(9), 1549-1552.

23. Jang, H. D., & Swaisgood, H. E. (1989). Disulfide bond formation between thermally denatured  $\beta$ -lactoglobulin and  $\kappa$ -casein in casein micelles. Journal of Dairy Science, 900-904.
24. Jensen, R. G. (2002). The composition of bovine milk lipids: January 1995 to December 2000. Journal of Dairy Science, 85, 295-350.
25. Kim, H. H. Y., & Jimenez-Flores, R. (1995). Heat-induced interactions between the proteins of milk fat globule membrane and skim milk. Journal of Dairy Science, 78, 24-35.
26. Kirchmeier, O. (1973). Arrangement of Components, Electric Charge and Interaction Energies of Casein Particles. Netherlands Milk and Dairy Journal, 27(2/3), 191-198.
27. Kontopidis, G., Holt, C., & Sawyer, L. (2004).  $\beta$ -lactoglobulin: Binding properties, structure and function. Journal of Dairy Science, 87, 785-796.
28. Lee, S. J., & Sherbon, J. W. (2002). Chemical changes in bovine milk fat globule membrane caused by heat treatment and homogenisation of whole milk. Journal of Dairy Research, 69, 555-567.
29. Lucey, J. A. (2002). Formation and Physical Properties of Milk Protein Gels. Journal of Dairy Science, 85( 2), 281-294.
30. Lucey, J. A., Dick, C., Singh, H., & Munro, P. A. (1997). Dissociation of Colloidal Calcium Phosphate-Depleted Casein Particles as Influenced by Ph and Concentration of Calcium and Phosphate. Milchwissenschaft- Milk Science International, 52(11), 603-606.
31. Lucey, J. A. , Johnson, M. E., & Home, D. S. (2003). Perspectives on the basis of the rheology and texture properties of cheese. Journal of Dairy Science, 86, 2725-2743.
32. Marchesseau, S., Mani, J.-C., Martineau, P., Roquet, F., Cuq, J.-L., & Pugniere, M. (2002). Casein interactions studies by the surface plasmon resonance technique. Journal of Dairy Science, 85, 2711-2721.

33. Mather, I. H. (2000). A review and proposed nomenclature for major proteins of the milk fat globule membrane. Journal of Dairy Science, **83**, 203-247.
34. McCrae, C. H., & Muir, D. D. (1991). Effect of surface protein concentration on the heat stability of systems containing homogenised fat globules from recombined milk. International Dairy Journal, **89**-100.
35. McMahon, D. J., & McManus, W. R. (1998). Rethinking casein micelle structure using electron microscopy. Journal of Dairy Science, **81**, 2985-2993.
36. Michalski, M. C., Cariou, R., Michel, F., & Garniert, C. (2002). Native vs. damaged milk fat globules: Membrane properties affect the viscoelasticity of milk gels. Journal of Dairy Science, **85**, 2451-2461.
37. Oldfield, D. J., Singh, H., & Taylor, M. W. (1998). Association of Beta-Lactoglobulin and Alpha-Lactalbumin With the Casein Micelles in Skim Milk Heated in an Ultra-High Temperature Plant. International Dairy Journal, **8**(9), 765-770.
38. Papiz, M. Z., Sawyer, L., Eliopoulos, E. E., North, A. C. T., Findlay, J. B. C., Sivaprasadarao, R., Jones, T. A., Newcomer, M. E., & Kraulis, P. J. (1986). The structure of  $\beta$ -lactoglobulin and its similarity to plasma retinol-binding protein. Nature, **324**, 383-385.
39. Rasmussen, L. K., Johnsen, L. B., Tsiara, A., Sorensen, E. S., Thomsen, J. K., Nielsen, N. C., Jakobsen, H. J., & Petersen, T. E. (1999). Disulphide-linked caseins and casein micelles. International Dairy Journal, **9**, 215-218.
40. Schmidt, D. G. (1982). Association of Caseins and Casein Micelle Structure. Developments in Dairy Chemistry, **1**, 61-86.
41. Schorsch, C., Jones, M. G., & Norton, I. T. (2002). Micellar casein gelation at high sucrose content. Journal of Dairy Science, **85**, 3155-3163.
42. Sharma, S. K., & Dalgleish, D. G. (1994). Effect of heat treatments on the

incorporation of milk serum proteins into the fat globule membrane of homogenised milk. Journal of Dairy Research, 61, 375-384.

43. Singh, H. (2004). Heat stability of milk. International Journal of Dairy Technology, 57(2-3), 111-119.
44. Singh, H., & Fox, P. F. (1987). Heat stability of milk: role of  $\beta$ -lactoglobulin in the pH-dependent dissociation of micellar  $\kappa$ -casein. Journal of Dairy Research, 54, 509-521.
45. Singh, H., Ye, A., & Havea, P. (2000). Milk protein interactions and functionality of dairy ingredients. The Australian Journal of Dairy Technology, 55, 71-77.
46. Slattery, C. W. (1976). Casein micelles structure; an examination of models. Journal of Dairy Science, 1545-1556.
47. Slattery, C. W., & Evard, R. (1973). A model for the formation and structure of casein micelles from subunits of variable composition. Biochim. Biophysics Acta, 317, 529-538.
48. Grotenhuis, E. T., Tuinier, R., & de Kruif, C. G. (2003). Phase stability of concentrated dairy products. Journal of Dairy Science, 86, 764-769.
49. Vasbinder, A. J., Rollema, H. S., Bot, A., & de Kruif, C. G. (2003). Gelation mechanism of milk as influenced by temperature and pH; studied by the use of transglutaminase cross-linked casein micelles. Journal of Dairy Science, 86, 1556-1563.
50. Vasbinder, A. J., van de Velde, F., & de Kruif, C. G. (2004). Gelation of casein-whey protein mixtures. Journal of Dairy Science, 87, 1167-1176.
51. Walstra, P. (1979). The Voluminosity of Bovine Casein Micelles and Some of Its Implications. Journal of Dairy Research, 46(2), 317-323.
52. Walstra, P. (1990). On the Stability of Casein Micelles. Journal of Dairy Science, 73(8), 1965-1979.

53. Walstra, P. (1999). Casein sub-micelles: do they exist? International Dairy Journal, 9, 189-192.
54. Walstra, P., & Jenness, R. (1984). Dairy Chemistry and Physics. New York: John Wiley.
55. Ye, A., Singh, H., Oldfield, D. J., & Anema, S. (2004). Kinetics of heat-induced association of  $\beta$ -lactoglobulin and  $\alpha$ -lactalbumin with milk fat globule membrane in whole milk. International Dairy Journal, 14, 389-398.

## **A.2 Time-dependent rheology: Thixotropy review**

Rheology is the study of the flow and deformation of matter (Borwankar, 1992; Lapasin & Pricl, 1995; Ma & Barbosa-Canovas, 1995; Fellows, 2000) i.e. the study of the internal response of materials to external applied forces (Cheremisinoff, 1993).

Time-dependent rheology is the most complex aspects of rheology and progress in this field has been reviewed regularly (Mewis, 1979; Cheng, 1987; Barnes, 1997). This review will concentrate on time-dependent rheology, covering three main aspects: definition and characterisation of thixotropy, modelling and rheometry. It is important to note that thixotropy is a subset of time-dependent behaviour, where the material displays shear thinning but time-dependent characteristics.

Rheological data are needed in the food industry for two main reasons:

- They directly affect the transport of heat, mass and momentum in unit operations and are required for the design of food manufacturing processes and equipment (Peeples, Gould, Jones, & Harper, 1962; Steffe, Mohamed, & Ford, 1984; Mohamed & Steffe, 1985; Dodeja, Sarma, & Abichandani, 1990; Carreau, Chhabra, & Cheng, 1993; Bhamidipati & Singh, 1995),
- Rheological behaviour is directly related to food structure. As such it correlates well with the texture and sensory properties of food and can be used for quality control

### **A.2.1 Strain and stress**

Stress and strain are two rheological terms which deal with the force applied and the resultant deformation respectively.

Stress is defined as a force per unit area, and expressed in Pascals ( $\text{N/m}^2$ ). Stress can be tensile (stretching force), compressive (compression) or shear (tangentially to a surface area). Tensile and compressive forces act perpendicularly to the surface area, i.e. normal forces. Shear force acts in parallel direction to the surface area (Steffe, 1992).

Strain is the measure of the deformation of a system. The strain rate (often called the shear rate in liquid rheology) is defined as the rate of change of strain.

### **A.2.2 Rheological models**

Rheological behavior is often analyzed through the use of a flow curve or rheogram, where the shear stress is plotted against the shear rate (Cheremisinoff, 1993). This plot is commonly used to describe the relationship between the two variables, which can be mathematically modelled using various functional relationships. Modelling is a powerful tool to represent and summarise a large quantity of data into a single equation where possible, and allows prediction of system behaviour. All liquid food systems fit one of two rheological model groups, Newtonian or non-Newtonian.

#### **A.2.2.1 Newtonian fluids**

Newtonian fluids have a straight line relationship between shear stress and shear rate with a zero intercept (Steffe, 1992), which can be expressed mathematically as

$$\tau = \mu \dot{\gamma} \quad (\text{A.1})$$

where  $\mu$  is the constant of proportionality, with the unit of Pascal-seconds (Pa.s).

$\tau$  shear stress in Pa

$\dot{\gamma}$  shear rate  $\text{s}^{-1}$

All fluids that do not exhibit this behaviour are called non-Newtonian.

The viscosity is dependent on temperature, and follows the well-known Arrhenius equation

$$\ln \mu = \frac{B}{T} + C \quad (\text{A.2})$$

where B and C are empirical constants and T is temperature in degree Kelvin. Thus an increase in temperature results in a decrease in viscosity.

### A.2.2.2 Non-Newtonian Time-independent fluids

The viscosity of many real fluids systems is not constant, but is a function of shear rate or shear stress applied. The apparent viscosity for non-Newtonian fluids has a precise definition. It is shear stress divided by shear rate (Steffe, 1992)

$$\mu_{app} = \frac{\tau}{\dot{\gamma}} \quad (A.3)$$

A plot of apparent viscosity curves for various non-Newtonian time-independent fluids is shown in Figure A.2. For Newtonian fluids, the apparent viscosity remains constant with shear. For non-Newtonian fluids, the apparent viscosity can either increase (shear thickening) or decrease (shear thinning) with an increase in shear.

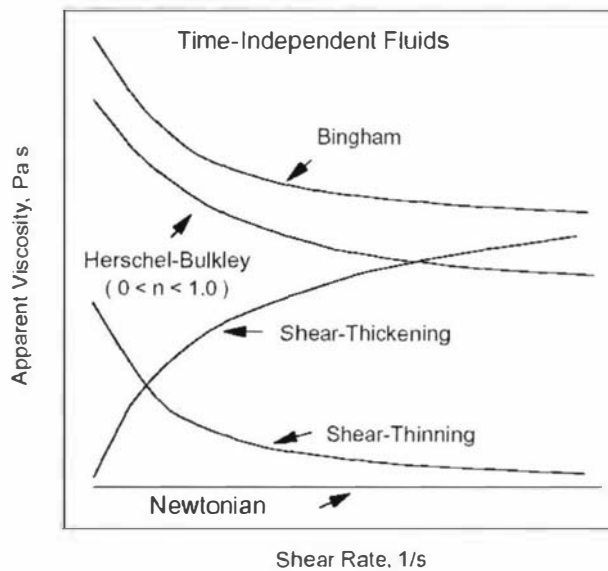


Figure A.2: Apparent viscosity of time-independent fluids (Steffe, 1992).

This illustrates the fundamental flaw in comparing rheological behaviour based on data obtained at just one shear rate value. In Figure A.2, if a single point test of two different fluids was carried out at the intersection between the shear thinning and thickening curves, the same viscosity would be obtained, indicating similar behaviour.

This is obviously wrong, as the two curves represent very different viscosity-shear rate behaviour. Thus, numerous data points across the shear range are required to evaluate the flow behaviour of non-Newtonian fluids.

For non-Newtonian fluids, there are many relationships that describe the relationship between shear stress and shear rate, from which viscosity values are obtained. Most of these non-Newtonian models are empirical models which were developed by fitting mathematical equations to experimental data.

A commonly used non-Newtonian time-independent model is the Herschel-Bulkley model (Herschel & Bulkley, 1926).

$$\tau = \tau_y + K(\dot{\gamma})^n \quad (\text{A.4})$$

where  $\tau_y$  is the yield stress (Pa)

$K$  is the consistency coefficient (Pa.s)

$n$  is the flow behaviour index (dimensionless)

Under special conditions, the Herschel-Bulkley model can be simplified into other models (Nguyen & Boger, 1992; Kokini, 1992) as summarised in Table A.1.

Table A.I: Newtonian, power law and Bingham plastic fluids as special cases of the Herschel-Bulkley model (Steffe, 1992).

Fluid	$K$	$n$	$\tau_y$
Herschel-Bulkley (Herschel & Bulkley, 1926)	$>0$	$0 < n < \infty$	$>0$
Newtonian	$>0$	1	0
Power law shear-thinning (pseudoplastic)	$>0$	$0 < n < 1$	0
Power law shear-thickening (dilatant)	$>0$	$1 < n < \infty$	0
Bingham plastic (Bingham, 1922)	$>0$	1	$>0$

Both the Herschel Bulkley and the Bingham plastic models incorporate a yield stress, which represents a minimum shear stress (force) required to induce flow. Below this value, the material exhibits solid-like characteristics. The topic of yield stress will be discussed in further detail in section 5. Halmos & Tiu (1981) and Dervisoglu & Kokini (1986) noted that the Bingham plastic model can be used to describe a Herschel-Bulkley fluid in the low shear rate region where Newtonian behaviour takes place, as discussed below.

In a rheogram for a typical non-Newtonian fluid, there are three distinct regions, a lower Newtonian region, a Power Law (middle) region, and an upper Newtonian region (Figure A.3). Sometimes more than one model is required to describe the complete rheological behaviour of a given system over a broad range of shear rates (Umeya, Isoda, Ishii, & Sawamura, 1969).

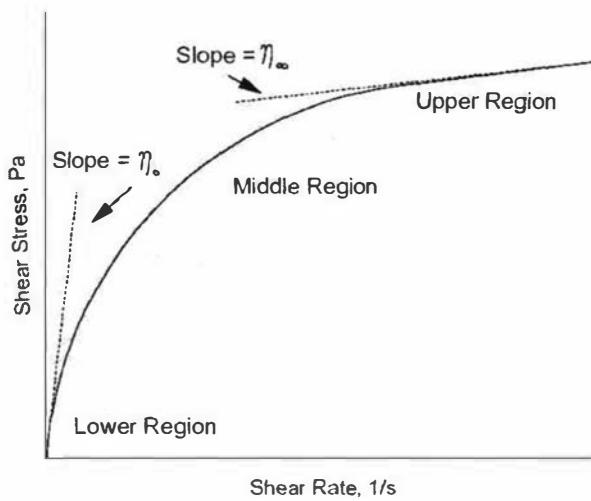


Figure A.3: Complete rheogram of idealised shear thinning behaviour (Steffe, 1992)

### A.2.2.3 Non-Newtonian Time-dependent fluids

In time dependent systems, for a given constant shear rate value, the shear stress changes with shearing time and can either decrease or increase. The rheological behaviour is dependent on the shear rate value, and more importantly on the shear history.

### A.2.3 Thixotropy

The definition of thixotropy varies widely in the literature and has changed with time. The term comes from the Greek words “thixis” (stirring or shaking) and trepo (turning or changing) (Barnes, 1997). Thixotropy was originally associated with the isothermal sol-gel transformation during storage and gel-sol transformation caused by mechanical shear (Barnes, 1997). This definition focuses on the extreme change of structure, with the transformation from liquid to solid and vice versa (Alexander, 1992). The definition assumed that the whole process is completely reversible and is practical in systems such as paint and adhesive.

In 1994, Pryce-Jones provided an alternative definition which stated that thixotropy describes “an increase of viscosity in a state of rest and a decrease of viscosity when

submitted to a constant shearing stress” (Barnes, 1997). In this definition, the change in viscosity during rest and during shearing is considered, but the change in the state of the system, either liquid or solid, is of less concern.

Kembloswki and Petera (1981) defined three conditions which a purely thixotropic system must fulfill:

- The liquid must be inelastic, i.e. unable to store internal energy without the change of entropy
- For any given shear level, when given sufficient time, the viscosity of the system will approach an equilibrium value
- The equilibrium viscosity function is monotonic.

Cheng (1987) listed five typical characteristics of thixotropic behaviour.

1. A decrease in viscosity with time under constant shear rate

- In a rested material, or
- When the shear rate is changed from a low to a high value. In this case the shear stress over shoots, and shows a steady decrease with time, until it reaches the equilibrium value (Figure A.4)

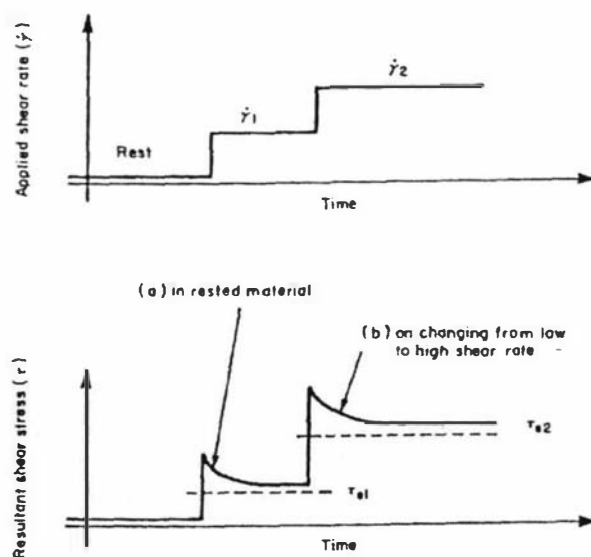


Figure A.4: Characteristics of thixotropic behaviour; decrease in shear stress or viscosity under constant shear rate. (Cheng, 1987)

2. The viscosity recovers with time

- In a material at rest, or
- When the shear rate is changed from a high to a low value. But this viscosity can be reduced again upon renewed shearing at high shear rate. (Figure A.5)

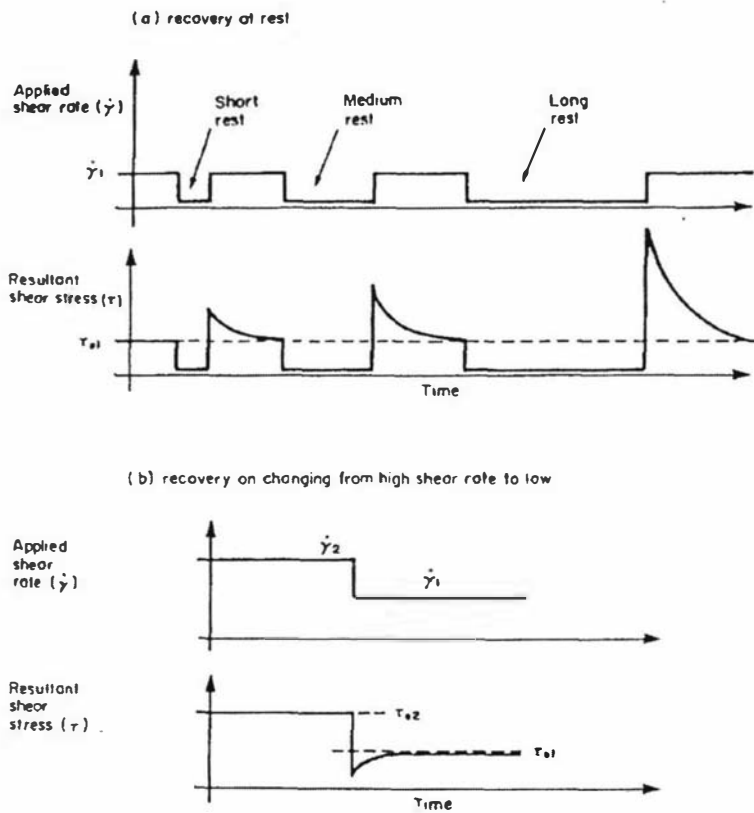


Figure A.5: Characteristics of thixotropic behaviour; shear stress or viscosity recovery. (Cheng, 1987)

3. An equilibrium flow curve is obtained when each applied shear rate is held until the shear stress attains the steady state value (Figure A.6)

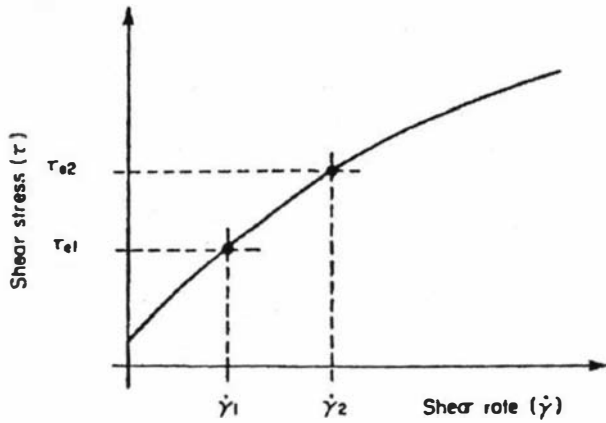


Figure A.6: Characteristics of thixotropic behaviour; equilibrium flow curve. (Cheng, 1987)

4. A hysteresis loop under cyclic shearing, ramped or oscillation

- In a rested material the first loop may show a more or less sharp peak. Subsequent loops on repeated cycling reduce in size and shift towards the shear rate axis;
- In a material that has been pre-sheared at a high shear rate, the repeated loops shift away from the shear rate axis (Figure A.7)

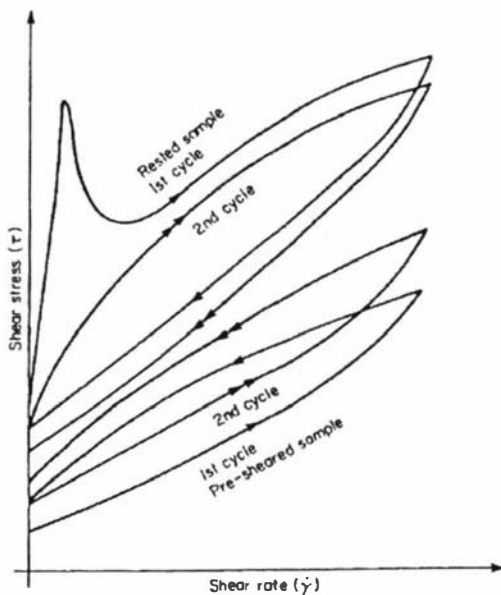


Figure A.7: Characteristics of thixotropic behaviour; hysteresis loop under cyclic shearing. (Cheng, 1987)

5. An equilibrium loop is obtained when the cyclic shearing is repeated indefinitely (Figure A.8)

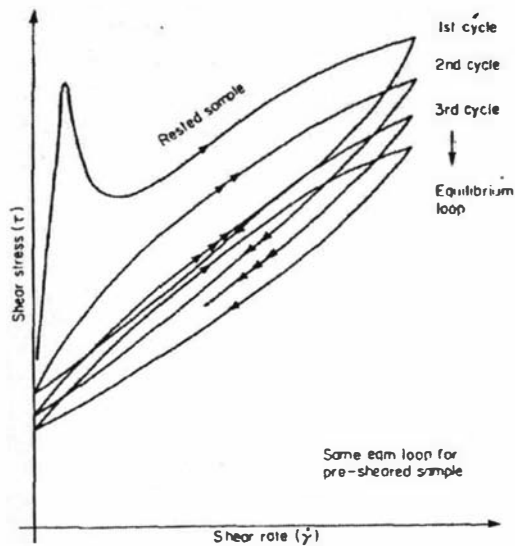


Figure A.8: Characteristics of thixotropic behaviour; equilibrium loop. (Cheng, 1987)

The peak in the first cycle is typical of the high level of shear needed to break down liquid solutions that have gelled to some extent. Such experimental observation cannot be accounted for by the definition of thixotropy of Kembloswki and Petera (1981). Thus some confusion will persist until there is a universally accepted definition of thixotropy. Time dependent behaviour, including thixotropy, arises because of the finite time required for any structural change to take place in response to an applied shear (Kembloswki & Petera, 1981; Barnes, 1994). Thus, any liquid with a microstructure can show thixotropy. It can also be said that all shear thinning materials are thixotropic, because the structure will always take a finite time to bring about change under the influence of shear. Time independent fluids simply have a very short timescale.

This brings the discussion on to the importance of the response time of the measuring instrument in comparison to the time scale of the structural changes in the system (Barnes, 1997; Quemada, 1999). If the time scale of the changes is shorter than the response time of the instrument, then any structural changes will be seen as an

instantaneous event. On the other hand, if the time scale of the changes is longer than the response time of the instrument, thixotropy can be measured where gradual changes between two structural states can be detected (Kokini, 1992; Ma & Barbosa-Canovas, 1995). A given material can behave like a solid or liquid depending on the time-scale of the applied stress (Lapasin & Priel, 1995).

A time-dependent system has a memory effect. This means that the shear history has a significant effect on the behaviour of the system (Dekee, Code, & Turcotte, 1983). The memory effect arises from the way energy is dissipated from a given system in a flow field. In the first mechanism, some energy can be stored in the system, and the elastic response is delayed by the viscous nature of the system. This is encountered in both viscoelastic solids and fluids. In the second mechanism, complete dissipation occurs and the delayed response arises from the time needed for structural changes of the material to take place (Kembloswki & Petera, 1981).

The change in structure is governed by the competition between the build up process caused by Brownian motion and in-flow collisions forces and the breakdown process caused by shear (Kembloswki & Petera, 1981; Barnes, 1994, 1997; Yziquel, Carreau, Moan, & Tanguy, 1999). The breakdown process actually involves two opposing processes. Shear force will break down the bonds interlinking the structural elements, as well as induce collisions of separated units to reform such bonds (Mujumdar, Beris, & Metzner, 2002).

It is possible for Brownian motion to cause break up of structural elements. In such situation, anti-thixotropy occurs (Barnes, 1997).

At rest, Brownian motion is the only rebuilding force present, which is usually much smaller than the shearing forces (Barnes, 1997). Thus, rebuilding can take a long time for the particles to rearrange and move into the most favourable position and structure.

Thixotropy is more pronounced in systems containing non-spherical particles as they have to find themselves in the best 3D structure by rotational as well as translational movement. The changes in the structure can be visualised with the aid of Figure A.9

from Barnes (1997), which plots a shear sweep curve overlaying a structural diagram. The dark line represents the equilibrium flow curve where the shear stress was allowed sufficient time to reach a constant equilibrium value for every shear rate. On this equilibrium flow curve, the equilibrium structure breaks down with an increase in shear rate. At a high enough shear value, the structure is broken down into its separate constituent primary particles.

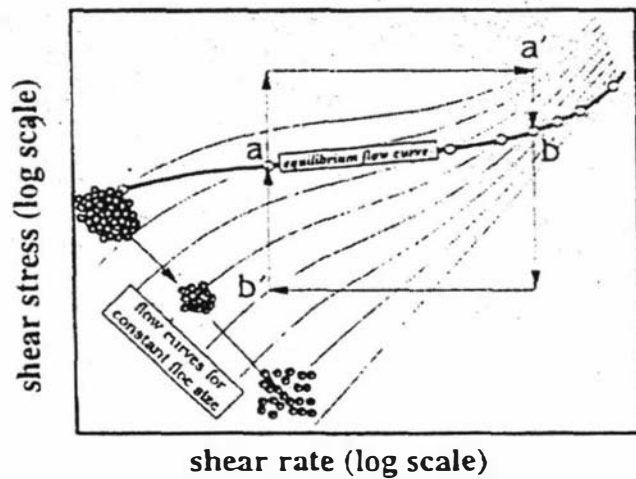


Figure A.9: Microstructure and flow curves of a flocculated suspension. (Barnes, 1997)

It is important to realise that the rate of break down and build up are different. The breakdown process occurs in a short period of time, from seconds to a few minutes depending on the system and shear rate level. The build-up process is much longer and can take hours to days and weeks. This is attributed to the small kinetic energy from Brownian motion available to the particles.

Shear changes the internal morphology of flocs, as well as breaking them down. Flocs consist of particles attracted to one other as well as entrapped liquid. Thus, when the flocs are deformed, the viscous dissipation within them has also to be taken into account.

When the flocs are big, the internal contribution to viscous energy is significant and includes the energy required to break or make the floc aggregates, flocs and flocculi,

stretching of bonds within the flocs, and viscous dissipation due to movement of particles through, and flow in, the occluded liquid (Cheng, 1987).

Particle size and distribution also have significant effects on the rheological behaviour. Small particles are less deformable which can affect the way they are packed in flocs (Barnes, 1994).

All of the above discussion is based on a very important assumption of a completely reversible recovery process. This has two consequences:

- For any given shear rate, there is only one equilibrium shear stress value.
- The use of an equilibrium state removes the effect of shear history

The development of rheological models is simplified significantly because of this assumption, as the shear history can be removed. Of course, the complete reversible recovery of structural changes is only applicable to a few classes of materials, such as clay (Alessandrini, Lapasin, & Sturzi, 1982).

The characterisation of thixotropy is essentially based on the measurement of viscosity changes with shear rate and time. In real time-dependent fluids, the formation and break down of structure in the dispersed phase is often accompanied by two other important phenomena, viscoelasticity and the presence of a yield stress. These phenomena are normally studied at low shear rates.

#### **A.2.3.1 Viscoelasticity**

Gelation is often monitored using dynamic oscillatory measurement techniques. The sample shear is varied sinusoidally with time and the deformations are kept small to keep the data in the linear viscoelastic range, where the strain is linearly dependent on the applied stress. For a viscoelastic system, the in-phase stress is related to the elastic response, while the out of phase stress is the viscous part (Hamley, 2000). If the frequency of deformation is  $\omega$  and time is  $t$ , the stress can be determined as follows

$$\tau = \tau'_o \sin \omega t + \tau''_o \cos \omega t \quad (\text{A.5})$$

Two shear moduli can be determined for the in phase ( $G'$ ) and out of phase ( $G''$ ) components.

$$G' = \frac{\tau'_o}{\gamma_o} \quad (\text{A.6})$$

$$G'' = \frac{\tau''_o}{\gamma_o} \quad (\text{A.7})$$

The two shear moduli are more commonly referred to as the storage modulus ( $G'$ ) and the loss modulus ( $G''$ ) (Hamley, Hamley, 2000; Curcio et al., 2001; Bower, 2002).

The loss tangent,  $\tan \delta$  (used to evaluate the gelling point, e.g. Curcio et al., 2001), which is defined as

$$\tan \delta = \frac{G''}{G'} \quad (\text{A.8})$$

where  $G''$  is the loss modulus, viscous properties

$G'$  is the storage modulus, elastic properties

Gelation could be evaluated as the point at which the loss tangent does not depend on frequency (Curcio et al., 2001). A typical plot of  $G'$ ,  $G''$  and  $\tan \delta$  with testing time is shown in Figure A.10. The second cross over point between the  $G'$  and  $G''$  can be considered a coagulation time which marks the transition from liquid-like to solid-like behaviour without invoking the onset of a gel (Lapasin & Prich, 1995). Ozer et al. (1998) provided an alternative method to define the gelling point, which is the time in minutes to attain a  $G'$  of 10 Pa.

$G'$  and  $G''$  become non-linear at larger strains as the frequency is increased. Beyond the linear region,  $G' < G''$ , the material becomes more dominantly viscous (Benezech & Maingonnat, 1994).

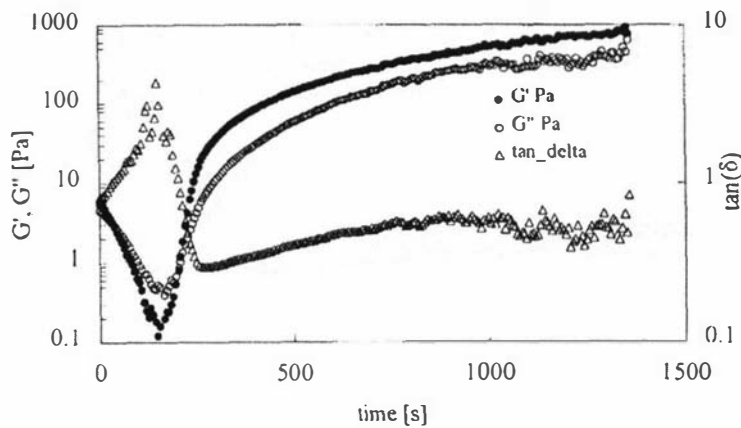


Figure A.10: A typical plot of  $G'$ ,  $G''$  and  $\tan \delta$ . (Curcio, et. al. 2001)

### A.2.3.2 Yield Stress

#### A.2.3.2.1 Definition

The yield stress is an important variable in industrial applications. A well recognised definition of yield stress is the minimum stress required to initiate permanent deformation in a given system (Dzuy & Boger, 1983, 1985; Cheng, 1984a; Hannote, Flores, Torres, & Galindo, 1991). When a stress less than the yield stress is applied, no permanent deformation takes place, i.e. no flow. On exceeding the yield stress, flow occurs (Bames & Walters, 1985). The yield stress is a measurement of the network structure, and the strength required to break this structure into elements that can be deformed under shear (Mewis, 1979).

Bames and Walters (1985) derived two new definitions, dynamic and static yield stresses. The dynamic yield stress is obtained from extrapolating flow curve data that has been obtained at equilibrium position, i.e. when the system was allowed to reach constant shear stress for a given shear rate level. The static yield stress is acquired after prolonged storage. The static yield stress can be higher than the dynamic yield stress in many cases. The static yield stress is more applicable in start up situations,

while the dynamic yield stress would be more appropriate for continuous flow applications (Barnes & Walters, 1985). The static yield stress has been sometimes referred as gel strength (Goodrich, Yoshimura, & Prudhomme, 1989; Keating & Hannant, 1989; Zhou, Solomon, Scales, & Boger, 1999).

There are many more definitions of yield stress that have been derived over the years; (Houwink, 1958; Dzuy & Boger, 1983; Evans, 1992; Schurz, 1992; Spaans & Williams, 1995).

#### **A.2.3.2.2 Yield stress measurement techniques**

There are three schools of thought regarding the measurement of yield stress: extrapolation of the flow curve to zero shear rate intercept, direct measurement at extremely low shear rates and curve fitting with rheological models with a yield stress (Lang & Rha, 1981; Dzuy & Boger, 1983; Hannote et al., 1991; Nguyen & Boger, 1992).

Under the classical definition of the yield stress as the minimum stress required to initiate permanent deformation, proof experiments would need to be carried out for infinite time to show that the shear rate at any given stress is actually zero (Evans, 1992). For example, Hartnett and Hu (1989) showed that a 3.2 mm diameter nylon ball with a density of  $1.16 \text{ g/cm}^3$  did not move by a measurable distance after 3 months of observation when immersed into a Carbopol solution. They believed that the yield stress is an engineering reality. However, they admitted that if given more time, a measurable deformation distance may have been obtained. Thus, patience of the experimenter becomes the bottle neck of the experiment (Spaans & Williams, 1995).

There are several methods that have been devised for direct measurement of yield stress. However, each technique has its own definition of yield stress, limitations and sensitivity (Nguyen & Boger, 1992). Techniques that approach the yield stress from below eliminate the effect of shear history. This means the shear stress is progressively increased to and above the yield stress. In this low region, only

reversible deformation takes place and thus shear history does not play a role in determining the rheological behaviour. These techniques include creep/recovery, stress growth and vane method. However, in methods such as stress relaxation and incline-plane tests, the fluid structure is permanently damaged by the preshearing actions. These tests are only suitable for time-independent systems.

The value of the yield stress is highly dependent on the equipment used and the testing parameters applied (Lang & Rha, 1981; Barnes & Walters, 1985; Yoshimura, Prud'homme, Princen, & Kiss, 1987; Chilton, Stainsby, & Thompson, 1996). Barnes and Walters (1985) pointed out that the yield stress is a time dependent property, and is dependent on two time scales, the elapsed time between the application of stress and the start of the observation period, and also the duration of the observation period itself. Thus, the yield stress does not have a unique value. Schurz (1992) proposed the use of an "apparent yield stress" which is dependent on the measuring time and the lowest accessible shear rate.

The use of data in the low shear region will be in danger of suffering wall slip and other defects during measurements (Wildemuth & Williams, 1985; Magnin & Piau, 1990). Slips are typically encountered in concentrated suspensions when the stresses are below the yield stress (Nguyen & Boger, 1992). During flow, breakdown of fluid structure can take place where the suspended particles move away from the wall region, leaving a low viscosity thin lubricating which forms a lubricating layer adjacent to the wall (Cokelet, Merrill, & Gilliland, 1963; Cheng, 1984a; Muller-Mohnssen, Weiss, & Tippe, 1990; Kokini, 1992; Nguyen & Boger, 1992). This effect can be negated by having rough surfaces on the inside of the capillary tubes (Nguyen & Boger, 1983). Independent analysis of the reliability of rheology data at low shear level for a given rheometer is imperative before any extrapolation can be carried out (Nguyen & Boger, 1992).

Whether a true yield stress exists or not, the presence of a marked change in rheological behaviour in the region of critical stress has been widely observed, e.g. (Nagase & Okada, 1986; Keating & Hannant, 1989; Hannote et al., 1991; Moore, Cossor, & Baker, 1995). Yield stress plays important roles in processes where some form of start up in flow is encountered, such as drilling (Jones & Hughes, 1996),

mixing (Moore et al., 1995) and pumping (Dzuy & Boger, 1983; Chilton et al., 1996). The determination of the critical stress region at the appropriate shear level as that encountered in practical applications would be of more importance than the definition of the true yield stress where greater accuracy is not required (Charm, 1963; Barnes & Walters, 1985).

As it is difficult to measure the shear stress at zero shear rate, extrapolation from the lowest shear rate value used in an experiment is commonly employed (Barnes & Walters, 1985). For non-linear data flow curves, the prediction of yield stress through extrapolation depends on the accuracy of the lowest shear rate measurement. Thus, an instrument with a lower reliable operating shear level would produce a lower yield stress value. This prompted Cheng (1984a) to argue that the yield stress is a myth, and given accurate enough measurements no yield stress will be observed, and that a second Newtonian plateau will be observed at low shear rates. The use of extrapolation techniques would mean that the yield stress is a model parameter, not a physical description of the system (Hannote et al., 1991; Nguyen & Boger, 1992).

The yield stress can also be estimated by fitting the experimental flow curve with a rheological model that includes a yield stress, such as the Herschel-Bulkley and the Casson models. The accuracy of the yield stress estimation is defined not only by the reliability of the rheological data, but also on the number of points and the shear range covered, in particular the lower shear rates range.

Astarita (1990) summarized the confusion about the existence of yield stress with a simple question. "What are a measurable distance and a practical time scale? Acknowledging the importance of the "practical time scale", Scott Blair (1933) and Coussot and Boyer (1995) required the yield stress to be observed during "usual experiments" which correspond to the conditions of practical applications.

There are still many arguments whether or not the yield stress exists as a well defined quantity (Doraiswamy et al., 1991) or whether the yield stress is nothing more than a fitted parameter in a rheological model. Thus the yield stress remains a controversial field of study because of the disagreement in the meaning of the term, and the

methods of measurement required in order to obtain an accurate value (Barnes & Walters, 1985; Evans, 1992).

#### **A.2.4 Rheological modelling**

Rheological models can be classified into one of three categories (Alessandrini et al., 1982; Nagase & Okada, 1986; Barnes, 1997), depending on the level of detail in the analysis of the structure of the system.

1. Structural models can be further subdivided into two groups
  - The first group includes those which attempt to derive some direct descriptions of the transient change of microstructure.
  - The second group analyses the change in structure as a whole, and a lumped structural parameter,  $\lambda$ , is introduced.
2. Empirical models of time dependency based on rheological data, such as shear stress-shear rate, as well as viscosity data.
3. Dynamic models, where the structure of the systems is described through detailed analysis of inter-particle forces

Dynamic models attempt to analyse structural changes from fundamental understanding, arising from simple physics of attraction and repulsive forces and statistical analysis. Many workers further attempt to explain these forces in terms of the chemical and thermodynamic behaviour of the components that make up the product.

##### **A.2.4.1 Structural Models**

Structural models deal with the relationship between rheological parameters measured and the evolution of the dispersed phase structure as a whole but do not investigate in detail the inter-particle forces that make up the structure, as well as the interactions between the dispersed and the aqueous phases.

In direct structure theories, the models view the structure as made up of aggregates, which are formed from primary particles. The structure is discussed with reference to

the rate equation for the kinetics of aggregation and segregation. In lumped structure models, a structural parameter,  $\lambda$ , is introduced which simplifies the situation even further by collating all forces that affect the structure into one variable.

Neither the direct nor lumped structure models require a discussion of the nature of inter-particle forces or the chemical behaviour of the individual elements that make up the structure. These models are most useful for industrial applications where the key rheological parameters are required for transport analysis and design and operation of plants. They do not allow any insight into product formulation and how that may affect rheological behaviour.

#### A.2.4.1.1 Direct structural theories

The structure of a system is related to the distribution of broken and unbroken bonds (Goodeve, 1939).

$$-\frac{d(\text{unbroken})}{dt} = k_a(\text{unbroken})^n - k_b(\text{broken})^m \quad (\text{A.9})$$

where  $k_a$  is the rate constant of breakdown and depends on the amount of unbroken bonds available.  $k_b$  is assumed to be independent of shear rate, and describes the rate constant of collision leading to structural build up caused by Brownian forces.

Similarly to the above expression, (Cross, 1965) derived his model based on the assumption that a structure is made up of flocs of randomly linked chains of particles.

$$\frac{dN}{dt} = k_2 P - (k_o + k_1 \dot{\gamma}^m) N \quad (\text{A.10})$$

where  $N$  is the average number of links per chain,  $k_2$  is a rate constant describing Brownian collision.  $k_o$  and  $k_1$  are rate constants for the Brownian and shear contributions to breakdown.  $P$  is the number of single particles per unit volume, and  $m$  is a constant less than unity.

At equilibrium, i.e. when  $\frac{dN}{dt} = 0$ , the above equation becomes

$$N_e = \frac{k_2 P}{k_o \left( 1 + \frac{k_1}{k_o} \dot{\gamma}^m \right)} \quad (\text{A.11})$$

Cross assumes that viscosity is given by a constant  $\mu_\infty$  plus a viscous structural contribution proportional to the number of bonds  $N_e$

$$\frac{\mu_e - \mu_\infty}{\mu_o - \mu_\infty} = \frac{1}{1 + \frac{k_1}{k_o} \dot{\gamma}^m} \quad (\text{A.12})$$

Yziquel et al. (1999) provided an alternative method for the analysis of structural changes in time-dependent colloidal suspensions. The evolution of their structural parameter was described following three possible kinetic processes:

- Structure changes due to the rate of shear
- Structure changes associated with stored elastic energy
- Structure changes related to the rate of energy dissipated

They found that the energy-dependent model provided excellent fit to the nonlinear behaviour of concentrated suspensions. The model describes yield and thixotropic phenomena, nonlinear viscoelastic behaviour during oscillatory measurements, and overshoots observed in stress growth experiments.

#### **A.2.4.1.2 Lumped parameter structural theories**

Moore F. (1959) introduced the idea of a structural parameter  $\lambda$  with his work on ceramic slips. He assigned two extreme values to  $\lambda$  for the two extreme states of structure in a flocculated system. When the structure is fully built up, i.e. when allowed to rest until equilibrium is reached,  $\lambda = 1$ . When the structure is fully broken

down, i.e. when sheared at infinite shear and the system is allowed to reach equilibrium,  $\lambda = 0$ .

Moore F. (1959) then derived the equation of state

$$\tau = (\mu_{\infty} + c\lambda)\dot{\gamma} \quad (\text{A.13})$$

The equation of rate is given as

$$\frac{d\lambda}{dt} = g = a(1 - \lambda) - b\lambda\dot{\gamma} \quad (\text{A.14})$$

Where  $-b\lambda\dot{\gamma}$  is the rate of structural break down

$a(1 - \lambda)$  is the rate of structural build up

A negative  $g$  value indicates breakdown, while a positive value means build up. A zero value denotes equilibrium state.

It is interesting to note that in this model the build up rate is not dependent on the shear rate. This implies that the build up process is only dependent on the Brownian motion, as a shear parameter is not included in the equation. This view is agreed by some authors (Mujumdar et al., 2002) and disagreed by others who prefer to include the dependence of shear rate in the build up rate equation (Alessandrini et al., 1982).

For any given shear rate, the structure value can be evaluated by integrating equation (A.14)

$$\lambda = \lambda_{eT} - (\lambda_{eT} - \lambda_o)\exp[-(a + b\dot{\gamma}_T)t] \quad (\text{A.15})$$

The equation uses the idea of equilibrium to predict the change in structure where the system is changed from one equilibrium state to another.

Combining the equations of state (A.13) and rate (A.14), Cheng (1987) gives,

$$\tau = \left( \mu_{\infty} + \frac{a-g}{a+b\dot{\gamma}} c \right) \dot{\gamma} \quad (\text{A.16})$$

This equation incorporates the time dependent effect into the viscosity variable. The time effect is not treated as an independent variable that can be multiplied with a basic relationship at time zero to obtain the rheology data.

A contour map can be plotted to illustrate constant  $\lambda$  and constant  $g$  lines (Cheng, 1987), as shown in Figure A.11. Moore F. (1959) gave a similar plot with shear rate on the y-axis and shear stress on the x-axis. As Newtonian behaviour was assumed, all constant  $\lambda$  lines represented straight-line relationship between shear stress and shear rate.

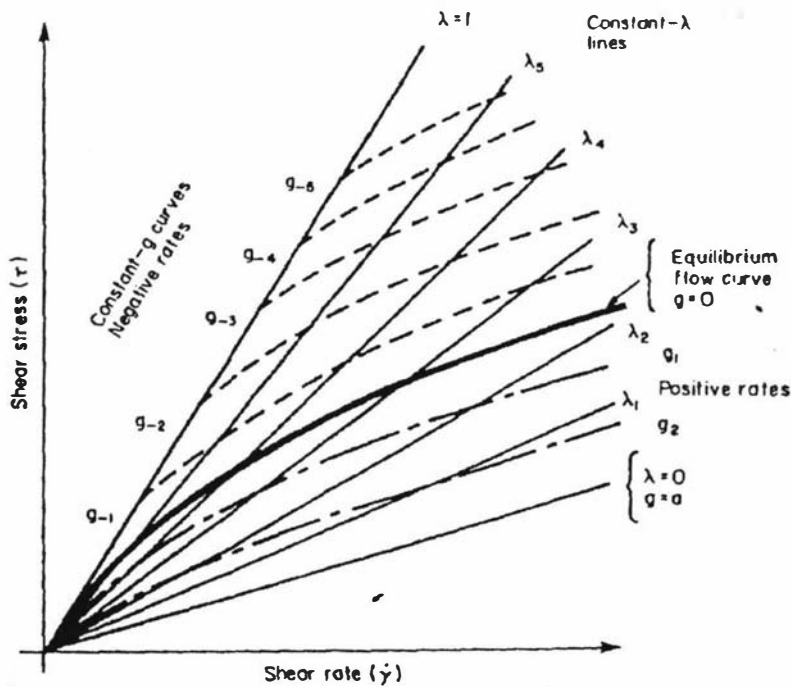


Figure A.11: Contour map of the Moore model. (Cheng, 1987).

A generalised model can be derived as follows, where no assumptions are made on the kinetics of the breakdown and build up processes (Cheng, 1987).

$$\tau = \tau(\dot{\gamma}, \lambda) \quad (\text{A.17})$$

$$\frac{d\lambda}{dt} = g(\dot{\gamma}, \lambda) \quad (\text{A.18})$$

Baravian, Quemada and Parker (1996) followed the same approach as Cheng, however, with a different relationship between viscosity and structure

$$\mu(\tau, t) = \mu(\lambda) = \frac{\mu_{\infty}}{(1 - K\lambda)^2}, \quad K = 1 - \left(\frac{\mu_{\infty}}{\mu_0}\right)^{\frac{1}{2}} \quad (\text{A.19})$$

The structural parameter can be written as

$$\lambda = \frac{1 - \left(\frac{\mu_{\infty}}{\mu}\right)^{\frac{1}{2}}}{K} \quad (\text{A.20})$$

There have been several modifications to the rate equation linking the rate of change in the structural parameter with the rates of break-down and build-up processes (Alessandrini et al., 1982; Schmitt, Ghnassia, Bimbenet, & Cuvelier, 1998; Mujumdar et al., 2002). Schmitt et al. (1998) went one step further and developed a model to predict the friction factor from viscosity flow data on yoghurt during transportation. All models were developed for fully reversible thixotropic systems due to the need of obtaining equilibrium rheological behaviour at a given shear rate to eliminate the effect of shear history (Alessandrini et al., 1982).

Tiu and Boger (1974) devised a different approach in the analysis of time dependent behaviour in their ambitious work titled “Complete rheological characterization of time-dependent food products. The equation of state was given as,

$$\tau = \lambda(\tau_y + K\dot{\gamma}^n) \quad (\text{A.21})$$

The instantaneous value of  $\lambda$  can be determined from the instantaneous apparent viscosity

$$\lambda = \frac{\mu\dot{\gamma}}{\tau_y + K\dot{\gamma}^n} \quad (\text{A.22})$$

The above equation is also valid at equilibrium with the substitution of  $\lambda_e$  and  $\mu_e$  in the appropriate locations.

On a graph of shear stress versus shear rate for mayonnaise, Tiu and Boger (1974) observed a non-linear relationship on a log-log plot. Interesting, these flow curves at different time periods of constant shear rates were almost parallel to each other. They claim that this observation suggests that the fluid systems could be described by a single rheological equation with time as a parameter, as stated in equation (A.21).

The equation treated the time dependent structural variable as an independent parameter that can be multiplied to a Herschel-Bulkley model to account for the time dependency. This equation implied that the structural changes had the same effect on each of the three Herschel-Bulkley parameters (Dekee et al., 1983).

The decay in the structural parameter was assumed to follow a second order equation

$$\frac{d\lambda}{dt} = -k_1(\lambda - \lambda_e)^2 \text{ for } \lambda > \lambda_e \quad (\text{A.23})$$

where  $k_1$  is the rate constant that is dependent on shear rate. More importantly, this equation can only be used to analyse the rate of breakdown in structure, as the equation specifically states that the equilibrium structure value must be less than the current value. The relationship between  $k_1$  and shear rate can be determined using the following equation

$$a_1(\dot{\gamma}) = \frac{k_1\dot{\gamma}}{\tau_y + K\dot{\gamma}^n} \quad (\text{A.24})$$

Both  $k_1$  and  $a_1$  increase with an increase in shear rate, indicating an increase in the rate of breakdown in structure with shear rate. Tiu & Boger (1974) fitted an exponential model to analyse the change in  $k_1$  and  $a_1$  with shear rate, while Benezech and Maingonnat (1993) utilised linear regression.

More importantly, Tiu and Boger believed that mayonnaise only has one equilibrium structural value which is independent of shear rate. This contradicts the definitions of thixotropy where the equilibrium structure would change with shear rate, as shown in Figure A.9.

O'Donnell and Butler (2002) showed the dependency of the equilibrium structural parameter and shear stress on shear rate in their experiments with yoghurt. They found that the yield stress, equilibrium shear stress and equilibrium structural parameter had a power law relationship with shear rate. The inclusion of this dependency of equilibrium structure on shear rate gave better model predictions against experimental data. Residual error between predicted and experimental data decreased with an increase in shear rate and measurement time during shear step tests.

The adoption of the lumped parameter principle in rheological modelling of food products is commonly encountered e.g. (Benezech & Maingonnat, 1993; Butler & McNulty, 1995; Power, Rodd, Paterson, & Boger, 1998) Many of these systems are multi-structured (more than one type and grade of microscopic and molecular species). The use of a single structural parameter is adequate to approximate the thixotropic behaviour of multi-structured systems (Cheng, 1974).

An alternative approach to the structural parameter is the use of volume fraction as an indication of the arrangement of particles. Einstein (1906) proposed the following relationship between viscosity and volume fraction for a system of spherical particles completely dispersed in a dilute aqueous suspension

$$\mu = 1 + 2.5\phi \tag{A.25}$$

where  $\phi$  is the volume fraction of the system

The Einstein equation has been modified over the years to express the effect of volume fraction on the viscosity of concentrated and non-spherical particles systems e.g. (Mooney, 1951; Krieger, 1972; Dames, Morrison, & Willenbacher, 2001; Usui, 2002). Due to the complexity of the interactions involved, many have preferred to restrict their work to simplified systems where interactions between components are better understood. These include:

- Mono-dispersed system (Tsenoglou, 1990)
- Bimodal spherical particle size distribution system (Gondret & Petit, 1997; Dames et al., 2001).
- Multimodal spherical particle size distribution system (Usui, 2002)

#### **A.2.4.2 Phenomenological models**

One of the main limitations of analysing the rheological behaviour of time-dependent fluids with the structural models is the requirement of an equilibrium state, which implies full reversibility. Many real time-dependent fluids, particularly emulsions and colloidal solutions encountered in the food industry, undergo permanent structural changes during storage. For example, recombined sweetened condensed milk (RSCM) is known to exhibit age thickening (Samel & Muers, 1962). Structural models cannot describe or explain these irreversible changes.

The existence of irreversible changes implies that such a time-dependent fluid cannot be fully characterised unless the full time-temperature-shear history is known, which is not normally the case. An approximate description, however, can be made by simply taking several snap shots of the flow curve at different points in time. This method only works if the measurement time is considerably shorter than the storage time of the sample.

The instantaneous flow curve can be described by phenomenological models. This approach derives mathematical models to describe the relationship between shear stress and shear rate and time. They do not connect directly to the basic processes

responsible for structural changes (Mujumdar et al., 2002). They are restricted to the product investigated and to the conditions under which the measurements were performed. Thus, these models are empirical and do not offer any insights into the physics and chemistry of the structure and its interaction with shear.

Time-independent rheological models used for these snapshots have been briefly discussed in section 2.2.3.2. Benezech and Maingonnat (1994) published a good review on the numerous rheological models used to characterise the rheological behaviour of yoghurt. The Herschel-Bulkley model has been widely used to capture the instantaneous flow curves of dairy systems e.g. (Benezech & Maingonnat, 1993; Velez-Ruiz & Barbosa-Canovas, 1997, 1998, 2000). The changes in the model parameters with time can be analysed to monitor the time-dependent behaviour.

An alternative approach is to follow the change in shear stress with time. One of the more widely used models of this type is the Weltmann model (Weltman, 1943).

$$\tau = A - B \ln(t) \quad (\text{A.26})$$

where A and B are constant parameters which are dependent on shear rate at which the test was conducted.

Many of those who have used the Weltmann model have made an assumption that the shear rate is constant with time (Hough, Moro, Segura, & Calvo, 1988). This is technically incorrect. In most commercial rheometers the rotational speed is kept constant with time but as the structure changes with shearing time, the flow behaviour index  $n$  changes and therefore the true shear rate also changes even when the rotational speed is constant.

Ramaswamy and Basak (1991) proposed a similar model to that of Weltman, where the time of measurement is normalized by the time,  $t_m$ , at which maximum shear stress is observed  $t_m$

$$\tau = A - B \ln\left(\frac{t}{t_m}\right) \text{ where } t \geq t_m \quad (\text{A.27})$$

$t_m$  was not defined as zero time, but instead as the time when the first reliable measurement of shear stress could be obtained. Because the fluid is shear thinning, this value would obviously be larger than all subsequent shear stress values.  $t_m$  is a function of the data acquisition and measuring system, and measuring time (Ramaswamy and Basak, 1991). A significant advantage of this model and the Weltman model is that an equilibrium parameter is not required to describe the rheological behaviour.

O'Donnell and Butler (2002) found that the Weltman model gave the best fit during rheological characterisation of yoghurt across the shear rate range of 5-700  $\text{s}^{-1}$  in comparison to the lumped parameter model proposed by Tiu and Boger (1974) and the modified version by O'donnell and Butler (2002) which takes into account the change in equilibrium structural parameter with shear rate.

Nguyen and Boger (1985, 1987) developed an alternative method to monitor the thixotropy behaviour by concentrating on the development of structure during storage at rest through the use of yield stress. Obviously, this brings in the issue of the determination of the yield as discussed in section 2.2.5.

### **A.2.4.3 Dynamic Models**

There is a vast amount of literature on the development of thixotropic models based on hydrodynamic (motion of particles) and thermodynamic approaches (Regirer & Shadrina, 1978; Heyes, 1988; Tuinier & de Kruif, 2002; Sohn & Rajagopalan, 2003). These models analyse the forces that govern the attraction and repulsion between particles, and how these affect the structure of the system. The models rarely deal with the chemistry details, such as the molecular make up, bonds and chemical reactions.

Ideally such a model should be explicit in a constitutive equation so that one can measure the evolution of the structure from the knowledge of hydrodynamics and thermodynamic interactions. Ultimately, the aim of rheological modeling is to provide engineers and technologists with a tool to predict the final morphology under a given flow field from the knowledge of the on-line rheological measurements (Yu, Bousmina, Grmela, Palieme, & Zhou, 2002).

Particles will attract or repulse each other depending on the nature of the inter-particle forces. Except when subjected to infinite shear where the structure is fully broken down into individual particles and the fluid behaves in a Newtonian manner, particles are attracted to one another and form flow units.

The structure of the flow units will change upon the application of shear. In order to analyse the continuous change in structure of the flow units, one has to know the inter-particle forces between the particles, the adsorbed macromolecular layer, as well as the interactions with the free macromolecules, surfactants and emulsifiers in the continuous phase if applicable. One also has to know the actual number of inter-particle bonds in the aggregated flow units (Kembloswki & Petera, 1981).

Next, the inter-particle forces between the flow units that lead to the break down and build up processes will have to be determined. The kinetics of the two processes are required, as well as the frequency of encounter. This provides information into the energy required for break down or aggregation processes to occur, and how these relate to energy imparted by Brownian motion and applied shear.

Then the effect of flow unit structure on the rheological behaviour of the system is analysed. Factors to be considered are shape, concentration, size distribution, shear and time.

In complex systems such as milk concentrates, there are thousands of components and interactions, which are often superimposed in a complicated manner to form these unit structures (Usui, 2002). In complex fluids, there are consequently multiple structural relaxation times contributing to a corresponding variation of the rheological behaviour with time scales over which they are measured (Sohn & Rajagopalan, 2003).

The use of model systems in the study of rheological behaviour is widely encountered. In these models, the number of components are limited, and the interactions between them are simplified and can be easily controlled (Sohn & Rajagopalan, 2003). Correlations between structure, particle interactions, and rheological behaviour can be determined more easily. Examples of model systems include mono-dispersed hard sphere (Sohn & Rajagopalan, 2003) such as gum, clay suspensions, polymer solutions and other colloidal system (Mills, Goodwin, & Grover, 1991). Brownian hard sphere systems are often encountered, which consist of stable hard spheres with Brownian motion, but without long-range inter-particle forces (Mewis, Frith, Strivens, & Russel, 1989).

An example of a dynamic model is found in the work of Tuinier and de Kruif (2002), de Kruif (1998,, 1999) on factors affecting the rheology of a milk system. Tuinier and de Kruif (2002) combined previously developed theories of hydrodynamics with chemistry understanding to model the rheological behaviour of dilute skim milk during renneting or acid induced coagulation. Firstly, from fundamental physics, they pointed out that the change in structure is governed by three forces: van der Waals forces, electrostatic repulsion and steric repulsion.

Van der Waals forces are the results of permanent dipole- permanent dipole, permanent dipole- induced dipole, and induced dipole- induced dipole interactions between molecules (Narsimhan, 1992; Dickinson & McClements, 1995; Schramm, 1996). Induced dipole-induced dipole interactions result from the rapidly fluctuating dipole moment of a neutral molecule which polarises other neighbouring molecules, and thus gives rise to an attractive force between the neighbouring molecules (Narsimhan, 1992). Van der Waals forces are weak, and act over a relatively long range in comparison to the steep steric and electrostatic repulsion between approaching molecules.

Electrostatic and steric repulsions are caused by the presence of a stabilised  $\kappa$ -casein layer on the surface of the casein micelles. The segment of the  $\kappa$ -casein protruding into the serum contains 15 weakly charged groups that give rise to the electrostatic

repulsion (Tuinier & de Kruif, 2002). The steric repulsion arises from the overlapping stabilised layer, which consists of  $\kappa$ -casein in milk systems, as two particles approach (Cheng, 1987). For steric repulsion, the model even accounts for the dissociation of the  $\kappa$ -casein from the casein micelles at low pH.

The total force is the sum of these three forces. Upon lowering pH, the model revealed the smaller contribution of electrostatic repulsion and the overwhelming effect of steric repulsion. Due to the dissociation of the  $\kappa$ -casein at low pH, the steric repulsion is short range. The system can thus be regarded as an adhesive hard sphere system (Tuinier & de Kruif, 2002).

### **A.2.5 Rheometry**

Measurement of rheology for non-Newtonian fluids always requires care and, more importantly, a thorough understanding of rheological behaviour, of the conditions under which the data is generated and the implication of the results.

Additional difficulties are encountered with time-dependent fluids because of the dependency of shear stress on time, as well as shear rate. The system constantly changes during preparation, storage, and measurement.

During measurement, even the simple task of filling and loading the sample in the rheometer imparts additional shear history that is often ignored or forgotten in data analysis. In cup and bob geometry, the gap between the parts is often of the order of several millimetres. The force required to push the solution through the gap is high, and can cause undesirable breakdown in the structure.

When working at high solids content, reproducibility is jeopardised by the difficulty in obtaining consistent solids contents, particle size distribution and particle packing structure (Cheng, 1984a). Many thixotropic systems are multi-structure (more than one type and grade of microscopic and molecular species (Cheng, 1974)). Reproducibility in these systems is difficult due to inadequate mixing, sedimentation, syneresis and inhomogeneity (Cheng, 1974).

Several methods can be utilised to establish a consistent initial condition in the sample during measurement, including fixed rest time after sample loading, pre-shear at a prescribed shear rate for a fixed time followed by a set rest period (Labropoulos, Palmer, & Lopez, 1981; Pamell-Clunies, Kakuda, Mullen, Amott, & Deman, 1986; Gassem & Frank, 1991). These methods however cannot completely eliminate the problem as the effect of prehistory on a previously untested sample is always unknown (Barnes, 1997).

Cheng (1987) utilises the theory of equilibrium to eliminate shear history effect on a sample. He suggests that a sample should be sheared at a low level until an equilibrium state is reached. Theoretically, the processes of breakdown and build up in thixotropic systems are fully reversible. Thus, for a given shear rate, the equilibrium state should be independent of shear history.

In systems where there are permanent changes to the structure with time, such as milk concentrates (Bienvenue, Jimenez-Flores, et al. 2003), a true equilibrium state does not really exist. The temperature and shear history of the sample becomes extremely important and the replication of measurements is impossible. In such cases, the system is not really thixotropic although the irreversible changes are sometimes much smaller than the thixotropic effects and an approximate rheological characterisation is still possible.

Mewis (1979) listed three fundamental types of experiments for the study of time-dependent rheology:

- a step function (shear step)
- consecutive linear increase and decrease in shear (shear sweep)
- a sinusoidal change in shear (oscillation)

The choice between the shear sweep or shear step test becomes the first immediate question. A shear sweep test involves a linear increase in shear rate or shear stress from zero to a set value, and then returns at the same rate to zero. The test is quick, easy to carry out and provides an indication of the degree of thixotropy (Benezech &

Maingonnat, 1994). The area between the up and down curve is sometimes taken as a measure of thixotropy.

Barnes (1997) listed several bad points associated with the shear sweep test:

- The test is often carried out too quickly, and thus introduces effects of equipment inertia that does not always get taken into account (Krieger, 1990; Baravian & Quemada, 1998). In more advanced rheometers, the instrument's inertia is taken into account in the software packages.
- The test varies both the shear and time variables at the same time. Ideally, these two variables should be manipulated independently. For example, if it is desirable to analyse the time dependent behaviour of a fluid over a shear rate range of  $0-10\text{s}^{-1}$ , ideally 10 identical samples would be required. Each sample is subjected to a step-wise experiment, with the first covering the shear rate range of  $0-1\text{s}^{-1}$ , the second over  $0-2\text{s}^{-1}$ , and so on. All samples should be measured simultaneously in identical equipment by operators working in exactly the same way. Obviously, this ideal exercise cannot be carried out.

In a shear sweep test, apart from the first point of measurement, all subsequent data points will be affected by the shear history created by the previous measurement points that will affect the way the system behaves at the current shear value. This makes it impossible to analyse the rheological behaviour in terms of each variable separately.

The shear step test is an alternative testing method, which involves subjecting the test material to a constant shear rate or stress for a predetermined period of time, before the shear level is changed to another constant value. The test needs to be repeated for different jumps in shear level. More importantly, the initial rheological behaviour must be similar between batches.

The results from these tests depend on the test parameters used, such as measurement interval, the shear range covered, number of data points. Rohm (1992) published a comprehensive study on the effect of measurement procedure on the rheological behaviour of yoghurt. Two sets of experiments were carried out. In the first set, the

range of shear rate in the shear sweep test remained constant, while the measurement time was varied. The hysteresis loop area was found to increase drastically with duration of test. In second experiment, the duration was kept constant, while the final shear rate was modified. The hysteresis loop area increased proportional to final shear rates when these were over  $100 \text{ s}^{-1}$ . Standardisation of experiment protocol is eminently desirable (Rohm, 1992).

Another issue is the choice between controlled shear stress and control shear rate mode. Barnes and Walters (1985) and Chilton et al. (1996) found that the controlled stress rheometer was more accurate at low shear strain rates. However, Krieger (1990) pointed out that controlled-stress rheometers contain much longer instrument inertial time delays of the order of 1 second that must be taken into account during measurement.

For most computerised rotational rheometers, the shear stress and shear rate are obtained from torque and spindle speed measurement with the assumption that the measured system is Newtonian. Chilton et al. (1996) acknowledged that this assumption can produce errors of up to 30% in the values for shear rate, and thus non-Newtonian corrections are required (Krieger & Elrod, 1953; Rao, Hamann, & Humphries, 1975).

Accurate temperature control is imperative during rheological measurement for any given systems (Barnes, 1994), particularly time-dependent systems. In systems such as milk concentrate where irreversible reactions take place under certain conditions, temperature control becomes even more important. At elevated temperature, drying of samples at exposed surfaces and edges provides additional complication in applications where only a small volume of sample is required, such as cone and plate.

In time-dependent systems, the change in rheological behaviour is a function of time. Thus, the response time of the rheometer must be faster than the time scale of the structural changes of the system in order to measure the time-dependent behaviour (Ma & Barbosacanos, 1995).

There are other problems during measurement that may also need to be addressed, including position dependent friction at low shear rate (Giles & Denn, 1990), instrument inertia (Cheng, 1987; Krieger, 1990; Baravian & Quemada, 1998), slips encountered in the high shear range and end effects correction (Bagley, 1957; Highgate & Whorlow, 1969; Princen, 1986).

### **A.2.5.1 Instruments**

#### **A.2.5.1.1 Capillary viscometers**

Fluid from a balance tank is forced through a small circular tube, and the resultant pressure drop and the flow rate are recorded (Ma & Barbosa-Canovas, 1995). The constitutive equation for capillary viscometry can be derived from first principles for time-independent non-Newtonian fluid (Nguyen & Boger, 1992; Ma & Barbosa-Canovas, 1995). End and wall effects are two main problems encountered with the use of capillary rheometers (Bagley, 1957; Vinogradov & Froishteter, 1978; Cheng, 1984b; Kokini, 1992; Nguyen & Boger, 1992).

In general the amount of sample required for capillary rheometers is quite large and the time taken for each measurement relatively lengthy making them less suited for the study of time-dependent fluids, except for special designs such as the gun rheometer developed by Cheng (1987).

#### **A.2.5.1.2 Concentric cylinder viscometers**

These are generally a cup and spindle design, where the spindle rotates and the cup is fixed. Shear is applied to the fluid located in the annulus between the two components. The narrow gap between the cup and spindle ensures a uniform deformation profile within the fluid system (Ma & Barbosa-Canovas, 1995).

The operation of computerised concentric cylinder rheometers with real time reporting of viscosity measurements is based on the assumption of Newtonian behaviour in the test fluid. Thus, the introduction of non-Newtonian behaviour, in particular the presence of a yield stress, gives rise to tedious procedures for data analysis (Darby, 1985; Nguyen & Boger, 1992).

Concentric cylinder rheometers also suffer from errors from end effects and apparent slip at the wall. End effects become more significant with non-Newtonian fluids, particularly those with a yield stress. End effects corrections can be easily applied by adding an extra equivalent length to the actual depth of submersion of the bob during data analysis (Highgate & Whorlow, 1969; Nguyen & Boger, 1992). Slip can be minimized through the introduction of rough surfaces.

The vane rheometer, an alternative form of concentric cylinder design, was introduced by Dzuy and Boger (1983) as a novel method to measure yield stress. The design has been widely applied to study the yield stress of a variety of systems (Keating & Hannant, 1989).

Because of their relative ease of operation and cleaning, rotational viscometers have come to be widely used for rheological characterisation.

#### **A.2.5.1.3 Cone and plate rheometers**

These rheometers consist of an inverted cone, the apex of which is in near contact with the plate (Quinzani & Valles, 1986; Nguyen & Boger, 1992; Cheremisinoff, 1993).

The shear rate in a cone and plate instrument is constant with radial position, which is a definite advantage in rheological studies. Data analysis with cone and plate design is less tedious than the other designs, provided the angle of the cone is sufficiently small (less than  $4^\circ$ ) (Hellingsa, Somsen, & Koenraads Jpjm, 1986; Nguyen & Boger, 1992; Barnes, 1994). In addition the cone and plate design requires very small samples making it well suited for small-strain oscillatory experiments often used to

study gel systems (Benezech & Maingonnat, 1994). The biggest problem is that the evaporation rate is high, especially at high temperatures because of the high surface to volume ratio and the small size of the sample making it difficult to keep the total solids concentration constant during measurement (Barnes, 1994). Slippage is a problem that must be endured, as experienced by other designs too.

#### **A.2.5.2 Sample preparation**

Sample preparation of time-dependent systems is difficult due to the continuous change in rheological behaviour with time (Boger & Tiu, 1974; Barnes & Walters, 1985; Cheng, 1987; Barnes, 1997; Corvisier, Nouar, Devienne, & Lebouche, 2001). It is important to either control or account for this change during preparation and subsequent measurements to ensure the collection of accurate, reliable and, more importantly, reproducible results. In the literature, numerous authors have developed techniques to overcome this reproducibility difficulty, with most methods utilizing the principle of equilibrium state (Park & Ree, 1971; Edwards, Godfrey, & Kashani, 1976; Cheng, 1987), which would eliminate the effect of shear history and achieve consistent initial testing condition for a time-dependent experiment. Table 2.2 lists various sample preparation and rheological measurement techniques cited in the literature.

The most obvious observation from Table 2.2 is the apparent lack of information provided by authors who analysed the rheological behaviour of time-dependent fluids. Rohm (1992) clearly showed the significant effects of measurement conditions on the rheological data of time-dependent reconcile the discrepancies that are often encountered between different published results.

As seen in Table A.2, a common technique during sample preparation is to rest the samples for a period of time before measurement commences. The resting period ranged from 1 hour (Lawrence, Clarke, & Augustin, 2001) to 1 day (Schelhass & Morris, 1985) to 5 days (Velez-Ruiz & Barbosa-Canovas, 1998). However, often there are no data to show that the initial rheological behaviours are similar between replicate samples.

Many authors have used high shear rate to achieve equilibrium state in time-dependent systems (Park & Ree, 1971; Edwards et al., 1976; Cheng, 1987; Steventon, Parkinson, Fryer, & Bottomley, 1990; Wolthers, Duits, Vandenende, & Mellema, 1996; Corvisier et al., 2001). Wolthers et al. (1996) and Corvisier et al. (2001) noted the possible use of high shear to break the structure down to its individual component and prohibit the build up process. Interestingly, Abu-Jdayil and Mohameed (2002) only applied a shear rate of  $47.43 \text{ s}^{-1}$  using a Haake VT 500 concentric cylinder viscometer to achieve complete break down of Labneh (concentrated yoghurt) samples after 2 hours of constant shear. However, this method would only allow the study of structural build up once this high shear force is removed

There are also other techniques developed to minimise replicate error. For example, Boger and Tiu (1974) and Power et al. (1998) degassed mayonnaise samples while Pradipasena and Rha (1977) shook  $\beta$ -lactoglobulin samples gently to ensure good repeatability of the data.

Table A.2: Sample preparation and measurement techniques from literature review

Authors	Title	Test description	Equip, model	Equip. type	Sample preparation	Test shear range ( $s^{-1}$ )	Model
(Ramaswamy & Basak, 1991)	Time dependent stress decay rheology of stirred yoghurt	Constant shear rate	Haake	Rotational	Storage at 2°C for 20 min	100-500	Weltman
(Abu-Jdayil & Mohameed, 2002)	Experimental and modelling studies of the flow properties of concentrated yoghurt as affected by the storage time		Haake	rotational		2-132	
(Alonso, Larrode, & Zapico, 1995)	Rheological behaviour of infant foods		Haake	rotational		0-230.4	
(Bloore & Boag, 1981)	Some factors affecting the viscosity of concentrated skim milk	Single point	Contraves AG	Inline, rotating bob		356 (at 200 rpm)	
(Kelly, 1982a)	The effect of preheat temperature and urea addition on the seasonal variation in the heat stability of skim milk powder	HCT at 120°C and 20%TS	N/A	N/A		N/A	No

Table A.2: Sample preparation and measurement techniques from literature review (continue)

Authors	Title	Test description	Equip. model	Equip. type	Sample preparation	Test shear range (s <sup>-1</sup> )	Model
(Kelly, 1982b)	Effect of seasonal-variation, urea addition and ultrafiltration on the heat-stability of skim-milk powder	HCT at 120°C and 20%TS	N/A	N/A		N/A	No
(Baldwin, Baucke, & Sanderson, 1980)	The effect of concentrate viscosity on the properties of spray dried skim milk powder	Single point	Brookfield RVT, spindle #2	Rotational		50 rpm	No
(Velez-Ruiz & Barbosa-Canovas, 2000)	Flow and structural characteristics of milk (whole)	25C, shear sweep	Paar Physica UM MC20	Concentric cylinder (Z1)	Evaporated samples stored at 4°C for 2-3 days	500-1000	Herschel-Bulkley
(Velez-Ruiz & Barbosa-Canovas, 1997)	Effects of concentration and temperature on the rheology of concentrated milk (whole)	Shear sweep	Paar Physica UM MC20	Concentric cylinder (Z1)	Evaporated samples stored at 4°C for maximum of 5 days	500-1000	Herschel-Bulkley

Table A.2: Sample preparation and measurement techniques from literature review (continue)

Authors	Title	Test description	Equip, model	Equip. type	Sample preparation	Test shear range (s <sup>-1</sup> )	Model
(Hough et al., 1988)	Flow properties of Dulce de Leche, a typical Argentine dairy product	Constant shear	Haake RV2	Concentric cylinder	Not given	32 rpm	Weltmann
(Lawrence et al., 2001)	Effects of heat treatment and homogenization pressure during sweetened condensed milk manufacture on product quality	Single point	Brookfield RVT	Cup and bob, rotary	RSCM from cans were stored at 25°C for 1 hour	20 rpm, spindle 4	None
(Velez-Ruiz & Barbosa-Canovas, 1998)	Rheological properties of concentrated milk as a function of concentration, temperature and storage time	Shear sweep	Paar Physica UM MC20	Concentric cylinder (Z1)	Evaporated samples stored at 4°C for maximum of 5 days	0-1000	Herschel-Bulkley
(Kocak & Zadow, 1985)	Process conditions affecting age-thickening and gelation of sterilised canned evaporated milk	Single point	Mojonnier viscosimeter	Torsional meter	Not mentioned	N/A	

### A.2.6 Summary

Thixotropy is a common rheological behaviour observed in many complex systems, in particularly the food industry. There are several definitions of thixotropy that are well established and the flow behaviours identified. Thixotropy is the destruction of structure when the shear rate is increased, or the build up of structure when the shear rate is decreased. Thixotropy arises because of the finite time required for any structural changes to take place.

The relationship between structure, its rate of change and rheological behaviour are still poorly understood. Models have been developed to provide more simple views of structure and its interaction with rheology. However, these models do not provide adequate information to improve the understanding of structure and its make up.

Dynamic models offer detailed insights into the physics of bonds formation and inter-particle potentials that have been derived from fundamental knowledge of forces. These models usually do not incorporate chemistry understanding.

Experimental techniques, including sampling, preparation and measurement, may contribute significantly to the discrepancies between published results on the thixotropic behaviour of many systems. Rohm (1992) clearly showed the effect of measurement parameters on the resultant rheological behaviour of time dependent system, and standardisation of experiment protocol is desirable.

Of course, such standardisation of experiment protocol is difficult when the results must be kept within the range of shear rate of practical applications. Thixotropy experiments have been carried out on a wide range of materials, ranging from simple colloidal system to complex food solutions. Each type of material has its own practical value in its industry, and its application is different from any other. For example, the rheology of paint deals with low shear level, with particular interest on the recovery of viscosity during resting, i.e. once the paint has been applied. In the oil industry, transportation

takes place at high shear. The yield stress is also of importance due to its effect during start up. Yield stress is a perfect example of a rheological parameter that has been devised to describe certain aspects of rheology with many practical benefits.

The evidence that irreversible changes occur during storage or processing of time-dependent fluids are largely anecdotal. More formal evidence has only begun to be reported recently. Such behaviour complicates immensely the problems in measurement techniques as well as modelling. It implies that the system can only be characterised if the full temperature-shear-time history of the product is known, which is extremely rare in the commercial/industrial context. There is barely any work at all in this area which remains one of the biggest challenges in the rheological study of time-dependent fluids.

#### A.2.7 References

1. Abu-Jdayil, B., & Mohameed, H. (2002). Experimental and Modelling Studies of the Flow Properties of Concentrated Yogurt as Affected by the Storage Time. Journal of Food Engineering, 52(4), 359-365.
2. Alessandrini, A., Lapasin, R., & Sturzi, F. (1982). The Kinetics of Thixotropic Behavior in Clay Kaolin Aqueous Suspensions. Chemical Engineering Communications, 17(1-6), 13-22.
3. Alexander, E. B. (1992). Dilatancy and thixotropy: commonly misused terms and confused phenomena. Soil Survey Horizons, 33: 2, 36-38.
4. Alonso, M. L. , Larrode, O., & Zapico, J. (1995). Rheological Behavior of Infant Foods. Journal of Texture Studies, 26(2), 193-202.
5. Astarita, G. (1990). The Engineering Reality of the Yield Stress. Journal of Rheology, 34(2), 275-277.
6. Bagley, E. B. (1957). End correction in the capillary flow of polyethylene. Journal of Applied Physics, 28, 624-627.

7. Baldwin, A. J., Baucke, A. G., & Sanderson, W. B. (1980). The effect of concentrate viscosity on the properties of spray dried skim milk powder. New Zealand Journal of Dairy Science & Technology, 15(3), 289-297.
8. Baravian, C., & Quemada, D. (1998). Correction of instrumental inertia effects in controlled stress rheometry. European Physical Journal-Applied Physics, Vol.2, No.2, 2 (2), 189-95.
9. Baravian, C., Quemada, D., & Parker, A. (1996). Modelling thixotropy using a novel structural kinetics approach: basis and application to a solution of iota carrageenan. Journal of Texture Study, 27, 371-390.
10. Barnes, H. A. (1994). Rheology of Emulsions - a Review. Colloids and Surfaces a- Physicochemical and Engineering Aspects, 91, 89-95.
11. Barnes, H. A. (1997). Thixotropy-a review. Journal of Non-Newtonian Fluid Mechanics, vol.69, no.2-3, pp.1-33.
12. Barnes, H. A., & Walters, K. (1985). The Yield Stress Myth. Rheologica Acta, 24(4), 323-326.
13. Benezech, T. , & Maingonnat, J. F. (1993). Flow properties of stirred yoghurt: structural parameter approach in describing time-dependency. Journal of Texture Studies, 24, 455-473.
14. Benezech, T. , & Maingonnat, J. F. (1994). Characterization of the Rheological Properties of Yogurt - a Review. Journal of Food Engineering, 21( 4), 447-472.
15. Bhamidipati, S., & Singh, R. K. (1995). Determination of Fluid-Particle Convective Heat-Transfer Coefficient. Transactions of the Asae, 38(3), 857-862.
16. Bienvenue, A., Jimenez-Flores, R., & Singh, H. (2003). Rheological properties of concentrated skim milk: Importance of soluble minerals in the changes in viscosity during storage. Journal of Dairy Science, 86, 3813-3821.

17. Bingham, E. C. (1922). Fluidity and Plasticity. New York: McGraw Hill.
18. Bloore, C. G., & Boag, I. F. (1981). Some factors affecting the viscosity of concentrated skim milk. New Zealand Journal of Dairy Science & Technology, 16(2), 143-154.
19. Boger, D. V. , & Tiu, C. (1974). Rheological properties of food products and their use in the design of flow systems. Food Technology in Australia ; 26(8), 325-335.
20. Borwankar, R. P. (1992). Food texture and rheology: A tutorial review. Journal of Food Engineering, 16, 1-16.
21. Bower, D. I. (2002). An Introduction to Polymer Physics. Cambridge, United Kingdom: Cambridge University Press.
22. Carreau, P. J., Chhabra, R. P., & Cheng, J. (1993). Effect of Rheological Properties on Power-Consumption With Helical Ribbon Agitators. AIChE Journal, 39(9), 1421-1430.
23. Charm, S. E. (1963). Effect of yield stress on the power law constants of fluid food materials determined in low shear rate viscometers. Industrial & Engineering Chemistry (I&EC) Process Design and Development, 2, 62-65.
24. Cheng, D. C. H. (1974). On the behaviour of thixotropic fluids with a distribution of structure. Journal of Physics D. Applied Physics, 7, L155-L158.
25. Cheng, D. C. H. (1984a). Further Observations on the Rheological Behavior of Dense Suspensions. Powder Technology, 37(JAN-), 255-273.
26. Cheng, D. C. H. (1984b). Further observations on the rheological behaviour of dense suspensions. Powder Technology, 35, 255-73.
27. Cheng, D. C. H. (1987). Thixotropy. International Journal of Cosmetic Science, 9(4), 151-191.

28. Cheremisinoff, N. P. (1993). An introduction to polymer rheology and processing. Florida, USA: CRC Press Inc.
29. Chilton, R., Stainsby, R., & Thompson, S. (1996). The design of sewage sludge pumping systems. Journal of Hydraulic Research, *34*(3), 395-408.
30. Cokelet, G. R., Merrill, E. W., & Gilliland, E. R. (1963). The rheology of human blood-measurement near and at zero shear rate. Transactions of the Society of Rheology VII, 303-317.
31. Corvisier, P., Nouar, C., Devienne, R., & Lebouche, M. (2001). Development of a thixotropic fluid flow in a pipe. Experiments in Fluids, *31*, 579-587.
32. Coussot, P., & Boyer, S. (1995). Determination of yield stress fluid behaviour from inclined plane test. Rheologica Acta., *34*(6 ), 534-543.
33. Cross, M. M. (1965). Rheology of non-Newtonian fluids: a new flow equation for pseudoplastic systems. Journal of Colloid Science, *20*, 417-437.
34. Curcio, S., Gabriele, D., Giordano, V., Calabro, V., de Cindio, B., & Iorio, G. (2001). A rheological approach to the study of concentrated milk clotting. Vol. 40, 154-161.
35. Dames, B., Morrison, B. R., & Willenbacher, N. (2001). An empirical model predicting the viscosity of highly concentrated, bimodal disperions with colloidal interactions. Rheologica Acta, *40*, 434-440.
36. Darby, R. (1985). Couette viscometer data reduction for materials with a yield stress. Journal of Rheology, *29*(4), 369-378.
37. de Kruif, C. G. (1998). Supra-aggregates of casein micelles as a prelude to coagulation. Journal of Dairy Science, *81*, 3019-3028.
38. de Kruif, C. G. (1999). Casein micelle interactions. International Dairy Journal, *9*, 183-188.

39. Dekee, D., Code, R. K., & Turcotte, G. (1983). Flow Properties of Time-Dependent Foodstuffs. Journal of Rheology, 27(6), 581-604.
40. Dervisoglu, M., & Kokini, J. L. (1986). Steady Shear Rheology and Fluid-Mechanics of 4 Semisolid Foods. Journal of Food Science, 51(3), 541-&.
41. Dickinson, E., & McClements, D. J. (1995). Advances in food colloids. Glasgow: Chapman & Hall.
42. Dodeja, A. K., Sarma, S. C., & Abichandani, J. (1990). Heat transfer during evaporation of milk to high solids in thin film scrapped surface heat exchanger. Journal of Food Process Engineering, 12, 211-225.
43. Doraiswamy, D., Mujumdar, A. N., Tsao, I., Beris, A. N., Danforth, S. C., & Metzner, A. B. (1991). The Cox-Merz Rule Extended - a Rheological Model for Concentrated Suspensions and Other Materials With a Yield Stress. Journal of Rheology, 35(4), 647-685.
44. Dzuy, N. Q., & Boger, D. V. (1983). Yield Stress Measurement for Concentrated Suspensions. Journal of Rheology, 27(4), 321-349.
45. Dzuy, N. Q., & Boger, D. V. (1985). Direct yield stress measurement with the Vane method. Journal of Rheology, 29(3), 335-347.
46. Edwards, M. F., Godfrey, J. C., & Kashani, M. M. (1976). Power requirement for the mixing of thixotropic liquids. Journal of Non-Newtonian Fluid Mechanics, Vol.1, No.4, Dec., 309-22.
47. Einstein, A. (1906). Eine nenu Bestimmung der Molekul-dimensionen. Annual Physik, 19, 289-306.
48. Evans, I. D. (1992). On the Nature of the Yield Stress . Journal of Rheology, 36(7), 1313-1316.
49. Fellows, P. (2000). Food processing technology. Cambridge: Woodhead Publishing

Limited.

50. Gasseem, M. A., & Frank, J. F. (1991). Physical-Properties of Yogurt Made From Milk Treated With Proteolytic-Enzymes. Journal of Dairy Science, *74*(5), 1503-1511.
51. Giles, D. W. , & Denn, M. M. (1990). Strain measurement error in a constant stress rheometer. Journal of Rheology, *34*(4), 603-608.
52. Gondret, P., & Petit, L. (1997). Dynamic Viscosity of Macroscopic Suspensions of Bimodal Sized Solid Spheres. Journal of Rheology , *41*(6), 1261-1274.
53. Goodeve, C. F. (1939). A general theory of thixotropy and viscosity. Transaction Faraday Society, *35*, 342-358.
54. Goodrich, K. , Yoshimura, A., & Prudhomme, R. K. (1989). Measurement of the modulus and yield strength of soft gels: experiments and numerical simulation. Journal of Rheology , *33*(2), 317-327.
55. Halmos, A. L., & Tiu, C. (1981). Liquid Foodstuffs Exhibiting Yield Stress and Shear-Degradability. Journal of Texture Studies, *12*(1), 39-46.
56. Hamley, I. W. (2000). Introduction to Soft Matter. Polymers, Colloids, Amphiphiles and Liquid Crystals. West Sussex, England: John Wiley & Sons, Ltd.
57. Hannote, M., Flores, F., Torres, L., & Galindo, E. (1991). Apparent Yield Stress Estimation in Xanthan Gum Solutions and Fermentation Broths Using a Low-Cost Viscometer. Chemical Engineering Journal and the Biochemical Engineering Journal, *45*(3), B49-B56 .
58. Hartnett, J. P., & Hu, R. Y. Z. (1989). The Yield Stress - an Engineering Reality. Journal of Rheology, *33*(4), 671-679.
59. Hellinga, C. , Somsen, D. J., & Koenraads Jpjm. (1986). Viscosity of Stirred Yogurt - Modern Techniques Useful in Analyzing and Improving Routine

- Measurements. Netherlands Milk and Dairy Journal, 40(2-3), 217-240.
60. Herschel, W. H., & Bulkley, R. (1926). Measurement of consistency as applied to rubber-benzene solutions. Proc. Am. Soc. Test. Matls, 26, 621-633.
61. Heyes, D. M. (1988). Shear thinning of dense suspensions modelled by Brownian dynamics. Physics Letters A, 132(8-9), 399-402.
62. Highgate, D. J., & Whorlow, R. W. (1969). End effects and particle migration effects in concentric cylinder rheometry. Rheologica Acta, 8, 142-151.
63. Hough, G., Moro, O., Segura, J., & Calvo, N. (1988). Flow Properties of Dulce-De-Leche, a Typical Argentine Dairy Product. Journal of Dairy Science, 71( 7), 1783-1788.
64. Houwink, R. (1958). Elasticity, plasticity and structure of matter. New York: Dover.
65. Jones, T. G. J., & Hughes, T. L. (1996). Drilling fluid suspensions. (Vol. 251pp. 463-564). 1155 SIXTEENTH ST NW, WASHINGTON, DC 20036: Amer Chemical Soc.
66. Keating, J., & Hannant, D. J. (1989). The effect of rotation rate on gel strength and dynamic yield strength of thixotropic oil well cements measured using a shear vane. Journal of Rheology, 33(7), 1011-1020.
67. Kelly, P. M. (1982a). The effect of preheat temperature and urea addition on the seasonal variation in the heat stability of skim-milk powder. Journal of Dairy Research, 49(2), 187-196.
68. Kelly, P. M. (1982b). Effect of seasonal-variation, urea addition and ultrafiltration on the heat-stability of skim-milk powder. Journal of Dairy Research, 49(1), 119-126.
69. Kembloski, Z., & Petera, J. (1981). Memory effects during the flow of thixotropic

- fluids in pipes. Rheologica Acta., vol.20, no.4. West Germany., 311-23.
70. Kocak, H. R. , & Zadow, J. G. (1985). Age gelation of UHT whole milk as influenced by storage temperature. The Australian Journal of Dairy Technology, 40(1), 14-21.
71. Kokini, L. J. (1992). Rheological properties of foods. New York: Marcel Dekker, Inc.
72. Krieger, I. M. (1972). Rheology of monodisperse latices. Advance Colloid Interface Science, 3, 111-136.
73. Krieger, I. M. (1990). The role of instrument inertia in controlled stress rheometers. Journal of Rheology, 34(4), 471-483.
74. Krieger, I. M., & Elrod, H. (1953). Direct determination of the flow curves of non-Newtonian fluids II. Shearing rate in the concentric cylinder viscometer. Journal of Applied Physics, 24(134-134).
75. Labropoulos, A. E., Palmer, J. K., & Lopez, A. (1981). Whey-Protein Denaturation of Uht Processed Milk and Its Effect on Rheology of Yogurt. Journal of Texture Studies, 12 (3), 365-374.
76. Lang, E. R., & Rha, C. (1981). Determination of the yield stress of hydrocolloid dispersions. Journal of Texture Studies, 12(1), 47-62.
77. Lapasin, R., & Prici, S. (1995). Rheology of industrial polysaccharides: Theory and applications. Cornwall, Great Britain: Chapman & Hall.
78. Lawrence, A. , Clarke, P. T., & Augustin, M. A. (2001). Effects of Heat Treatment and Homogenisation Pressure During Sweetened Condensed Milk Manufacture on Product Quality. Australian Journal of Dairy Technology, 56(3), 192-197.
79. Ma, L., & Barbosa-Canovas, G. V. (1995). Instrumentation for the Rheological

Characterization of Foods. Food Science and Technology International,  
1(1), 3-17.

80. Magnin, A., & Piau, J. M. (1990). Cone-and-Plate Rheometry of Yield Stress Fluids - Study of an Aqueous Gel. Journal of Non-Newtonian Fluid Mechanics, 36, 85-108.
81. Markovitz, H. (1985). Rheology: in the beginning. Journal of Rheology, 29(6), 777-798.
82. Mewis, J. (1979). Thixotropy-a general review. Journal of Non-Newtonian Fluid Mechanics, 6(1), 1-20.
83. Mewis, J., Frith, W. J., Strivens, T. A., & Russel, W. B. (1989). The Rheology of Suspensions Containing Polymerically Stabilized Particles. Aiche Journal, 35(3), 415-422.
84. Mills, P. D. A., Goodwin, J. W., & Grover, B. W. (1991). Shear field modification of strongly flocculated suspensions. aggregate morphology. Colloid Polymer Science , 269, 949-963.
85. Mohamed, I. O., & Steffe, J. F. (1985). Sensitivity of Flow-Rate Calculations to the Rheological Properties of Herschel-Bulkley Fluids. Transactions of the ASAE, 28 (4), 1349-1352.
86. Mooney, M. (1951). The viscosity of a concentrated suspension of spherical particles. Journal of Colloid Science, 6, 162-170.
87. Moore F. (1959). The Rheology of ceramic slips and bodies. Vol. 58, 470-492.
88. Moore, I. P. T., Cossor, G., & Baker, M. R. (1995). Velocity Distributions in a Stirred-Tank Containing a Yield Stress Fluid. Chemical Engineering Science, 50(15), 2467-2481.
89. Mujumdar, A. , Beris, A. N., & Metzner, A. B. (2002). Transient Phenomena in

Thixotropic Systems. Journal of Non-Newtonian Fluid Mechanics, 102(2), 157-178.

90. Muller-Mohnssen, H., Weiss, D., & Tippe, A. (1990). Concentration dependent changes of apparent slip in polymer solution flow. Journal of Rheology, 34(2), 223-244.
91. Nagase, Y., & Okada, K. (1986). Heterogeneous behavior after yielding of solid suspensions. Journal of Rheology, Vol.30, No.6, Dec. , 30(6), 1123-42.
92. Narsimhan, G. (1992). Emulsions. Physical chemistry of foods . New York: Marcel Dekker, Inc.
93. Nguyen, Q. D., & Boger, D. V. (1983). Yield stress measurement for concentrated suspensions. Journal of Rheology, 27(4), 321-329.
94. Nguyen, Q. D., & Boger, D. V. (1992). Measuring the flow properties of yield stress fluids. Annual Review in Fluid Mechanics, 24, 47-88.
95. O'donnell, H. J., & Butler, F. (2002). Time-Dependent Viscosity of Stirred Yogurt. Part I: Couette Flow. Journal of Food Engineering, 51(3), 249-254.
96. Park, K., & Ree, T. (1971). Kinetics of thixotropy of aqueous bentonite suspension. Journal of the Korean Chemical Society, 15(6), 293-303.
97. Pamell-Clunies, E., Kakuda, Y., Mullen, K., Arnott, D. R., & Deman, J. M. (1986). Physical properties of yoghurt; a comparison of vat versus continuous heating systems of milk. Journal of Dairy Science, 69, 2593-603.
98. Peeples, M. L., Gould, I. A., Jones, C. D., & Harper, W. J. (1962). Forced convection heat transfer characteristics of fluid milk products. Journal of Dairy Science, 45, 303-310.
99. Power, D. J. , Rodd, A. B., Paterson, L., & Boger, D. V. (1998). Gel transition studies on nonideal polymer networks using small amplitude oscillatory

rheometry. Journal of Rheology, 42(5), 1021-1037.

100. Pradipasena, P., & Rha, C. (1977). Pseudoplastic and rheopectic properties of a globular protein ( beta -lactoglobulin) solution. Journal of Texture Studies., 8: 3, 311-325.
101. Princen, H. M. (1986). A novel design to eliminate end effects in a concentric cylinder viscometer. Journal of Rheology, 30(2), 271-283.
102. Quemada, D. (1999). Rheological Modelling of Complex Fluids: Iv: Thixotropic and "Thixoelastic" Behaviour. Start-up and Stress Relaxation, Creep Tests and Hysteresis Cycles. European Physical Journal-Applied Physics, 5(2), 191-207.
103. Quinzani, L. M., & Valles, E. M. (1986). The use of a modified cone and plate geometry (MCP) in a rotational rheometer for the measurement of material functions. Journal of Rheology, 30(S), S1-S21.
104. Ramaswamy, H. S., & Basak, S. (1991). Time dependent stress decay rheology of stirred yogurt. International Dairy Journal., 2: 1, 17-31.
105. Rao, V. N. M., Hamann, D. D., & Humphries, E. G. (1975). Flow behavior of sweet potato puree and its relation to mouth feel quality. Journal of Texture Studies., 6(2), 197-209.
106. Regirer, S. A., & Shadrina, N. Kh. (1978). On models of thixotropic fluids. Journal of Applied Mathematics and Mechanics, 42(5 ), 925-936.
107. Rohm, H. (1992). Viscosity determination of stirred yoghurt. Vol. 25, 297-301.
108. Samel, R., & Muers M. M. (1962). The age-thickening of sweetened condensed milk. I. Rheological properties. Journal of Dairy Research, 29, 249-258.
109. Schelhass, S. M., & Morris, H. A. (1985). Rheological and scanning electron microscopic examinatin of skim milk gels obtained by fermenting with ropy

and non-ropy strains of lactic acid bacteria. Vol. 4, 279-87.

110. Schmitt, L. , Ghnassia, G., Bimbenet, J. J., & Cuvelier, G. (1998). Flow properties of stirred yogurt: calculation of the pressure drop for a thixotropic fluid. Journal of Food Engineering, 37, 367-388.
111. Schramm, L. L. (1996). Suspensions: Basic principles. (Vol. 251pp. 3-44). 1155 Sixteenth St Nw, Washington, DC 20036: Amer Chemical Soc.
112. Schurz, J. (1992). A yield value in a true solution. Journal of Rheology, 36(7), 1319-1321.
113. Scott Blair, G. W. (1933). On the nature of yield value. Physics, 4, 113.
114. Sohn, I. S. , & Rajagopalan, R. (2003). Microrheology of model quasi-hard-sphere dispersions. Journal of Rheology, 48(1), 117-142.
115. Spaans, R. D., & Williams, M. C. (1995). At Last, a True Liquid-Phase Yield Stress. Journal of Rheology, 39(1), 241-246.
116. Steffe, J. F. (1992). Rheological methods in food process engineering. Michigan, USA: Freeman Press.
117. Steffe, J. F., Mohamed, I. O., & Ford, E. W. (1984). Pressure-Drop Across Valves and Fittings for Pseudoplastic Fluids in Laminar-Flow. Transactions of the Asae, 27(2), 616-619.
118. Steventon, A. J., Parkinson, C. J., Fryer, P. J., & Bottomley, R. C. (1990). The rheology of yoghurt. R. E. Carter (Editor), Rheology of food, pharmaceutical and biological materials with general rheology (pp. 196-210). London: Elsevier Applied Science.
119. Tiu, C., & Boger, D. V. (1974). Complete rheological characterization of time-dependent food products. Journal of Texture Studies, 5(3), 329-338.
120. Tsenoglou, C. (1990). Scaling concepts in suspension rheology. Journal of

Rheology, 34(1), 15-29.

121. Tuinier, R., & de Kruif, C. G. (2002). Stability of casein micelles in milk. Journal of Chemical Physics, 117(3), 1290-1295.
122. Umeya, K., Isoda, T., Ishii, T., & Sawamura, K. (1969). Some observations on the flow properties of disperse systems. Powder Technology, 3, 259-66.
123. Usui, H. (2002). Prediction of dispersion characteristics and rheology in dense slurries. Journal of Chemical Engineering of Japan, 35(9), 815-829.
124. Velez-Ruiz, J. F., & Barbosa-Canovas, G. V. (1997). Effects of concentration and temperature on the rheology of concentrated milk. Transactions of the ASAE, 40(4), 1113-1118.
125. Velez-Ruiz, J. F., & Barbosa-Canovas, G. V. (1998). Rheological Properties of Concentrated Milk as a Function of Concentration, Temperature and Storage Time. Journal of Food Engineering, 35(2), 177-190.
126. Velez-Ruiz, J. F., & Barbosa-Canovas, G. V. (2000). Flow and Structural Characteristics of Concentrated Milk. Journal of Texture Studies, 31( 3), 315-333.
127. Vinogradov, G. V., & Froishteter, G. B. T. K. K. (1978). The generalised theory of flow of plastic disperse systems with account of wall effect. Rheologica Acta, 17, 156-165.
128. Weltman, R. N. (1943). Breakdown of thixotropic structure as a function of time. Journal of Applied Physics, 14, 343-350.
129. Wildemuth, C. R., & Williams, M. C. (1985). A new interpretation of viscosity and yield stress in dense slurries: coal and other irregular particles. Rheologica Acta, 24, 75-91.
130. Wolthers, W., Duits, M. H. G., Vandenende, D., & Mellema, J. (1996). Shear

history dependence of the viscosity of aggregated colloidal dispersions. Journal of Rheology, 40(5), 799-811.

131. Yoshimura, A. S., Prud'homme, R. K., Princen, H. M., & Kiss, A. D. (1987). A comparison of techniques for measuring yield stresses. Journal of Rheology, 31(8), 699-710.
132. Yu, W., Bousmina, M., Grmela, M., Palieme, J. F., & Zhou, C. (2002). Quantitative relationship between rheology and morphology in emulsions. Journal of Rheology, 46(6).
133. Yziquel, F. , Carreau, P. J., Moan, M., & Tanguy, P. A. (1999). Rheological Modeling of Concentrated Colloidal Suspensions. Journal of Non-Newtonian Fluid Mechanics, 86(1-2), 133-155.
134. Zhou, Z., Solomon, M. J., Scales, P. J., & Boger, D. V. (1999). The yield stress of concentrated flocculated suspensions of size distributed particles. Journal of Rheology, 43(3), 651-671.

### A.3 Ratios of change in the Herschel-Bulkley parameters during age thickening

All the storage runs in this work showed that the value of  $n$  decreases with storage time during age-thickening. This is also observed by Velez-Ruiz and Barbosa-Canovas (1997) in fresh milk concentrates. The ratio of increase in  $\tau_y$  and  $K$ , and the ratio of decrease in  $n$  can be determined and plotted against storage time. Figure A13 plots the changes in  $\tau_y/\tau_{y,0}$ ,  $K/K_0$ , and  $n/n_0$  against storage time for run C100. The ratios of increase in  $\tau_y$  and  $K$  with storage time are quite different in Figure A13 and therefore cannot be modelled by a unique multiplier. This trend was also observed with the data from Velez-Ruiz and Barbosa-Canovas (1997) when similar graphs were plotted. These results validate the argument put forth by Trinh and Schraekenrad (2002) that separate time factor should be coupled with each model parameter to account for the independent variation with time.

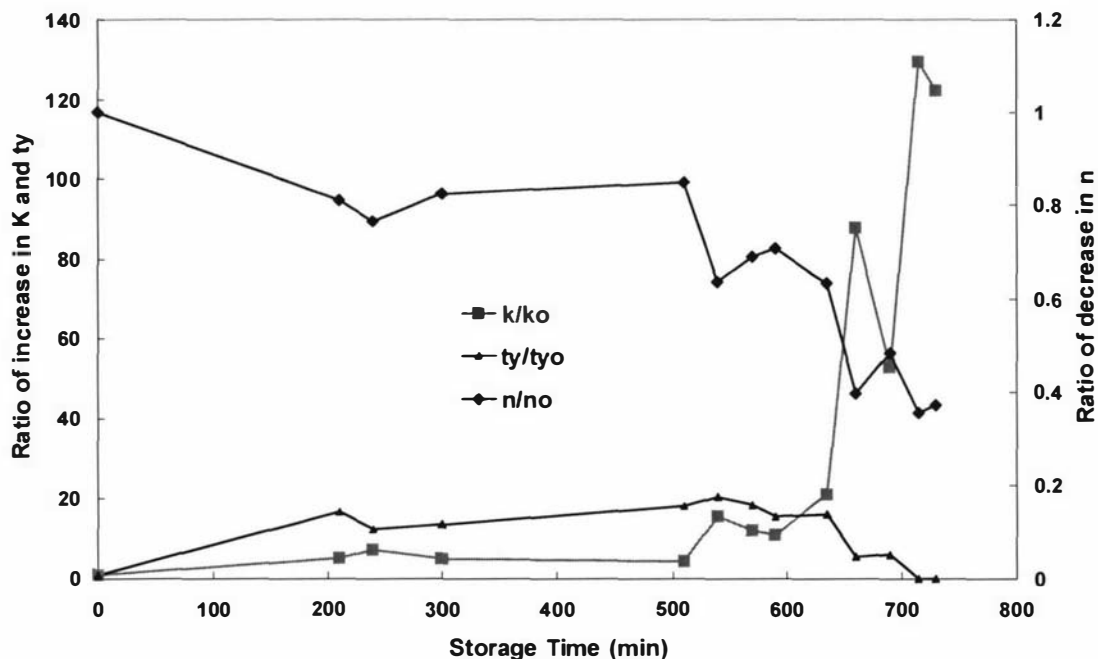


Figure A.12: Changes in  $\tau_y/\tau_{y,0}$ ,  $K/K_0$ , and  $n/n_0$  with storage time during age thickening. Run C100, powder B, 50%TS, 75°C.

As stated previous, the structure of a time-dependent fluid at any time is the result two competitive processes: build up and breakdown which can be expressed in the equation derived from the Moore model (Moore, 1959)

$$\frac{d\lambda}{dt} = g = a(1 - \lambda) - b\lambda\dot{\gamma} \quad (\text{A.28})$$

The method of Tiu and Boger (1974) assumed that the parameter  $a$  is zero and thus structural build up is non-existent. Even when there is a net breakdown of structure at a given shear rate, it is not conceptually correct to assume that collisions of particles by Brownian motion and agitation do not result in some structural build up. Therefore the parameter measured by Tiu and Boger (1974) is not quite the same as the breakdown coefficient in the Moore model.

### A.3.1 Reference List

1. Moore F. (1959). The Rheology of ceramic slips and bodies. Vol. 58, 470-492.
2. Tiu, C., & Boger, D. V. (1974). Complete rheological characterization of time-dependent food products. Journal of Texture Studies, 5(3), 329-338.
3. Trinh, K. T., & Schraekenrad, H. (2002). Effect of heating on the rheological properties of milk concentrates. Paper #401 in 9th APCCChE Congress and Chemeca, Christchurch, New Zealand .
4. Velez-Ruiz, J. F., & Barbosa-Canovas, G. V. (1997). Effects of concentration and temperature on the rheology of concentrated milk. Transactions of the ASAE, 40(4), 1113-1118.

#### A.4 Comparison of consistency coefficient versus apparent viscosity

As observed in sections 5.4-5.7, the consistency coefficient was found to follow similar trends to the apparent viscosity during age thickening in reconstituted concentrates made from powder B. An example of the similarity between the trends in  $K$  and  $\mu_{app}$  for run C100 is shown in Figure A.14.

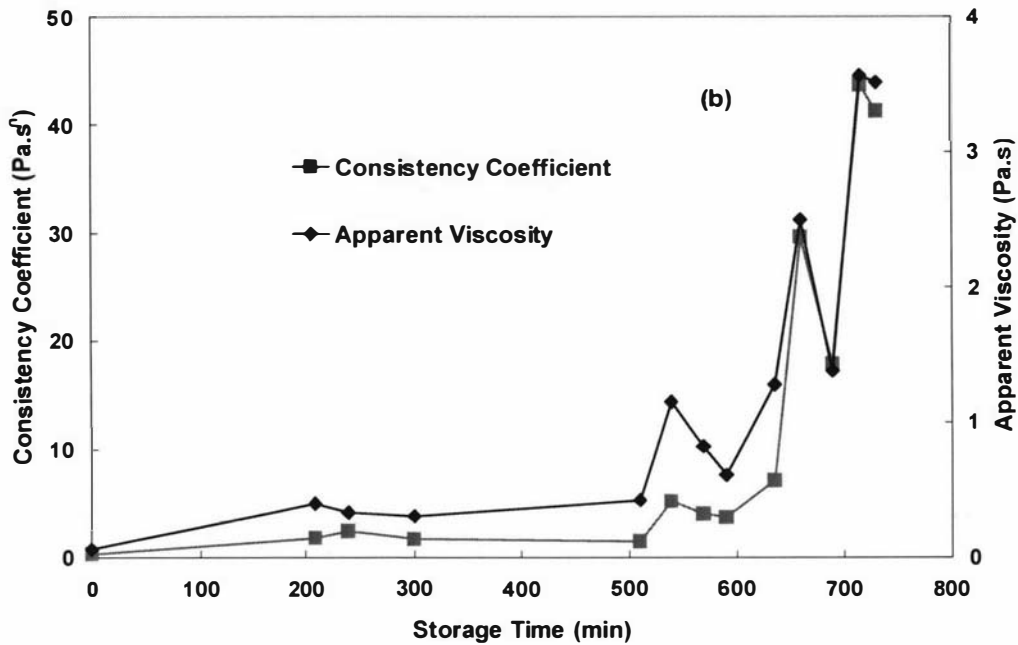


Figure A.13: Comparison in the changes in  $K$  and  $\mu_{app}$  with storage time during age thickening. Run C100, powder B, 50%TS, 75°C.

The trends in yield stress and apparent viscosity were quite different. As the apparent viscosity is determined by

$$\mu_{app} = \frac{\tau}{\dot{\gamma}} \quad (\text{A.3})$$

it is be more appropriate to plot the changes in  $\frac{\tau_y}{\dot{\gamma}}$  with storage time and compare the trend with that of the apparent viscosity.  $\frac{\tau_y}{\dot{\gamma}}$ ,  $\mu_{app}$  and  $K$  were normalised against the time-zero value for run C100 and the results are shown in Figure A15.

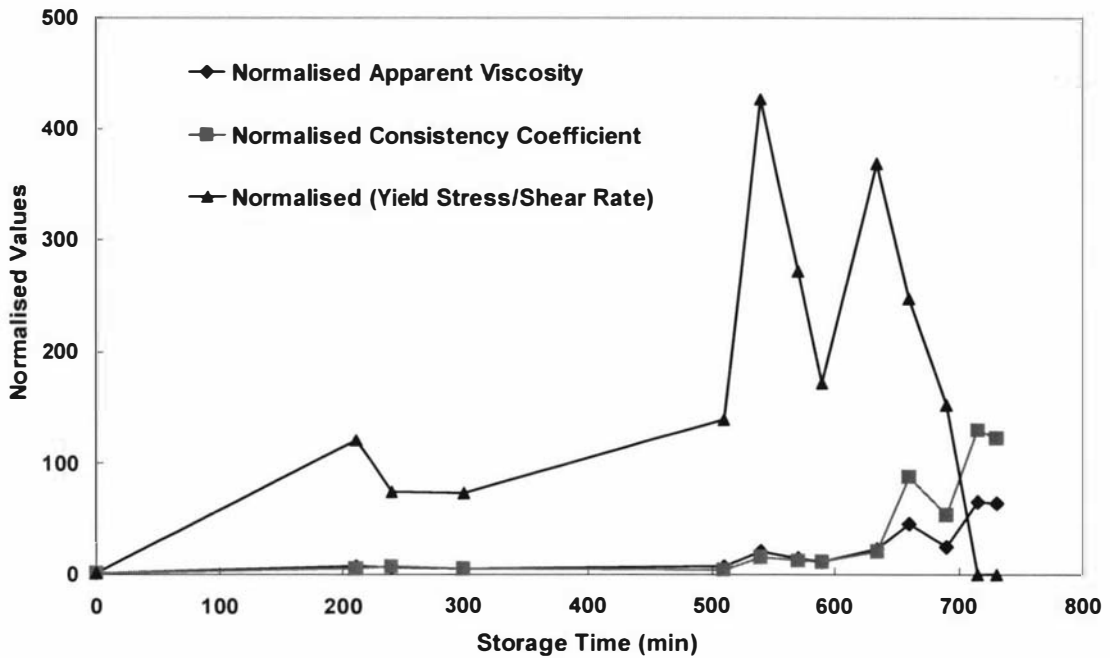


Figure A.14: Comparison between the changes in the normalized  $\frac{\tau}{\dot{\gamma}}$ ,  $\frac{\tau_y}{\dot{\gamma}}$  and  $K$  with storage time during age thickening.

The trend of the yield stress did not agree with that of the apparent viscosity. It seems that the change in viscosity with storage time during age thickening was driven much more by the consistency of the fluid than its yield stress.